DOCTOR OF PHILOSOPHY

Relative sea level change in the Forth and Tay Estuaries: past changes informing future trends

Powell, Victoria Alicia

Award date:
2012

DOCTOR OF PHILOSOPHY

Relative sea level change in the Forth and Tay Estuaries: past changes informing future trends

Victoria Alicia Powell

2012

University of Dundee

Relative Sea Level Change in the Forth and Tay Estuaries: Past Changes Informing Future Trends.

Victoria Alicia Powell

PhD

University of Dundee

January 2013

Table of Contents

List of Figures

List of Tables

Acknowledgements

I would like to thank everyone who has supported me throughout my studies at the University of Dundee and, in particular, the following individuals and organisations for providing essential data, information and support throughout my studies:

- My supervisors, Rob Duck and Derek McGlashan, for their tireless support and guidance;
- Forth Ports, the primary funding body, and SNH for providing additional funding;
- Peter Crawley at Forth Ports and all Forth Ports staff, for providing essential background information, support and guidance about tide gauges, levelling and port operations;
- The staff at the Port of Dundee, for supporting me while I transcribed data for several weeks at the Port Office, and likewise the staff at UKHO in Taunton, for supporting me and providing additional information while I transcribed data at their office;
- PSMSL, TERC, UKHO, BODC/NTSLF, SEPA, Perth Harbour Authority, Forth Ports and Dunbar Harbour Trust for providing tide gauge data and background information;
- The following specialists for their personal communications: Phillip Woodworth, Kevin Horsburgh, Christopher Jones; as well as other mentioned in the text;
- Jonathan Powell for his guidance with Excel macro creation for data extraction;
- The MathWorks and the University of Dundee for providing additional training events in specialist areas that have helped me develop a greater knowledge of software packages and the subject area;
- My family, colleagues and friends for their support.

Declaration

The candidate:

I declare that I am the author of this thesis; unless otherwise stated, I have consulted all references cited; the work of which the thesis is a record has been carried out and composed by myself; and that the work has not been accepted in fulfilment of the requirements of any other degree or professional qualification.

…….

Victoria Powell

Supervisors:

I certify that Victoria Powell has satisfied the conditions of the Ordinance and Regulations and is qualified to submit this dissertation in application for the degree of PhD.

…….

Professor Robert Duck

…….

Dr. Derek McGlashan

Abstract

This thesis introduces new relative sea level datasets from the Forth and Tay Estuaries dating between 1900 and 2010 and uses these to analyse sea level oscillations, surge components and to influence future sea level projections. Prior to this research, relative sea levels had not been analysed across this region. These datasets were collated and corrected using renowned methods and investigated using Shennan *et al.*'s (2012) GIA corrections, Torrence and Compo's (1998) Morlet wavelet transform and Graff's (1981) sea level maxima analysis. The relative sea level data were then used to support adaptations of two sea level projection models to 2100; the UK Climate Projections 2009 (UKCP09) probabilistic model and Vermeer and Rahmstorf's (2009) temperature-sea level relationship projections model. These models were, in turn, used to project the impact of extreme relative sea levels on local infrastructure by 2100.

This research revealed that relative sea level in the Forth and Tay Estuaries between 1900 and 2010 rose at a rate of 0.27 to 0.56 mm a^{-1}, which is smaller than the global average of 1.7 mm a^{-1} (Church and White, 2011). Tidal residuals were commonly observed to be approximately 0.4 and 0.7 m at Leith and Dundee between 2003 and 2010, whilst the highest sea level maxima across 5 ports in the region ranged between 3.27 and 4.13 m above OD. Adaptions of the UKCP09 model reduced the original projections for 2100 of between 31.3 and 35.1 cm to between 24.3 and 27.5 cm above the 1990 mean. Similarly, adaptions of the Vermeer and Rahmstorf (2009) model reduced projections from 107.5 cm to between 50.9 and 54.2 cm above the 1990 mean. These adapted projections, when added to the extreme 2100 sea level calculations, suggests that the highest extreme sea level by 2100 could reach the present day quayside heights at selected locations in the Forth and Tay Estuaries. The approach and results are replicable across other regions, thereby refining projections made by previous authors.

Chapter 1 - Introduction

1.1 Introduction

> '*Global sea level rise and its resultant impacts on the coastal zone has been identified as one of the major challenges facing humankind in the twenty-first century. Impacts on the environment, the economy, and societies in the coastal zone will likely be large,*' Woodworth *et al.* (2010:1).

Sea level change and storm surge events have been identified as two important elements of climate change by the Intergovernmental Panel on Climate Change (IPCC) (Houghton *et al.*, 2001). The IPCC Fourth Assessment Report (AR4) projected 2100 global sea levels to be between 18 and 59 cm higher than that in 1990 (Solomon *et al.*, 2007). Increasing sea levels can have devastating effects on coastal infrastructure and the environment (*cf.* Woodworth *et al.*, 2010).

Historically, global tide gauge data indicate that global sea level rose at a rate of 1.7 mm a^{-1} between 1900 and 2000 (Church and White, 2006). However, sea level is not globally consistent and Gerhels and Long (2008) suggest that the IPCC values should be substituted with regional information that takes into account land movement rates, changes in tidal range, storm surges and changes in sea-surface topography. There are decadal and multi-decadal cycles that impact sea level change rates, such as those fragmented by short-term satellite altimetry data (3.1 mm a^{-1} between 1993 and 2003) in IPCC AR4 (Cazenave and Nerem, 2004; Leuliette *et al.*, 2004; Solomon *et al.*, 2007).

The area studied in this thesis, including the Forth and Tay Estuaries of eastern Scotland (Figure 1.1; Chapter 3), has not previously been subject to regional scale relative mean sea level (MSL) analyses since 1900. This gap in scientific knowledge of the area is one of the main motivations behind this thesis. Parts of the Forth Estuary have been included in maxima sea level studies conducted by Graff (1981), who studied many ports along the British coast purely for storm surge event analysis. This prior knowledge of the area prompted this thesis to continued the study of storm surge activity in this location. Prior to 1900 both estuaries have been analysed on geological timescales (Sissons *et al.*, 1966).

Both estuaries contain industrial-scale ports and smaller harbours, which introduced another motivation behind this thesis. This thesis was initiated and funded by Forth Ports Limited (formerly Forth Ports PLC and referred to here as Forth Ports), the largest port operator and the largest Port Authority in the region. This study benefits the ports by providing detailed analysis of past relative sea level trends and projections of how the ports and harbours may be affected by future extreme high sea level events, which would likewise benefit the scientific community. This thesis would

also use methods of relative sea level change database compilation for estuary regions that can be repeated across similar regions. These motivations are listed in more detail in Section 1.2.

Forth Ports provided tide gauge datasets from Grangemouth, Rosyth, Leith, Methil and Dundee. Their tide gauge data have been corrected and combined in this thesis with data from international, national and local sources, forming a unique historic relative sea level database across a regional scale.

Figure 1.1. Location Map – Map of Scotland highlighting the Forth Estuary (south) and Tay Estuary (north).

As well as historical relative sea level, storm surges have been analysed in this region. Storm surges have caused major flood events along the British coastline, including the January 1953 coastal flooding event that caused extensive flood damage and many deaths along the east coast of Britain, The Netherlands and southern North Sea generally (Hickey, 2001). With increasing relative sea levels local planners need to accommodate for additional flooding, inundation and inland retreat (Chowdhury *et al.*, 2008; Jenkins *et al.*, 2007). Several sea level models have been produced for global or national projections (Solomon *et al.*, 2007; Department for the Environment, Food and Rural Affairs (DEFRA), 2011a), but few areas have access to local scale models and few include surge projections relative to specific local areas.

Studies of surge and sea level maxima, through the comparison of predicted sea levels and tide gauge observed sea level data, have been conducted previously in this region, including Graff's (1981) maxima height study of the UK. In the Forth and Tay Estuaries region, Graff (1981) analysed maxima frequencies at Grangemouth, Methil, Kirkcaldy, Rosyth and Leith. However, these results are now outdated due to the availability of more comprehensive records. Retrospectively, there is little sea level information currently published about the present day status of the Forth and Tay Estuaries. Therefore, local planners and policy-makers currently refer to national data that may not be relevant at a local scale.

1.2 Motivation

A number of motivations inspired the creation of this thesis, which will impact sea level science, sea level projections and regional application:

- The tide gauge data collected from Forth Ports facilities have never been analysed before, therefore this thesis is producing a unique local sea level database. This information should be analysed and presented for the benefit of academia and local stakeholders.
- Unlike coastal areas to the south, this area of the Scottish coastline is thought to be still experiencing glacio-isostatic uplift at a rate of 1.0 to 1.3 mm a^{-1} (Shennan *et al.*, 2009). Shennan *et al.* (2009) rely on geological data compiled from a number of geological surveys across the UK, resulting in an evidence-based map. This near north-south divide across Britain means southern England relative sea level trends may vary significantly from the relative sea level trends from the Forth and Tay Estuaries.
- Two studies have already produced flood maps for the Forth and Tay Estuaries area, focusing on coastal flood events with a frequency greater than 0.5% (SEPA, 2006; Fife Council, 2011). Neither of the flood maps represents the actual defence structure heights and the digital terrain models are either grossly inaccurate or the accuracy has been omitted (SEPA, 2006; Fife Council, 2011). These maps are presently being used by local government, stakeholders and academia as an evidence base, despite their flaws. Therefore, this motivates this thesis to produce projections that create more accurate relative sea level projections.
- In the Forth and Tay Estuaries region, Graff (1981) analysed maxima frequencies at Grangemouth, Methil, Kirkcaldy, Rosyth and Leith. Most datasets were of an intermittent quality and between 20 and 30 years in length. Graff (1981) did not intend for these data to be used to project future flood frequencies, therefore the data are only relevant for the time of

acquisition (around 1980). This thesis aims to update some of the results produced by Graff (1981).

- With the rate of eustatic sea level rise projected to increase over the twenty-first century, present day relative sea level trends and storm surge heights are considered likely to increase comparatively (DEFRA, 2011a). As the rate of sea level rise is expected to increase in line with climate change connected temperature increase, it is essential that coastal adaptation and new developments are appropriate (Nicholls, 2010). As projections of future sea level change vary due to uncertainties in future emissions and the processes by which the main sea level change contributors will change in the future (Woodworth *et al.*, 2010) it is very important to understand the local settings and how relative sea levels intereact with the coast.
- Historical tide gauge records are being used to construct and validate global and regional relative sea level models for 2100 projections, which includes internationally renowned climate change models such as the UK Meteorological Office (UKMO) series (HadCM3 etc., explained in Chapter 8) (UKMO, 2011). As most climate models are constructed on a global or national scale that is too coarse a resolution to identify changes in the Forth and Tay Estuaries their projections of 2100 relative sea levels are likely to have significant errors (Gehrels and Long, 2008). All models have an element of uncertainty, but localised studies should reduce uncertainties about land movement and localised surge characteristics. The Forth and Tay Estuaries have not been subject to localised relative sea level projections on a 100 year timescale, but these would benefit future studies.
- Along with the five data ports, Forth Ports owns and manages several other ports, harbours and marine facilities in the two estuaries. Forth Ports are required to maintain the infrastructure at these sites. If relative sea levels are thought to pose a risk to port infrastructure, significant capital investment would be required. As with all development projects, Forth Ports have given support to this project to gain more information about historical relative sea level trends, storm surges and to obtain projections of future sea level trends that may aid coastal and infrastructure management decisions in the near future.

1.3 Aims

The main aims of this research are to:

- Identify the appropriate evaluation processes needed for accurate tide gauge data correction and explain these;

- Develop appropriate methods to create a process to assimilate regional sea level trend(s) from multiple datasets;
- Evaluate, analyse and explore the use of local tide gauge data for historical sea level analysis, surge and maxima analysis, sea level oscillation identification and sea level projections;
- Review existing sea level projections generated by international and national sea level models adapted for the Forth and Tay Estuaries;
- Identify if areas of the Forth and Tay Estuaries would be under threat from future sea level flooding; and
- Examine the spatial and temporal scales of future sea level flooding in the Forth and Tay Estuaries region.

1.4 Hypotheses

- Tide gauge data from the Forth and Tay Estuaries can be used to form a reliable dataset between 1900 and 2010;
- Relative sea level data can identify multi-annual to multi-decadal sea level trends and surge events;
- Multiple short datasets can be used to create a longer regional time series that allows for enough data for genuine relative sea level histories to be created, leading to sufficiently robust data for future projections.

1.5 Structure of Thesis

The thesis begins with a comprehensive review of literature surrounding the subject of sea level change. The literature review (Chapter 2) introduces sea level change, ocean mechanics and estuarine influences before discussing sea level oscillations, glacio-isostasy, storm surges, tidal measurement and tidal prediction. This essential introduction to sea level change theory is designed to prepare readers for the technical science discussed later.

Chapter 3 introduces the two estuaries, the Forth and the Tay Estuaries and include detailed descriptions that highlight their unique attributes and the significant differences between their water bodies. The estuaries function on different scales, varying in catchment area, estuary area and population densities. Both estuaries have areas of environmental and financial importance, such as

the Grangemouth Refinery, Forth Island SPA and the Tay Estuary protected seal colony. Both chapters include information on the local geology, geomorphology, sediment dynamics, estuary characteristics, data locations, tidal influences, currents and historical background.

A methodological review (Chapter 4) was produced to fully assess the current sea level analysis methods alongside development of the methods used in this investigation. This includes background information on tide gauge use, data collection (including data characteristics and errors), data correction, sea level data analysis, storm surge data analysis and simple modelling methods.

Chapter 5 is the first results/data processing chapter, which describes how tide gauge data changes throughout the correction stage. Datum jumps of only a few centimetres can result in disfiguration of a sea level trend, resulting in implied steepening of sea level rise or fall rates. In full, the local sea level results chapter presents the tide gauge sources, pre-corrected data, daily tide gauge sea level curves for each location, datum-corrected data relative to OD (Newlyn), glacio-isostatic adjustment (GIA) analysis and data corrected for GIA.

This dataset is the most accurate historical sea level record for the local area and the most relevant reference for future sea level studies in the Forth and Tay. Chapter 5 is followed by the local sea level data interpretation chapter (Chapter 6), which explains the trends in 1900 to 2010 local data and compare these to global sea level and non-sea level trends prior to discussing these relationships. Oscillations and cycles in the local sea level data are analysed, highlighting their importance in the local area.

In addition to information on past relative sea level, information is needed on past storm surge levels. In Chapter 7, past surge events are discussed and compared with tide gauge recorded residual heights. Maxima and surge data are compiled to form an extreme water level baseline, which can be used in future projections of sea level.

The entire ensemble of past sea level and extreme water level data are compiled in Chapter 8, the modelling chapter. After the baseline is set, the chapter introduces various sea level projection models that have previously been used for global and national studies that have included the Forth and Tay Estuaries in their geographical coverage. Two of these models are chosen for simplistic adaptation, which focuses around either correcting or adding GIA correction for the local area.

Several sea level projection models have been adapted for use by this thesis and are either compared with or adapted with the use of local tide gauge data. The model results include still water relative sea levels, surge heights and development freeboard levels, which are compared against present day coastal defence heights. These models are essentially basic tools that can identify areas of the Forth and Tay Estuaries that will be at risk from extreme water level coastal overtopping.

Chapter 2 - Literature Review

2.1 Introduction

Climate change has become one of the most important global issues today, due to our increasing awareness of its potential impacts, including global warming, changes in precipitation, global sea level rise and changes to the pattern of extreme (Houghton *et al.*, 2001). Examples of extreme events considered by some to be induced by climate change include the UK 2003 heat wave, 2009 Cumbria floods and 2007 Gloucestershire floods, which were severe events that caused severe damage to infrastructure, farmland and human health (Stedman, 2004; Blackburn *et al.*, 2008; Sibley, 2010).

Historically, coastal areas across the globe have become population hot spots as the idyllic nature of the sea attracts large populations to the coast and the easy-access, low-lying land has brought in industries. The sea has been utilised for thousands of years as a food source, a transport link and, more recently, an area for recreation. Industrialisation of the coast started centuries ago, for example the tidal dockyard discovered in Lothal, Ahmedabad, India, dating back as far as 2450 BC, which is acclaimed to be oldest dockyard yet discovered (Hardisty, 2007:62; Gaur and Vora, 1999).

In Scotland 20% of the population live within 1 km of the coast and 70% live within 10 km of the coast (Scottish Executive, 2005; Hadley, 2009). In addition, ~25% of all businesses (10% of the national turnover) are located within 1 km of the coast (Scottish Executive, 2005; Hadley, 2009). Coastal towns and cities expand as their populations increase, which can force new development to spread seaward of towns onto previously undeveloped coastal land that could potentially be vulnerable to flooding and erosion.

The coast itself is constantly changing and is subject to geological and geomorphological changes (tilting, folding, faulting), tectonic and glacial changes (uplift, subsidence), sediment transport (eroding, accreting), weathering, wind and water regimes, diverse vegetation and fauna patterns, tides, and oceanographic factors (sea surface temperature, salinity) (Shennan *et al.*, 2012; Hesp, 2002; Ruessink and Jueken, 2002; Aagaard *et al.*, 2002). A moderate increase in mean global sea level of between 20 and 30 cm could result in flooding, erosion and saltwater intrusion in low-lying areas (Chowdhury *et al.*, 2008).

The natural environment can be vulnerable to sea level rise with beaches, dunes and wetlands potentially suffering and attempting to retreat inland (Jenkins *et al.*, 2007). Coral reefs would be abandoned if the sea rose faster than the reefs could sustain (ibid). Coastal flooding, algal blooms and pollution could all increase whilst fishing, aquaculture, shipping and tourism are adversely impacted (ibid).

This literature review explains in the following sections the present knowledge behind sea level change, prediction and management. Basic wave and tide theory is explained before explaining sea level change, sea level oscillations, glacio-isostatic adjustment (GIA), estuarine impacts, storm surges, prediction and management.

Before entering an in depth theory of climate and sea level change there are several terms that need to be introduced:

- *Eustasy* – 'the absolute change in global sea level' (Haslett, 2008:136). Eustasy accounts for the actual sea level change without reference to the land and is sometimes called global sea level, however a specific reference to eustatic sea level acknowledges that it represents the level of the oceans if the Earth were not rotating and if the oceans were level (Shennan *et al.*, 2011; Mitrovica and Milne, 2003).

- *Isostasy* – 'the vertical movement of land due to local geological factors' (Haslett, 2008: 136). Isostasy is the movement of the land due to influences such as glacial (glacio-isostasy), hydro-isostasy, plate tectonic, mining etc.

- *Relative sea level* – the balance between eustasy and isostasy at a given location on the coast producing observed sea level changes (Haslett, 2008). At one point on the coast 'it is never certain whether the sea is rising or falling or the land is subsiding or being uplifted, or both,' Maul *et al.* (1996:84).

- *Mean sea level* – the average sea level over a given time period; typically daily, monthly or annually.

- *Steric sea level* - 'sea level change resulting from density variations' (Haslett, 2008:155), i.e. global warming increases the ocean temperature, which decreases the ocean density leading to an increase in ocean volume. These may also be brought about by saline or pressure variations (Haslett, 2008; Antonov *et al.*, 2002).These steric differences result in msl being 0.20m higher in the Pacific Ocean than the Mediterranean Sea/Atlantic Ocean at either ends of the Panama Canal (Pugh, 2004).

- *Glacio-eustasy* – during 'glacial stages water is extracted from the oceans and transferred to ice sheets where it is locked up for the duration of the glacial stage' (Haslett, 2008: 137). This restriction is followed by the release of water into the oceans from glaciers during inter-glacial stages.

- *Glacio-isostasy* – the same ice sheets that control glacio-eustasy grow over land 'exert great overburden pressure, causing the land to isostatically subside', which is known as glacio-

isostasy (Haslett, 2008: 137). The land then relaxes after the ice sheets melt, which is known as isostatic rebound or uplift (Haslett, 2008: 137).

2.2 Waves and Tides

Two elements of ocean mechanics are reviewed in this section, specifically waves and tides. Oceanic waves have sine wave patterns with definable wavelengths, amplitudes, crests, troughs, heights and celerities (Figure 2.1). Numerous long and short frequency waves occur to create the ever changing nature of sea level.

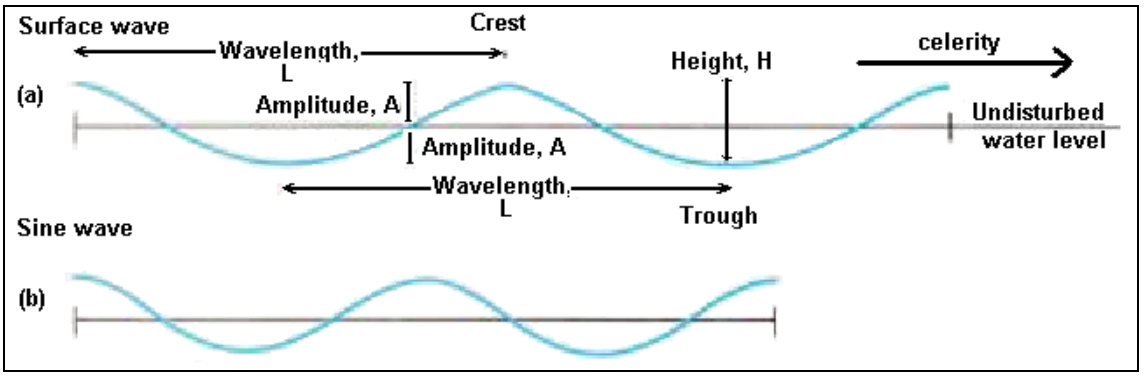

Figure 2.1. Wave characteristics (adapted from University of Maine, 2003).

It is important to remember that tides themselves are long, fixed-frequency waves caused by the gravitational pull of the Moon and Sun (Bearman, 1999). Smaller frequency and amplitude surface waves, generally referred to as waves or wind waves, can be developed by wind over long or short fetches, producing variable amplitudes depending on the wind speed and direction in relation to the coastline (Fragherazzi and Wiberg, 2009).

Tsunami, seiches, storm surges and cyclonic weather systems can generate long wave frequencies of $1x10^{-5}$ s^{-1} which translates to frequencies of up to 2.5 hours (Figure 2.2) (Bearman, 1999), although only storm surges commonly occur in UK coastal waters. Tsunami are sometimes referred to as tidal waves by the press, but tsunami are significantly different in form from a classic oceanic wave and tend to be caused by earthquakes, significant land movement such as a submerged landslide or large meteor impacts (Gisler, 2008). They are not controlled by astronomic or atmospheric actions.

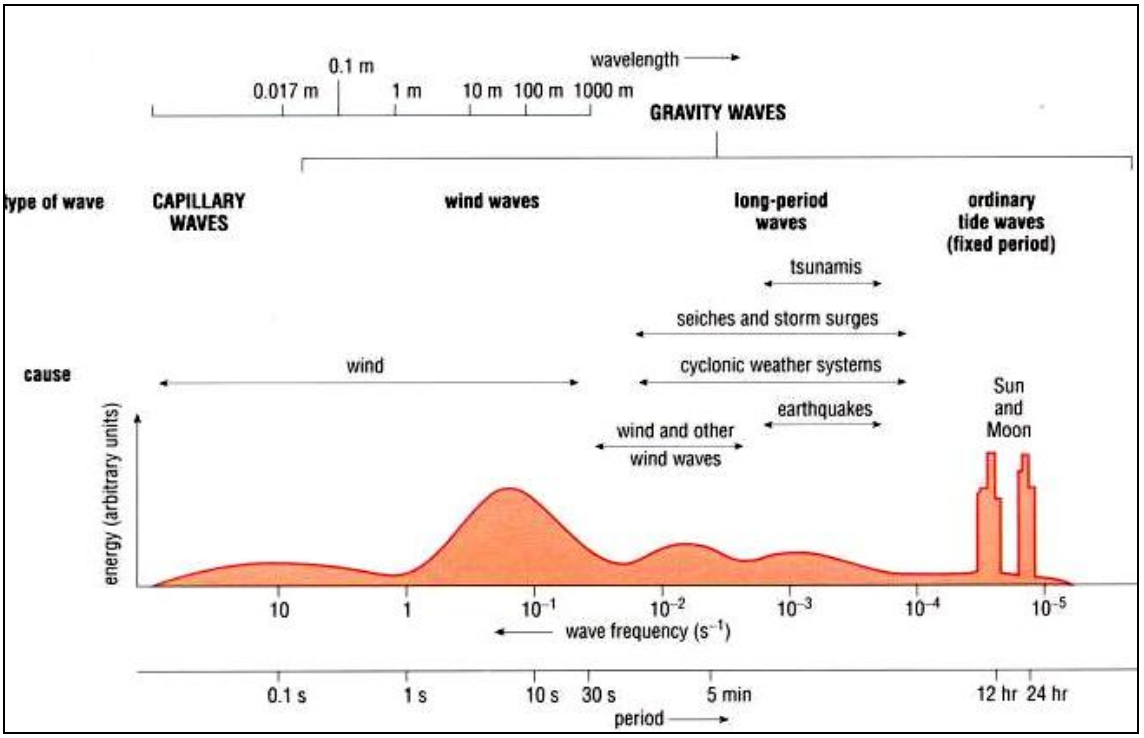

Figure 2.2. Types of Waves (Bearman, 1999:13).

2.2.1 Waves

As seen in Figure 2.2, there are a variety of short frequency waves (e.g. wind waves) and long frequency waves (e.g. tsunami). Wind interacts with the surface of the ocean, displacing the surface of the water and developing a cyclical motion in the near-surface area (Phillips, 1957; Mitsuyasu, 2002). The nearshore wave regime includes all of these waves overlapping, interacting and coming from different directions.

A wave profile may consist of multiple waves with varying wavelengths, amplitudes and celerities, therefore mutating the wave to seem inconstant. However, models have been developed to recognise individual cycles (i.e. tidal harmonics, Section 2.9). Linear wave theory can be used to calculate oceanic wave propagation along a straight coastline and assumes that a 2-dimensional progressive surface gravity wave has:

- Wave depth and length greater than amplitude (Hudspeth, 2006; Sorensen 1993);
- Wave particle velocity relating to amplitude;
- Wave depth and length controlling wave celerity; and
- Wave celerity larger than wave particle velocity (Sorensen 1993).

Waves transform from their open-sea state through the interactions with boundary condition near the shore (Sorensen, 1993). Shallowing and narrowing of the seabed in the nearshore introduces non-dissipative forces, such as refraction and shoaling, as well as dissipative forces, such as bottom friction, wave breaking and wind generation (Collins, 1972; Abbott and Price, 1994) (Figure 2.3).

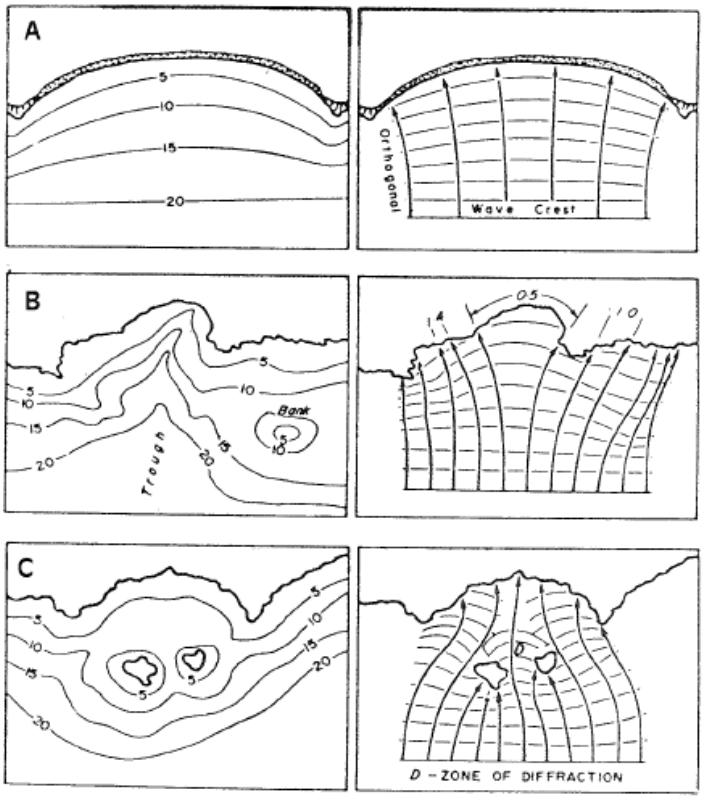

Figure 2.3. 'Wave refraction diagrams in relation to submarine topography. A) refraction of waves moving into a bay, B) refraction of waves moving over a trough (refraction coefficients indicated, C) refraction around and diffraction between offshore islands' (Bird, 2000:11).

As waves move into coastal areas, where waves interact with the bottom topography, their orbital movements diminish until they approach a minimum where the water depth is significantly minimal enough to cause the wave to collapse (Collins, 1972). Backwash and swash characteristics are also influenced by the beach slope (Masselink and Anthony, 2001). The energy of the wave and the breaking pattern of the wave (surging, plunging, collapsing or spilling) can generate either erosive or accretive processes (Galvin, 1968). Sediment can be transported along the coast by waves. The backwash of these waves can pull the sediment offshore and longshore drift pushes it back onshore in a zigzag pattern that prevalently follows the direction of the wind (Ingle, 1966).

Understanding how a wave works increases the effectiveness of shoreline defences against wave attack. Coastal defences are required for high energy waves due to the serious impact waves have on the coastline.

2.2.2 Tides

The lunar cycle produces two high and low tides each day (lunar semi-diurnal tide), as seen strongly in the Atlantic Ocean (Hicks *et al.*, 1965; Hendershott, 2012). The solar cycle produces one high and low tide each day (solar diurnal tide), as seen along the Antarctic coast (Hicks *et al.*, 1965; Hendershott, 2012). The lunar and solar influences dominate different areas of the Earth's oceans with large areas of the Indian Oceans experiencing mixed tidal influences where the solar influences are large and the East Indies experiencing dominant lunar semi diurnal tides (Chapman and Westfold, 1956). Mixed tides will have two high and low tide during the average day, but with one large high and low tide and one small high and low tide each day.

Along most coastlines tides are the largest movements of sea level, however tidal ranges vary over small geographical areas. There are four classes of tidal range; microtidal (0 to 2 m), mesotidal (2 to 4 m), macrotidal (4 to 6 m) and megatidal (over 6 m) (Masselink and Short, 1993). In the mid-ocean sea level varies minimally due to tidal influences, but this is amplified in shallowwater and additionally in funnel-shaped embayments (Soo An, 1997). The British coastline is predominantly macrotidal (Short, 1991) with areas of microtidal ranges in central southern England, megatidal in the Bristol Channel and the North Wales Irish Sea, and mesotidal along areas of western and northern Scotland and south eastern England.

The tidal range is dictated by the coastline orientation to its nearest amphidromic point, due to Coriolis Effect (McDonald, 1952). Gaspard Gustave de Coriolis discovered oceanic circulation patterns, which he discovered were the orientation points around which objects in the sea and air followed the direction of the Earth's rotation rather than following straight lines (McCully, 2006). The eye of each circulatory pattern is called an amphidromic point (Figure 2.4). For fluids, the direction of the circulation is anticlockwise in the Northern Hemisphere and clockwise in the Southern Hemisphere (Lydolf, 1985).

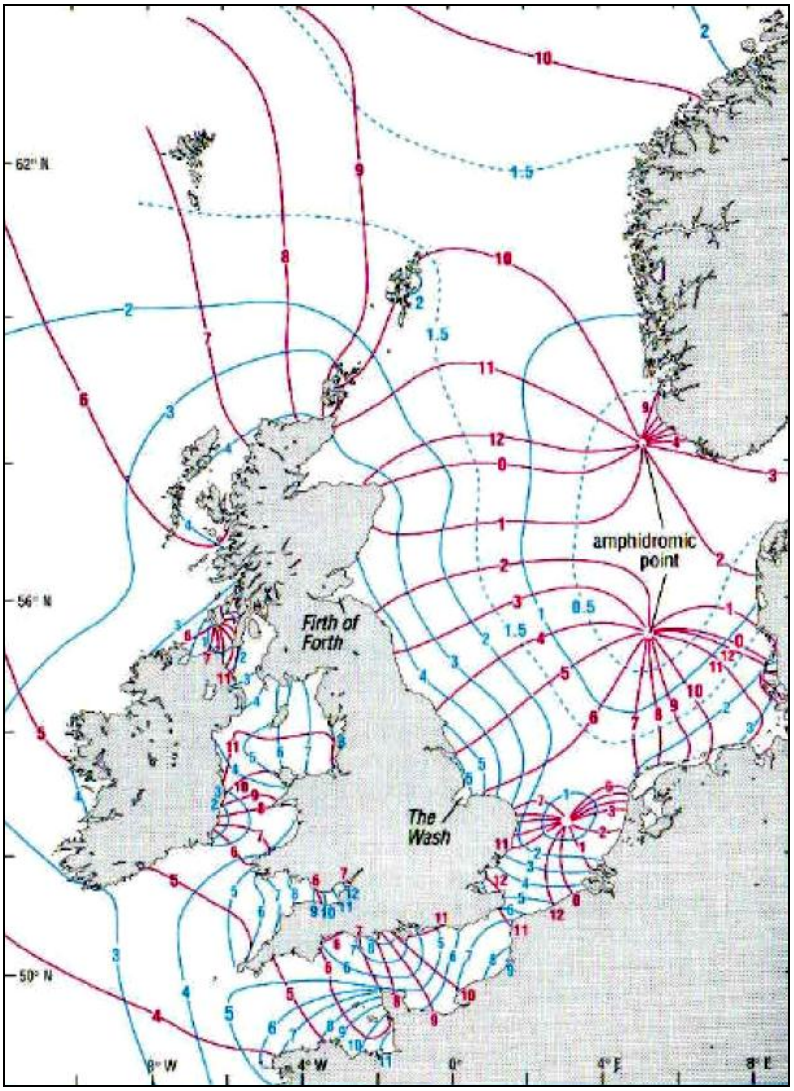

Figure 2.4. Amphidromic points and cotidal lines off the coast of North West Europe (Bearman, 1999:70).

Coriolis Force is a very important control factor of atmospheric and oceanic parameters, controlling the direction of pressure gradients in anticyclones and depressions (Pinet, 2008). The British east coast has three amphidromic points, around which the sea circulates anticlockwise, creating a southwards circulation across the British east coast (Figure 2.4) (Haslett, 2008). The amphidromic point positioned off the south Norwegian coast controls the rotational direction of the tide off the eastern Scottish coast.

The Earth's tidal bulges are now recognised as the daily (24.07 hours) and monthly (27.56 days) tidal movements, the extremes being called spring and neap tides (23.78 days) (Figure 2.5) (Bearman, 1999). Spring tides occur when the Sun and Moon are in alignment with the Earth, therefore creating the greatest tidal bulge during this period, i.e. the highest high tide and the lowest low tide. Neap tides are the result of the Moon's gravitational pull being 90° from that of the Sun,

therefore pulling in a perpendicular direction and creating the lowest high tide and the highest low tide (Bearman, 1999).

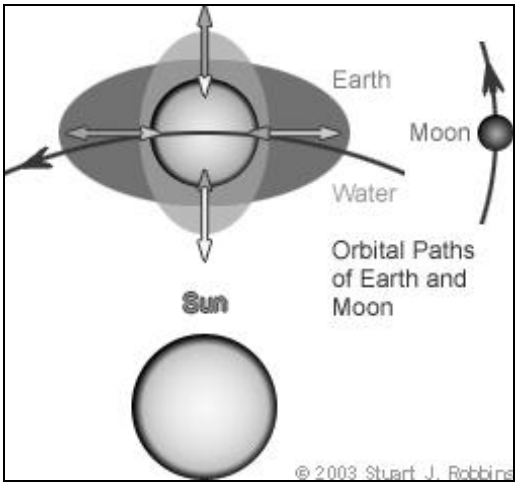

Figure 2.5. Tidal bulges from the Moon and Sun (Journey through the Galaxy, 2006).

Solar tidal waves are half the height of lunar tidal waves. Due to the elliptical nature of Earth's orbit the lunar and solar declination displacement is not equally exerted across both hemispheres (Figure 2.6). The Earth rotates around the Sun, which, along with the solar exertion having a 23.5° displacement beyond the equator, results in six month hemispherical cycling of tidal displacement strength (McCully, 2006). The lunar declination cycles between hemispheres every two weeks, resulting in a fortnightly tidal displacement cycle. Solar declination cycles reside in each hemisphere long enough to form hemisphere-wide diurnal solar tide patterns (McCully, 2006).

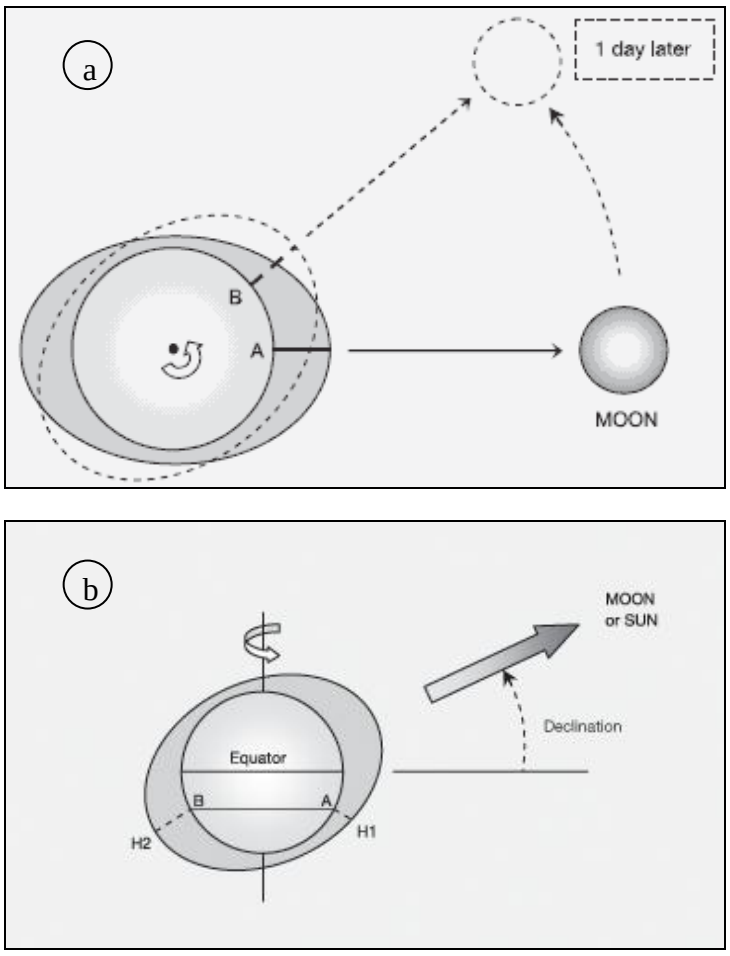

Figure 2.6. Movement of the tidal bulge driven by the Moon and Sun daily (Land Information New Zealand, 2009). a) Movement of the tidal bulge in relation to the Moon and the Earth's axis over one day. b) Relation of the tidal bulge in relation to the Moon-Sun (when in line) and the Earth's equator, highlighting the declination and sea level variance (H1-H2).

Tides, being regulated by astronomical cycles, are predictable far in advance. Tides produce tidal currents, with semi-diurnal tides producing the greatest currents due to the more frequent change in the tidal direction. Macrotidal and megatidal ranges produce the greatest currents as well as the largest intertidal areas with the beach forming near the coastline (Masselink and Anthony, 1991). The currents control sediment movement in the nearshore and intertidal regions.

The sea surface can be split into several long-frequency tidal waves, which are called tidal constituents within harmonic analysis. Some of these have been highlighted in Table A2.1 (Appendix 2), including the lunar semi-diurnal and solar semi-diurnal cycles that are dominant along the open coast (Maul *et al.*, 1996). The tidal harmonics highlighted in Table 2.1 are the *primary harmonics*, which can explain 90% of variance. When the additional *secondary harmonics* are added to the analysis, 99% of variance can be explained (Chowdhury *et al.*, 2008).

		Period of cycle	*Coefficient ratio (M_2 = 100)*
S_a	Solar annual	364.96 days	1.27
S_{sa}	Solar semi-annual	182.7 days	8.02
	Lunar sinusoidal month	29.5 days	
M_m	Lunar monthly	661.3 hours/27.555 days	8.25#
M_f	Lunar fortnightly	327.86 hours/13.661 days	17.2#
Q_1	Lunar diurnal elliptic	26.868 hours	7.22#
M_1/ O_1	Lunar diurnal/Principal lunar	25.82 hours/1.035 days	41.51
S_1/ P_1	Solar diurnal/Principal solar	24.07 hours	19.32
k_1	Luni-solar diurnal declination	23.93 hours	58.38
N_2	Larger Lunar ellipse semi-diurnal	12.66 hours	19.15
M_2	Lunar semi-diurnal	12.42 hours	100
S_2	Solar semi-diurnal	12 hours	46.52
k_2	Luni-solar semi-diurnal	11.97 hours	12.66
M_4	Lunar quarter-diurnal	6.21 hours	

Table 2.1. Solar and Lunar Inter-Annual Cycles (Sources: Hardisty, 2007; Bearman, 1999; Pugh, 2004; Marchuk and Kagan, 1989). The coefficient ratios are the tidal power in relation to the M_2. # values relative to a M_2 cycle with a power of 90.81.

Lunar cycles also influence the tide over longer time periods through cycles including the:

- 18.6 year declination/nodal cycle – inversely influences the amplitude of the lunar semi-diurnal cycle (Burroughs, 2003; Denny and Paine, 1998; Gratiot *et al.*, 2008; Kaye and Stuckey, 1973), influences sedimentation along the coast (Oost *et al.*, 1993) and has had maxima in February 1969, October 1987 and May 2006 (Gratiot *et al.*, 2008). Several studies have identified a strong correlation between this cycle and the oscillating sea level along the east coast of the United States of America, with recent influence estimated to be between 4 and 6 cm (Kaye and Stuckey, 1973; Gratiot *et al.*, 2008);
- 8.85 year lunar perigee cycle – influences the lunar elliptical modulator (L_2) harmonic constituent (Pugh, 2004).

2.3 Sea Level Oscillations

Sea levels, in addition to waves and tides, are impacted by long and short frequency cycles. Glacial-scale and multi-centennial cycles include Milankovitch Cycles and Heinrich Event (Broecker, 1998; Hunt and Malin, 1998). Although these cycles are very important over hundreds and thousands of years, they would not appear in tide gauge data.

In tide gauge records, the longest of which are around 200 years in length, several different oscillation types can be identified in the mid-latitude North Atlantic region, e.g. pressure anomaly, solar, sunspot, lunar and other astronomical cycles. Pressure anomaly cycles, i.e. geographical pressure-gradient dependent cycles, include the North Atlantic Oscillation (NAO), Arctic Oscillation (AO), NAO Low-Frequency Oscillation (LFO) and the Atlantic Multi-Decadal Oscillation (AMO) (Czaja and Marshall, 2001; Polyakov and Johnson, 2000; Knight *et al.*, 2006). Each oscillation is measured to its individual indices, which can suggest the annual influence of each oscillation on sea level through positive or negative values. The relative impact each oscillation has on sea level varies from location to location.

The NAO (Figure 2.7) is characterised as 10 and 30 year cycles (Czaja and Marshall, 2001; Kravtsov *et al.*, 2007) with a decadal pattern being confirmed in Greenland ice cores (Hurrell, 1995). It is the most dominant oscillation in its region with positive NAO Index values increasing localised sea levels (Kravtsov *et al.*, 2007). In the North Atlantic around Great Britain the NAO influences winter storminess, ocean wave heights, rainfall, temperature and ecological cycles (Marshall *et al.*, 2001).

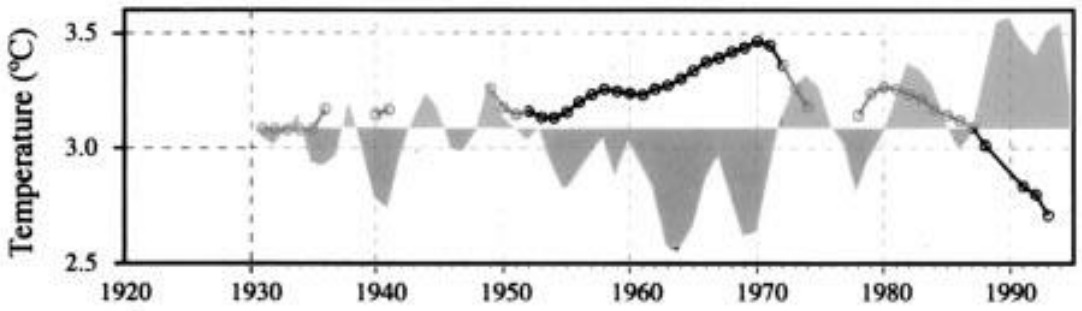

Figure 2.7. Temperature of the Labrador Sea Water (points and line) with the NAO index (shaded), showing an inverted relationship between temperature and the NAO (McCarney et al., 1997:21).

The AO (Figure 2.8) is a cycle with a ~10 year frequency, which is nearly indistinguishable from the NAO (Polyakov and Johnson, 2000). It also has a positive impact on localised sea level in relation to its indices results. The LFO is a 60 to 80 year frequency cycle characterised as fluctuations in the NAO oscillation with a positive relationship between the indices and sea level (Polyakov and Johnson, 2000). The Atlantic Multi-Decadal Oscillation (AMO) (Figure 2.9) is a 60

to 100 year frequency cycle identified in the Atlantic sea surface temperature (SST) (Knight *et al.*, 2006; Gray *et al.*, 2004).

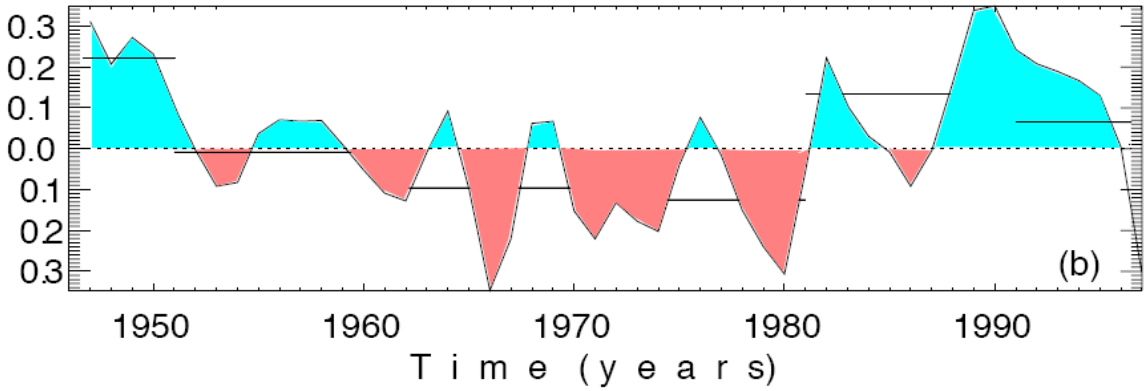

Figure 2.8. Calculated atmospheric vortex over the central Arctic Ocean, identifying both decadal AO variation and 60 to 80 year LFO dependence (Polyakov and Johnson, 2000).

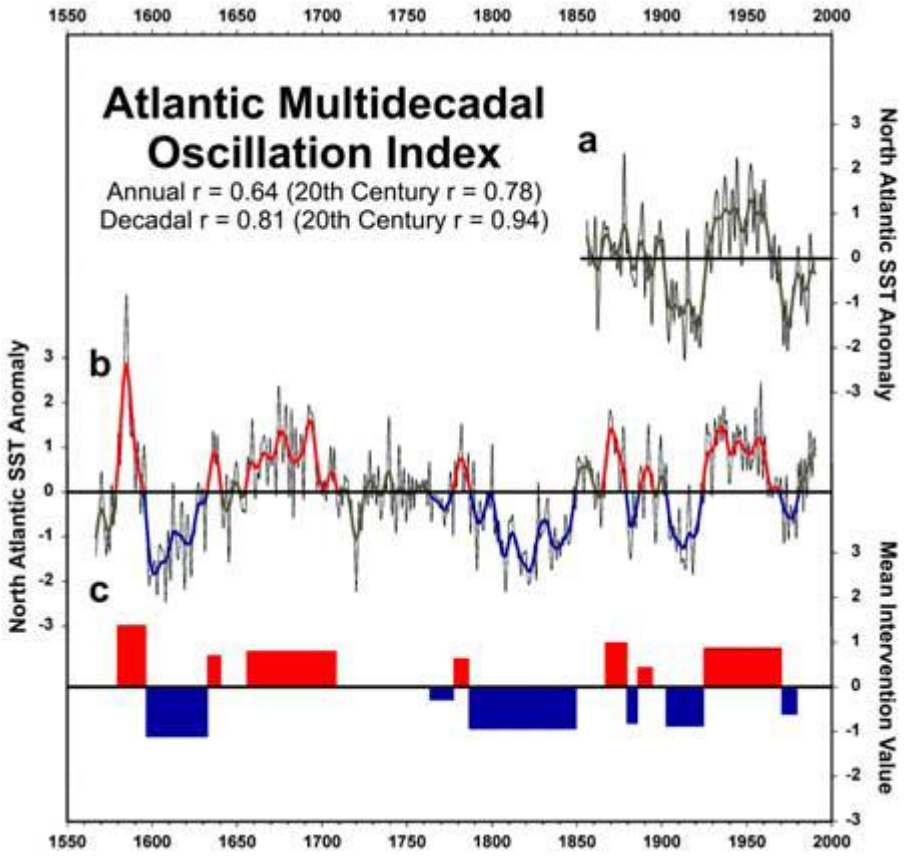

Figure 2.9. (a) Annual sea surface temperature anomalies (dark grey line) and 10 year AMO Index running mean (black line), 1856-1900 AD. (b) Tree ring chronologies 1567-1990 (dark grey line) and 10 year AMO Index running mean (black line). AMO warm regimes in red, cold regimes in blue and insignificant periods in grey. (c) mean sea surface temperature anomaly value and durations of warm (red) and cold (blue) regimes (Gray *et al.*, 2004).

Several long-frequency solar and sunspot cycles can have an impact on sea level amplitude:

- 87 year Gleissberg solar cycle (Singer and Avery, 2008) – sometimes referred to as the Centennial Gleissberg Cycle, this cycle has been active since 1710 and present debate about this cycle suggests that it was at its minimum at the start of the nineteenth century and its most recent minima may have coincided with the 22-year sunspot cycle minima around 2009 (Feynman and Ruzmaikin, 2011),
- 210 year De Vries-Suess solar cycle (Singer and Avery, 2008) – a cycle first identified by De Vries and linked to solar cycles by Suess in 1978 through the analysis of dendrochronology data (Berger, 2012),
- 22 year double sunspot (Hale) cycle, which has 11 year extreme influences (Burroughs, 2003; Camuffo, 1999; Livingston and Penn, 2009). The peak years of the sunspot cycles often correspond with the negative stage of the El Nino cycle, demonstrating a potential relationship (Roy and Haigh, 2010);
- Various other short cycles.

Astronomical cycles, excluding lunar and solar cycles:

- 19.9 year Saturn-Jupiter cycle (Camuffo, 1999).

Analysing the amplitudes of these cycles would have to be conducted on a site-by-site basis due to local characteristics. Frequencies of pressure anomaly cycles have been modelled by studies including that of Yan *et al.* (2004). Most studies conclude that further research is needed in this field; this is especially so regarding the observed increase in some cycle amplitudes, e.g. the 3.5 to 13.9 year frequency oscillations observed by Jevrejeva *et al.* (2006). Their study suggested the cycles in this band's amplitudes have been increasing since 1940, when global sea levels witnessed several decades of increased sea level and temperature rise (Yan *et al.*, 2004).

Studies including those by Rennie and Hansom (2011) and Pethick (1999) have analysed 15 years of sea level records. Trend analyses of less than 30 years will not include the full LFO, NAO and AO cycles, which are dominant in the North Atlantic around the UK. Rennie and Hansom (2011) used tide gauge data as evidence of accelerating sea level rise since 1993. These data were extracted from the first 15 years after an extreme high NAO and AO combined event in 1991 to project sea level until 2100. In 1991 NAO and AO cycles were individually at their highest point in their indices since the beginning of the twentieth century, which influenced temperature and sea level inversely (Figure 2.10) (McCartney *et al.*, 1997; Mashall *et al.*, 2001).

2.4 Past Acceleration of Sea Level Rise

Previous studies have suggested eustatic sea level rise is accelerating. Pethick (1999) used some of the same data and methods as Rennie and Hansom (2011) to deduce this. Accelerations appearing within short decadal timescales have been discussed by Holgate and Woodworth (2004), but Woodworth *et al.* (2007) analysed longer sea level records that were several decades in length, which should include more of the sea level oscillations.

Woodworth *et al.* (2007) confirmed that there have been accelerations in the rate of global sea level rise since 1870, but their observations did not confirm one overall acceleration trend. Woodworth *et al.* (2007) confirmed accelerations around the 1920s and 1960s, which could be associated with the AMO or LFO, and the NAO and AO are suspected to be very influential. As well as sea level rise accelerations, there have been sea level rise minima periods and sea level falls. They conclude that more data are needed to confirm any acceleration of sea level rise, as most of the studies that have investigated sea level acceleration have used the same data collected by either Church and White (2006) or Jevrejeva *et al.* (2006).

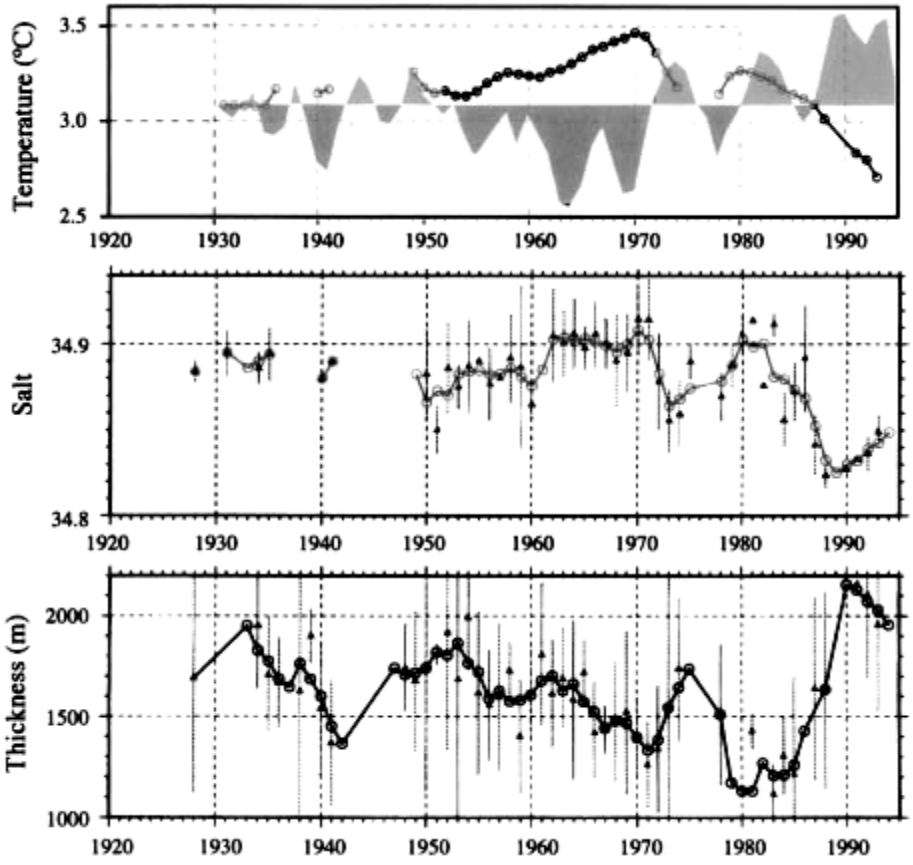

Figure 2.10. Records dating between 1920 and 2000 of (Top) temperature of the Labrador Sea Water (LSW) with the NAO index-shaded; (middle) salinity in the Labrador Sea; (bottom) thickness of LSW core. As the NAO strengthened the LSW became colder, fresher and more voluminous. (McCartney *et*

***al.*, 1997; Marshall *et al.*, 2001). Labrador Sea Water is a subpolar water mass that is formed by air-sea exchanges in the North Atlantic and is a major contributor to deep water formation (McCartney *et al.*, 1997).**

In summary, the AMO, AO, NAO and LFO cycles are recorded as the most influential of the oscillations in the North Atlantic. Due to their multidecadal cyclic nature, sea level datasets shorter than 30 years would intersect the oscillation trends.

2.5 Non-Tidal Influenced Storm Surges

A surge is a heightening or lowering of a water body primarily caused by changes in atmospheric pressure and strong winds (Haslett, 2000; Lowe *et al*., 2001; Sorensen, 2006). Various other local and atmospheric influences affect the behaviour of surges as they approach the coastline (Sorensen, 2006). Surge event duration and height ranges vary depending on the local sea bed topography, fetch and atmospheric characteristics. Several examples of catastrophic surge events and defensive constructions are given in Chapter 7 along with additional local storm surge literature (Lamb, 1991; Smith 1993; Hickey, 2000; Gill, 1982).

The IPCC Fourth Assessment Report and the MCCIP predicted that storms will decrease in number, but increase in intensity (Jenkins et al., 2007), although the possibility of change to flood frequency and intensity has been debated by several other studies (Hickey, 1997; Lozano *et al*., 2004; Ball *et al.*, 2008; Werritty *et al.*, 2002; Haigh *et al.*, 2010). Storm periods, with reduced atmospheric pressure and increased winds, produce the highest surge events and can combine with increased precipitation runoff in estuaries (Liu, 2000).

High fluvial discharge and coastal storm surges can converge at the tidal limit. This leads to estuary head urban development, agriculture and the natural environment being at risk from more intense convergence flood events (Liu, 2000). Atmospheric pressure and sea level hold a close relationship with a rise of 1 mb of pressure equating to a fall of 1 cm in sea level; the inverse barometer effect (Gil and de Toro, 2005; Chelton and Davis, 1982). The influence from atmospheric low pressure can cause sea levels to rise over 1 m above the predicted height, which can result in flooding of low-lying areas (Bretaña, 1987).

Coastal flooding has been recorded for hundreds of years and several sources have attempted to build databases of coastal flood events in the UK. The British Hydrological Society' Chronology of British Hydrological Events is a large database of fluvial, pluvial and coastal flooding events that have been recorded historically (Law *et al.*, 2010; Black and Law, 2004). Several large estuaries

have been included in the survey, including the Forth and Tay Estuaries. These events are good identifiers of past maxima levels, but surge heights are not likely to be their sole cause.

The interlinking nature between sea level oscillations and severe high water levels has been identified by several studies. For example, the NAO cycle has a positive influence on flood cycles, sea level and storminess (Hickey, 1997; Lozano *et al.*, 2004; Woodworth *et al.*, 2007; Ball *et al.*, 2009). Other flood prevalent cycles have been identified by Black and Burns (2002) and Macdonald *et al.* (2006), which are discussed further in Chapter 7.

Unfortunately, most of the historical flooding data do not include enough information about each flooding event to accurately measure the surge height against a specific location. Some methods of surge analysis use recent residual tide gauge data to identify surge events. These residual data points are constructed by subtracting the predicted harmonic tidal level from the observed tidal level. Spurious large positive and negative surges can be created as artefacts of malfunctioning gauges or gauges with timing-errors (Figure 2.11) (Dixon and Tawn, 1994). The residual data now also include harmonic tidal analysis errors and human errors. More details are presented in Chapter 7.

Storm surge analysis and prediction methods are discussed in Chapter 4, including sea level maxima analyses (Graff, 1981; Lennon, 1963; Suthons, 1963), the Proudman Oceanographic Laboratory tide-surge models (Dixon and Tawn, 1994; 1997; Flather *et al.*, 2001; Williams and Flather, 2004; Jones and Davies, 2009) and several adapted analysis methods used in this thesis. In

After the major surge event in January 1953, which caused damage along the length of the east coast of Britain, several tidal maxima studies were initiated. Lennon (1963) and Suthons (1963) produced studies for the west and southeast coasts of Britain regarding the extreme value analysis method on the use of frequency curves of storm surges. Both Lennon (1963) and Suthons (1963) used different forms of frequency distribution analysis.

Graff (1981), following Lennon (1963), presented data from 67 ports across the Great Britain following a study of 80, 13 of which were removed due to data limitations. This study used a frequency distribution method compiled by Jenkinson (1955) through 5 year mean trends; a running mean where one data point represents the average of the neighbouring five annual means. This method has been used for both open coast and estuarine regions, and produces frequency distribution curves. Graff (1981) suggested that there was an increasing trend in maxima across the UK.

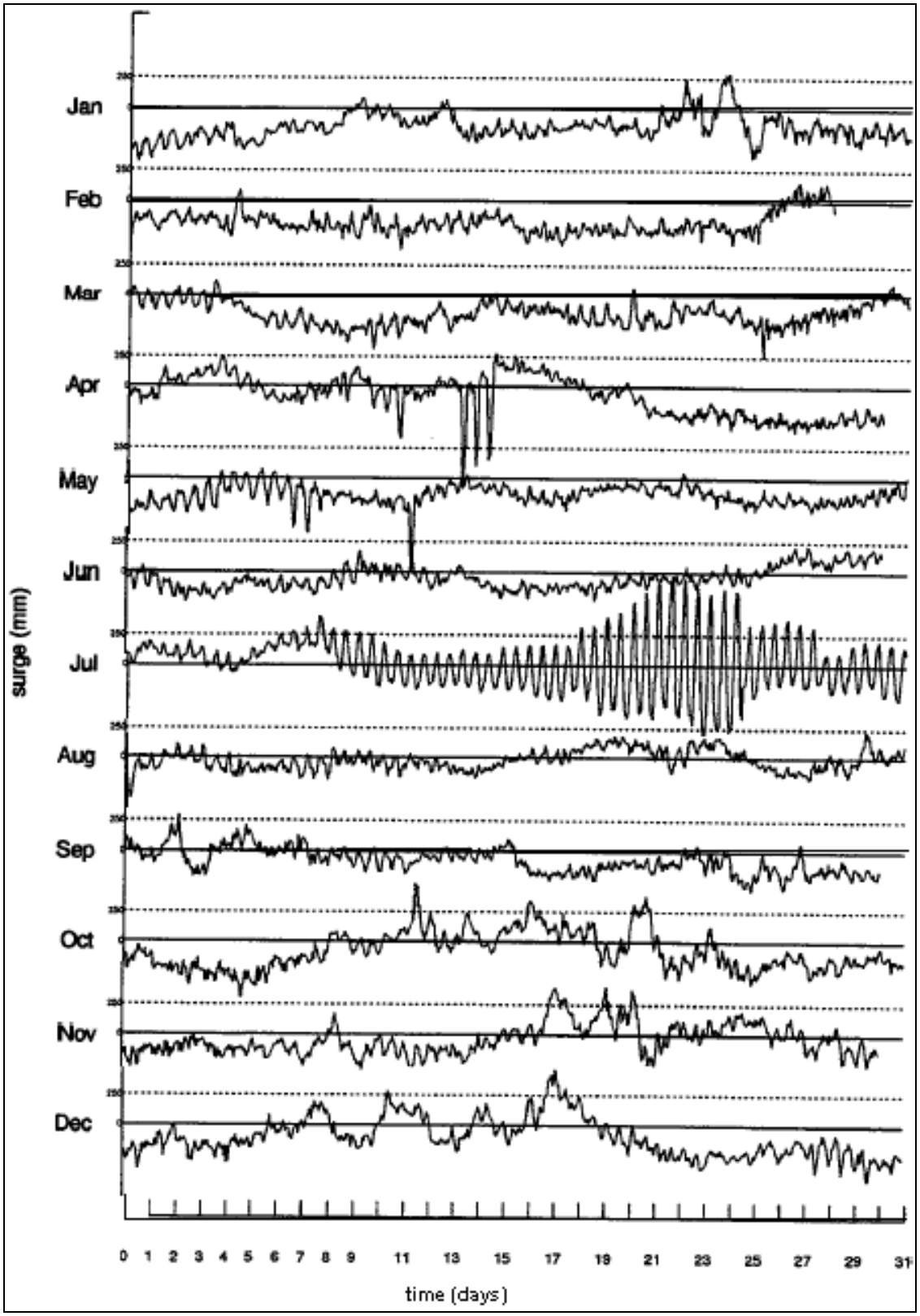

Figure 2.11. Examples of erroneous hourly surge data: Newlyn 1944 (Dixon and Tawn, 1994:37).

Graff (1981) did not intend for these data to be used for long term relative mean sea level trend analysis, but purely for contemporary (1980s) extreme sea level frequency analysis. However,

Pethick (1999) and Rennie and Hansom (2011) both used the Graff (1981) Scottish maxima dataset in support of their sea level trend reversal theory, suggesting that glacio-isostatic adjustment decreased suddenly in the mid-1970s. However, this was actually a turning point in the 30 year Arctic Oscillation Low-Frequency Oscillation (LFO) that was more evident in the longer timescale English maxima records. Gehrel and Long (2008) warned that the 1993 to 2003 3.1 mm a^{-1} rate of eustatic sea level rise could be influenced by the positive trend of a 20 to 30 year sea level cycle and cannot as yet be designated an acceleration in the long term rate of sea level change. Unfortunately, this trend is what Pethick (1999) and Rennie and Hansom (2011) observed in the mid-1970s.

Graff (1981:420) '*although the earlier diagrams show a wide and varied range in estimates of the 1/100 year level, one should bear in mind that these ranges encompass equivalent frequency estimates derived from time series of different lengths, and for many ports we have already seen evidence to suggest such frequency estimates are time dependent.*'

Graff (1981) used Lennon's (1963) method of calculating the intensity of extreme sea levels for 1/100 year events between 1945 and 1980 in order to eradicate time dependent frequency errors:

$$\frac{\text{Extreme level} - \text{Mean high water spring level}}{\text{Spring range}}$$

The general pattern of extreme level intensity identified in Figure 2.12, with higher intensities on the north-west and south-east British coastlines and lower intensities on the north-east and south-west coastlines. The lower intensities along the eastern Scottish coastline appear as shallower curves in the flood frequency curves than those along the western Scottish coastline (Graff, 1981).

Prediction of storm surges has been investigated on a national scale by previous studies (Williams and Flather, 2004). Storm surge models used by UK NGOs have been created by POL. These models work with POL's oceanic model, UK Meteorological Office (UKMO) meteorological data and NTSLF sea level data. The final product, a storm surge warning, is fed to the Storm and Tide Forecasting Service (STFS), the Environment Agency and the Scottish Environment Protection Agency (SEPA) (Williams and Flather, 2004). Substantial increases in high water surge heights have been calculated for the Bristol Channel and the east Irish Sea by the POL "CS3" tide-surge model (Flather *et al.*, 2001) (Figure 2.13). This model is independent of any timescale, representing only the potential surge change relative to sea level change.

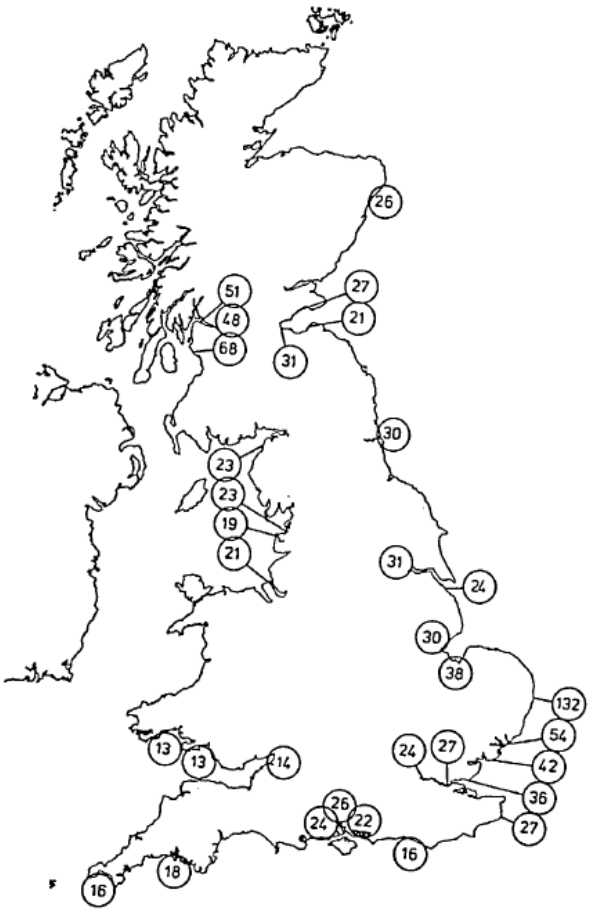

Figure 2.12. Map showing the distribution Graff's (1981) data sites around Great Britain (Graff, 1981:427).

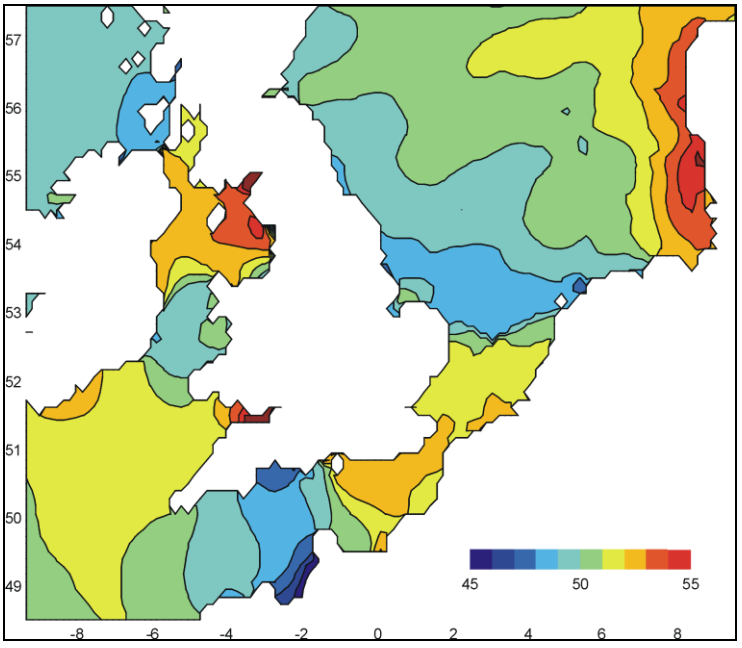

Figure 2.13. Computed change in mean high water (cm) due to a 50 cm rise in MSL (Flather *et al.*, 2001:11). Computed by the POL CS3 tide-surge model.

Some localised management plans, such as the Fife Shoreline Management Plan (Fife Council 2011), have included projections of future extreme sea level, which are essential for the longevity of coastal management plans. For 2100 projections to be completely functional they must include surge calculations as mean sea level projections would only account for still water levels.

2.6 Climate and Sea Level Change

Sea level, being influenced by atmospheric pressure, winds, tides, ocean currents and temperature, is greatly affected by climate change on both short-term and long-term timescales (Barbosa *et al.*, 2006). Both global sea level and temperature have been increasing since 1800 AD (Mortari, 2004) (Figure 2.14; Figure A2.1, A2.2 and A2.3, in Appendix 2). The oceans, as well as increasing in volume due to the impacts of increasing temperatures, absorb large quantities of CO_2 and act as an effective carbon sink (Revelle and Seuss, 1957; The Royal Society, 2005). These levels have been increasing over the last two centuries, causing acidification (Figure 2.14) (Revelle and Seuss, 1957; National Research Council of the National Academies, 2011; The Royal Society, 2005).

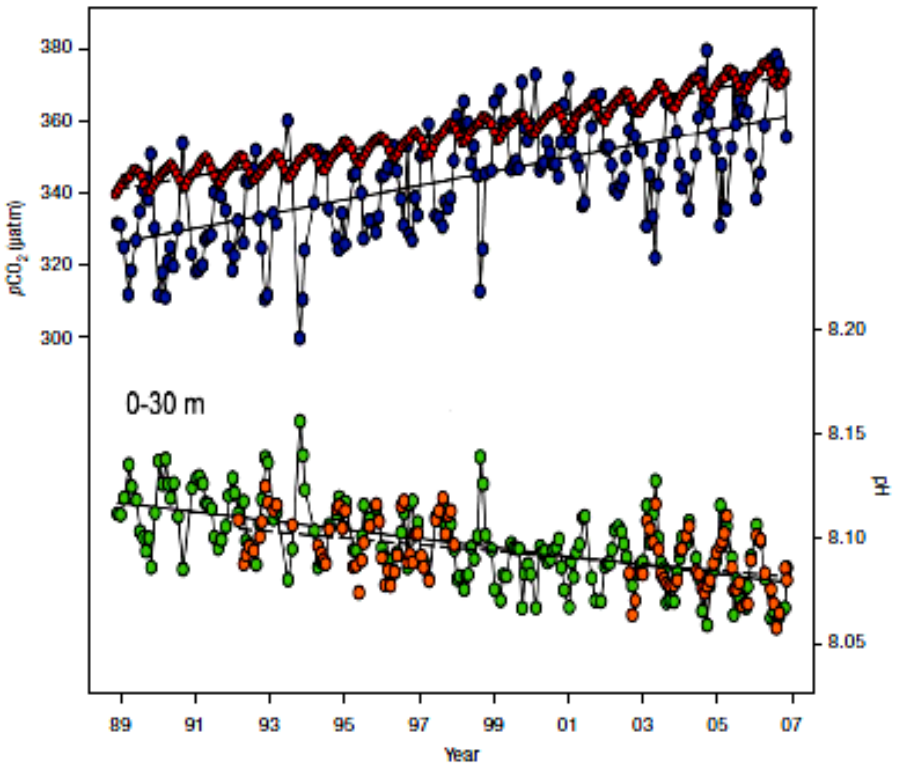

Figure 2.14. 'Ocean carbon dioxide and pH measurements near Hawaii at Station ALOHA 1988-2007. This figure demonstrates that as carbon dioxide in the air and ocean increases over time, the pH in the seawater decreases (Dore et al., 2009). Top: Calculated partial pressure of carbon dioxide in seawater (blue •), and in air at nearby Mauna Loa (red •). Bottom: Direct measurement of pH in surface

seawater (orange •) compared with calculated pH (green •).' National Research Council of the National Academies (2011).

Sea level rise has been monitored for over two hundred years through the use of various tidal measurement systems. A brief overview of sea level measurement and past and present sea level change is given in Sections 2.4.1 and 2.4.2.

2.6.1 Sea Level Measurement

To produce accurate projections the tide gauge records must be corrected and validated. Sea level recordings can be generated from tide gauge or satellite altimetry data. Tide gauges, which are discussed in detail in Section 4.2, are used for navigation, shipping and scientific analysis purposes. Various types of tide gauge are available, ranging from the basic tide board (Figure 2.15), float gauge, pressure gauge, acoustic gauge and the RADAR gauge (Hardisty, 2007).

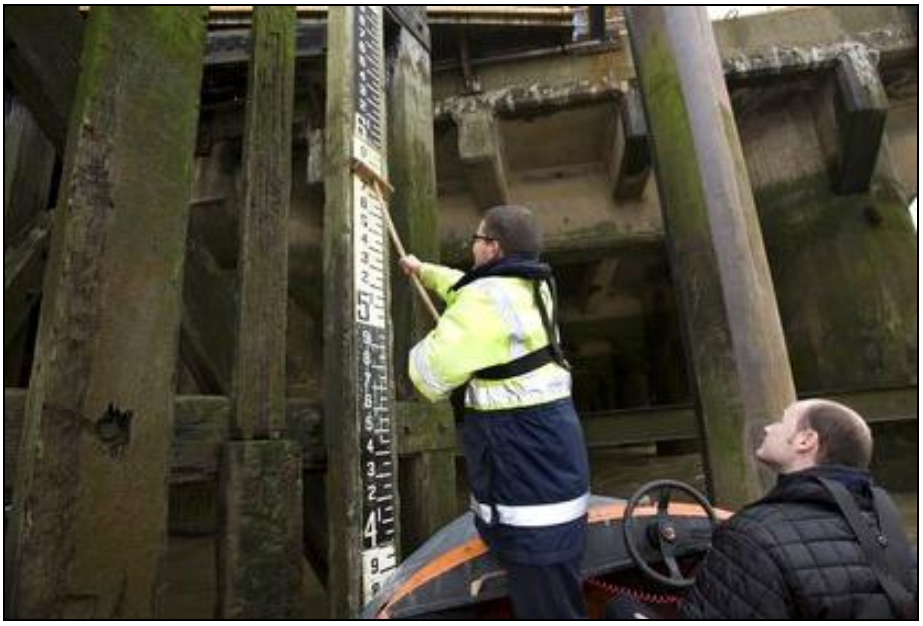

Figure 2.15. Photograph of a tide gauge maintained by the Port of London Authority (2011).

Float gauges were the original automatic recording gauges initially designed by Moray in the seventeenth century, but first engineered by Palmer in the nineteenth century (Hardisty, 2007). Pressure gauges measure hydrostatic pressure in comparison with air pressure to calculate sea level (Hardisty, 2007). Acoustic gauges measure water level off the reflected surface and RADAR gauges measure the time taken for a RADAR pulse to return from a reflected surface (Proudman Oceanographic Laboratory (POL), 2008).

Stilling wells are often used to reduce wave oscillation impact on float, pressure and acoustic readings. All of these systems can be linked to a DATARING data logger to created timed data

merged potentially with external factors, i.e. GPS or meteorological data (DATARING being an acronym for Data Acquisition for Tidal Applications by the Remote Interrogation of Network Gauges) (POL, 2008).

Tide gauges are not installed on a spatially uniform basis across the globe (Figure 2.16), making comprehensive global sea level estimates bias towards Northern Hemispherical trends (Church and White, 2004; Woodroffe, 1993). Local conditions, such as vertical glacio-isostatic movement, have a great impact on pre-corrected global sea level trends (Nakada and Inoue, 2005). Other issues that affect the quality of tide gauge data include instrumental failure (leading to gaps, spikes and jumps in the records), reference datum change, human error, vandalism, tectonic land movement, human induced land movement and inadequate maintenance regimes (Gil and De Toro, 2005; Holgate, 2007; Woodworth *et al.*, 1999; Powell *et al.*, 2011). New tide gauges are preferably fitted with GPS recorders to remove land movement errors (Wöppelmann *et al.*, 2007).

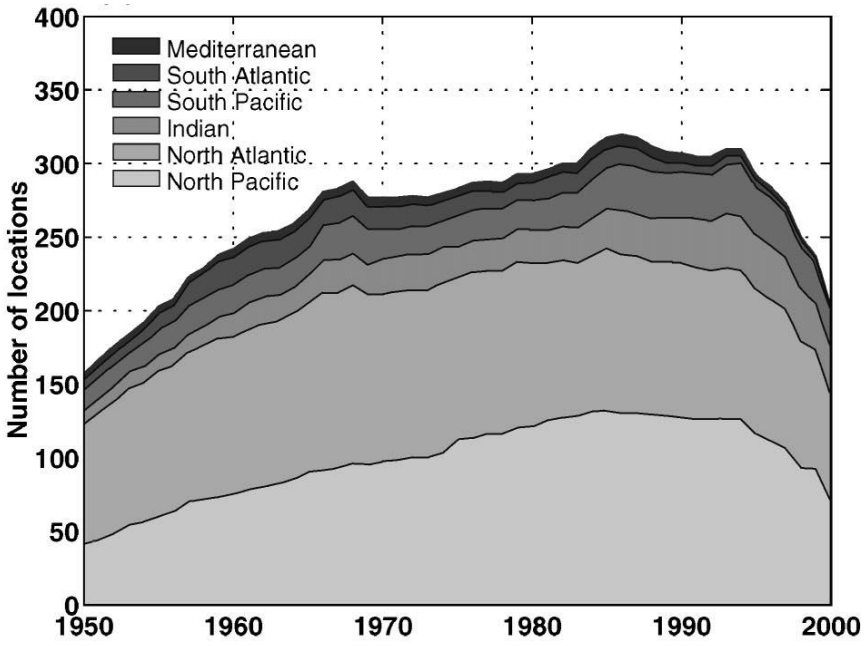

Figure 2.16. Number of tide gauge locations and the regional distribution between 1950 and 2000 (Church and White, 2004: 2612).

Tide gauges are installed and maintained for various reasons. In general, port authorities that install tide gauges need high accuracy to ensure the safety of the ships passing through their operational areas. Some local authorities install tide gauges to monitor surge conditions for coastal flooding of estuaries or low-lying coastal land and do not intend for the data to be used for long-term sea level analysis. Scientific bodies install tide gauges for various reasons, including for coastal flooding purposes. Often, only the port authority would have the human resources to monitor a tide gauge

more frequently than once a day. The accuracy and maintenance regimes vary for these reasons depending on the owner and/or operator of the gauge (Powell *et al.*, 2011).

Historic tide gauge records are available from several research organisations, including the British Oceanographic Data Centre (BODC), the Permanent Service for Mean Sea Level (PSMSL), the UK Hydrographic Office (UKHO), the National Tidal and Sea Level Facility (NTSLF), the Scottish Environment Protection Agency (SEPA) and several port authorities. Some of these authorities provide corrected data, which have been corrected for datum errors, recording errors and human errors. Even these datasets should be re-checked in order to certify data accuracy (Powell *et al.*, 2011).

Unlike satellite altimetry, which measures the eustatic movement of the ocean from a satellite, tide gauges measure the relative motion of the sea with respect to the land on which they are fixed (Maul *et al.*, 1996). This results in tide gauges measuring relative sea level, which includes both eustatic sea level and isostatic land movement. Satellite altimetry technologies, such as the TOPEX and POSEIDON satellites, are perceived to be more accurate than tide gauges (Mitchum, 2004). However, the satellite data span less than twenty years (Watson *et al.*, 2008; Leuliette *et al*. 2004).

The two methods, satellite altimetry and tide gauge recording, record different global averages as the tide gauge data are restricted to coastal shelf areas and the satellite altimetry data cover the entire global oceans (Marcos *et al.*, 2007). Gehrels and Long (2008) explained that sea level is not constant across the globe with some areas experiencing higher levels than others. The inclusion of large areas of open ocean in the satellite altimetry data could include large oceanic areas of higher sea level, which would result in the satellite altimetry data producing higher global sea level averages. Only tide gauge data are used in this thesis to produce past sea level records.

2.6.2 Historical Sea Level Changes

The main contributors to sea level change are identified as thermal expansion of the oceans and water mass increase due to land-ice melt (Solomon *et al.*, 2007). Solomon *et al.* (2007) calculated the sea level contributions of thermal expansion and glacier-ice cap input to be 0.42 mm a^{-1} and 0.50 mm a^{-1} respectively. These statistics vary slightly between models, for example global tide gauge data compiled by Nakada and Inoue (2005) suggests contributions of 0.40 mm a^{-1} from thermal expansion and 0.50 mm a^{-1} from glacier-ice cap input. ‘IPCC suggest that projected changes in sea level as a result of climate change will be a dominant factor in sea level change by the latter half of this century’ (UKCIP, 2006).

Examples of individual site sea level records include those at Aberdeen, North Shields, Sheerness, Newlyn and Liverpool (Figure 2.17). Each of these locations has witnessed rising sea levels since the beginning of sea level recording. Aberdeen is a good example of a sea level recording site witnessing glacio-isostatic uplift, resulting in the sea level rise trend appearing to be slower than at the other sites (Flather *et al.*, 2001; PSMSL, 2011).

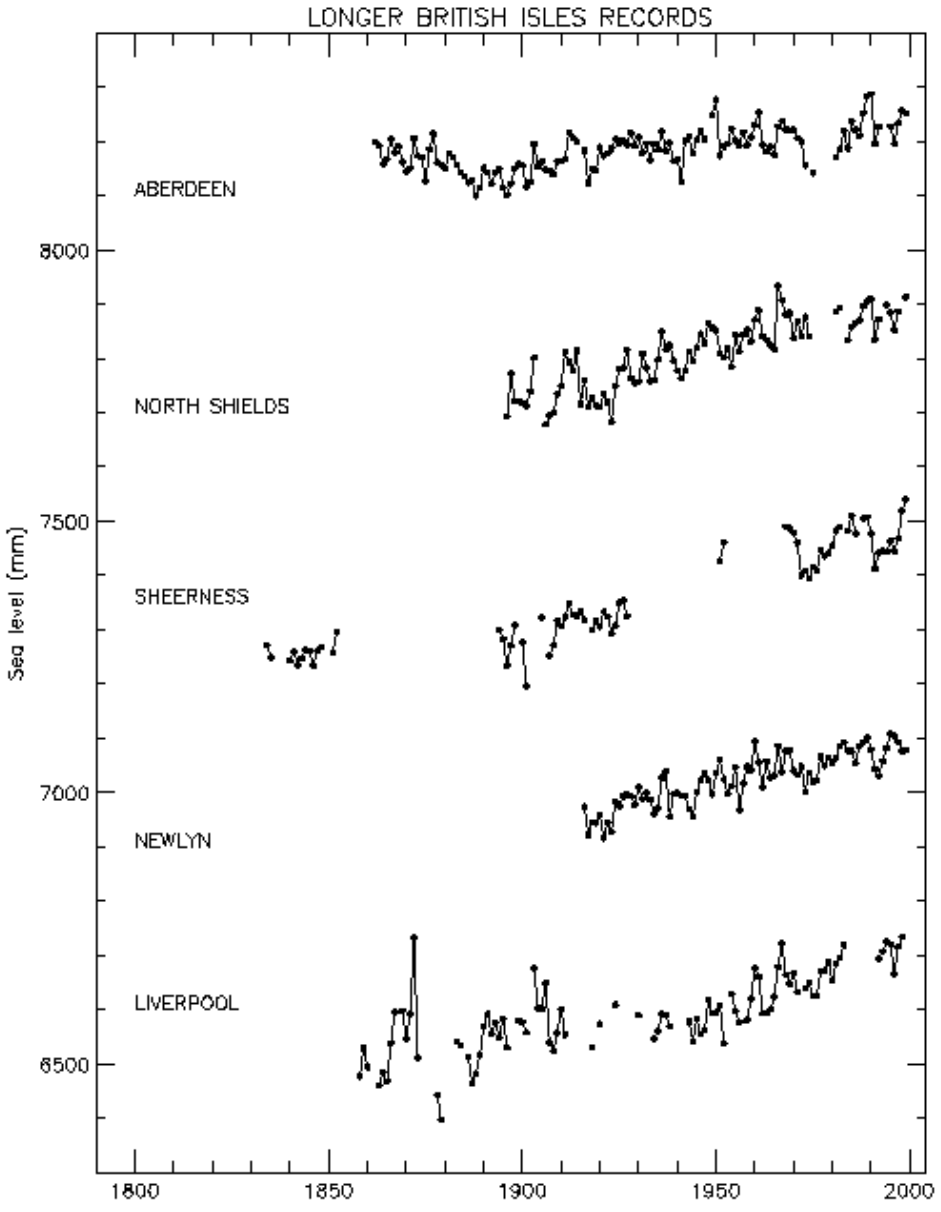

Figure 2.17. Long term changes in sea level at UK sites with long records (Flather *et al.*, 2001:6).

The Marine Climate Change Impact Partnership (MCCIP) studied marine sea surface and air temperature, observing that they are increasing by 0.2 to 0.6°C per decade across the UK except near the Scottish Continental Shelf waters where rates are lower (MCCIP, 2008). The UK

Government aims to limit temperature increase to 2 °C by 2100 from the 1990 benchmark. However, models of future climate change suggest that temperature could increase by 1.1 to 6.4 °C (Solomon *et al.*, 2007). This variance depends on how emissions are controlled in the near future and relies upon global cooperation.

The Department for the Environment Food and Rural Affairs' (DEFRA) climate change policy recognises several signs of climate change, including relative sea level rise along the UK coastline of ~1 mm a^{-1} during the twentieth century, decreasing Arctic summer sea ice since 1979 and an average warming of the Earth's surface of 0.4 °C a^{-1} since records began in 1970 (DEFRA, 2011b). The positive correlations between sea level and temperature withincreasing twentieth century global trends, and negative correlations between temperature and snow melt, suggest close relationships between sea level rise, temperature increase and Northern Hemisphere snow cover (Figure 2.18).

Global eustatic sea level rise has been calculated by several approaches. Douglas (1997) used data from 24 tide gauge records held by PSMSL. These data records were qualified to represent global sea level, because they were all over 60 years in length, were not located at convergent plate boundaries, were at least 80% complete, showed agreement with nearby gauges and were not located in regions of high glacio-isostatic movement. The corresponding data indicated an average global sea level rise of ~1.8 mm a^{-1} since 1900 (Douglas, 1997).

Miller and Douglas (2006) suggested that some of the longest tide gauge records indicate there has been a small positive sea level acceleration of 0.01 mm a^{-1} in the nineteenth century and no discernable rate of acceleration through the twentieth century. This followed their review of analyses undertaken by Woodworth (1990), Kearney & Stephenson (1991) and Donnelly *et al.* (2004). After their review Miller and Douglas (2006) agreed with the original results and methods given by Douglas (1992) and Woodworth (1990), both of which used data with long timescales. However, Jevrejeva *et al.* (2008) analysed datasets from the past 300 years and agreed with Church and White (2006) that there has been significant, continuous global sea level rise acceleration of 0.01 mm a^{-1} since 1800.

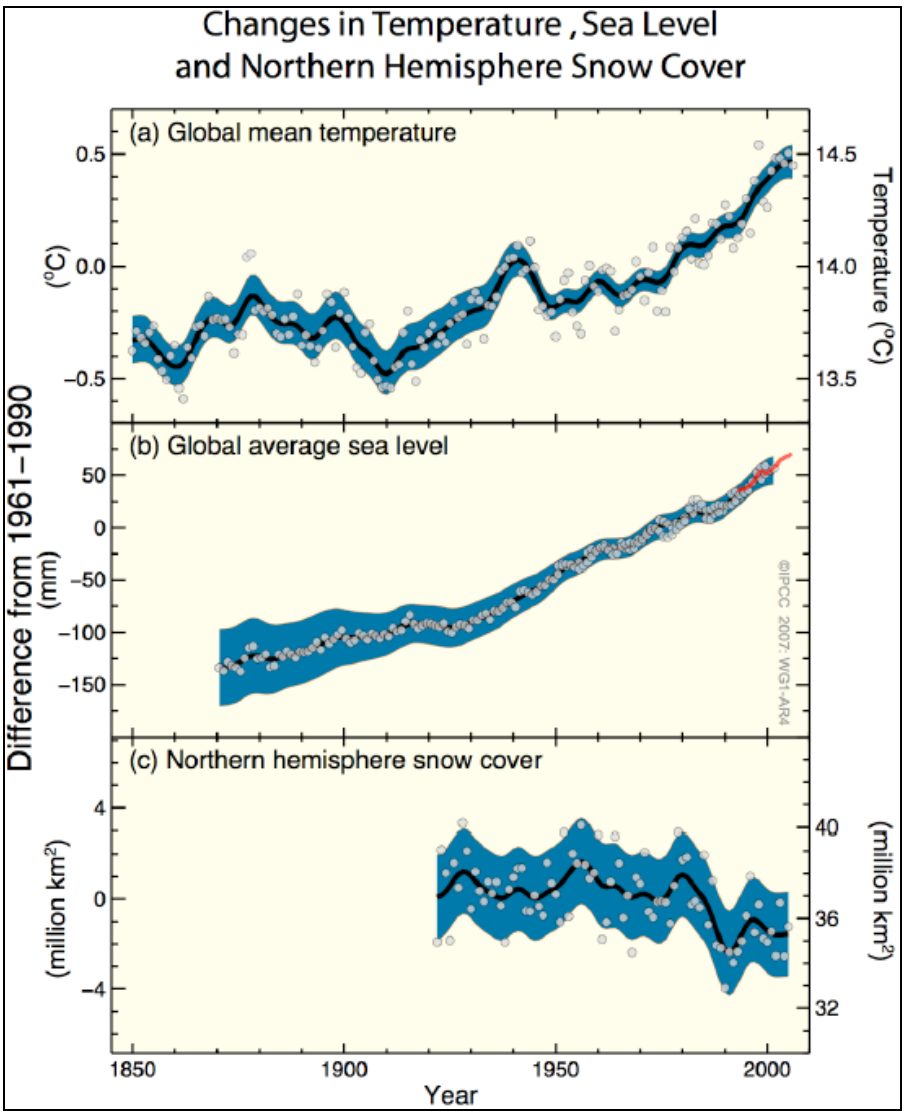

Figure 2.18. Changes in (a) global mean temperature, (b) global average sea level and (c) Northern Hemisphere snow cover between 1850 and 2005 (Solomon *et al.*, 2007:17). This figure identifies that there is a relationship between global temperature rise, global sea level rise and northern hemisphere snow cover reduction.

Jevrejeva *et al.* (2008) produced global sea level data that suggest sea level rose by 6 cm in the nineteenth century, 19 cm in the twentieth century and, if the causes of sea level acceleration continue, sea level could rise by 34 cm in the twenty-first century. These calculations presume climate change is the predominant cause of this acceleration in sea level rise, which is theoretically supported by the timing of acceleration start, at the beginning of the Second Industrial Revolution (~1850 AD). Modelling of future sea levels is discussed in Sections 2.9, 4.7 and Chapter 8.

Church and White (2006) produced a global sea level average dataset for the period 1870 to 2004. Their data suggested a rise in sea level of 19.5 cm across the time period, a twentieth century global sea level rise rate of 1.7 ± 0.3 mm a^{-1} and a global sea level rise acceleration of 0.013 ± 0.006 mm a^{-}

^{2}. Church and White (2006) speculated that if the acceleration rate continued until 2100 then the 1990 to 2100 sea level rise total would be between 28 and 34 cm.

Church and White (2011) reported updated calculations, using tide gauge and satellite altimetry data from 1880 to 2009 and 1993 to 2009 respectively. After glacio-isostatic adjustment (GIA) correction the global rate of sea level rise between 1880 and 2009 was 1.7 ± 0.2 mm a^{-1}. Church and White (2011) acknowledged the variability in the twentieth century sea level rise rate and a reduction in the global sea level rise acceleration rate to 0.009 ± 0.004 mm a^{-2} since 1900 in the tide gauge data and 0.009 ± 0.003 mm a^{-2} in the altimetry data. An overall rise of 21 cm occurred between 1880 and 2009 (Church and White, 2011).

Sea level rise fluctuations should not be assumed to be synchronous and equal in amplitude along every coast, not even within the limited region of the southern North Sea (Weerts *et al.*, 2005). Some relative sea level records, such as analysis of coastal sediments, cannot be correlated with global climate change indicators due to local and regional processes (Bungenstock and Schäfer, 2009). Therefore, regional issues and estuarine impact must be considered when undertaking local and regional research.

In summary, eustatic sea levels have been recorded as having risen by 6 cm in the nineteenth century, 18.5 to 19 cm in the twentieth century and are projected to rise at a greater rate in the twenty-first century. The increasing rate of sea level rise could have a dramatic impact on the coast.

2.7 Estuaries and Sea Level Change

Estuaries are semi-enclosed water bodies attached to the coast with a freshwater input and tidal nature (Dyer, 1997). The definition of estuaries generally includes fiards, fjords, firths and all other freshwater river mouths with tidal elements. Firths are studied in this thesis. Firths, known as ‘the arms of the sea’, are formerly-glaciated, funnel-shaped, drowned river valleys, similar in definition to fiards (Bird, 2008).

Their fluvial input variations, geomorphic characteristics and tidal contributions create unique conditions. This uniqueness adds complications to holistic analysis of estuaries and direct comparison between model output of individual estuaries. Every estuary works differently to another with constantly changing river discharge, tidal movement, waves, sediment exchange and meteorology in addition to sea level change and storm surge parameters (Dyer, 1997; Reeves and Karunarathna, 2009).

Tide waves in estuaries are not the near perfect sine waves exhibited in the open ocean (Kjerve, 1988). Estuaries are generally shallow upstream and deep at the mouth (van Rijn, 1990). In the

typical estuary, seabed friction and shallowing encourage distortion in the wave pattern (Figure 2.19) (Dyer, 1997; van Rijn, 1990). This distortion also warps the lunar diurnal and semi-diurnal cycles (Table A2.1) creating asymmetry in the tidal curve in estuaries (Dyer, 1997). Friction rates are variable depending on the estuary sediment type, width and depth (Sylvester, 1974).

Of the tidal harmonics discussed in Section 2.9, the most dominant lunar and solar semi-diurnal frequencies can be overridden by shorter-frequency quarter-diurnal cycles in areas where shallowing interrupts the dominant longer-frequency cycles (Liu, 2000). More information about the various tidal harmonics can be found in Section 2.9 and Table A2.1.

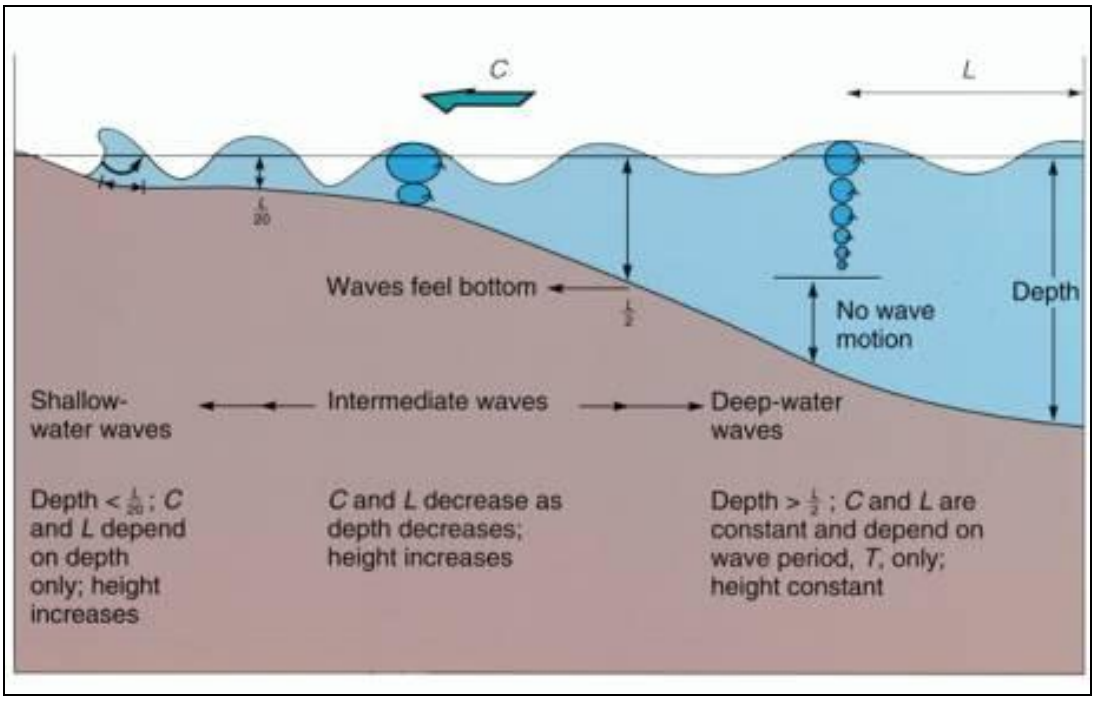

Figure 2.19. Wind wave pattern change in a shallowing environment (University of Maine, 2003).

Bottom topography greatly affects waves approaching the shoreline (Besley *et al.*, 1998). Obstacles, such as sandbanks and spits, reduce the water depth further. Waves refract as they slow and adapt to bottom topography contours in the narrowing and shallowing waters, eventually slowing and breaking (Liu, 2000). This reduces wave energy and tidal currents in the upper estuary. Besley *et al.* (2009) stated that seawalls should be designed to use the coastal bathymetry to the advantage of coastal engineering.

In funnel-shape estuaries, bathymetric changes can produce double high and low tides (Bearman, 1999). The Forth Estuary, observes double high and low tides, which are locally known as lackie tides. This is an example of the lunar quarter-diurnal (M_4), 1/6th-diurnal (M_6) and 1/8th-durnal (M_8) tidal harmonics overriding the longer frequency, more dominant lunar semi-diurnal (M_2) cycle.

Where an estuary narrows and shallows quickly, known as convergence, the shallowed wave is forced upwards and forwards to compensate and house the water volume. A significant convergence can form a tidal bore, which is a small wall of water forced forward by a shock wave to propagate above the shallow-water depth (Bearman, 1999; Webb and Metcalfe, 1987). Both of these events, forced by sudden shallowing and narrowing, appear in daily tide gauge records and can present tidal measurements higher than the daily high tide.

A tidal wave that spends most of its energy travelling up the estuary is called a progressive wave (Dyer, 1997). Progressive waves produce high water levels and currents near the mouth, but act as a standing wave at the upper limit of the estuary (Bearman, 1999). Both the estuaries in this thesis observe progressive tidal waves where the water stands upriver and slowly returns to the sea, visualised as an asymmetrical tidal cycle in tidal records (Dobereiner, 1982). This is another friction dominated impact on tidal waves in estuaries with particular bathymetric qualities (Hardisty, 2007).

Fluvial discharge can have a significant impact on tidal amplitude and penetration, but this depends on the fluvial-marine discharge ratio. A large fluvial discharge into a small microtidal estuary would have a larger dominance than a small fluvial discharge into a large megatidal or macrotidal estuary (van Rijn, 1990; Bearman, 1999), such as the firths found in Scotland. Even these firths vary significantly in their seawater-fluvial discharge ratios.

Estuary mouths can experience saltwater wedge fronts, where a large discharge of fluvial freshwater meets saltwater. A saltwater-freshwater wedge would typically appear due to large quantities of both water types meeting and the denser saltwater advancing along the seabed faster than at the surface (Geyer and Farmer, 1989; Friedrichs and Aubrey, 1988; Hardisty, 2007). Some mixing may occur over the front, which is not perpendicular across the estuary cross-section, but follows the bottom topography in the shallows and bends with the tidal inflow and outflow (Hardisty, 2007). These fronts can be identified by foam lines at the water surface in some estuaries. A front is less likely to occur in estuaries with a small fluvial discharge, where increased mixing occurs furthers upstream (Geyer and Farmer, 1989; Hardisty, 2007). Wedges can have control over the location of fluvial sediment deposition, marine sediment deposition and overall sediment retention (Kostaschuk *et al.*, 1992).

Estuary channels are controlled by ebb and flow tidal currents (Robinson, 1960). The currents change the position and dimension of the channels, necessitating port dredging where navigation is impacted by channel dynamics. Estuaries are generally areas of high sedimentation. The rate depends on the original size of the drowned river valley area, volume of the mouth, river sediment yield, downwash from bordering slopes, shore erosion and sediment inflow from the sea (Friedrichs

and Aubrey, 1988). Estuaries on emerging coasts infill more rapidly, due to wave and current action, compared to those on submerging coasts (Teasdale *et al.*, 2011).

The tidal range in the estuary can shape the estuary mouth and intertidal area significantly. A microtidal estuary will be dominated by wave action and river currents with narrow intertidal areas and potentially steeper slopes and narrower beaches (Dyer, 1997). The estuary will be more exposed to surge events as the sea will be close to the shoreline for long periods of time. Mesotidal estuaries will have stronger tidal currents than microtidal estuaries, as well as larger intertidal zones. Macrotidal and megatidal estuaries will be dominated by tides and tidal currents, funnel-shaped with large intertidal flats and deeper channels (Hardisty, 2007).

Estuaries have the additional complication that they are a 'nexus of human activity' (Reeves and Karunarathna, 2009:938). Estuaries are commonly used by heavy industry, agriculture, domestic housing, fish and shellfish farming, leisure and tourism. They are also habitats for rare bird, aquatic fauna and flora in the mid-estuary, marshlands and tidal flats (Mclusky, 1987). Both the human and natural environment can be threatened by fluvial and coastal flooding, erosion and sediment mobilisation.

In summary, estuarine morphology is manipulated by tides and tidal currents. Sea level rise could cause significant changes to the tidal range, penetration and tidal currents in estuaries. This may result in estuarine sediment mobilisation, flooding and erosion. Increased tidal ranges will result in present day intertidal zones being submerged for longer periods of time and potential translocation of intertidal flats into neighbouring areas. The firths discussed in this thesis are post-glacial formations, therefore additional isostatic elements need to be investigated.

2.8 Ice and Glacio-isostasy

Over thousand of years Milankovitch cycles, such as the precession of the equinoxes, eccentricity and obliquity of the Earth's axis (Figure 2.20), manipulate the Earth's precession and rotation around the Sun, being almost exclusively responsible for the continuous cyclic periods of hot and cold events, known as glacial and interglacial periods, which last of approximately 100 ka and 10 ka^{-1}, respectively (Masselink and Hughes, 2003). Shorter hot and cold periods that last for up to 1 ka^{-1} are known as interstadials and stadials (Masselink and Hughes, 2003). The last glacial period, known as the Holocene or Flandrian in the UK, ended approximately 10 to 12 ka^{-1} BP (Masselink and Hughes, 2003). Since that time the global ice sheets have been melting and the land is continuing to recover from partial ice sheet coverage.

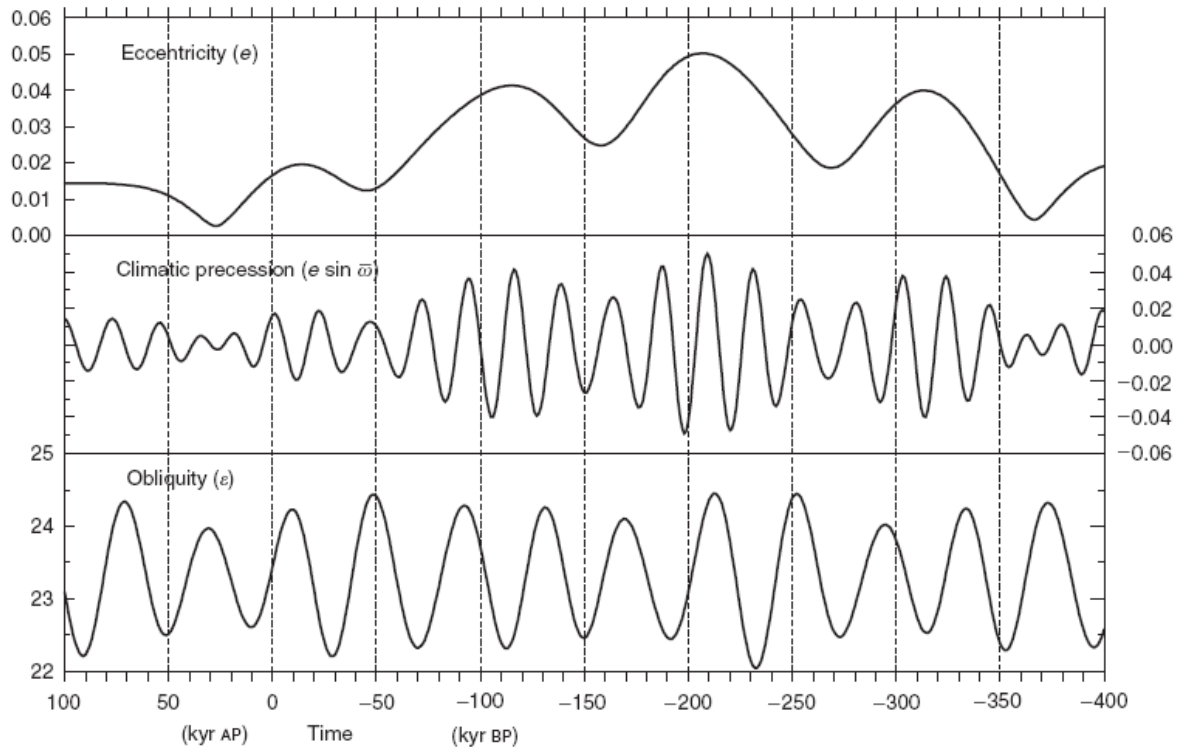

Figure 2.20. 'Long-term variations of eccentricity, climatic precession and obliquity from 400 000 years ago to 100 000 years into the future (Curry *et al.*, 2003).

Glacio-isostasy is the term used for land movement after or during ice sheet melt in interglacial periods and glacio-isostatic adjustment (GIA) is the term used for postglacial rebound of depressed areas of land that were once beneath ice. In GIA areas, the central area of the ice sheet, where the ice was thickest, heaviest and depressed the land greatest and for longest, witnesses the greatest uplift in comparison with the periphery (Firth and Stewart, 2000). During the creation of an ice sheet, 'the mantle material below the crust under the ice sheet is displaced leading to a rising of the crust around the ice sheet periphery (glacial forebulge)' (Jenkins, 2007). This forebulge would witness subsidence during the next interglacial. In areas where isostatic land movement is equal to the eustatic sea level change the sea level will appear to be stable (Figure 2.21). This is know as sea level stillstand (Haslett, 2008).

Historically, evidence suggests that sea levels have been 125 m below the present level and if all the Earth's ice melted, global sea level may rise by an additional 70 m (Dyer, 1997), although this level of melt is unlikely over centennial scales. During the last twenty thousand years, continental ice has decreased by 70%, occurring alongside the rise in sea level (Milne *et al.*, 2006). Titus *et al.* (1991) states that during the previous interstadial period sea levels were approximately 6 m higher than they were in 1991, which implies what the potential height of sea level could be from ice sheet melt and thermal expansion sometime in the future.

Cullingford (1966), Cullingford *et al.* (1966) and McManus *et al.* (1993) recognised raised beaches along the Forth and Tay Estuaries, which range from 6.1 to 14.8 m above present Ordnance Datum level. These raised beaches were products of post-glacial land level rise combined with eustatic sea level fall since the Last Glacial Maxima (Sissons, Smith and Cullingford, 1966). Pedoja *et al.* (2011) suggest that global continental uplift may have had an impact on beach uplift due to slow plate tectonic interactions.

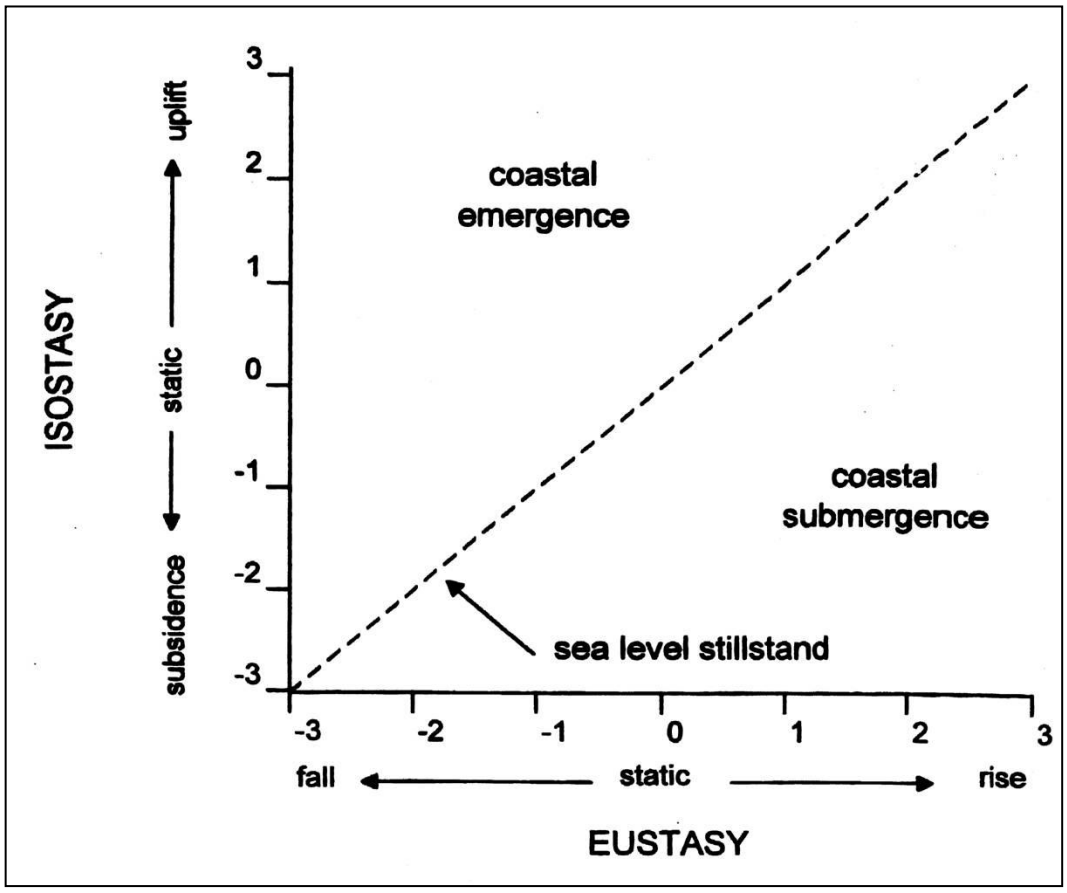

Figure 2.21. The balance between isostasy and eustasy; potentially resulting in coastal emergence, subsidence or stillstand (Haslett, 2008:137).

In the next few millennia glacial scale cycles suggest the next glacial period (ice age) should begin (Maul *et al.*, 1996). If this occurred there would be a 5 to 15 °C drop in temperature at sea level, decreasing sea levels, increased ice formations, greater need for fuel and reduced food production in the upper latitudes (Titus *et al.*, 1991; Singer and Avery, 2008). The initiation of stadials can be fairly swift, as demonstrated by the Younger Dryas initiation and closure, with this one thousand year event both starting and ending in only a few decades (Severinghaus *et al.*, 1998). However, temperatures are predicted to continue to increase and are over 1 °C higher now than they were during the last interglacial period, suggesting that a new stadial or glacial period may not be imminent (Titus *et al.*, 1991).

Attempts to quantify glacio-isostatic movement along coasts include methods such as:

- Construction of GIA global ice models – e.g. the ICE-5G series;
- Compilation of geological datasets – e.g. Shennan *et al.* (2009);
- Geodetic tide gauge use – i.e. GPS measurement or Continuous GPS (CGPS) recording alongside tide gauge measurement;
- Woodworth and Jarvis' (1991) Master Station approach.

GIA models of the Flandrian Ice Sheet are composed of an isostatic Earth simulation model, a Late Pleistocene ice history model and an ocean-ice distribution model (Milne *et al.*, 2006). The first GIA model for the UK was published by Lambeck (1993) in the early 1990s (Milne *et al.*, 2006). Boulton and Hagdorn (2006) produced a Late Pleistocene ice model of the British ice sheet, which suggests that the ice sheet had a relatively low summit with long marginal lobes. The exact location of the Late Devensian ice sheet extent over Britain is unknown, but Boulton and Hagdorn (2006) reviewed several other models and estimated the average modelled ice limits to be 1400 m high and approximately 100 km into the sea from the Scottish east coast.

GIA modelling is in its infancy with several studies suggesting significant improvements are needed to eradicate the gaps and misfits in the UK upland results (Bradley *et al.*, 2009). 'There is a clear uncertainty surrounding estimations of rates of isostatic adjustment' (UKCIP, 2006). Lithosphere thickness is one of the parameters that can negatively impact on GIA model output in upland areas (Shennan *et al.*, 2002).

The UKCP09 sea level projections use Bradley *et al.*'s (2009) GIA modelled uplift rate. Bradley *et al.* (2009:17) states their GIA model has a 'good fit to the regional sea level data base' of Shennan *et al.* (2006), however the fit between the Bradley *et al.* (2009) GIA model and the Shennan *et al.* (2009) data for eastern Scotland is poor, with the Shennan *et al.* (2009) GIA rates being nearly twice as large as the Bradley *et al.* (2009) rates.

Shennan *et al.* (2006) criticised the ICE-4G model, which is the improved version of ICE-3G, for timing errors concerning the major ice melt in Scotland. They also noticed the ICE-4G model predicted raised shorelines in areas where none are observed. Tide gauge studies have used models such as the ICE-3G series to correct vertical motion (Berge-Nguyen *et al.*, 2008). The current version of this model is ICE-5G.

Shennan *et al.* (2009) used a combination of various geological carbon-dating studies (Table A2.2, Appendix). The compiled geological data are considered very accurate along the UK coastline. Generally, the Shennan *et al.*'s (2009) UK results suggest most areas of Scotland are experiencing glacio-isostatic uplift and some parts of southeast and southwest England are experiencing

subsidence. An earlier version of the Shennan *et al.* (2009) model has been used in the UKCP09 sea level projections, which are discussed in Section 2.9.

Shennan, with several other authors, produced a series of GIA models based on radio-carbon dated geological survey data from various locations along the British coastline (e.g. Shennan, 1989; Shennan and Horton, 2002; Shennan *et al.*, 2002; Shennan *et al.*, 2006; Shennan *et al.*, 2009; Bradley *et al.*, 2011; Shennan *et al.*, 2011; Shennan *et al.*, 2012). Amongst these papers, Shennan and Horton (2002) produced an equation to define relative sea level rise (Eq. 1).

$$\Delta\zeta\mathbf{RSL}\ (t, \varphi) = \Delta\zeta\mathbf{EUS}\ (t) + \Delta\zeta\mathbf{ISO}\ (t, \varphi) + \Delta\zeta\mathbf{TECT}\ (t, \varphi) + \Delta\zeta\mathbf{LOCAL}\ (t, \varphi) \quad \text{(Eq. 1)}$$

Where $\Delta\zeta$RSL is relative sea level change, t is time, φ is location, $\Delta\zeta$EUS (t) is the time-dependent eustatic function, $\Delta\zeta$ISO (t, φ) is the total isostatic effect of the glacial rebound process including both the ice (glacio-isostatic) and water (hydroisostatic) load contributions, $\Delta\zeta$TECT (t, φ) is any tectonic effect, and $\Delta\zeta$LOCAL (t, φ) is the total effect of local processes at the site involved (Shennan and Horton, 2002). Since that time Shennan *et al.* (2011) have improved this equation (Eq. 2).

Shennan *et al.* (2011) highlighted the important fact that the terms relative sea level, relative land level and vertical land motion/movement (VLM) are commonly misunderstood. Shennan *et al.* (2011) defines sea level as the elevation of the geoid (sea surface averaged over several decades) relative to the solid surface of the Earth at a given time; generally the present.

Shennan *et al.* (2011) used some of the equations constructed by Mitrovica and Milne (2003) to explain sea level; i.e. Eq. 2, 'sea level is the difference between the geoid and the solid surface of the Earth, both measured relative to the centre of the Earth' with each geographical location (φ), the geoid (G), the solid, rock surface (R) and time (t), being intrinsic to the calculation of sea level (SL) (Figure 2.22):

$$\mathbf{SL}\ (\varphi, t) = \mathbf{G}\ (\varphi, t) - \mathbf{R}\ (\varphi, t) \quad \text{(Eq. 2)}$$

As seen in Figure 2.22, significant changes to the Shennan *et al.* (2011) model since its development stage when it was published by Shennan and Horton (2002). In 2002, the GIA model estimated GIA rates of between 1.0 and 1.6 mm a^{-1} across the Forth and Tay Estuaries. The models were created from a database of radiocarbon dated sea level index points from across the UK (Shennan and Horton, 2002). As the models have included new geological data sites and improved in accuracy, the estimated GIA rates in the Forth and Tay Estuaries have decreased. This is not an overall trend for the UK as figures for some areas have increased or remained constant (Shennan *et al.*, 2011).

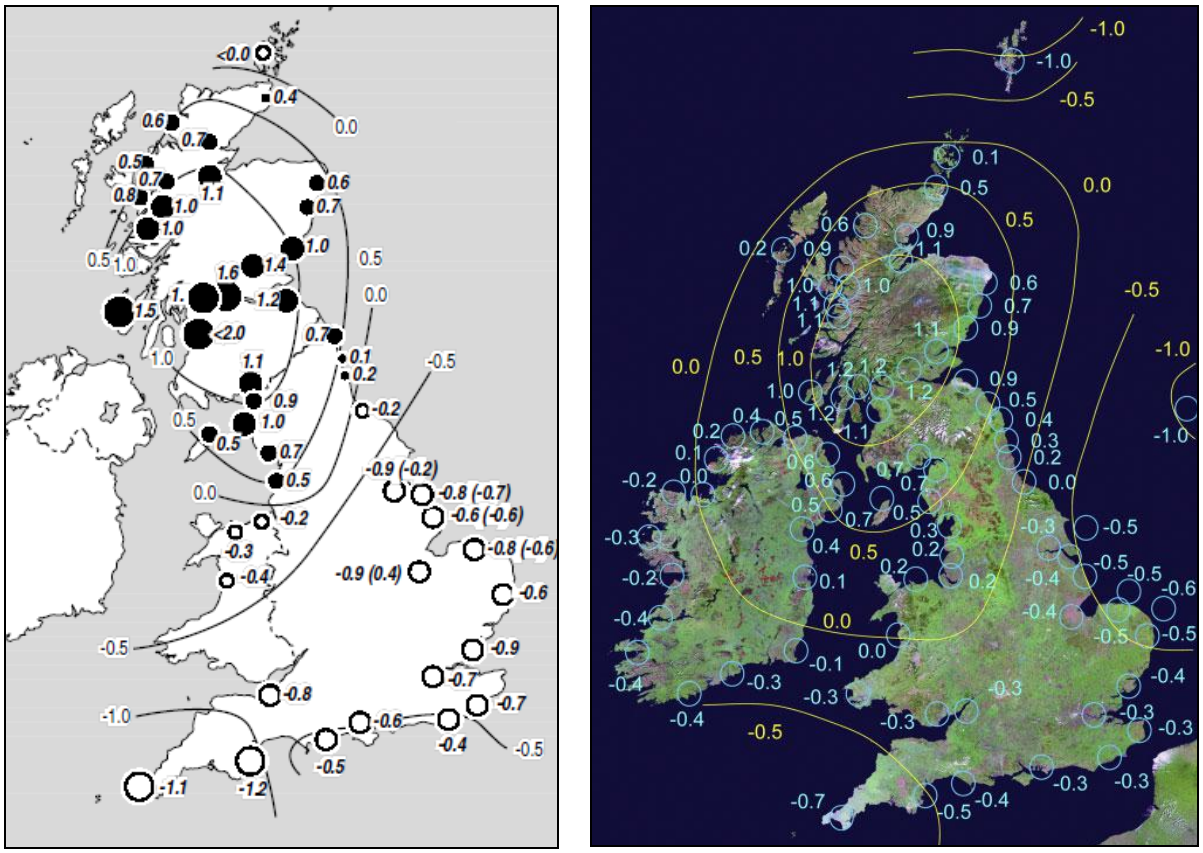

Figure 2.22. Late Holocene relative land/sea level changes (mm a^{-1}) in Great Britain taken fron a) Shennan and Horton (2002), and b) Shennan *et al.* (2011); positive values indicate relative land uplift or sea level fall, negative values are relative land subsidence or sea level rise. Figures in parentheses are the trends that take into account modelled changes in tidal range during the Holocene. Contours are drawn by eye as a summary sketch of the spatial pattern of change.

At this point, it is important to understand that models can calculate either VLM or relative land level change. VLM, as described by Shennan *et al.* (2011), is the change in the elevation of the rock surface relative to the centre of the Earth and is not limited to previously glaciated areas. Shennan *et al.* (2011) modelled relative land level change (RLLC) (Figure 2.23a), taking into account the contributions from vertical land motion (VLM) (Figure 2.23b) and the mean sea surface change (Figure 2.23c). These RLLC projections are presented in Figure 2.24, with the new present-day estimation being slightly reduced compared to previous calculations made by Shennan *et al.* (2009) and Shennan *et al.* (2006).

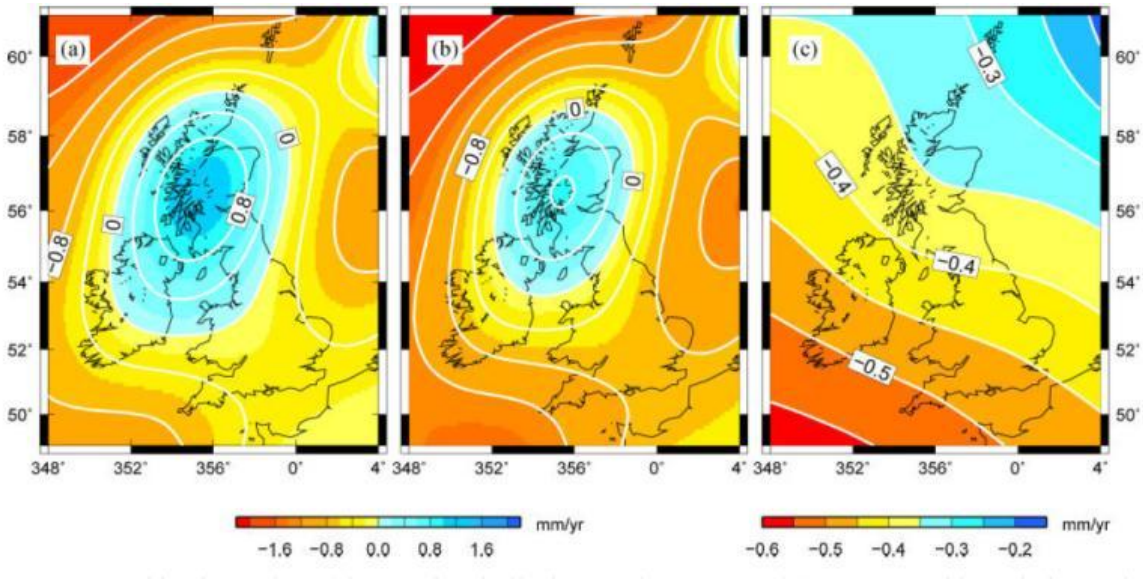

Figure 2.23. '(a) Model predictions of rates of change in relative height (Δ T (*φ*, *t*)/ Δ *t*, i.e. - Δ SL (*φ*, *t*) Δ *t*) at present around the British Isles using the model of Bradley *et al.* (2011); (b, c) The contribution to this signal from vertical motion of the solid earth (sea floor or land, - Δ R (*φ*, *t*)/ Δ *t*) and mean sea surface (over several decades this approximates the ocean geoid, - Δ G (*φ*, *t*)/ Δ *t*), respectively,' (Shennan *et al.*, 2011:6).

Land level or 'topography', T, is the negative of sea level (Eq. 3 and 4; Figure 2.22) (Shennan *et al.*, 2011).

$$\mathbf{T}(\varphi, t) = \mathbf{R}(\varphi, t) - \mathbf{G}(\varphi, \mathrm{t}) \quad \text{(Eq. 3)}$$

$$= -\mathbf{SL}(\varphi, t) \quad \text{(Eq. 4)}$$

Sea level change Δ SL, is calculate by subtracting the change in solid surface height from the change in sea surface height over time (t_0 as the chosen reference time) in the geographical area (Eq. 5; Figure 2.22).

$$\Delta\,\mathbf{SL}(\varphi, t) = \Delta\,\mathbf{G}(\varphi, t) - \Delta\,\mathbf{R}(\varphi, t) \quad \text{(Eq. 5)}$$

Where:

$$\Delta\,\mathbf{G}(\varphi, t) = \mathbf{G}(\varphi, t) - \mathbf{G}(\varphi, t_0) \quad \text{(Eq. 5a)}$$

$$\Delta\,\mathbf{R}(\varphi, t) = \mathbf{R}(\varphi, t) - \mathbf{R}(\varphi, t_0) \quad \text{(Eq. 5b)}$$

GIA models can project Holocene relative sea level change for any time in the past, where t_{past} is time before present (Equation 6).

$$\mathbf{RSL}(\varphi, t_{past}) = \mathbf{SL}(\varphi, t_{past}) - \mathbf{SL}(\varphi, t_{present}) \quad \text{(Eq. 6)}$$

> '*GIA and geological usages of the term 'relative sea level change' only coincide for consideration of change at the zero time datum. The rate of relative sea level change at* t_0,

as expressed in Eq. (4), is the same as describing the relative vertical motion between the solid earth surface and the sea surface (ocean geoid) at the shoreline. The rate of present relative sea level change is the negative of the rate of present relative land level (topography) change (Eq. 3). Importantly, this is very different to the change in the elevation of the rock surface relative to the centre of the Earth, ΔR (φ, t), commonly termed 'vertical land motion',' (Shennan *et al.*, 2011:5).

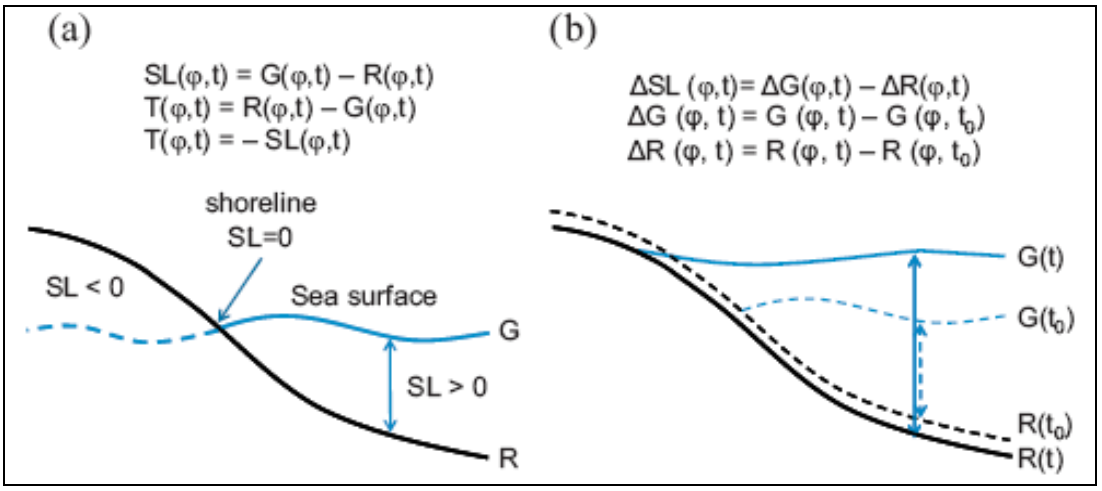

Figure 2.24. 'Definition of sea level change and associated variables common in the GIA modelling community: (a) sea level (SL), topography (T), sea surface or geoid (G, the time-averaged sea surface, over several decades, approximates the ocean geoid) and solid, or rock surface (R), all measured relative to the centre of the Earth, for geographical location ((*φ*) and time (*t*); (b) sea level change (ΔSL), for example at the location of the arrows, is the length of the solid arrow minus the length of the dashed arrow and t_0 is a chosen reference time,' (Shennan *et al.*, 2011:2).

Rennie and Hansom (2011) reviewed several papers on GIA, including Bradley *et al.* (2009), Bingley *et al.* (2007), Firth and Stewart (2000), Shennan *et al.* (2002; 2009), Teferle *et al.* (2009) and Woodworth *et al.* (1999). These papers, some of which are discussed in more detail below, give a comprehensive knowledge of GIA models on a UK scale. Unfortunately, there have been some misleading errors included in Rennie and Hansom's (2011) study, which suggest that short timescale trends that intersect sea level oscillations can represent long timescale projection.

Primarly, the most significant error in Rennie and Hansom's (2011) paper is that some of the important results from Bingley *et al.* (2007) have been transcribed incorrectly and some datasets referenced to Bingley *et al.* (2007) are not in the original paper. Secondly, both charts in Rennie and Hansom's (2010) Figure 3, depicting 'relative sea level rates in the UK' and 'vertical land movement rates with continuous geographical positioning system (CGPS) estimates' respectively, are labelled incorrectly and should actually be labelled 'relative land level change rates' and 'modelled VLM uplift rates without CGPS estimates' from Bradley *et al.* (2009). Rennie and

Hansom (2011) is an example of a study that does not correctly represent the difference between relative land level change and VLM (Shennan *et al.*, 2011). The Bradley model used by Rennie and Hansom (2011), was directly compared with CGPS data in Bradley *et al.* (2009), where it was suggested that the Bradley model was not accurate to the eastern Scotland coast CGPS land level recordings (Figure 2.22). This inaccuracy was confirmed for areas of Scotland projected by both the Shennan *et al.* (2011) and Bradley *et al.* (2011) model adaptations in Shennan *et al.* (2011).

Furthermore, Rennie and Hansom (2011) focused on short-term fluctuations, between 1992 and 2007, and use these trends to predict a large linear sea level rise until 2100. Figure 2.25 for Aberdeen illustrates how this short 15 year trend could misconstrue long term trends, depending on where along the timeline the trend is located (Dawson *et al.*, 2012). It is curious that their predictions were made in spite of their own warning that 'the clear dangers in extrapolating long-term trends from short-term data since sea level changes are subject to significant inter-annual, decadal and inter-decadal variability' (Rennie and Hansom, 2011:197). Unfortunately, many figures have not been referenced at their source, resulting in changes as they are adapted and re-adapted from the work of others.

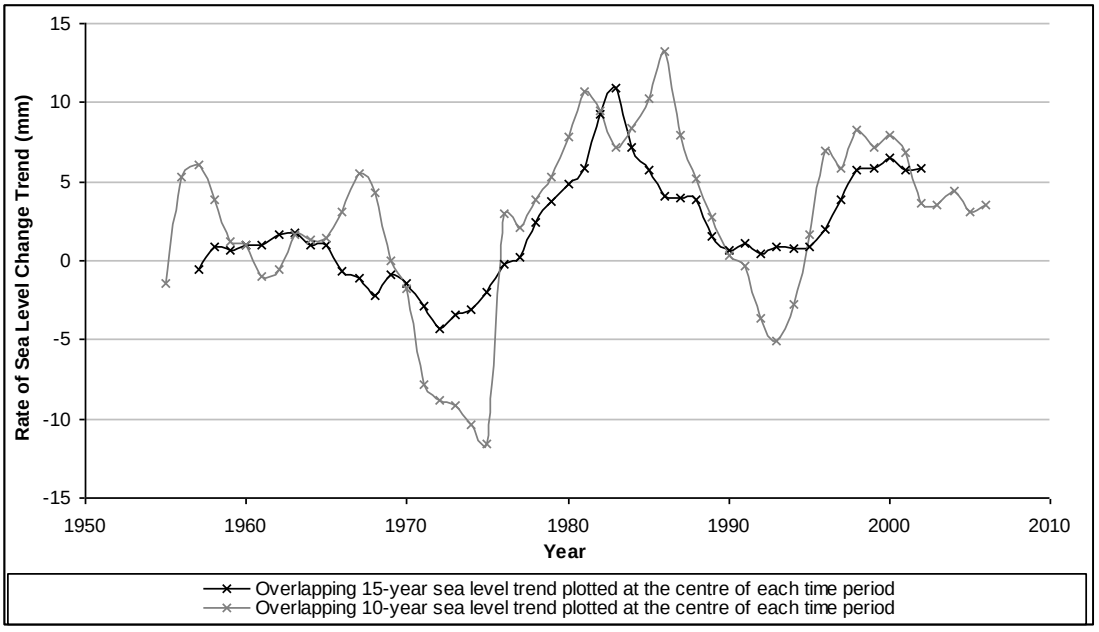

Figure 2.25. Observed changes in 10 year and 15 year the rates of sea level change between 1950 and 2009 from Aberdeen RLR monthly data. 1966-1969 data are missing and trends beginning or ending in these years have been omitted.

Separate to GIA models, geodetic tide gauge networks have been constructed, which provide sea level data from tide gauges that are monitored by GPS equipment or tide gauge benchmarks. POL are responsible for maintaining the A Class National Network; a national geodetic tide gauge-benchmark network (Woodworth *et al.*, 1999). Data at sites designated as A Class site are

considered more geodetically accurate, because the tide gauge stability is regularly checked against a benchmark. Benchmarks must be checked with GPS equipment for isostatic movement and human interference at appropriate intervals, such as an annual inspection.

Bingley *et al.* (2007) used CGPS, absolute gravimetry (AG) and persistent scatter interferometry (PSI) land movement measurement equipment to monitor land movement at tide gauge stations along the British coastline. The CGPS and AG land movement estimates confirmed continuing rising GIA levels of 1 to 2 mm a^{-1} in Scotland, whilst southern England experienced subsidence rates of up to 1.2 mm a^{-1} (Bingley *et al.*, 2007). In areas where CGPS tide gauges are stationed Bradley *et al.*'s (2009) CGPS contour map of vertical rates over the UK region agrees with Bingley *et al.*'s (2007) conclusions.

Woodworth and Jarvis (1991) suggested a method called the Master Station approach, using a tide gauge-GPS system at one site to correct land movement at nearby tide gauge stations (Woodworth *et al.*, 1999). This technique can be used to correct short time series in close proximity to the Master Station where similar cyclical trends occur and can be used to construct localised datasets from several different sites with overlapping timescales (Woodworth *et al.*, 1999).

Tide gauges with continuous GPS recordings are the ideal records for sea level trend analysis. Only 16 out of 130 CGPS stations in the UK that Bradley *et al.* (2009) analysed were accurate enough for vertical sea level measurement. Bradley *et al.* (2009) constructed four separate GIA models applied to the UK (Figure 2.26). These four models explain in greater details some aspects that are involved in constructing an accurate regional GIA model.

As well as glaciers and ice caps, land-stored water in ground-reservoirs, lakes and rivers limit the potential water mass in the oceans (Dyer, 1997). Chao *et al.* (2008) calculated the global levels of water impoundment between 1900 and 2007 and concluded that water impoundment in reservoirs, including seepage, had increased significantly in that time period. This equates to present day global sea levels being 30 mm lower than if the impounded water had been allowed to enter the oceans since 1900 (Chao *et al.*, 2008). Wada *et al.* (2010) suggest that Chao *et al.* (2008) do not take into account groundwater depletion due to groundwater abstraction. Groundwater abstraction has increased since 1900, thereby contributing more water to the oceans and partially compensating for water impoundment. However, groundwater abstraction can cause localised subsidence, which would cause further sea level change problems in coastal areas (Wada *et al.*, 2010).

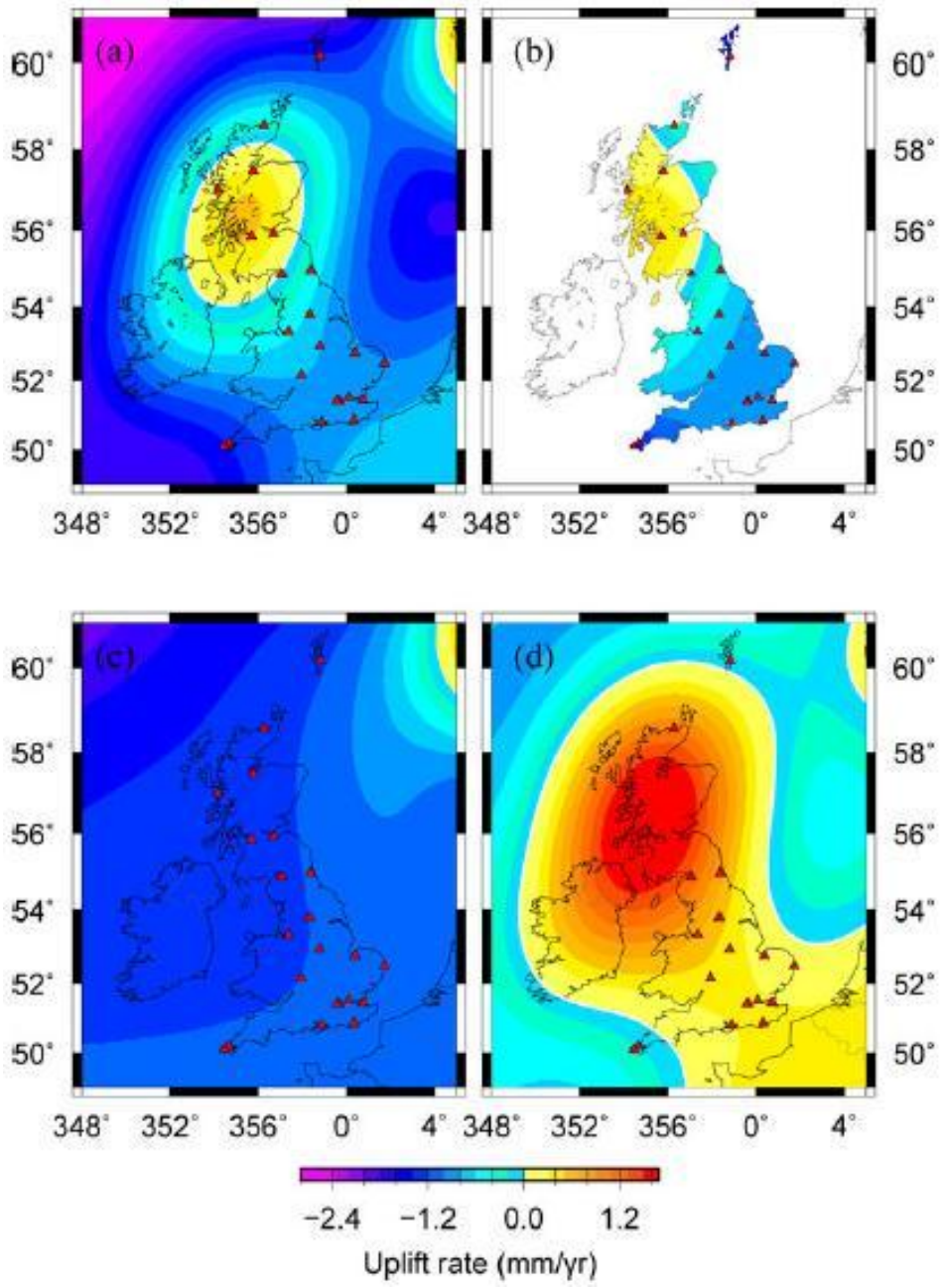

Figure 2.26. (a) Predictions of uplift rate on a 5 km by 5 km grid for the reference ice model and an Earth viscosity model that, when combined with the reference ice model, provides a good fit to the regional sea-level data base (Shennan *et al.* 2006b). This model adopts a 71 km lithosphere thickness, and a upper and lower mantle viscosity of 5 × 1020 Pa s and 1 × 1022 Pa s, respectively. The large positive uplift rates shown in the top right of the frame are associated with the deglaciation of the Fennoscandian component of the adopted ice model, i.e. the influence of ice melt from the neighbouring Fennoscandian Ice Sheet. (b) Same as (a) except that predicted velocity field sampled only at GPS site locations. (c) Component of total predicted signal (a) associated with non-local ice sheet loading. (d) Component of total predicted signal (a) associated with local (British–Irish) ice sheet and ocean loading (Bradley *et al.*, 2009:17).

In summary, on a global-scale where it is impossible to use geological databases to model GIA, global GIA models such as ICE-4G are available. Upland areas should be analysed with caution, as errors have been found in the Scottish upland area of the ICE-4G model. There is evidence of GIA still occurring in Scotland, illustrated in the Shennan *et al.* (2009) paper. On a UK scale the Shennan *et al.* (2009) GIA map from geological data can be used. Future global sea level projections should take water impoundment (Chao *et al.*, 2008) and groundwater depletion (Wada *et al.*, 2010) into account.

2.9 Sea Level Projection and Predictions

The inception of recording tide gauges led to deeper investigation of tidal movement and ultimately tidal harmonics. Harmonic analysis of tides is still an important prediction method of regular tidal cycles. There are eleven primary tidal constituents that measure over 0.03 m in amplitude relative to the location (Phillips, 2009). Each named constituent's cycle period and coefficient ratio are listed in Table A2.1 (Appendix).

Each constituent discussed in this section has a shorter frequency than 365 days and lower tidal amplitude influence than the lunar semi-diurnal cycle, M_2. According to Woodworth *et al.* (1999), the most important tidal constituents for short prediction are the Q_1, O_1, P_1, k_1, N_2, M_2, S_2 and k_2 harmonics (fully named in Table A2.1, Appendix). 'Records as short as 29 days can be used to determine the ratio between the amplitude and phase of each constituent' (Maul *et al.*, 1996:100).

Lord Kelvin designed the first tidal machine for harmonic prediction in 1867. Tidal harmonics can be complicated to analyse if the complete collection of several hundred harmonics are used. The more tidal constituents used the more accurate the prediction will be and harmonics change considerably from site to site. Five tidal harmonic models are presented in Figure 2.27. Each time an additional constituent is added, the model becomes more complex and more accurate.

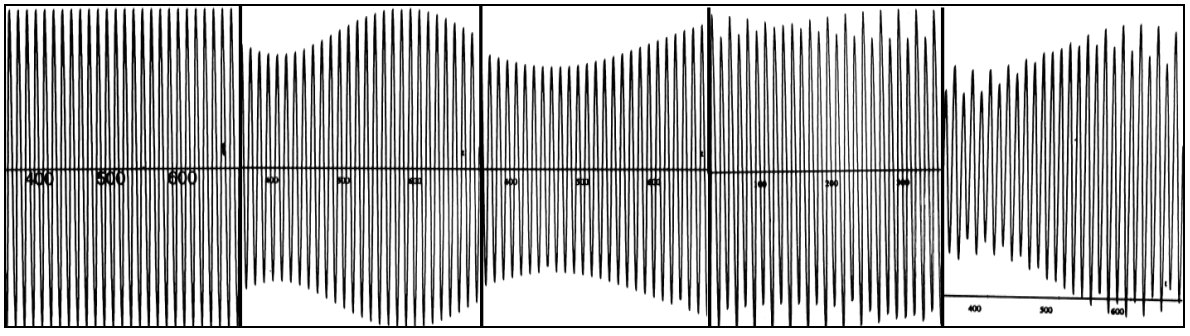

Figure 2.27. Examples of tide prediction using M_2, M_2+S_2, M_2+N_2, M_2+k_2, and a compilation of eleven tidal constituents for Bridgeport, USA (Phillips, 2009).

Sea level projection models are built to predict the future, but should be able to accurately represent the past environment as well. Most of the models discussed later in the chapter produced good projections of past sea levels. Some of the projection validation methods and potential errors are discussed here. To test the validity of the Hadley Centre's Ocean-Atmosphere General Circulation Model (GCM), Hadley Cell Climate Model 3 (HadCM3), Gregory *et al.* (2006) reviewed its projections of the past 500 years anthropogenic and natural forcings of climate change. Although the temperature projections were well reproduced, the global sea level prior to the past few decades did not follow observed estimates. The suspected reasoning behind this is the late installation of the anthropogenic acceleration of sea level rise.

Jevrejeva *et al.* (2009) constructed a delayed response statistical model to replicate sea level variability from the past millennia, specifically in relation to anthropogenic and natural forcings. Their findings suggested that prior to 1800 volcanic and solar radiation were the main drivers of sea level change. Since then 14 ± 1.5 cm (75%) of global sea level rise has been due to anthropogenic forcings and 4 ± 1.5 cm (25%) has been due to natural forcings (Jevrejeva *et al.*, 2009).

Lombard *et al.* (2009) constructed a global eddy-admitting ocean/sea-ice simulation based on the Nucleus for European Models of the Oceans code at ¼° resolution. This simulation, performed by the DRAKKAR project, ran over the time period 1958 to 2004, allowing the daily atmospheric forcings to be used in the spatial patterns analysis of sea level change between 1993 and 2001 (Lombard *et al.*, 2009). The simulation does not assimilate data, but produces accurate regional sea level trend patterns compared to satellite altimetry data. The simulations were compared against a second model, MERCATOR, which uses a shorter integration length and ultimately produces less accurate results (Lombard *et al.*, 2009).

Twenty-first century sea level models should, in best practice, be constructed from sea level datasets holding more than fifteen years of data, although thirty years and over are needed to determine secular sea level trends with 0.5 mm a^{-1} standard error (Woodworth *et al.*, 1999). Fifty years are needed for a standard error of 0.3 mm a^{-1}, due to interannual to multi-decadal variability of sea level (Woodworth *et al.*, 1999). Maul *et al.* (1996) recognised the 18.6 year lunar nodal cycle and suggested that nineteen years of data are needed to register this trend. The IPCC suggested fifty years of data are needed to create reliable sea level scenarios, although their Fourth Assessment Report refers to global tide gauge data between 1961 and 1990 (29 years) (Houghton *et al.*, 2001).

The maximum modelled level of potential sea level rise in the twenty-first century varies considerably between studies. The IPCC predictions have changed noticeably from the initial publication of the IPCC First Assessment Report in 1990 to the Fourth Assessment Report in 2007 due to improvements in data availability and the computing power (Solomon *et al.*, 2007). The

present predictions by the IPCC are more conservative than previous modelled results, for which they have been criticised (Masters, 2010; Vermeer and Rahmstorf, 2009) (Figure 2.28).

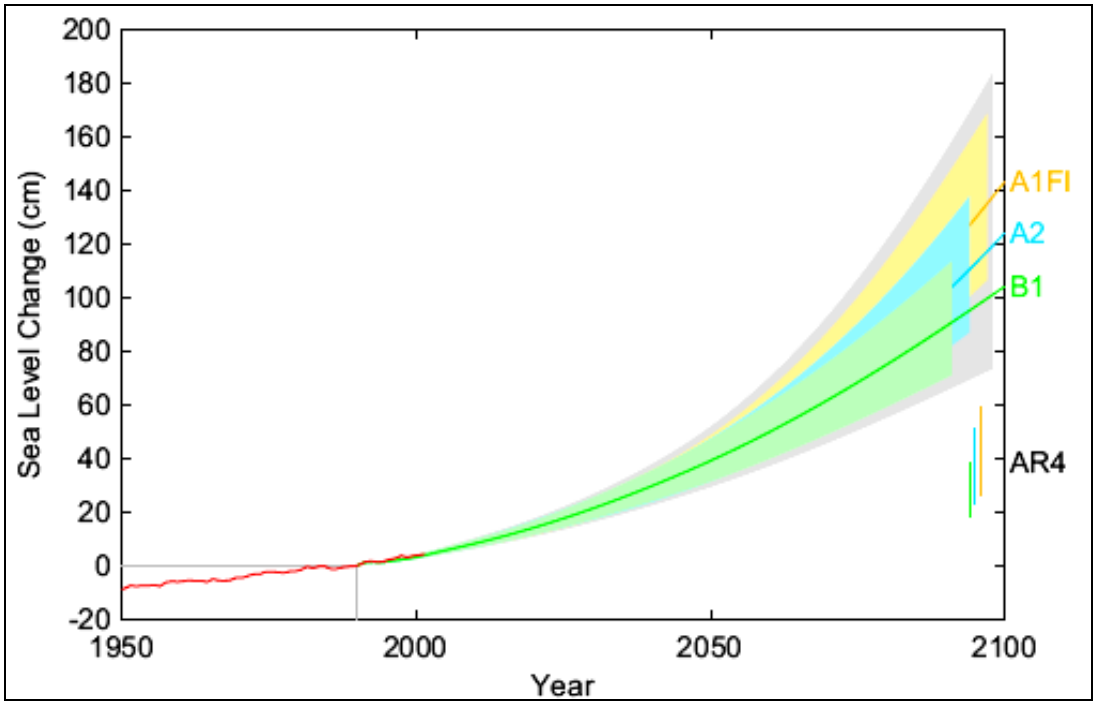

Figure 2.28. 'Projection of sea-level rise from 1990 to 2100, based on IPCC temperature projections for three different emission scenarios (labeled on right, see Projections of Future Sea Level for explanation of uncertainty ranges). The sea-level range projected in the IPCC AR4 (2) for these scenarios is shown for comparison in the bars on the bottom right. Also shown is the observations-based annual global sea-level data (18) (red) including artificial reservoir correction' Vermeer and Rahmstorf (2009:21531).

A number of scientists believe that the IPCC scenarios do not adequately account for ice melt and other relationships. Masters (2010) investigated the Rahmstorf (2007), Pfeffer *et al.* (2008) and IPCC (Solomon *et al.*, 2007) predictions of future sea level (Figure 2.29). There are large variances between the predictions, depending on ice models and other climate change parameters.

The UK Climate Impact Programme 2002 (UKCIP02) uses some of the same UK Meteorological Office (UKMO) Unified Models (MetUM) as were used by the IPCC Third Assessment Report (TAR), as well as three of the IPCC TAR emission scenarios (Table 2.2 and Figure 2.30) (UKCIP, 2006). The UK Climate Projections 2009 (UKCP09) is an improved version of UKCIP02. The UKCP09 projections incorporate local interaction more comprehensively than IPCC AR4 (Jenkins et al., 2007).

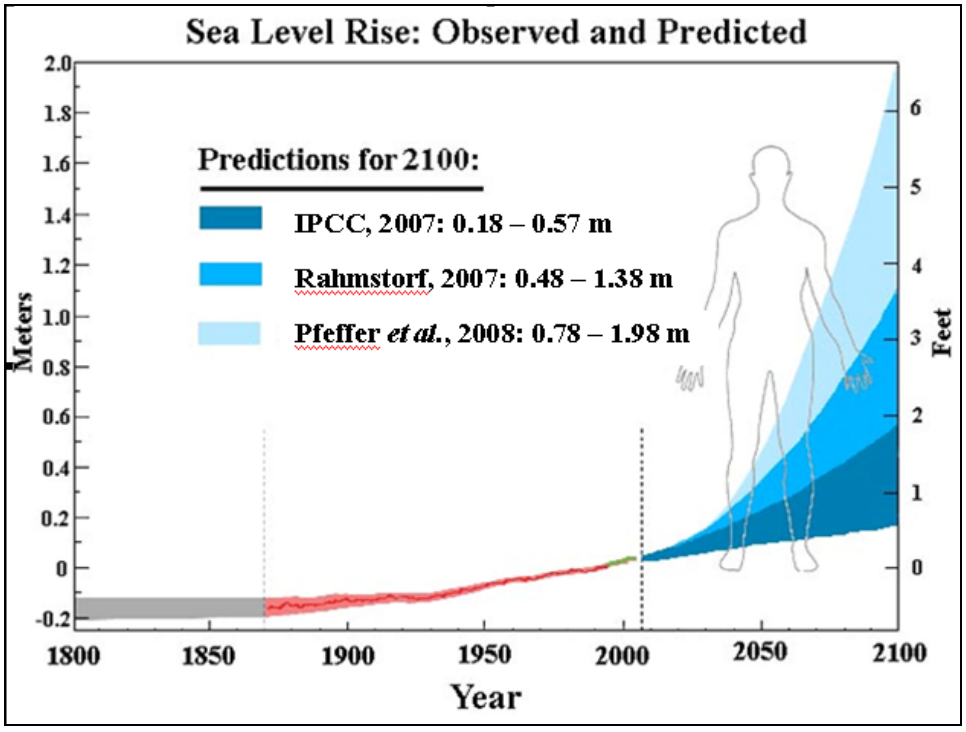

Figure 2.29. 'Observed global sea level from tide gauges (red line, pink colour is the uncertainty range) and satellite measurements (green line), with forecasts for the future. The blue colours show the range of projections for three different forecasts (the forecasts overlap, but this overlap is not shown). Image modified from U.S. EPA,' Masters (2010).

UKCIP provide an online user interface to help planners and academics construct graphs of regional or specific parameter output from UKCP09 (UKCIP, 2010; DEFRA, 2011a). This tool allows users to select numerous timescales and emissions scenarios for application with numerous climate change parameters and allows GIA corrections from Bradley *et al.* (2009). Passing the decision making aspect of scenario building to users allows selective use of emissions scenarios and potential for misuse of the extreme scenarios. UKCP09 projected the high, medium and low emission scenarios central estimates of relative sea level rise for the four capital cities in the UK (Table 2.3). Across the scenarios the 2100 relative sea level range was 23.4 to 53.1 cm (DEFRA, 2011a).

	Regional Isostatic Uplift (+ve) or Subsidence (-ve) (mm/yr)	Net Sea-level Change (cm) Relative to 1961-1990					
		Low Emissions 'Low' IPCC Estimate			High Emissions 'High' IPCC Estimate		
		2020s	2050s	2080s	2020s	2050s	2080s
London	-0.8	8	13	17	18	42	77
Scotland	0.8	0	1	0	10	30	60
Wales	-0.5	6	11	14	16	40	74

Table 2.2. Vertical land movement due to isostatic adjustment for the administrative regions of England and the devolved administrations of Wales and Scotland [Source: estimate from Shennan and Horton, 2002] and predicted relative sea-level change for the 2020s, 2050s and 2080s based on the UKCIP02 Low Emissions and High Emissions Scenarios (UKCIP, 2006).

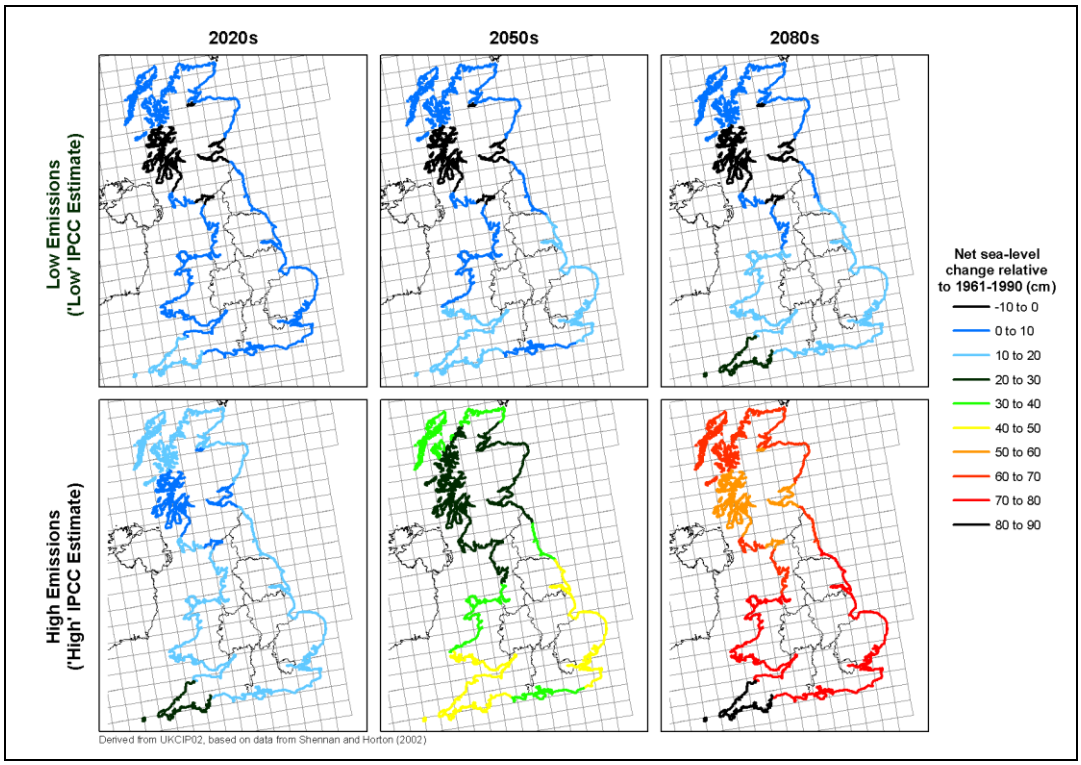

Figure 2.30. Predictions of sea level change based on Shennan and Horton (2002) and adapted by UKCIP (2006).

	London			Cardiff			Edinburgh			Belfast		
	High	**Med**	**Low**	**High**	**Med**	**Low**	**High**	**Med**	**Low**	**High**	**Med**	**Low**
2000	3.5	3.0	2.5	3.5	2.9	2.5	2.2	1.6	1.2	2.3	1.7	1.3
2010	7.3	6.2	5.3	7.3	6.2	5.3	4.7	3.5	2.6	4.9	3.8	2.8
2020	11.5	9.7	8.2	11.5	9.7	8.2	7.5	5.7	4.3	7.8	6.0	4.6
2030	16.0	13.5	11.4	15.9	13.4	11.4	10.7	8.2	6.1	11.1	8.6	6.6
2040	20.8	17.5	14.8	20.8	17.5	14.8	14.2	10.9	8.2	14.7	11.4	8.7
2050	25.8	21.8	18.4	25.9	21.8	18.4	18.0	13.9	10.5	18.6	14.5	11.1
2060	31.4	26.3	22.2	31.4	26.3	22.2	22.1	17.1	13.0	22.9	17.8	13.7
2070	37.2	31.2	26.3	37.1	31.1	26.3	26.6	20.6	15.7	27.4	21.4	16.5
2080	43.3	36.3	30.5	43.3	36.2	30.5	31.4	24.4	18.6	32.3	25.3	19.6
2090	49.7	41.6	35.0	49.7	41.6	35.0	36.5	28.4	21.8	37.6	29.4	22.8
2095	53.1	44.4	37.3	53.1	44.4	37.3	39.2	30.5	23.4	40.3	31.6	24.5

Table 2.3. Central estimates for each decade of relative sea level change (cm) with respect to 1990 levels (DEFRA, 2011a).

An inverse statistical model was used by Jevrejeva *et al.* (2010:1) to 'examine potential response in sea level to changes in natural and anthropogenic forcings by 2100'. Six of the IPCC Special Report on Emissiosn Scenarios (SRES) emission scenarios were used to project global sea level rise of between 0.6 and 1.6 m (0.59 and 1.8 m within confidence limits) (Jevrejeva *et al.*, 2010). Natural forcings were calculated to be responsible for up to 5% of global sea level rise.

> '*As alternatives to the IPCC projections, even the most intense century of volcanic forcing from the past 1000 years would result in 10 to 15 cm potential reduction of sea level rise. Stratospheric injections of SO_2 equivalent to a Pinatubo eruption every 4 years would effectively just delay sea level rise by 12 to 20 years. A twenty-first century with the lowest level of solar irradiance over the last 9,300 years results in negligible difference to sea level rise forcings by 2100. With six IPCC radiative forcing scenarios we estimate sea level rise of 0.6 to 1.6 m, with confidence limits of 0.59 m and 1.8 m. Projected impacts of solar and volcanic radiative forcings account only for, at maximum, 5% of total sea level rise, with anthropogenic greenhouse gases being the dominant forcing*,' (Jevrejeva *et al.*, 2010:1).

Grinsted *et al.* (2010) used a four parameter linear response equation to link global temperature and sea level between 200 and 2100 AD. The study used Monte Carlo inversion to estimate likelihood distributions of the equation parameters to visualise projected sea level scenarios. 'The model has good predictive power when calibrated on the pre-1990 period and validated against the high rates of sea level rise from the satellite altimetry,' (Grinsted *et al.*, 2010:461). Between 1990 and 2100

sea level is predicted to rise by between 0.9 and 1.3 m along the IPCC A1B scenario (Grinsted *et al.*, 2010).

The final example of a sea level projection model comes from Vermeer and Rahmstorf (2009), who refined the simple global temperature-sea level relationship model that had been presented by Rahmstorf (2007). Their model relies on Goddard Institute for Space Science (GISS) global temperature data and Church and White (2006) data between 1880 and 2000 and is tested on data produced by a global climate model covering the past millennia and the twenty-first century (Vermeer and Rahmstorf, 2009). Hindcast comparison with global sea level data between 1880 and 2000 indicates as correlation of over 0.99. Vermeer and Rahmstorf (2009) used the IPCC emission scenarios global temperature statistics to calculate sea level rise between 1990 and 2100, suggesting a global sea level rise range of between 0.75 and 1.9 m.

The twenty-first century sea level projections made by Rahmstorf (2007), Vermeer and Rahmstorf (2009), Grinsted *et al.* (2010) and several others have been compared in Figure 2.31. A significant variance can be seen between them, due to the range of input parameters and cycle accuracy applied.

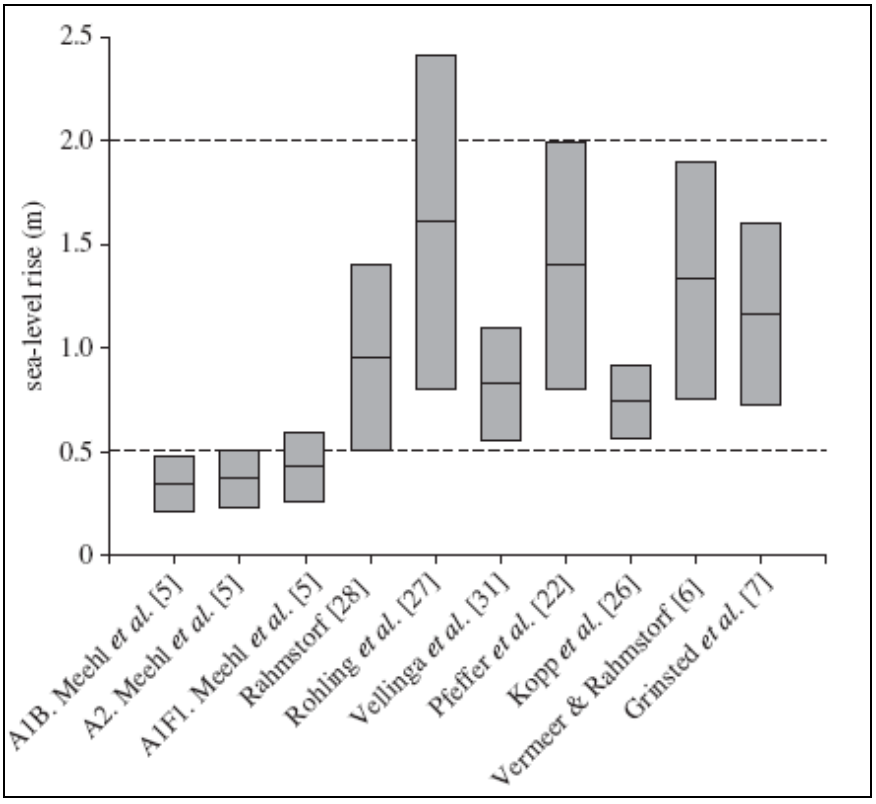

Figure 2.31. 'A graphical summary of the range of IPCC AR4 [5] sea-level-rise scenarios (for 2090-2099) and post-AR4 projections possible in a 4◦C world. The dotted lines represent the minimum (0.5 m) and maximum (2.0 m) bounds considered in terms of impacts' in the Nicholls *et al.* (2011:164) study. Additional sources include Meehl *et al.* (2007), Rahmstorf (2007), Rohling *et al.* (2008), Vellinga *et al.*

(2008), Pfeffer *et al.* (2008), Kopp *et al.* (2009), Vermeer and Rahmstorf (2009) and Grinsted *et al.* (2010).

New tide gauge data are continuously becoming available as port authorities provide access to their data to research bodies for scientific research and as researchers themselves install their own gauges. As data correction and modelling techniques become more sophisticated scientific predictions hope to become more accurate. The main discrepancy across modelling techniques lies with the glacio-eustatic input from ice cap and glacier meltwater (Solomon *et al.*, 2007; Pfeffer *et al.*, 2008). Presently the IPCC models are commonly referred to. The next report, IPCC Fifth Assessment Report, is due for publication in 2014.

In summary, IPCC and UKCIP results suggest 2100 sea levels are not likely to reach 1 m above the 1990 level. This is contrary to a large number of studies that suggest sea level rise may be between 1 and 2 m (Grinsted *et al.*, 2010; Vermeer and Rahmstorf, 2009).

2.10 Conclusions

Climate change induced sea level change will impact on a large percentage of the global population by potentially causing damage to their infrastructure, agriculture, health and local environment (De la Vega-Leinert and Nicholls, 2008). In the UK government has responded by attempting to reduce climate change contributions through legislative means and constructing defence structures along the coastline. Various soft and hard engineering techniques have been recommended over time, but a site-by-site approach is necessary to ensure structures are robust enough in high energy areas and aesthetically appropriate in locations with landscape sensitivities.

Ocean mechanics, including waves and tides, are the most visible of all oscillations in sea level. Short-frequency, surface waves driven by wind can be generated over long or short fetches and can vary significantly in amplitude (French, 2001). Tides are fixed-period waves influenced by astronomical cycles and adequately calculated by harmonic analysis. The M^2 and S^2 harmonics are dominant with other short-frequency waves interacting to form the natural tidal curve (Chowdhury *et al.*, 2008).

Sea level is influenced by numerous oscillations, those with frequencies less than 210 years are detectable in tide gauge data (Singer and Avery, 2008). Due to the temporal limitations of most sea level records only the 1 to 30 year oscillations would be detectable. Several studies have used sea level record of 15 years or shorter to predict twenty-first century sea level (Rennie and Hanson, 2010), which are inaccurate due to the studies not acknowledging longer cycles such as NAO and

AO cycles and their resultant levels in their calculations. For more accurate prediction rates, 30 years of historic sea level data must be used.

Global sea level and temperature have been rising at an increased rate since 1800 AD (Mortari, 2004). Various studies have compiled global sea level datasets to calculate the global sea level trend (Solomon *et al.*, 2007; Flather *et al.*, 2001). The average calculated global sea level rise is 18 to 19 cm between 1900 and 2000 (Solomon *et al.*, 2007; Jevrejeva *et al.*, 2008). The main contributors to sea level change are thermal expansion of the oceans and water mass increase due to land-ice melt. The average observed rates of global sea level are ~1.8 mm a^{-1} between 1900 and 2000 (from tide gauge data) and 3.1 mm a^{-1} since 1993 (from satellite altimetry data) (Solomon *et al.*, 2007). Although tide gauge data indicate a short-term increase since 1993, there are uncertainties as to the reliability of comparing long-term tide gauge data with satellite altimetry data, in addition to the unreliability of using data since 1993 due to resultant fragmentation of the NAO and AO 30 year cycles.

Estuaries and shallow coastal areas change the nature of open ocean waves by introducing seabed friction and space limitation. Each estuary must be analysed individually due to the unique nature of estuarine parameters (van Rijn, 1990). The M_2 tide harmonic is overtaken by the shorter frequency M_4, M_6 and M_8 harmonics, which change the tidal nature in an estuary (Kjerve, 1988, Bearman, 1999, Camuffo, 1999). Bathymetric variation and sedimentary obstacles reduce wave energy with convergence producing tidal bores in some funnel-shaped estuaries (Besley *et al.*, 2009; Webb and Metcalfe, 1987).

In the UK, glacio-isostasy has produced wide variations in land movement with parts of Scotland experiencing land emergence and parts of southern England experiencing land submergence (Shennan *et al.*, 2009). Various models have been produced to calculate global GIA levels (Bradley *et al.*, 2009; Nakada and Inoue, 2005). Shennan *et al.* (2009) produced a basic glacio-isostasy map from a compilation of carbon-dating studies. Although Shennan *et al.*'s (2009) work features some data referencing issues, the compiled geological data are considered accurate across most parts of the UK.

Estuaries that stretch deep inland can experience variable rates of glacio-isostatic movement. In Scotland, several estuaries stretch 50 km or more inland. Over that distance, isostatic rebound can vary by up to 0.5 mm a^{-1} (Shennan *et al.*, 2009). The Forth Estuary, for example, currently experiences 1.3 mm a^{-1} of GIA at the estuary head and 1.0 mm a^{-1} at the mouth (Shennan *et al.*, 2009).

Tsunami are not common in UK waters, but other long-period single event waves, including storm surges, threaten damage to property and infrastructure. Storm surges of over 1 m have occurred

along the UK coastline in the past. Various models have been produced to predict surge events over the short-term using tide gauge warning systems (Flather *et al.*, 2001; Dixon and Tawn, 1994). Basic maxima studies have identified increasing maxima levels, although most of the datasets are of less than 30 years (Graff, 1981).

Various sea level measurement and modelling techniques are available. The most revered sea level models are the IPCC Fourth Assessment Report (Solomon *et al.*, 2007) and the UKCP09 Projections (Jenkins et al., 2007). The UKCP09 user interface allows regional analyses of sea level predictions with GIA corrections. Simplistic global models have been constructed by several models to correct the IPCC land-ice rates, which are considered too conservative. Vermeer and Rahmstorf (2009) instead modelled the sea level change using the relationship between temperature and sea level. As seen in Figure 2.24, comparison between the IPCC (Solomon *et al.*, 2007), Pfeffer *et al.* (2008) and the first version of Rahmstorf's (2007) model, there are large differences depending on the land-ice melt predicted. The work of Vermeer and Rahmstorf (2009) is discussed further in Chapter 8.

Tide gauge data are assets essential to understanding historic and future sea level changes. Additional information regarding sea level variation around the UK coast could benefit future studies. Investigation into pressure anomaly oscillations and their influence on sea level height around the UK would improve tidal prediction.

Chapter 3 – The Estuaries

3.1 Introduction

The Forth and Tay Estuaries are situated on the east coast of Scotland and share some physical characteristics. This chapter is structured so as to present these shared characteristics before focusing on the estuaries separately. Within this first section the focus is principally on the large scale geological, geomorphological, generic tidal information, palaeo-historical and historical events. Later in the chapter the focus turns to variations in the tidal and sediment dynamics throughout the estuaries, as well as modern port infrastructure and conservation status.

Both estuaries are tidally-dominant, macrotidal, funnel-shaped estuaries with a large mouth, although the Tay has a smaller mouth than that of the Forth Estuary (Jenkins *et al.*, 2002). The estuaries lie in the Midland Valley of Scotland between the Highland Boundary Fault and the Southern Upland Fault (Hansom and McGlashan, 2005; Armstrong *et al.*, 1985; Buller and McManus, 1971).

During the Devensian glacial period, 100,000 years BP to 12,000 years BP, large parts of Scotland were covered by ice; estimated to have been between 1,000 and 2,000 m thick, depending on the ice cap characteristics (Sissons, 1967; Boulton and Hagdorn, 2006). Once the ice melted, the land rebounded before slowing to its present day rate (Firth and Stewart, 2000). Figure 3.1 highlights the land movement within the upper, middle and lower Forth Estuary from 12,000 BP to 4,000 BP (Smith *et al.*, 2010). This figure relies on records of emergent features and illustrates fluctuations in the relative sea level trend due to decreasing glacio-isostatic uplift and glacio-eustatic sea level rise (Firth and Stewart, 2000). Locally, the estuaries have been studied at various locations for glacio-isostatic uplift as well as Holocene sea level change. Studies such as Sissons *et al.* (1966) and Smith *et al.* (2010) outlined the evidence uplift of the Forth and Tay Estuaries shoreline by mapping the uplift of raised beaches along the coast by at least 34 m above the present day shoreline in the inner estuary.

Areas of Scotland are experiencing continued glacio-isostatic uplift, including the Forth and Tay Estuaries (Shennan *et al.*, 2009). Glacio-isostatic uplift rates at Perth and Montrose are 1.2 mm a^{-1} and 1.0 mm a^{-1}, respectively (Shennan *et al.*, 2009), and 1.07 ± 0.35 mm a^{-1} at Leith (UKCIP, 2006), 1.0 mm a^{-1} at Dunbar and 1.3 mm a^{-1} at Stirling (Shennan *et al.*, 2009). Localised uplift and block uplift (in comparison with differential tilting) do occur (Firth and Stewart, 2000), but are not known to cause significant sudden changes in land movement rates over the course of the Tay or Forth Estuaries with only 0.1 mm a^{-1} to 0.2 mm a^{-1} of glacio-isostatic adjustment (GIA) variance

calculated (Shennan *et al.*, 2009). These uplift rates compensate for a percentage of the eustatic sea level rise that has occurred over the past 100 years around the British coastline (Chapter 2).

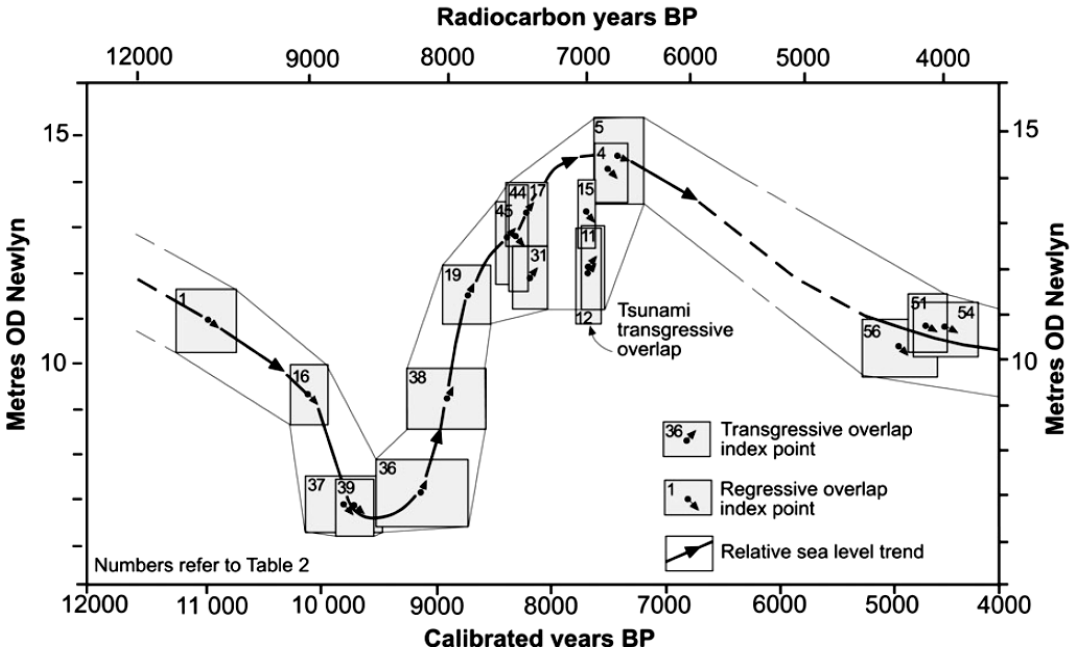

Figure 3.1. Forth Holocene sea level curve for the Forth Valley at Wester Flanders Moss (Smith *et al.*, 2010:2399).

3.2 The Tay Estuary

The Tay Estuary, also known as the Firth of Tay, is the shorter of the two estuaries studied in this thesis at 50 km in length from tidal limit in the west to the mouth in the east. Perth lies at the head of the estuary and Buddon Ness (north) and Tentsmuir Point (south) lie at the estuary mouth (Figure 3.2). From river source to mouth, the Tay is the longest river in Scotland at 193 km with a drainage basin covering *c.*6,500 km^2 (McManus, 1985; Buller *et al.*, 1971). The main tributaries of the Tay include the Earn, Almond, Isla, Braan, Tummel and Lyon (Figure 3.3). All but the Earn join the Tay before reaching the Perth Gap at the estuary head. The Earn joins the estuary on the south bank along its upper reaches (McManus, 1998).

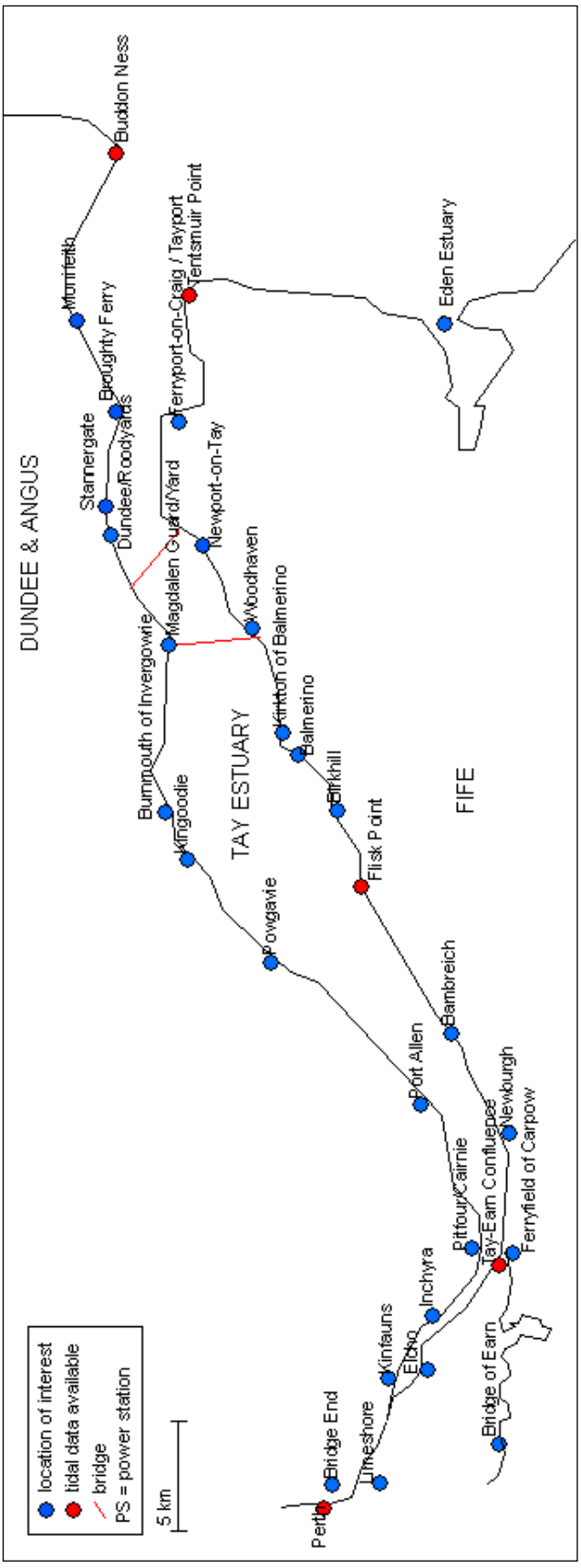

Figure 3.2. Map of the Tay Estuary.

The Tay Estuary has a spring tidal range of 5.0 m, neap tidal range of 2.5 m and an equinoctial tidal range of 6.0 m (McManus, 1998). It has previously been studied for various characteristics involving its sediment dynamics, estuarial currents, tidal influences and biology. Investigations within the estuary have used remote sensing and sonar mapping techniques (Buller and McManus, 1975; Charlton *et al.*, 1975; Khayrallah and Jones, 1975; Anderson, 1989).

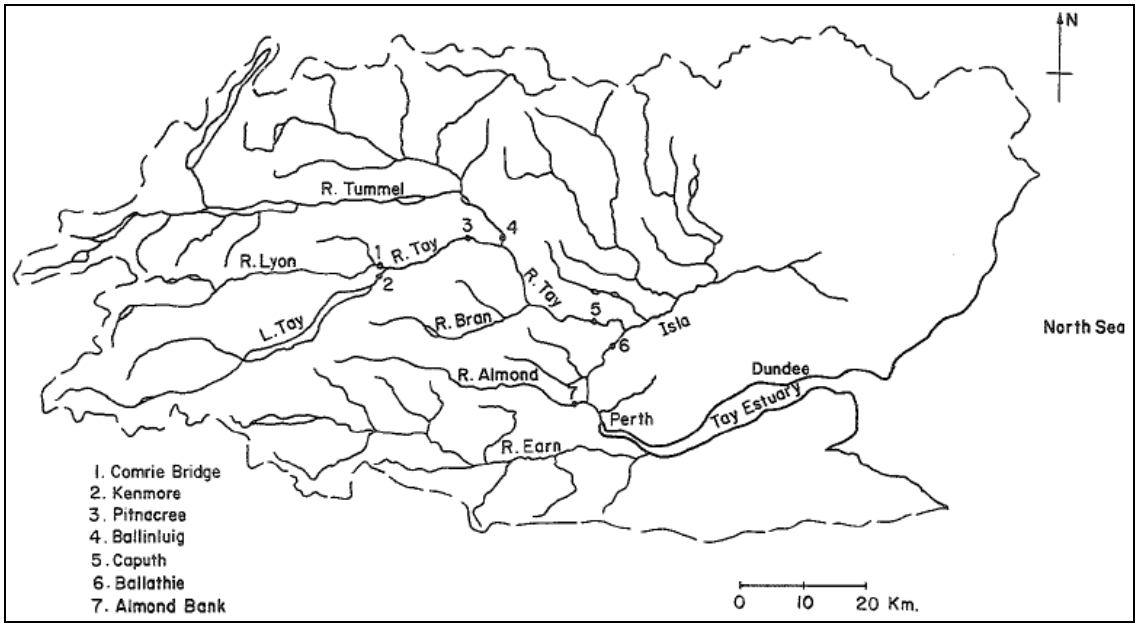

Figure 3.3. The Tay catchment (Al-Jabbari *et al.*, 1978:18). The numbers refer to the locations of gauging stations.

To understand the morphology of the Tay Estuary, background information has been collected focusing on local geology, sea level history, tidal forcings, currents and sediment dynamics. The estuary has several settlements along its coast, which, as with the majority of the coast, could be affected by rising sea levels.

3.2.1 Geology and Geomorphology

The Tay Estuary lies along the axis of the Sidlaw Ochil Anticline in the Midland Valley (Hansom and McGlashan, 2005; Armstrong *et al.*, 1985; Buller and McManus, 1971). The Carse of Gowrie is located along the northern shore, between the Sidlaw Hills and the estuary, with the Ochil Hills trending along the Fife coast (Figure 3.4). The coastline is dominated by red sandstone and andesite lava bedrock of Lower Devonian age (Armstrong *et al.*, 1985) (Figure 3.4).

At the beginning of the Flandrian Transgression the Tay Estuary was a deep drowned river valley, which intermittently shallowed over thousands of years as sea level fell (Sissons, 1967; Dyer, 1997). Ice that had covered the whole area left behind a layer of glacial till over the Old Red

Sandstone (i.e. Devonian) outcrops after it melted. The hills were eroded smooth and the channel lay almost 60 m below today's sea level, but has since been naturally filled (McManus, 1970; Buller and McManus, 1971) (Figure 3.5).

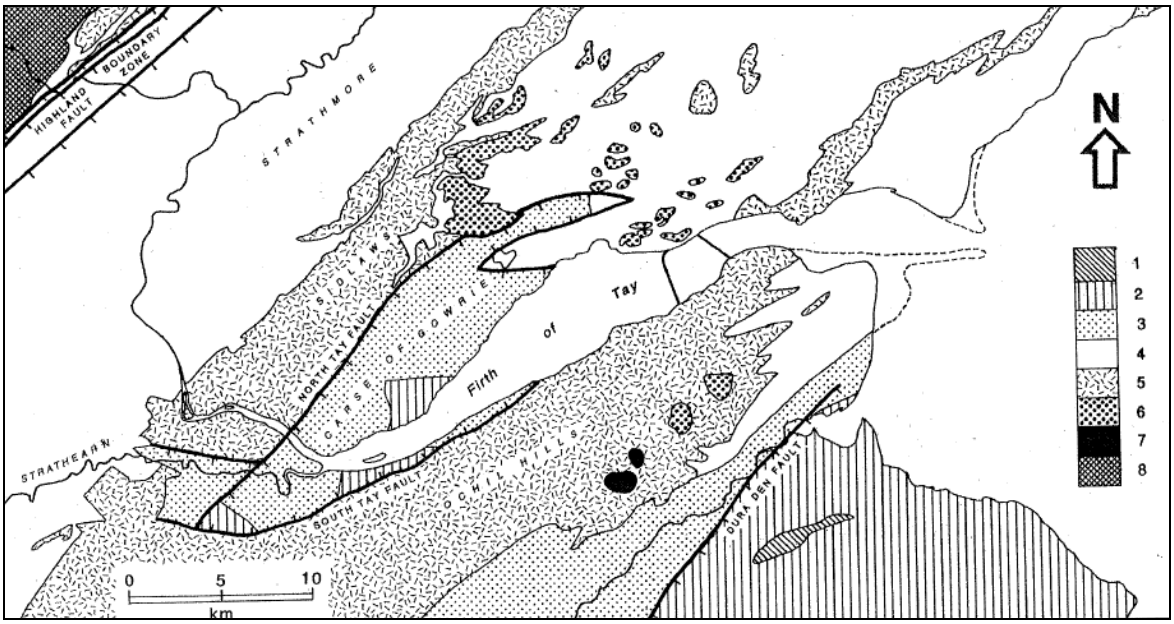

Figure 3.4. Solid geology of the Tay Estuary. Key: (1) Namurian (Carboniferous); (2) Dinantian (Carboniferous); (3) Upper Devonian; (4) Lower Devonian sedimentary rocks; (5) Lower Devonian lavas and volcanic conglomerates; (6) Lower Devonian intrusions; (7) possible vents; (8) Dalradian metamorphic rocks. Bold lines denote faults, with ticks indicating the downthrow side (Armstrong *et al.*, 1985).

Post-glacial sea level fall is evident along the Tay Estuary coast where raised beaches still remain (Figure 3.6). Raised beaches are presently found along the south coast of the estuary, evident between Tayport and the Tay Road Bridge with evidence of raised beaches and estuarine flats extending to the Carse of Gowrie, Perth. In the upper estuary the raised estuarine flats dominate the area. These beaches are also present along the north coast parallel to those on the south. However, along the coast at Dundee, major landscaping works and development schemes have either remodelled the topography or partially hidden these features from view.

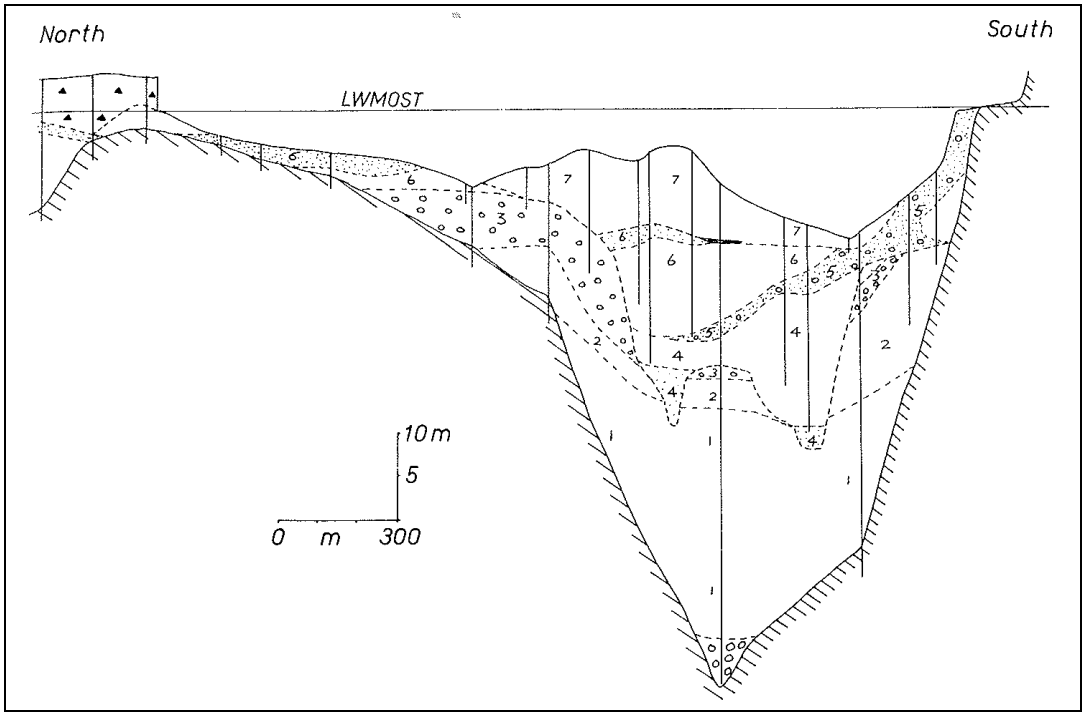

Figure 3.5. Geological section along the Tay Road Bridge at Dundee (Buller and McManus, 1971:229). "Vertical lines represent boreholes; diagonal lines: bedrock; dashed lined: lithological boundaries and erosional surfaces; open circles: cobbles; dots: sandy gravels; solid black: peat; black triangles: artificial fill; blank: fine sediments (sand, silt and clay). Stratigraphy: Basal boulder bed is the lodgement till of the Aberdeen-Lammermuir Ice. 1: ablation tills of the retreating Aberdeen-Lammermuir Ice; 2 and 3: deposits of the Perth re-advance; 4: fill of the first post-glacial estuary; 5: gravels of the Flandrian transgression (approx. 6,000 B.P.); 6: fill of the second estuary culminating with peat (approx. 5,500 B.P.); 7: modern sands. LWMOST = low water mark of spring tides".

Figure 3.6. Raised beaches along the coastline between Tayport and Newport-on-Tay (courtesy of Professor R. Duck and Christie, 1980).

3.2.2 Historical Background

Historically, two large settlements have been located along the Tay Estuary since before the Medieval Period. The City of Dundee, located on the northern coast near the estuary mouth, was founded as a seaport (McKean *et al.*, 2009). Perth, located at the head of the estuary, was a powerful city as Dundee began to develop as a seaport. In the Medieval Period, Perth was established as the county town; it was the resident city of the Scottish Monarchy and is referred to as the Fair City of Perth (Bellenden, 1822). The two cities rivalled about rights to moor along the river, which could have destroyed the Dundee industries if Perth had successfully fought for rights along the river's entire length (Bellenden, 1822). Since then Perth has lost its city status and Dundee has become the prominent settlement along the Tay Estuary.

Dundee lies on the north bank, opposite Newport-on-Tay and Wormit where both the Tay Railway Bridge and the Tay Road Bridge presently cross the estuary. The estuary at Dundee formed a natural harbour, which was in use during the Medieval Period. Shipping orientated around Castle Rock, where St. Paul's Cathedral is located today in Dundee City Centre (Graham, 1979). The Dundee City records were destroyed in 1547 during the English occupation, which included all the historical information about port and harbour use for hundreds of years (Graham, 1979). However, trade information can be derived from external records, highlighting wine trade between Bordeaux and Forfar through the Port of Dundee during this period (Graham, 1979).

Dundee's waterfront has regularly been advanced or remodelled since the fifteenth century through land claim, dock development and waterfront regeneration (Figure 3.7 and Figure 3.8). The harbour suffered from structural failures and weaknesses before the eighteenth century when wooden bulwarks, piers and defensive structures were common (Graham, 1979).

Development of the large wet docks began after 1814 when several docks were designed by Robert Stevenson of Edinburgh and Thomas Telford. These included the King William IV Dock and Earl Grey Dock (Graham, 1979), which have since been infilled during the construction of the land fall of the Tay Road Bridge. The two surviving wet docks, Victoria Dock and Camperdown Dock, are no longer used for the purpose they were built for in the mid-nineteenth century (Section 3.2.2). All of these docks were essential for the Jute industry that flourished in Dundee, importing raw materials through the port.

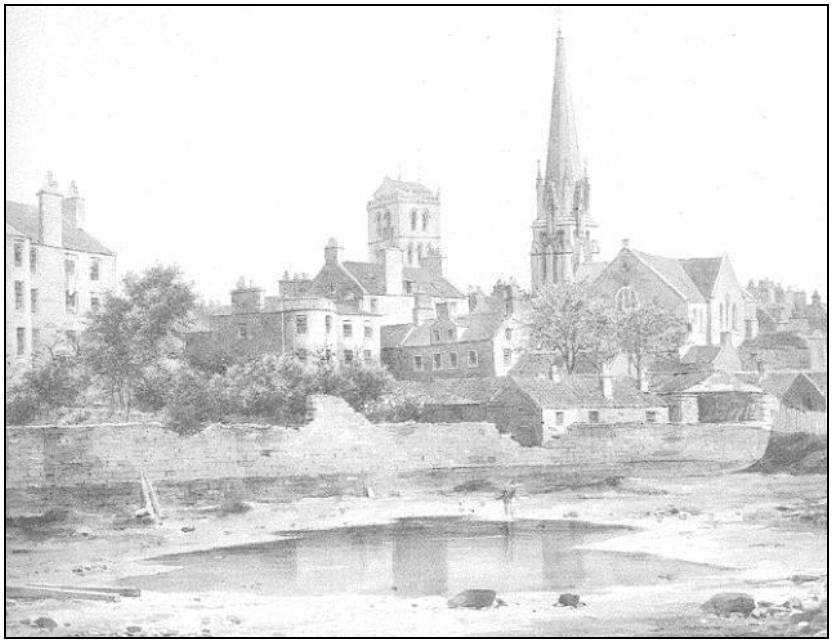

Figure 3.7. Image of the city's edge against the old seawall captured from the railway causeway in the early 1850s. This image emphasises the condition of the intermediate land (McKean and Whatley, 2010). A similar image of the Arbroath railway depicted the railway causeway, 7 m above low tide, with the sea to the right and the inland areas to the left, described as 'foetid lagoons' (Whatley *et al.*, 2011; Plate 38).

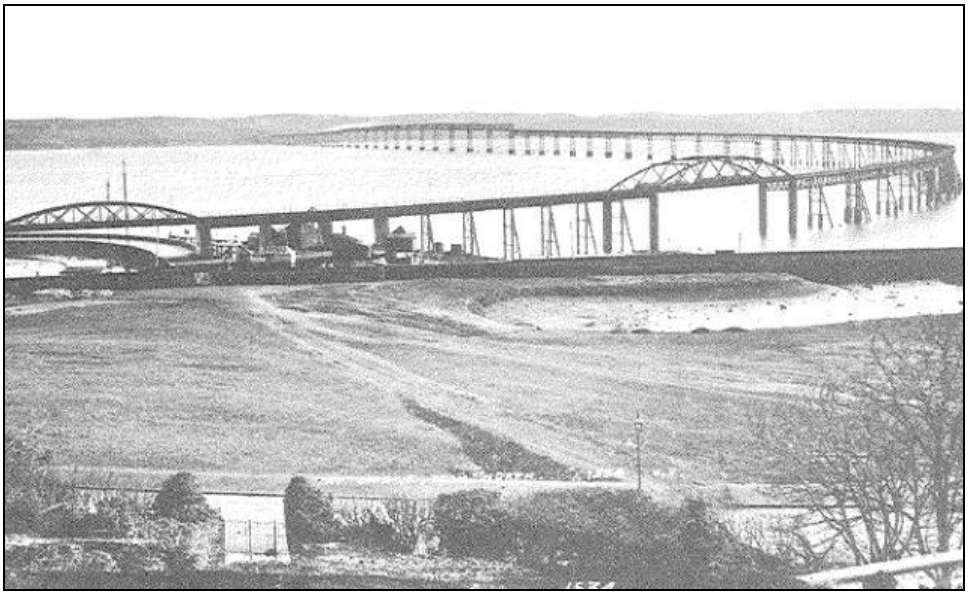

Figure 3.8. Photograph of the first Tay Rail Bridge, built in June 1878 and collapsed in December 1879. A remnant of the former Magdalen Green beach is in the foreground, cut off from the Tay (Whatley *et al.*, 2011).

During the last three centuries, development along the estuary has included several land claim ventures for agricultural, housing and shipping operation expansion. Two examples of land claim in

the Tay include the coastline at Pitfour, near the Earn confluence, and a large amount of land along the Dundee waterfront (Richardson, 1839). Pitfour is an agricultural area with a low population opposite the Earn confluence, where the estuary narrows upstream. Between 1826 and 1833 two embankments were erected to enclose 0.275 km^2 (27.5 ha) for agricultural use (Richardson, 1839). This land continues to be used for agricultural purposes up to the present day.

The Dundee waterfront has migrated seaward through land claim projects over hundreds of years. One particular realignment scheme along this coastline was analysed by Cunningham (1887) a few years afterwards to assess the impact that it had had on the estuary. This realignment involved the continued construction of the docks, railway works and a river training wall. Parts of the seawall lay 0.53 km further seaward than before the works, limiting the channel to 2.41 km in width, i.e. the land claim equalled approximately one-sixth of the previous channel width (Cunningham, 1887). This scheme aimed to promote faster currents to naturally relocate Middle Bank and Ballast Bank from their positions close to Dundee's expanding docklands. However, Ballast Bank shifted east from Magdalen Green to the area around the Port of Dundee (Table 3.1; Figure 3.2) (Cunningham, 1895).

Another large nineteenth century engineering project, which changed the estuary's morphology, focused on the extraction of large quantities of sediment from the channel between Newburgh and Perth. The dredging scheme was coordinated by 'Mr Stevenson of Edinburgh' in 1835 (Beardmore, 1862) to remove sediment including postglacial boulders, large quantities of sand and areas used as fords and salmon weirs (Beardmore, 1862). The previously natural, shallow channels in the inner estuary limited the potential use of Perth as a harbour for large shipping around this time of industrial development. The extraction of sediment increased customs at the harbour six fold between 1833 and 1844 (Beardmore, 1862).

Some of the excess dredged material was deposited onto Mugdrum Island near the Newburgh shore (Figure 3.2). The channel presently splits and flows around the island (McManus, 1985). After the 'improvements' to the upper Tay Estuary the time of spring high tide arrival at Perth was brought forward by 50 minutes (Table 3.2). In this case the spring tidal flood period has been shortened without increasing or decreasing the tidal height (Beardmore, 1862). However, in the intervening time, between the channel excavation in the upper estuary in 1835 and the Dundee waterfront expansion in 1887, the estuary had seen a sediment influx of 120 million cubic metres (Cunningham, 1887). It is not known whether this changed the high tide timing between Perth and Newburgh.

Location	Evidence of Sediment Movement
Chequer Buoy (near Dundee Harbour)	Sediment accumulation outside harbour area, possibly from Middle Bank
Middle Bank	Middle Bank measured 130 acres above LW in 1833 and disappeared by 1887. This produced better depths for harbour access on the south side of river
Ballast Bank	Ballast Bank moved 1½ miles downstream to partially position in front of Dundee Harbour
Birkhill Bank	More northerly and 1½ miles downstream
Balmerino Bank	Increased dimensions and 1 mile downstream
'Eppies Taes'	Previously near Balinbreich Castle, moved 1 ½ miles downstream
Tay Bar, Abertay Sands and Gaa Sands	Shoaling areas are reduced as to not be a threat to shipping
Lady Buoy, Outer Bar and Horseshoe Bank	Shoaling heights reduced to -14 ft MSLW, -18 ft MSLW and -13 ft MSLW respectively

Table 3.1. Observations of sediment movement within the Tay Estuary from Cunningham (1887).

	Newburgh 1833+44 (h:mm)	Perth 1833 (h:mm)	Perth 1844 (h:mm)
Spring tide flood	4:20	2:20	3:10
Spring tide ebb	7:20	7:00	7:10
Neap tide flood	3:30	3:15	3:10
Neap tide ebb	6:45	7:00	7:00

Table 3.2. Tidal variance from Beardmore (1862).

3.2.3 Tidal Influence and Currents

With regards to the tidal limit, two limits can be discussed; that of saline intrusion and that of water height. Salinity in the Tay Estuary varies from 35 psu (practical salinity units) at the mouth, to 25 psu at Newport Pier on the opposite bank to Dundee, 25 psu at the Tay Railway Bridge, 10 psu near Balmerino near the centre of the estuary, and to ~5 psu at Newburgh just below the Tay-Earn confluence (McManus, 1998).

The tidal height limit, as shown on Ordnance Survey maps, in the River Tay lies at Scone and in the River Earn lies 2 km above the Bridge of Earn (Dobereiner 1982, McManus, 1985). The tidal range in the estuary rises until Flisk, but then quickly contracts before Newburgh (Table 3.3).

Station	Datum (m)	Tidal amplitude (m)	Tidal delay (h:mm)
Port of Dundee	-2.90 m O.D.	5	0:00
Tay Rail Bridge	-2.32m O.D.	5	0:00
Flisk Point	-2.32m O.D.	5.5	0:20
Newburgh Quay	-1.00m O.D.	4.2	0:30
Inchyra Pier	-0.5m O.D.	3.8	0:40
Perth	-0.0m O.D.		0:50

Table 3.3. Tidal heights and delays for stations along the Tay Estuary (Bates *et al.*, 2004; Dobereiner, 1982; Angus Council, 2010). The Tay Railway Bridge and Flisk Point Datums are equal to the old Dundee Datum before its conversion to LAT.

As the tide progresses into the estuary, the tidal wave is squeezed into a narrower and shallower channel. This convergence of the tide causes the tidal height to increase in the middle reaches of the estuary (Figure 3.9) (Webb and Metcalfe, 1987; Jenkins, 2003). This transition of channel range and depth along the estuary forces an increase in the high tide level in the upper estuary (Table 3.4 and Figure 3.10).

Source	Change in elevation of high water (m) on a spring tide			
	Buddon	**Dundee**	**Newburgh**	**Perth**
Cunningham (1895)	0	-1.10	+0.22	+0.45
Allen (1945)	0	+0.10	+0.45	+0.80
TERC (1972)	0	+0.18	+0.70	+0.80

Table 3.4. Comparative tidal high water levels along the Tay Estuary (Charlton *et al.*, 1975).

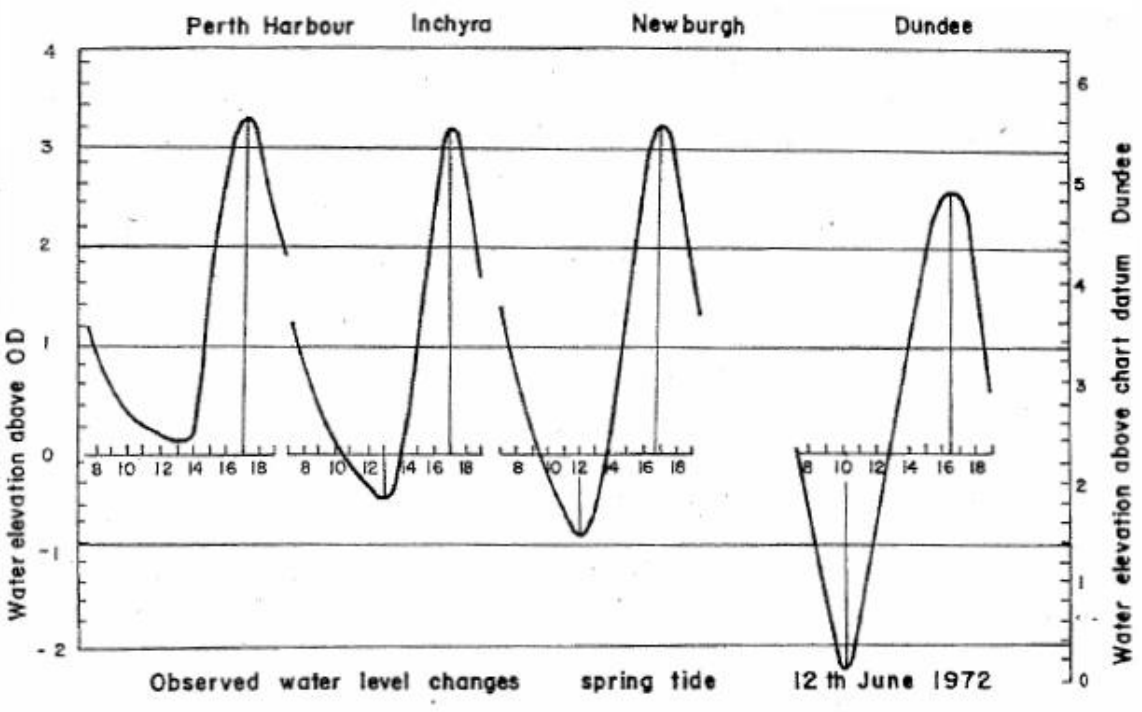

Figure 3.9. Tidal profiles at various locations along the Tay Estuary observed on the spring tide of 12 June 1972 (McManus, 1998).

In the Tay Estuary, tidal prediction calculations can be made for Dundee and Arbroath from the Admiralty tidal harmonic constant values published by the UK Hydrographic Office (UKHO) (Table 3.5). These predictions take into account the progression of the tidal range within the estuary.

	ML	Harmonic Constants				Zone UT				S. W. Corrections			
	z_0	M_2		S_2		k_1		O_1		f_4	F_4	f_6	F_6
	(m)	g°	H.m	g°	H.m	g°	H.m	g°	H.m				
Dundee	3.25	064	1.68	108	0.54	226	0.12	072	0.14	149	0.010	046	0.008
Arbroath	3.13	045	1.64	083	0.56	219	0.15	055	0.16	109	0.013	054	0.003

Table 3.5. Harmonic constants taken from the UKHO Admiralty Tide Tables 2008 Part III (UKHO, 2008:340). ML = predicted tidal height relative to Chart Datum at the specified locations.

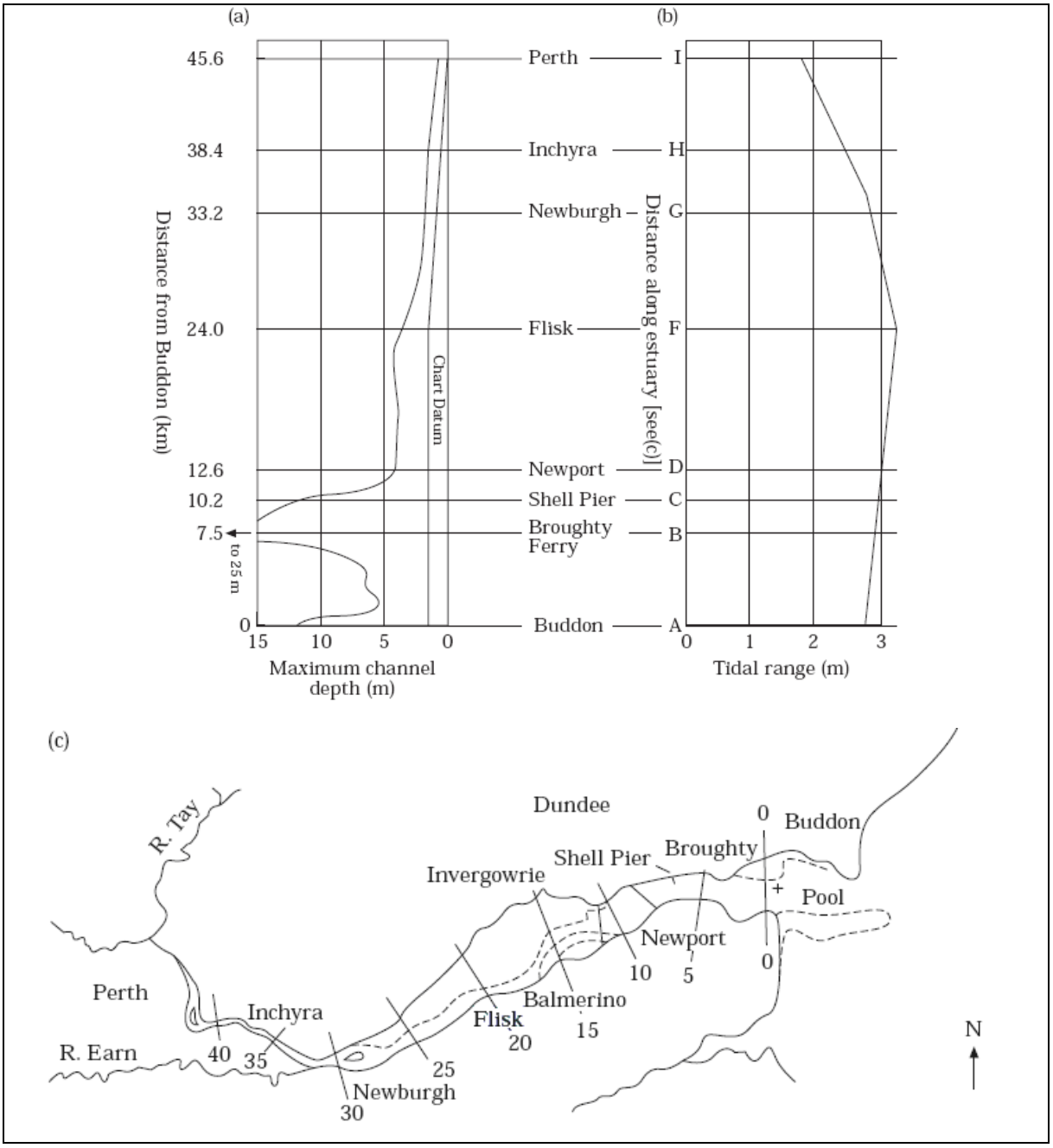

Figure 3.10. (a) Maximum channel depth along the estuary, (b) tidal range along the estuary, and (c) map of Tay Estuary with cross-section locations of sediment sampling (Williams and West, 1975).

The spring tidal volume is estimated at 623 x 10^6 m^3 and the neap tidal volume at 130 x 10^6 m^3 (Table 3.6) (Dobereiner, 1982). There is an estimated ratio of 2:1 between tidal and fresh water during a neap tide cycle compared with 10:1 during a spring tide. A ratio of 50:1 or even 200:1 may occur during a spring tide with a low freshwater input (Dobereiner, 1982).

Tidal range	Tidal exchange volume (10^6 m^3) upstream of:		
	Stannergate (D)	**Broughty Ferry**	**Buddon**
5.94 Extreme spring (Cunningham, 1895)	-	-	623
5.00 Ordinary spring tide	271.8	286.5	380.5
2.44 Ordinary neap tide	152.3	161.0	213.3
1.09 Extreme neap (Cunningham, 1895)	-	-	130

Table 3.6. Tidal exchange volumes for various tidal ranges (Charlton *et al.*, 1975). (D) represents Dundee.

The flood-ebb cycle in the Tay is asymmetrical in form with long ebb periods and short floods (Dobereiner, 1982). Up to 60% of the ebb flow volume is exchanged in each tide (Charlton, 1980). The sea currents, measured by recording buoy markers, circulate in an anti-clockwise motion southwards across the estuary's mouth during the flood and northwards during the ebb (Dobereiner, 1982; Charlton, 1980) (Figure 3.11).

Tidal velocity in the upper estuary can be slowed and increased by hydrological flow. Hydrographic gauges have captured river flow data from above Perth since 1947 for early-warning flood information between Ballathie, Caputh and Perth (Macdonald *et al.*, 2006). The river produces a variable flow depending on the fluvial input at that time with a long-term average daily disharge of 198 m^3s^{-1}; 167 m^3s^{-1} from the River Tay and 31 m^3s^{-1} from the River Earn (McManus, 1985; Richardson, 1839; Jenkins *et al.*, 2002). A 40 year flood from the Rivers Tay and Earn can produce a disharge of 1,550 m^3s^{-1}, whereas the summer disharge can be as little as 15 m^3s^{-1}. The Earn contributes 16% of the overall hydrological input with the remaining 84% from the River Tay above Perth (McManus, 1998).

In January 1993 the peak discharge measured 2,269 m^3s^{-1} at Ballathie on the River Tay and 415 m^3s^{-1} on the River Earn (Black and Anderson, 1994). Jenkins (2003) suggested that the peak instantaneous discharge for the Tay-Earn system should be estimated at 2500 ± 100 m^3s^{-1}. The average monthly fresh water inflow for both estuaries is shown in Figure 3.12. Information on storm induced surges is presented in Chapter 7.

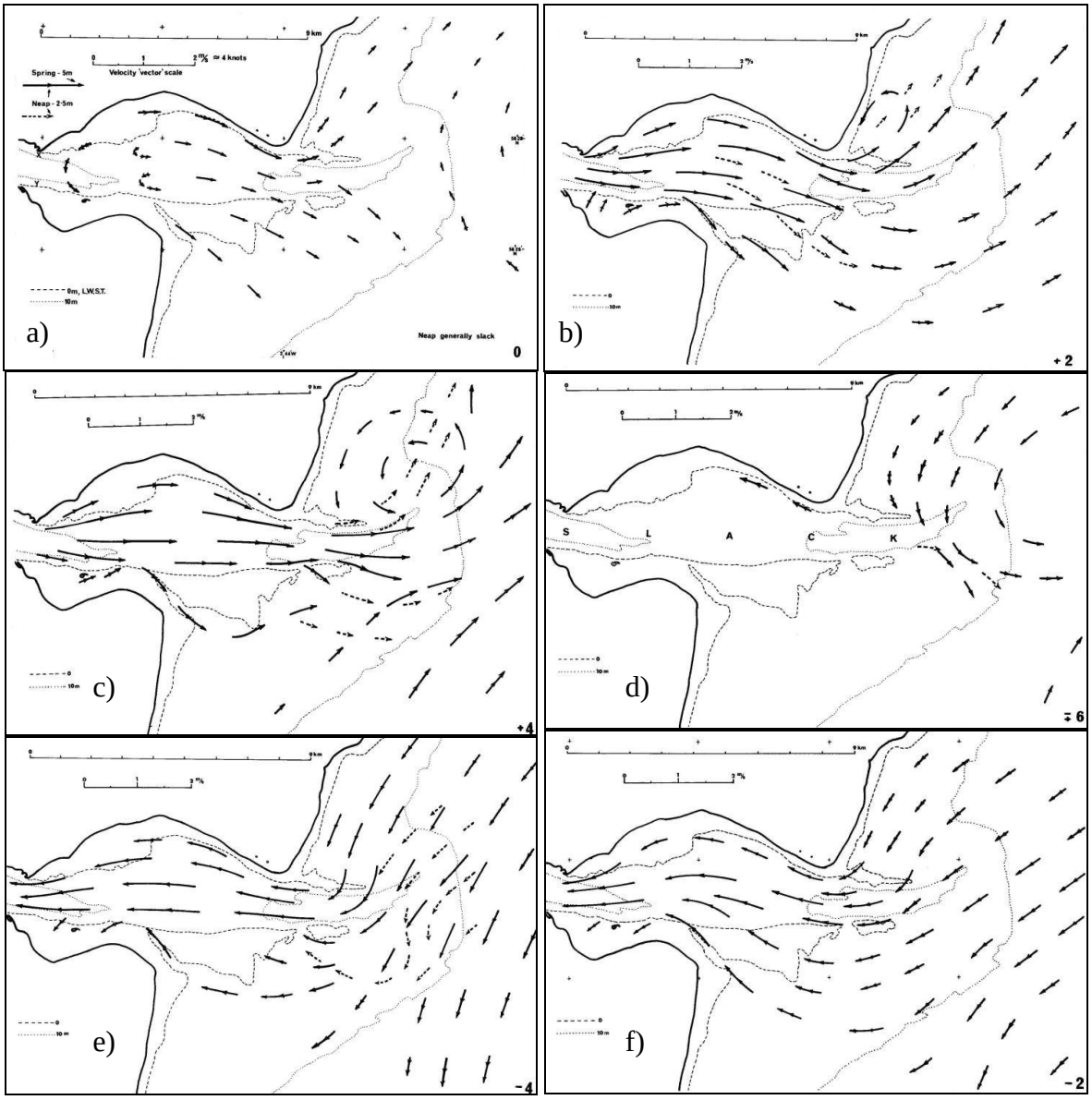

Figure 3.11. Tidal currents of the outer Tay Estuary at high water Dundee a) (t = 0); b) (t= +2); c) (t= +4); d) (t= +/-6); e) (t= -4); f) (t= -2) (Charlton, 1980:37-42).

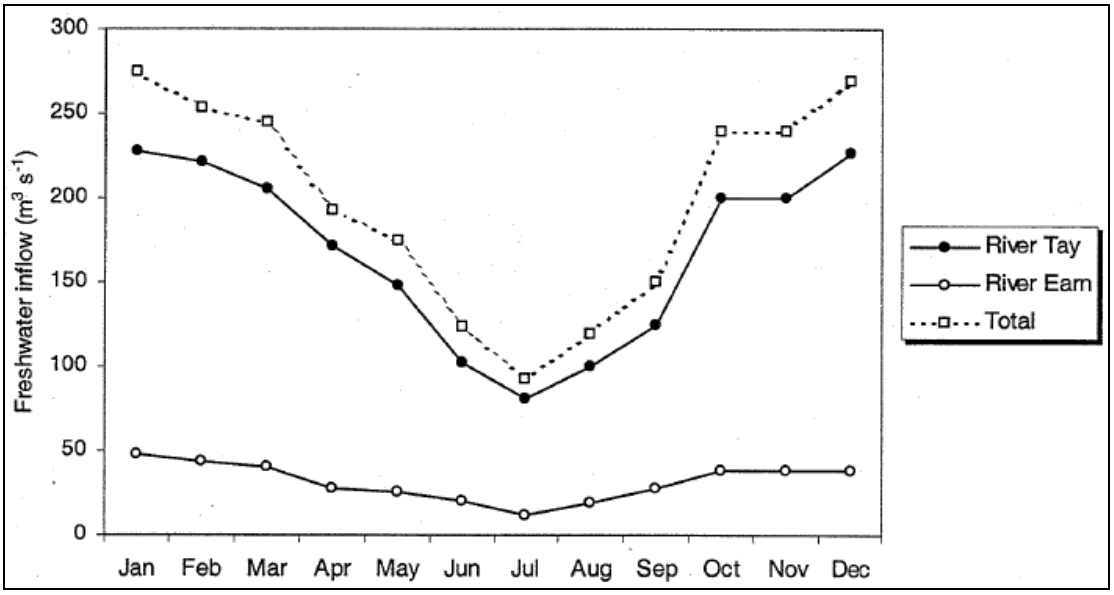

Figure 3.12. Hydrograph showing the monthly average inflow of fresh water to the Tay Estuary (Pontin and Reid, 1975).

The flow of the river into the estuary is impeded by the flood tide and increased during the ebb. The spring and neap tides add their own unique influences to the rate of hydrological flow. The tidal velocity is likewise influenced by the fluvial discharge in the upper estuary and by the tidal lunar cycle. Tidal velocity variances at Perth include those presented in Table 3.7. At Perth these rates are significantly impacted by the freshwater input from the River Tay, especially during flood events when alteration to the tidal flood velocity and the ebb velocity can seriously impact shipping travelling upstream to Perth Harbour.

	Half-ebb	**Half-flood**
Spring tide	2.31 ms^{-1} (4.5 knots)	1.54 ms^{-1} (3 knots)
Neap tide	1.54 ms^{-1} (3 knots)	0.77 ms^{-1} (1.5 knots)

Table 3.7. Tidal velocity variation at Perth (Perth Harbour Authority, 2010).

Although this thesis does not focus on the influence of waves, it is worth acknowledging studies that have looked at the wave environment in the Tay Estuary, as wave have an additional impact on the coast. The Angus Council Shoreline Management Plan has compiled data on wind and wave characteristics at the mouth of the Tay Estuary. Their survey indicated a predominantly north eastern direction wind environment. Within Ramsay and Brampton's (2000) 1986 to 1994 survey offshore of Carnoustie the majority of waves, including swell waves, were sourced from the north east. Over 40% of waves measured less than 1 m with the majority of all waves measuring less than 2 m in height.

3.2.4 Estuarine Sediment Dynamics and Bathymetry

The Tay Estuary's morphology can be split into three sections, intertidal flats, mid-estuary sandbanks and channels (Buller *et al.*, 1971). The deepest part of the Tay lies between Tayport and Broughty Ferry in the outer estuary (Bates *et al.*, 2004). These characteristics are evident in bathymetric maps (Figure 3.13 to Figure 3.15).

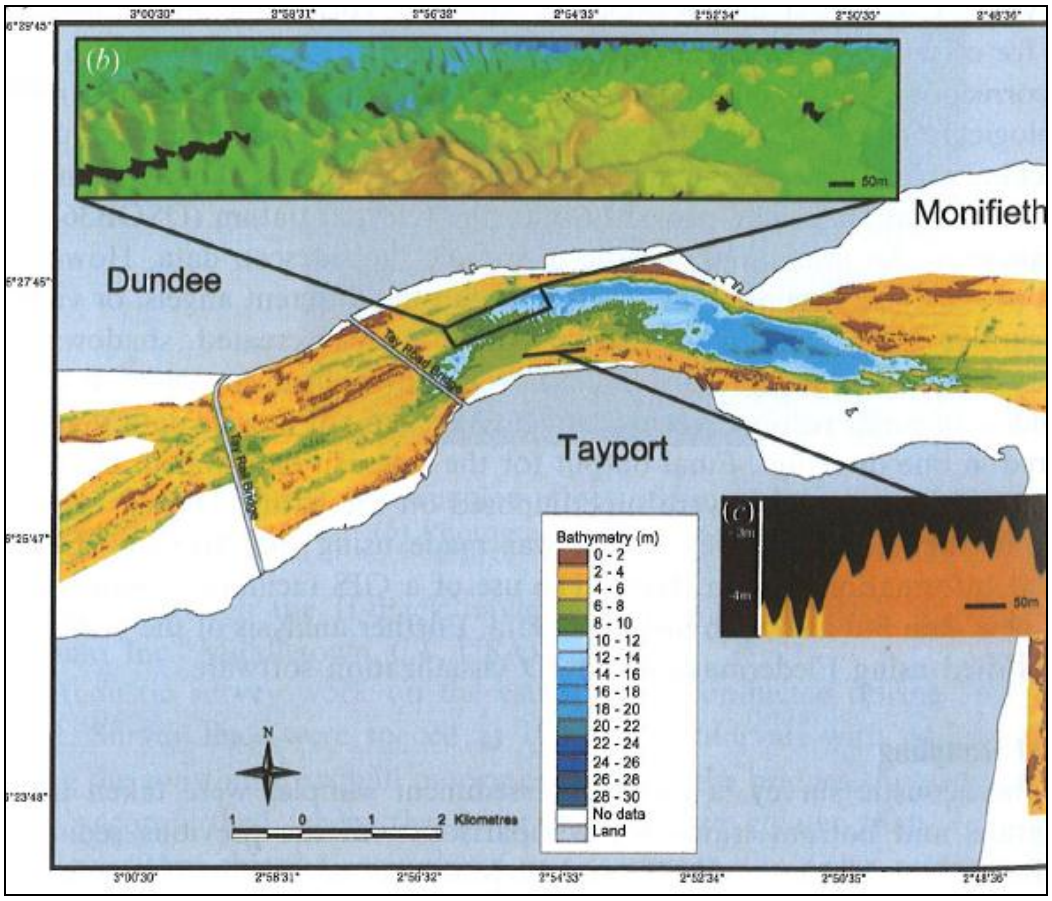

Figure 3.13. 'Bathymetry for Tay Estuary and Eden Estuary candidate Special Area of Conservation (cSAC) determined using Submetrix System 2000 bathymetric sidescan' (McManus, 1985).

Bathymetric surveys of the Tay Estuary were conducted by Bates *et al.* (2004) using swath-bathymetric sidescan sonar survey equipment. The survey was not comprehensive of the entire estuary and omits areas that were inaccessible due to the position of exposed or shallow sandbanks at the time of the survey. To the west of the Tay Railway Bridge the survey is limited to the shipping channel westward of Flisk where it terminates (Figure 3.15). The survey does highlight deep areas near Broughty Ferry and in the central channel between Broughty Ferry and the Port of Dundee river berths (Bates *et al.*, 2004).

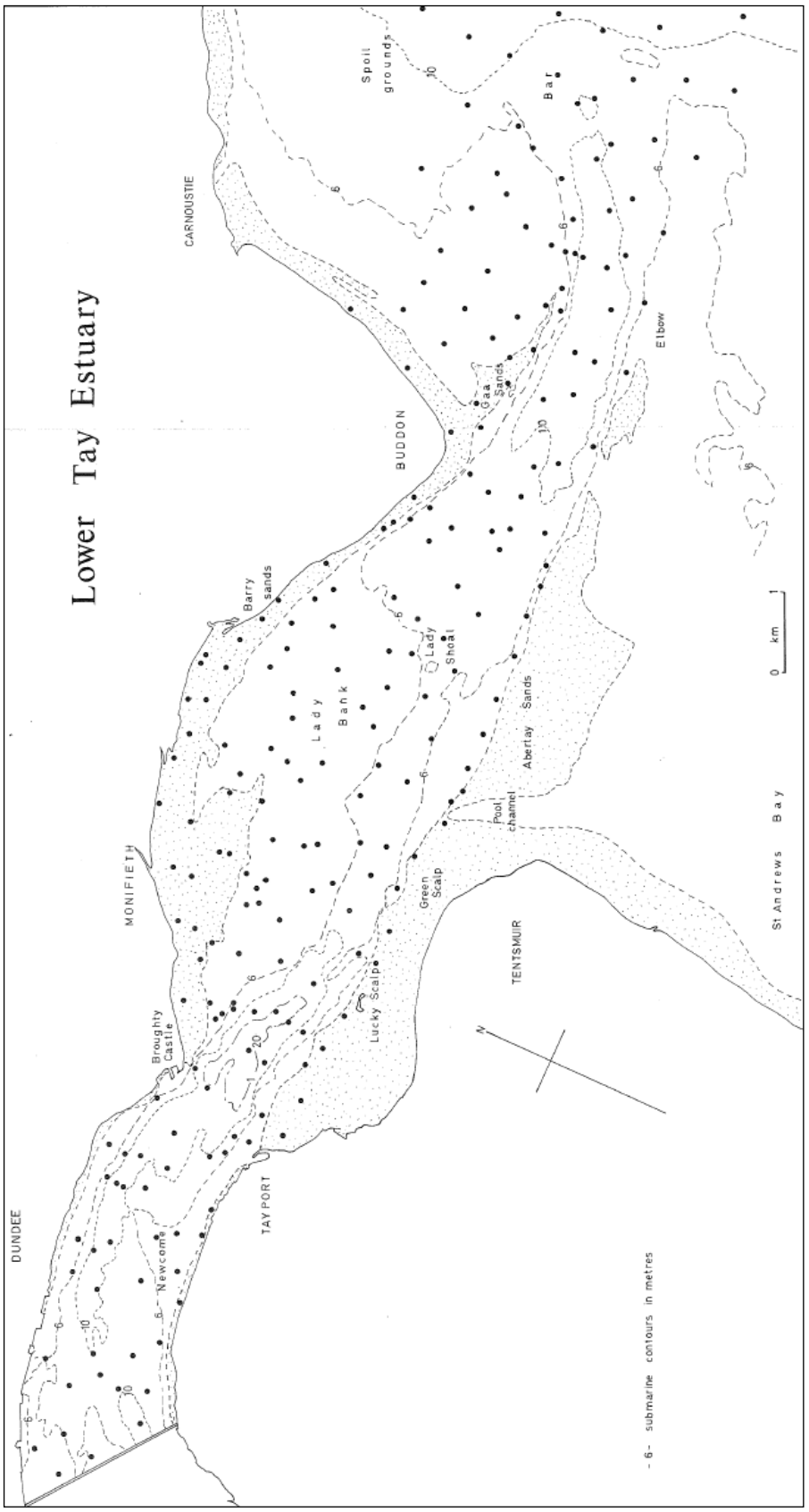

Figure 3.14. Locality map showing bottom sediment sampling locations and submarine bathymetry contours (based in Admiralty Chart No. 1481) (McManus *et al.*, 1980:134a).

The rivers entering the Tay Estuary feed in ten time more sediment than those entering the Forth Estuary (McManus, 1986), with the Tay Estuary having few rock outcrops exposed along the coastline. In some areas present day sediment has been scoured to reveal post-glacial boulders, pebbles, peat, compact black clay and red late-glacial Arctic clay. In the channel, fine sediments are limited with coarse sands replacing the smaller grain sizes with shell content, boulders and pebbles increasing seaward (Buller *et al.*, 1971).

In the upper estuary, muds and silts are the most common grain size with larger grain size material, including boulders, appearing along the beaches and estuarine shores (Figure 3.13 to Figure 3.19) (Buller *et al.*, 1971). Throughout the estuary there are extensive sandbanks, especially to the north of the maintained shipping channel. The primary sandbank formation process is driven by the estuarial currents (Charlton, 1980).

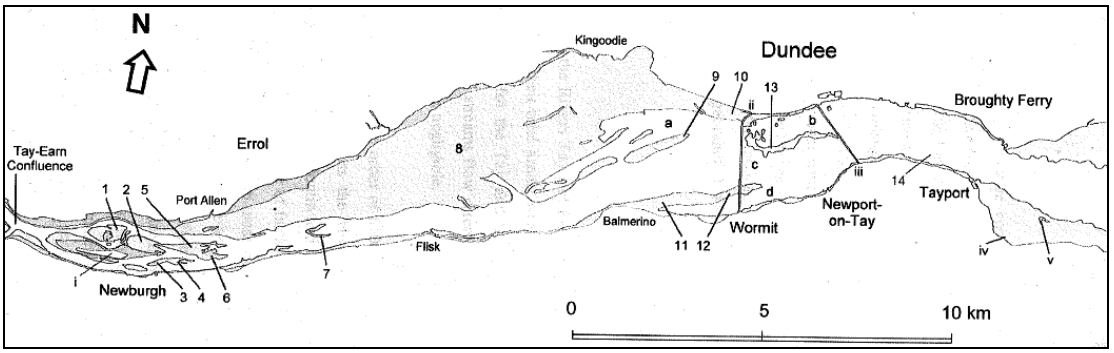

Figure 3.15. Bottom topography of the Tay Estuary. Areas of reed beds are shaded in dark grey, areas between high and low water marks are shaded in mid-grey and areas below the low water mark are shaded in pale grey.' Jenkins (2003:40) key: (1) Kerewhip Bank; (2) The Turk; (3) Litte Bank; (4) Bells Bank; (5) Johnston Bank; (6) Haggis Bank; (7) Deil Bank; (8) Dog Bank; (9) Old Channel Bank; (10) My Lord's Bank; (11) Naughton Bank; (12) Wormit Bank; (13) Middle Bank; (14) Newcombe Shoal; (a) Kingoodie Channel; (b) Queen's Road Channel; (c) Navigational Channel; (d) Wormit Channel; (i) Mugdrum Island; (ii) Tay Railway Bridge; (iii) Tay Road Bridge; (iv) Tayport Bay saltmarsh; (v) Lucky Scalp.

Two islands formed by sediment deposition in the Tay Estuary lie in the western extent with Friarton/Moncreiffe Island in the Perth Gap and Mugdrum Island (marked as *i* on Figure 3.16) in the channel north of Newburgh. Two Devonian age andesite bodies form small islands near the northern bank at Dundee, called Fowler Rock and Beacon Rock.

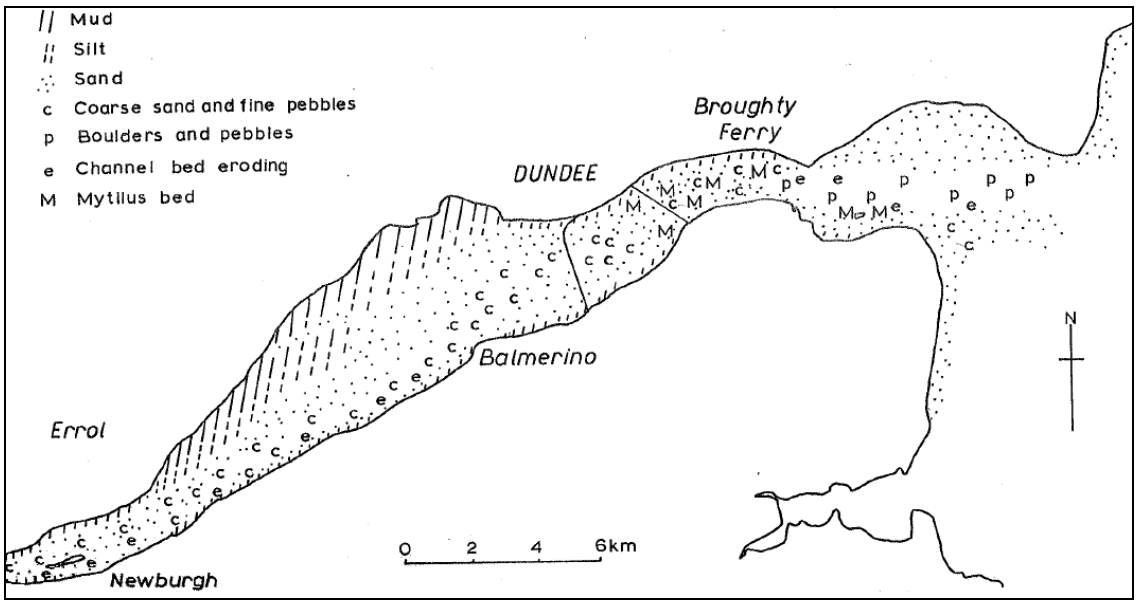

Figure 3.16. 'Distribution of modern day sediments in the Tay Estuary' (Buller *et al.*, 1971:20).

The estuary has several biological and geological conservation designation allocated to it, including Sites of Special Scientific Interest (SSSI), Nature Conservation Review (NCR) sites, Geological Conservation Review (GCR) sites, a National Nature Reserve (NNR), a Special Area of Conservation (SAC), a proposed Local Nature Reserve (LNR), one proposed Ramsar site and one proposed Special Protection Area (SPA) (SNH, 2010). The sandbanks in the Tay Estuary form an important habitat for wading birds, molluscs and other fauna and flora, but these sandbanks can be challenging for water transport in the upper estuary. At the estuary mouth, Tentsmuir Point is the fastest accreting area of the UK, although erosion is occurring along the Kinshaldy/Tentsmuir Sands shoreline to the south (Whittington, 1996). This is primarily due to longshore movement of sediment from the south where the shoreline extends from the Eden Estuary to Tentsmuir Point.

Jenkins *et al.* (2005) conducted an analysis of sediment provenance in the Tay Estuary using a sediment fingerprinting technique, which determined the magnetic susceptibilities of sediment samples from the River Tay, the River Earn and from beaches in Angus and Fife. They concluded that approximately 78% ± 10% of the sediment is derived from marine sources, 18% ± 10% from the River Tay and 4% ± 10% from the River Earn.

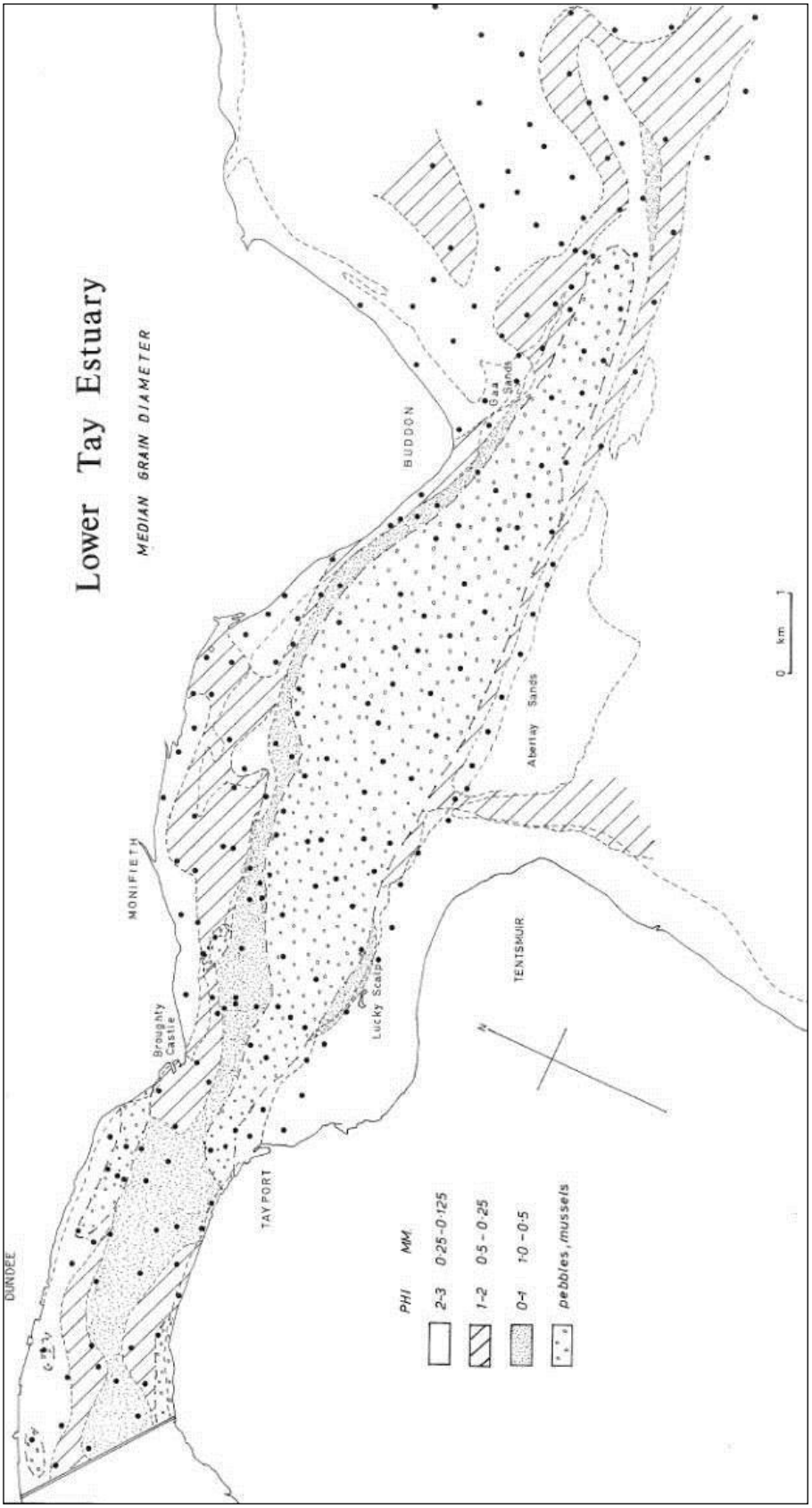

Figure 3.17. Distribution of median grain diameter in the Lower and Outer Tay Estuary (McManus *et al.*, 1980:136b).

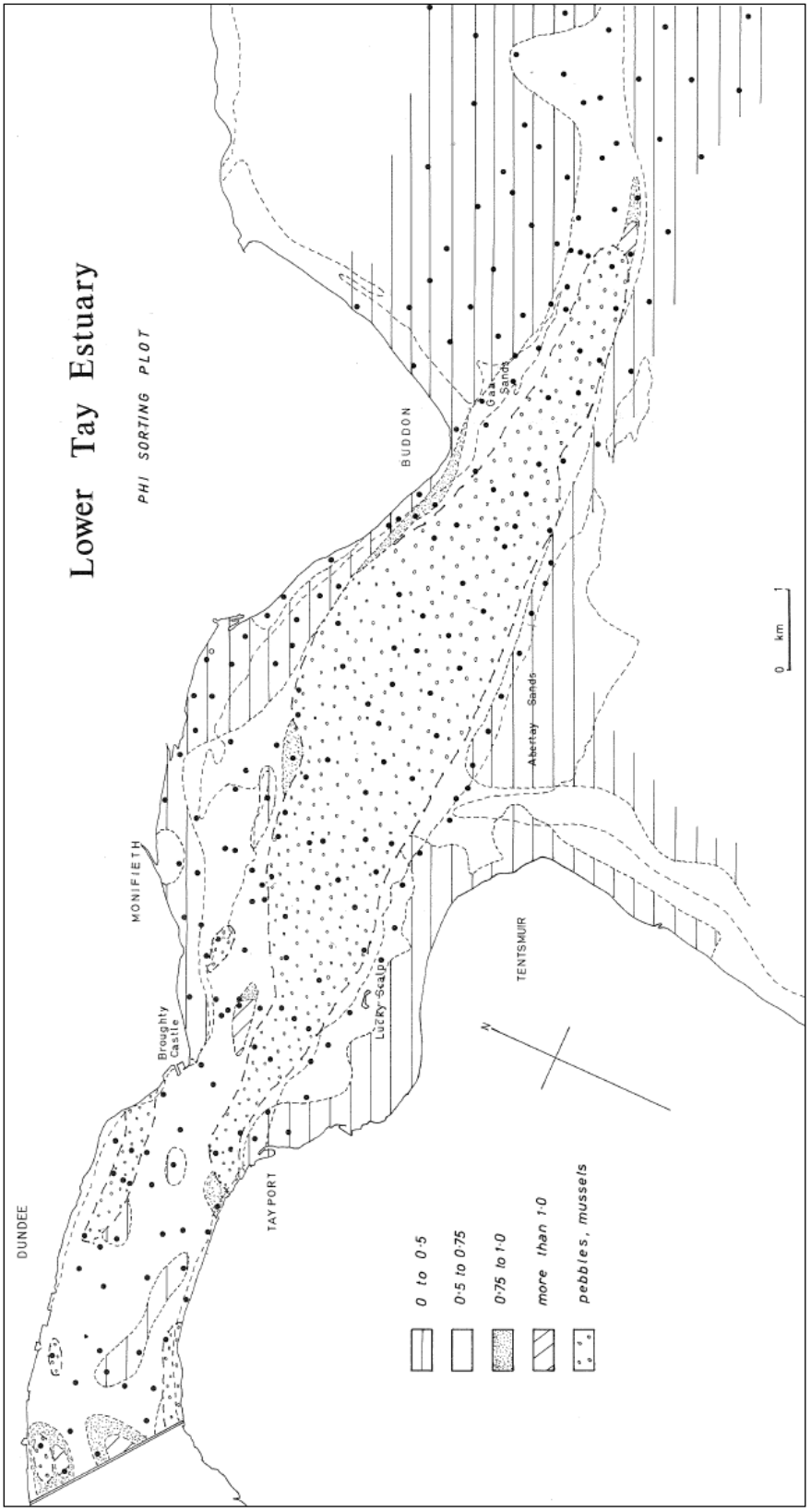

Figure 3.18. Sorting characteristics of sediment in the Lower and Outer Tay Estuary (McManus *et al.*, 1980:138a).

The sandbanks at the mouth of the estuary, the Abertay and Gaa Sands, act like offshore breakwaters and serve to minimise wave heights entering the estuary (McManus, 1985). The middle estuary sediments, near the Tay Railway Bridge, are very unstable with sandbank movement and channel migration evident (Duck, 2005) (Figure 3.20). This instability occurs in the outer estuary as well. Several lighthouse designs were constructed to serve Barry Links over the fifteenth, sixteenth and seventeenth centuries (McGlashan, 2003). The instability of the sediment around that area led to the first designs being built on rollers, but two stone lighthouses were built by the Stevensons in 1866. Unfortunately, the migrations of the estuary channel resulted in both lighthouses becoming redundant, necessitating the movement of the smaller lighthouse in 1884 by 63 m north eastwards (McGlashan, 2003). Ultimately, this lighthouse became redundant again and was replaced by a lightship (McGlashan, 2003).

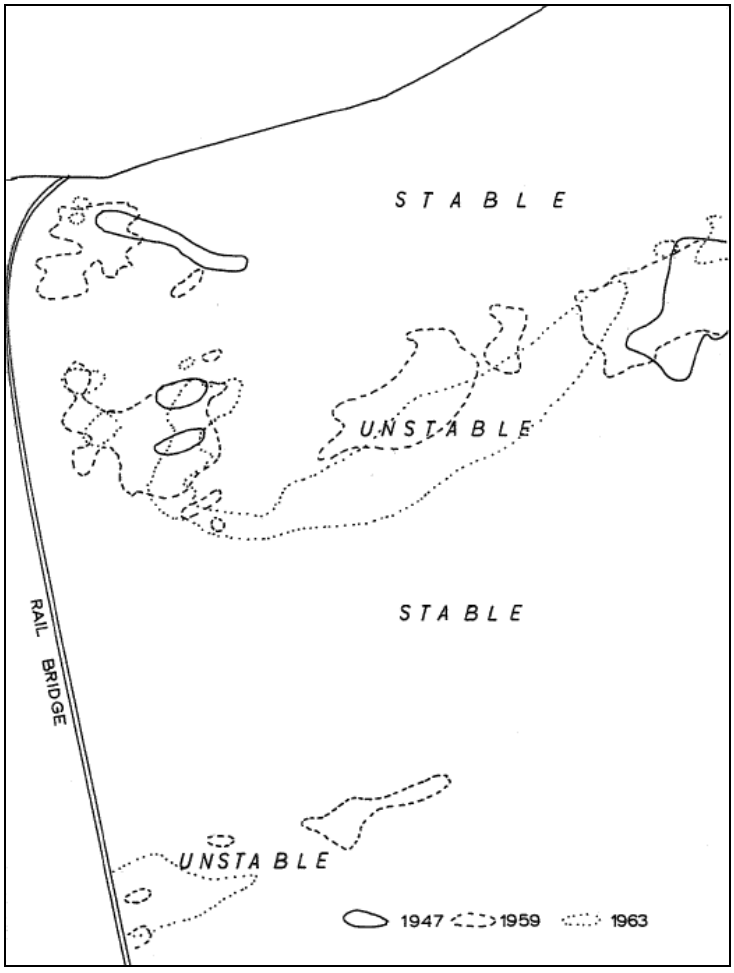

Figure 3.19. 'Low water mark of Middle and Birkhill Banks for various years to show stable and unstable areas' from Buller *et al.* (1971:33).

3.2.5 Modern Port Infrastructure

Dundee is the largest city along the Tay Estuary. Within a 60 minute drive, the Dundee catchment, had a population of 628,468 people in 2011, including areas in Perthshire, Kinross-shire, Fife and Angus. In March 2011, 144,290 people were registered as residing within the Dundee City Council boundaries, of which 94,750 were of working age and 72,300 were economically active (Dundee City Council, 2011).

Perth, at the head of the Tay Estuary, is the second largest settlement on the Tay with 43,501 people living within the limits of Perth during the 2001 Census (Perth & Kinross Council, 2007). Unfortunately more recent census estimates are not yet available for this new city, but county estimates suggest there have been continuous increases in population since 2001, with an additional *c.*13,000 people living in the county (147,780 in total by 2010) (Perth & Kinross Council, 2011). Perth was awarded city status in 2012.

There are a number of recreational activities along the Tay as well as industrial and commercial activities. Several infrastructural features along the Tay are highlighted in Figure 3.20. Along the Tay Estuary, tourism activities include cetacean watching, beach activities, cliff walking, heritage sites, sailing and recreational fishing.

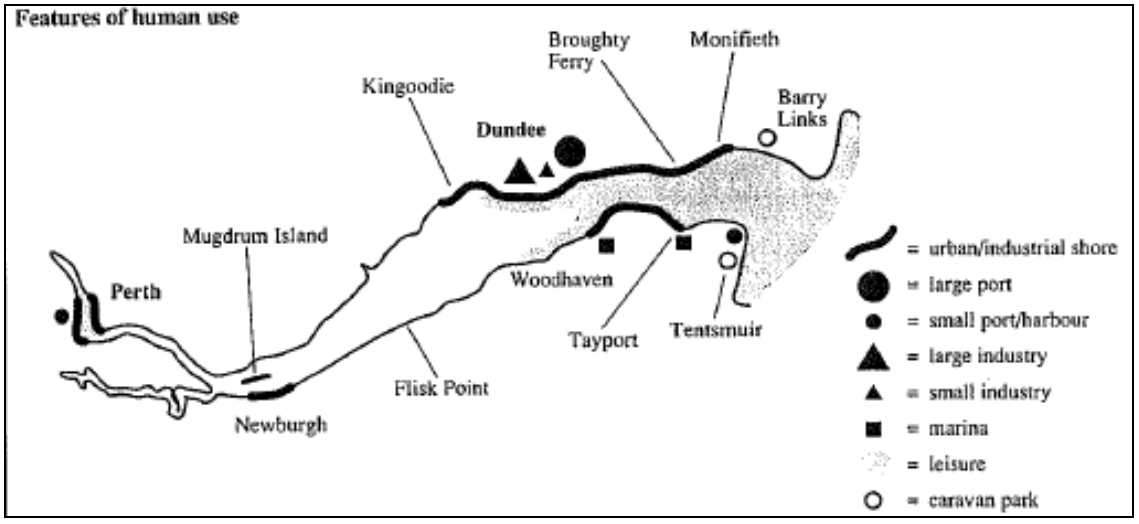

Figure 3.20. Features of human management in the Tay Estuary (SNH, 2010:86.5).

Gas and oil pipelines lie beneath the estuary bed at Elcho, Inchyra and Monifieth. An incident occurred on 30 October 2008 when a ship heading for Perth ran aground in the estuary, resting on the pipeline near Elcho. On this occasion no damage was done to the pipeline (Smith, 2008). This event may have been due to either an unpredicted lowering of the tide or human navigation error, but this illustrates the importance of thorough understanding of tides.

Thirty seven outfalls released wastewater into the Tay Estuary on the northern shore between Invergowrie and Arbroath before completion of the Tay Wastewater Project in 2001, 33 of which were short sea outfalls with the other four being long sea outfalls (Finan, 2007). Part of this project involved constructing a series of pumping stations along the northern outer Tay Estuary coastline to pump wastewater from Dundee, Broughty Ferry, Monifieth, Carnoustie and Arbroath to the Hatton Wastewater Treatment Plant, between Carnoustie and Arbroath. This system has greatly improved the quality of water released into the estuary (Finan, 2007; Scottish Government, 2000).

In the estuary today there are two commercial ports, the large Port of Dundee and small Perth Harbour (Section 3.2.5). In addition there are several fishing and leisure harbours, two of which are Tayport Harbour and Broughty Ferry Harbour. Smaller harbours and landing places are numerous, for example Arbroath Harbour, famous for its Arbroath Smokies, on the North Sea coast immediately north of the estuary mouth.

Referring back to the commercial Port of Dundee, the area surrounding Victoria and Camperdown Docks has been under development over the past 600 years and redevelopment into a residential and commercial area in the last 20 years. This includes the closure of the stretch of river berths between the Tay Road Bridge and Camperdown Dock gate. The Port of Dundee was purchased by Forth Ports Limited in 1995.

Dundee has a deep quayside maintained through an annual dredging campaign (Table 3.8). The Port of Dundee handles liquid bulks, cruise liners, dry bulk, general cargo, forest products, grain and renewable energy products. Dundee has roll-on roll-off facilities, a tidal basin and 1.3 km of collective river berth length split over six key ‘wharfs’ (Figure 3.21) (Forth Ports, 2010).

Berths	Maximum Depth	Quayside Length
King George V Wharf	8.5m	445m
Caledon West Wharf	9.5m	76m
Princess Alexandra Wharf	8m	256m
Eastern Wharf	8m	213m
Prince Charles Wharf West	9.6m	114m
Prince Charles Wharf East	9m	200m

Table 3.8. Port of Dundee Berths (Forth Ports, 2010).

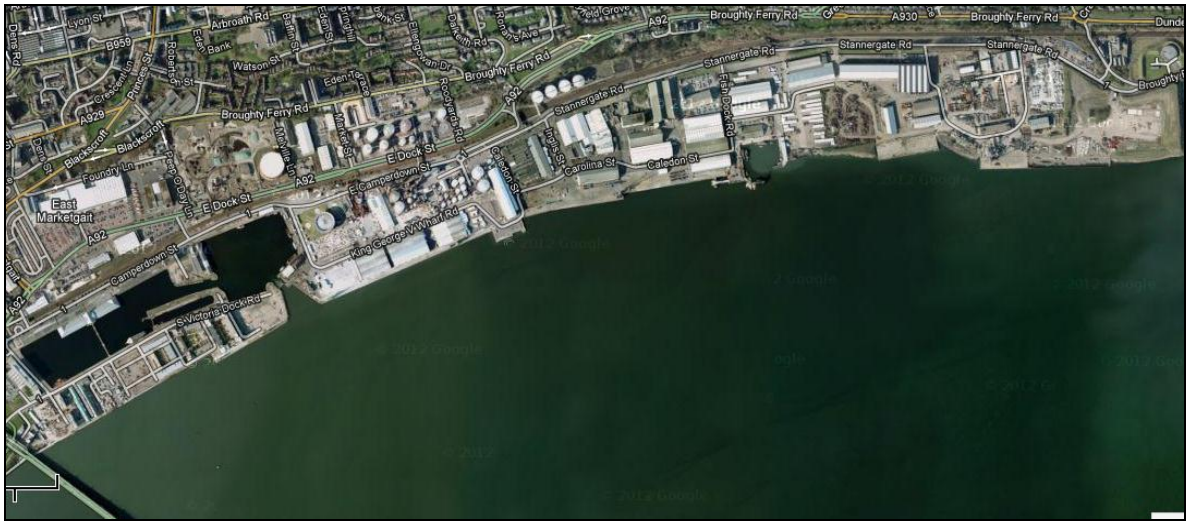

Figure 3.21. Port of Dundee (Google Maps, 2012).

The underlying geology and estuary bed sediments make the port suitable for jack-up oil rig drilling platforms, which can dominate the skyline impressively (Figure 3.22 and Figure 3.23), as well as their service ships. Training operations for oil installation safety are conducted at the port (Forth Ports, 2010).

Figure 3.22. Jack-Up Oil Rig – Rowan Gorilla VII – 1, photographed from the south shore of the Tay Estuary within 1 km east of the Tay Road Bridge (Talk Photography, 2011).

Figure 3.23. Jack-Up Oil Rig – Rowan Gorilla VII – 2, photographed from Dundee Law, central Dundee (Talk Photography, 2011).

Presently Perth Harbour can hold ships up to 90 m in length with a total dockside berthing length of 418 m (Figure 3.24) (Perth Harbour Authority, 2010). The harbour is currently used by ships transporting bulk and liquids such as animal feedstuffs, fertilisers, timber, chemicals and barite ore (Perth Harbour Authority, 2010).

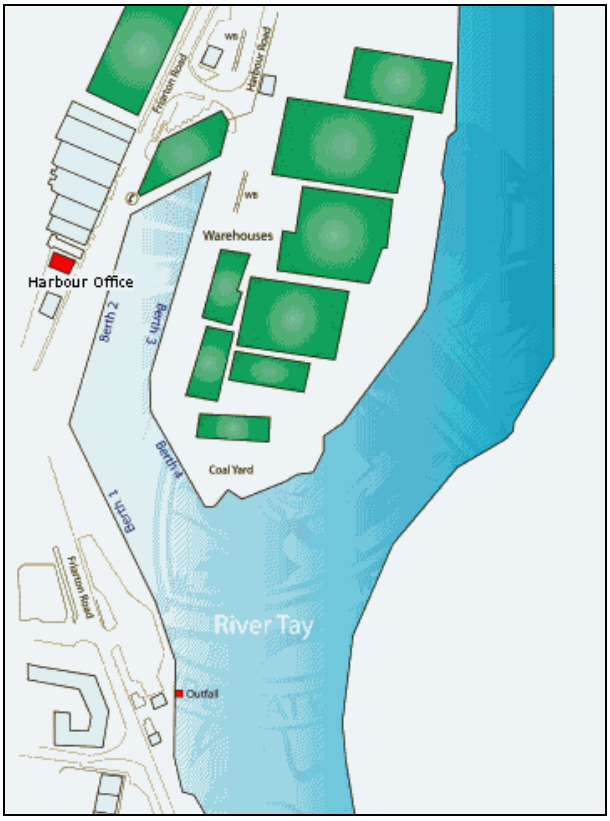

Figure 3.24. Perth Harbour plan (Perth Harbour Authority, 2010).

Perth Harbour is more susceptible to the impacts of sea level change and storm surge events, due to its location at the estuary head. Shipping at this location is already affected by the difficult conditions found at estuary heads, i.e. sediment migration and potential combined fluvial and coastal surge events. Perth Harbour Authority (2010) insists that although pilotage is not compulsory for large ships approaching Perth, it is highly recommended landward of the Tay bridges to avoid the inner estuary sandbanks.

The maximum depth in the harbour is 4.6 m at MHWS, which designates it suitable only for ships that can rest on the river bottom; classified as Not Always Afloat But Safe Aground (NAABSA) (Perth Harbour Authority, 2010). Ships were seen waiting in the outer estuary for several days during the 2010/2011 winter period when ice floes in the estuary made shipping precarious, especially in the Perth Gap area.

3.2.6 Conservation Status

To manage some areas of the Tay Estuary for conservation, several designations have been imposed. The estuary is ecologically important for its diverse wetland habitats including areas of marine environments (65.45 km^2), saltmarsh (5.02 km^2), sandflats/mudflats (52.18 km^2) and shingle (SNH, 2010) habitats. One geologically important site has been designated in the Arbroath Cliffs area.

Amongst the designations for biological and geological conservation are Sites of Special Scientific Interest (SSSI), Nature Conservation Review (NCR) sites, Geological Conservation Review (GCR) sites, a National Nature Reserve (NNR), a Special Area of Conservation (SAC), a proposed Local Nature Reserve (LNR), one proposed Ramsar site and one proposed Special Protection Area (SPA) (SNH, 2010). More information about these designations can be found on the Scottish Natural Heritage interactive website pages (SNH, 2011). The locations of these areas include Monifieth Bay, Flisk Wood, Inner Tay Estuary, Barry Links, Tayport-Tentsmuir Shore, Balmerino-Wormit Shore, Carey (near Abernethy on the River Earn) and one designation includes the entire Tay Estuary (Figure 3.26).

There have been 33,600 recorded wintering birds including redshank, bar-tailed godwit, eider, sanderling, grey plover, dunlin and oystercatcher with breeding birds including black-headed gull, arctic tern, herring gull and ringed plover. The Tay Estuary is also a roosting point for the pink-footed goose (SNH, 2010). There are several notable species of invertebrate, fish and mammal species, including salmon, smelt, otter, grey seal and common seal.

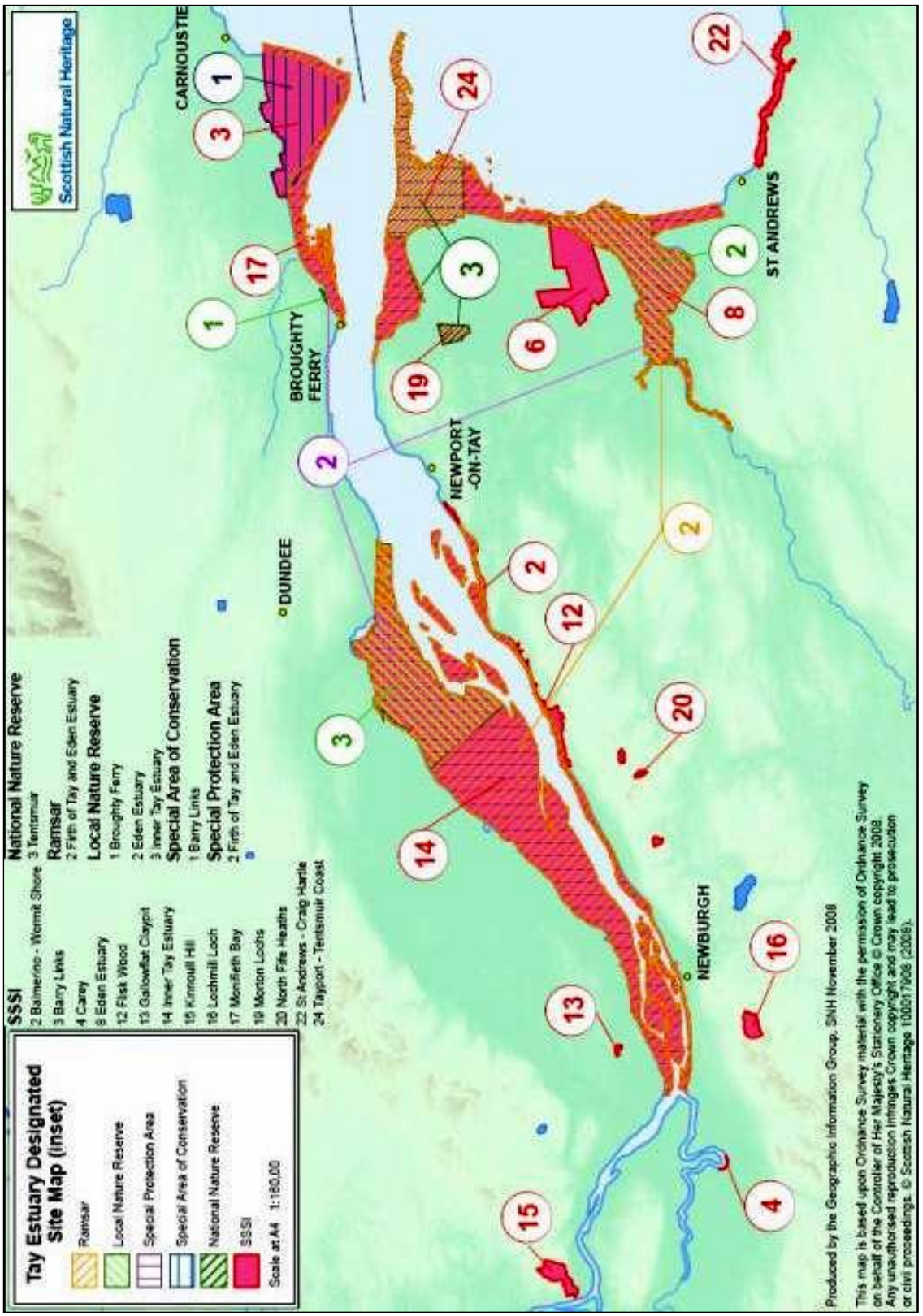

Figure 3.25. Conservation status within the outer Tay Estuary and Eden Estuary (Tay Estuary Forum, 2009:14). This figure was constructed from the Scottish Natural Heritage interactive map and reproduced in this format for the Tay Estuary Forum Management Plan (2011).

3.3 The Firth of Forth and Forth Estuary

The Firth of Forth is 96 km long from the tidal limit at Stirling to the mouth of the firth between Fife Ness on the northern coast and Dunbar on the southern coast (Clarke and Elliott, 1998; Steers, 1973; Forth Estuary Forum, 2010). This area covers 1,670 km^2 and the firth is 19 km wide at its broadest point (Figure 3.26) (Firth and Stewart, 2000).

This estuary has separate distinctive areas that have been nominally classified by the Forth River Purification Board (1995) as the estuarine and firth areas; this approach has been adopted here and is generally accepted. The estuary is located to the west between Stirling and the bridges at Queensferry. The upper reaches are heavily protected and areas of land claim are retained by embankments prohibiting landward movement of the sea. The area between the bridges at Queensferry and the Forth Estuary mouth is generally considered the firth (Figure 3.27: Firth *et al*., 1997). The firth has distinct differences from the estuarine area in bathymetric topography, salinity, tidal currents and various other characteristic. The term Forth Estuary is some times used to refer to the entire tidal Forth area.

The estuary and firth have a combined 4,655 km^2 drainage basin (Clarke and Elliott, 1998; Firth *et al.*, 1997; Elliott and Neill, 2007; Dobson *et al.*, 2000). Eleven major source rivers enter the Firth of Forth at different location along its course, including the Tyne, Esk, Water of Leith, Almond, Avon, Carron and Forth on the south coast and the Teith, Allan, Devon and Leven on the north coast (Figure 3.28) (Browne, 1987).

Unlike the Tay Estuary, which has the depths and sediment supply of a sediment-filled drowned river valley, the Firth of Forth is better compared to a fjord; a deep tidal inlet with rocky sides (Pethick, 1999). Firths are commonly described as drowned river valleys and were flooded during the Flandrian Trangression (Dyer, 1997; Hardisty, 2007; Reeves and Karunarathna, 2009). Depths of up to 70 m have been recorded within the channel of the firth (Elliott and Neill, 2007). The Firth of Forth has a similar tidal range to the Tay Estuary, 5 m at spring tide, 2.5 m at neap tide and 6 m at equinoctial tides.

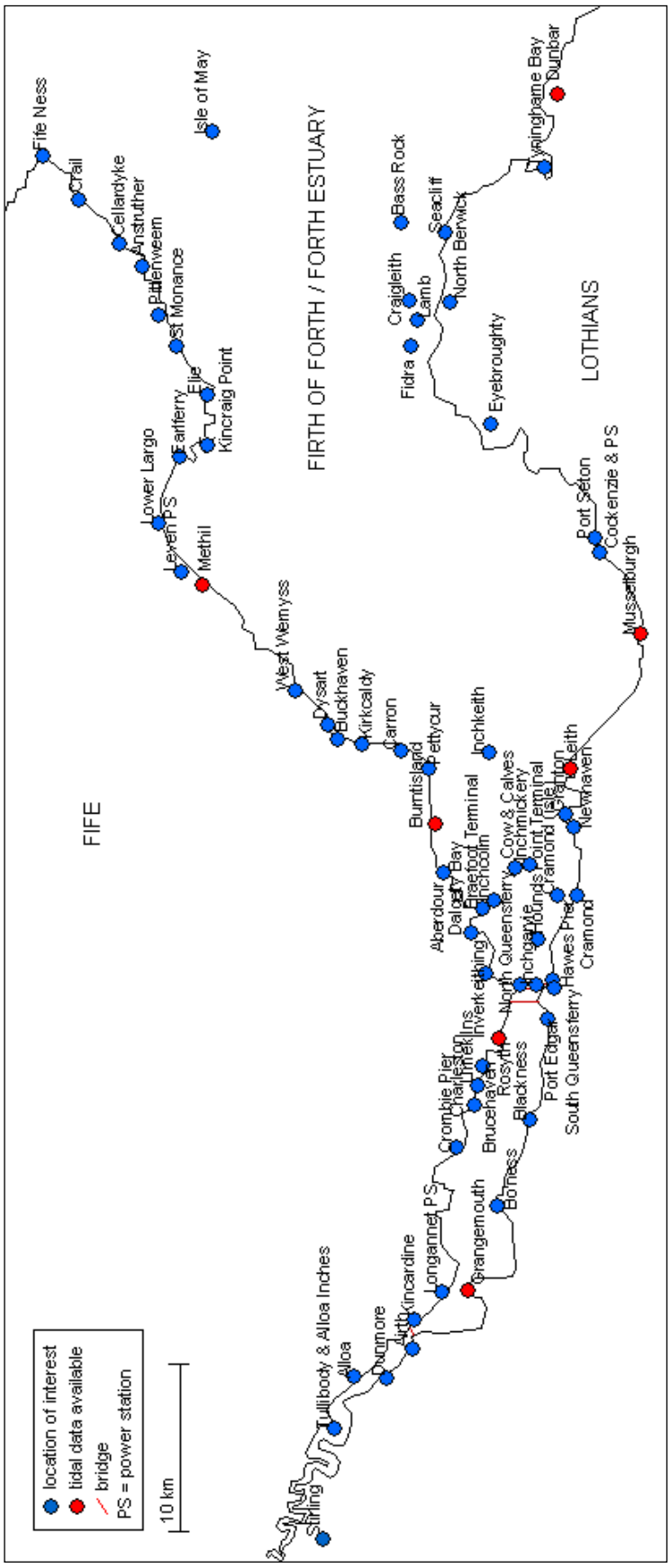

Figure 3.26. Map of the Firth of Forth.

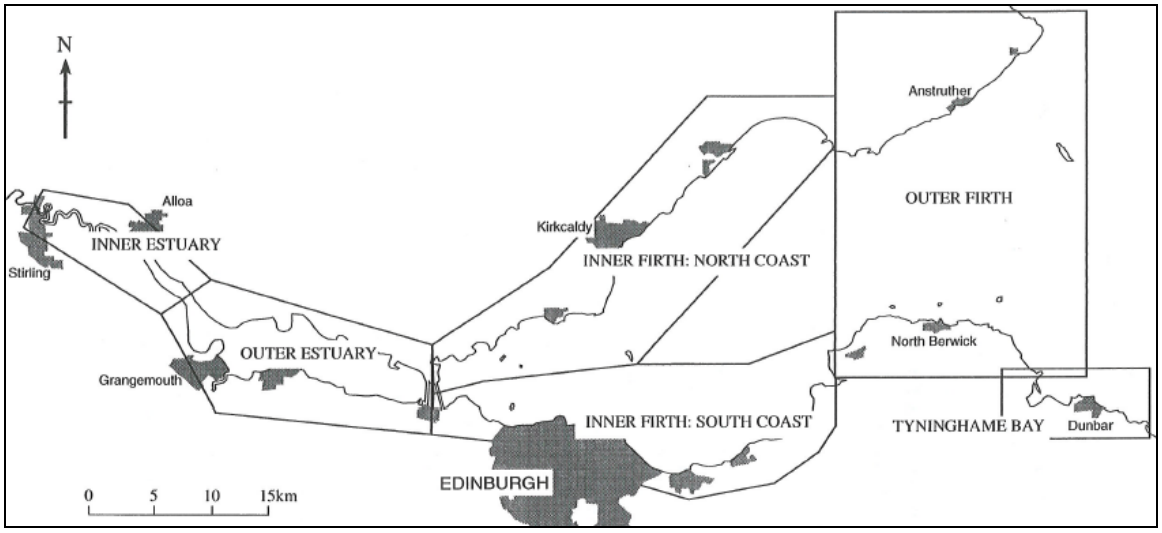

Figure 3.27. The Firth of Forth sub-regions (Firth *et al.*, 1997:26).

3.3.1 Geology and Geomorphology

The drainage basin is sourced in the Highlands, Ochil Hills, Cleish Hills, Lomond Hills, Gargunnock Hills, Bathgate Hills and Pentland Hills, which are contained in a small region surrounding the estuary (Figure 3.28). The coastal region of the Firth of Forth is generally formed of Carboniferous Limestone (Woodward, 1904; Firth *et al.*, 1997). Some areas of igneous rocks occur throughout the site, especially along the North Berwick coastline on the south-eastern shore. Coal Measures occur centrally on both north and south coasts around Methil, Musselburgh and at the head of the estuary (Figure 3.29) (Firth *et al.*, 1997). Figure 3.29 also shows the geology of east central Scotland, illustrating a marked difference in the geology of the Forth and immediately northern Tay.

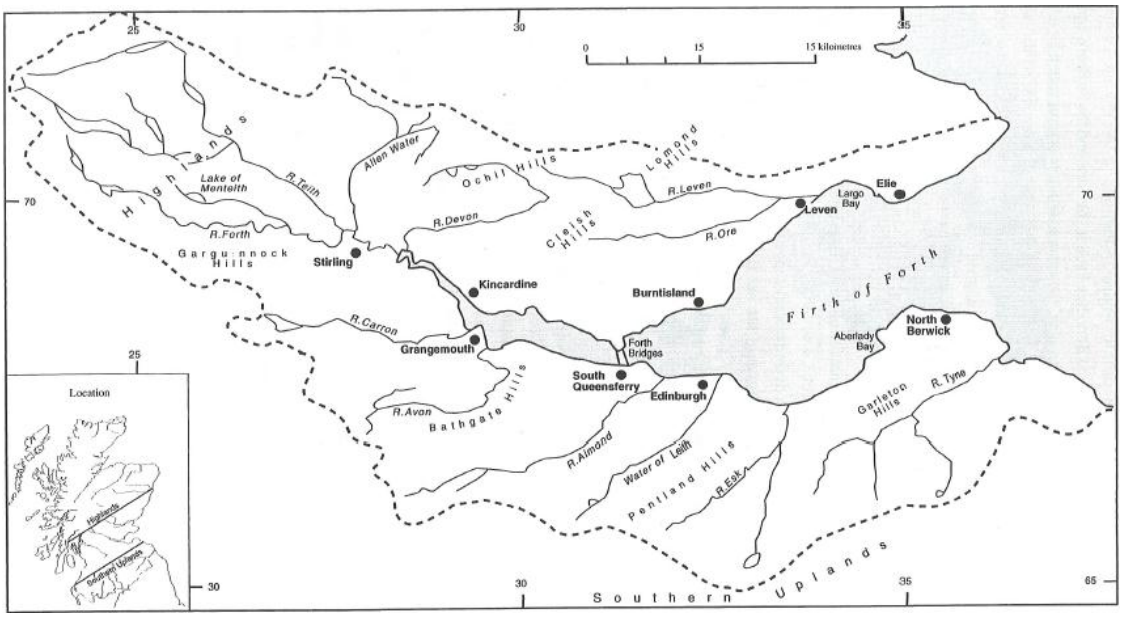

Figure 3.28. Forth Drainage Basin (Firth *et al.*, 1997:5).

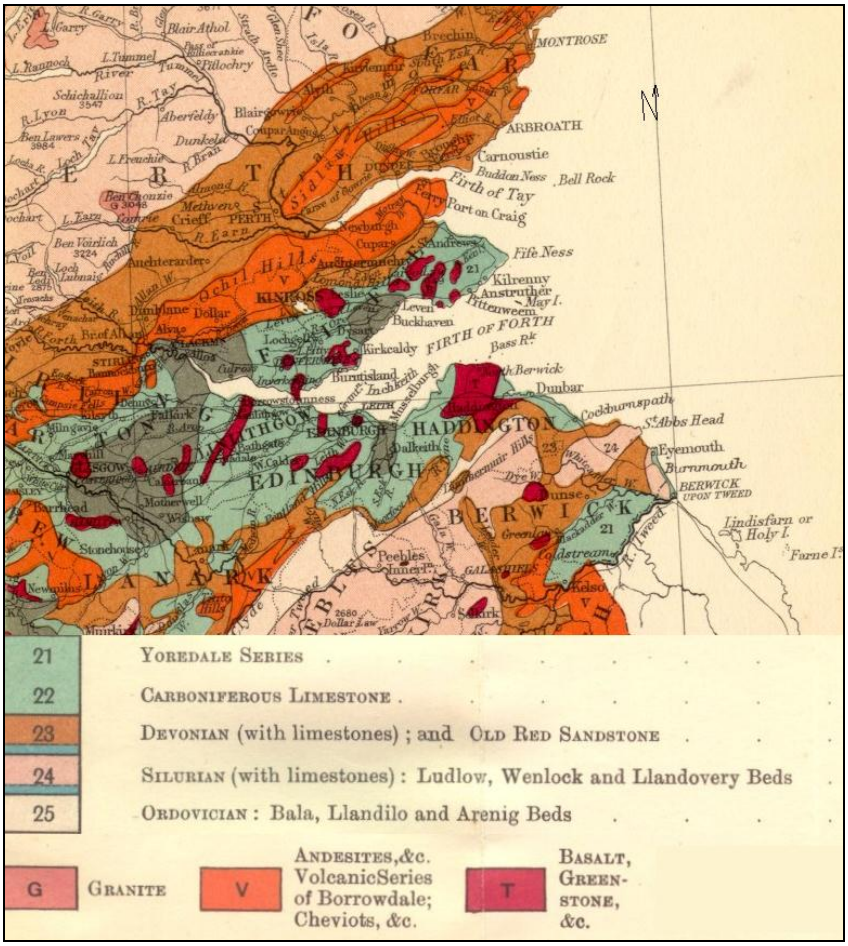

Figure 3.29. Solid geology of East Central Scotland (Woodward, 1904).

The inner estuary is constrained by the geology, resulting in narrow areas between Stirling and Kincardine Bridge (Firth *et al.*, 1997). Estimated depths at Alloa are 5 m, compared to ~20 m at Rosyth, ~70 m in the channel under the Queensferry bridges and ~40 m in the firth (Elliott and Neill, 2007). Two SSSIs are designated in the meanders west of Alloa, namely Alloa Inch and Tullibody Inch (Firth *et al.*, 1997). Navigation within this upper region is regulated to the tidal limit, but it is closed to commercial freight traffic with sedimentation in this area especially above the Alloa Inches.

In this area, low-lying cliffs of Carboniferous and Devonian age sandstones are prevalent with shore platforms, large sand banks, lowland marsh and raised beaches (Bates and Oakley, 2004; Bates *et al.*, 2004). The Firth of Forth has large areas of rock outcrops that were moulded in the direction of ice movement during the Late Devensian (GeoWise Ltd and CRGGU, 1999). The outer firth coastline has sporadic shore platforms and low-sediment bays. On the northern shore vertical bedrock cliffs are normally fronted by a cliff-edged raised beach system behind a shore platform (Firth *et al.*, 1997). The River Tyne enters the sea at Tyninghame Bay on the outer edge of the firth with its own independent estuarine system (Firth *et al.*, 1997).

Around 12,000 to 10,000 BP, when the last glacial period ended, a short period of glacial readvance named the Youger Dryas (or the Loch Lomond Re-advance) formed the Loch Lomond and Loch Menteith moraines (Gray and Brooks, 1971). Shell materials were found inside the moraines (Gray and Brooks, 1971) suggesting the head of the Forth Estuary, where the Loch Menteith moraines lie, was underwater at this time.

3.3.2 Historical Background

Edinburgh is the primary city in the Forth catchment, being Scotland's capital city, located centrally along the southern shore. Stirling, at the head of the estuary, is the secondary city. In the Forth Estuary basin 1.4 million people live (Dobson *et al.*, 2000), which is a quarter of the Scottish population. A significant portion of Scotland's industry is based around the Forth Estuary, which relies on good transport links to Scotland and the rest of Europe (Dobson *et al.*, 2000).

The natural harbour characteristics throughout the Forth Estuary have promoted water transport for hundreds of years. Small sailing ships harboured at Stirling Harbour between the eleventh and nineteenth centuries and traded regularly with Europe. Alloa, Airth and Elphinstone (Dunmore) also traded with Holland in the seventeenth century through the transport of coal (GeoWise Ltd and CRGGU, 1999).

Burntisland is one of several natural harbours in the Firth of Forth with historical records supporting claims of its utilisation as a shipping harbour for nearly two thousand years. Julius Agricola recognised its natural potential in 83 AD (Murray, 1983). Oliver Cromwell used the harbour for his head quarter in 1651. The harbour was used from 1844 as a ferry port to Granton until the Forth Railway Bridge opened. It was further used as a coal export facility and ship building with the surrounding area famed as a holiday destination for a while (Murray, 1983). It is still used as an industrial port today by Forth Ports.

Sea embankments were widespread across the Firth of Forth during the seventeenth century (Cadell, 1913; Firth *et al.*, 1997). During the Medieval Period land claim was already occurring at Airth, in the upper estuary opposite Kincardine. A basic seawall was constructed at Inch Ferryton at about 1636. Large areas of land were created by Dutch immigrants, including areas of Skinflats, near Grangemouth, in the eighteenth century (Cadell, 1913).

A total of 28.6 km^2 of intertidal mudflats or sandflats were converted into usable land between 1600 and 2008 (51% of the total intertidal land in the estuary) (Figure 3.30) (GeoWise Ltd and CRGGU, 1999; Hansom and McGlashan, 2005). Between 1600 and 1851 13.75 km^2 of the intertidal zone was claimed (24.5% of total inter-tidal zone) (Table 3.9). Between 1851 and 2008 14.85 km^2 of the intertidal zone was reclaimed (26.4% of the total intertidal zone). One such area that was claimed during this time period was for the development of the Port of Grangemouth.

	Estimated 1600 total intertidal area	**1851 total intertidal area**	**1999 intertidal area**	**Estimated loss 1600-1810**	**Estimated loss 1850-1999**
Lower estuary	11.4	10.80	7.39	0.60	3.41
Middle estuary	37.94	27.83	18.11	10.11	9.72
Upper estuary	6.72	2.58	1.96	4.14	0.62
Total	56.12	41.21	27.46	14.85	13.75
Percentage of original area	100%	73.46%	49.0%	26.4%	24.5%

Table 3.9. Estimated areas of intertidal change over the last 400 years in km^2 in comparison with change in the last 150 years (GeoWise Ltd and CRGGU, 1999:18).

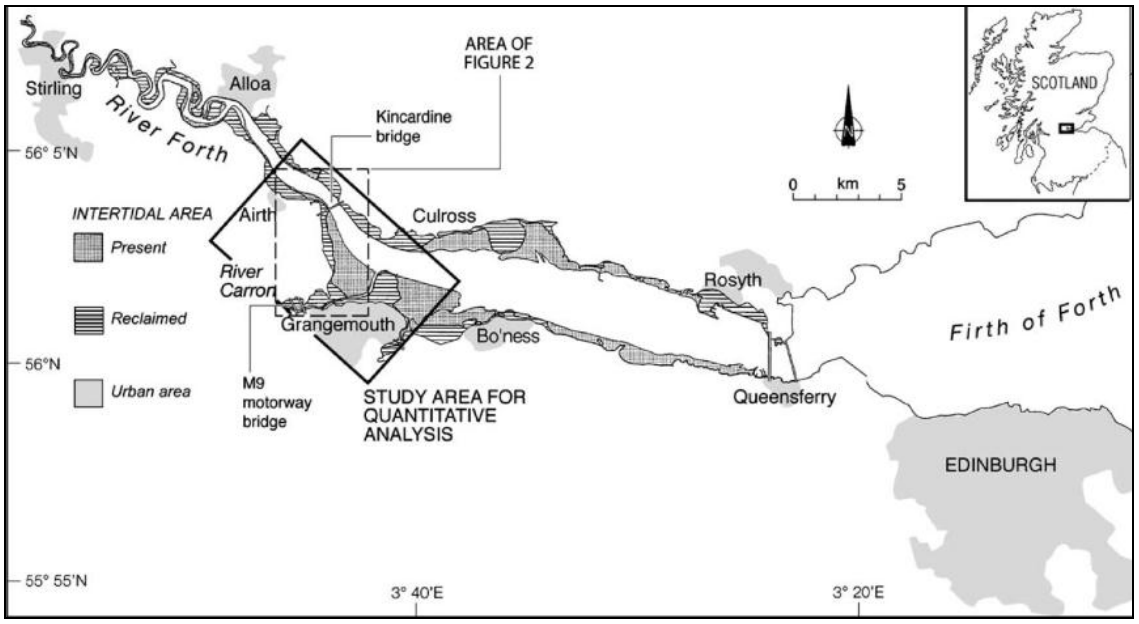

Figure 3.30. The intertidal reclaimed land within the estuary between Stirling and the Queensferry bridges (Givear *et al.*, 2004:381). Land claim is predominantly located in the upper estuary above Queensferry.

Land claim had a dramatic effect on the ecological value of the estuary. Loss of half of the intertidal zone resulted in the large percentages of the natural habitats being removed, which would have provided for protected and non-protected species today. The fish species of the estuary may have suffered as 24% of natural fish habitats and 40% of the fish food supplies were lost (McLusky *et al.*, 1992). Bird habitats were reduced, which included habitats required by the protected dunlin and bar-tailed godwit (McLusky *et al.*, 1992).

Greenwood and Hill (2003) estimated that only 22.62 km^2 of intertidal mudflats remain unclaimed in the estuary, the largest of which is at Kinneil (5.71 km^2 at MHWS and 6.42 km^2 at MHWN). Areas close to claimed land, Kinneil and Skinflats, are host to several populations of fish including flounder, plaice, whiting, gobies, eelpout, cod, and common dab (Greenwood and Hill, 2003).

Scottish tide gauges are not affected by major tectonic movement (Shennan *et al.*, 2002); however mining subsidence has been an issue in some areas. These coal mining activities were prevalent in the Forth Estuary and Firth of Forth, but not the Tay Estuary. All underground mining activity has ceased with the last deep mine at Longannet closed in 2002. The Coal Authority (2010a;b;c;d) asserted that all mining subsidence in the locations directly surrounding local tide gauges has stopped (Appendix 3).The Forth has a long history of underground and open cast mining, which has led to subsidence in some areas including under the channel, saltmarshes and mudflats. In the inner estuary the worst affected areas are near Alloa, Fallin (Polmaise Mine), the Inch Ferryton area, South Clackmannan and Airth (GeoWise Ltd and CRGGU, 1999).

There have been mining activities within the Dysart-Buckhaven area of the firth for over 800 years, both opencast and underground (Saiu *et al.*, 1994). Underground mining, which was initially limited by water ingress, became more productive in Dysart from 1791 and Wemyss from 1838 when steam pumps were introduced (Saiu *et al.*, 1994). Powerful haulage and windings meant that in the 1860s coal was being mined to depth of 915 m.

Extraction techniques associated with this area, according to Saiu *et al.* (1994), included 'stoop and room' and 'longwall'. Stoop and room consisted of leaving coal pillars to support the roof. Longwall mining consisted of removing large areas of coal and allowing immediate roof collapse. Subsidence was less likely to occur with stoop and room, but if subsidence did occur it could happen at any point within the next 100 years. The longwall mining technique would result in immediate subsidence with a 6 month residual period (Saiu *et al.*, 1994).

The maximum level of subsidence would be equal to 80% of coal extracted from each seam where there may be over ten seams that have been worked. Between Dysart and Buckhaven 19 seams have been worked with depths ranging from 30.48 m to 457.20 m (Saiu *et al.*, 1994). It is unlikely that these seams lie directly above one another, therefore the potential for 19 seams worth of subsidence at one location is low. The likelihood that these seems would subside now after this time is low, as already stated by Saiu *et al*. (1994).

The largest collieries within the Dysart-Buckhaven area were the Wellesley, Michael and Frances. The waste material from their mines were heaped onto rock platforms on the coastline. These waste piles were known as 'bings' (Saiu *et al.*, 1994). Each bing had its own characteristics depending on the method of construction and the impact of the tide. Bing sediments were distributed in both directions by the tide forming mantles of shale and sandstone that could be 2.0 to 5.0 m thick on top of foreshores and cliff footings (Saiu *et al.*, 1994). One of the Michael colliery bings was shaped to raise land levels behind the foreshore for railway sidings and workshops (Saiu *et al.*, 1994). This work resulted in the sedimentation of West Wemyss Harbour, which had been a popular industrial port previously (Saiu *et al.*, 1994). Dysart Harbour was likewise affected by the longshore transport of sediment from the Frances Colliery bing (Saiu *et al.*, 1994).

In 1947, during the period of mining nationalisation, the Michael Colliery produced the largest output at 562,455 tonnes a^{-1}, the Wellesley Colliery produced 32,659 tonnes a^{-1}, and the Frances Colliery produced 279,413 tonnes a^{-1}. By the early 1960s the Michael Colliery had increased capacity to 719,397 tonnes a^{-1}, the Wellesley Colliery to 436,356 tonnes a^{-1} and the Frances Colliery to 412,769 tonnes a^{-1}. All producing more waste to deposit along their bings. However when these three collieries each closed in 1968, 1967 and 1984, respectively, the waste material that had been acting as coastal protection was stopped (Saiu *et al.*, 1994).

The Wellesley bing was partially in the wave action zone and when eroded sediment was transported in both directions with large quantities of sediment moving with the south-eastern waves onto the Buckhaven foreshore. Prior to mining Buckhaven lay on a headland, had a substantial harbour and tourist industry. Between 1893 and 1926 Buckhaven experienced 66 to 100 m accretion rates (Saiu *et al.*, 1994). The Port of Methil, previously known as Methil Harbour, became the Wellesley Colliery harbour in 1907, then known as the Wellesley Harbour (RPA Smith, 2011). It was converted into a graving-dock for the construction of large offshore oil platforms in the early 1970s after the closure of the Wellesley Colliery, which required the shoring up of the Wellesley bing with coarse doleritic rip-rap to prevent sedimentation (Saiu *et al.*, 1994). However, this stopped sediment provision to the Buckhaven foreshore, where accreted land had been redeveloped a short period before (Saiu *et al.*, 1994).

The Michael Colliery area experienced erosion after colliery waste stopped being supplied. By 1990 only the Michael bing remained of the colliery waste between East and West Wemyss. West of the bing consistent erosion has been occurring and concrete slabs from the colliery remnants were deposited on the foreshore. Works near the Wemyss Caves have been threatened by coastal erosion since the mining works stopped (Saiu *et al.*, 1994). After the closure of Frances Colliery the bing extended beyond the cliff by 200 m and lay parallel to the coast for 760 m, but was defended by wooden structures and wire mesh in 1974 to prevent movement by the tide. Dysart Harbour was reopened around this time for recreational purposes (Saiu *et al.*, 1994). Ultimately, the decline of mining east of Kirkcaldy has reduced the amount of coal waste being deposited on the beaches as coastal protection (McManus *et al.*, 1993). This has led to coastal erosion in areas of high population and tourism (McManus *et al.*, 1993).

Much of the traditional sea trades and transport needs, such as fishing and coal mining, have declined in the last one hundred years leaving ports derelict (McManus *et al.*, 1993). Previous to this, the Forth thrived as the southern Fife coastline was heavily mined for coal and ores. The local ports facilitated transport of goods to power stations and industries along the river as well as access to ferries used to transport pedestrians, cars and trains across the Firth of Forth, east of Queensferry (Saiu *et al.*, 1994; McKean, 2006).

3.3.3 Tidal Influence and Currents

The spring tidal range within the Firth of Forth varies from 4.5 m at Tyninghame Bay to 5.3 m at Alloa (Table 3.10) (Firth *et al.*, 1997; McManus, 1998). During the daily tidal cycle the tidal flood is stronger near the northern shore and the ebb tide is stronger on the southern shore (Figure 3.31), which is due to the bathymetry and not the Coriolis Effect (Webb and Metcalfe, 1987). Tidal

calculations can be made using the harmonic constants values published by the UKHO (2008) (Table 4.3).

Site	MHWS	MLWS	Spring tide range	MHWN	MLWN	Neap tide range
Dunbar	5.4	0.9	4.5	4.2	2.0	2.2
Leith*	5.6	0.8	4.8	4.5	2.1	2.4
Rosyth	5.8	0.8	5.0	4.7	2.2	2.5
Grangemouth	5.7#	0.5#	5.2	4.5#	1.9#	2.6
Kincardine	5.8	0.6	5.2	4.8	2.3	2.5

Table 3.10. Predicted tidal range at a selection of ports in the Firth of Forth (Firth *et al.*, 1997:17).

	ML	Harmonic Constants								S. W. Corrections			
	z_0	M_2		S_2		k_1		O_1		f_4	F_4	f_6	F_6
	(m)	g^o	H.m	g^o	H.m	g^o	H.m	g^o	H.m				
Dunbar	3.03	057	1.61	097	0.55	222	0.11	069	0.15	070	0.018	070	0.003
Fidra	3.04	055	1.71	097	0.60	219	013	061	0.14	069	0.020	098	0.006
Leith	3.19	055	1.79	096	0.61	221	0.12	065	0.14	103	0.016	125	0.006
Rosyth	3.26	056	1.90	097	0.65	221	0.12	067	0.14	098	0.018	146	0.008
Grangemouth	3.10	056	2.00	101	0.68	225	0.12	064	0.15	106	0.016	156	0.011
Kincardine	3.10	060	2.21	101	0.60	219	0.13	070	0.15	065	0.018	177	0.018
Burntisland	3.26	055	1.77	095	0.59	220	0.11	071	0.13	064	0.027	129	0.012
Kirkcaldy	2.88	054	1.77	095	0.63	218	0.13	064	0.14	083	0.022	116	0.008
Methil	3.10	055	1.77	095	0.60	222	0.13	066	0.14	106	0.014	106	0.004
Anstruther Easter	3.07	052	1.62	092	0.57	217	0.13	061	0.15	132	0.011	060	0.003

Table 3.11. Harmonic constants taken from the UKHO Admiralty Tide Tables 2008 Part III (UKHO, 2008:340).

Rapid salinity reduction only begins to occur west of the bridges at Queensferry with a drop from 25 psu at Queensferry to 10 psu at Alloa with 5 psu signifying the saline isohaline, i.e. the saline tidal limit, between 5 and 20 km east of Stirling (Firth *et al.*, 1997; McManus, 1998). The Firth of Forth is generally well-mixed. In the outer area of the firth 30% of the fish species are marine

juveniles and 15% are seasonal marine species. Further into the estuary, in the inner firth where the salinity drops to under 30 psu, marine juveniles decrease and marine seasonal species (Greenwood and Hill, 2003).

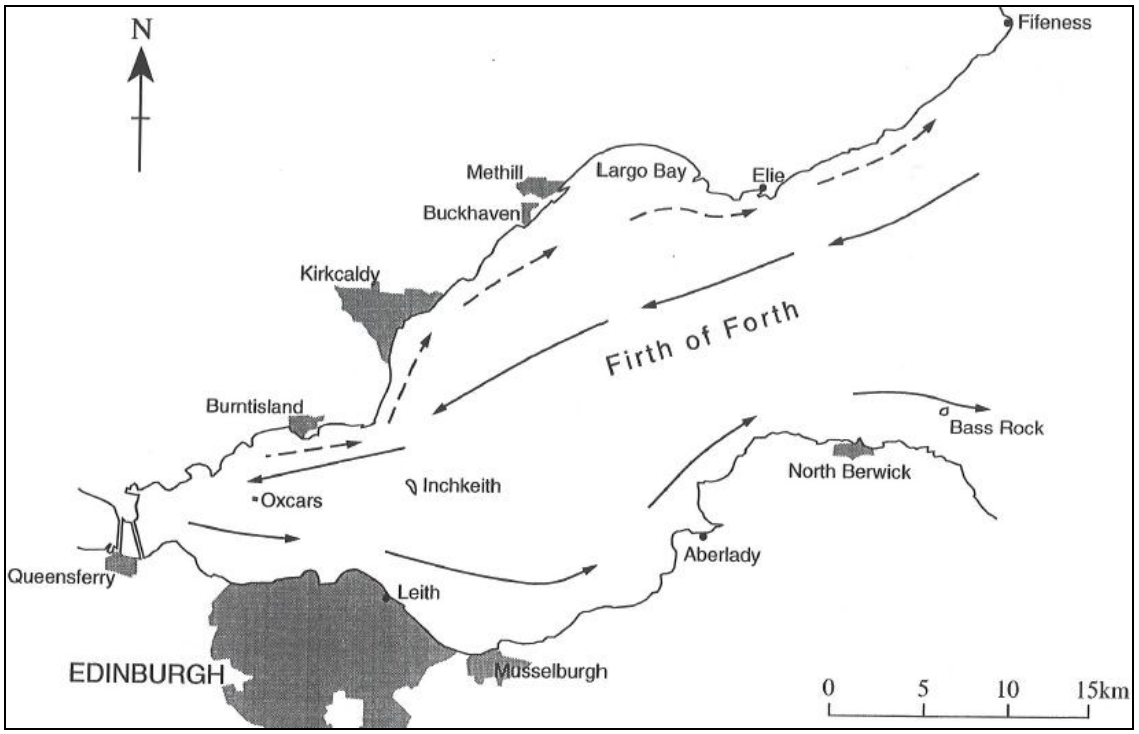

Figure 3.31. Tidal currents in the Firth of Forth (Firth *et al.*, 1997:22).

Tidal stream velocities have been calculated by the UKHO based on high water at Leith (Imray Laurie Norie & Wilson Ltd., 2007). A large variety of locations have been measured within the Firth of Forth including areas near North Carr Lightship, Bass Rock, Kirkcaldy, Leith and Rosyth (Imray Laurie Norie & Wilson Ltd., 2007).

Within this estuary, as with most estuaries, the tidal cycle is skewed by local characteristics. For example, there is a mean flow velocity of 0.8 to 1.1 ms^{-1} during an ebb tide and 0.5 to 0.8 ms^{-1} during a flood tide (Clarke and Elliott, 1998; Elliott and Neill, 2007). Above Grangemouth the tidal curve is skewed by shallow water properties that advance the low tide and delay the high tide (Webb and Metcalfe, 1987). Another example is that in the lower reaches of the Forth a slack period occurs at low water (Webb and Metcalfe, 1987).

The major rivers supplying 75% of the fluvial flow to the estuary are the Rivers Forth, Teith and Allan to the west, which together contribute an average daily flow rate of 61 m^3s^{-1} (Firth *et al.*, 1997; Clarke and Elliott, 1998; Dyke, 1987). According to Dobson *et al.* (2000) the mean river daily discharge is 5.1 x 10^6 m^3 and the mean tidal influx is 5.1 x 10^8 m^3, which is with a estuarine river flow rate of 59.0 m^3s^{-1} compared with 5902.7 m^3s^{-1} tidal.

As the wave is squeezed into a narrowing and shallowing estuarine environment it is forced upwards and forwards into the estuary. If an estuary narrows or steepens significantly over a short distance the tidal range increases enough to form a tidal bore, a shock wave that is forced forward in order to propagate above the shallow water depth, which happens 6 km east of Alloa (Webb and Metcalfe, 1987).

The Lackie tide is an unusual example of shallow water anomaly that can be seen at slack tide as double high tide and low tide in the inner estuary between Grangemouth and Stirling (Firth *et al.*, 1997; Elliott and Neill, 2007; Webb and Metcalfe, 1987). Fundamentally, the semi-diurnal wave that imposes the twice daily tides is superimposed by a higher frequency harmonics wave by the shallow water mechanics (Webb and Metcalfe, 1987). Unusually, even though the double high water tides occur up the estuary to Stirling the double low water tides cease at Kincardine Bridge.

Some studies, such as 'Hydroacoustic Communications in the Firth of Forth' by the University of Bangor and Heriot-Watt University, set up temporary tide gauge stations for short term study. The University of Bangor (2009) set up a tide gauge at North Berwick in the outer firth for 3 months in 1995. While these results are too short for long term study or tidal prediction they can be used to identify tidal harmonics and establish the elevation and boundary conditions (University of Bangor, 2009). Where the estuary narrows at the Queensferry headland, the river and tidal current forced through the narrowed space are concentrated, which leads to an increased scour effect resulting in a localised increase in depth.

The surface wave environment can impact the coast, therefore information about the predominant direction of wind and surface waves was collected. Unlike the Tay Estuary, which has a predominant north eastern wind and surface wave direction, the Forth Estuary predominantly has wind approaching from the south west (Harrison, 1987). The wind roses produced by Harrison (1987) suggested that not only was this the most consistent direction for wind, but also the direction from which the strongest gusts of wind came from. This suggests that waves from this direction may potentially be large, however this wind is coming over-land, so there is no opportunity for a build up of wave energy over a long fetch.

3.3.4 Estuarine Sediment Dynamics and Bathymetry

The River Forth is the primary supplier of fluvially-derived sediment, supplying over 311,000 m^3 (99,790 tonnes) more than the Teith (76,455.49 m^3 or 24,494 tonnes) and the Allan (35396.06 m^3 or 11,340 tonnes) of solute and sediment load (Firth *et al.*, 1997). A large percentage of the River Forth sediment is fine-grained, which feeds the upper estuary mudflats (Firth *et al.*, 1997). Within

the estuary fine sediments are prevalent with boulders, pebbles, sands and silts along the beaches and shore edges (Figure 3.32) (Firth *et al.*, 1997).

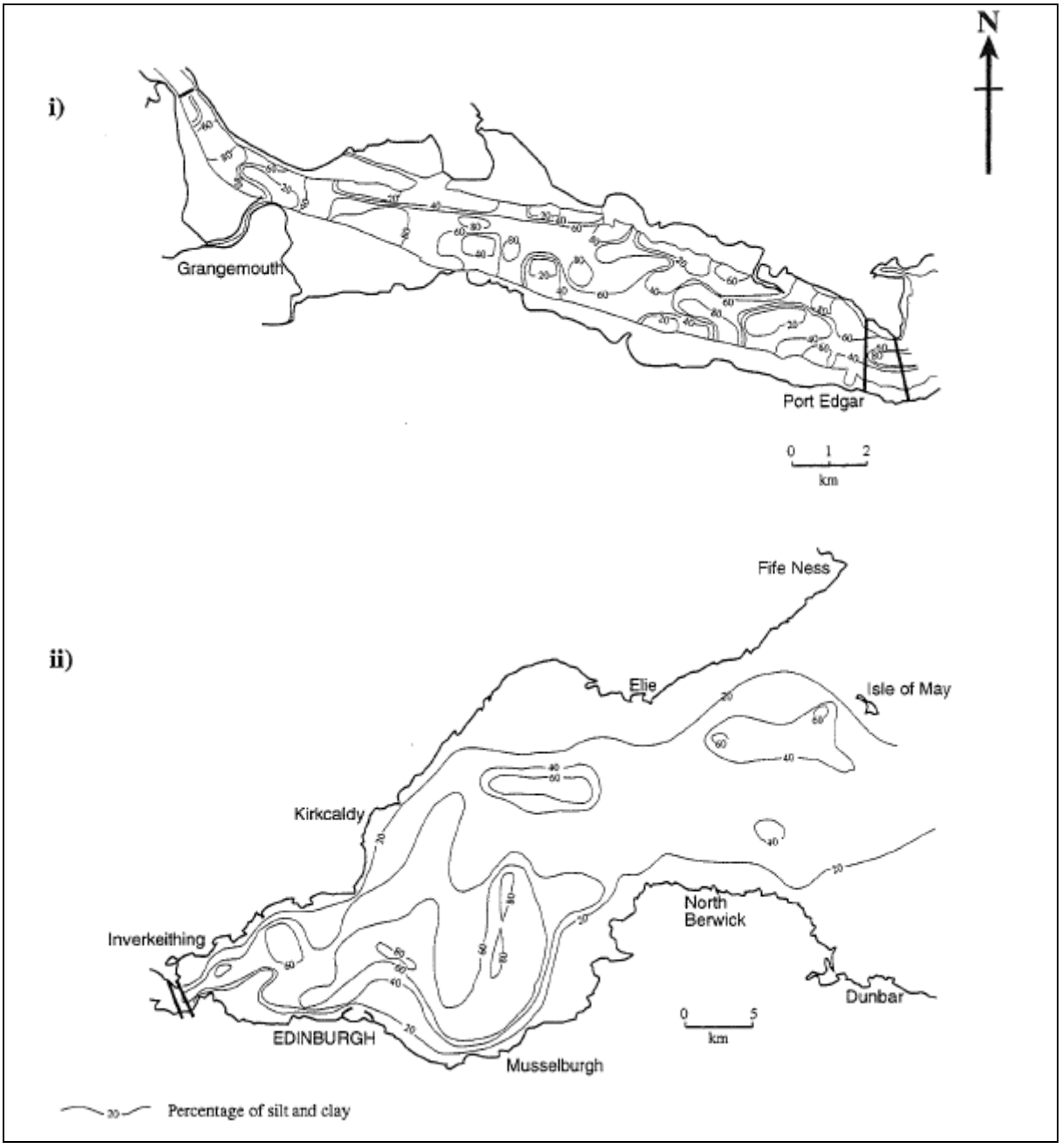

Figure 3.32. Seabed sediments in the Firth of Forth (Firth *et al.*, 1997:23).

Several bathymetry studies of the Firth of Forth have been conducted, with most studies focusing on the area around the Forth Road Bridge and Forth Railway Bridge at Queensferry (Baxter *et al.*, 2008). Dawson *et al.* (2007) presented a bathymetry map, which focused on the bathymetry of the Firth of Forth with an overlap into part of the estuary (Figure 3.33). The University of Bangor (2009) created a bathymetric model of the entire Firth of Forth between Queensferry and North Berwick, which also focused at a higher resolution on the two bridges at Queensferry (Figure 3.33).

These bathymetric maps agree on areas as deep as 60 m in the channel off the coast of North Berwick as well as in the inner Firth of Forth shipping channel seaward of the bridges at Queensferry.

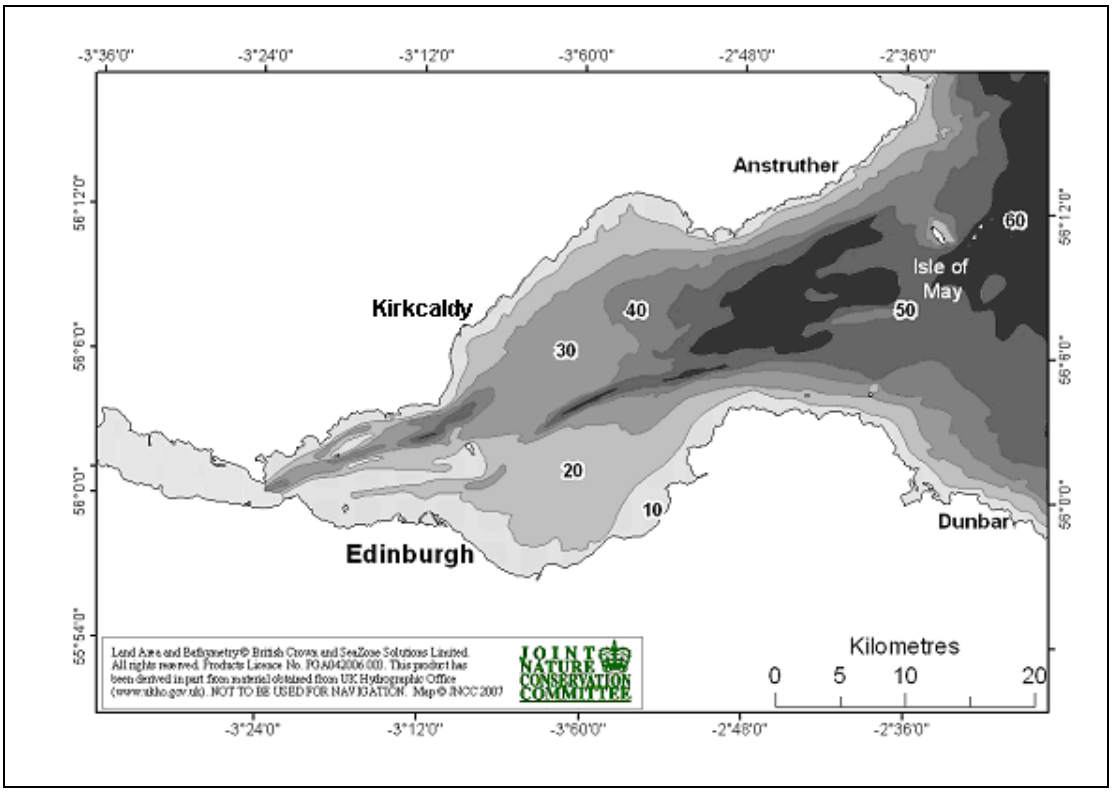

Figure 3.33. Firth of Forth bathymetry in metres (Dawson *et al.*, 2007:9).

Sand within the system can be found on fine-sediment bayhead beaches and dunes, which are both active and relict dunes in the outer firth. Dune systems are more prominent on the southern coast (Firth *et al.*, 1997). In the inner firth, between the bridges at Queensferry and Kincraig Point on northern shore and Eyebroughty on the southern coast (Figure 3.28; Figure 3.27), there are extensive areas of intertidal sediments. Along the southern coast stretches of gravels and coarse sand form the sandflats at the heavily sedimented mouth of the River Esk in the inner firth and a large sand stretch known as Drum Sands lies at the tidal mouth of the River Almond.

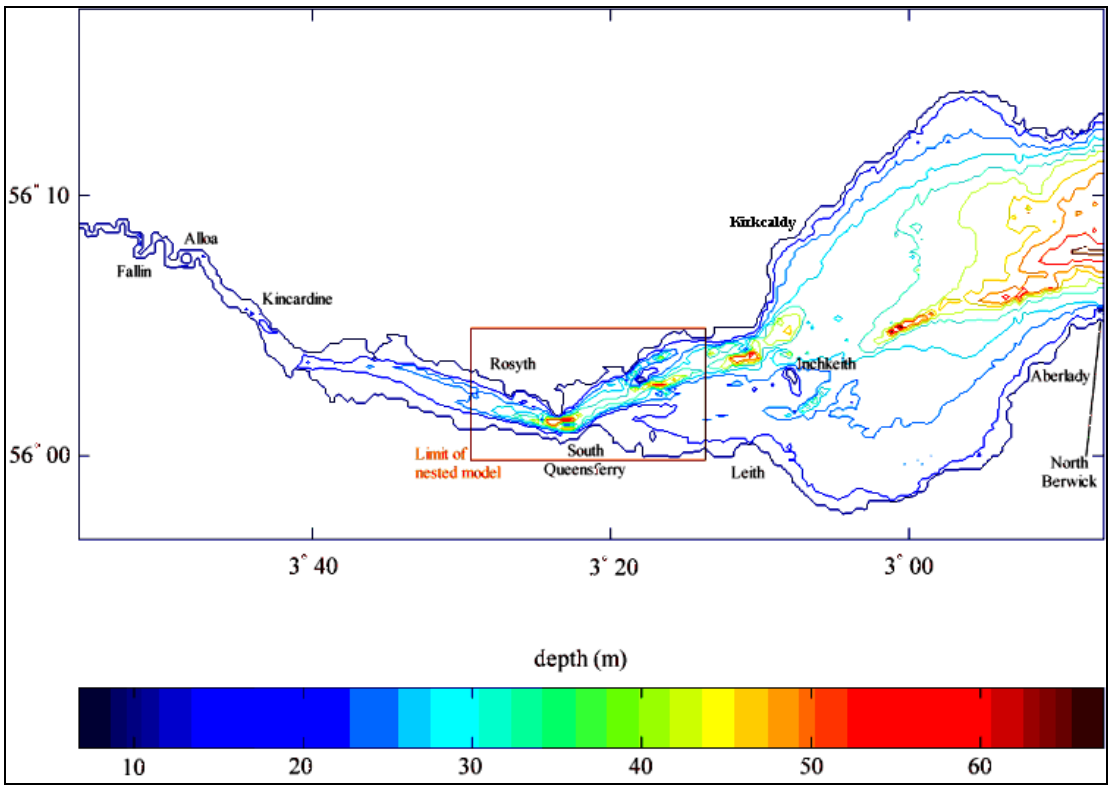

Figure 3.34. Bathymetry of Firth of Forth Tidal Limit (University of Bangor, 2009).

On the north shore of the firth, erosion is occurring and the only river, the River Leven, is only a minor source of fluvially-derived sediment (Firth *et al.*, 1997). This shore has narrow beach stretches with some dune fields to the east. The dune fields are mainly stable with some peripheral erosion (Firth *et al.*, 1997). Around the bridge piers, foundations and nearby seawalls fine sediment accumulates, whilst the channels remain clear (Firth *et al.*, 1997). Figure 3.35 illustrates the rock outcrops that the Firth of Forth bridges at Queensferry rest on and the unusual fluctuation in seabed depth, caused by glacial and postglacial processes.

Within the estuary between Stirling and the Queensferry bridges sandbanks can dry to +1 m OD with channel depths near Alloa of -9.28 m OD (TERC, 1991). The outer estuary, between Kincardine Bridge and the Queensferry bridges, is characterised by a number of embayments and promontories (Firth *et al.*, 1997). Some of these promontories were created through centuries of land claim. The Rivers Carron and Avon join the estuary at Grangemouth on the south side. Mudflats are continuous on the south side of the estuary, fluctuating from a width of 2 km at Grangemouth to 200 m at Bo'ness. Saltmarsh backs the mudflats, although some parts of the saltmarsh on the channel margin are eroded periodically (Firth *et al.*, 1997).

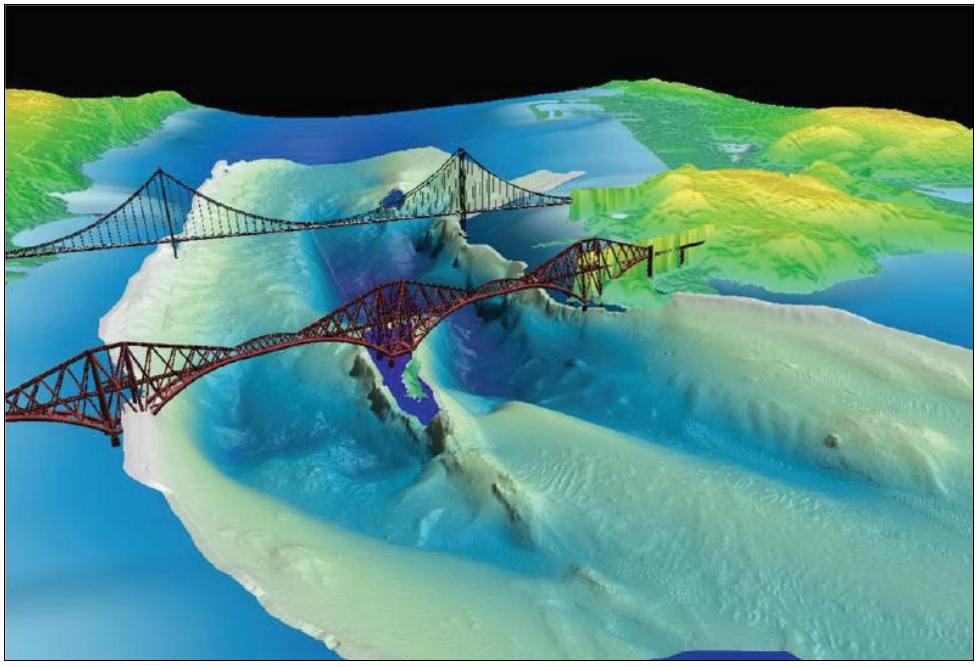

Figure 3.35. 'Rock outcrops used to support the Firth of Forth bridges obtained using multi-beam echo-sounders' (Baxter *et al.*, 2008:29).

The north coast in the outer estuary is characterised by mudflats and intertidal shore platforms. There are fewer harbour facilities in the estuary, but seawalls and earth embankments to facilitate land claim are almost continuous along the coastline (Firth *et al.*, 1997). There are no seawalls in the Kincardine Bridge area where the saltmarsh is extensive (Firth *et al.*, 1997) except to protect the Kincardine Power Station.

3.3.5 Modern Port Facilities and Conservation Features

Some of the ports in the Forth Estuary (Table 3.12) have been redeveloped into leisure ports. However, several industrial ports remain with Grangemouth being a major oil refinery and container terminal and other sites along the estuary maintaining major transportation links and renewable energy units (McLusky, 1987).

In the firth, the Port of Leith, in the mouth of the Water of Leith, is ideally situated as a shelter against oceanic storms. Leith has a colourful history dating back to before 1544 when the Earl of Hereford constructed the first pier (Mackintosh, 2010). The first wet dock was completed in 1806, Old East Dock, with Victoria Dock, Albert Dock, Edinburgh Dock and Imperial Dock all in use by 1902 (Mackintosh, 2010). Additional to these, the Port of Leith also has the Prince of Wales Dock and Western Harbour through which all traffic navigate (Figure 3.36; Table 3.13).

Crail,	Dysart,	Aberdour,	Charleston,	Cramond,
Cellardyke,	Port Seton,	Braefoot Terminal,	Alloa,	Newhaven,
Anstruther Easter,	Buckhaven,	Dalgety Bay,	Stirling,	Granton,
Pittenweem,	Kirkcaldy,	North Berwick,	Grangemouth,	Leith,
St. Monans,	Carron,	Inverkeithing,	Cockenzie,	Fisherrow,
Elie, Earlsferry,	Seacliff,	North Queensferry,	Blackness,	Cove
Lower Largo,	Dunbar	Rosyth,	Port Edgar,	(Figure 3.27)
Methil,	Pettycur,	Brucehaven,	Hawes Pier,	
West Wemyss,	Burntisland,	Limekilns,	South Queensferry,	

Table 3.12. Ports and harbours in the Forth Estuary (Mackintosh, 2009).

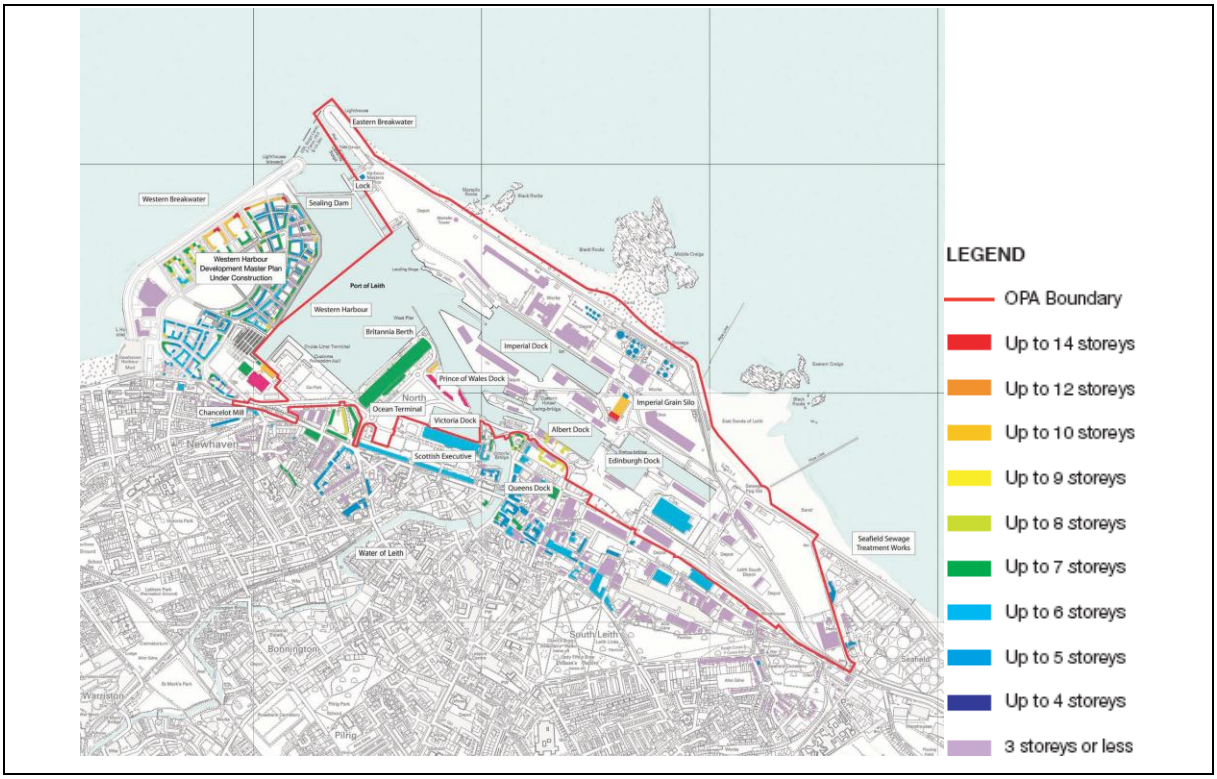

Figure 3.36. Leith development area (Ove Arup & Partners Scotland Ltd, 2007).

Forth Ports at the Port of Leith is accountable for managing the water level within the impounded port to prevent flooding in the local area. Potential flood risk is higher here due to the additional water input from the Water of Leith into the impounded port. Effective prediction of tidal and fluvial water levels is needed to ensure the impounded water depth is deep enough for ship draft and shallow enough to accommodate fluvial flow throughout the high tide period, which is a unique challenge for impounded docks. Fluvial flows are released from Western Harbour through culverts, the shipping lock and penstock valves.

Berths	Maximum Depth	Quayside Length
Imperial Dock	9.15m	1,396m
Imperial Basin	9.5m	200m
Albert Dock	7.2m	840m
Edinburgh Dock	7.2m	1,200m
Harbour Berth No 6	7.2m	150m
Harbour Berth No 8-12	9.5m	305m
Cruise Berth	9.75m	570m

Table 3.13. Port of Leith Berths (Forth Ports, 2010).

Leith accepts cruise liners, dry bulk, general cargo and grain products, with a designated cruise liner berth. Leith is also a site of recent development with Victoria Quay Scottish Government buildings and Ocean Terminal shopping centre, and plans for several urban villages to be developed on previously active areas of the port (Figure 3.37) (Forth Ports, 2010; Mackintosh, 2010), though this has been superseded at the time of writing by cargo handling requirements and the residential and retail aspirations have been reduced to allow for renewables manufacturing opportunities.

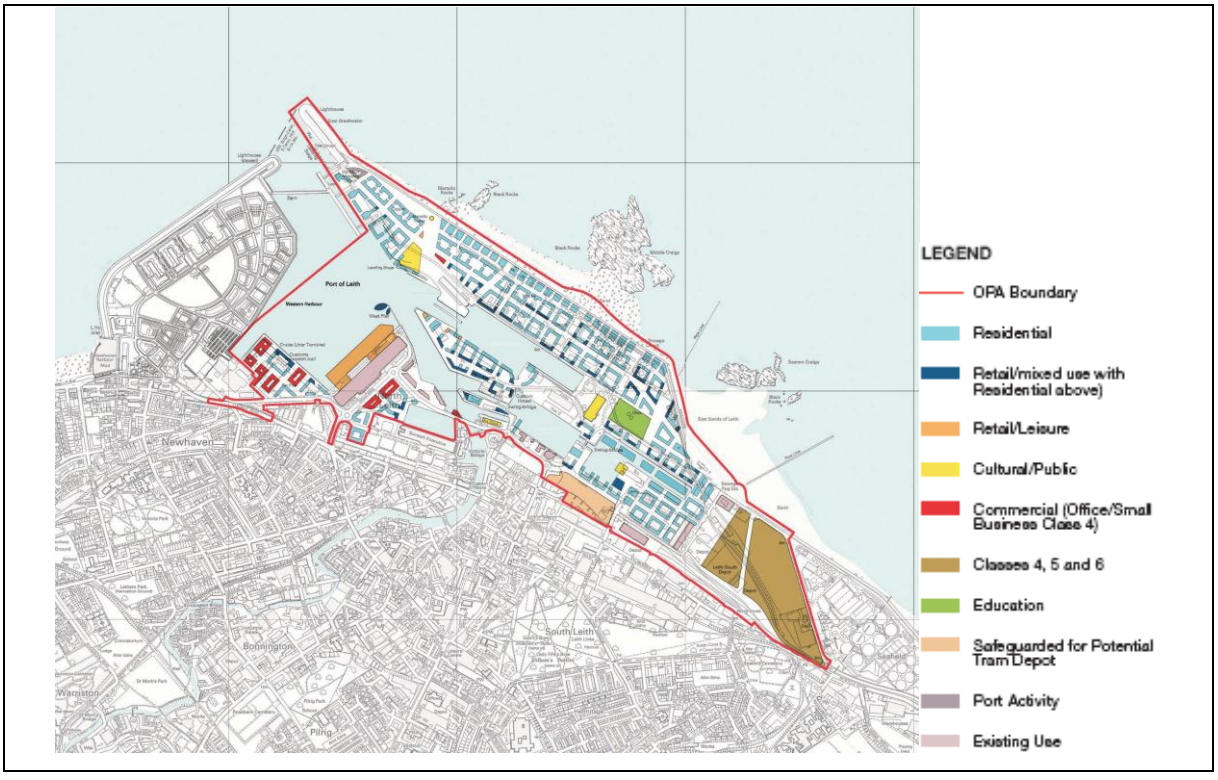

Figure 3.37. Leith proposed development (Ove Arup & Partners Scotland Ltd, 2007).

In the Forth Estuary the Port of Grangemouth is of considerable size (Figure 3.38) with a lock entrance 237.6 m long by 29.1 m wide (Forth Ports, 2010). The port has three main operational areas: the hydrocarbons basin, the Grange Dock and Carron Dock: handling a range of cargos from hydrocarbons and edible oils to forest products (Table 3.14). This port can handle liquid bulk,

containers, dry bulk, general cargo, forest products and grain. The port has the largest capacity for containers in Scotland with a threshold of 400,000 TEU per annum (Forth Ports, 2010).

Figure 3.38. Port of Grangemouth (Google Maps, 2012).

Berths	Maximum Depth	Quayside Length
Carron Dock	5.0m to 6.4m	355m
Forest Products Berth	7.5m	600m
Eastern Channel:-	-	-
1 - Common User Jetty	10.0m	-
4 - Private Jetties	11.0m	-
1 - Private Jetties	6.7m	-
1 - LPG Private Berth	8.0m	-
Grange Dock	7.7m	2,175m

Table 3.14. Port of Grangemouth Berths (Forth Ports, 2010).

Sedimentation of harbours can be a major issue. Nicholson and O'Connor (1986) modelled a sedimentation problem at the Port of Grangemouth harbour gate, which came about after the installation of a new gate in the 1970s. The harbour authority authorised several sedimentation studies around the harbour gate and approach channel in the late 1970s and early 1980s to improve their knowledge of sedimentation in the area (O'Connor, 1994). Present day sedimentation in the Port of Grangemouth area is controlled by the port dredging regime.

Christopher Jones of the UKHO Tides Department (pers. comm.) commented on a well-known sedimentation issue at Dunbar Harbour. In this circumstance Dunbar was one of three sites being

assessed for potentially replacing Liverpool as the Ordnance Datum reference site. However, Newlyn in Cornwall was not suffering from sedimentation problems and was chosen instead.

3.3.6 Conservation Status

The environmental importance of the area has been highlighted by the Ramsar designation covering the entire Firth of Forth between the Alloa Inches and the estuary mouth. The reasoning behind this designation includes the 1988 and 1993 surveys of the Firth of Forth recording 79,000 waterfowl including 37,000 wildfowl and 42,000 waders (GeoWise Ltd and Coastal Research Group, Glasgow University (CRGGU), 1999).

This area is also covered by SPA and SSSI designations. The Forth islands of Inchmickery, Isle of May, Fidra, Lamb, Craigleith, Bass Rock and Long Craig are protected by SPA and four SSSIs (including individual designations for Inchmickery, Isle of May and Bass Rock). A third SPA protects a breeding population of tern around Imperial Dock Lock at Leith (Figure 3.39) (Jennings *et al.*, 2010).

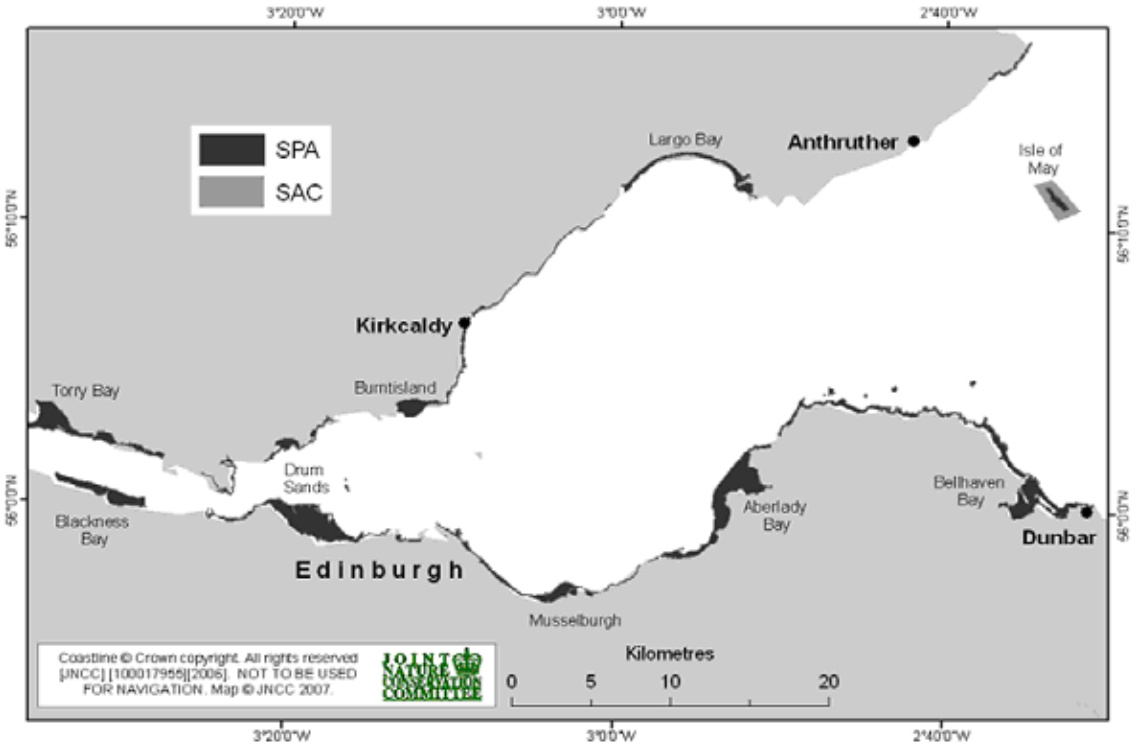

Figure 3.39. SPAs and SACs in the Firth of Forth (Dawson *et al.*, 2007).

The final two of the seven SSSIs in the Firth of Forth cover areas of the Barns Ness coast (south of Dunbar) and the Fife Ness coast for their saltmarsh and geological importance (Firth *et al*., 1997). There are two Country Parks in this region based at Tyninghame Bay (John Muir) and Long Craig

Island. LNRs include Torry Bay, Skinflats, Kinneil Kerse, Aberlady Bay and Bass Rock. RSPB sites can be found on Inchmickery, Lamb and at Skinflats. There are also several Scottish Wildlife Reserves in the Firth of Forth, including on Inchkeith and Long Craig amongst others (Firth *et al.*, 1997).

3.4 Conclusions

Both estuaries share some physical characteristics, due to their location on the east coast of Scotland and their firth geomorphology. Both estuaries are macrotidal, funnel-shaped and have a spring tidal range of approximately 5 m at the mouth. The tidal range and high water level progressively change within the estuaries; tidal heights are greater in the inner estuary, whilst the tidal range decreases between the middle and inner estuary.

The Forth Estuary is very different to the Tay Estuary in its morphology, but shares similar tidal influences and has a similar historic background. The Forth Estuary coastline is rich in intertidal shore platforms, with fine- and coarse-sediment beaches and dune systems occurring in places. Throughout the Tay Estuary, mudflats and sandbanks are common with dune systems near the mouth. In the Forth Estuary there is a significant change between the *firth* and the *estuary*, with shallow-water characteristics appearing above the bridges at Queensferry where mudflats and sandbanks prevail in contrast to the firth. This sudden transition is not apparent in the Tay Estuary.

Eleven rivers enter the Forth Estuary at staggered locations along its course, providing low amounts of freshwater and sediment from across the catchment. The Tay Estuary has two rivers at the head of the estuary supplying freshwater and sediment that are of insignificant quantities compared to those provided from marine sources, but considerably greater than that supplied to the Forth Estuary (Jenkins *et al.*, 2002).

Human interaction with the both estuaries for sea transport has been documented for nearly two thousand years. Both estuaries have been morphologically adapted through land claim, but areas of the upper Forth Estuary have also been utilised for coal extraction. Both estuaries are still used for industrial port operations, up to Grangemouth in the Forth Estuary and Perth in the Tay Estuary.

Chapter 4 - Methods

4.1 Research Design

The methods used in this thesis were selected after creating a research design, which focused in the thesis aims. Principally the research design was driven by the need for accurate and effective methods for tide gauge data collection, tide gauge data validation, data analysis for land movement, sea level oscillation identification, storm surge identification and relative sea level adaptation. The methods implemented in this thesis are discussed in the following sections, the most important of which include:

- Tide gauge data collection – collecting data from ports and institutions though site visits, logging the high and low tides into Excel spreadsheets from records recorded on paper, and using Excel macros to find high and low tides from records recorded in a digital format;
- Tide gauge data validation – manually checking records of errors, reviewing data maintenance and calibration records, and converting data from the local datum to Ordnance Datum;
- Data analysis of land movement influence on relative sea levels – investigating the Shennan *et al.* (2011) glacio-isostatic levels for the locality, and converting the relative sea level trend from 1900 to the local eustatic sea level trend using the glacio-isostatic values to illustrate the influence of glacio-isostasy;
- Sea level oscillation identification – using Morlet wavelet analysis proposed by Torrence and Compo (1998) to identify the power of sea level cycles and their time locality;
- Storm surge identification – extracting information from historical records of surge events and flooding, analysing sea level maxima using the method applied by Graff (1981), and analysing residual tide gauge data for surge events over 400mm;
- Relative sea level model adaptation – adapting the UKCP09 probabilistic projections model so that it included the updated Shennan *et al.* (2011) relative-land level glacio-isostatic levels for the locality, adapting the Vermeer and Rahmstorf (2009) temperature-sea level relationship model to include the Shennan *et al.* (2011) glacio-isostatic rates and the Wada *et al.* (2010) groundwater extraction rates, comparing the pre-adaptation and post-adaptation rates, and comparing the post-adaptation rates against present day infrastructure rates following a method used by Forth Energy (2010) at a port in this region.

4.2 Data Collection

4.2.1 Local Tide Gauge Data

Data have been recorded by various tide gauges in the Forth and Tay Estuaries and Aberdeen since 1862 (Figure 4.1; Table 4.1). Aberdeen data have been included for data validation because of the port's proximity to the study site, its recording longevity and its reputation as a stable tide gauge site (Woodworth *et al.*, 1999).

Data records that are used in this thesis are described as either:

- Paper records - records that were originally recorded directly onto paper and have not previously been transposed into a computerised format. The high and low tide from the paper records were manually transcribed from the paper records into Excel spreadsheets, which is referred to in this section as *digitised*. These records are subject to minimal potential human errors during transcription; or
- Digital (electronic) records - any form of tidal data provided in a computerised format. Some of these datasets may have originally been recorded onto paper and then transposed into a digital format and corrected by the data provider. The Forth Ports data was provided in minute-by-minute frequency in Excel spreadsheets, which were then processed using an Excel Macro that extracted the turning points.

	Type of Sensor	Sensor Model	Start Year	End Year	Provider
Aberdeen	Float	-	1862	1930	PSMSL
Aberdeen	Float	Cary-Porter	1930	1967	PSMSL
Aberdeen	Pressure		1931	1963	BODC-PSMSL
	(1930-67)	Cary-Porter			
	(1967-80)	Munro			
	(80-present)	Dataring/Digiquartz			
Aberdeen	Float	Munro	1967	1975	PSMSL
Aberdeen	Pressure	Neyrpic Bubbler	1975	1976	PSMSL-
Aberdeen	Float	Munro	1979	1985	PSMSL
Aberdeen	Pressure	'A Class' Bubbler	1985	1993	PSMSL
Aberdeen	Pressure	'A Class' Bubbler	1994	2008	PSMSL
Arbroath	Pressure	Impress	2007	2009	SEPA
Bridge of Earn	Pressure	Impress	1992	2009	SEPA
Dunbar	Float	Cary-Porter	1913	1951	PSMSL-OS
Dunbar	-	-	1973	1974	PSMSL
Dunbar	-	-	1974	1979	UKHO
Dundee	Float	-	1897	1912	PSMSL
Dundee	Pressure	Valeport 710	1987	2008	FP
Dundee	Pressure	VMT	2008	2011	FP
Earn Confluence	Pressure	Valeport 710	2008	2009	PKC
Grangemouth	Float	Munro	1979	1997	FP
Grangemouth	Pressure	Valeport 710	2003	2008	FP
Grangemouth	Pressure	Valeport MIDAS TMS (VMT)	2008	2011	FP
Leith	-	-	1949	1954	PSMSL/BODC -
Leith	Float	A. Lege	1954	1979	PSMSL/BODC
Leith	Float	Munro	1979	1980	PSMSL/BODC -
Leith	-	-	1980	1981	UKHO
Leith	Pressure	(A.) Ott	1980	1981	PSMSL-BODC
Leith	Pressure	(A.) Ott	1981	1981	BODC
Leith	Float	Munro	1981	1989	BODC*
Leith	-	Potentiometer	1988	2008	PSMSL
Leith	Pressure	FT Bubbler	1990	2008	BODC

Leith	Pressure	Valeport 710	2003	2008	FP
Leith	Pressure	MT Bubbler 2nd FT Bubbler	2006	2008	BODC
Leith	Pressure	VMT	2008	2011	FP
Methil	Pressure	Valeport 710	2003	2008	FP
Methil	Pressure	VMT	2008	2011	FP
Musselburgh	Pressure	SEPA 5 m transducer	2006	2008	SEPA
Newburgh	Pressure	Valeport 710	2007	2009	PKC
Newport-on-Tay	-	-	1972	1990	TERC
Newport-on-Tay	Pressure	Impress	1995	2009	SEPA
Perth	Pressure	Valeport 710	1991	2009	SEPA-PKC
Perth	Pressure	Valeport 710	2006	2009	PKC
Rosyth	Float	-	1912	1920	UKHO
Rosyth	Float	Cary-Porter	1955	1995	PSMSL/UKHO
Rosyth	Pressure	Valeport 710	2003	2008	FP
Rosyth	Pressure	VMT	2008	2011	FP
Stannergate	-	-	1978	1990	TERC

Table 4.1. Types of gauges (format taken from Watson *et al.*, 2008) (MT = Mid-Tide; FT = Full-Tide; - = tide gauge information lost; FP = Forth Ports). For information about different types of tide gauge sensors refer to Box A5.1 in Appendix 5.

Several organisations hold tidal data relevant to the Forth and Tay Estuaries. Data were collected from the Permanent Service for Mean Sea Level (PSMSL), the British Oceanographic Data Centre (BODC)/National Tidal and Sea Level Facility (NTSLF), the Scottish Environment Protection Agency (SEPA), Perth and Kinross Council (PKC), the UK Hydrographic Office (UKHO), Forth Ports and the former Tay Estuary Research Centre (TERC) of the University of Dundee.

Some sources allow free access to their data via the Internet, including the PSMSL with the NTSLF (through the Proudman Oceanographic Laboratory (POL) or the National Oceanography Centre (NOC)) and the BODC, although data requests are needed for high frequency data. All other data sources require direct data requests for all data access. Each source has its own format for presenting data; in fact some sources have more than one format and may include variations in recording frequencies, meteorological data inclusion and associated background information.

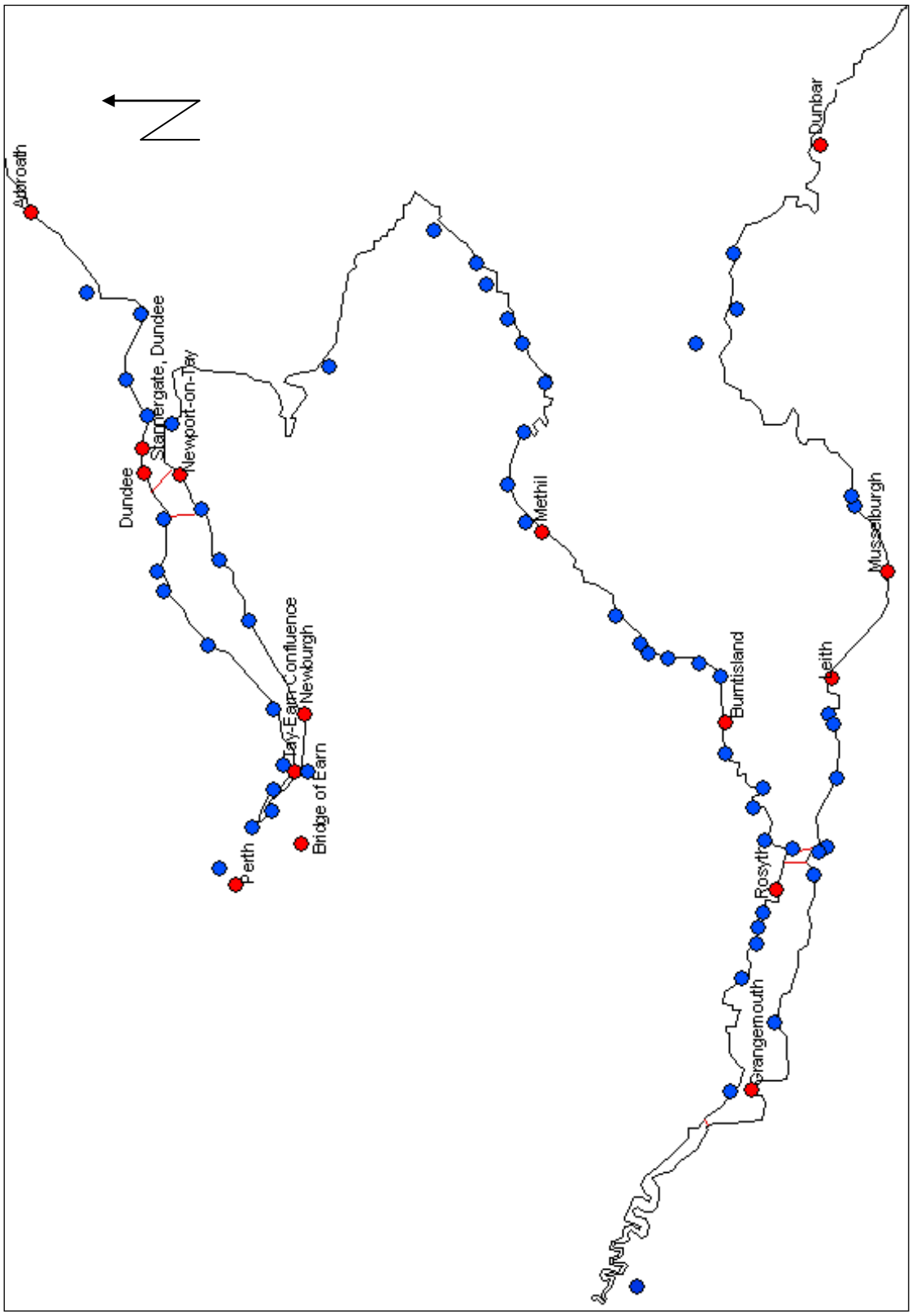

Figure 4.1. Location map. Blue = Current or historical ports, harbours or landing areas where no data have been found, Red = Ports, harbours or landing areas where data have been found (some locations taken from Duncan, 1996).

Data collected from the PSMSL, through POL, were available online in monthly or annual frequencies complete within one file. These data were copied from their webpage into a word or text file. Additional collection information as was provided online and in metadata files. For some datasets, data were available in minute-by-minute or higher frequency formats by request, but this detail was not required in this study for long term relative sea level analyses.

Data collected from the BODC are provided online in text files (Figure 4.2), but can be easily imported into Microsoft Excel (Figure 4.2) and a MATLAB function is available for fast data analysis. This source provides data for Leith and Aberdeen, spanning 19 and 60 years, respectively.

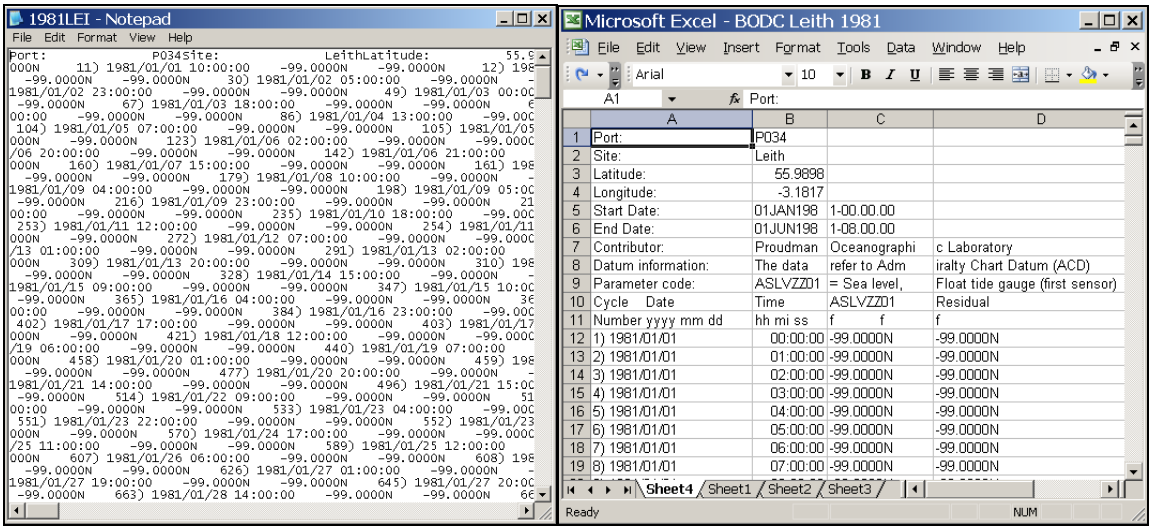

Figure 4.2. BODC Leith 1981 text file and BODC Leith 1981 Excel file.

SEPA has provided data from several gauges in the Forth and Tay Estuaries, but some are from gauges located too far upstream in the tributaries to observe accurate tidal components. These data are provided in 15 minute intervals with each spreadsheet representing one calendar year. They were then converted into daily and monthly averages (Table 4.2; Figure 4.3).

The SEPA sites all use the Impress model pressure tide gauges with a Hawk model datalogger or '5 m transducers' (Una Thom, pers. comm., Julie Carter, pers. comm.). The sites were levelled using Ordnance Survey benchmarks and temporarily allocated SEPA benchmarks or stage posts. SEPA ascertains that these data were not intended for relative sea level data analysis and so have been used only for comparison with other local gauge records in this study. The Bridge of Earn, Musselburgh and Perth (Scone) data lie on the upper limits of the tidal range due to the gauge locations on tributary rivers.

Site	**Musselburgh (River Esk)**	**Perth (Scone)**	**Arbroath**	**Bridge of Earn (River Earn)**	**Newport-on-Tay**
No. of years	4	19	3	18	5

Table 4.2. SEPA tide gauge locations and the number of years with data.

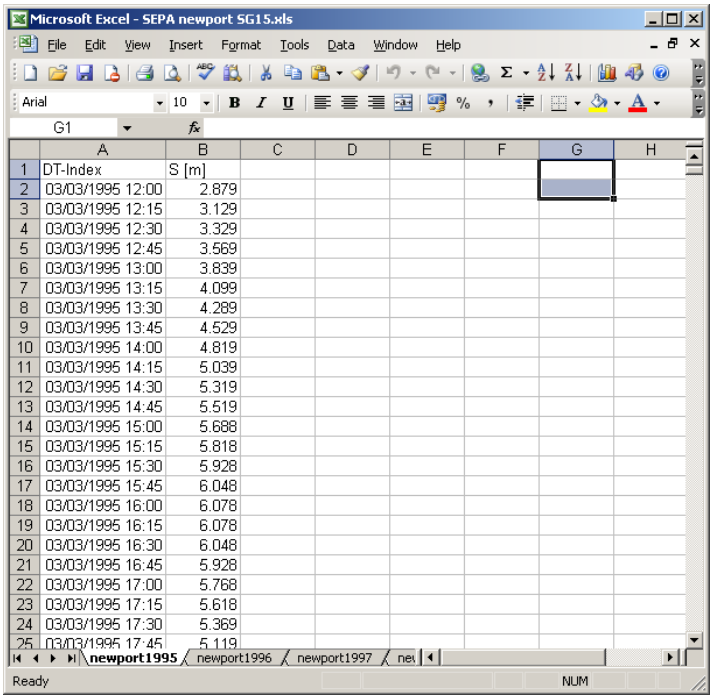

Figure 4.3. SEPA Newport-on-Tay data.

PKC, specifically Perth Harbour Authority, have collected digital and paper records of tidal data for three sites near Perth, although two datasets are very intermittent in their logging regime and may not have recorded for days or weeks at a time. The digital dataset was collected directly from Perth Harbour Authority (Table 4.3).

Site	**Perth Harbour**	**Tay-Earn Confluence (Ribny Beacon)**	**Bridge of Earn (River Earn)**
No. of years	4	3	3

Table 4.3. PKC tide gauge locations and the number of years with data.

The UKHO have collected paper tidal data from three sites with Munro-style float gauge recorders within the Forth and Tay Estuaries area (Table 4.4).

Data still available at the UKHO with Munro recorded format include:

- Leith –1980-1988, 8 years (converted from the paper record by UKHO);

- Rosyth – 1945-46, 1956-57, 1974-1980, 1996, 2000-08 intermittently, 21 years (converted from the paper record by UKHO).

Site	**Rosyth**	**Dunbar**	**Leith**
No. of years	8	5	2

Table 4.4. UKHO tide gauge locations and the number of years with data.

Data still available at the UKHO in digital hourly format include:

- Burntisland – 2000, 1 year (no data available from other sources);
- Grangemouth – 1996-1998 intermittently, 3 years;
- Methil – 1996-1998 intermittently, 3 years;
- Leith – 1996-1998 intermittently, 3 years;
- Dundee - 1996-1998 intermittently, 3 years.

All data are held at the UKHO conservancy site in Taunton, Somerset. Data were collected by the author visiting the UKHO and transposing high and low tides from paper records, similar to those in Figure 4.6, which were in a fragile state. Some age-related damage, along with original errors and time limitations, prevented a more comprehensive digital copy. The digital copy was constructed by averaging the high and low tides (Figure 4.4).

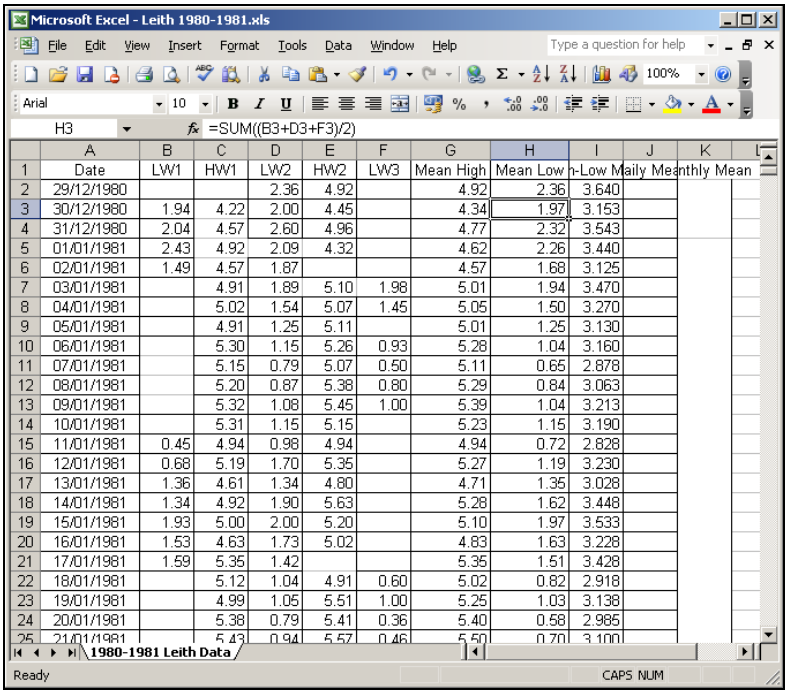

	A	B	C	D	E	F	G	H	I	J	K
1	Date	LW1	HW1	LW2	HW2	LW3	Mean High	Mean Low	n-Low Maily Mean	Monthly Mean	
2	29/12/1980			2.36	4.92		4.92	2.36	3.640		
3	30/12/1980	1.94	4.22	2.00	4.45		4.34	1.97	3.153		
4	31/12/1980	2.04	4.57	2.60	4.96		4.77	2.32	3.543		
5	01/01/1981	2.43	4.92	2.09	4.32		4.62	2.26	3.440		
6	02/01/1981	1.49	4.57	1.87			4.57	1.68	3.125		
7	03/01/1981		4.91	1.89	5.10	1.98	5.01	1.94	3.470		
8	04/01/1981		5.02	1.54	5.07	1.45	5.05	1.50	3.270		
9	05/01/1981		4.91	1.25	5.11		5.01	1.25	3.130		
10	06/01/1981		5.30	1.15	5.26	0.93	5.28	1.04	3.160		
11	07/01/1981		5.15	0.79	5.07	0.50	5.11	0.65	2.878		
12	08/01/1981		5.20	0.87	5.38	0.80	5.29	0.84	3.063		
13	09/01/1981		5.32	1.08	5.45	1.00	5.39	1.04	3.213		
14	10/01/1981		5.31	1.15	5.15		5.23	1.15	3.190		
15	11/01/1981	0.45	4.94	0.98	4.94		4.94	0.72	2.828		
16	12/01/1981	0.68	5.19	1.70	5.35		5.27	1.19	3.230		
17	13/01/1981	1.36	4.61	1.34	4.80		4.71	1.35	3.028		
18	14/01/1981	1.34	4.92	1.90	5.63		5.28	1.62	3.448		
19	15/01/1981	1.93	5.00	2.00	5.20		5.10	1.97	3.533		
20	16/01/1981	1.53	4.63	1.73	5.02		4.83	1.63	3.228		
21	17/01/1981	1.59	5.35	1.42			5.35	1.51	3.428		
22	18/01/1981		5.12	1.04	4.91	0.60	5.02	0.82	2.918		
23	19/01/1981		4.99	1.05	5.51	1.00	5.25	1.03	3.138		
24	20/01/1981		5.38	0.79	5.41	0.36	5.40	0.58	2.985		
25	21/01/1981		5.43	0.94	5.57	0.46	5.50	0.70	3.100		

Figure 4.4. Forth Ports high and low tide data from paper records. The spreadsheet illustrates the high and low tides for each day. Due to the orbital pattern of the moon and surge events there can be 1 or 2

high tides and 1 to 3 low tides within 24 hours. Recording errors or omissions can leave gaps in the data, such as cell F9 above. In this case the gap was less than 6 hours, but in cases where more than one turning point was missing the days data was excluded. Columns H and I use equations to calculate the daily average high and low tides.

Forth Ports data (Table 4.5) were recorded by four different gauge systems since 1979. The paper records from Grangemouth were created by a Munro gauge with a paper output; drawing a continuous line for a week onto marked square paper (similar to that seen in Figure 4.6). This type of gauge would be manually corrected by comparing the recorder readout with a quayside tide board.

Site	**Grangemouth**	**Dundee**	**Rosyth**	**Methil**	**Leith**
No. of years	22	24	8	8	8

Table 4.5. Forth Ports tide gauge locations and the number of years with data.

Digital and paper records were collected from Peter Crawley (Dredging and Conservancy Superintendent, Forth Ports). The Dundee paper dataset from 1987 was captured with a Valeport 710 pressure transducer and recorded onto a paper output recorder. A precision potentiometer was used at the Port of Grangemouth throughout the duration of the Munro gauge's residence. The precision potentiometer transmitted data from the gauge to a dot-matrix recorder at a different location on the port. Data from this gauge are available from 1979. Since then two gauges have been used, the Valeport 710 and Valeport MIDAS TMS, which were also used consecutively at four other Forth Ports sites.

Forth Ports data are presented in three digital formats. Each digital record presents near minute-by-minute records including date, time and tidal height in metres for one day. The most detailed digital records (Figure 4.5) also include predicted tide height, surge height, wind direction, wind speed, maximum gust speed, air pressure and air temperature.

Several port visits have taken place since October 2008 in order to observe the position of tidal gauges, understand port operations and meet the operations staff at Forth Ports. Several visits to the port premises were needed to transpose Dundee and Grangemouth tidal data from paper documents (Figure 4.6).

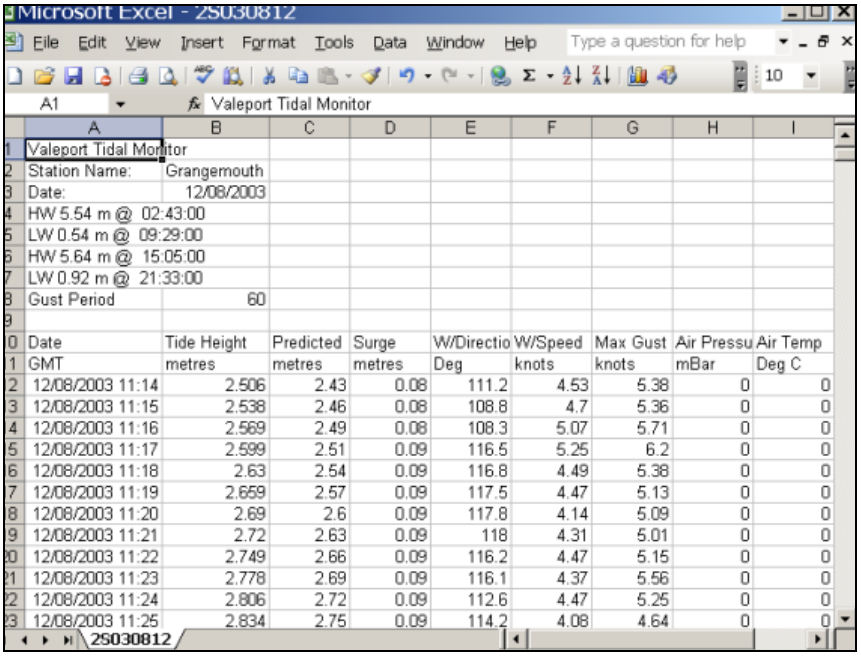

Microsoft Excel - 25030812

File Edit View Insert Format Tools Data Window Help Type a question for help

A1 Valeport Tidal Monitor

	A	B	C	D	E	F	G	H	I
1	Valeport Tidal Monitor								
2	Station Name:	Grangemouth							
3	Date:	12/08/2003							
4	HW 5.54 m @	02:43:00							
5	LW 0.54 m @	09:29:00							
6	HW 5.64 m @	15:05:00							
7	LW 0.92 m @	21:33:00							
8	Gust Period	60							
9									
10	Date	Tide Height	Predicted	Surge	W/Directio	W/Speed	Max Gust	Air Pressu	Air Temp
11	GMT	metres	metres	metres	Deg	knots	knots	mBar	Deg C
12	12/08/2003 11:14	2.506	2.43	0.08	111.2	4.53	5.38	0	0
13	12/08/2003 11:15	2.538	2.46	0.08	108.8	4.7	5.36	0	0
14	12/08/2003 11:16	2.569	2.49	0.08	108.3	5.07	5.71	0	0
15	12/08/2003 11:17	2.599	2.51	0.09	116.5	5.25	6.2	0	0
16	12/08/2003 11:18	2.63	2.54	0.09	116.8	4.49	5.38	0	0
17	12/08/2003 11:19	2.659	2.57	0.09	117.5	4.47	5.13	0	0
18	12/08/2003 11:20	2.69	2.6	0.09	117.8	4.14	5.09	0	0
19	12/08/2003 11:21	2.72	2.63	0.09	118	4.31	5.01	0	0
20	12/08/2003 11:22	2.749	2.66	0.09	116.2	4.47	5.15	0	0
21	12/08/2003 11:23	2.778	2.69	0.09	116.1	4.37	5.56	0	0
22	12/08/2003 11:24	2.806	2.72	0.09	112.6	4.47	5.25	0	0
23	12/08/2003 11:25	2.834	2.75	0.09	114.2	4.08	4.64	0	0

25030812

Figure 4.5. Example of an Excel spreadsheet automatically created by the Valeport gauge software.

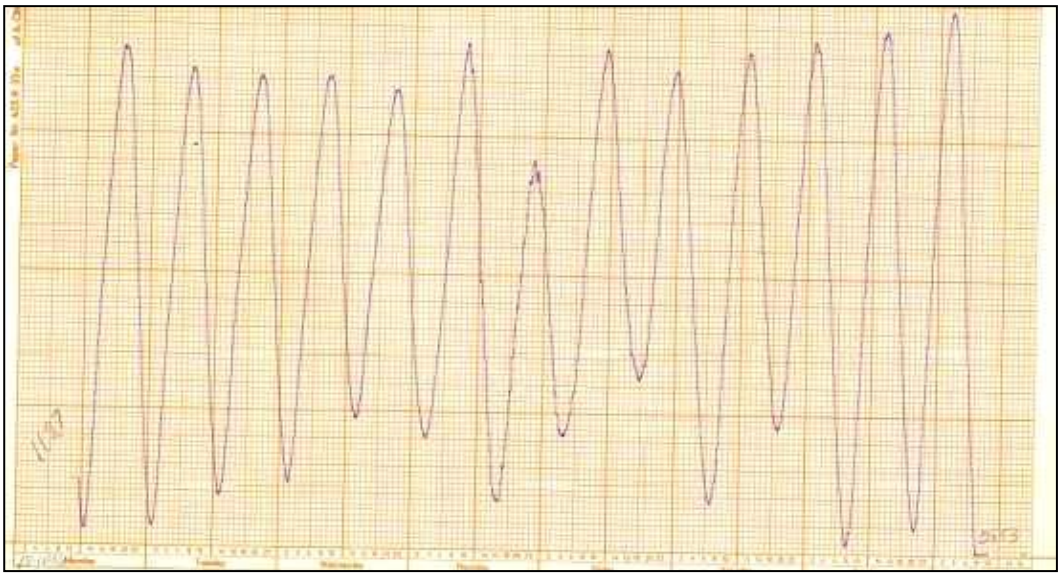

Figure 4.6. Example of paper dataset, similar to Grangemouth, taken from the TERC Newport-on-Tay dataset.

TERC was a local research centre of the University of Dundee. TERC operated a tide gauge at Newport-on-Tay and another at Stannergate, the easternmost point of the Port of Dundee, to study tidal characteristics in the outer Tay Estuary. The Newport-on-Tay tide gauge was adopted by SEPA, but data produced before SEPA's involvement have been retained by the University of Dundee. The two tide gauges were monitored by TERC between 1972 and 1990, although data are also available for 2000 at Newport-on-Tay (Table 4.6 and Figure 4.7). All of these data were collated by the author for validation.

Site	**Newport-on-Tay**	**Stannergate, Dundee**
No. of years	19	6

Table 4.6. TERC tide gauge locations and the number of years with data.

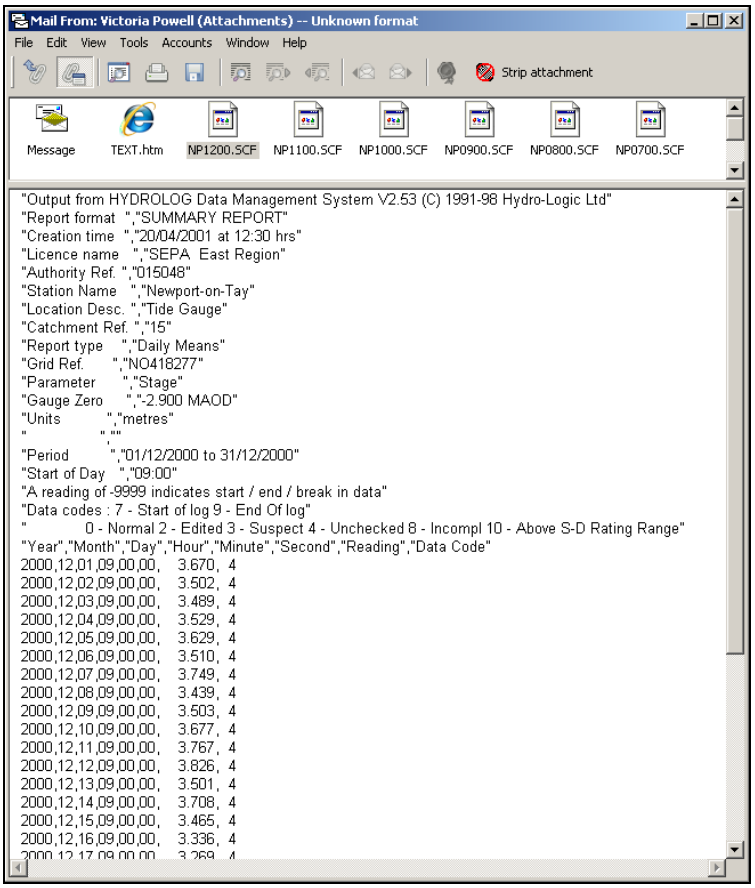

Figure 4.7. An example of TERC Newport-on-Tay data.

4.2.2 Local Storm Surge and Maxima Data Collection

Additional data were collected from secondary sources, such as local riparian authority reports and academic papers, to support primary tide gauge data analysis of storm surge patterns. These methods are described in Section 4.6.

4.3 Data Validation

4.3.1 Dataset Errors and Inaccuracies

Paper records

As with most of the paper records, certain practicalities need to be taken into account:

- Several UKHO datasets were transcribed from weekly recorded sea level paper charts, similar in appearance to those of the TERC data (Figure 4.6). Each page of data needed to be adjusted for variations in the placement of the pen, which changes the datum. This adjustment is not common and can be corrected through pen mark comparisons with the previous and next pages, reading annotations made by the gauge operator and by making comparisons with the tidal harmonic predictions for the week. If all of the high and low tides share a common variance between predicted tides and observed tides there may be a generic error.
- The UKHO data include several datasets that were recorded during or just after the First and Second World Wars. During these periods of austerity measures, the paper quality used to record the Rosyth and Dunbar records was vastly reduced, which meant that when the paper datasets were transcribed by the author in 2009 the sheets had become brittle and extremely fragile. Some of the weekly pages had partially disintegrated or become considerably discoloured, whilst other pages were missing completely.
- Some paper records are affected by amplitude limitation of the pen arm, which cut off the extreme high and low tides at a fixed point; the extreme reach of the arm. An example of this occurring can be seen in the TERC Newport-on-Tay record in Figure 4.6, specifically in the final low tide recording. This cutting off of the low tide recording occurs frequently at that particular site. The artificial increase in the low tide appears as an increase in the daily average.

The daily averages produced from extracted high and low tide levels are comparable with hourly frequency daily averages at a well-maintained tide gauge site and can be used to form sea level trends and sea level maxima heights, whilst avoiding potential data loss from short gaps. In situations where the low tide height has been cut off by sedimentation or gauge malfunction, neither technique would provide an accurate representation and conversion of the data into a daily mean may lead future users to believe the data are accurate. Neither form of daily mean are reliable for storm surge studies with minute-by-minute frequency data needed for this purpose.

Digital records

To speed up transcription of high and low tides from digital datasets into a daily format, a Microsoft Excel macro was created that extracts the high and low tide turning points in each file (Figure 4.8; Box A5.2 in Appendix 5). The way the macro finds the turning points requires each high and low point to be greater or less than ten recordings either side of it.

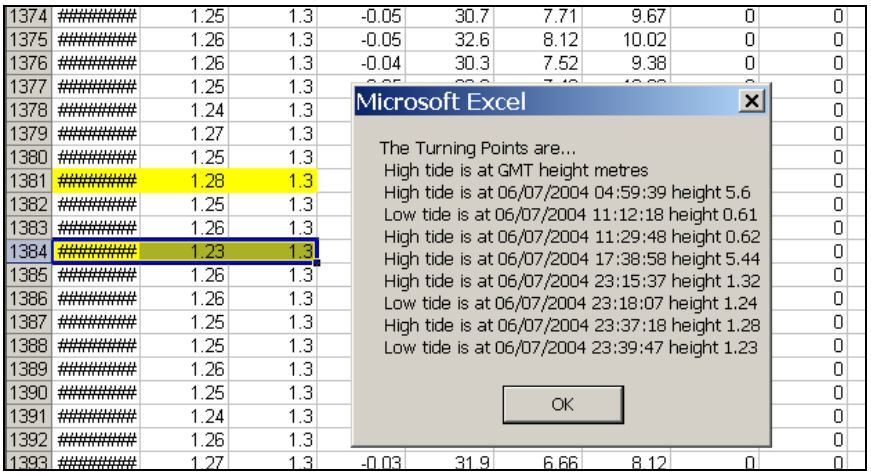

Figure 4.8. An Excel Spreadsheet with tidal height 'turning points' extracted using 'Final Macro.xls'. This macro searches for the high and low tides in minute-by-minute and 15 minute interval data. Each turning point must be greater than the ten data points adjacent to it. If the data experience high fluctuations due to poor weather conditions or surge events then the macro may extract additional data points that need to be corrected manually.

Spikes, Gaps, Steps and Time Shifts

Combining two datasets from different sources or tide gauge system variations in the collection method may produce a selection of errors and inaccuracies. The most common of these are datum changes, but there may also be mechanical errors, human errors and natural variations. Gil and De Toro (2005) state that mechanical error can appear in tidal data as:

- Spikes – a vertical shift/anomaly of a single data point;
- Gaps – a section of missing data along a timeline;
- Steps (i.e. jumps) – a sudden jump or fall in the height of the data, which could be caused by mechanical errors or a change to the site datum; and
- Time Shifts – an anomaly that occurs when the tide gauge clock is out of synchronisation, mainly impacting datasets recorded more frequently than daily, which would cause observed data to appear to lag behind or be in advance of the predicted tide.

In Figure 4.9, there is an example of at least one datum jump in the Grangemouth paper dataset before 1991 and digital dataset after 2003, which was corrected by the author by referring back to historical information about datum change and converting the older dataset to the new datum level (see Section 4.3.2). There are also three gaps in the data and several individual positive or negative spike events. Gaps can be interpolated if enough data are available to provide accurate projection. In this study it was decided not to interpolate as the data were intended for comparison with future sea level model projections. Spikes were identified manually at a high resolution by pin-pointing individual data points that were more than 20 cm higher or lower than the neighbouring point within daily data. Spikes were removed so that they would not impact upon trend analysis. Without correction of errors at each site there cannot be accurate comparison between datasets.

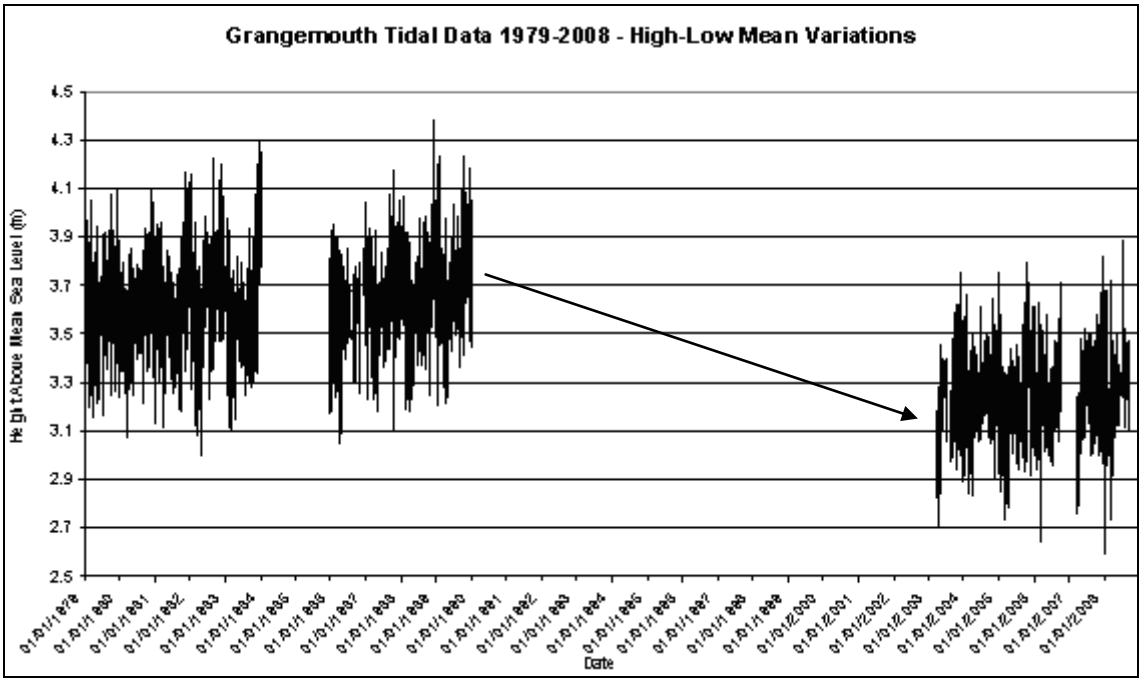

Figure 4.9. Forth Ports Grangemouth tidal data between 1979 and 2008. The arrow indicates a negative trend produced by the lowering of the site datum some time between 1990 and 2003.

Gauge Accuracy

Gauge accuracies were investigated through consultation with various gauge operators and gauge manufacturer publications (See Chapter 5). Taking into account potential accuracy changes due to local calibration approximation, Tables A4.1 and A4.2 (in the Appendix) illustrate the calculated error margins and confidence margins for each gauge. Additional information taken from background records can highlight potential shortcomings in accuracy. For example, some types of

gauges are less accurate than others due to their recording method and gauge replacement may be because of gauge failure or inaccuracy over a long period.

Background information from the BODC and PSMSL have been provided on their webpages. These records highlight instrument changes and data completeness. However, these records lack information on gauge accuracy and the PSMSL website does not give information on every type of gauge that it has collected data from. This information is only available through personal communication with the institutions.

Maintenance schedules were thus requested for all of the data sites from the data. Scientific gauges monitored by the NTSLF at other locations are expected to be maintained very accurately. The frequency of tide gauge system maintenance influences long term accuracy. Ideally, all calibration dates, times and heights should be identified before datum correction. However, none of the tide gauge operators have accessible calibration records.

4.3.2 Datum Correction

A datum is a horizontal level relative to which all levels of the land and/or sea are measured by a local or national authority. For example, in the UK the UKHO have set Ordnance Datum (OD) as the standard height of sea level to be the mean sea level at Newlyn, Cornwall, between the years 1915 and 1920. Prior to the designation of OD Newlyn in 1921, Ordnance Datum was initiated in Liverpool in 1841 with ground zero based 30.5 m below a benchmark bolt on St. Johns Church. However, in 1844 OD was changed to the mean sea level of Victoria Dock, Liverpool, after a nine day survey (denoted as 'OD other' on Figure 4.10).

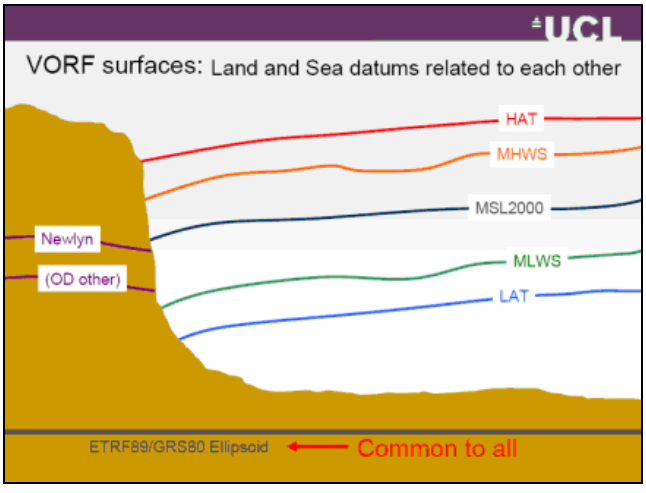

Figure 4.10. Vertical Offshore Reference Frame (VORF) surfaces: land and sea datum related to each other (Ziebart and Iliffe, 2007) CD tends to be greater than or equal to LAT at ports in the Forth and Tay Estuaries.

At each port it is common for a unique datum to be used, known as Chart Datum (CD). CD is commonly lower than OD and since the 1970s CD has coincided with Lowest Astronomical Tide (LAT) at the nearest Standard Port and, therefore, most of the tide is observed above 0 m CD (Figure 4.10). All tidal data in this thesis were converted to Ordnance Datum (Newlyn) (ODN) for comparison.

CD and LAT to ODN datum conversions for each site are available in Table A5.1 and Box 5.3 (in Appendix 5). These conversion factors were taken from individual port and harbour records of datum levels as well as historical survey records kept by the UKHO (Figure 4.11) (Christopher Jones, Head of Tides at UKHO, pers. comm.). Older records may vary due to tide gauge record deterioration, but they may also differ from other site trends due to glacio-isostatic variations.

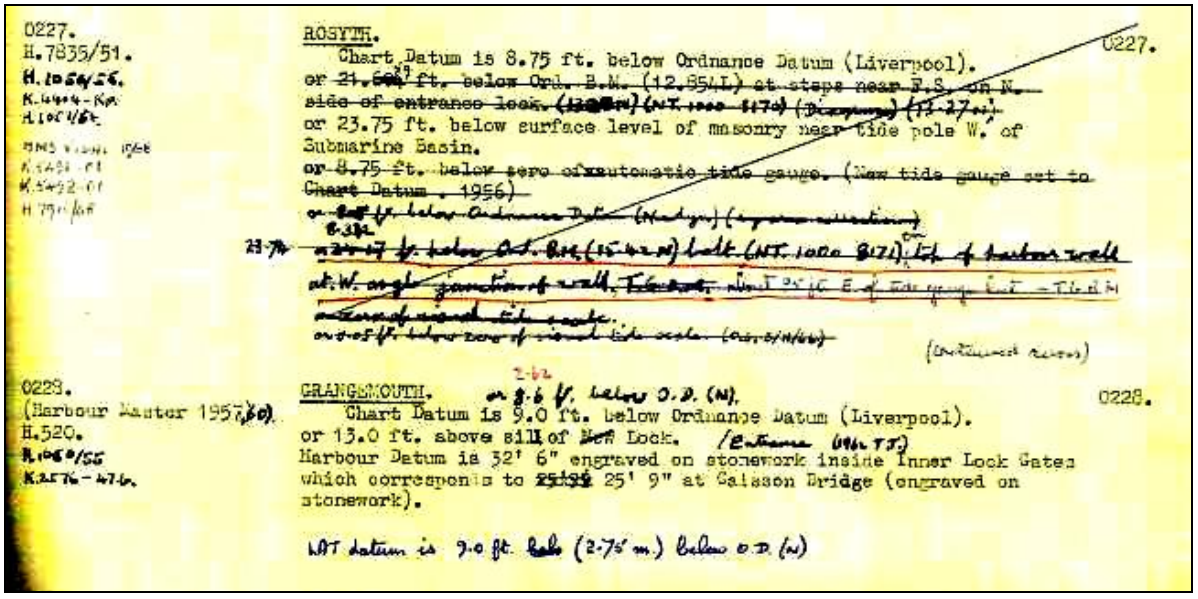
0227.
H.7835/51.
ROSYTH.
Chart Datum is 8.75 ft. below Ordnance Datum (Liverpool).
0227.
or 23.75 ft. below surface level of masonry near tide pole W. of Submarine Basin.
0228.
(Harbour Master 1957)
H.520.
GRANGEMOUTH.
Chart Datum is 9.0 ft. below Ordnance Datum (Liverpool).
or 13.0 ft. above sill of Lock.
Harbour Datum is 32' 6" engraved on stonework inside Inner Lock Gates which corresponds to 25' 9" at Caisson Bridge (engraved on stonework).
LAT datum is 9.0 ft. (2.75 m.) below O.D. (N)

Figure 4.11. An example of the datum information stored at the UKHO for Rosyth and Grangemouth (Christopher Jones, pers. comm.). The levels were recorded during surveys of the estuary, not when the datum changed.

The PSMSL provide Metric data and Revised Local Reference (RLR) data. The main difference between the two is that RLR data have been converted so that all relative sea level data are recorded relative to a single datum (See Section 4.3.2). These RLR data, including data from all PSMSL sites used other than Dundee, have a datum conversion chart provided (Figures A5.1 to A5.6, Appendix).

Most ports may have changed from one datum to another during their tide level recording period. It is possible to erroneously overlook small jumps in the data, which could greatly impact on sea level trend analysis. All data in this thesis were analysed closely for datum change firstly by comparing the tide gauge datasets to historical records of datum change and secondly by manually analysing the tide gauge data over long timescales and high-resolutions for changes in datum height.

For regional analyses, all of the chosen datasets were converted to a different datum. To avoid regional trends being skewed by variation in height across the estuary length, each dataset was converted to a datum that equalled its 1990 average. This method produces datasets that all intersect at 0 m above the datum during 1990. These datasets are then comparable for cross site relative sea level analyses and, when combined, form representative GIA-corrected trends for the region. However, to fully appreciate the comparison between the sites at the 1990 average datum the results must been seen. Refer to the results in Chapter 5.

4.4 Land Movement

There are various causes of land movement that can change relative sea level (Figure 4.12) (King *et al.*, 2009). The main causes that the Forth and Tay Estuaries may be experiencing include glacio-isostatic adjustment (GIA), sedimentation, natural subsidence and infrastructural subsidence. Sedimentation is a local issue that has been discussed in Chapter 3. Therefore only GIA and other forms of land subsidence are discussed here.

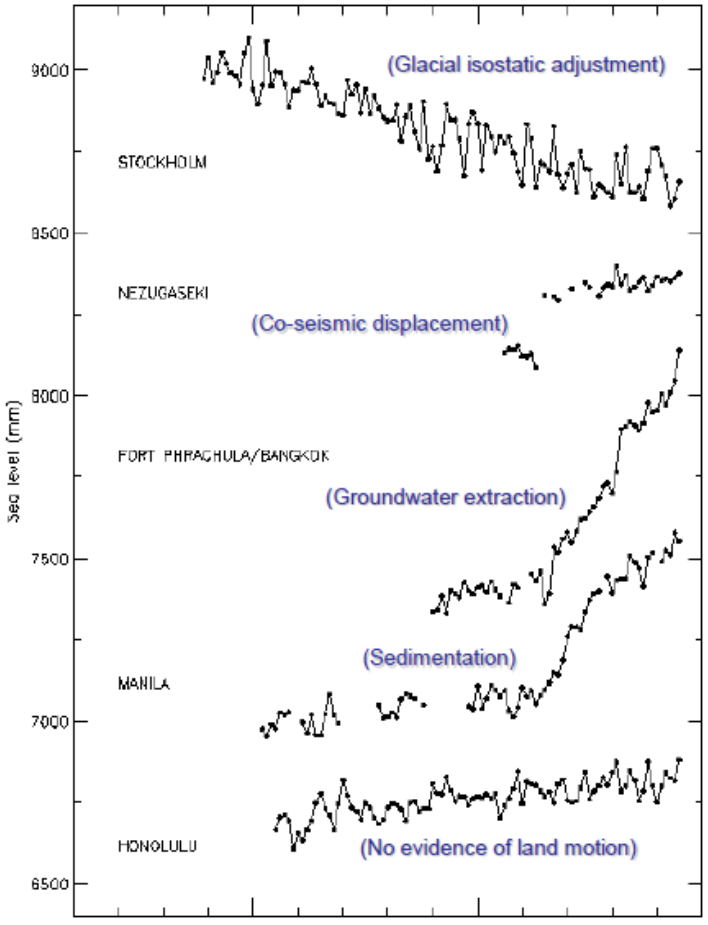

Figure 4.12. Examples of tide gauge data affected by land movement (King *et al.*, 2009).

4.4.1 Glacio-Isostatic Adjustment

The degree of GIA, land level change caused by land ice induced pressure changes, significantly differs across the UK. Parts of Scotland are rising at a relative rate of 1 mm a^{-1} (Shennan *et al.*, 2011) or more. For this reason this study used the relative land level change rates produced by Shennan *et al.* (2011) to estimate present day land level change (see Chapter 5). Each site used the GIA rates specified on Shennan *et al.*'s (2011) map of relative land level change rates. The specific rates were 1.0 mm a^{-1} for Dundee, Leith and Rosyth; 1.1 mm a^{-1} for Perth, 1.2 mm a^{-1} for Grangemouth and 0.9 mm a^{-1} for Dunbar.

To estimate what regional sea level rates potentially may have been if GIA had been negligible, GIA was removed from relative sea level rates. These converted data are referred to as GIA-corrected datasets in the thesis. These relative land level change rates have also been applied to future sea level projections (see Chapter 8).

4.4.2 Natural and Infrastructural Subsidence

Natural subsidence due to coastal erosion, fluvial sediment redistribution, mining or land instability can appear as gradual or sharp changes in sea level in tide gauge datasets. There are four methods to identify these causes of natural subsidence:

- Conduct site investigations looking for evidence of movement and ask local site managers;
- Review historical records, including photography and GPS surveys, and compare with present day records;
- Consult local experts, such as the Scottish Mining Museum, to obtain records of past land instability at each location; and
- Review tide gauge background information for acknowledgement of land movement (some tide gauges may have connected GPS recorders).

Mining operations are logged at the Scottish Mining Museum, British Geological Survey and the Coal Authority. The Scottish Mining Museum was able to advise that Musselburgh, Prestonpans and Methil were sites of high colliery activities over the past 150 years (G. Archibald, pers. comm.). The British Geological Survey provided *Ground Stability Reports*, such as the results of a Coal Mining Report from the Coal Authority (2010a; b; c; d), that encompass several different causes of subsidence. According to the Coal Authority, most of the data collection sites did not require a *Coal Mining Report*, as no activity had taken place there (Coal Authority, 2010a; b; c; d). *Coal Mining Reports* were requested for four locations in the Forth and Tay Estuaries.

Land movement caused by infrastructural subsidence was investigated at the tide gauge site at Newport Pier, Newport-on-Tay, using photographic evidence and GPS surveys. Photographic evidence dating from the late 1970s illustrated continuous movement along the western side of the stonewall pier (Section 5.4.2). This evidence was supported by two GPS surveys of the pier using two Leica GPS systems, one used as a base station and the other as a roaming station. The survey involved taking spot measurements along transects across the width of the pier at approximately 1.5 m intervals and along the length of the pier where cracks are visible. Transects across the width of the pier were taken from low tide level up to the pier buildings on the landward boundary. These provide information on the variation in infrastructural subsidence along the length of the pier, which can be represented by elevation change or angle at given spot heights across a cross-section.

At the end of this process the tide gauge data at all sites have been subjected to GIA corrections and are now available in both relative sea level and GIA-corrected formats. The data are not referred to as eustatic sea level data, as some of the relative land level changes may have been inadvertently omitted. Further analyses can either use the locally relevant relative sea level data or the GIA-corrected data.

4.5 Sea Level Oscillation Identification

The sea level trends observed over annual to multi-decadal timescales are influenced by overlapping cycles of various frequencies. Identification of the cycles occurring in the Forth and Tay Estuaries led to a greater understanding of when these cycles could have had the greatest combined influence over sea levels and how they would have impacted short timescale trends.

A commonly used method of identifying wavelets is through Fourier transform (Massal, 2001). Fourier transform can obtain the frequency spectrum of stable cycles using comparable sine waves, but cannot obtain these values for cycles with oscillating frequencies (Massal, 2001). For this thesis the Torrence and Compo (1998) wavelet analysis method was used. The benefit of this method in comparison to the Fourier transform method is the additional accuracy at identifying the temporal locality and scaling of each of the major wavelets, know as the *mother* wavelets (Massal, 2001; Lee and Yamamato, 1994).

The simplest wavelet is the Haar wavelet, which is an orthogonal wavelet that produces linear output (Figure 4.13). This wavelet can project equal to the Fourier transform, but in addition is able to split the identification of wavelet cycles over a timescale. The Mexican Hat wavelet smooths the analysis, allowing for a closer relationship between the wavelet and the data. For oceanic waves and cycles the Morlet wavelet is the most appropriate as it is progressive, it can be used in time

frequency analysis, it can analyse both positive and negative frequencies, the phase is adaptable to fit variable frequencies and it has been used in previous sea level studies (Figure 4.14).

Torrence and Compo (1998) and Massal (2001) both used the Morlet mother wavelet within their wavelet analysis. Other wavelets may be more appropriate for non-oceanic signal analysis, including the Meyer, Mallat, Daubechies and Ricker (Mexican Hat) mother wavelets (Massal, 2001; Jevrejeva *et al.*, 2006). These wavelets are used with transform equations to multiply an inputted signal, so specific wavelets are chosen for their comparability with features in the time series to be analysed (Massal, 2001).

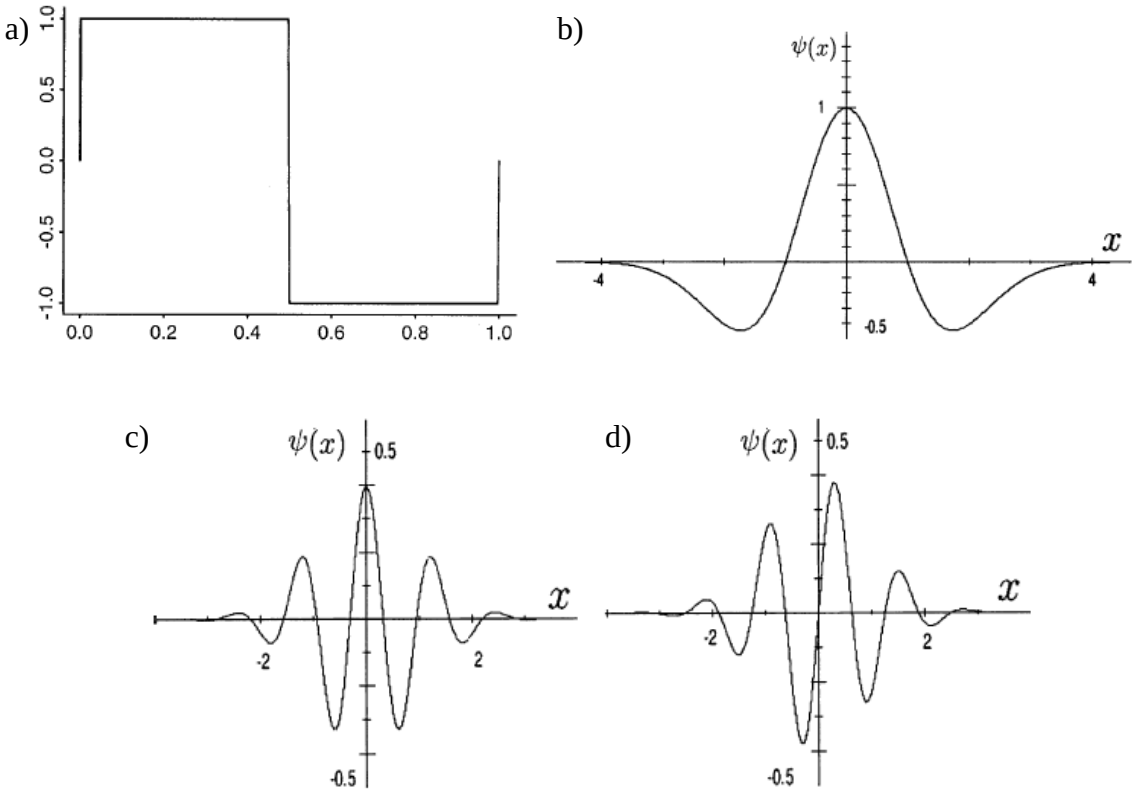

Figure 4.13. A selection of wavelets ranging from a) a simple orthogonal wavelet with linear output known as the Haar wavelet; b) the Mexican Hat wavelet, also known as a Ricker or DOG wavelet; c) and d) two component of a Morlet wavelet, the *real* and *complex* parts (Kumar and Foufoula-Georgiou, 1997; Domingues *et al.*, 2005).

The Morlet wavelet (see equation) is representative of a plane frequency wave:

$$g(t) = \exp(-\tfrac{1}{2} t^2) \exp(ict)$$

Where g(t) is the mother wavelet and c is the plane wave of frequency modulated by a Gaussian envelope.

The benefit of using Morlet wavelet analysis can be seen in Figures 4.14 and 4.15, which demonstrates how both stable and changing signals can be interpreted over a given timeline. In

Figure 4.14 there are three clear frequency bands on the *scale b* axis, identifying the dominant signals to be 2, 5 and 10.5 seconds in frequency. Contrastingly, the same method identified frequencies of 2, 5 and 10.5 seconds between confined time periods in Figure 4.15.

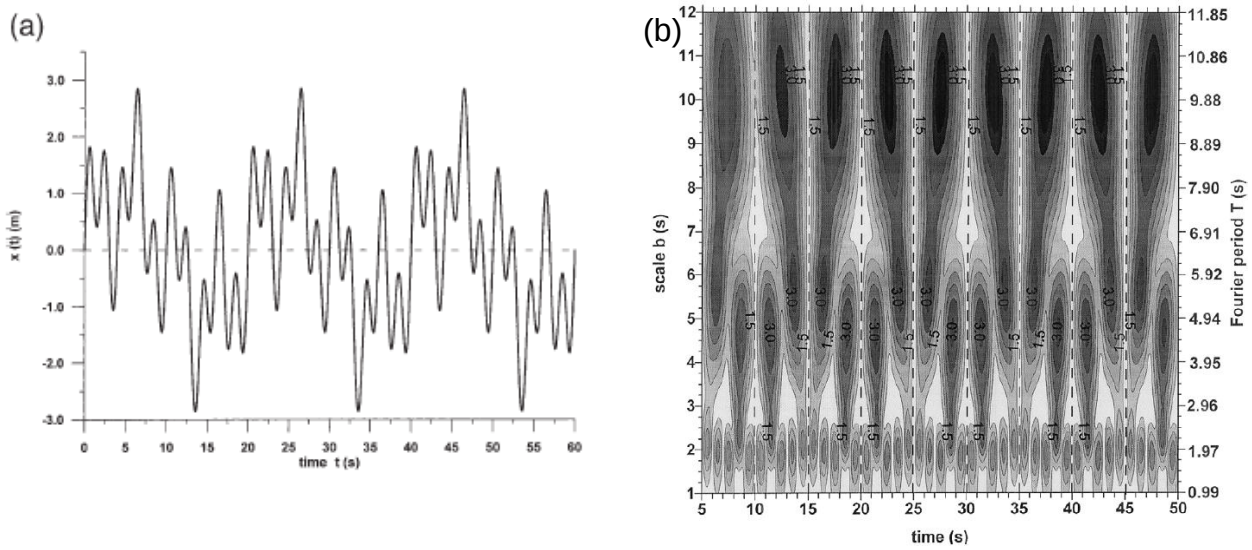

Figure 4.14. (a) a signal representative of three overlapping sinusoidal signals with stable frequencies; (b) the Morlet wavelet analysis ouput for a) illustrating three consistent signals with strong power outputs (Massel, 2001:960, 973).

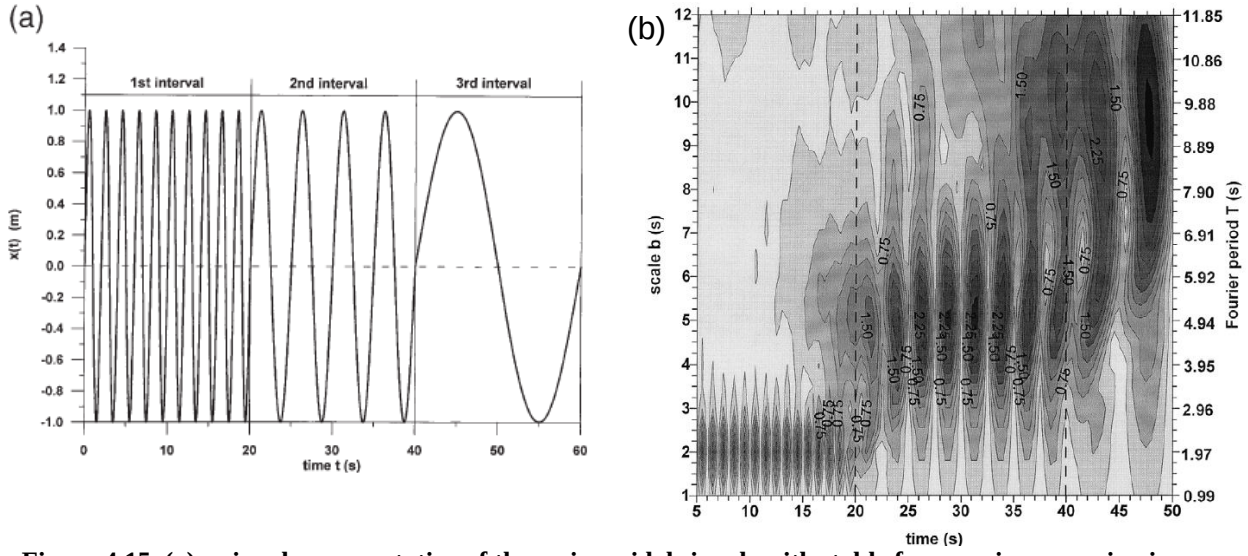

Figure 4.15. (a) a signal representative of three sinusoidal signals with stable frequencies occurring in series; (b) the Morlet wavelet analysis ouput for a) illustrating the transition between the three signals with strong power outputs (Massel, 2001:961, 974).

In their example, Torrence and Compo (1998) fitted the Morlet wavelet to identify El Niño trends within temperature data using the wavelet transform, which is now available as the m-file wavelet.m (Figure 4.16). The Department of Atmospheric and Oceanic Sciences at the University of Colorado (ATOC, 2011) describe high power (amplitude) frequencies, including 2-7 years (due to El Niño), which "hints of a 16 year oscillation" and progression of a 3 year period to a 5 year period between 1965 and 1980.

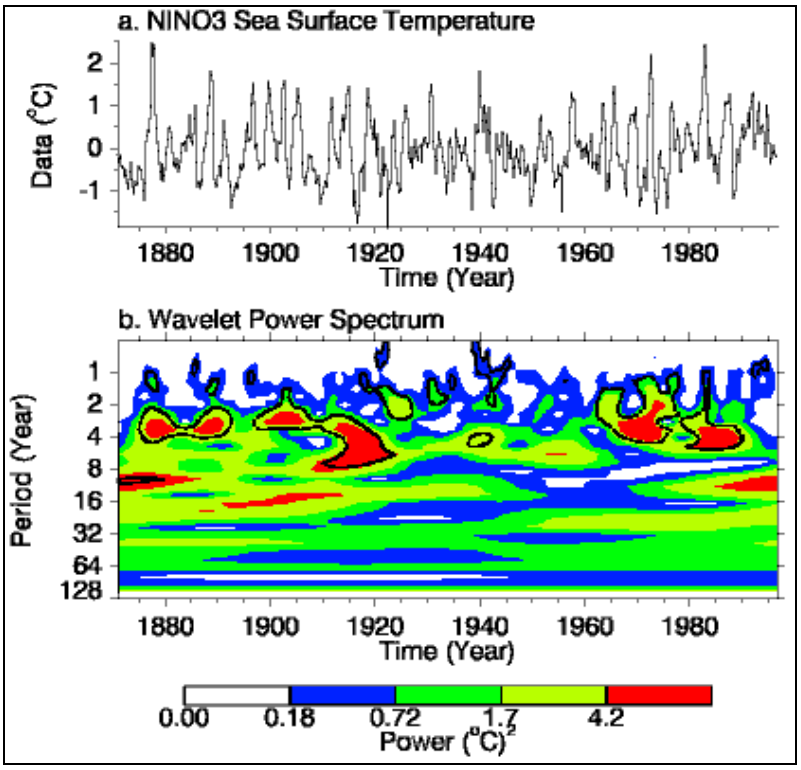

Figure 4.16. "(a) Time series of El Niño SST. (b) The wavelet power spectrum, using the Morlet wavelet. The *x*-axis is the wavelet location in time. The *y*-axis is the wavelet period in years. The black contours are the 10% significance regions, using a red-noise background spectrum. The red areas indicate that high El Niño activity occurred during 1880-1920 and 1965-present, while 1920-1960 was relatively calm" ATOC (2011). Consistent oscillations are identified where colours are near stable at a set periodicity across the timeline (ATOC, 2011).

The algorithms explained by ATOC (2011) were applied to data in the thesis using MATLAB m-files published by ATOC (2011), specifically wavetest.m, wavelet.m, wave_bases.m and wave_signif.m. To produce accurate wavelet analysis output for this thesis the only adaptation needed to the m-files was to remove the original dataset and replace it with site-specific relative sea level data. The results then identified the most dominant sea level oscillations within the analysed sea level data.

4.6 Storm Surge Analysis

Storm surges can increase the sea level considerably with storm surges of over 1 m being precedent in the Forth and Tay Estuaries. The surges, when combined with high tides and waves, could result in overtopping and flooding of coastal areas. For this reason several methods were used to analyse past records for surge data. Storm surges can be identified within tide gauge data and extracted from various historical records. The chosen methods for storm surge analyses were:

- Historical records from databases, journals, local riparian authority documents and other secondary sources (see Section 7.2);
- Sea level maxima analysis, adapted from Graff (1981) (see Section 7.4);
- Residual tide gauge data analysis, using a 400 mm threshold (see Section 7.5).

4.6.1 Historical Surge Records

Knowledge of historical events in the Forth and Tay Estuaries date back sporadically to the thirteenth century (McEwen, 2006) and have been used to create background information about some of the worst flood events in the last nine hundred years. Most of the historical 'flood' records for the Forth and Tay Estuaries do not, however, document whether flooding was due to marine, fluvial or pluvial events and their heights have not been recorded (Law *et al.*, 2010).

More recent storm surge events appear within local riparian authority flood reports, including Dundee City Council's biennial *Flood Prevention Reports* (1997; 1999; 2001; 2003; 2005; 2007; 2009). For some of these events it is difficult to determine whether they were caused by fluvial or marine flooding, as the documents rarely differentiate. Some local newspapers have also documented flooding events (e.g. *The Courier*, 2011; Carrell, 2011) particularly around Perth, which has suffered from combined fluvial and marine flood events in the recent past.

Recorded dates when flooding has occurred in the two estuaries have been compared with sea level maxima events and periods of residual tidal heights to confirm if the flood events occurred concurrently with extreme events and surge periods.

4.6.2 Sea Level Maxima

Sea level maxima are the highest high tides recorded by a tide gauge over a multi-annual timeframe. These heights are hypothesised to be influenced by surge events and may include tides occurring at

periods of high astronomical influence. These are the tides that will have the greatest hazard potential along the coastline.

Sea level maxima are records of past high water level events, providing a precedent for the future. Data were collected from Forth Ports and BODC tide gauges with the aim of investigating different methods of analysing sea level maxima trends. The data were compiled into three datasets for trend analysis:

- Highest 20 maxima across the multi-annual timescale;
- Highest 10 maxima per annum (Figure 7.9 shows the highest 10 maxima per annum for all the sites);
- Graff's (1981) analysis of the 5 year running mean.

The highest 20 maxima across the timescale would identify if the dataset is skewed towards a specific time period when storminess was prevalent. However, this method does not present data in a clear form if the dataset has gaps in the timeline or there are any datum jumps, spikes or other anomalies. In this case using the highest 10 maxima per annum would include a greater number of data point and would clearly indicate where data were missing. Graff (1981) instead used a 5-year running mean of the highest 10 maxima per annum, which could more easily be interpreted and removed the potential for annual influence in the overall trend.

Tide gauge data were taken from the complete Grangemouth dataset (1979 to 2010), part of the Leith dataset (1990 to 2010) and part of the Dundee dataset (1987 to 2010). Both the highest 20 maxima method and the highest 10 maxima per annum method were utilised for each of these datasets. These results were analysed individually for sea level maxima trend identification before comparing patterns in sea level maxima across sites.

Data from five ports within Graff's (1981) study of sea level maxima across the UK have been used in this study: Methil, Kirkcaldy, Rosyth, Grangemouth and Leith. Graff (1981) compiled annual extreme maxima data into 5 year running means for each site in order to present smoothed datasets, which were used to illustrate sea level maxima trends.Graff's analysis of maxima data has been continued until the present day using the primary tide gauge data from Grangemouth and Leith between 1979 and 2010. These data were converted to 5 year running means to compare directly with the Graff (1981) data.

4.6.3 Residual Tide Gauge Data

Residual tidal levels are the height difference between predicted and observed tidal levels. The main reason why tide gauge residual height levels can differ from surge levels is due to the potential for tidal prediction software to include errors. Residual data have been used in the following storm surge analysis methods and rely on prediction software supplied by the tide gauge manufacturers.

Forth Ports have provided five datasets for five different sites, each with at least five years of data collected by tide gauges attached to dataloggers. Five years of tide gauge data in minute-by-minute format were compared with predicted tidal levels. Periods where high residual readings are observed did not necessarily coincide with high water levels, due to the tidal cycle. However, these recordings were observed using the following methods to identify what potential these residual surge periods could have had if combined with a high tide. Like the sea level maxima analysis, this method is preferable to modelling, as the results produced are observations of past events providing a precedent for future surge levels.

Several methods have been used to identify storm surge events in this study:

1. A threshold of 400 mm has been used, so that all residual tide gauge heights over this are deemed significant storm surge events. The reasons why 400mm was chosen as the threshold is because from analysis of data from Dundee and Leith it was observed that below this value surges occurred frequently;
2. Analysis of actual tide gauge maxima with the extreme high water level as a threshold; and
3. Analysis of actual tide gauge maxima with the berth or lock gate heights as a threshold.

Initially, point 1 was used in this study to highlight storm surge numbers. Comparison between sites during individual storm events that occurred across the entire region illustrated how storms changed as they travelled across the Forth and Tay Estuaries and progress up the Forth Estuary.

Point 3, above, identified the five highest tidal heights at each port throughout their recording period and compared these to berth and lock gate heights at selected ports. This comparison identified whether past maxima tidal levels would have caused still water level overtopping.

Events that have been identified by local riparian authorities and independent sources as having been affected by coastal high water levels are discussed in Chapter 7. Tide gauge residuals were analysed on these dates to assess if storm surge components were one of the causes of the observed coastal high water levels within the Forth and Tay Estuaries. These events could otherwise have been driven by extreme water levels caused by astronomical tidal cycles or by wave overtopping.

4.7 Sea Level Modelling

Most sea level models are integrated into either a simplified climate change model or a General Circulation Model (GCM). Simplified models are constructed using an observed relationship between two or more climate variables as the primary tool. For example, a relationship between sea surface temperatures and sea level change has been identified, suggesting a positive correlation. If the future trend of temperature were known then an estimation of future sea level change could be calculated (Rahmstorf, 2007). GCMs attempt to simulate as many different variables to the highest quality possible, which involves manipulation of equations within reasonable limits until the model fits the observed trends to the best possible degree of accuracy (Climateprediction.net, 2010). GCMs are considered more accurate than simplified models due to their intensive modelling and boundary conditions, but simplified models are quicker and easier to replicate.

Two sea level modelling methods have been adapted for use across the Forth and Tay Estuaries, i.e. the UK Climate Projections 2009 (UKCP09) regional sea level model and the Vermeer and Rahmstorf (2009) global sea level-temperature relationship model. Both of these underwent simplistic transformations for projection of relative sea level, converting the original absolute sea level projections by subtraction of local GIA rates (Chapter 8).

UKCP09 is a General Circulation Model (GCM), which uses a multi-scenario approach to project future changes to climate variables, including sea level change. Vermeer and Rahmstorf (2009) is a simplistic model that uses projected temperature changes for the future and the observed relationship temperature and sea level change to project future sea level change. These two approaches vary in their complexity.

The UK Climate Impact Partnership (UKCIP), the creators of UKCP09, provides an online User Interface that registered users can utilise to download raw data projections and adapt graphs of various climate variables and scenarios. For this thesis, relative and absolute sea level data projections were collected for the 5^{th}, 50^{th} and 95^{th} percentiles of the low, medium and high emission scenarios up to 2095. In particular, the mean of the projections, the 50^{th} percentile, is focused upon with the upper and lower extremes being presented for a representative interpretations of the projected potential levels. These statistics are geographically limited to grid squares of 1.25° latitude by 1.25° longitude (DEFRA, 2011a) (Figure 4.17).

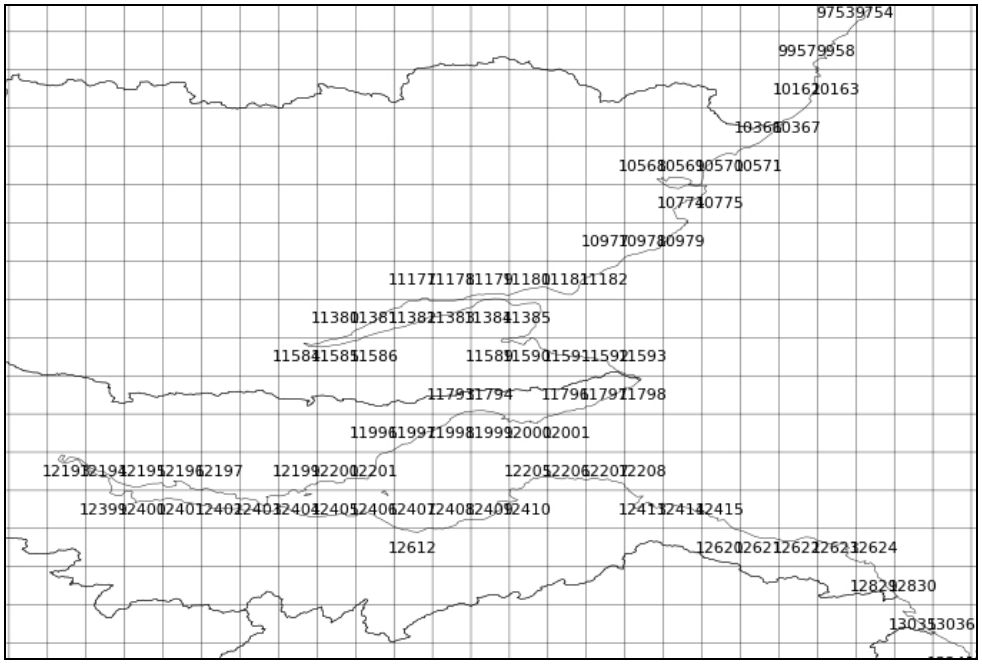

Figure 4.17. Illustration of 1.25° x 1.25° grid box IDs superimposed over the UKCP09 River Basins (DEFRA, 2011a).

The UKCP09 projected relative sea level change for three tide gauge recording sites, namely Dundee, Dunbar and Grangemouth, were compared for relative sea level projection trends (Figure 4.18). The UKCP09 produced relative sea level data for these sites using Bradley *et al.*'s (2009) vertical land motion (VLM) GIA rates for each grid square (DEFRA, 2011a). Relative sea level was additionally projected for the Forth and Tay Estuary, as an average, using the Shennan *et al.* (2011) relative land-level change (RLLC) GIA rates, for comparison with the VLM rates.

The Vermeer and Rahmstorf (2009) sea level model uses the Goddard Institute of Space Science (GISS) (2011) global temperature record and the Church and White (2006) global sea level record to project future global sea level from reliable IPCC (Solomon *et al.*, 2007) temperature projections until 2100. The simple analysis Excel spreadsheet by Moriarty (2011), replicating the Vermeer and Rahmstorf (2009) model, has been used in this thesis for model adaptation. Firstly the GISS (2011) global temperature data were adapted to project future temperatures that match the IPCC (Solomon *et al.*, 2007) projections. To project realistic decadal oscillations in temperature, the temperature pattern between 1980 and 2009 was copied and plotted repeatedly to project this multi-annual oscillating temperature pattern until 2100. A 0.22 °C a^{-1} increase for the medium emission scenario and a 0.25 °C a^{-1} increase with a 0.02 °C jump every 5 years for the high emission scenario was imposed on the projected temperature data to achieve their IPCC projected temperatures (Figure 4.18). Figure 4.19 illustrates the resultant impact on the annual rate of absolute sea level change.

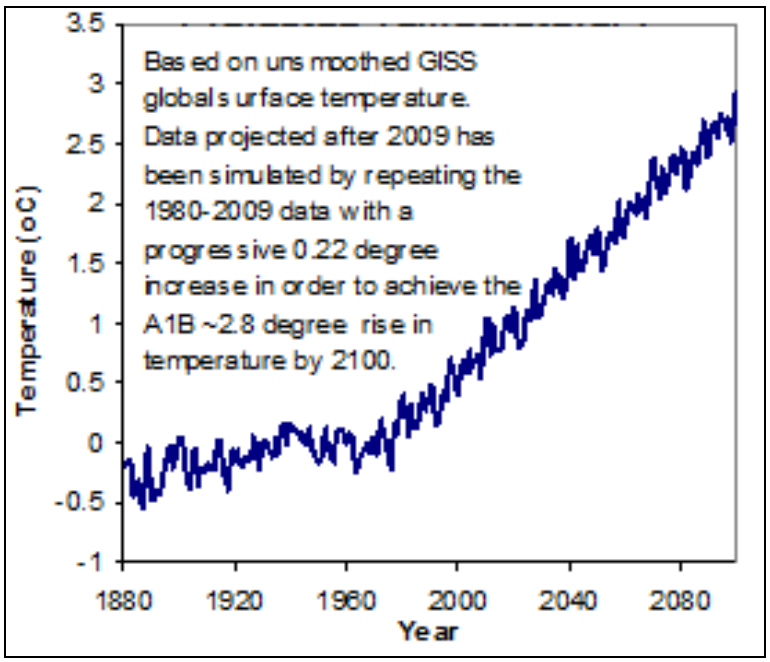

Figure 4.18. Vermeer and Rahmstorf (2009) temperature scenario used to predict sea level change until 2100 (Moriarty, 2011; GISS, 2011).

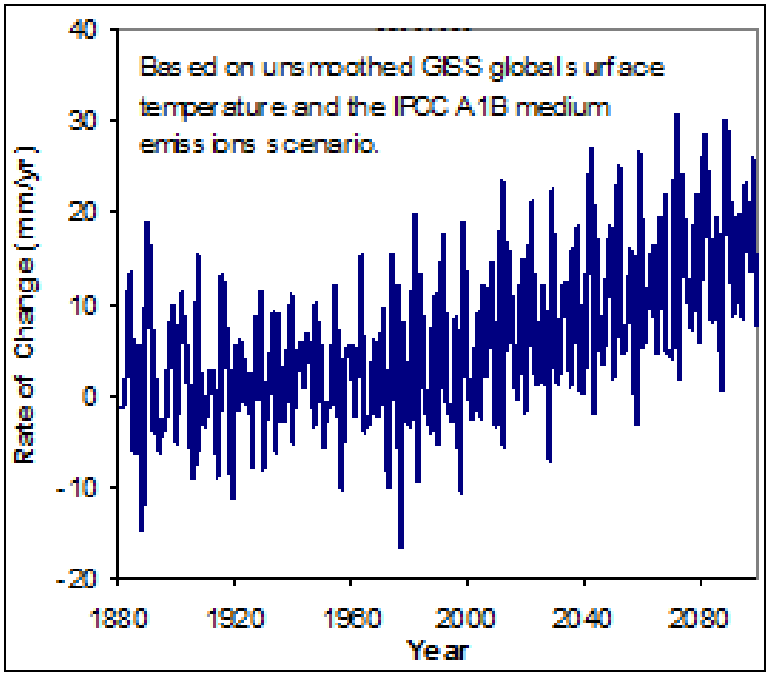

Figure 4.19. Projected sea level rise rate calculated with Vermeer and Rahmstorf (2009) (Moriarty, 2011; GISS, 2011).

Wada *et al.*'s (2010) groundwater depletion calculations were added to the Vermeer and Rahmstorf's (2009) model adaptation results in this thesis by integrating the calculations into the Excel spreadsheet constructed by Moriarty (2011). These global sea level results were then corrected for GIA to estimate relative sea level change in the Forth and Tay Estuaries by adding the Shennan *et al.* (2011) RLLC GIA annual rate to the global sea level projections. Both the UKCP09 (UKCIP, 2009) and Vermeer and Rahmstorf (2009) methods have been used to estimate future extreme sea levels. The results produced from storm surge analyses, focusing on surge comparison with quayside heights, were then combined with these future sea level projections to calculate potential future still water levels in relation to local infrastructure.

4.8 Conclusions

This chapter has introduced the methods used to transform raw tide gauge data into validated relative sea level data suitable for analyses of historical sea level trends, sea level oscillations and storm surge trends. Specific adaptation methods were used to convert multiple datasets to a singular datum for comparison. GIA rates were also used to project the sea levels that could have been observed in this region if GIA had had a negligible effect.

Some of these data are unique to this study, with several datasets being corrected and analysed for the first time as part of the study. The calculated extreme sea level data, additionally combined with future sea level projections, were compared with the heights of local coastal infrastructure. This method provides estimates of present day and 2100 projected extreme still water levels. These levels, which have not been calculated for this region before, summarise the extreme overtopping potential that may occur.

Chapter 5 - Local Sea Level Data Processing

5.1 Introduction

This thesis has three results chapters; namely *Local Sea Level Data Results*, *Storm Surge Events* and *Modelling the Impact of Relative Sea Level Change* (Chapters 5, 7 and 8). In this chapter, local tide gauge data have been corrected to produce a long term record of relative sea level in the Forth and Tay Estuaries. Some of these data have been processed for the first time and are suitable for additional use in storm surge analyses and sea level modelling (Chapters 7 and 8). The data presented here are analysed in Chapter 6.

With regards to future use of these data, care should be taken when extracting pre-corrected results. Ultimately, all results presented in this chapter should be considered in conjunction with data analyses presented in Chapter 6.

5.2 Location

Data were collected from the seven institutions that hold tide gauge data from the Forth and Tay Estuaries as well as neighbouring locations; Forth Ports, the Scottish Environment Protection Agency (SEPA), the former Tay Estuary Research Centre (TERC), Perth & Kinross Council (PKC), the Permanent Service for Mean Sea Level (PSMSL), the UK Hydrographic Office (UKHO), and the National Tidal and Sea Level Facility combined with the British Oceanographic Data Centre (NTSLF/BODC). Some of these institutions act as national or international conservators and have collected data from the Forth and Tay Estuaries dating back to the late nineteenth century, which are discussed in more detail in Section 5.3. Each institution may have data available in a variety of different formats and presentation styles, i.e. the data may have been recorded onto paper or digitally (Chapter 4), data also differed in their available frequency. All of the pre-corrected sea level data are discussed in this section.

The various institutions have collectively conserved data from 16 locations across the Forth and Tay Estuaries, counting some neighbouring locations. These include seven sites in the Tay Estuary, specifically Perth (at Scone), Perth Harbour, Ribny Beacon upstream of the confluence with the River Earn, Newburgh, Newport-on-Tay, the Port of Dundee and Stannergate (inside the eastern boundary of the Port of Dundee); six sites in the Forth Estuary, specifically Grangemouth, Rosyth, Methil, Leith, Musselburgh and Dunbar; Arbroath, which lies 15 km to the northeast of the Tay Estuary; Bridge of Earn in the lower reaches of the River Earn; and Aberdeen, which is located 100 km north of the Tay Estuary and has a well-studied, near-complete, 150 year tide gauge record.

The 16 sites (Figures 3.2 and 3.27) in the study region may each have a number of tide gauge recording frequencies and data qualities subject to different gauge accuracies and maintenance regimes (see Table A4.1, Table A4.2, in the Appendix). To understand more about the data quality, investigations have been made into aspects of the gauge location. The location characteristic of a tide gauge can include information about the tidal properities and the infrastructure to which the gauge was attached. Maps and photographs of each tide gauge position and tidal curves are included in Sections 5.2.1 to 5.2.15 to illustrate the variations in tidal range between sites.

5.2.1 Scone, Perth (SEPA)

This SEPA site is located furthest upstream in the Tay Estuary, c.1 km below the tidal limit at Scone Palace. The gauge is attached to the northeast bank. The SEPA stage post, to which the tide gauge is referred, is located at [NO 11605 25332] and the tidal curve is shown in Figure 5.1 (SEPA, 2010).

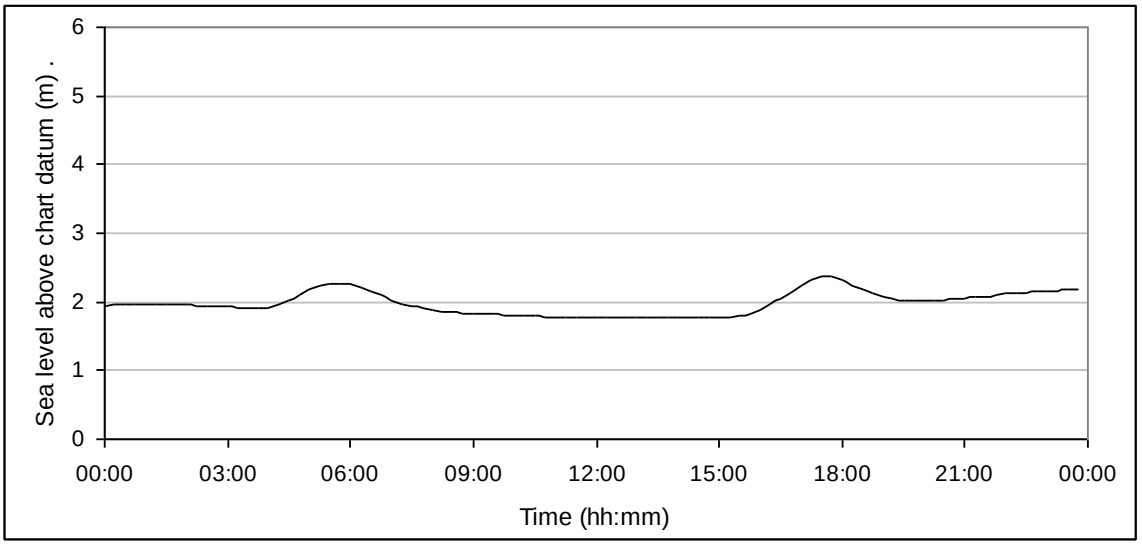

Figure 5.1. Sea level curve at the SEPA Perth site on 10/03/2008, during a spring tide, illustrating a spring tidal range of c.0.5 m. MHWS and MLWS unknown at this location.

The Perth (Scone) gauge is described as a fluvial flood warning tide gauge location and is influenced by fluvial flooding events. As with the other SEPA tide gauge sites, the data here have not been corrected for sea level trend representation (Figure 5.2), but have been included for comparison purposes.

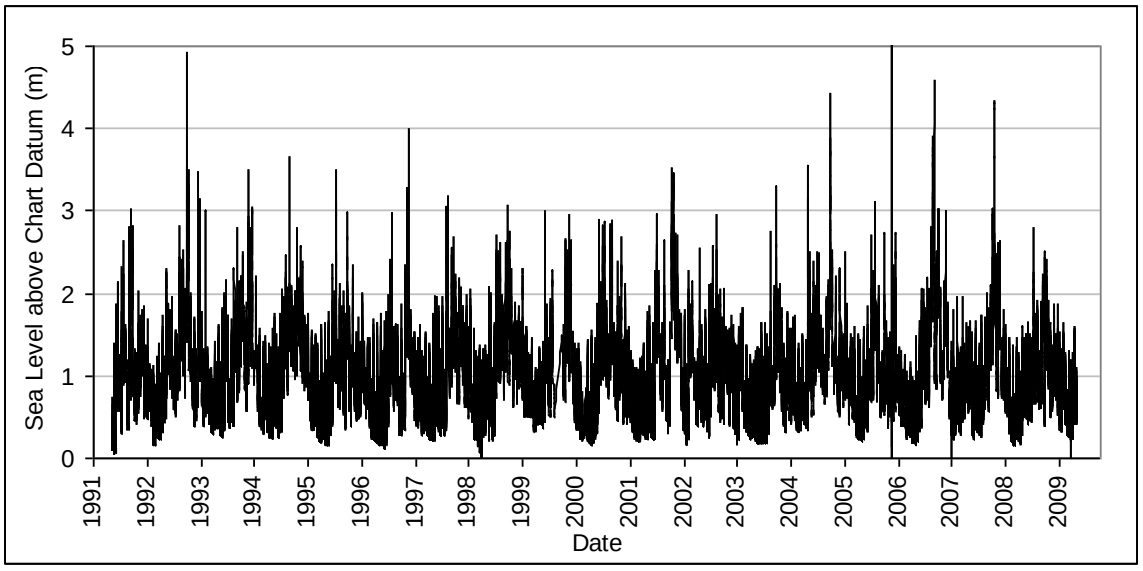

Figure 5.2. SEPA Perth hourly frequency sea level record from 15 minute sea level data between 1991 and 2009. The monthly mean data are not representative of sea level trends due to errors.

5.2.2 Perth Harbour (PKC)

At Perth Harbour, to the eastern, seaward side of the town of Perth (NO 11796 21899), the tidal influence is considerably greater (Figure 5.3). This gauge is attached to the harbour wall.

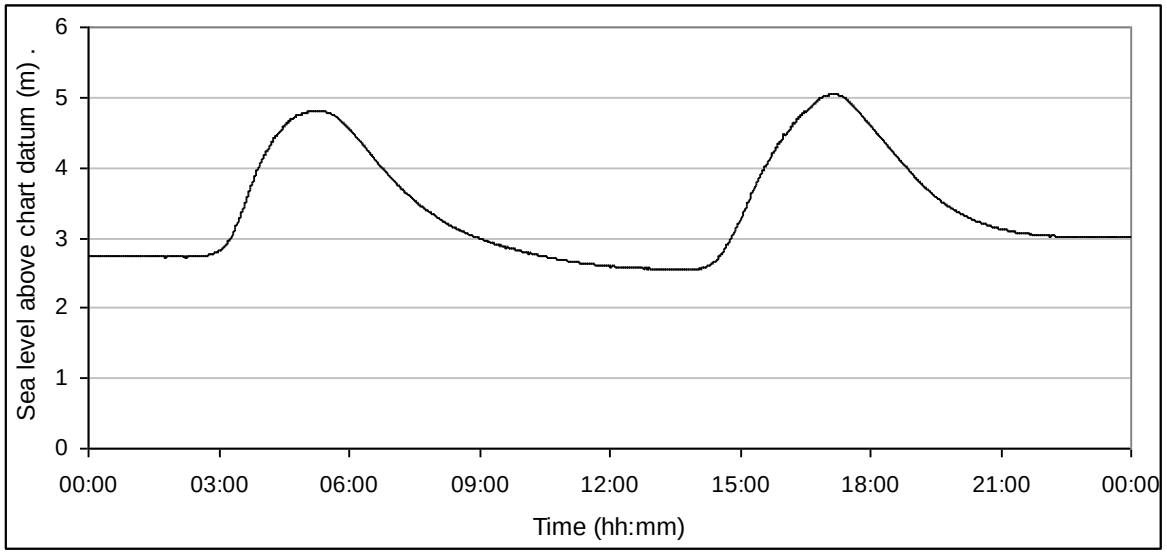

Figure 5.3. Sea level curve at the PKC Perth site on 10/03/2008, during a spring tide, illustrating a spring tidal range of c.2.5 m. MHWS is 5m and MLWS is 2.5m.

PKC data are collected by Perth Harbour Authority from one static tide gauge and two navigation beacons gauges located in the channel of the Tay Estuary (Figure 5.4).

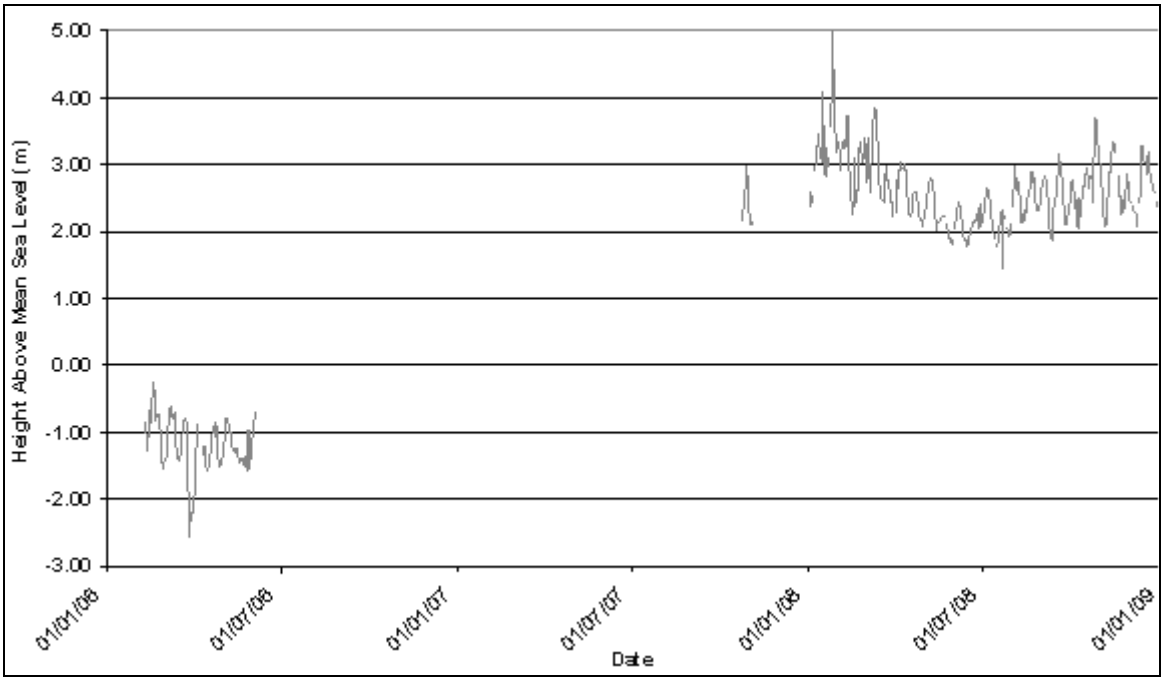

Figure 5.4. PKC Perth average daily mean sea level compiled from 15 minute sea level data between 2007 and 2009.

5.2.3 Bridge of Earn (SEPA)

The Bridge of Earn SEPA site is located above a meandering stretch of the River Earn. It is located at [NO 13415 18371] (Figure 5.5) (SEPA, 2010) and the gauge is mounted onto the northern bank.

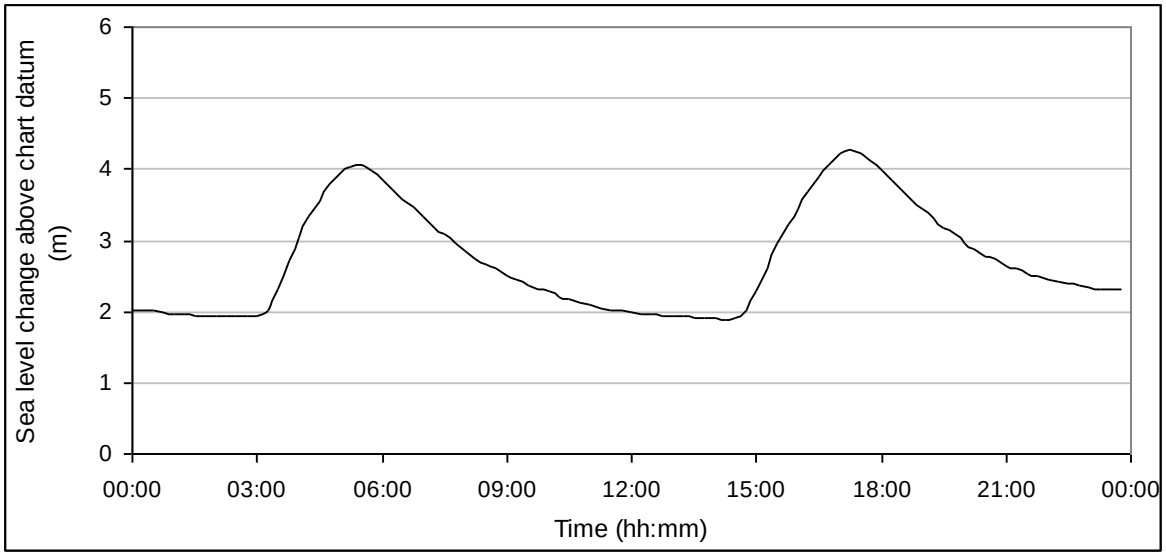

Figure 5.5. Sea level curve at the SEPA Bridge of Earn site on 10/03/2008, during a spring tide, illustrating a spring tidal range of c.2 m. MHWS and MLWS unknown at this location.

The Bridge of Earn SEPA site is described as a fluvial flood warning data collection site. However, Bridge of Earn experiences tidal fluctuations as it is within the tidal reach of the River Earn. In Figure 5.6, seasonal variances appear with spikes that could be associated with fluvial flood events. This dataset is available between 1992 and 2010; however data from 2008 onwards appear different from data recorded previously. This is due to the replacement of the datalogger. No additional information is available on whether the gauge was moved at this time. Therefore, the data here are not representative of the sea level trend.

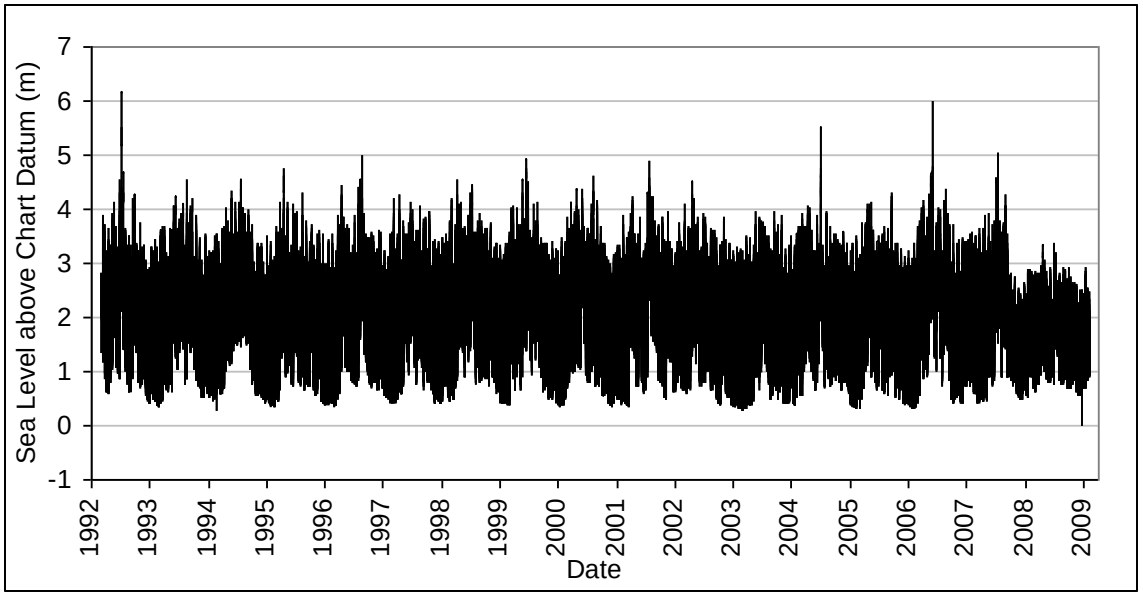

Figure 5.6. SEPA Bridge of Earn hourly frequency sea level record from 15 minute sea level data between 1992 and 2009. The monthly mean data are not representative of sea level trends due to unexpected anomalies, such as the unexpected reduction in tidal range after 2008.

5.2.4 Ribny Beacon, Tay Estuary-River Earn Confluence (PKC)

Ribny Beacon is a shipping channel navigation beacon located near the northern bank of the Tay Estuary between Elcho Castle (south bank) and Inchyra (north bank), c. 3.5 km west of the Tay-Earn confluence, with the closest settlement being St Madoes. Ribny Beacon is located at [NO 17700 20326] (Perth Harbour Authority, 2010b). The record bottoms out at just below 2 m, due to the positioning of the beacon (see Section 5.2) (Figure 5.7).

The Ribny and Newburgh Head beacons are navigational beacons that have been fitted with telecommunication devices that can transmit real-time sea level measurements to the Perth Harbour Authority. Due to the expensive nature of transmitting data between the beacons and Perth Harbour

Authority, they are active only part-time during transit of large ships between Newburgh and Perth. Therefore, the datasets are not extensive enough to form representative sea level trends (Figure 5.8).

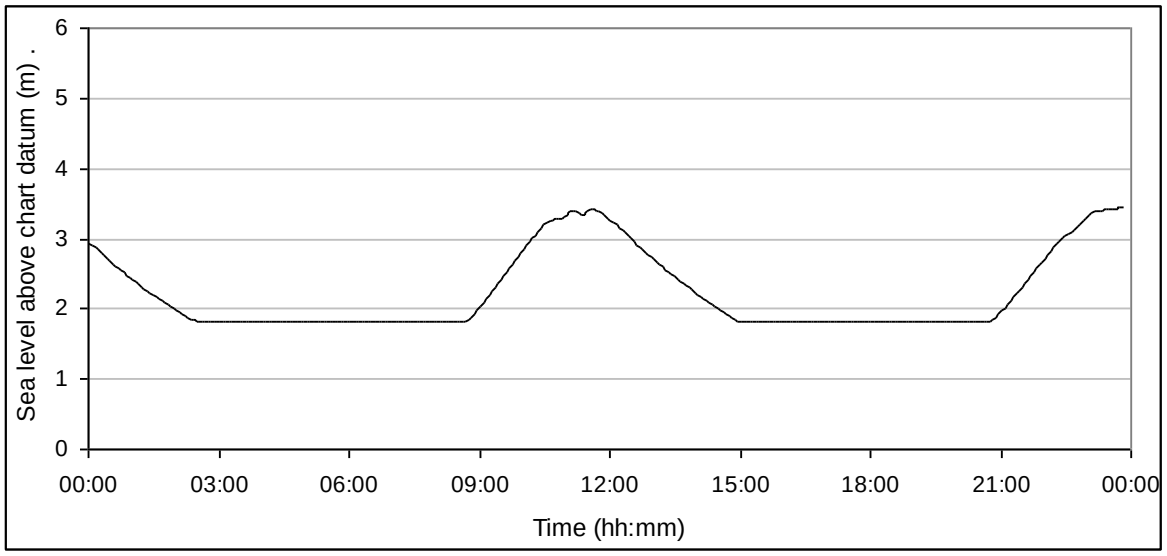

Figure 5.7. Sea level curve at the PKC Earn Confluence (Ribny Beacon) site on 21/11/2008. Data collected during a neap tide. The tidal range presented here is not comparable with those calculated for other sites, because this tide gauge is operated for short periods, approximately 2 hours, as ships pass the location. MHWS and MLWS unknown at this location.

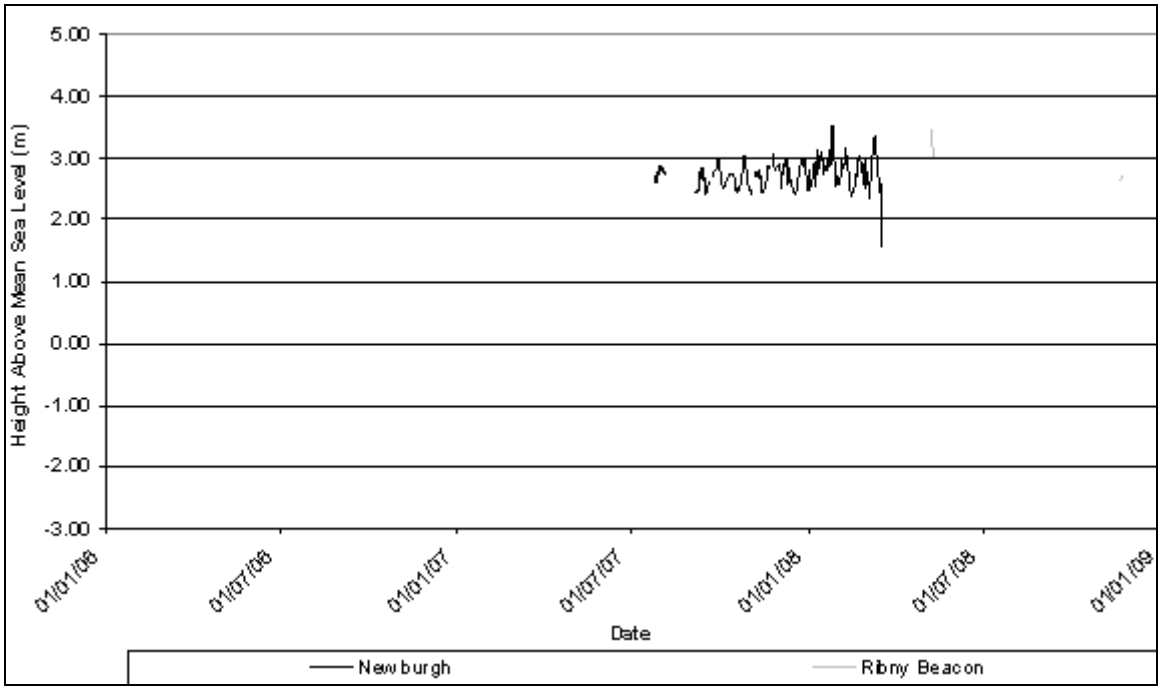

Figure 5.8. PKC Newburgh and Earn Confluence average daily mean sea level compiled from 15 minute sea level data.

5.2.5 Newburgh (PKC)

Newburgh Head Beacon is located in the channel near the southern coast of the Tay, east of Newburgh. This beacon can be found at [NO 24787 18339] (Perth Harbour Authority, 2010b). It is surrounded by several banks and shallow water areas, the closest being Little Bank and The Hard. The tidal data are minimalistic due to the intermittency of the data collection method (Figure 5.9).

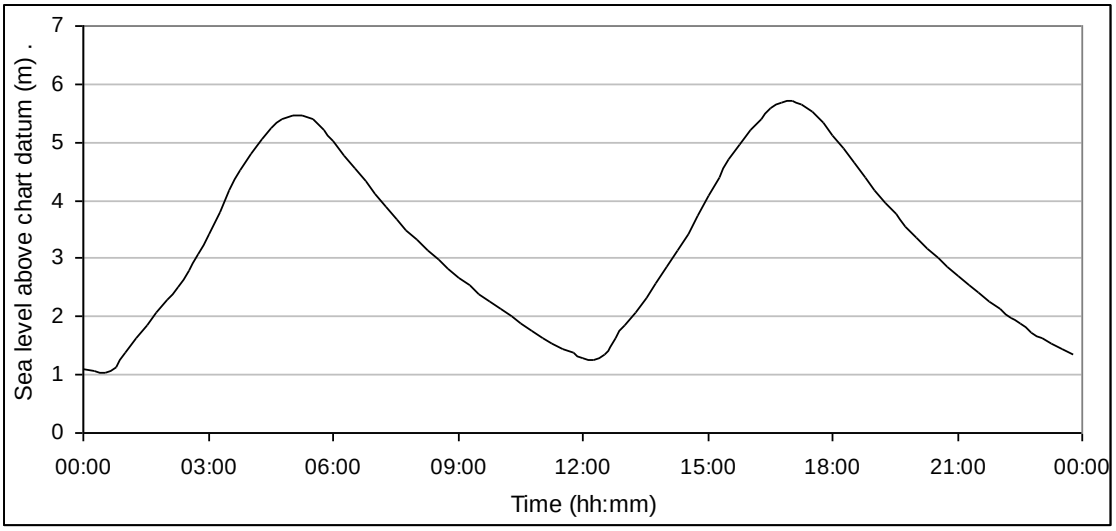

Figure 5.9. Sea level curve at the PKC Newburgh site on 10/03/2008, during a spring tide, illustrating a spring tidal range of c.4.5 m. MHWS is 5.5m and MLWS is 1.5m.

5.2.6 Newport-on-Tay (SEPA; TERC)

Newport Pier, in Newport-on-Tay, is a busy pier currently owned by David Anderson Marine and used for leisure craft mooring, craft maintenance and goods transport. The SEPA and TERC gauges operated from the same location on the pier; [NO 41790 27649] (Figure 5.10) (SEPA, 2010).

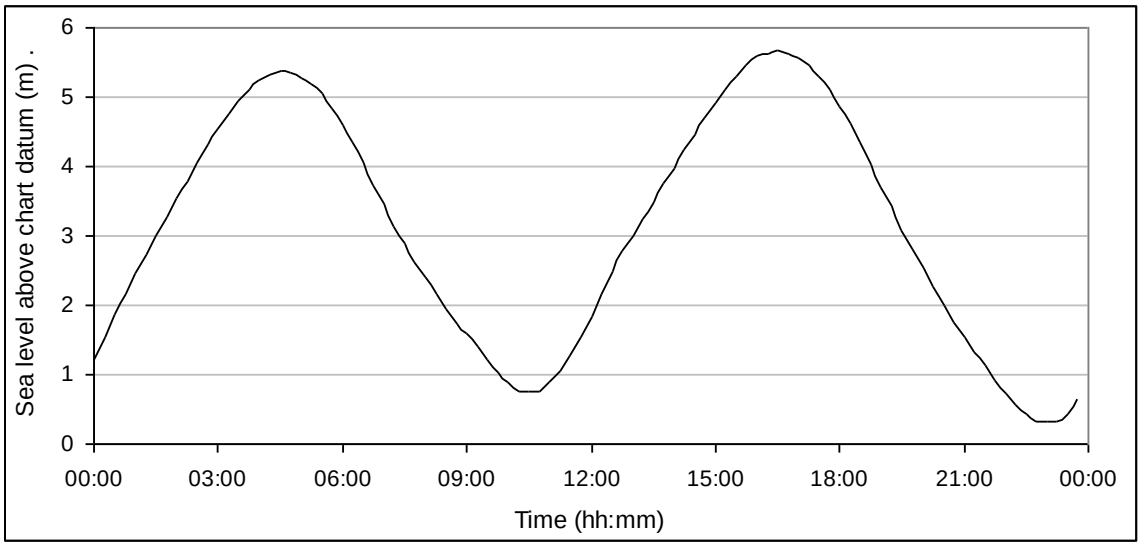

Figure 5.10. Sea level curve at the SEPA Newport-on-Tay site on 10/03/2008, during a spring tide, illustrating a spring tidal range of c.5 m. MHWS is 0.5m and MLWS is 5.5m.

SEPA's second line of coastal flooding detection for the Tay Estuary is situated at Newport-on-Tay. In Figure 5.11, the Newport-on-Tay data between 1995 and 2009 indicate a lowering of sea level (see Section 5.4.2).

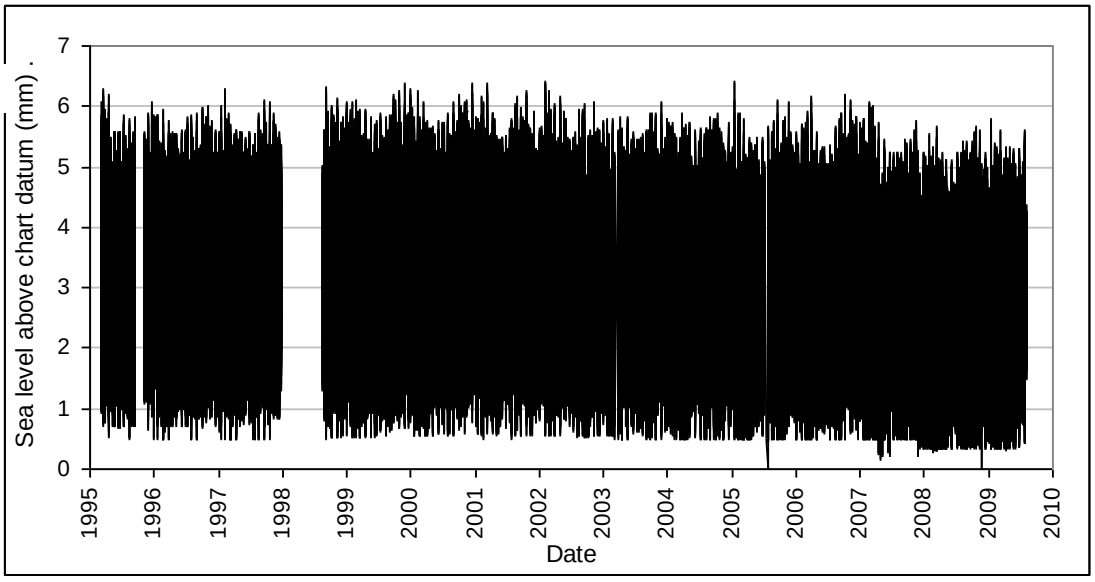

Figure 5.11. SEPA Newport-on-Tay hourly frequency sea level record from 15 minute sea level data between 1995 and 2009. Seven months of data are missing during 1998 as the data received did not show tidal patterns. These data were not representative of daily mean, as the value rapidly rose from 2.8 m to 4.8 m across the time period. The monthly mean data are not representative of sea level trends due to errors.

TERC initiated the collection of tide gauge data at two sites in the Tay Estuary, at Newport Pier and Stannergate. Both of these tide gauges recorded paper datasets, most of which were retained by the

University of Dundee. Few annotations were added to the paper records to indicate tidal height; this made it difficult to convert the paper recordings into a digital format and masked recording errors. Newport Pier was taken over as a tide gauge site by SEPA when TERC closed.

Newport Pier is of a stonewall construction with infill and a concrete extension on the western side where the tide gauge is situated. Large parts of the data transcription are incomplete where tidal heights could not be distinguished due to lack of height references on individual paper records. For this reason this dataset has been excluded here.

5.2.7 Dundee (Forth Ports; PSMSL)

The Port of Dundee is located to the south east of the City of Dundee and has been described in more detail within Chapter 3. Dundee tide gauge is situated centrally within the Port of Dundee's river berths (NO 42505 30834; Figure 5.12).

The Port of Dundee is the largest port in the Tay Estuary and the most northerly of those owned by Forth Ports. Tide gauge data from this site are currently available from Forth Ports dating back to 1986. The data are primarily available in paper records obtained between 1986 and 1997 and digitally since 1997. All Forth Ports sea level data have been processed (pre-correction) to produce daily mean sea level records from average high and low water level values (Figure 5.13).

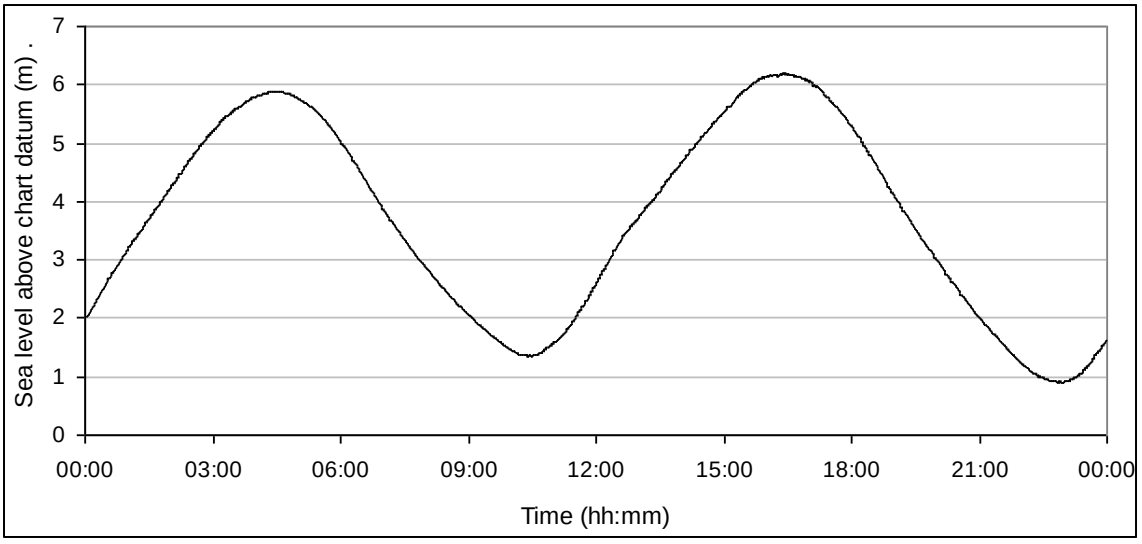

Figure 5.12. Sea level curve at the Forth Ports Dundee site on 10/03/2008, during a spring tide, illustrating a spring tidal range of c.5 m. MHWS is 0.5m and MLWS is 5.5m.

The PSMSL Dundee dataset is available only in Metric format. This monthly mean sea level dataset extends between 1897 and 1913 in a continuous record (Figure 5.14).

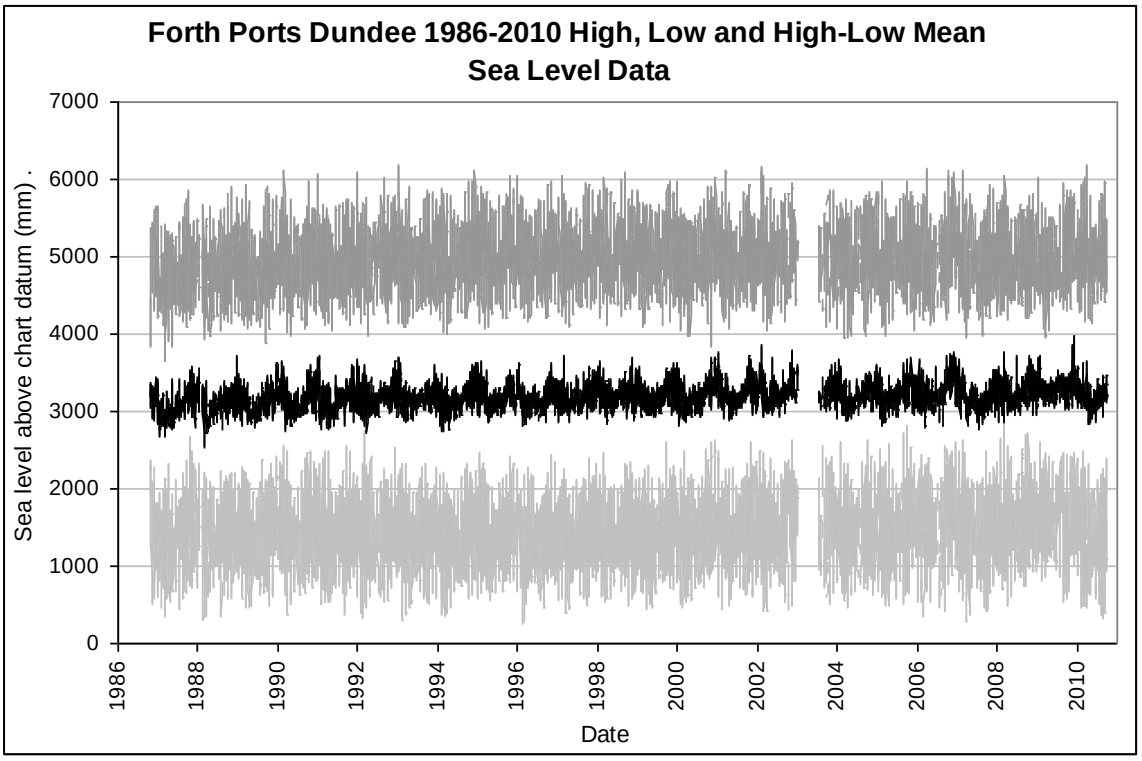

Figure 5.13. Forth Ports Dundee average daily high water level, average daily low water level and daily mean sea level between 1986 and 2010. The calculated mean sea level trend for this period from these data is an increase of 5.9 mm a^{-1}.

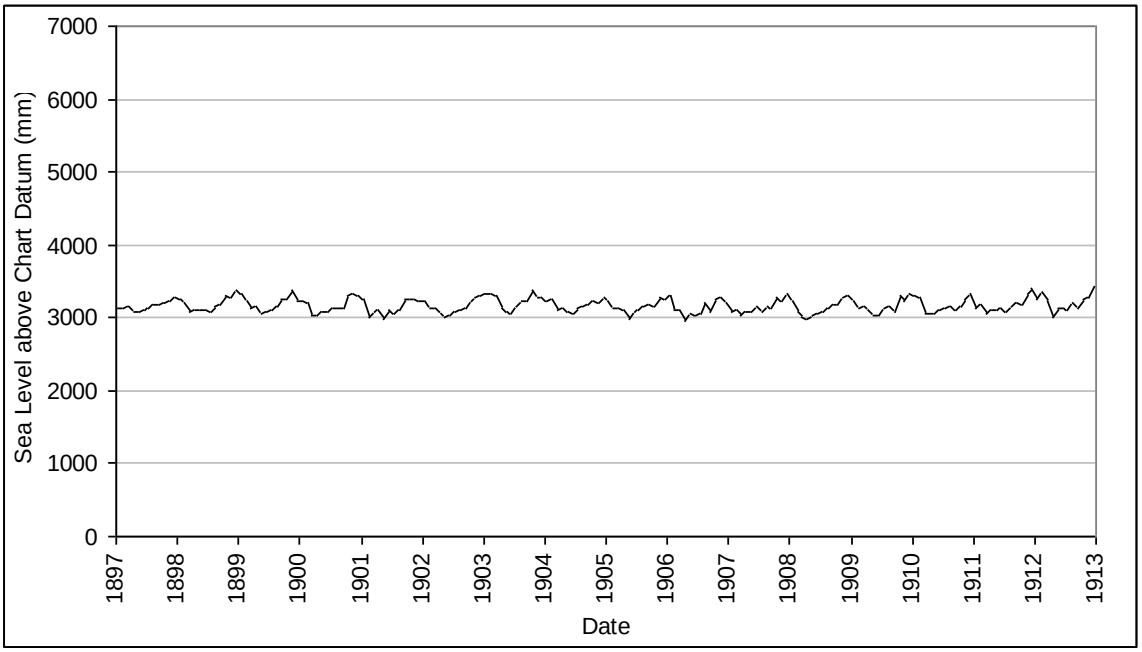

Figure 5.14. PSMSL Dundee monthly mean sea level data from Metric hourly sea level data between 1897 and 1913. Calculated mean sea level trend for this period from these data is 0.38 mm a^{-1}.

5.2.8 Stannergate, Dundee (TERC)

Stannergate lies on the eastern edge of the Port of Dundee on the north coast of the Tay Estuary between Dundee and Broughty Ferry (NO 43429 31026). The TERC Stannergate dataset is available in paper format as shown in Figure 5.15.

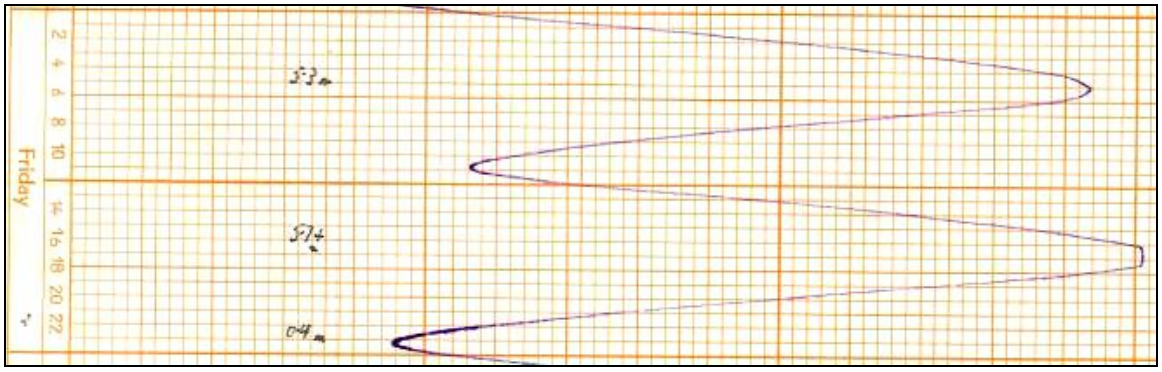

Figure 5.15. Sea level curve at the TERC Stannergate tide gauge, Dundee, during a spring tide, illustrating a spring tidal range of c.5 m. The height ranges from 0 m above Chart Datum towards the left of the page to approximately 5.85 m above Chart Datum on the far right of the page. However, the pen was not aligned to a set height scale on the page, making transcription of data particularly difficult on chart where heights have not been regularly recorded. MHWS is 0.5m and MLWS is 5.5m.

A tide gauge was situated on Shell Pier, Stannergate by TERC. The pier has since been demolished, making way for river berth improvements. The paper datasets for this site are of equally poor quality to those of Newport-on-Tay and have been excluded here.

5.2.9 Arbroath (SEPA)

The Arbroath gauge is located in Arbroath Harbour (NO 64236 40659), which is home to a lifeboat station, recreational craft and fishing vessels. The 15 minute data collected at this site suggest longer slack periods at Arbroath than in the outer Tay Estuary (Figure 5.16).

The Arbroath tide gauge, the most easterly of the SEPA gauges, acts as the first point of coastal flood warning detection for the Tay Estuary. Data are available from this gauge between 2007 and 2009 in 15 minute format. As shown in Figure 5.17, the data are not consistently accurate with tides, varying considerably between April 2008 and August 2008 (Figure 5.17). Spring low tides are also cut off throughout the dataset with the datum shifting by over 20 cm in early 2009. A trend was not calculated for this site due to these inaccuracies.

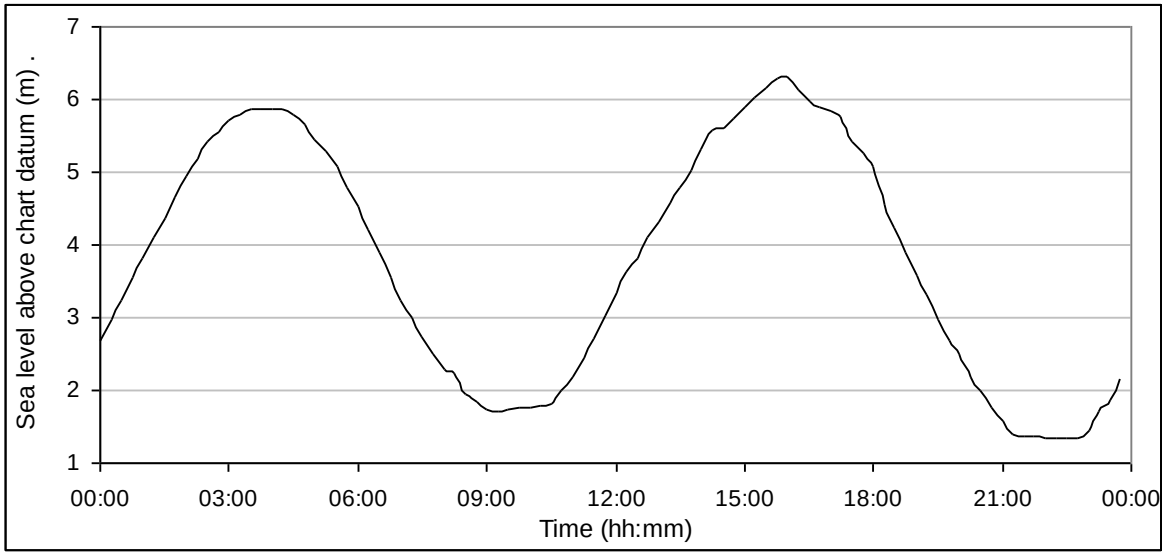

Figure 5.16. Sea level curve at the SEPA Arbroath site on 10/03/2008, during a spring tide, illustrating a spring tidal range of c.5 m. MHWS is 0.5m and MLWS is 5.5m.

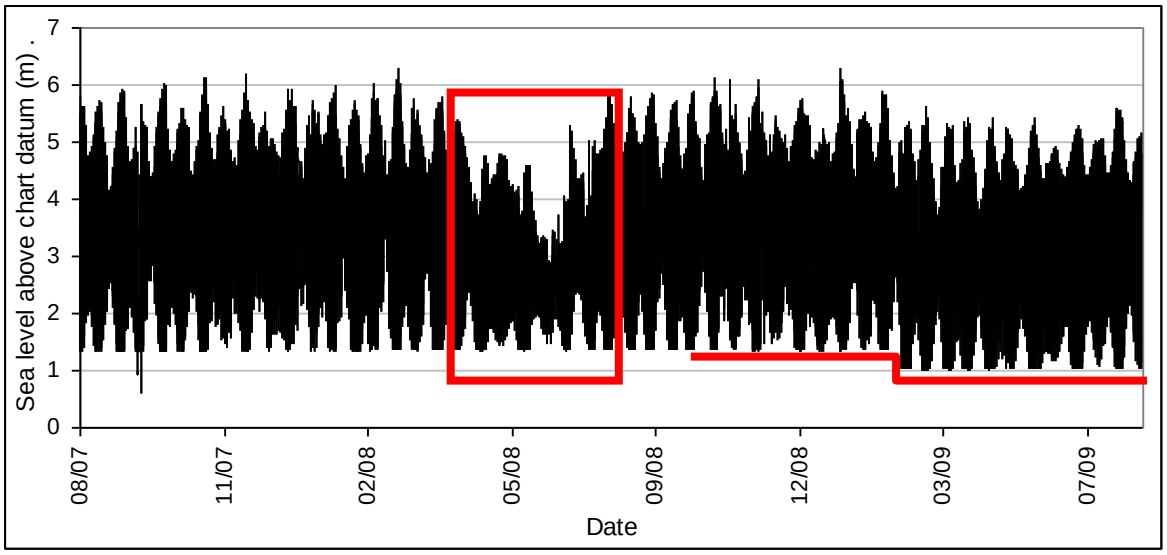

Figure 5.17. SEPA Arbroath hourly frequency sea level record from 15 minute sea level data between 2007 and 2009. The monthly mean data are not representative of sea level trends due to unexpected anomalies including areas within the red block and the datum change indicted by the line.

5.2.10 Grangemouth (Forth Ports)

Grangemouth is one of the large commercial-scale operable ports along the Forth and is located on the southern bank, opposite Longannet Power Station (NS 93824 82465). The tide gauge observes the entire tidal cycle, including the lackie, double high and low tides (see Chapter 3) (Figure 5.18).

The Port of Grangemouth data, given by Forth Ports, are available from the Grangemouth tide gauge from 1979 intermittently until 2010. Several gauges have been used during this time. All recordings prior to 1998 were made onto paper. Since then, the entire 1979 to 2010 data series has been converted into mean daily high-low sea level datasets. The high water, low water and mean daily high-low sea level are presented within Figure 5.19.

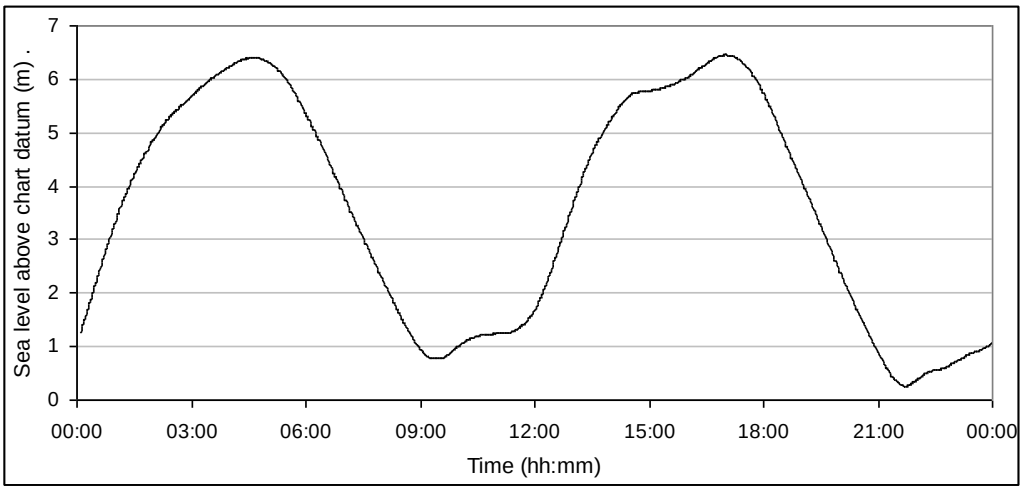

Figure 5.18. Sea level curve at the Forth Ports Grangemouth site on 10/03/2008, during a spring tide, illustrating a spring tidal range of c.6.0 m. MHWS is 0.5m and MLWS is 6.0m.

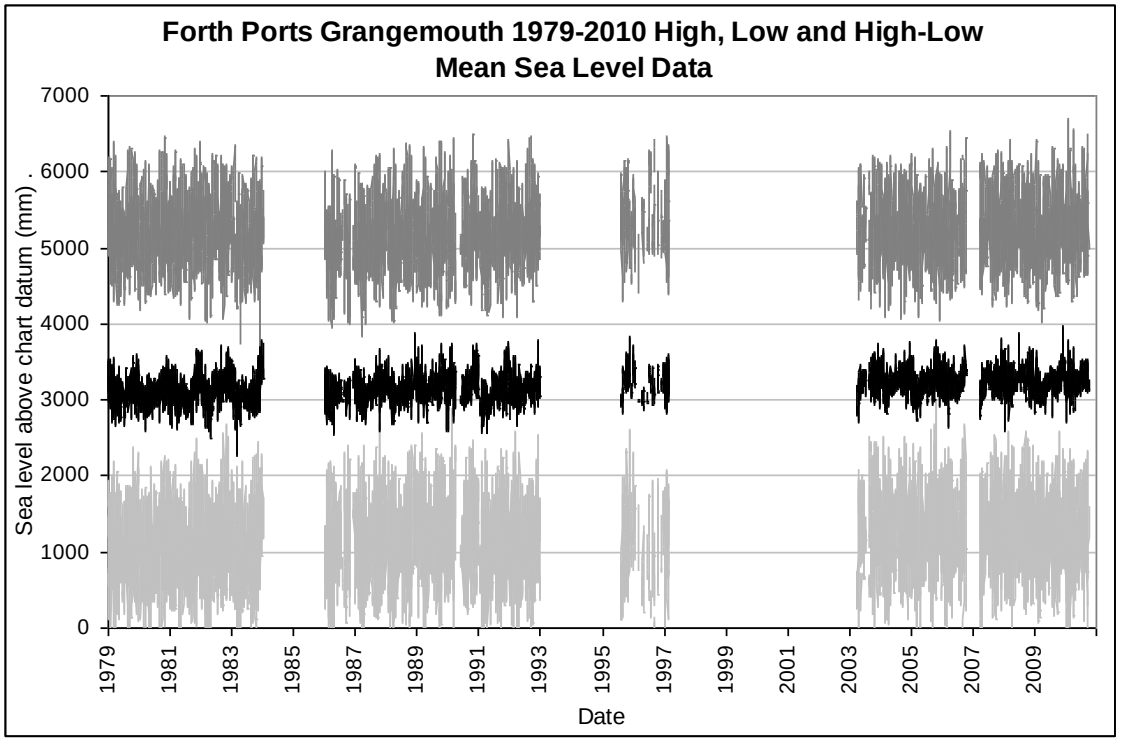

Figure 5.19. Forth Ports Grangemouth average daily high water level, average daily low water level and daily mean sea level between 1979 and 2010. The calculated mean sea level trend for this period from these data is an increase of 5.7 mm a^{-1}.

5.2.11 Rosyth (Forth Ports; PSMSL; UKHO)

The data from Rosyth are derived from two separate tide gauges. The UKHO and PSMSL tide gauge is located within the Babcock Rosyth Dockyard limits on the southern pier, whereas the Forth Ports tide gauge is located on the corner of one of the river berths (NT 10448 82064; Figure 5.20).

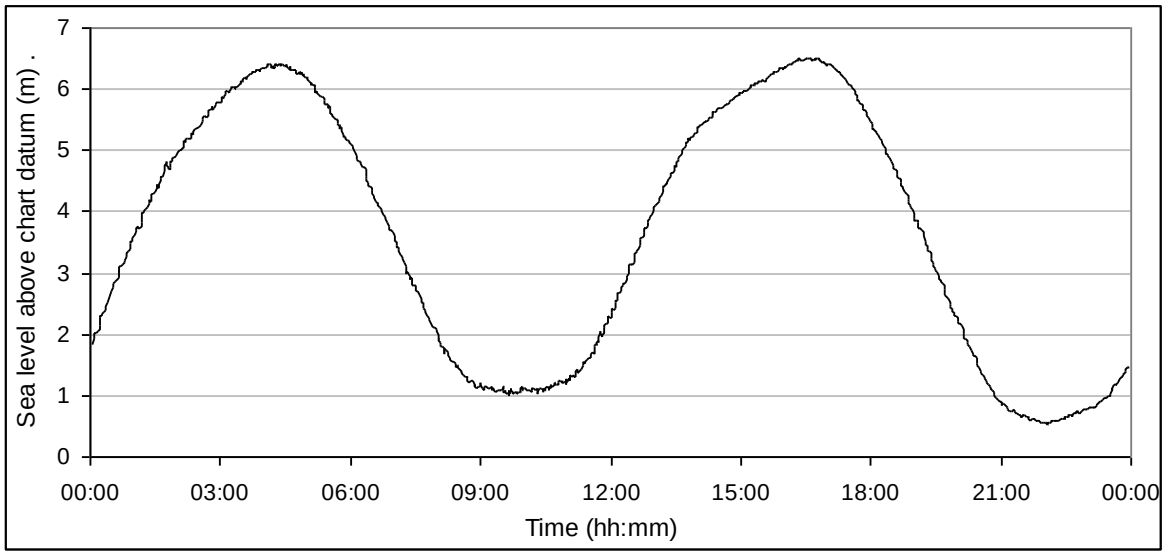

Figure 5.20. Sea level curve at the Forth Ports Rosyth site on 10/03/2008, during a spring tide, illustrating a spring tidal range of c.5.5 m. MHWS is 1.0m and MLWS is 5.5m.

The Port of Rosyth data between 2003 and 2010 are available from the Forth Ports tide gauge. Figure 5.21 highlights the daily high water, low water and mean daily high-low sea level data. These data are stable with no spikes or long-term skews appearing. PSMSL's Rosyth dataset is available online in monthly and annual Metric format, as well as monthly RLR format between 1964 and 1993 (Figure 5.22 to Figure 5.24).

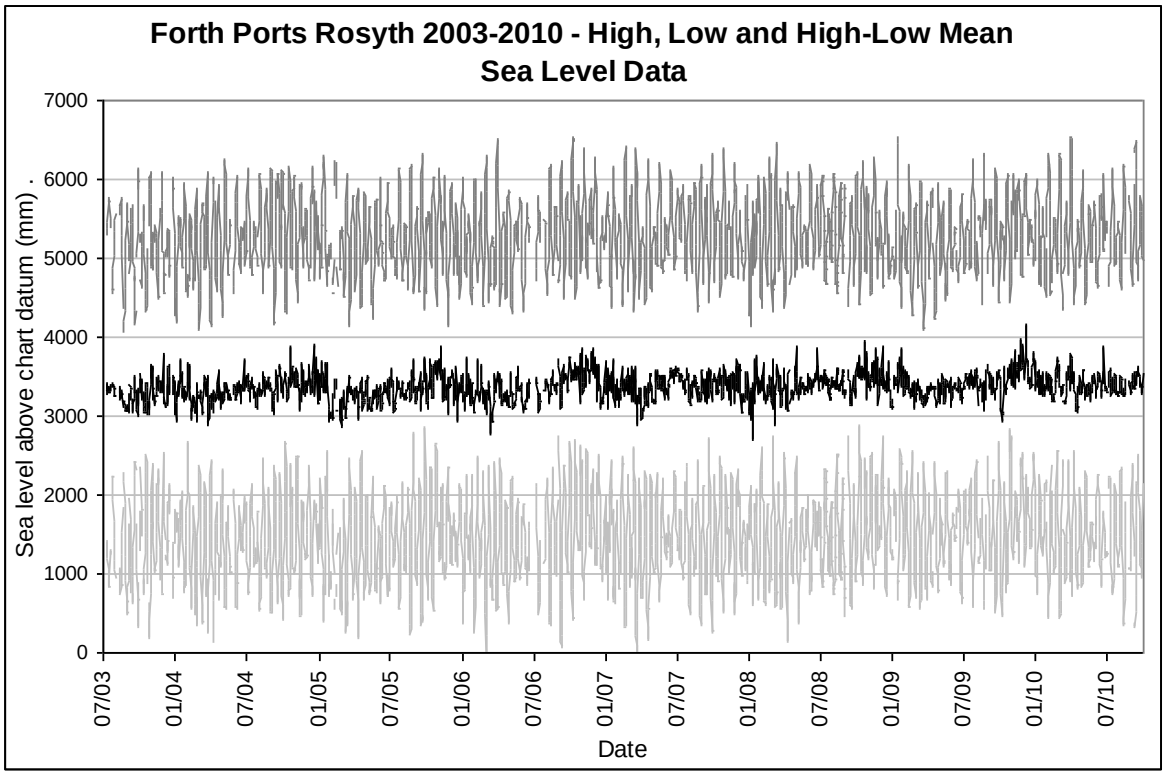

Figure 5.21. Forth Ports Rosyth average daily high water level, average daily low water level and daily mean sea level between 2003 and 2010. The calculated mean sea level trend for this period from these data is an increase of 20 mm a^{-1}.

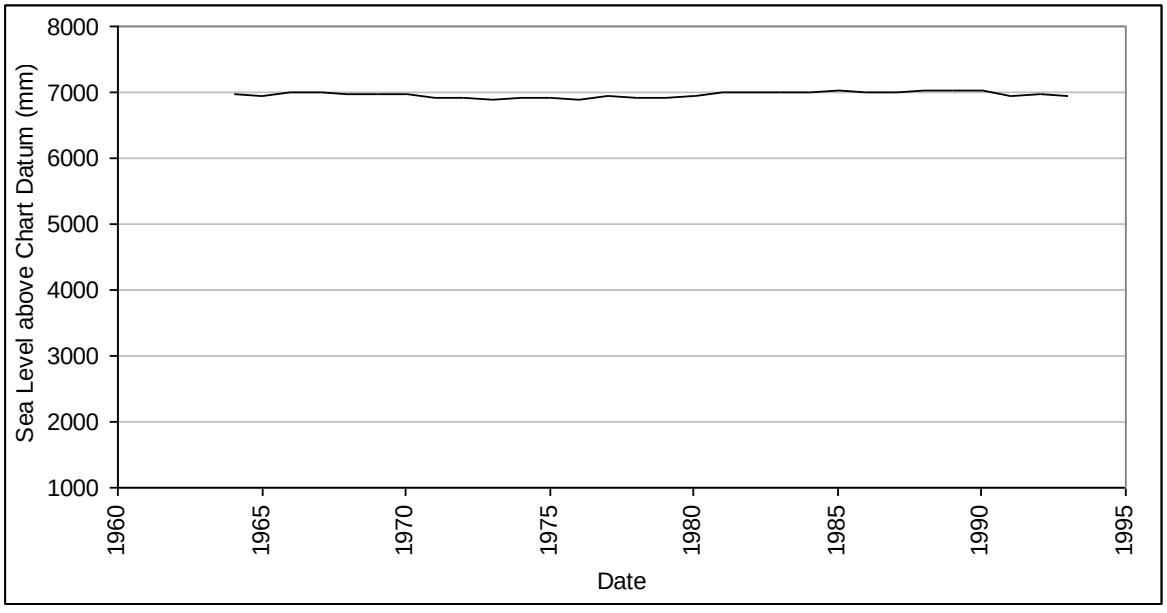

Figure 5.22. PSMSL Rosyth annual mean sea level data from Metric hourly sea level data between 1964 and 1993. Calculated mean sea level trend for this period from these data is 1.67 mm a^{-1}.

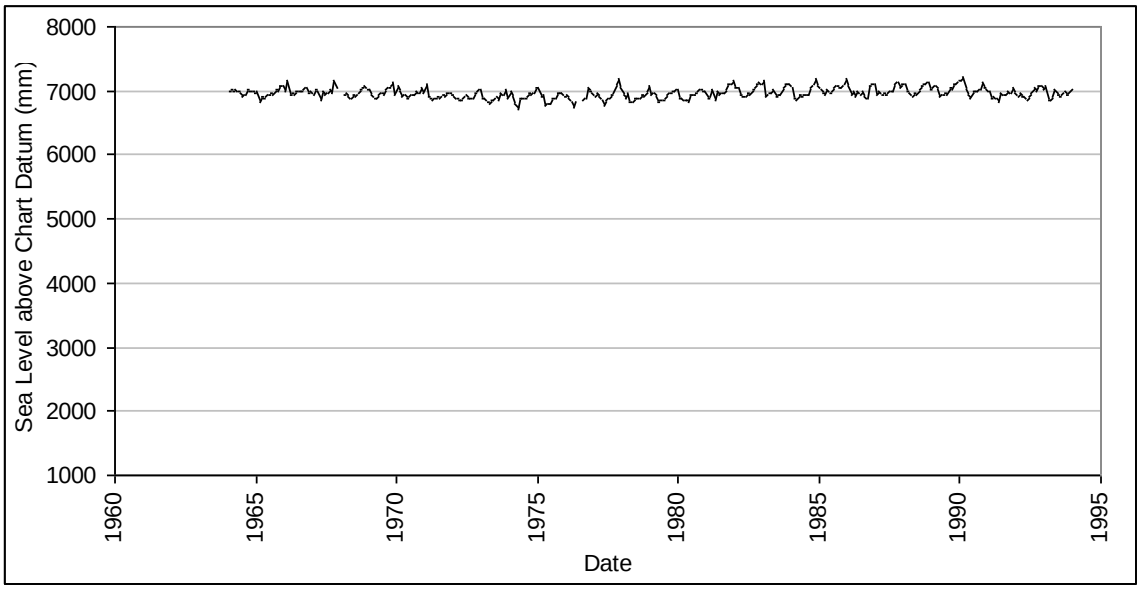

Figure 5.23. PSMSL Rosyth monthly mean sea level data from Metric hourly sea level data between 1964 and 1993. Calculated mean sea level trend for this period from these data is 1.67 mm a^{-1}.

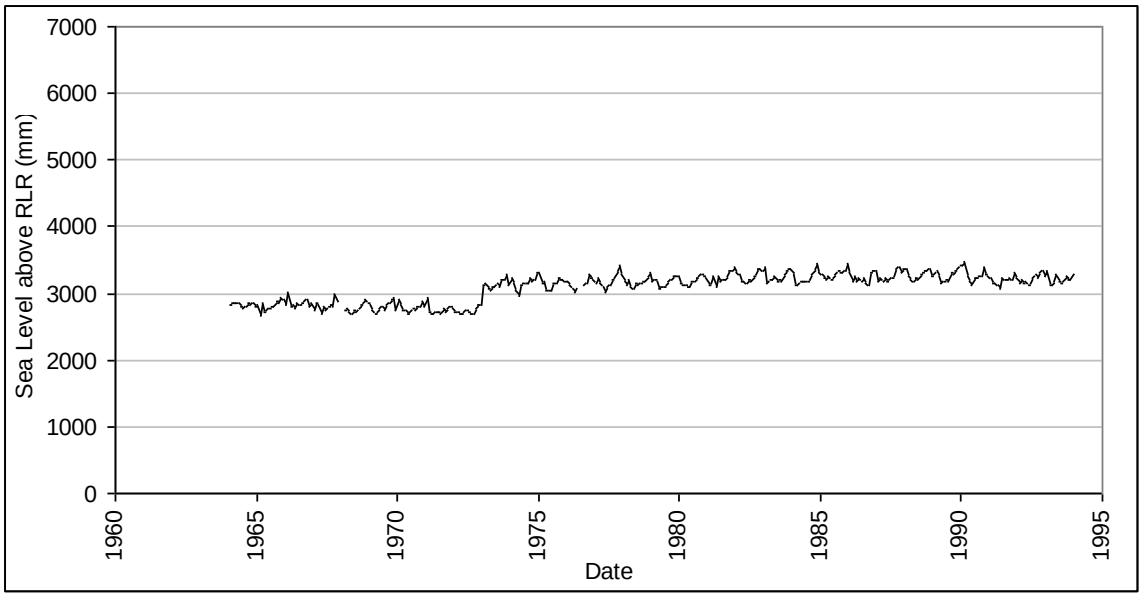

Figure 5.24. PSMSL Rosyth annual mean sea level data from RLR hourly sea level data between 1964 and 1993. The monthly mean data are not representative of sea level trends due to errors.

The UK Hydrographic Office (UKHO) allows access to all Forth and Tay data held at their Taunton facility. They currently hold data for Dunbar, Leith and Rosyth, amongst other UK datasets. Data were collected from paper records and the high and low tide heights were used to calculate the daily means for each site.

The UKHO Rosyth dataset includes data from 1912 and 1914 to 1920 (Figure 5.25). These data were recorded at what is now the Babcock Rosyth Dockyard, which is the enclosed dock and piers

of the western section of the former Rosyth Naval Dockyard area. Tidal trends here are calculated to be decreasing by 5.28 mm a^{-1} for this short period.

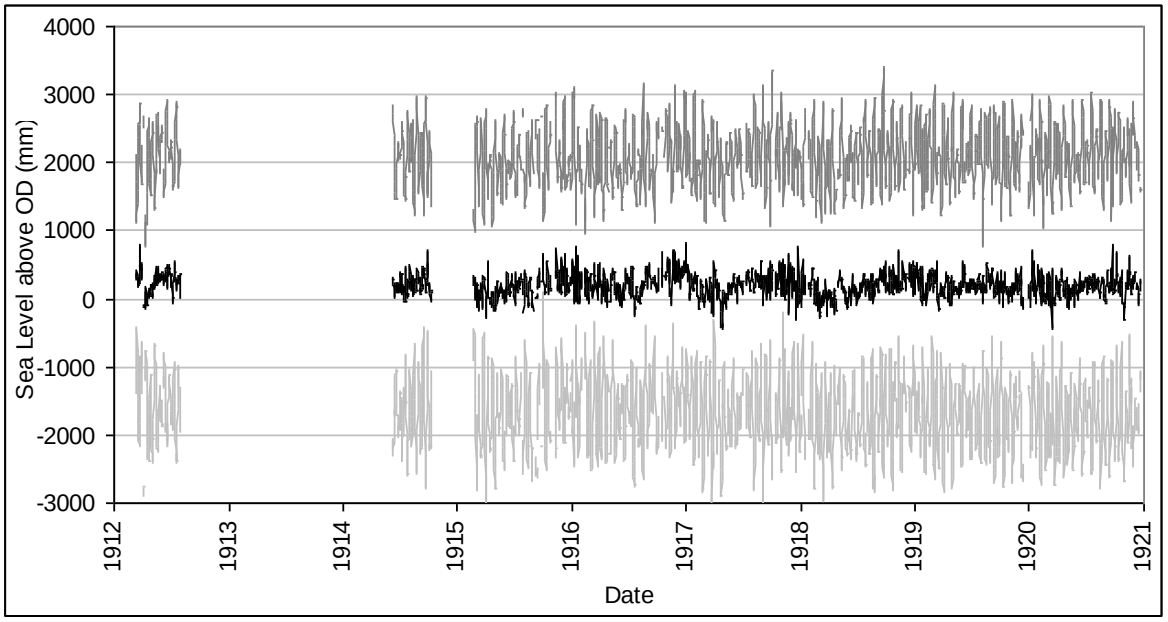

Figure 5.25. UKHO Rosyth daily mean high sea level, daily mean low sea level and daily mean sea level data between 1912 and 1920. Calculated mean sea level trend for this period is -5.28 mm a^{-1}.

5.2.12 Methil (Forth Ports)

The Port of Methil, the smallest of the Forth Ports sites with an operating tide gauge, is located on the north coast of the inner Firth of Forth. The tide gauge is located at the harbour mouth (NT 27707 99649; Figure 5.26).

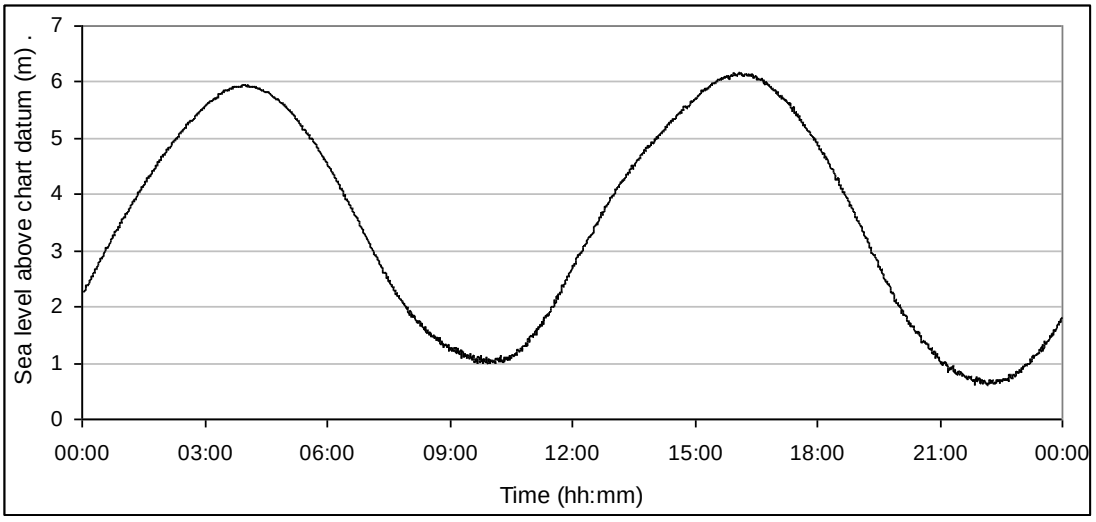

Figure 5.26. Sea level curve at the Forth Ports Methil site on 10/03/2008, during a spring tide, illustrating a spring tidal range of c.5.5 m. MHWS is 1.0m and MLWS is 5.5m.

The Port of Methil data from Forth Ports are available between 2003 and 2010; however the data presented here are sporadic (Figure 5.27) partly due to vandalism of the gauge hardware.

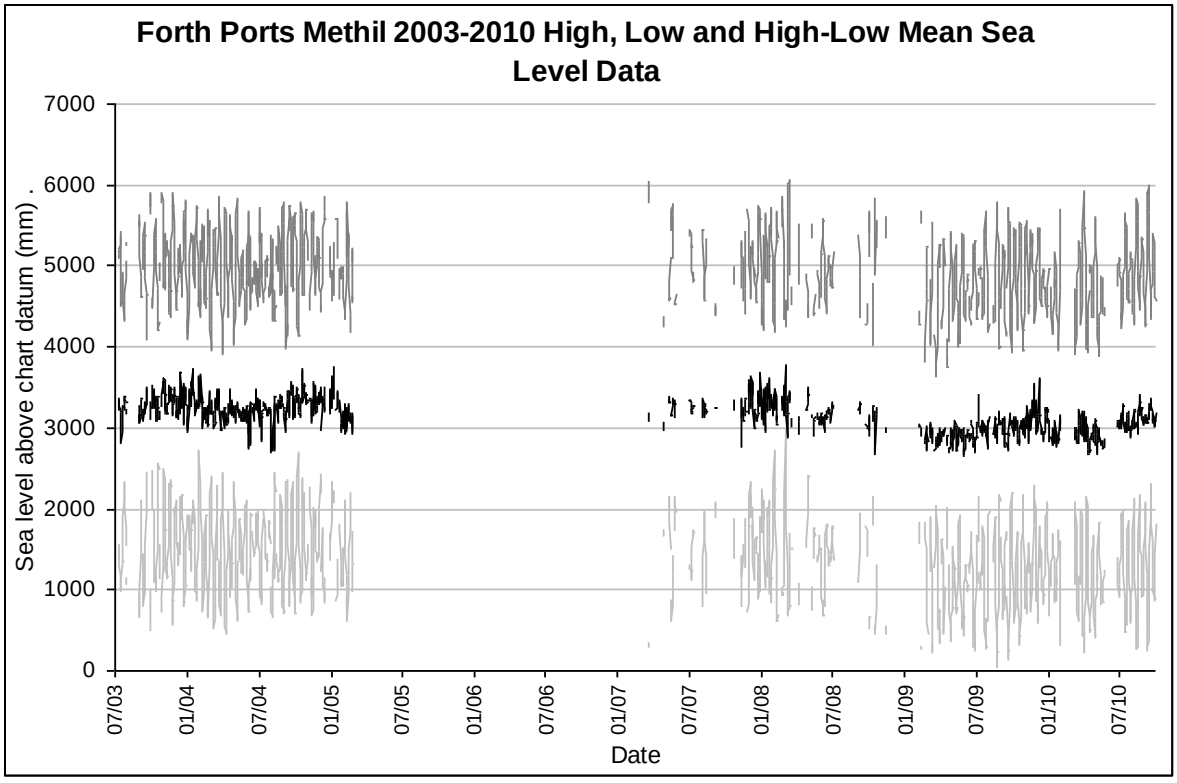

Figure 5.27. Forth Ports Methil average daily high water level, average daily low water level and daily mean sea level between 2003 and 2010. The calculated mean sea level trend for this period from these data is a decrease of 41.4 mm a^{-1}. This decreasing trend is likely to be due to gauge inaccuracy.

5.2.13 Leith (Forth Ports; PSMSL(1); PSMSL(2); UKHO; NTSLF/BODC)

The Port of Leith has recorded tide gauge data for several organisations. All of these tide gauges have been located at [NT 26798 77488]. The NTSLF/BODC, two PSMSL and UKHO gauges are likely to be the same gauge series, with the NTSLF and the PSMSL institutions adopting their data from the UKHO. The UKHO may have been gifted these data by the previous owners of the Port of Leith, as Forth Ports continue to do so for data from all of their tide gauge operating ports (Figure 5.28). The PSMSL datasets, Leith 1 and Leith 2 (see Table 4.1 for data timescales and gauge details), are both available in Metric and Revised Local Reference (RLR) formats (Table 5.1).

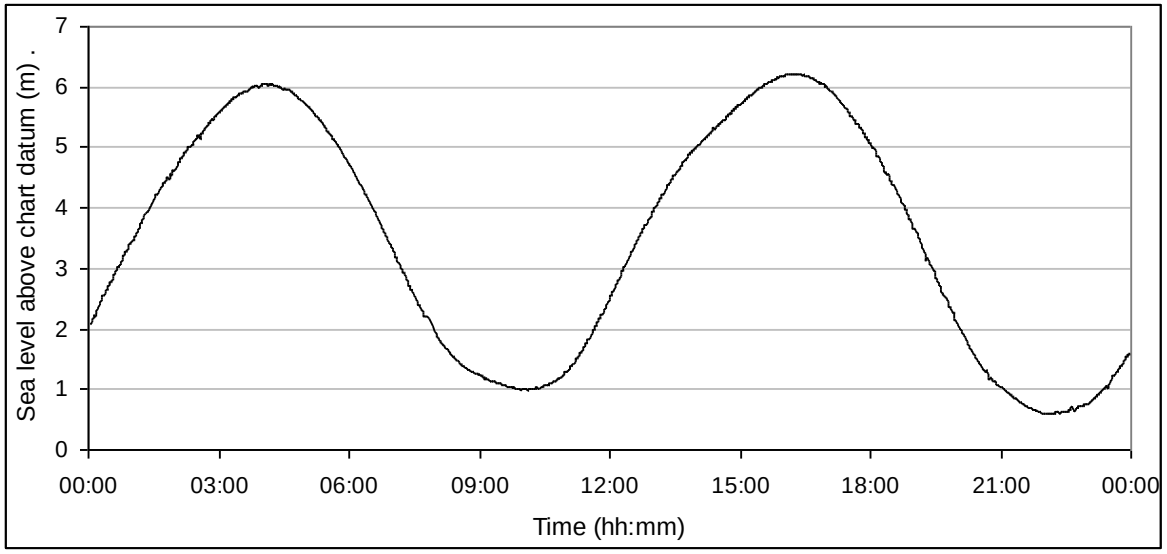

Figure 5.28. Sea level curve at the Forth Ports Leith site on 10/03/2008, during a spring tide, illustrating a spring tidal range of c.5.5 m. MHWS is 1.0m and MLWS is 5.5m.

The Port of Leith is the port for the City of Edinburgh. Tide gauge data are available from Forth Ports for this site between 2003 and 2010. These data are presented in Figure 5.29.

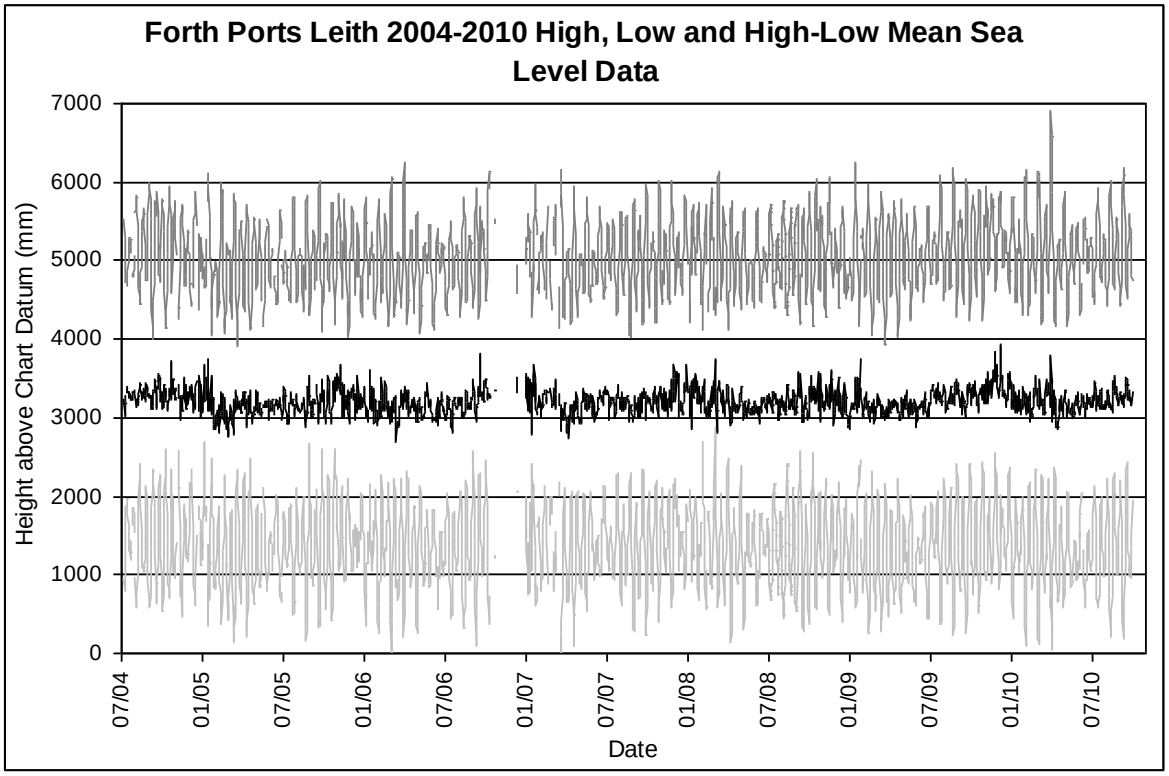

Figure 5.29. Forth Ports Leith average daily high water level, average daily low water level and daily mean sea level between 2004 and 2010. The calculated mean sea level trend for this period from these data is an increase of 5.5 mm a^{-1}.

Two datasets are available online from PSMSL at the Leith site. The Leith 1 Metric and RLR datasets extend between 1956 and 1971. Both datasets appear stable (Figure 5.30 and Figure 5.31).

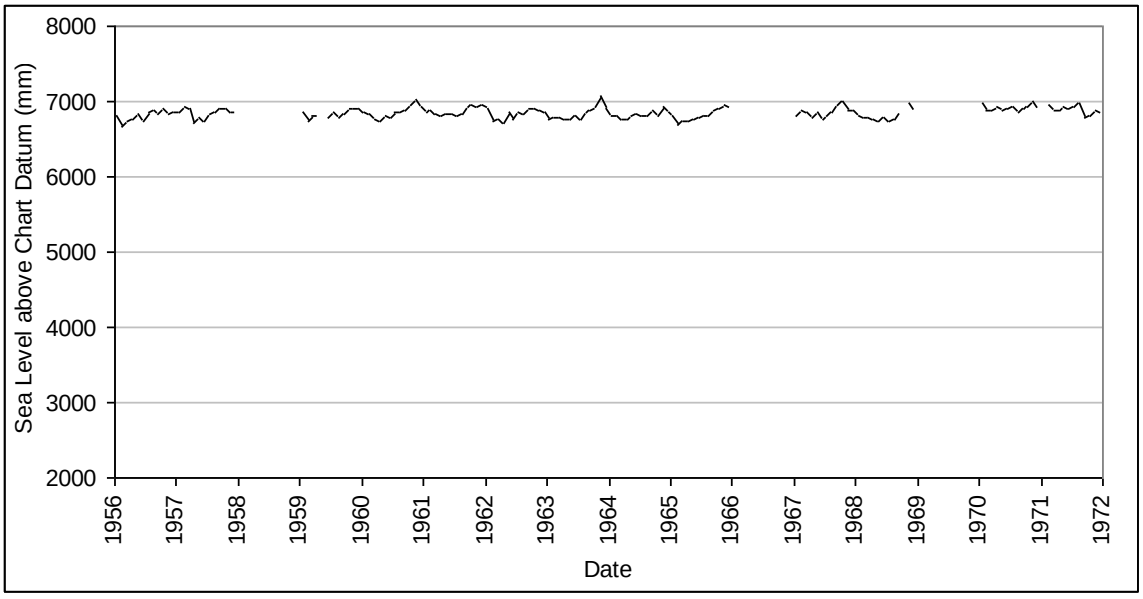

Figure 5.30. PSMSL Leith 1 monthly mean sea level data from Metric hourly sea level data between 1956 and 1971. Calculated mean sea level trend for this period from these data is 3.75 mm a^{-1}.

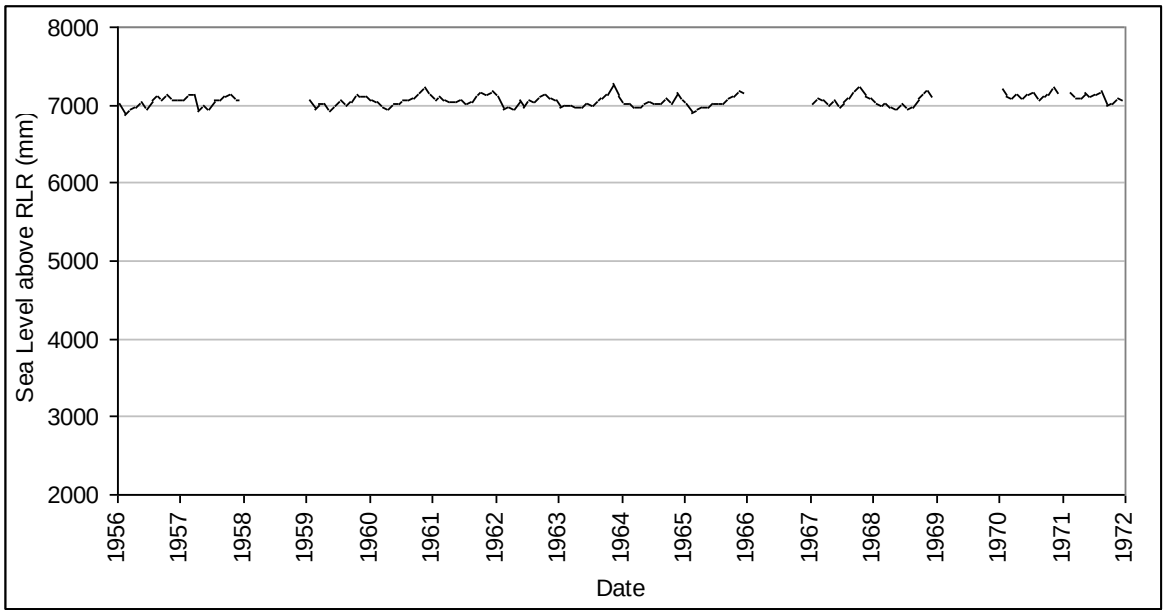

Figure 5.31. PSMSL Leith 1 monthly mean sea level data from RLR hourly sea level data between 1956 and 1971. Calculated mean sea level trend for this period from these data is 4.06 mm a^{-1}.

The longer Leith 2 Metric and RLR datasets extend from 1981 to 2009 (Figure 5.32 and Figure 5.33).

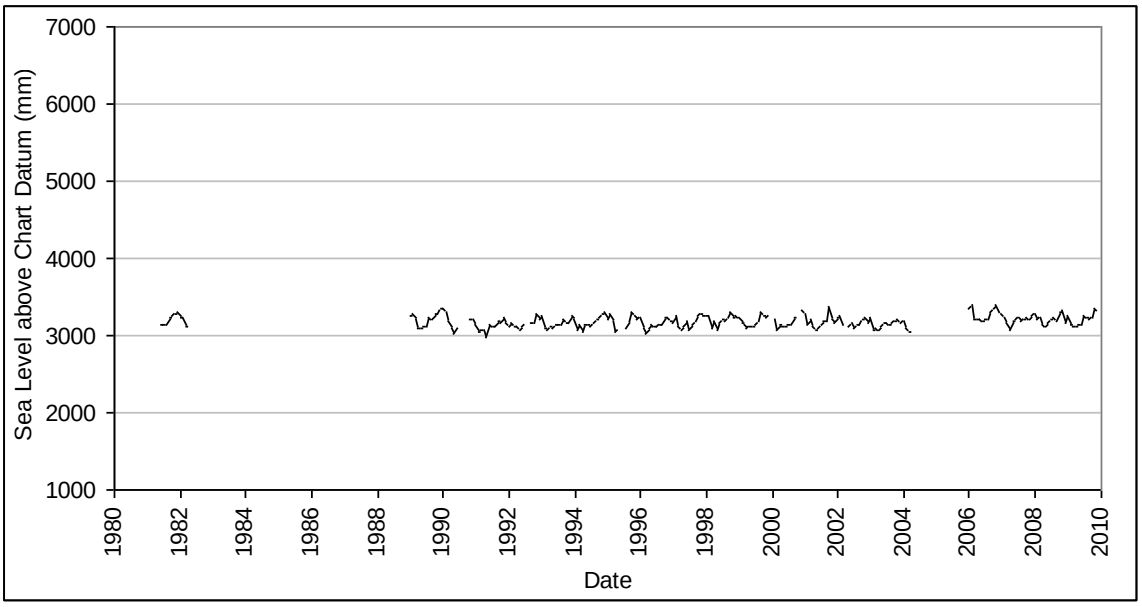

Figure 5.32. PSMSL Leith 2 monthly mean sea level data from Metric hourly sea level data between 1981 and 2009. The monthly mean data are not representative of sea level trends between 2005 and 2010. Calculated mean sea level trend for the period between 1990 and 2004 is -0.18 mm a^{-1}.

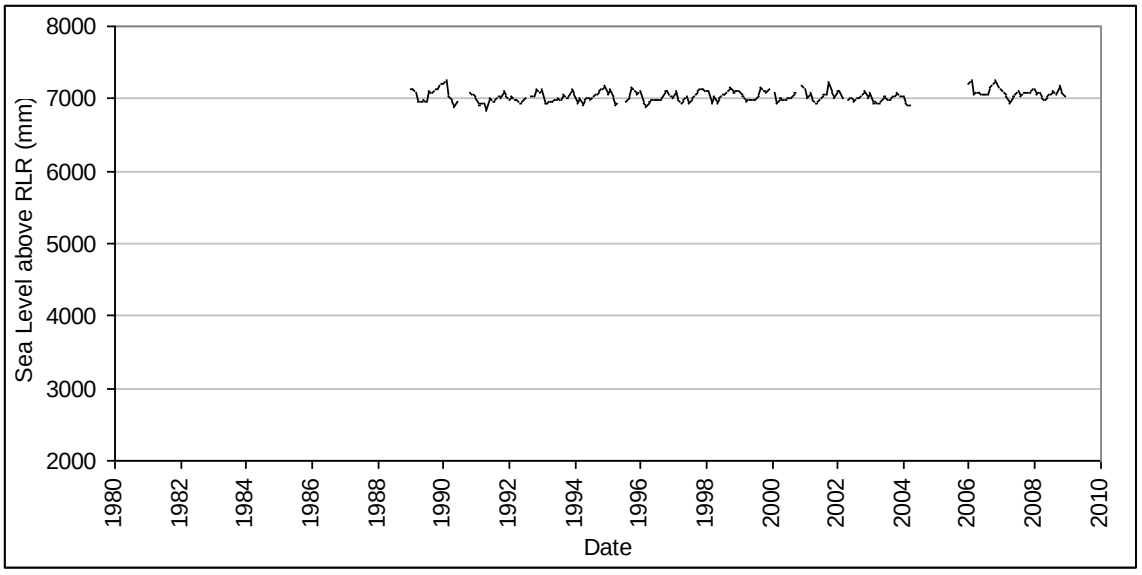

Figure 5.33. PSMSL Leith 2 monthly mean sea level data from RLR hourly sea level data between 1981 and 2009. The monthly mean data are not representative of sea level trends between 2005 and 2010. Calculated mean sea level trend for the period between 1990 and 2004 data is -0.34 mm a^{-1}.

The Leith dataset extends from 1980 to 1981 (Figure 5.34). Without supporting data from PSMSL, BODC and Forth Ports, the data would be over too short a timescale and would not be suitable for sea level analysis as errors could not be discounted. The calculated trend from this dataset is not representative due to the short timescale, but it may be representative of a sea level cycle and can be verified against neighbouring data sites.

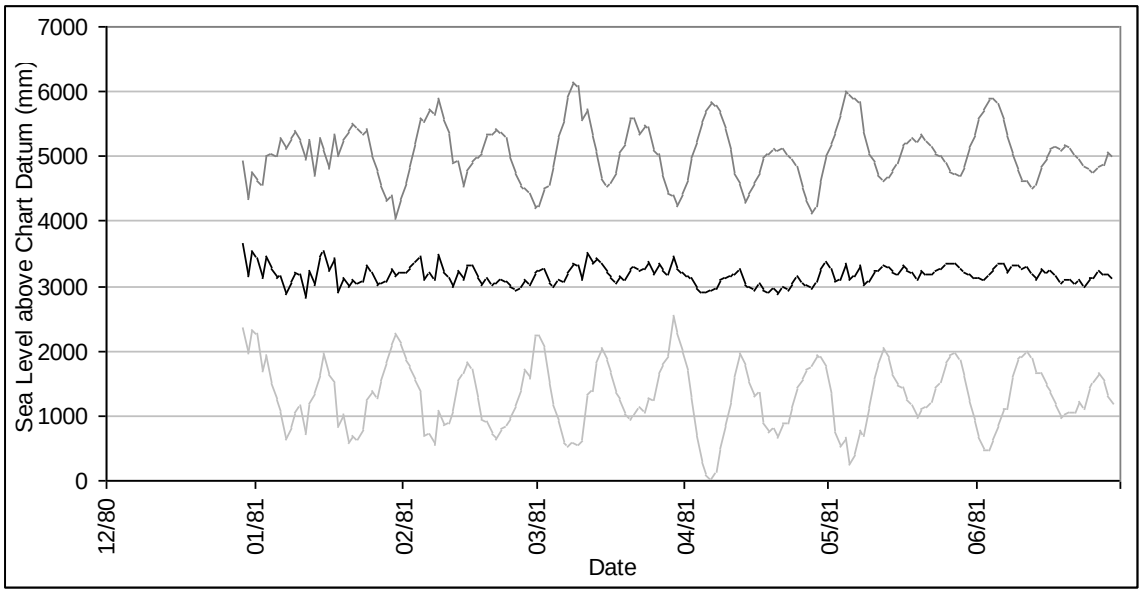

Figure 5.34. UKHO Leith average daily high water level, average daily low water level and daily mean sea level between 1980 and 1981. Calculated mean sea level trend for this period is -55.8 mm a^{-1}.

NTSLF collect raw tide gauge data from across the UK and are closely connected with BODC and PSMSL. These data are then processed for datum and long-term errors by the BODC, who publish the corrected data. There are two datasets within this study area that have been corrected by the BODC; those from Aberdeen and Leith. The data from Leith are available between 1990 and 2010 with a significant gap between 2004 and 2006 (Figure 5.35). This dataset overlaps with the Forth Ports Leith dataset, allowing comparison for analysis and correction.

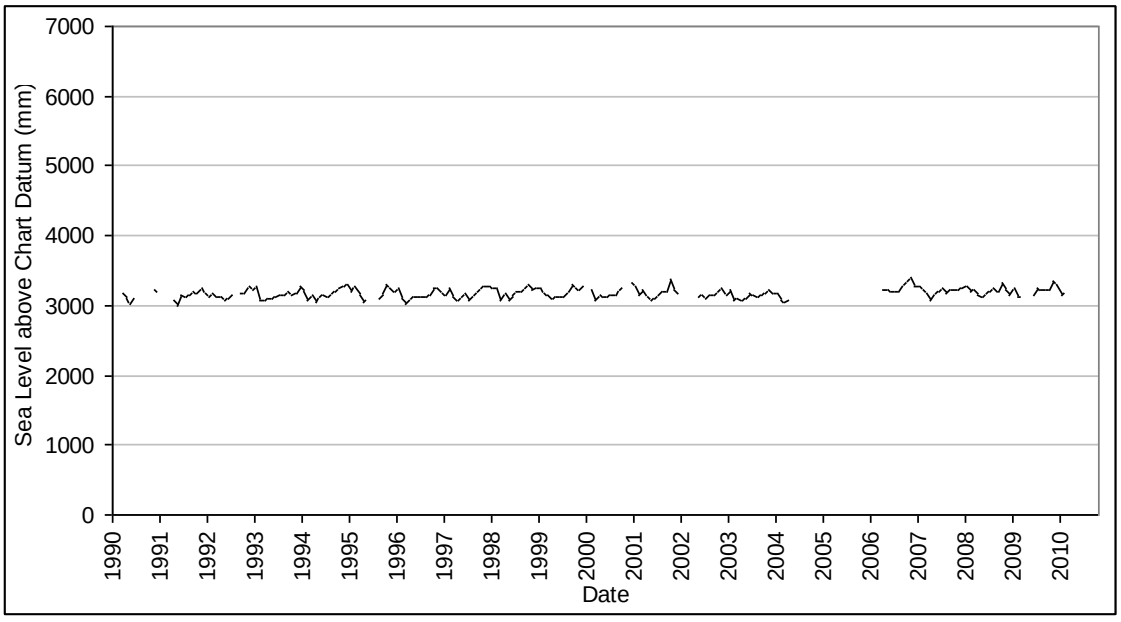

Figure 5.35. BODC/NTSLF Leith monthly mean sea level data from hourly sea level data between 1975 and 2010. Calculated mean sea level trend for this period from these data is 3.19 mm a^{-1}.

5.2.14 Musselburgh (SEPA)

Musselburgh, located east of Leith on the south coast of the Firth of Forth, has a tide gauge located on the east side of the River Esk in a kiosk with the stilling tubes extending vertically down the bank wall to the water (Julie Carty, pers. comm.). This gauge is located at [NO 34608 73184] (SEPA, 2010). Figure 5.37 highlights the minimal vertical tidal influence that is measured at this point within the River Esk.

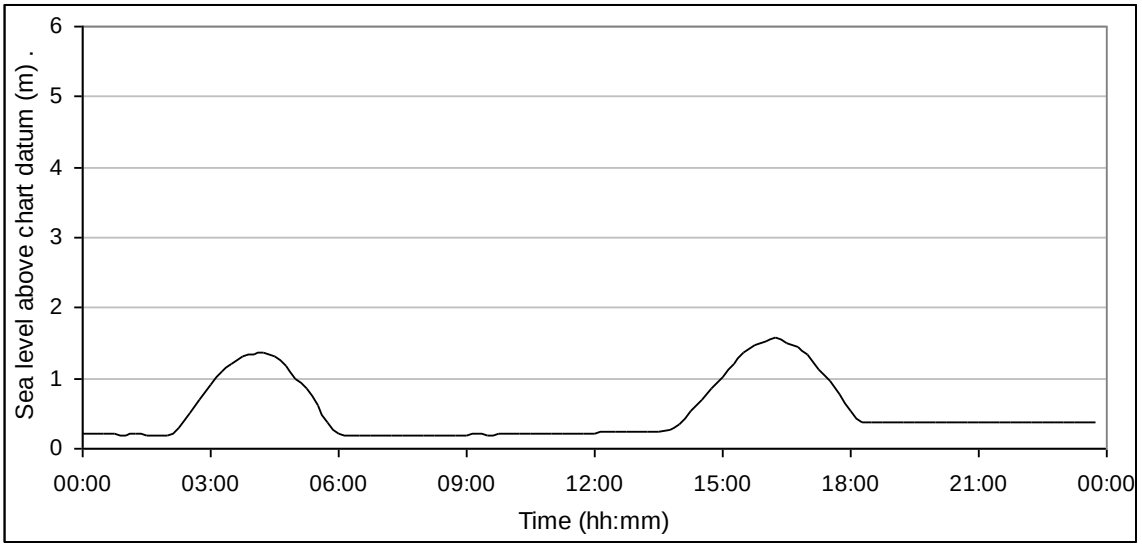

Figure 5.36. Sea level curve at the SEPA Musselburgh site on 05/09/2009 (data were not available on 10/03/2008), during a spring tide, illustrating a spring tidal range of c.0.5 m. MHWS and MLWS unknown at this location.

The Musselburgh SEPA gauge cannot record the low tide, with a long slack water period artificially appearing in the tidal cycle (Figure 5,37). This artificial slack water period could be due to either:

- The gauge being positioned too high, therefore resulting in the gauge being mechanically unable to record the lower portion of the tidal cycle;
- The gauge being designed to measure a range smaller than the natural tidal cycle at that point in the River Esk; or
- The slack water could represent the fluvial element of the water level from the River Esk.

A sister gauge lies to the south in the River South Esk monitoring the fluvial discharge.

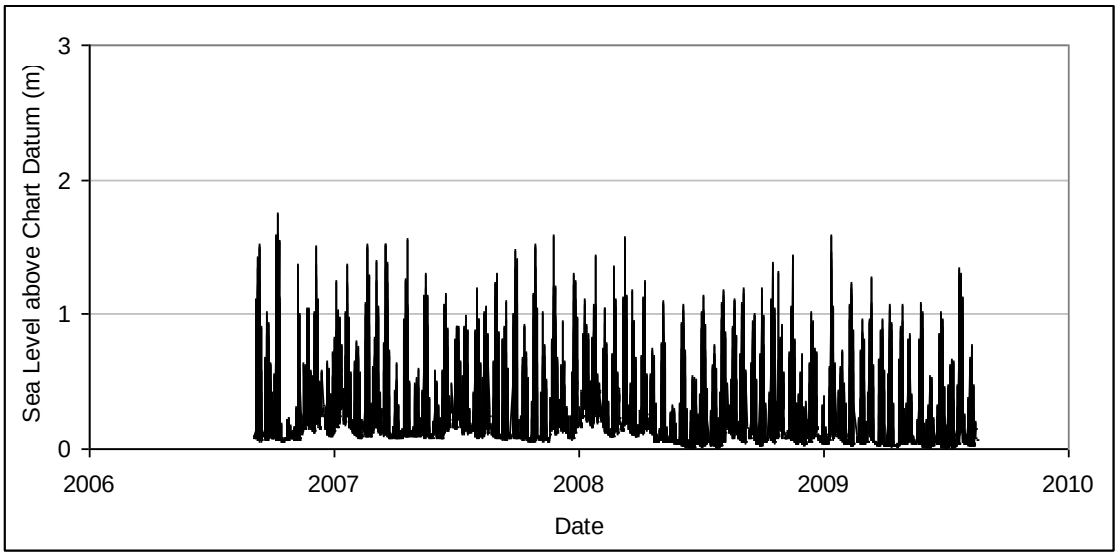

Figure 5.37. SEPA Musselburgh hourly frequency sea level record from 15 minute sea level data between 2006 and 2009. The monthly mean data are not representative of sea level trends.

5.2.15 Dunbar (PSMSL; UKHO)

Dunbar Harbour is located outside the Firth of Forth on the south coast (NT 67410 79080). Due to the monthly frequency of the data provided no tidal curve can be plotted. The port no longer records tidal heights. The PSMSL data for Dunbar are available online in both Metric and RLR format between 1913 and 1950 (Figure 5.38 and Figure 5.39).

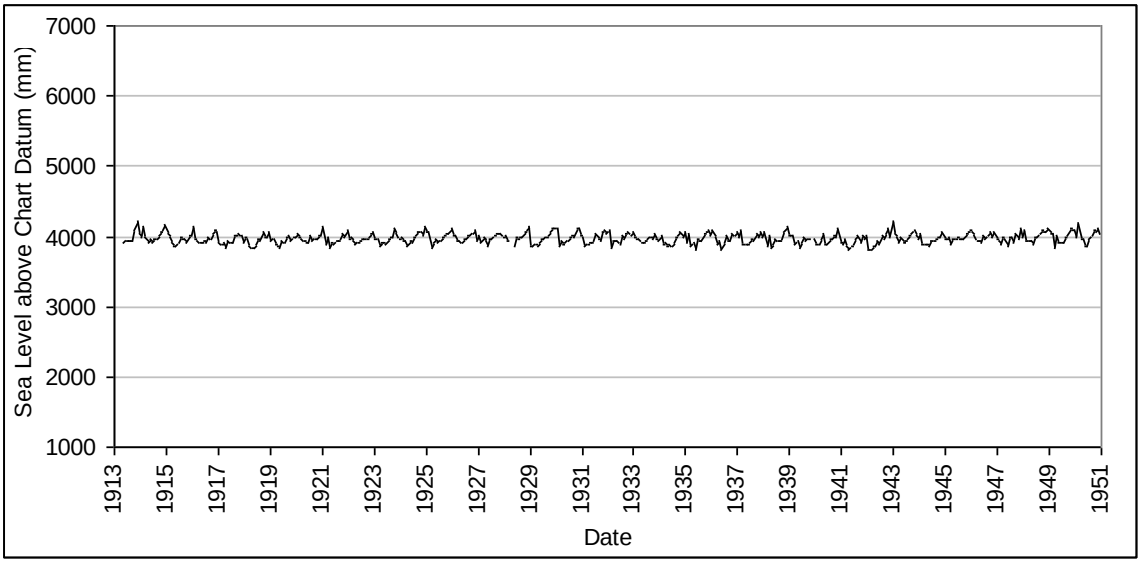

Figure 5.38. PSMSL Dunbar monthly mean sea level data from Metric hourly sea level data between 1913 and 1950. Calculated mean sea level trend for this period from these data is 0.37 mm a^{-1}.

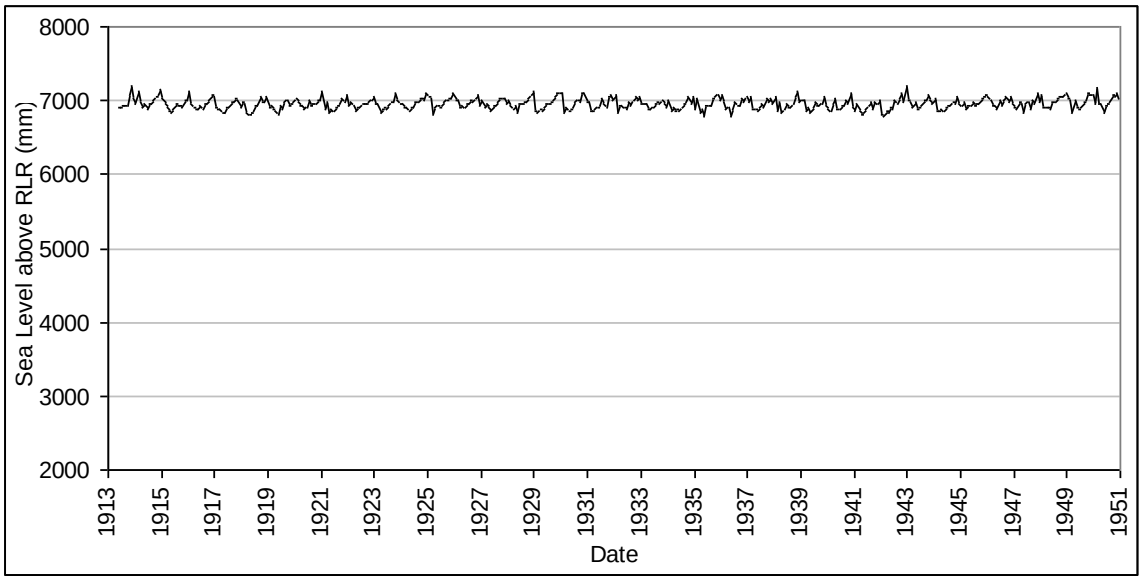

Figure 5.39. PSMSL Dunbar monthly mean sea level data from RLR hourly sea level data between 1913 and 1950. Calculated mean sea level trend for this period from these data is 0.45 mm a^{-1}.

Dunbar's UKHO data extend from 1975 to 1979 (Figure 5.40). This dataset was 'suspicious' as the Dunbar Harbour Trust were not aware of any tide gauge recordings taking place after 1950, but have since been confirmed as being part of a PSMSL dataset (PSMSL, pers. comm.). This short dataset appears to be stable in its monthly format, but has not been used in this study due to its short timescale.

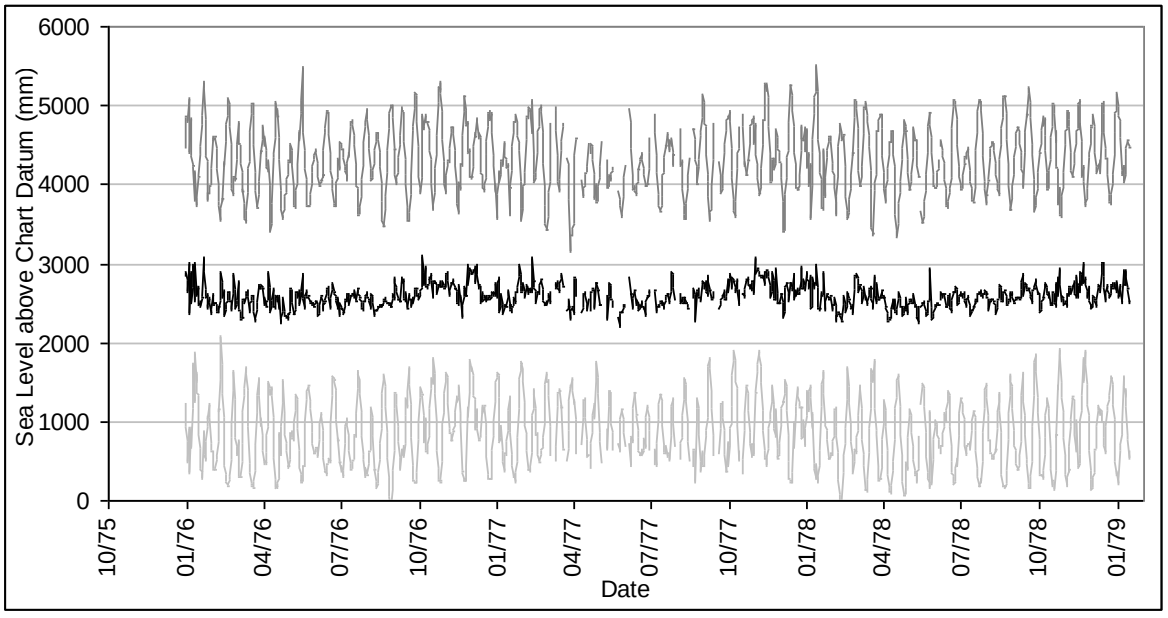

Figure 5.40. UKHO Dunbar average daily high water level, average daily low water level and daily mean sea level between 1975 and 1979. Calculated mean sea level trend for this period is 11.67 mm a^{-1}.

5.2.16 Aberdeen (PSMSL(1); PSMSL(2); NTSLF/BODC)

Aberdeen Harbour is located 100 km north of the Tay Estuary. The tide gauge managed by Aberdeen Harbour is located next to the present PSMSL tide gauge at [NJ 94444 06166] (Aberdeen 1, see Table 4.1). The harbour tide gauge does not record and is used purely for real-time navigation. PSMSL have two datasets from tide gauges at Aberdeen (with Aberdeen 2 being the earlier record shown in Table 4.1), both of which are available in Metric and RLR formats (see Table 5.1). The NTSLF/BODC collected data originated from a tide gauge managed by the PSMSL Tide Gauge Inspectorate (Figure 5.41).

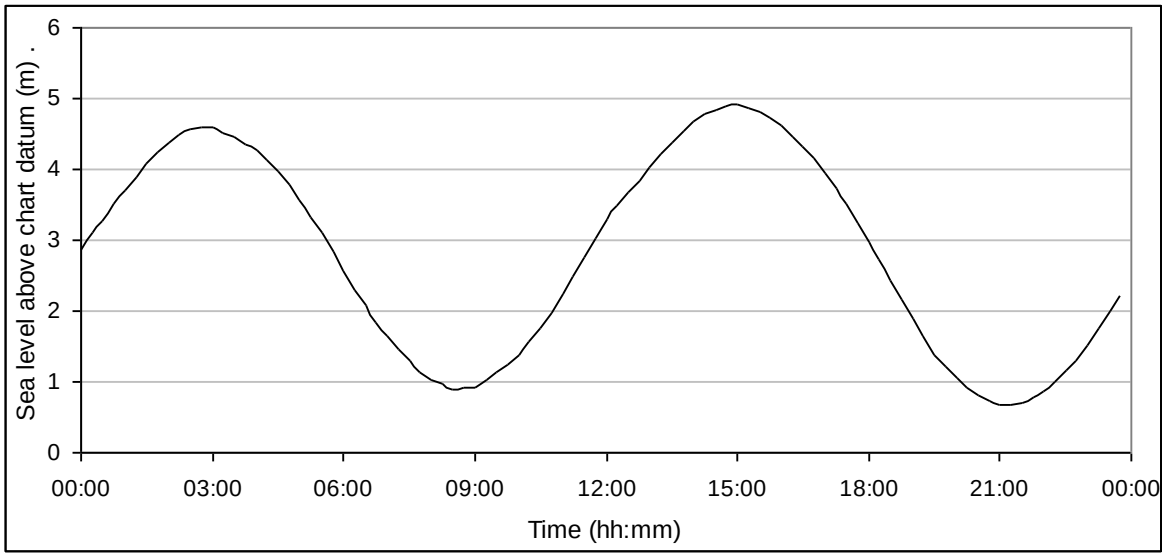

Figure 5.41. Sea level curve at the BODC/NTSLF Aberdeen site on 10/03/2008, during a spring tide, illustrating a spring tidal range of between c.4.0 m and 4.5 m.

PSMSL has collected various datasets from the Forth and Tay Estuaries. Two long datasets from Aberdeen have been used for comparison with the Forth and Tay Estuaries data to remove obviously erroneous datasets. The PSMSL are one of several organisations that correct tide gauge data gifted by their original sources as well as data directly from tide gauge under their management. Some of the PSMSL datasets are available in more than one format; Metric and RLR (see Chapter 4).

The PSMSL provide two datasets from Aberdeen, one of which extends between 1862 and 1965 (Aberdeen 2) with the other extending between 1931 and 2010 (Aberdeen 1). Both datasets are available in Metric and RLR format. From these partially-corrected datasets two trends have been calculated (Figure 5.42 to Figure 5.45).

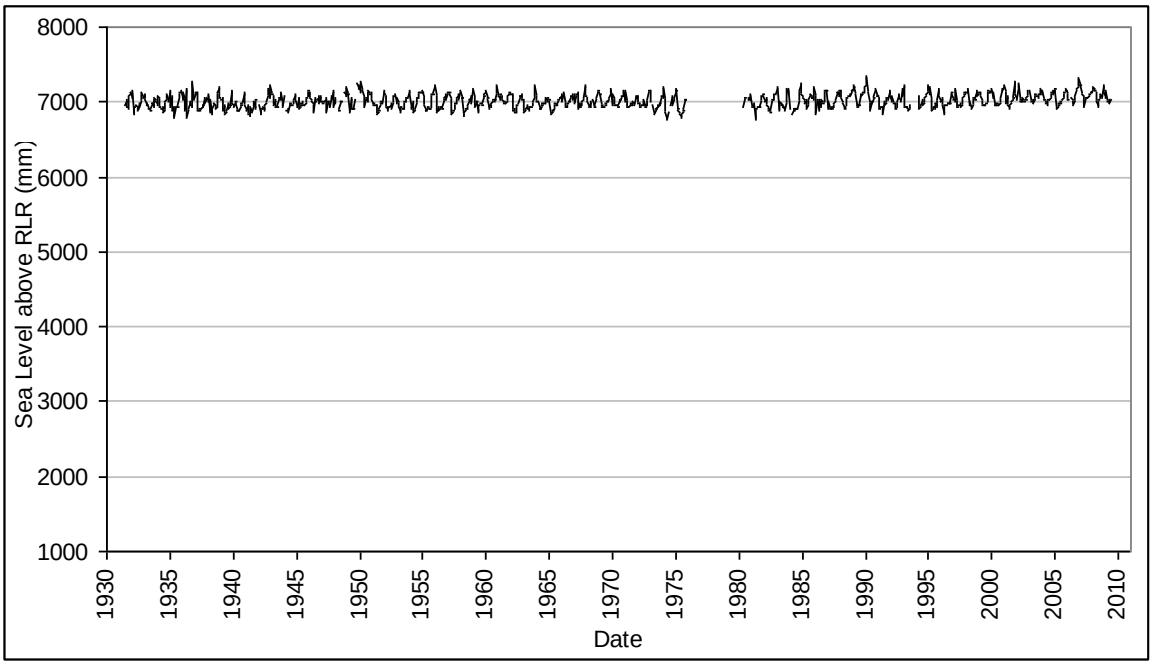

Figure 5.42. PSMSL Aberdeen 1 monthly mean sea level data from RLR hourly sea level data between 1931 and 2010. Calculated mean sea level trend for this period from these data is 0.96 mm a^{-1}.

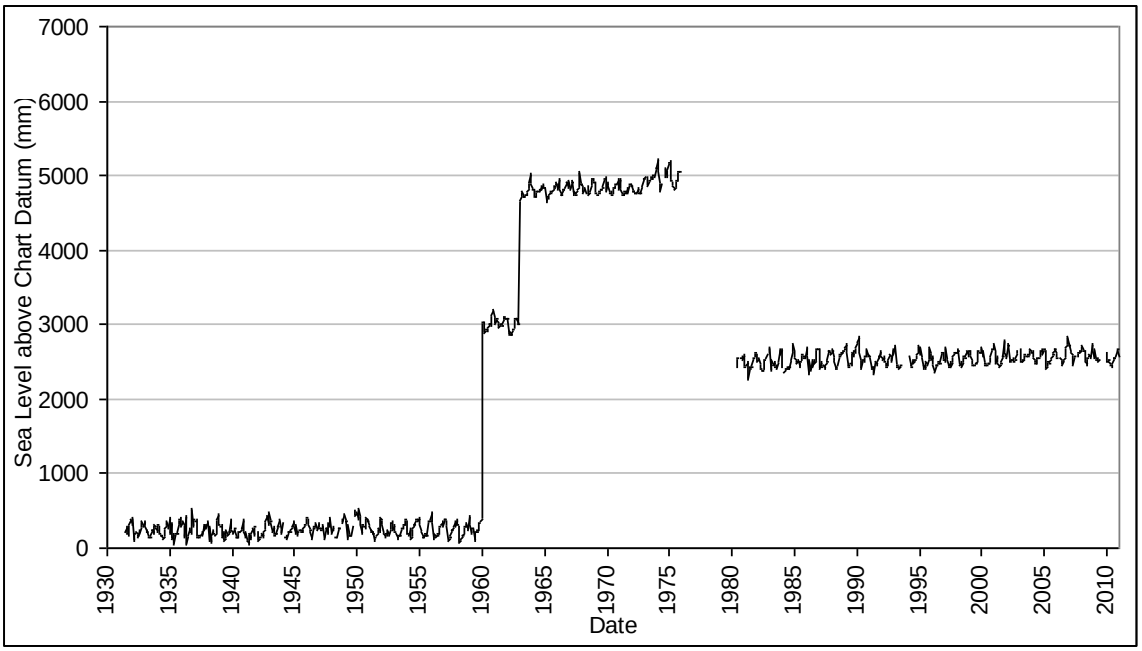

Figure 5.43. PSMSL Aberdeen 1 monthly mean sea level data from Metric hourly sea level data between 1931 and 2010. The monthly mean data are not representative of sea level trends due to errors.

Aberdeen's NTSLF data, which can be used for comparison with the Forth and Tay data, are available from 1930 to 2010 and replicate those of the PSMSL dataset (Figure 5.46). This dataset can be used for long-term trend analysis, because it extends for more than thirty years.

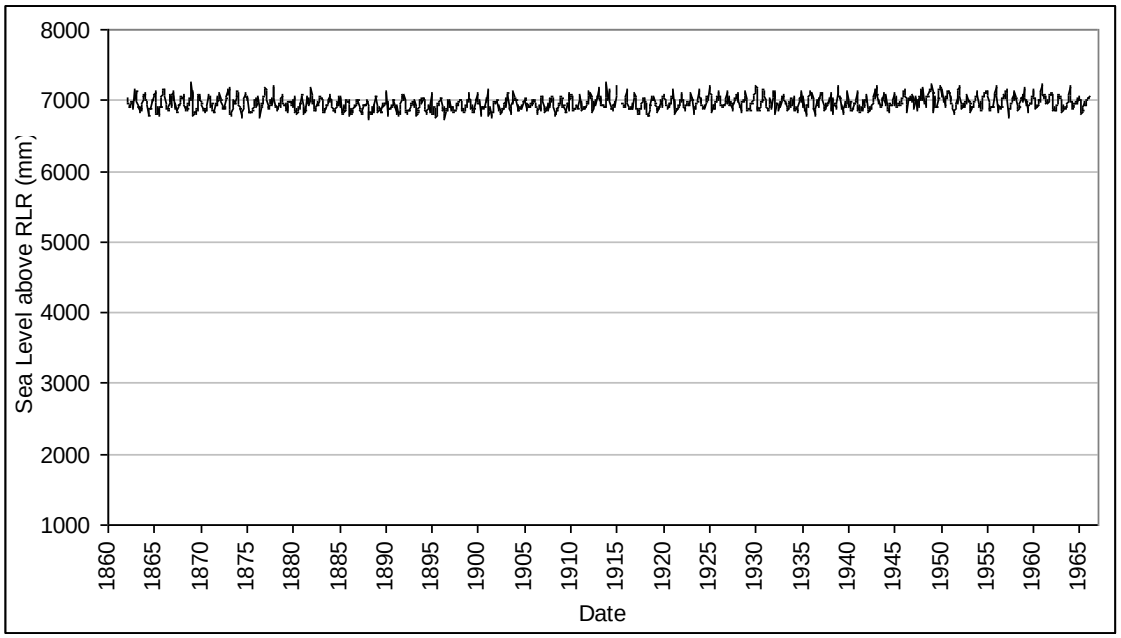

Figure 5.44. PSMSL Aberdeen 2 monthly mean sea level data from RLR hourly sea level data between 1862 and 1965. Calculated mean sea level trend for this period from these data is 0.98 mm a^{-1}.

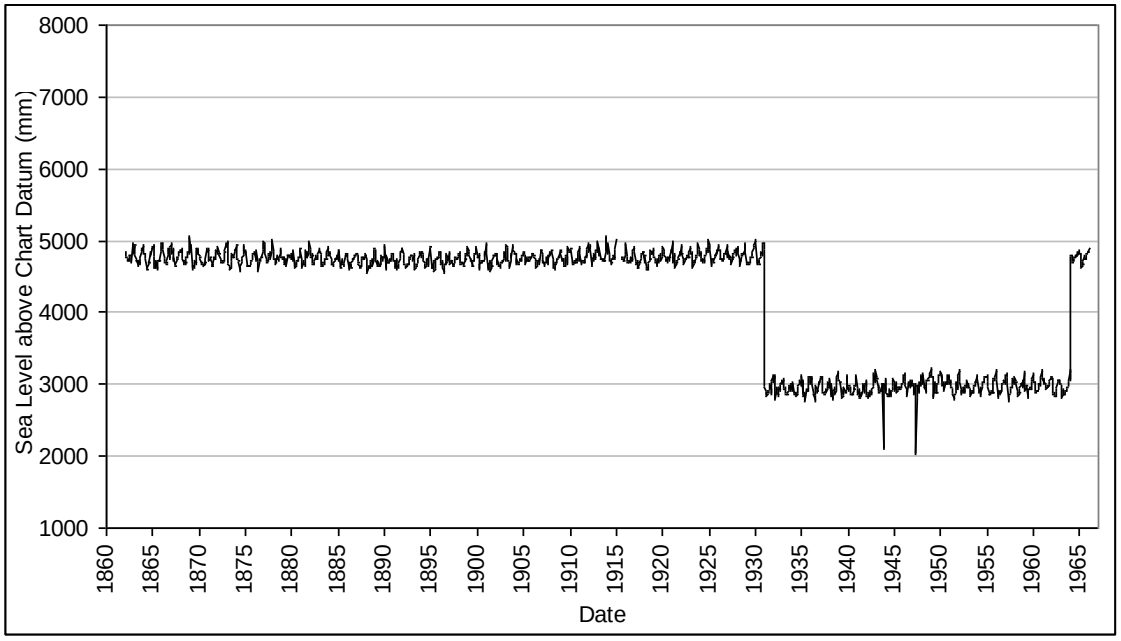

Figure 5.45. PSMSL Aberdeen 2 monthly mean sea level data from Metric hourly sea level data between 1862 and 1965. The monthly mean data are not representative of sea level trends due to errors.

5.4 Datum Correction to ODN

The Forth and Tay Estuary data were initially corrected for datum fluctuations on a site by site basis. Before the data for each site were converted to a single datum, the sea level datasets appeared as in Figure 5.46. The first conversions of these datasets were to their local Chart Datum or the

PSMSL RLR datum. To correct the sites to Ordnance Datum (OD), based at Newlyn in Cornwall, each site's background history and documentation of datum level change have been investigated and are described in the following sub-sections. Spikes have been manually removed from the datasets during datum correction.

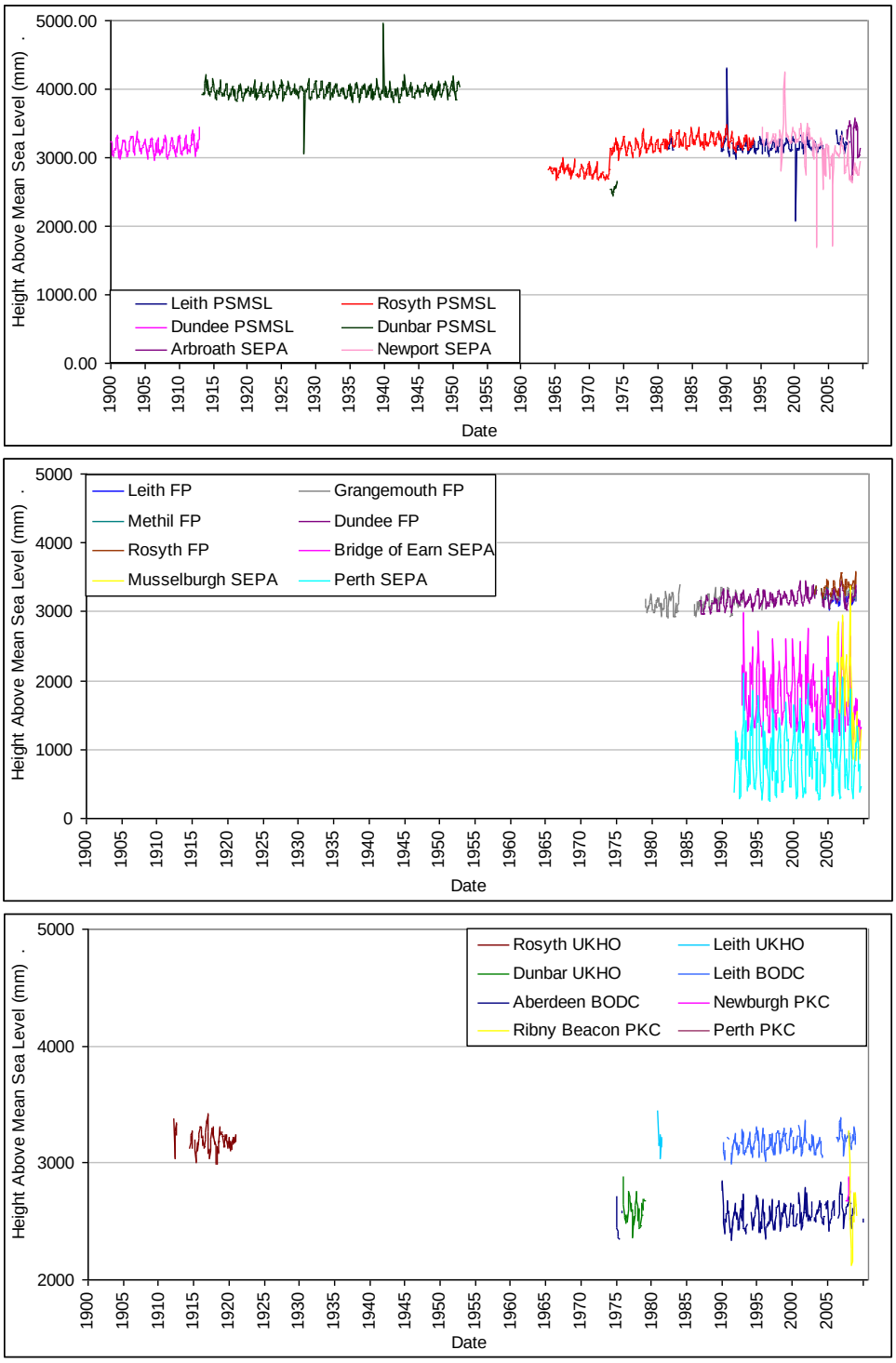

Figure 5.46. Complete datasets for the Forth and Tay Estuaries prior to spike and primary datum correction. The three charts above are organised by their data source institution with some separation

of institutional data for presentation purposes; PSMSL and SEPA, Forth Ports and SEPA, UKHO, BODC and PKC.

To reduce data overlap within visual presentations in this section, the study area has been divided into five sub-areas; sites outside the study region, the inner Tay Estuary, the outer Tay Estuary, the Forth Estuary and the Firth of Forth.

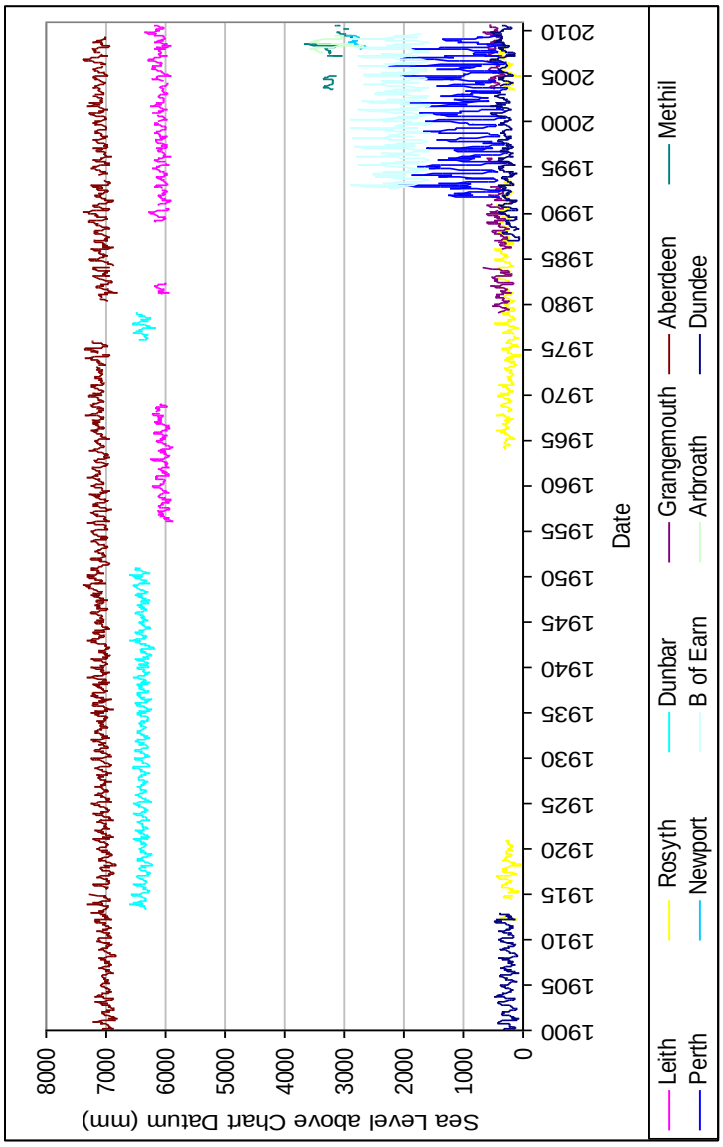

Figure 5.47. Complete datasets for the Forth and Tay Estuaries prior to final datum correction.

5.3.1 Sites Outside The Study Region

The Aberdeen datasets have benefited from connection with the PSMSL through the production of two RLR datum conversion maps for Aberdeen 1 and Aberdeen 2 (PSMSL, 2010). These maps (Figure A5.1 and Figure A5.2, in the Appendix) highlight the RLR datum, harbour datum, ODN,

various other local short-term datum and tide gauge benchmarks (TGBM). These datum levels can be used to convert from RLR to ODN, mean sea level or mean tide level very simply. Correction of the Metric data is not advised where RLR are available as the additional datum corrections can be avoided if RLR data are used.

The Aberdeen datasets needed additional correction to match up the PSMSL Aberdeen 1 mean sea level data with the Aberdeen 2 mean tide level data (as explained in Chapter 4) (Figure 5.48).

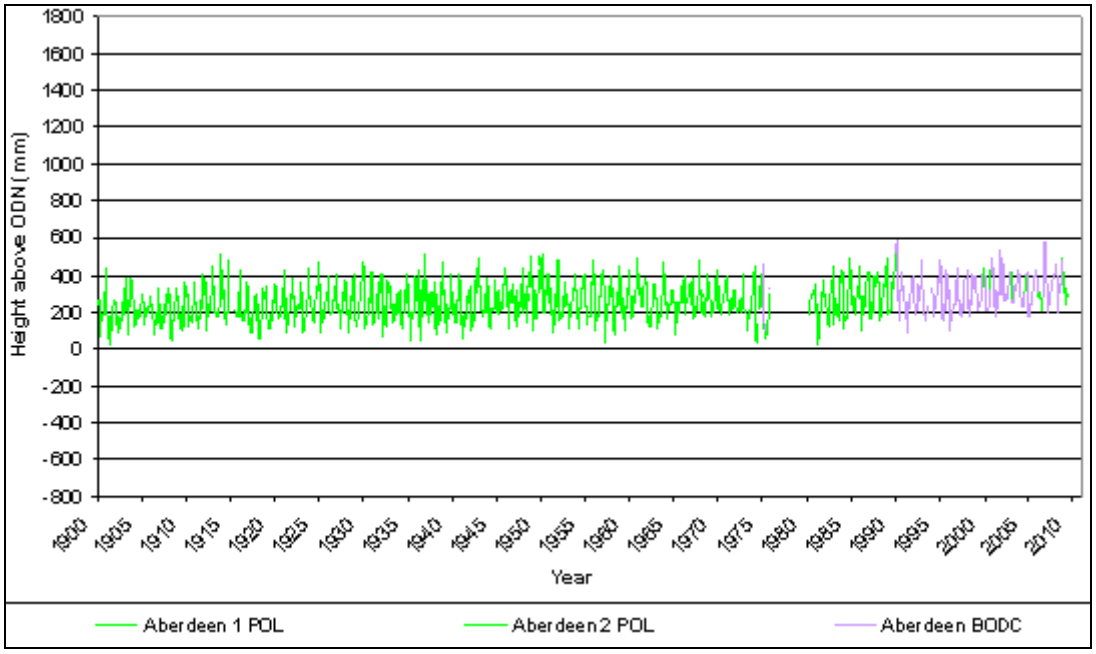

Figure 5.48. PSMSL Aberdeen 2 RLR data and BODC Aberdeen data converted for datum error (PSMSL, 2010); includes a 14 mm addition to the Aberdeen II data, as suggested by Woodworth *et al.* (1999).

5.3.2 The Inner Tay Estuary Sites

The Inner Tay Estuary data sites include Perth (Scone), Perth Harbour, Bridge of Earn, Ribny Beacon and Newburgh. Most of these sites have inadequate data for the needs of this study or have erroneous datasets. Due to data frequency limitations, Ribny Beacon and Newburgh have been removed from the analyses. The Perth (Scone), Perth Harbour and Bridge of Earn datasets have been corrected for datum errors (Figure 5.49). A secondary correction was made to correct the raised datum at Perth, which involved subtracting the difference between the Perth Harbour datum and the Perth datum from the higher Perth data (Figure 5.50).

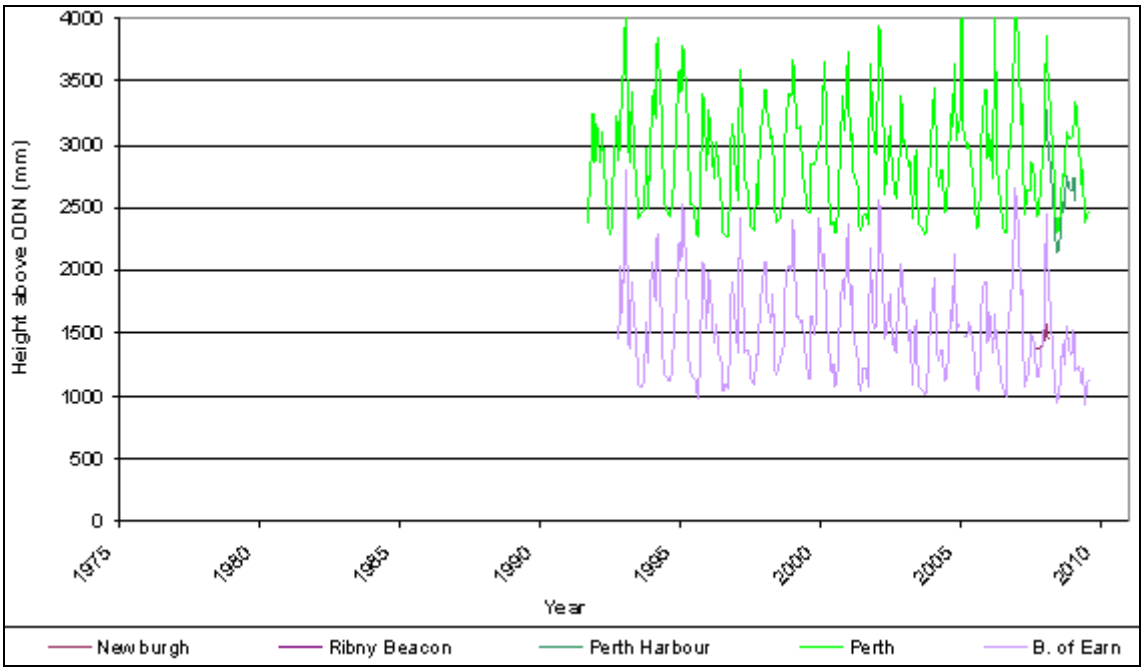

Figure 5.49. Data from the inner Tay Estuary that has been provisionally corrected for datum error, converting all sites to ODN using the guidance notes provided with data and additional corrections. Sites produced here include Perth, Perth Harbour and Bridge of Earn.

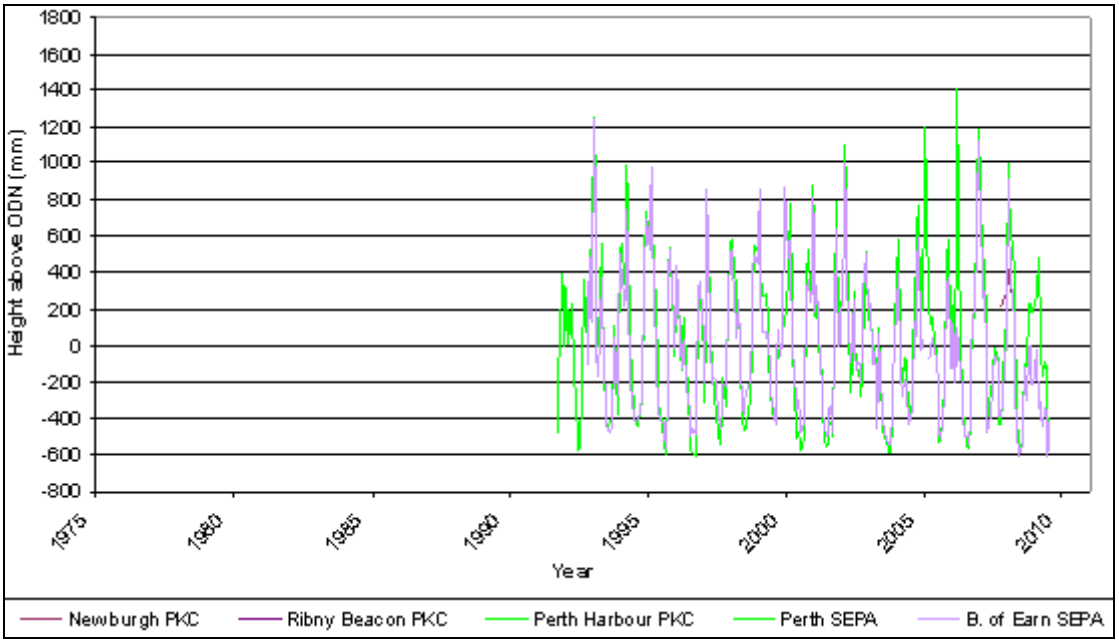

Figure 5.50. Secondary correction of data from the inner Tay Estuary that have been provisionally corrected for datum error, converting Perth Harbour to ODN with Perth and Bridge of Earn converted to mean sea level.

5.33 The Outer Tay Estuary Sites

The data sites in the outer Tay Estuary are Newport-on-Tay, Dundee, Stannergate and Arbroath (outside the Tay Estuary). All sites have been corrected for datum errors, although Stannergate and part of the Newport-on-Tay dataset have been discarded due to data replication limitations, as described above. The remaining datasets are presented in Figure 5.51. The PSMSL dataset for Dundee is in Metric format, meaning that PSMSL have not produced a datum conversion chart.

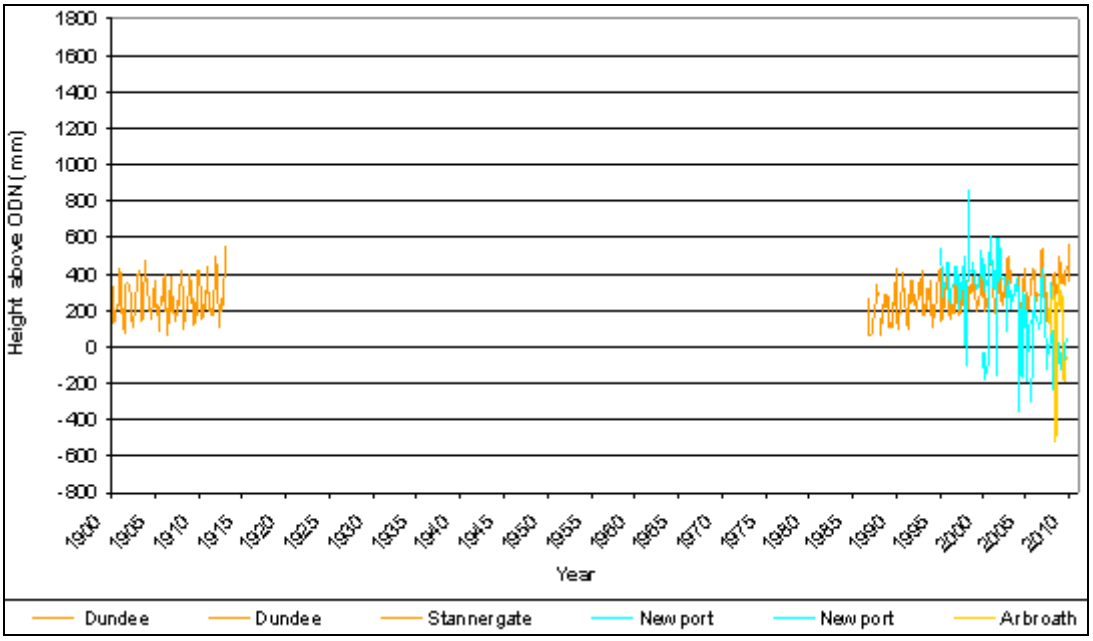

Figure 5.51. Data from the outer Tay Estuary that were corrected for datum error, converting all sites to ODN using the guidance notes provided with data and additional corrections. Sites here include Newport-on-Tay, Dundee and Arbroath.

Certain errors occur in the preliminary datum-corrected SEPA data for Arbroath and Newport-on-Tay. At Arbroath, a negative jump of 20 cm occurred in early 2009, which may be due to an active decision by the gauge operators to change the datum level or, as the gauge is in an active marine transport area, the gauge may have been intercepted by a ship or tampered with. At Newport-on-Tay there was a gradual lowering of the high water levels in the dataset, as well as sudden negative datum jumps in late 2006 and mid 2007. These datasets have thus been discarded due to the progressive movement within the data along the length of tide gauge recording.

5.3.4 The Forth Estuary Sites

The Forth Estuary data, here limited to the geographical region between Stirling and the bridges at Queensferry, incorporate Grangemouth and Rosyth. All datasets have been corrected to ODN. For

Rosyth this included using three different datum conversions for the UKHO, PSMSL and Forth Ports datasets. The PSMSL dataset, in RLR format, was converted using the Rosyth datum conversion chart (Figure A5.6, in the Appendix). The corrected Forth Estuary datasets are presented in Figure 5.52.

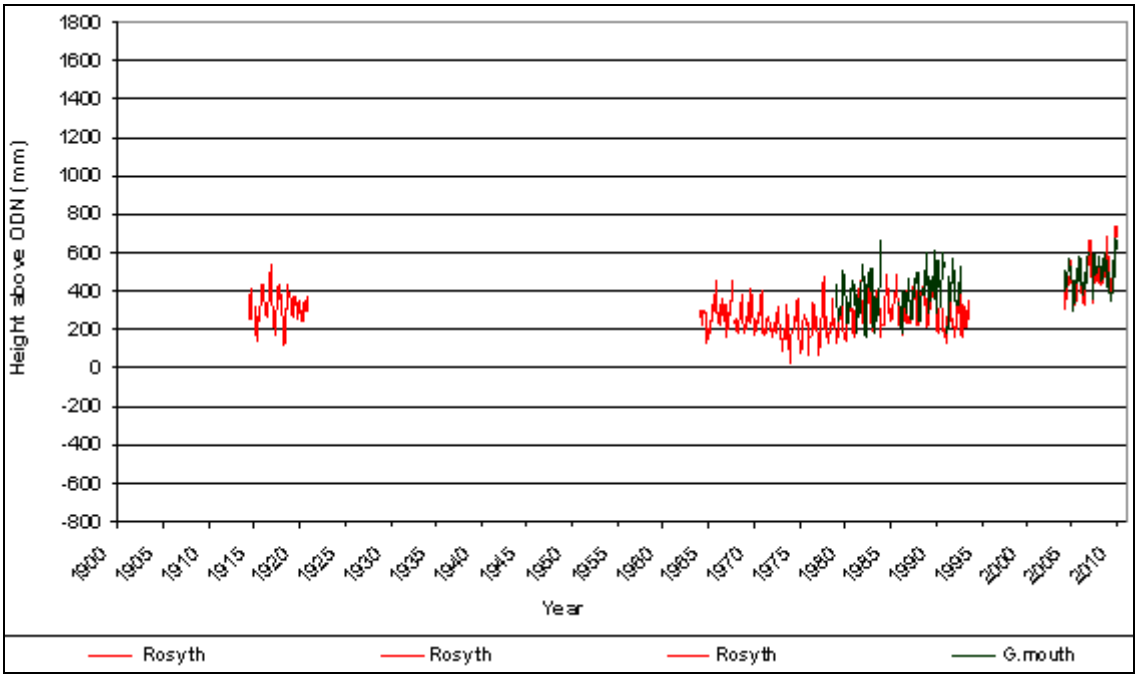

Figure 5.52. Data from the Forth Estuary that have been corrected for datum error, converting all sites to ODN using the guidance notes provided with data and additional corrections. Sites here include Grangemouth and Rosyth.

5.3.5 The Firth of Forth Sites

The data sites in the Firth of Forth, here limited to the geographical area between the bridges at Queensferry and the firth mouth, include Methil, Leith, Musselburgh and Dunbar. PSMSL RLR datum conversion maps are available for the Leith 1, Leith 2 and Dunbar PSMSL datasets (Figures A5.3, A5.4 and A5.5, in the Appendix). All sites have been corrected to OD using information given by the data authorities (Figure 5.53).

The Musselburgh datum correction applied in Figure 5.53 does not remove the datum jump that occurred in May 2008 and the Musselburgh data are still considerably higher above OD than the Leith, Dunbar and Methil data. Therefore an additional correction was made to convert the Musselburgh datum to the level of recorded mean sea level (Figure 5.54).

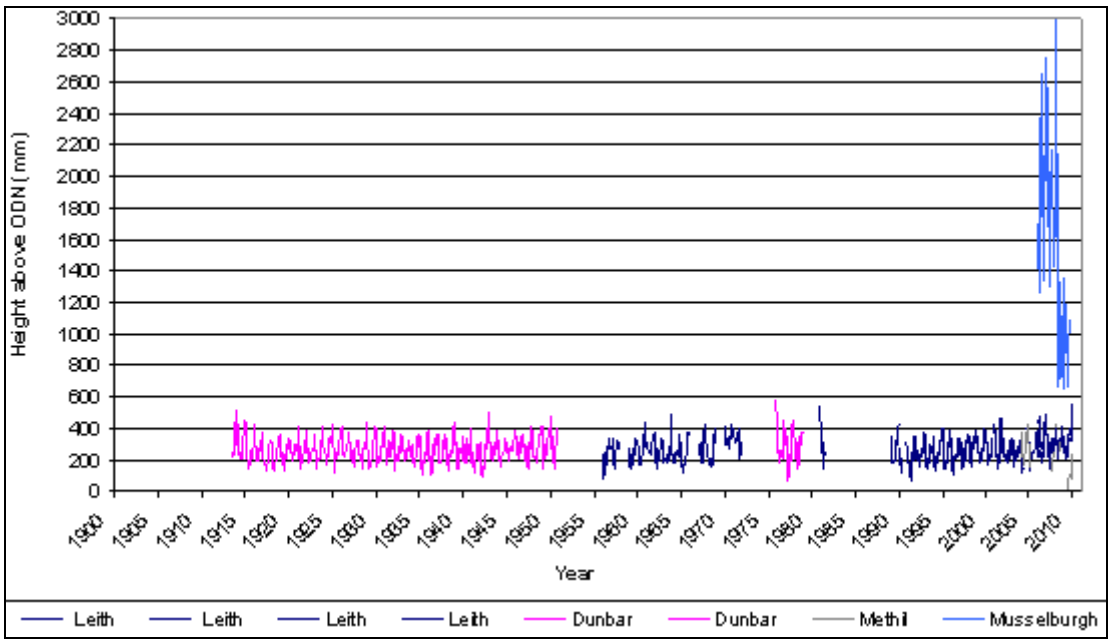

Figure 5.53. Data from the Firth of Forth that have been provisionally corrected for datum error, converting all sites to ODN using the guidance notes provided with data and additional corrections. Sites here include Methil, Leith, Musselburgh and Dunbar.

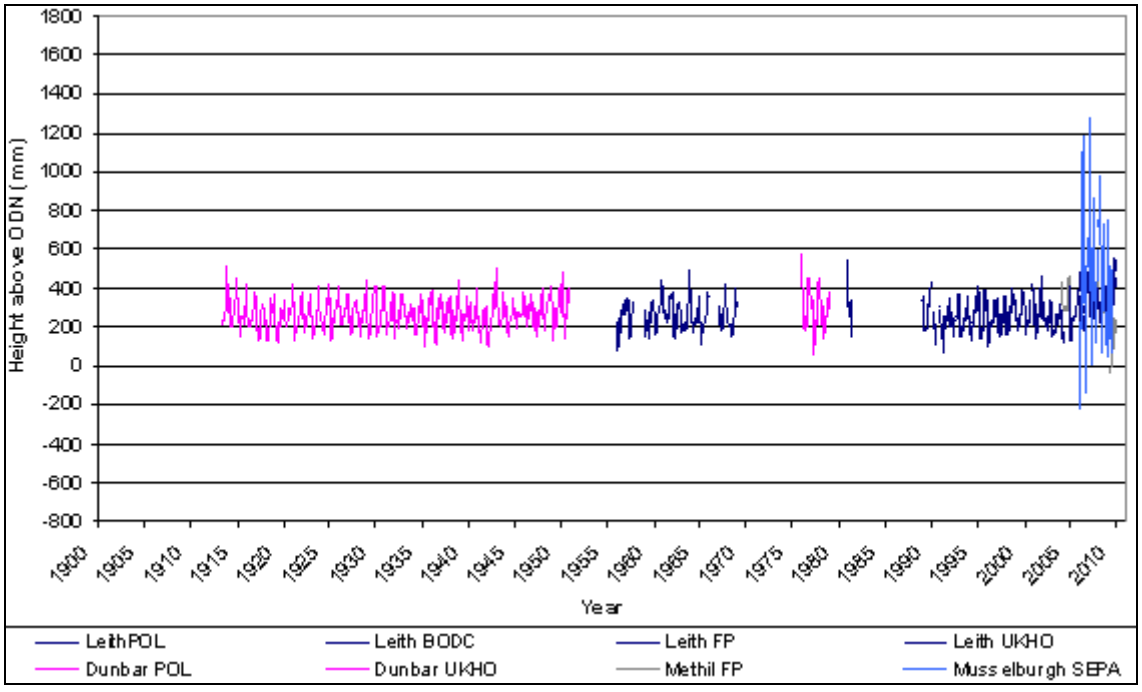

Figure 5.54. Additional correction of data from the Firth of Forth that have been provisionally corrected for datum error, converting Methil, Leith and Dunbar to ODN with Musselburgh converted to MSL.

5.3.6 Combined Datum Results

After reviewing the datasets that were corrected for datum variability, several datasets have revealed underlying datum fluctuations that make them unsuitable for sea level analysis. More information on the reasoning behind removing them from further analysis is presented in Chapter 6. These include all the SEPA, PKC and TERC data as well as the Methil dataset (Figure 5.55, 5.56 and 5.57). Therefore, although some of these datasets may be referred to in Section 5.4, they are not analysed further. As a result, Figure 5.58 was produced illustrating the remaining datasets from the Tay and Forth Estuaries converted to ODN. The conversion of all datasets to ODN has highlighted that the mean tidal height at Grangemouth is between 100 and 200 mm higher than those recorded further downstream in the Forth Estuary and in the outer Tay Estuary (Figure 5.58). As discussed in Section 2.7, this increased water height is due to the funnelling behaviour of estuaries, where the narrowing and shallowing nature of the estuary forces the incoming tidal prism to expand vertically to compensate for the decreasing space and increasing estuary bed height.

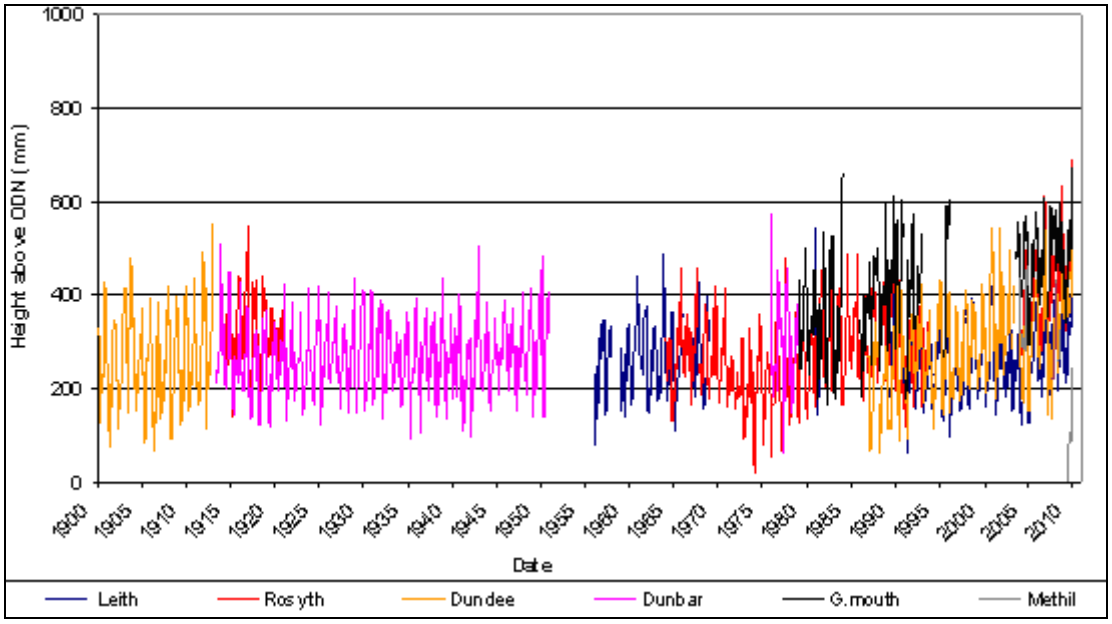

Figure 5.55. Data from the Tay and Forth Estuaries that have been corrected for datum error, excluding all PKC, TERC and SEPA data.

5.4 Land Movement

This section investigates potential causes of land movement in the Forth and Tay Estuaries. Coal Authority *Coal Mining Reports* (2010a-2010d) indicate that there were no issues with mining subsidence at any of the data sites, including Rosyth, Methil, Musselburgh and Grangemouth, but

other sources of land movement can include glacio-isostatic adjustment (GIA), infrastructural subsidence and other forms of natural subsidence.

5.4.1 GIA Identification and Correction

GIA relative land level change (RLLC) rates in the study area have been identified using the Shennan *et al*. (2011) study, as described in the Chapter 4. The difference between Vertical Land Motion (VLM) and RLLC is described in Chapter 4; essentially the VLM rates are the change in the rock surface relative to the centre of the Earth and relative land level change includes a spatial element in relation to the sea surface. The RLLC rates are 0.7 mm a^{-1} at Aberdeen, 0.9 mm a^{-1} at Montrose, 1.1 mm a^{-1} in the Tay, 0.9 mm a^{-1} in the outer Firth of Forth and 1.2 mm a^{-1} in the inner Forth Estuary. To compare sea level and RLLC rates between sites, each site has been converted to its 1990 mean datum using annual data, ensuring that all sites have identical relative sea levels at that time (Figure 5.56; see Section 4.3).

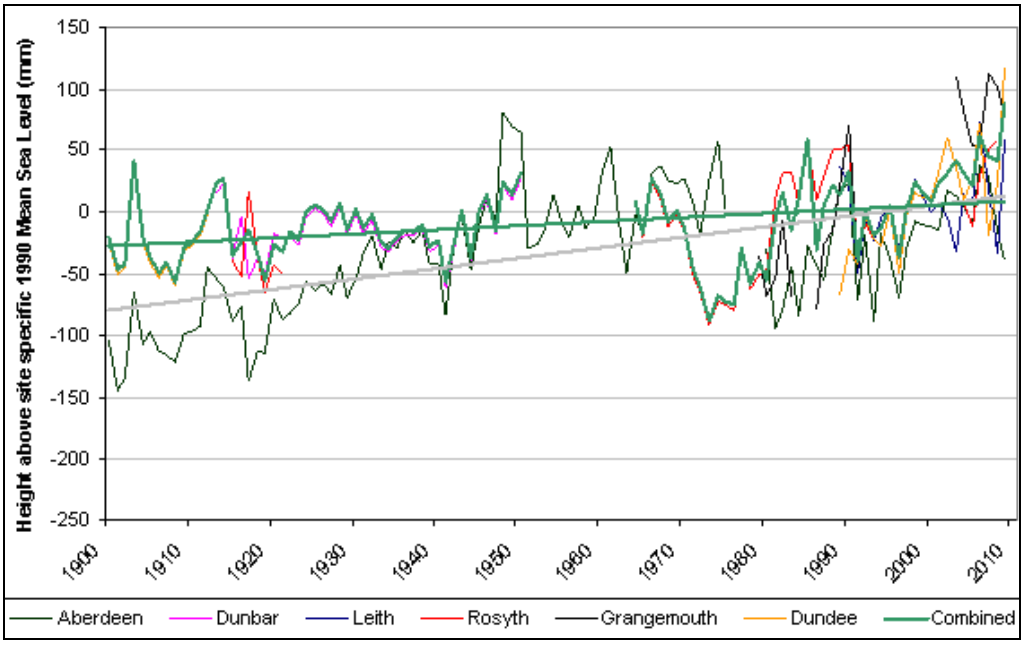

Figure 5.56. All datasets were converted from ODN to a datum constructed individually, equal to each site's 1990 mean sea level, i.e. datums were adjusted so that the linear trend line intercepted the y-axis 0 at 1990. Aberdeen, Dunbar, Leith, Rosyth, Grangemouth and Dundee are the main data sites used to represent this technique. This graph should be compared with Figure 5.57, which presents RLLC correction.

The following RLLC rates have been used in Figure 5.57; 0.7 mm a^{-1} in Aberdeen, 0.9 mm a^{-1} in Dunbar, 1.1 mm a^{-1} in Leith and Rosyth, 1.0 mm a^{-1} in Dundee, and 1.2 mm a^{-1} in Grangemouth. The combined estuaries dataset was adapted to fit the RLLC-corrected data by subtracting the

median GIA rate for the region from the 1900 to 2010 relative sea level combined estuaries dataset (Figure 5.57) (see Section 4.3). The gaps between the sea level height of the longest sea level datasets, Aberdeen, Dunbar and Dundee, were greatly reduced using this method. Figure 5.58 was also created to analyse the impact of including the Grangemouth data in the combined estuaries dataset. The fluctuating patterns of the Tay Estuary and Forth Estuary datasets are similar, with both datasets appearing to have coincident sea level peaks and troughs.

The Grangemouth dataset, which has a higher than average relative sea level trend in Figure 5.59, is shown to be not too dissimilar to the other datasets found in the two estuaries in Figure 5.58. The high relative sea level trend in Figure 5.57 could be due to the gaps in the dataset altering the overall trend. These gaps should not impact a combined estuary trend, as the regional sea level trend would be supported by neighbouring datasets.

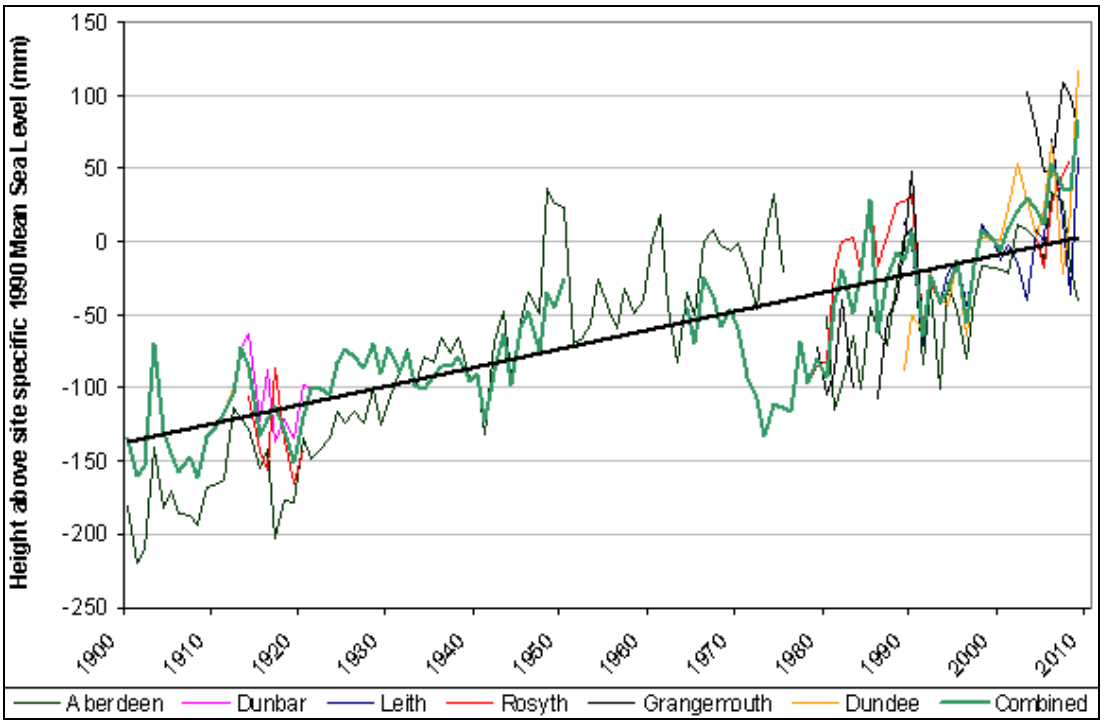

Figure 5.57. All datasets corrected for datum errors and RLLC. RLLC corrections have been hindcast to represent how the sea level trends would be presented if Shennan *et al.*'s (2011) RLLC rates were imposed linearly. Aberdeen, Dunbar, Leith, Rosyth, Grangemouth and Dundee are the main data sites used to represent this technique. This graph should be compared with Figure 5.56, which presents datum correction.

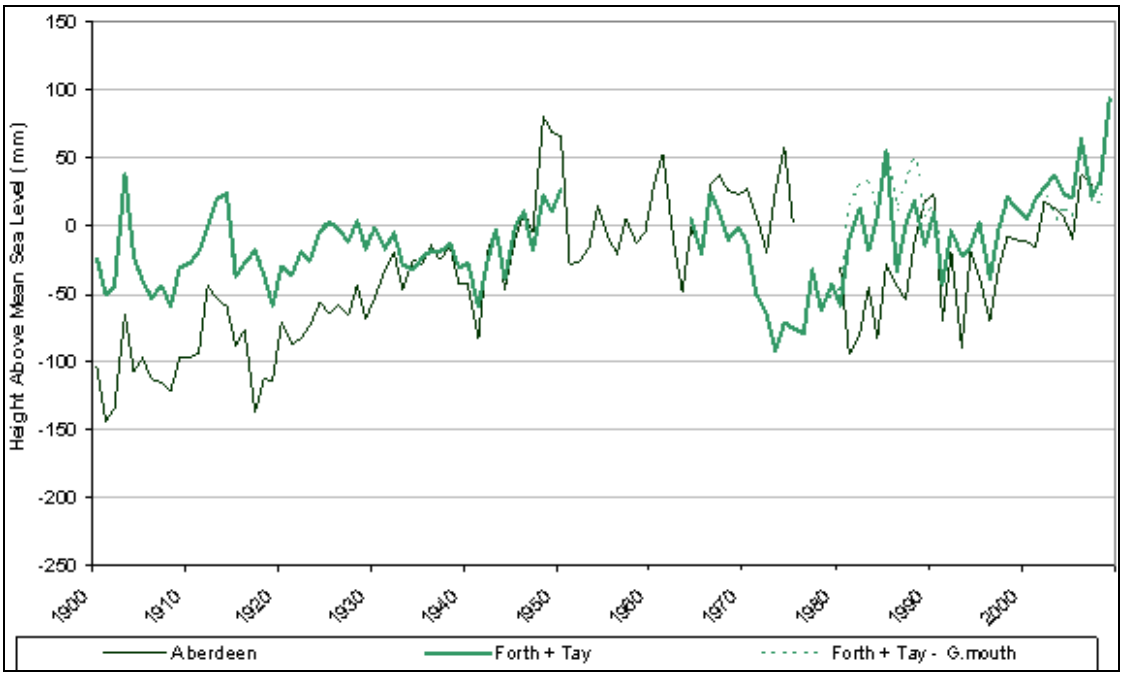

Figure 5.58. Sea level data for the Forth and Tay Estuaries adjusted to their individual 1990 sea level average datum. Grangemouth was temporarily removed from the combined dataset to test its data produced a large skew. As most of the datasets had a large increasing sea level trend, Grangemouth's data are suitable for short term trend analysis.

5.4.2 Site Specific Subsidence Identification

Musselburgh's gauge is close to six coal seams between 200 m and 1040 m in depth that were last worked in 1986 (Coal Authority, 2010a), whilst Methil's gauge is close to five coal seams 250 m to 660 m in depth that were last worked in 1963 (Coal Authority, 2010b). Only Grangemouth's gauge is close to an area where there is a live licence for underground mining, although this site is not likely to be affected by current mining developments (Coal Authority, 2010c). None of the sites have submitted damage claims regarding subsidence since 1984 (Coal Authority, 2010a; b; c; d).

One example of a structure suspected of subsiding while supporting a tide gauge system is Newport Pier. Newport Pier was constructed as a ferry pier in 1823 and still operates today. It was built by Thomas Telford, has been used as a ferry terminal and now as a boat servicing facility (Figure 5.59).

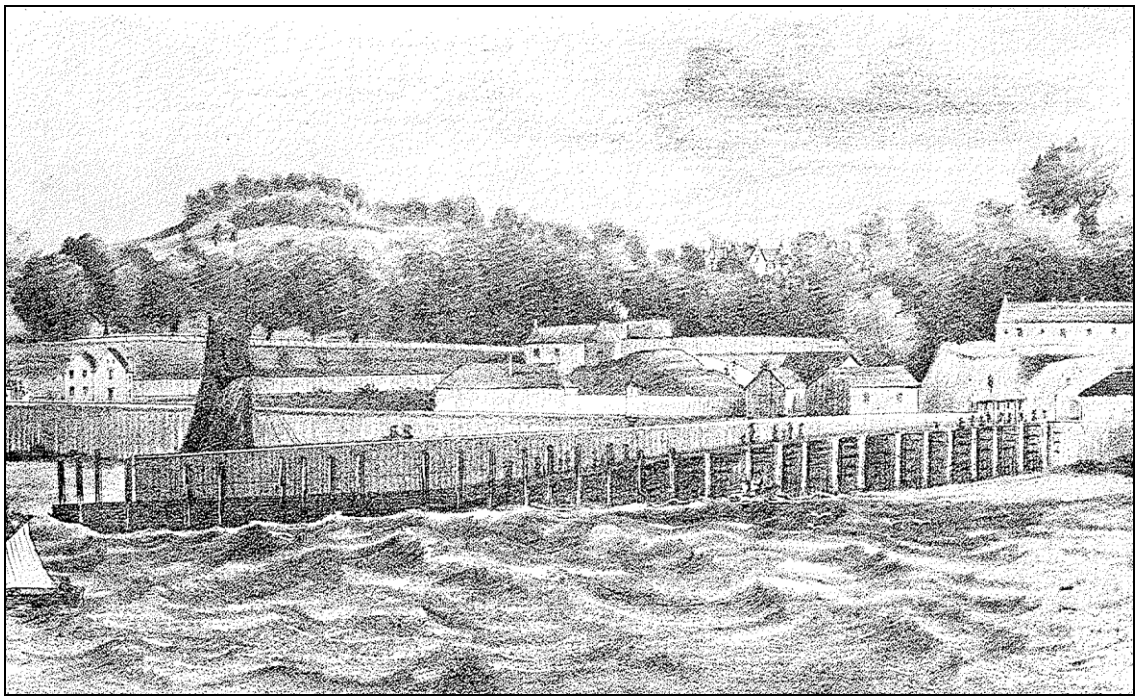

Figure 5.59. Image of Newport Pier in 1824 facing southeast (Ritchie and Thompson, 1930).

The pier was originally constructed with a solid dimension stone exterior, filled with waste stone and earth materials and capped with sett stones. This traditional construction approach is durable, but if the exterior is damaged the fine matrix fill can be winnowed out over time, potentially leading to internal or differential settlement. The western side of the pier was extended in 1928 (Figure 5.59). Since then the western side has suffered differential subsidence and slopes westwards. The eastern side of the pier is structurally sound with no visible subsidence (Figure 5.60).

Photographic evidence of structural movement is available from November 1979, January 1982, February 1990, March 1994 and June 2002 (R. Duck, pers. comm.). Five of these photographs, from 1979, 1982, 1990 and 2002, are collated in Appendix 6 (Figures A6.1 to A6.5). The oldest photographs, from 1979 and 1982 (Figure A6.1 and Figure A6.2), show cracks that measures over 2.5 cm in width between the 1928 concrete extension and the older section of the pier, which has more recently been filled with concrete.

In late February 1990 a large storm event caused major damage to the central stone wall and western brick wall (Figure A6.3). The tide gauge had been located on the corner of the western brick wall for several decades and its housing can be seen in Figure A6.4 attached to what remains of that wall. Photographs of the damage also reveal evidence of subsidence cracking at that time (Figure 5.62).

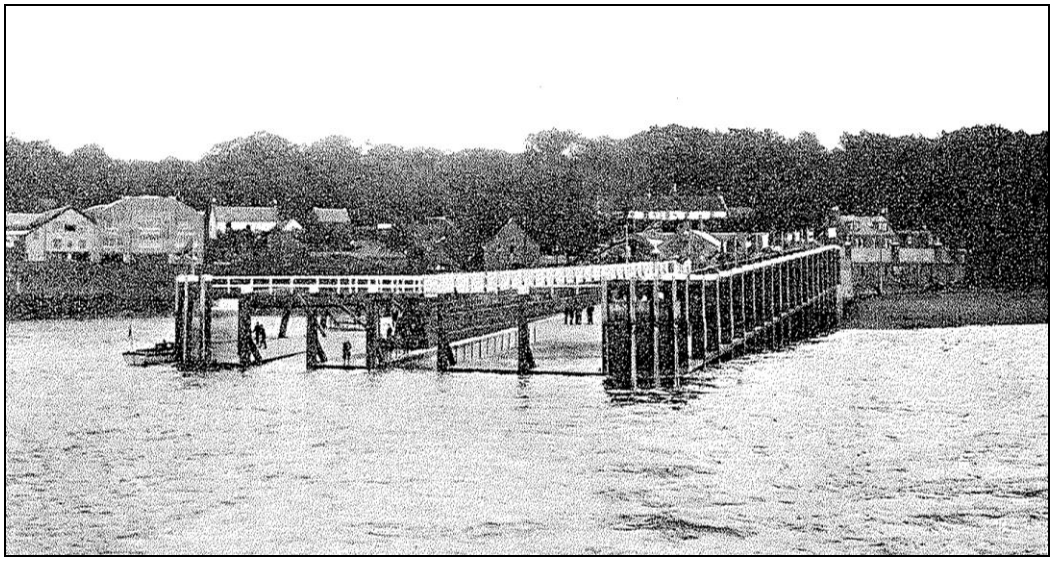

Figure 5.60. Image of Newport Pier in 1930; two years after the extension works (Ritchie and Thompson, 1930). The pier was constructed to be level across its width, except at the toe where split ramps allowed landing at variable tidal heights.

Figure 5.61. Images of the west and east sides of Newport Pier highlighting the cracks along the western side (left) and the stability of the eastern side (right) taken in September 2010.

Figure 5.62. Photograph of the west side of Newport Pier in February 1990 showing some of the damage caused by a storm event. The fork of a subsidence crack has been highlighted by the positioning of a piece of driftwood (courtesy of R. Duck).

By 1994 the central pier wall had been reconstructed. Figure 5.63 illustrates the tarmac repair patches fitted along the lines of subsidence cracks on the lower part of the pier's western side in 1994. Figure A6.5 (in the Appendix), taken in 2002, highlights the progression of subsidence in an area of the 1994 photograph (Figure 5,64). Large areas of this part of the pier have been patched and cracks filled.

By September 2010, cracks had opened up to 4 cm in width in places. Several large repair patches were cracking and the central area at the head of the pier was experiencing high levels of variance in the surface height (Figure 5.65). At least five large cracks extended from near the head of the pier to near the toe (Figure 5.66). Other minor cracks were also present independent of and linking with the major cracks. Some of these occurred in the major internal subsidence hollows that were visible along the length of the pier (Figure 6.65).

Figure 5.63. Photograph of the west side of Newport Pier in March 1994. The two dark areas have subsided, most noticeably on the left side of the photograph (courtesy of R. Duck).

Figure 5.64. Photograph of the west side of Newport Pier in September 2010. Red lines highlight cracks along the pier surface. There are substantial drops in height between the central crack and the central-right crack on the upper part of the pier.

Figure 5.65. Three photographs of the west side of Newport Pier in September 2010 illustrating three of the largest crack formations from west to east. The crack in the central part of the image covered in debris links up with the central right crack in Figure 5.64 and the right image here links with the central image in Figure 5.65.

To determine subsidence rates, two GPS surveys were conducted along Newport Pier in October 2010 and March 2011 measuring the height (in metres above the lowest recording) of the pier surface. After datum corrections (see Section 4.4.2) the GPS data were plotted using ArcMap and ArcScene, creating a 3-D image of the western half of the pier (Figure 5.66 and Figure 5.67). At any point along the pier length the surface height along the pier width should vary by less than 10 cm, as occurs along the pier east of the central wall. However, along the pier west of the central wall, the pier surface decreases in height westwards between the central wall and western edge by ~0.5 to ~1.0 m, with internal subsidence patches occurring along the length of the pier (Figures 5.66, 5.67 and 4.68).

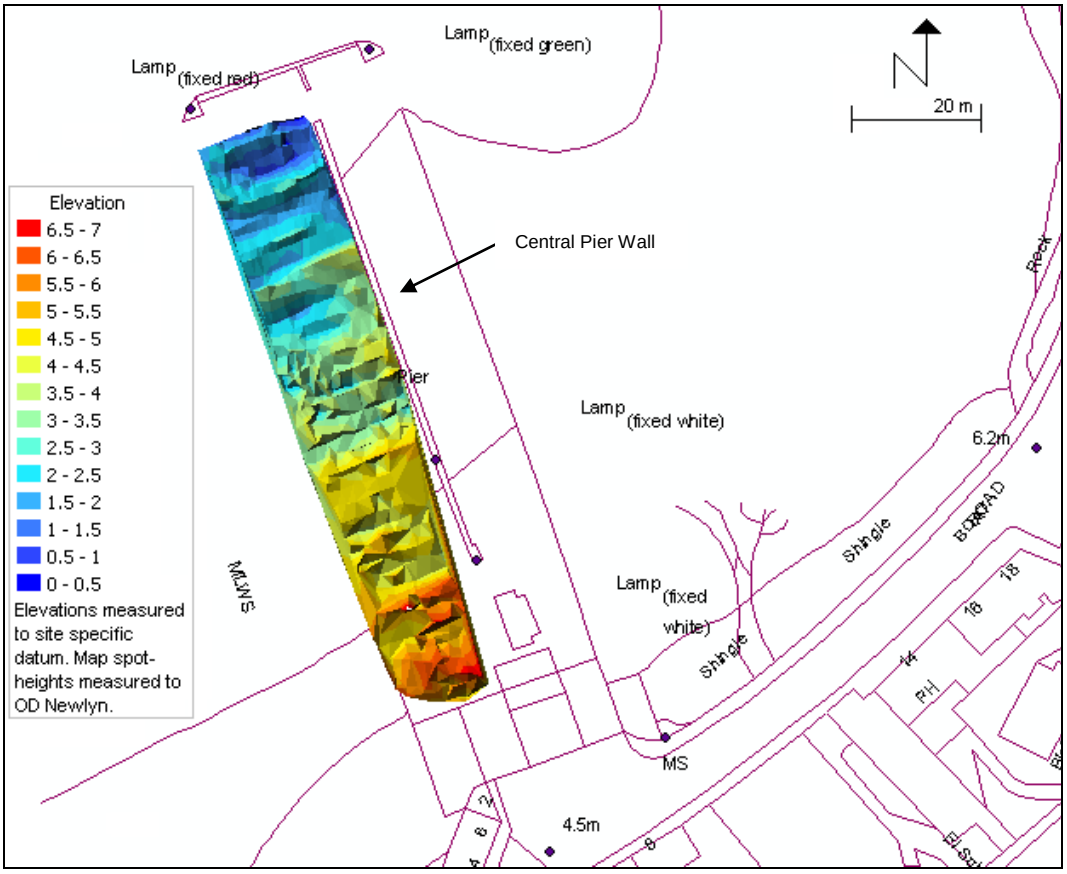

Figure 5.66. GPS results for Newport Pier as presented on ArcMap, with an alternative view in Figure 5.67. Elevations are measured in metres above the lowest recording. Analysis of the data identifies lower heights on the western edge compared to near the central wall. Exclusions to this rule include areas near the toe where a split ramp system occurs.

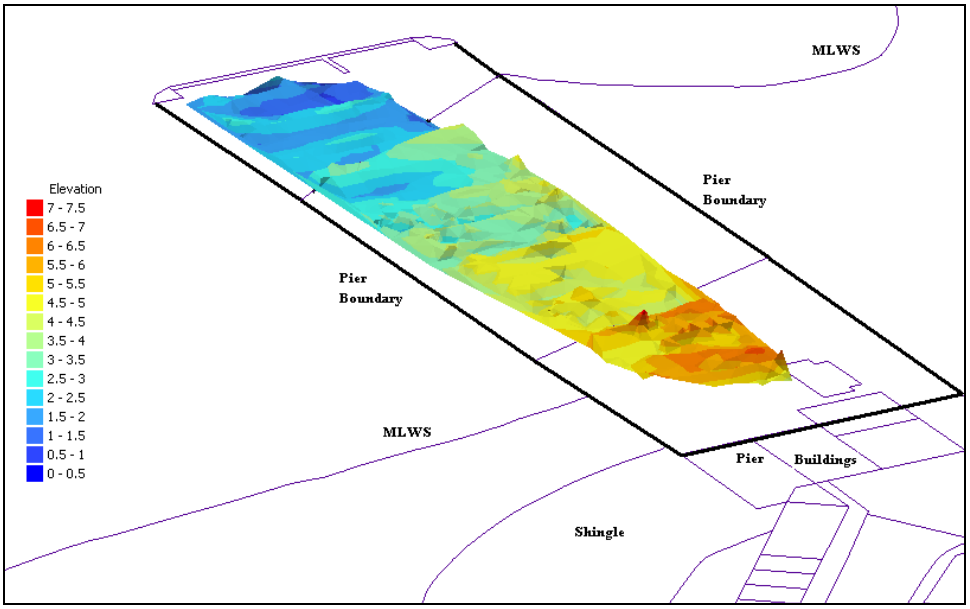

Figure 5.67. GPS results for Newport Pier as presented on ArcScene, with an alternative view in Figure 5.66. Elevations are measured in metres above the lowest recording. The 3-D elevations lie on top of a 2-

D map. Analysis of the data identifies lower heights on the western edge compared to near the central wall. Exclusions to this rule include areas near the toe where a split ramp system occurs. Some areas were automatically interpolated by the ArcGIS software where obstacles prevented direct data collection.

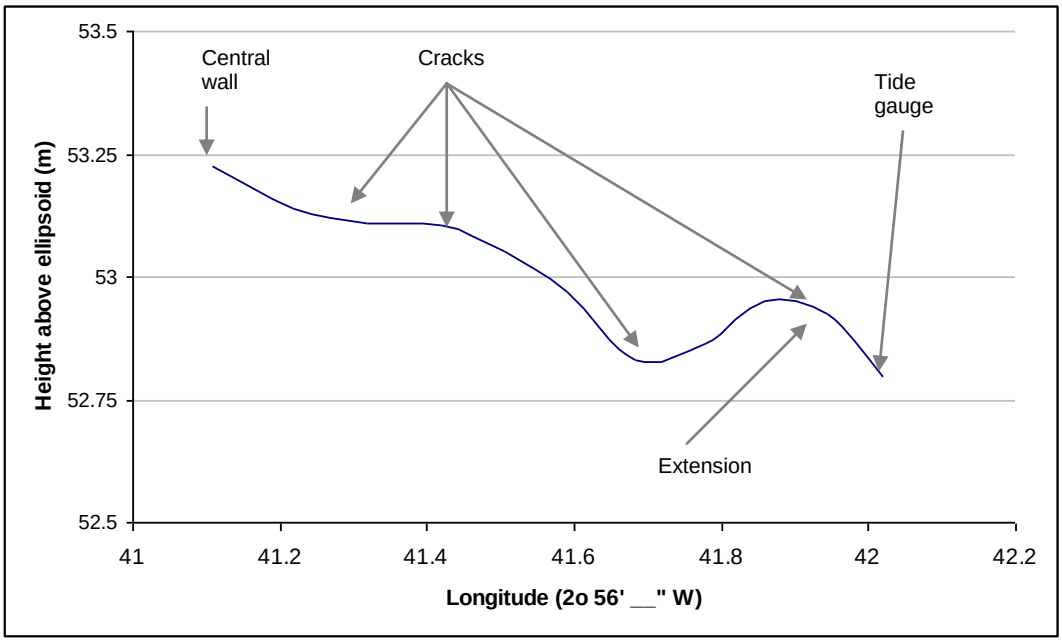

Figure 5.68. Surface height difference between central wall of Newport Pier (left) and the western edge (right), measured in metres above the lowest recording at Newport Pier.

Newport Pier is a prime example of infrastructural subsidence that could be occurring at any other tide gauge site globally. All sites within this study have been visited and investigated for signs of infrastructural instability. The data from Newport Pier was excluded due to the unpredictability of the infrastructure movement. All data providers have been asked for maintenance, calibration and gauge replacement heights, dates and additional information. Therefore, there should be no other sites within the final data suite that are suffering from subsidence.

5.5 Discussion

The main product of this thesis is a relative sea level record from local tide gauge data. The existing data are geographically spread equally across the Tay Estuary with datasets at the head and mouth of the estuary, whereas in the Forth Estuary there are data sites throughout the mid-estuary, few in the outer estuary and none at the head. Grangemouth is the nearest data site to the tidal limit (25 km away). Reliable data are not available at the head of the Tay Estuary due to the uncertainty of the Perth, Newburgh and Ribny Beacon datasets (Table 5.1) (see Sections 5.3.2 and 5.3.4).

Location	**Dataset**	**Timespan**	**Pre-corrected (mm a^{-1})**	**Datum-corrected (mm a^{-1})**	**GIA-corrected (mm a^{-1})**
Aberdeen	PSMSL-RLR1	1931-2010	0.96	0.88	1.54
	PSMSL-M1	1931-2010	-		
	PSMSL-RLR2	1862-1965	0.98		
	PSMSL-M2	1862-1965	-		
Dundee	Forth Ports	1986-2010	5.9	0.41	1.45
	PSMSL-M	1897-1912	0.38		
Dunbar	PSMSL-M	1913-1950	0.37	0.27	1.22
	PSMSL-RLR	1913-1950	0.45		
	BODC	1965-1979	11.67		
Grangemouth	Forth Ports	1979-2010	5.74	5.74	6.46
Rosyth	Forth Ports	2003-2010	20.00	0.64	1.60
	PSMSL-M	1964-1993	1.67		
	UKHO	1912-1920	-5.28		
Methil	Forth Ports	2003-2010	-41.4	-	-
Leith	Forth Ports	2004-2010	5.5	1.06	1.91
	PSMSL-M1	1956-1971	3.75		
	PSMSL-RLR1	1956-1971	4.06		
	PSMSL-M2	1981-2010	-0.18		
	PSMSL-RLR2	1981-2010	-0.34		
	UKHO	1980-1981	-55.8		
	BODC	1975-2010	5.19		
Arbroath	SEPA	2007-2009	-	-	-
Newport-on-Tay	SEPA	1995-2009	-	-	-
	TERC	1973-2000	-		
Bridge of Earn	SEPA	1992-2009	-	-	-
Scone, Perth	SEPA	1991-2009	-	-	-
Musselburgh	SEPA	1995-2009	-	-	-
Perth Harbour	PKC	2007-2009	-	-	-
Newburgh	PKC	2007-2009	-	-	-
Earn Confluence	PKC	2007-2009	-	-	-
Stannergate	TERC	1978-1990	-	-	-
Combined		**1900-2010**	**-**	**0.33**	**1.26**

Table 5.1. Pre-corrected relative sea level change, datum-corrected relative sea level change and GIA-corrected sea level change in Aberdeen and the Forth and Tay Estuaries between 1862 and 2010, calculated from local tide gauge data. Several tide gauge data could not be corrected for datum errors or recording errors and their trends are omitted from this table. Several sites experience large short term sea level change trends in their pre-corrected data, including Rosyth (Forth Ports), Methil (Forth

Ports) and Leith (UKHO). These trends are representative of short term trends and each dataset aligns with the overall long term trend of sea level change for the respective site. Ultimately, each datum-corrected dataset identifies a long term relative sea level rise of 1.06 mm a^{-1} or lower between 1900 and 2010, except Grangemouth. Grangemouth has been included in the corrected dataset due to the similarities with the short term sea level changes at Dundee during this time, but the Grangemouth dataset should not be used for long term sea level projection use. The table includes the relative datum-corrected and GIA-corrected sea level change trends between 1900 and 2010.

All pre-corrected relative, datum-corrected relative and GIA-corrected sea level change trends for Aberdeen and the Forth and Tay Estuaries are presented in Table 5.1. The combined dataset trend for the Forth and Tay Estuaries, representative of the entire 1900 to 2010 timescale, is considerably lower compared with some of the shorter timescale individual site trends. Some of the potential causes for the variations in long term and short term sea level trends are discussed in Chapter 6, which reviews several regional sea level oscillations, global sea level trends and the interactions between sea level and other climatic variables.

5.6 Conclusions

Seventeen of the 32 datasets collected for this study were corrected for recording errors and datum change. As presented in Figure 5.69, a combined relative sea level dataset from the Forth and Tay Estuaries provides a near continuous record between 1900 and 2010, with less than 10 years of data missing in the 1950s.

After datum-correction, GIA rates were applied to the datasets. Table 5.1 outlines the range datum-corrected relative and GIA-corrected sea level change trends across the Forth and Tay Estuaries. Excluding Grangemouth, between 1900 and 2010 the datum-corrected relative sea level change trends range from 0.27 to 1.06 mm a^{-1}. Across the same time span, the GIA-corrected sea level change trends range from 1.22 to 1.91 mm a^{-1}. Short term trends were discussed in Section 5.5 and are analysed further in Chapter 6, where the impacts of sea level cycles on short term trends are discussed.

This chapter investigated potential land movement, such as infrastructural subsidence. No such movement is suspected in any of the datum-corrected datasets. However, structural movement was observed at Newport Pier, Newport-on-Tay, which, for this reason, has not been successfully datum-corrected (Section 5.4.2).

Care must be taken when using these corrected datasets, as some elements of sea level behaviour have yet to be explained thoroughly, such as sea level oscillations (Chapter 6) and storm surge

events (Chapter 7). The long term regional sea level statistics produced in this chapter are compared with short term and global sea level trends in Chapter 6, explaining in greater detail how long term trends can be misconstrued by studies that exclude analyses of regional characteristics and multi-decadal sea level oscillations.

Chapter 6 – Local Sea Level Trend Analysis

6.1 Introduction

Global sea level change is a complex combination of naturally oscillating cycles, thermal expansion/contraction and land-based water reservoir transference. Relative sea level data have an added complication, with potential land level change, compared to eustatic sea level. This chapter analyses relative sea level at five ports and harbours in the Forth and Tay Estuaries. The data from these five sites are presented in Chapter 5.

All data derived from tide gauges include oscillations of varying frequency that can influence short-term sea level trends. This chapter analyses oscillations in the data using wavelet analysis methods. Oscillations are then identified by comparing their frequencies with known oscillations.

Comparisons between local data and global historical sea level trends are made, indicating whether local records vary greatly from global records and are likely to differ from the 2100 global model average. Both the Intergovernmental Panel on Climate Change (IPCC) Fourth Assessment Report (AR4) and the UK Climate Impact Partnership (UKCIP) UK Climate Projections ’09 (UKCP09) are interpreted here with regards to their collection of historical sea level data.

Finally, forcings, such as sea surface temperatures (SST), global ice mass, anthropogenic, volcanic and solar influences, are analysed. These elements are important factors affecting sea levels at both global and local scales. SST is hypothesised to have a positive relationship with sea level change.

6.2 Trends in Twentieth and Twenty-First Century Local Data

Linear trends were calculated for five sites in the Forth and Tay Estuaries; Dunbar, Dundee, Rosyth, Leith and Grangemouth (Figures 6.1 to 6.5). Linear trends overlook the osciallations that occur in the sea level data, therefore linear trends should only be used for datasets that covering more than twenty years. These sites have datasets longer than 30 years in duration, therefore accounting for most of the sea level trend influences imposed by short-term cycles. These datasets have been hindcast and forecast with linear interpolation to produce basic linear trend lines from 1900 to 2010. Four of the sites reveal relative sea level trends of between +0.23 and +0.56 mm a^{-1}.

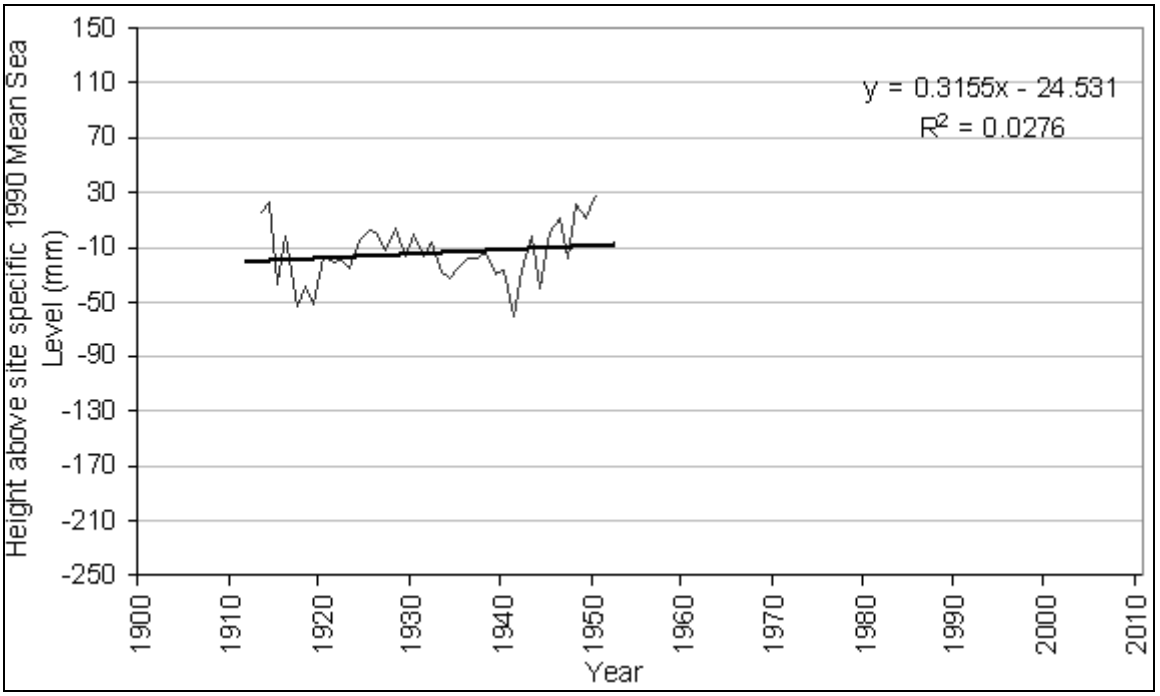

Figure 6.1. Dunbar annual linear trend 1900-2010.

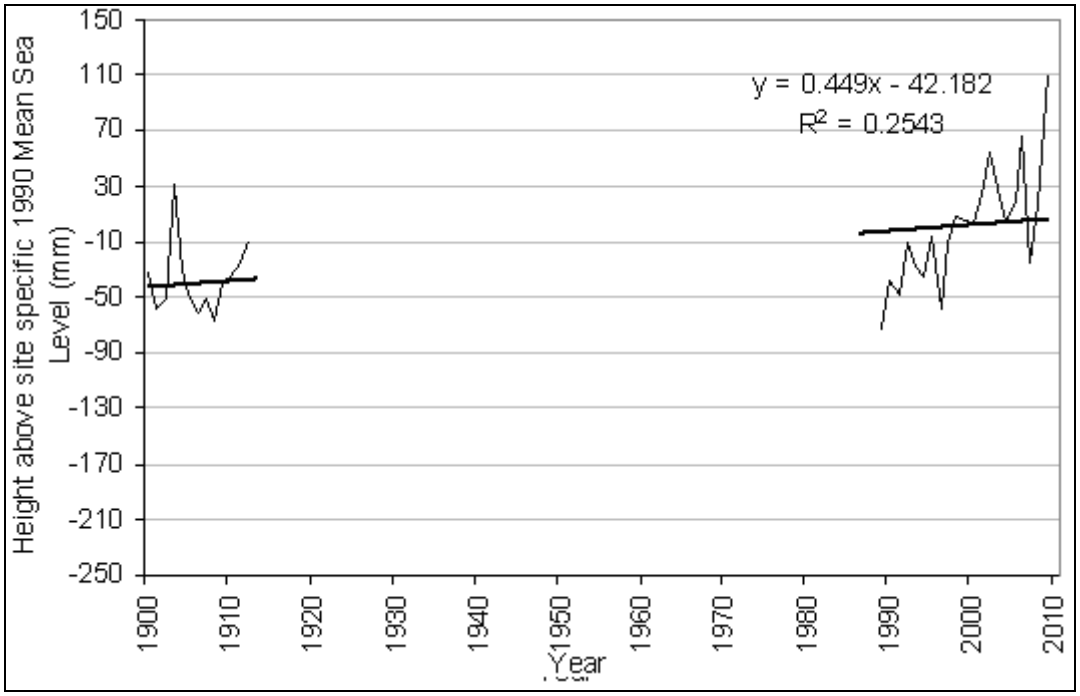

Figure 6.2. Dundee annual linear trend 1900-2010.

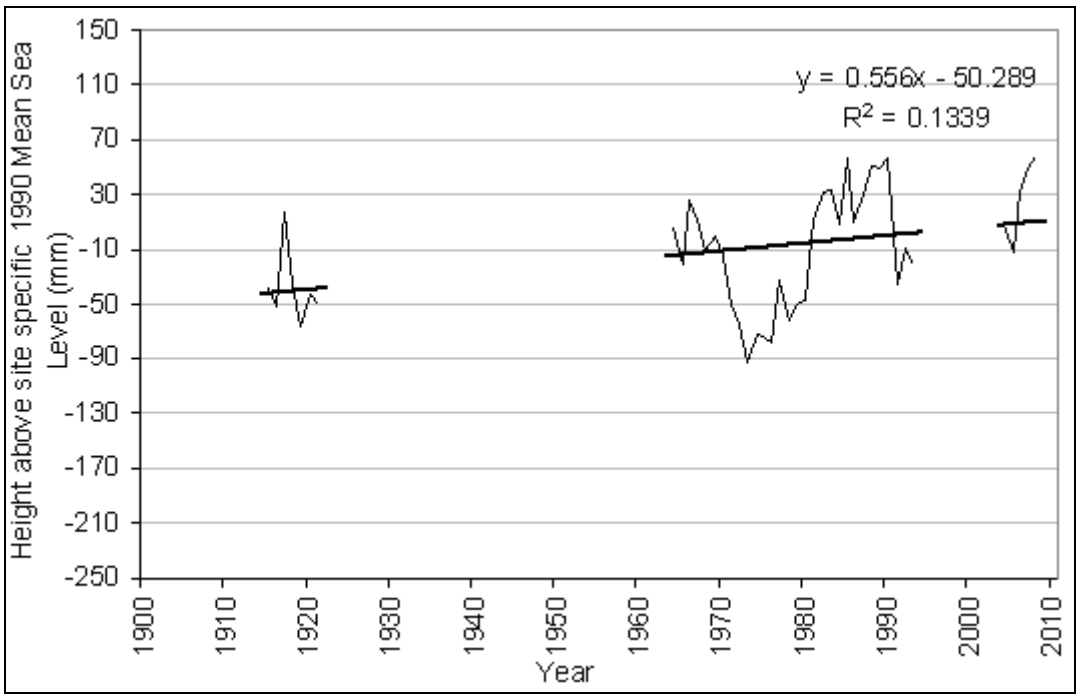

Figure 6.3. Rosyth annual linear trend 1900-2010.

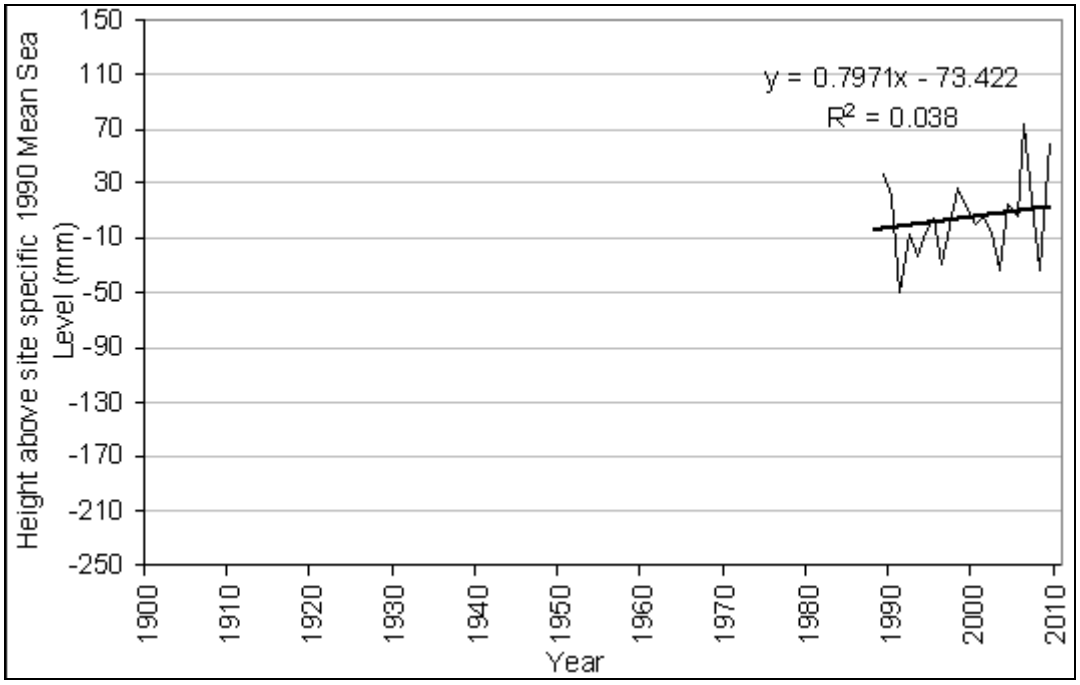

Figure 6.4. Leith annual linear trend 1900-2010.

Grangemouth is the only anomalous dataset with a trend of +5.56 mm a^{-1} between 1979 and 2010 (Figure 6.5). The intermittent nature of the dataset, due to missing data, may have masked parts of the natural sea level cycles that would have reduced the calculated sea level trend. The upper estuarine area of the Forth and Tay Estuaries may be experiencing a greater rise in sea level due to

estuarine funnelling effects. If the Perth datasets had been of better quality then the rates of rise at both Perth and Grangemouth could have been compared to identify if this is the case.

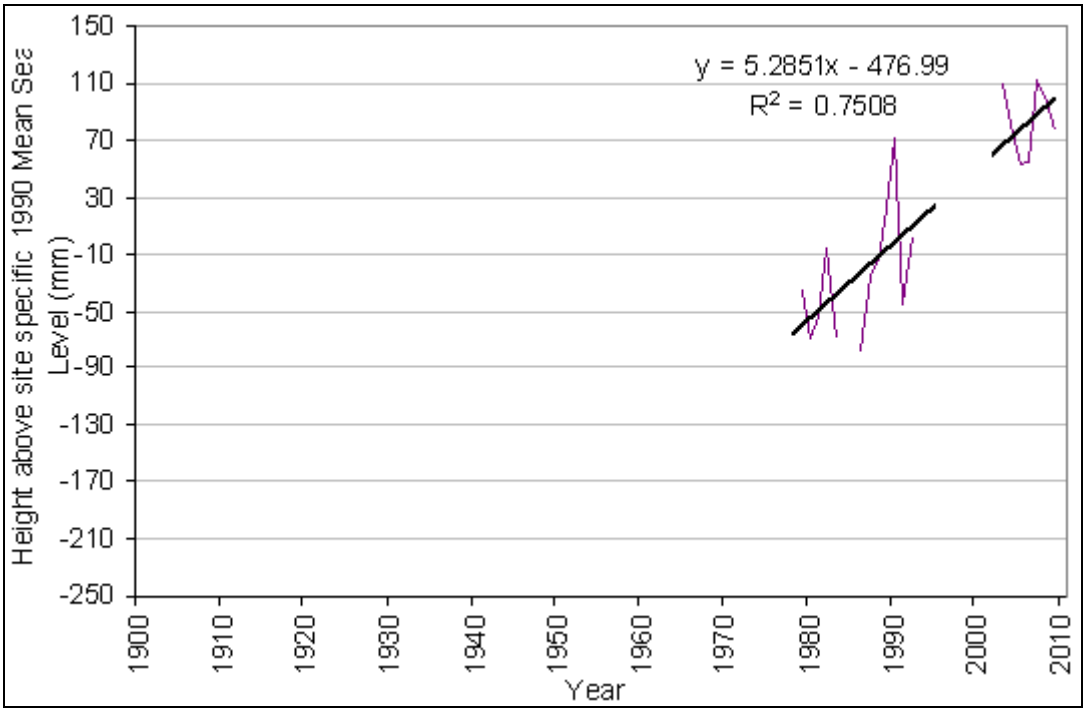

Figure 6.5. Grangemouth annual linear trend 1900-2010.

The linear trend for Dundee, between 1993 and 2008, is +3.86 mm a^{-1} with a total increase along the linear average of 87.38 mm between 1989 and 2008. The Rosyth dataset, between 1993 and 2008, illustrates an average trend of 5.2 mm a^{-1} (Table 6.1). These 15 year short timescale trends divide a known oscillation, the NAO, and are considerably different to the long timescale trends.

	Dunbar	Dundee	Rosyth	Leith	Grangemouth	Global
1900-2008	0.3155	0. 3775	0.556	0.2508	5.1166*	1.8
1993-2008		3.8631	4.5679*	1.4906	9.1756*	3.1

Table 6.1. Local sea level trends (mm a^{-1}) for Dunbar, Dundee, Rosyth, Leith and Grangemouth 1900-2008 and 1993-2008. The 1993-2008 trends are heavily influenced by decadal and multidecadal astronomical and pressure anomaly oscillations. The global average rate has been included as a comparison. * Some data points are missing, as illustrated in Figures 6.1 to 6.5.

6.3 Oscillation Identification

Natural oscillations in sea level have a significant impact on short-term sea level trends. To identify the influence that multiannual cycles can have on decadal sea level trends, the IPCC AR4 included a graph presenting several series of overlapping decadal sea level trend averages between 1950 and

2001 (Figure 6.6) (Solomon *et al.*, 2007). The data included two tide gauge datasets from Holgate and Woodworth (2004) and Church and White (2006), one satellite altimetry dataset from Cazenave and Nerem (2004), two thermal expansion datasets from Ishii *et al.* (2006) and Antonov *et al.* (2005) as well as one climate-driven land water storage dataset from Ngo-Duc *et al.* (2005). Figure 6.6 reveals that decadal cycles in sea level are prominent, even within these smoothed datasets.

Techniques to identify oscillatory cycles of 1 to 34 year frequencies should identify all medium-length astronomical oscillations. Longer frequency cycles would not be identifiable due to the timescale limitations of the datasets.

Decadal and 15 year sea level trends for Aberdeen and the Forth and Tay Estuaries are plotted in Figures 6.7 and 6.8. Both graphs show the variation in these short-term sea level trends along the lengths of the datasets. Both the Aberdeen and the Forth and Tay Estuaries datasets experience near regular periods of increasing and decreasing sea level over 18 to 20-year cycles, for example the Aberdeen dataset has minima in the late 1910s, 1930s, 1950s, 1970s and 1990s.

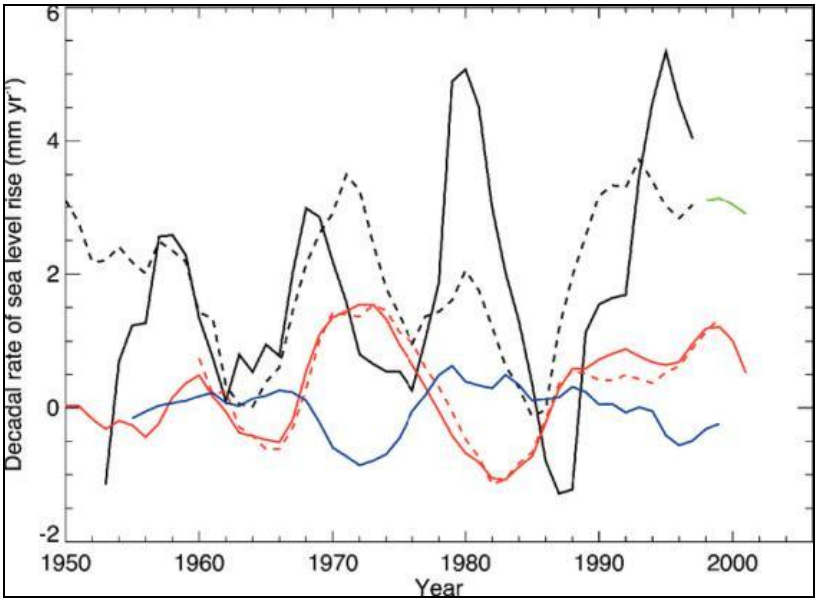

Figure 6.6. "Overlapping 10-year rates of global sea level change from tide gauge data sets (Holgate and Woodworth, 2004, in solid black; Church and White, 2006, in dashed black) and satellite altimetry (updated from Cazenave and Nerem, 2004, in green), and contributions to global sea level change from thermal expansion (Ishii *et al.*, 2006, in solid red; Antonov *et al.*, 2005, in dashed red) and climate-driven land water storage (Ngo-Duc *et al.*, 2005, in blue). Each rate is plotted against the middle of its 10-year period," Solomon *et al.* (2007).

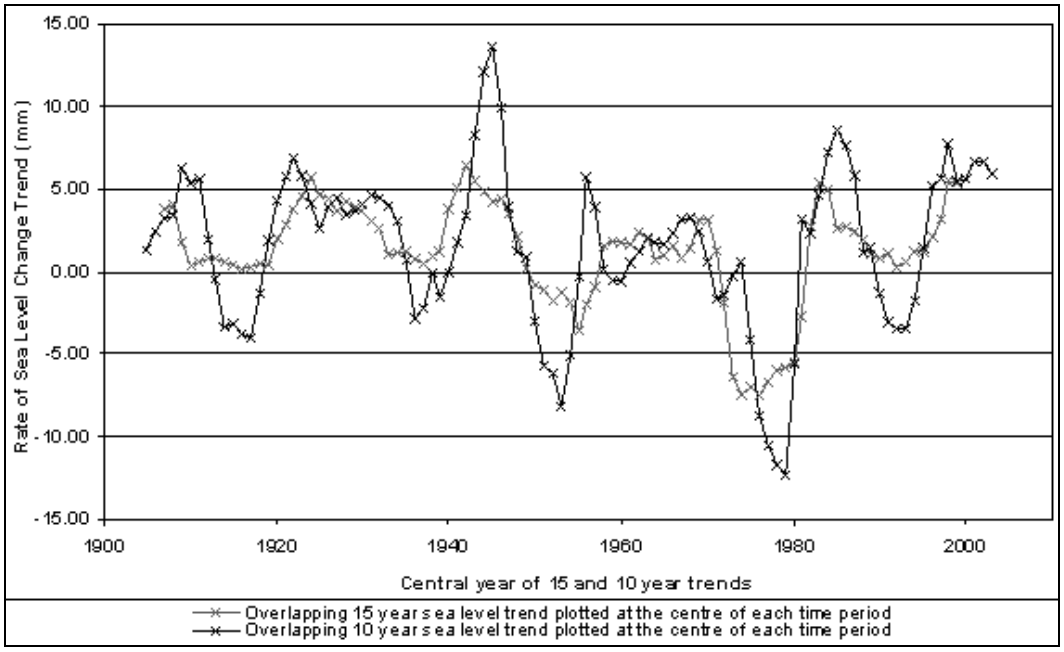

Figure 6.7. Observed changes in relative sea level change trends over 15 and 10 year periods at Aberdeen between 1900 and 2010.

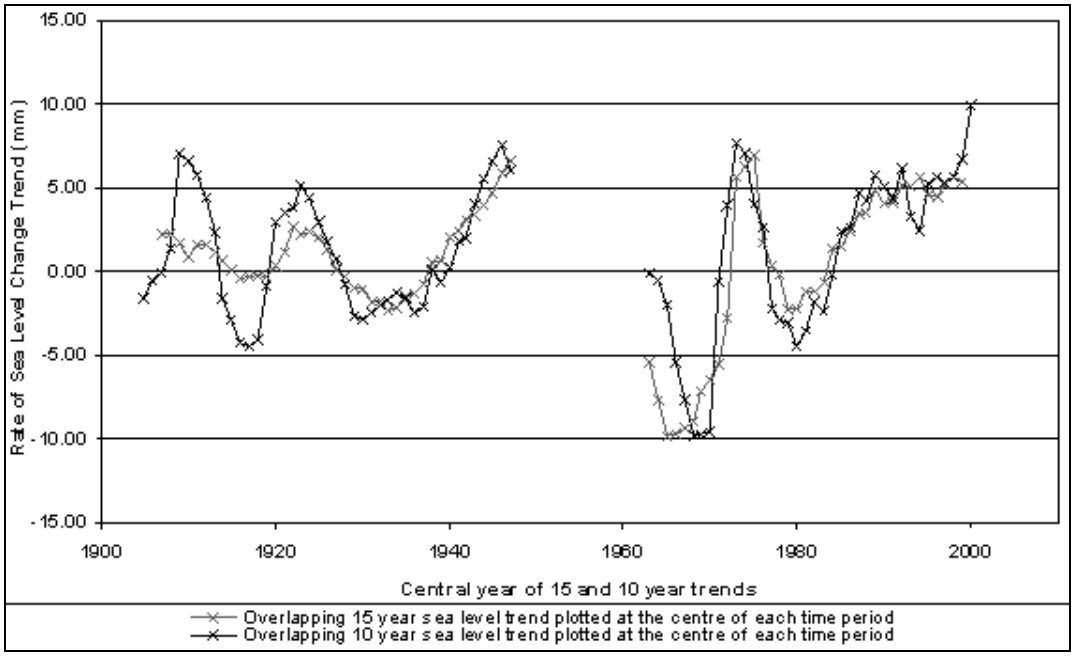

Figure 6.8. Observed changes in relative sea level change trends over 15 and 10 year periods across the Forth and Tay Estuaries using the combined estuary dataset between 1900 and 2010.

This thesis, similar to Jevrejeva *et al.* (2006), uses the Morlet wavelet analysis to identify long-term sea level oscillations (see Chapter 4). Figure 6.9 displays the wavelet power spectrum of 4 global regional sea level series with the cycle period (frequency) plotted against time. Jevrejeva *et al.* (2006) described Figure 6.9 as illustrating an increase in the cycle power between the 2 and 30 year periods between 1940 and 2006, with the normalised variance represented in colour from dark blue

(low) to dark red (high). Sea level oscillations are identified where variance is consistently low at a set periodicity along the timeline; where a periodicity appear to have a consistently low variance. An oscillation at a set frequency may appear to weaken or strengthen in parts along a timeline do to fluctuations in the cycles. The semi-circle appearing on each graph (Figure 6.9) is called the cone of significance, outside of which the significance is calculated to be less than 5% and therefore not reliable.

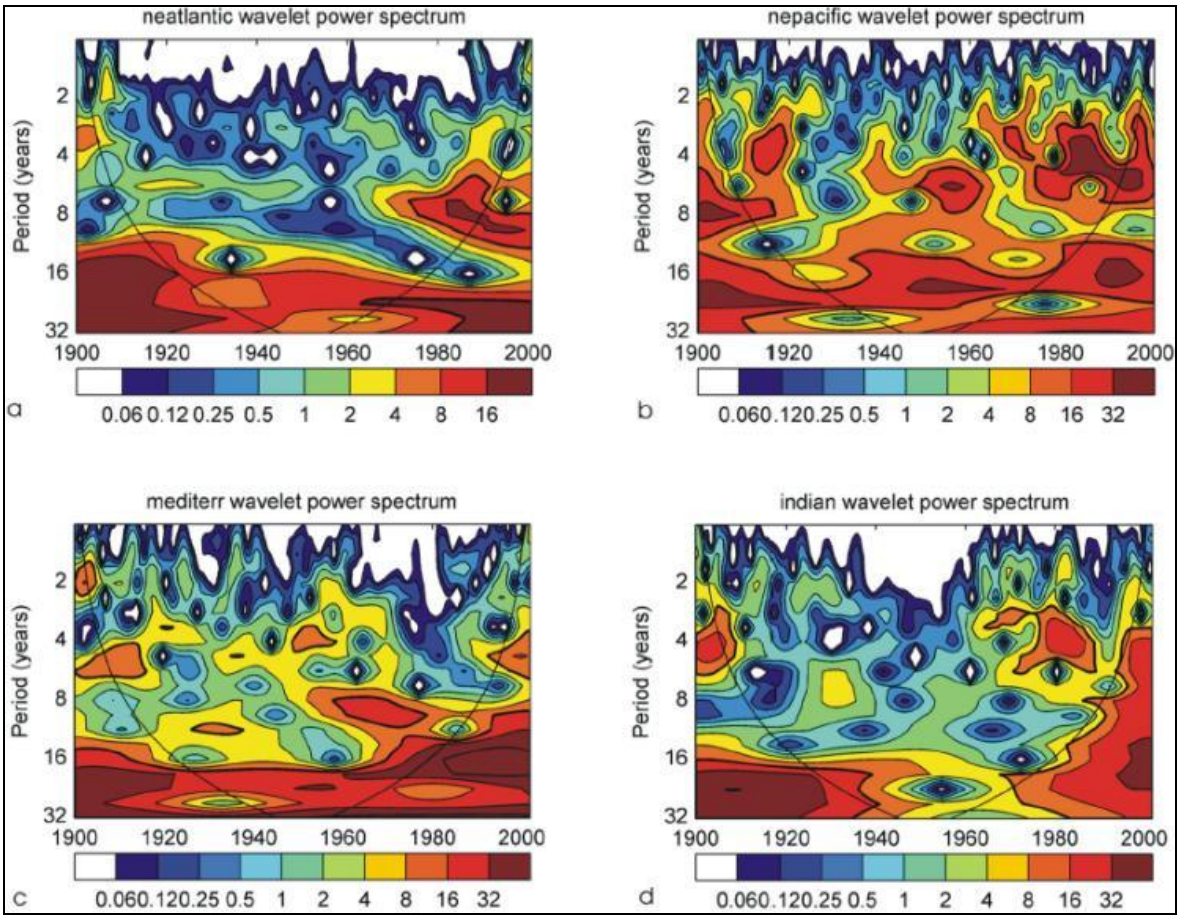

Figure 6.9. Wavelet power spectrum (Morlet) of monthly mean sea level for the (a) north eastern Atlantic Ocean; (b) north eastern Pacific Ocean; (c) Mediterranean Sea; (d) Indian Ocean. Contours are in variance units. In all panels the black thick line is the 5% significance level using the red noise model; solid line indicates the cone of influence. The color bar represents normalized variances. All of the time series show an increase of power in the wavelet power spectrum at 2–30 year periods since 1940s as can be seen by the spread of the red and yellow shading to the upper rights of the panels (Jevrejeva *et al.*, 2006:8). A more detailed explanation is included in the text.

Using the north eastern Pacific Ocean as an example, cycles of between 2 and 5 years in frequency can be seen as having low variance across most of the timescale. Longer periodicity oscillations appear to fluctuate more, but are identified by connecting periods of low variance at set frequency

levels. In the north eastern Atlantic Ocean these periodicity bands include 2-4, ~8 and ~15 years. Some of these oscillations are shared across all four of the examples.

Jevrejeva *et al.* (2006) identified that 5-20% of the signal variability occurred within the 3.5-13.9 year band. This suggests that several overlapping oscillations across the globe lie within this frequency band. Several oscillations were also found within the 13-30 year band. The periods with the greatest influence on sea level height include the period frequencies 3.5, 5.2-5.7, 7-8.5 and 10-13.9 years (Jevrejeva *et al.*, 2006; Unal and Ghil, 1995), which have all experienced an increase in amplitude since the 1940s (Jevrejeva *et al.*, 2006).

"Oscillations in the 2.2–7.8 year band in individual sea level records have been associated with large scale atmospheric circulation signals" (Jevrejeva *et al.*, 2006:6). These atmospherically driven oscillations have been observed in oceanic circulation and sea level changes. Jevrejeva *et al.* (2006) commented on the impacts of the Antarctic Annular Mode/Oscillation (AAM or AAO) and the Southern Ocean Index (SOI) in particular. In the North Atlantic region around the UK, other oceanic circulation and local atmospheric systems take precedence, such as the North Atlantic Oscillation (NAO) and Arctic Oscillation (AO).

In order to identify co-varying sea level and atmospheric frequency bands, Jevrejeva *et al.* (2006) used a wavelet coherency method. Figure 6.10 illustrates the influence of the AO on the variability of the North Atlantic and the influence of the SOI on three other regions. The North Atlantic region graph shows good correlation with the 2.2-13.9 year signals found in individual records. The north eastern Pacific has been increasingly influenced by the SOI and the Pacific Decadal Oscillation (PDO) over the last 60 years across the 2-30 year cycle periods (Jevrejeva *et al.*, 2006).

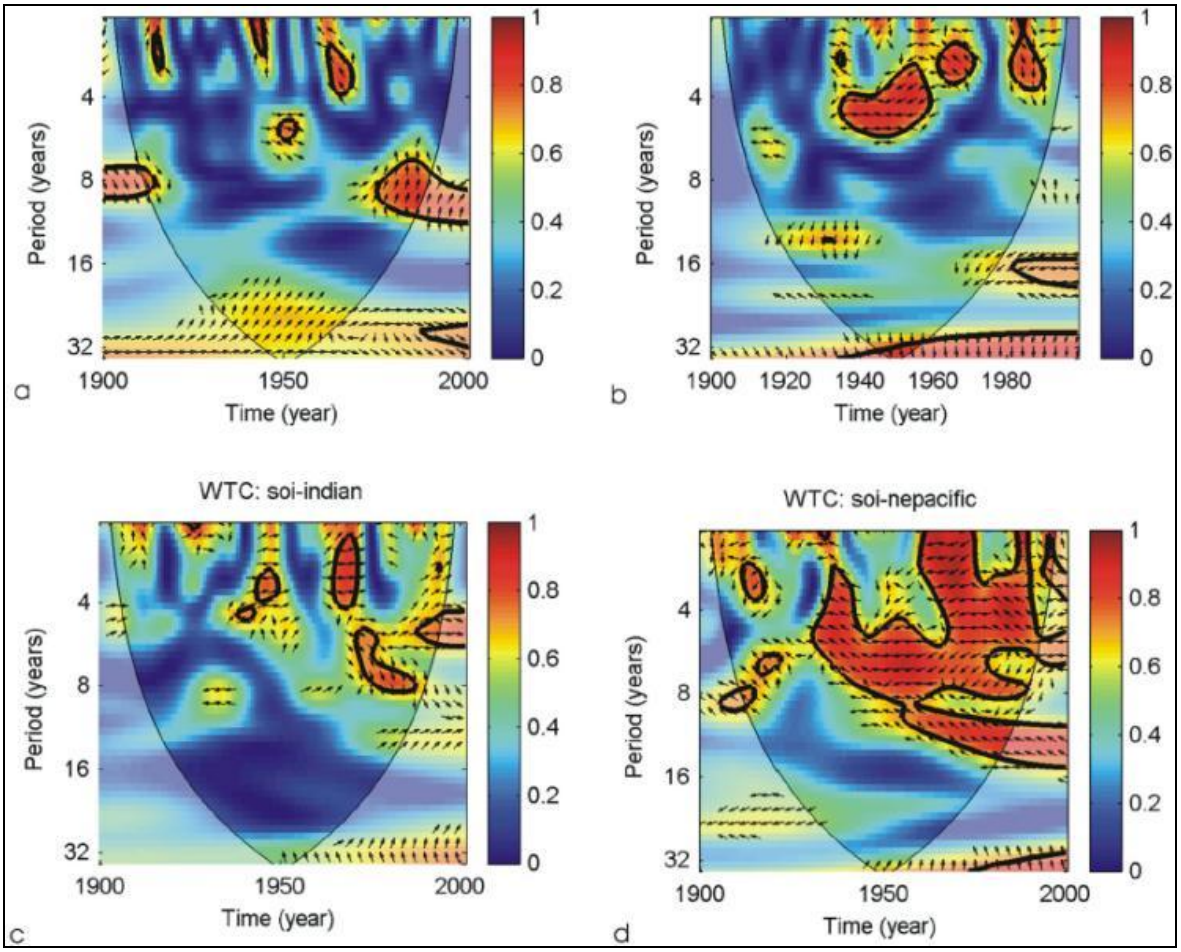

Figure 6.10. "(a) Wavelet coherency between AO/sea level in the north eastern Atlantic; (b) the same for the NAO/Mediterranean sea level; (c) the same for the SOI/Indian Ocean sea level; (d) the same for the SOI/ north eastern Pacific sea level. Contours are wavelet squared coherencies. The vectors indicate the phase difference (a horizontal arrow pointing from left to right signifies in-phase, and an arrow pointing vertically upward means the second series lags the first by 90° (i.e., the phase angle is 270°)). In all panels the black thick line is the 5% significance level using the red noise model. Data analysed are annual sea level," Jevrejeva *et al.* (2006:9).

6.4 Local Sea Level Wavelet Analysis

The wavelet analyses follow the Torrence and Compo (1998) methodology, which has been applied to all five datasets (see Chapter 4). As examples, Figures 6.11 to 6.13 illustrate the variance of wavelet analyses output at one location over different timescales. The graphs depict the sea level time series, contoured Morlet wavelet power spectrum, and variance graphs indicating variance over the time series length. With regards to part (b) of the graphs, the Morlet wavelet analysis, low power signals throughout the duration of the time series at a stable period suggest periods of low variance and therefore significant stable oscillatory cycles.

The three Aberdeen wavelet analysis graphs (Figures 6.11 to 6.13) represent the same dataset over different timescales. Several datasets have been analysed in this fashion to identify if the wavelet analysis is affected by timescale length. Figure 6.11 illustrates the wavelet analysis over nearly 150 years at Aberdeen. The main findings revealed in part (b) of Figure 6.11, the wavelet power spectrum, are that there are oscillations with low variability at frequencies between 2 and 4, 8 and 15 years. In Figure 6.11 and Figure 6.12 wavelet power spectra, an increase in the wavelet variability can be seen after 1940 by the introduction of the yellow coloured higher variability contours.

Wavelet analysis has been applied to monthly and annual data from Dunbar, Dundee, Grangemouth, Leith and Rosyth. The wavelet power spectra for Dunbar's monthly and annual data are similar to those at Aberdeen (Figures A7.1 and A7.2, in Appendix 7) highlighting peaks in the spectra during the same periods. Analysis of the Dundee data included separate wavelet analyses for the 1897 to 1912 data and 1988 to 2008 data, due to the large time gap. The analysis revealed large differences in variance between annual and monthly data as well as between the two time periods. However, the position of the high variance points in relation to period and the timeline are in agreement with the Aberdeen data (Figures A7.3 to A7.6). This suggests the difference in variance between the two time periods may be due to an increase in sea level oscillation magnitudes after 1940, which is consistent across all sites (discussed further in Section 6.3).

The Grangemouth results, though originating from results with missing data, illustrate the same relationship as that in the Aberdeen oscillation frequencies of 5 and 10 years (Figures A7.7 and A7.8, in Appendix 7). The Leith data were split into three timescales, 1954 to 2008, 1954 to 1965 and 1988 to 2008, in order to analyse the temporal impact on wavelet analysis. Within these wavelet power spectra the 3 to 4, 8, 10 and 20 year oscillation frequencies appeared as near consistent cycles, although these results are dependent on the timescale length of the dataset (Figures A7.9 to A7.14, in Appendix 7). The temporal variance between datasets had little impact on the

identification of periodicity, but did suggest a variance reduction in the longer analysis in Figures A7.9 and A7.12 (Appendix).

Wavelet analysis has been applied to the time periods 1912-1920, 1964-1993 and 1964-2008 at Rosyth. Most of the wavelet spectra highlight high variance periods associated with the oscillation frequencies 10 and 20 years. Some of the analyses have identified the 5 to 7 year periods (Figures A7.15 to A7.20, in the Appendix). These results suggest that sea levels within the Forth and Tay Estuaries are affected by the same cycles as identified in the Aberdeen dataset.

Three combined datasets for the 'Tay', 'Forth' and 'Forth & Tay' Estuaries have been analysed and wavelet power spectra produced. The Tay (Figure 6.14) is split into two wavelet power spectra due to missing data. These spectra do not appear to agree with each other, but the Tay spectrum as a whole is in agreement with the periodicity and timeline of the Forth Wavelet Power Spectrum (Figure 6.15).

Comparison between the Forth Estuary and Tay Estuary spectra emphasises similarities in the distribution of wavelet power across the periods. In that sense the variation between the Forth Estuary wavelet power spectrum (Figure 6.15) and the combined Forth and Tay Estuaries wavelet power spectrum (Figure 6.16) is minimal.

All of the long timescale analyses imply an increase in the variance across all periods after 1940. The combined Forth and Tay Estuary wavelet spectrum in Figure 6.16 illustrates the consistent 5 to 7, 10 and 20 year cycle periods across both estuaries. Table 6.3 illustrates the difference in variance within each wavelet spectrum discussed above.

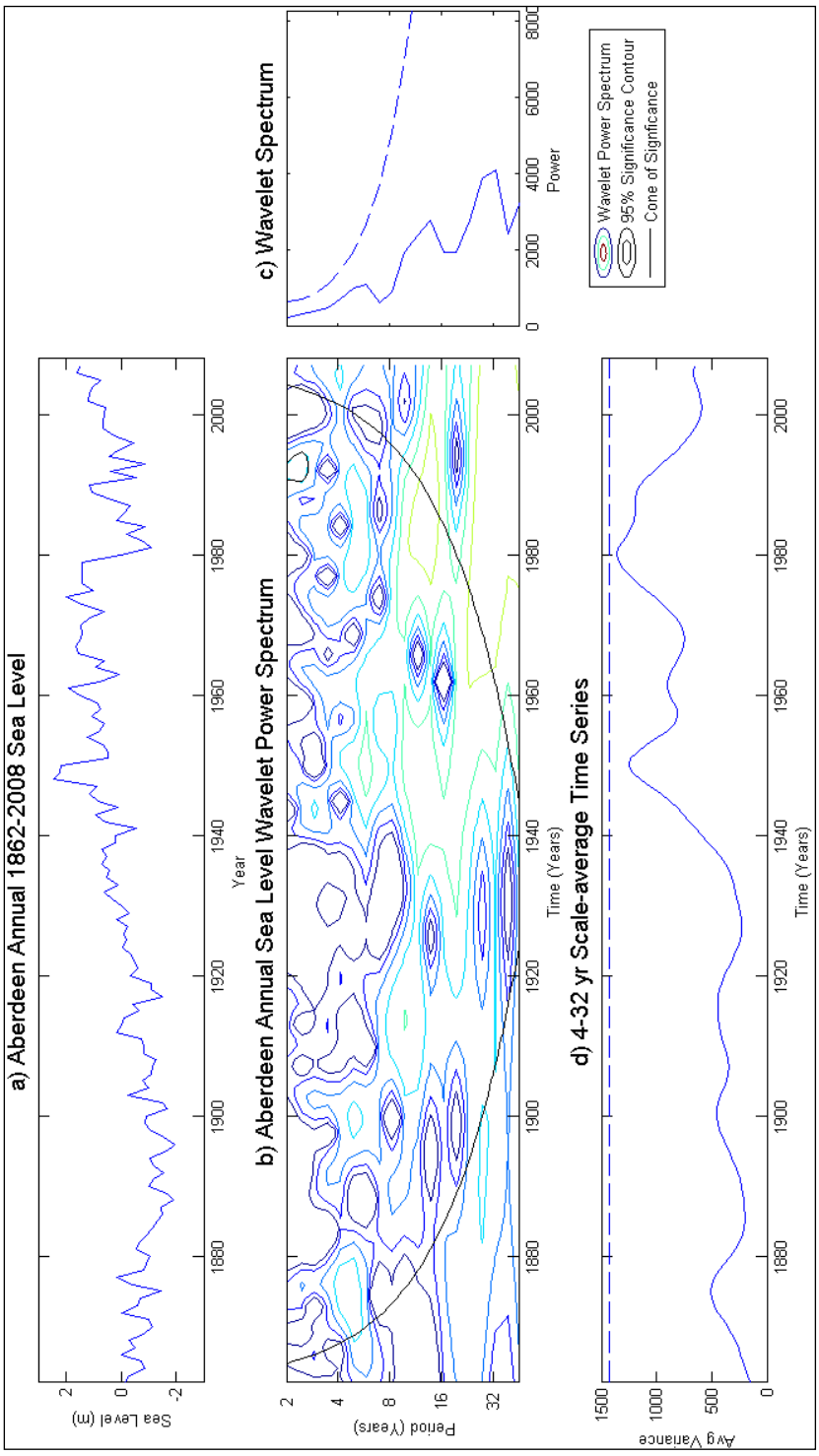

Figure 6.11. Wavelet analysis using the Torrence and Compo (1998) wavelet software. a) Complete Aberdeen time series sea level data. b) Aberdeen annual sea level power spectrum with attached legend explaining the wavelet power spectrum contours, 95% significance contours and the cone of significance. Contours coloured red and yellow are of high significance. c) The wavelet spectrum illustrates the spikes in variance in relation to the wavelet power spectrum (graph b). The y-axis is shared with graph b. d) The 4-32 year scale-average time series illustrates the smoothed variance in the data along the time series from the scale-average.

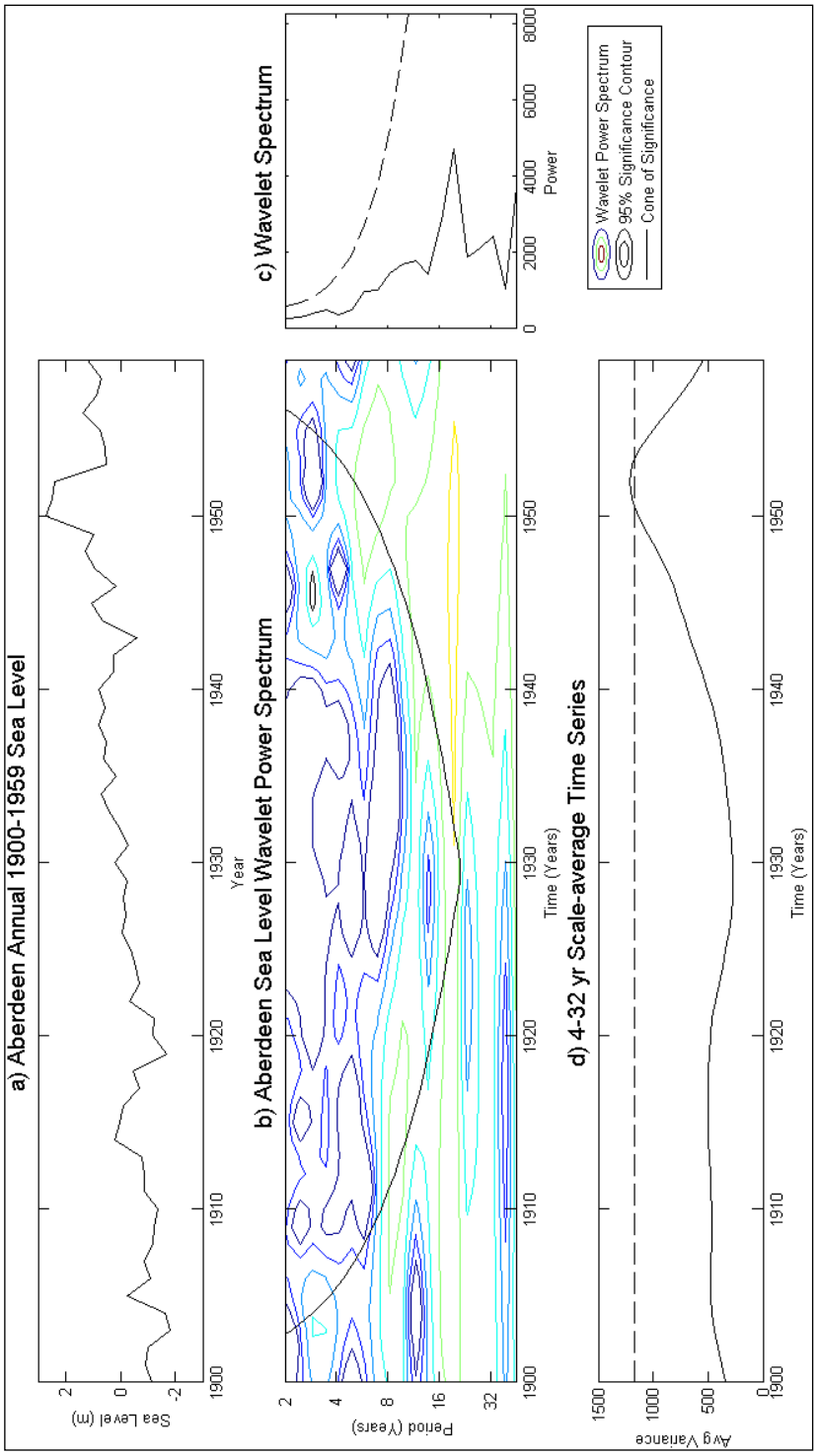

Figure 6.12. Wavelet analysis using the Torrence and Compo (1998) wavelet software. a) Aberdeen 1900-1959 time series sea level data. b) Aberdeen annual sea level power spectrum with attached legend explaining the wavelet power spectrum contours, 95% significance contours and the cone of significance. Contours coloured red and yellow are of high significance. c) The wavelet spectrum illustrates the spikes in variance in relation to the wavelet power spectrum (graph b). The y-axis is shared with graph b. d) The 4-32 year scale-average time series illustrates the smoothed variance in the data along the time series from the scale-average.

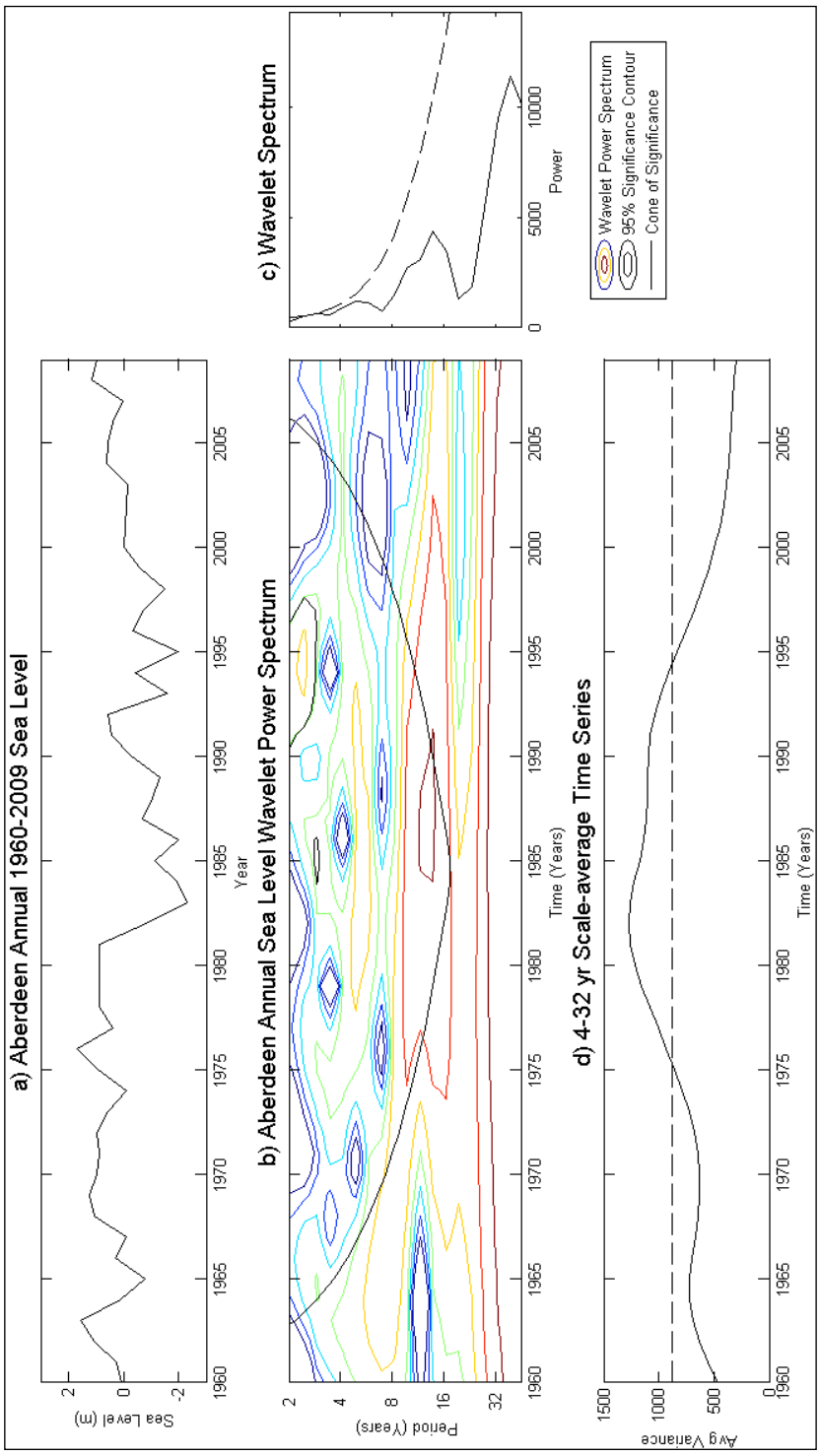

Figure 6.13. Wavelet analysis using the Torrence and Compo (1998) wavelet software. a) Aberdeen 1960-2009 time series sea level data. b) Aberdeen annual sea level power spectrum with attached legend explaining the wavelet power spectrum contours, 95% significance contours and the cone of significance. Contours coloured red and yellow are of high significance. c) The wavelet spectrum illustrates the spikes in variance in relation to the wavelet power spectrum (graph b). The y-axis is shared with graph b. d) The 4-32 year scale-average time series illustrates the smoothed variance in the data along the time series from the scale-average.

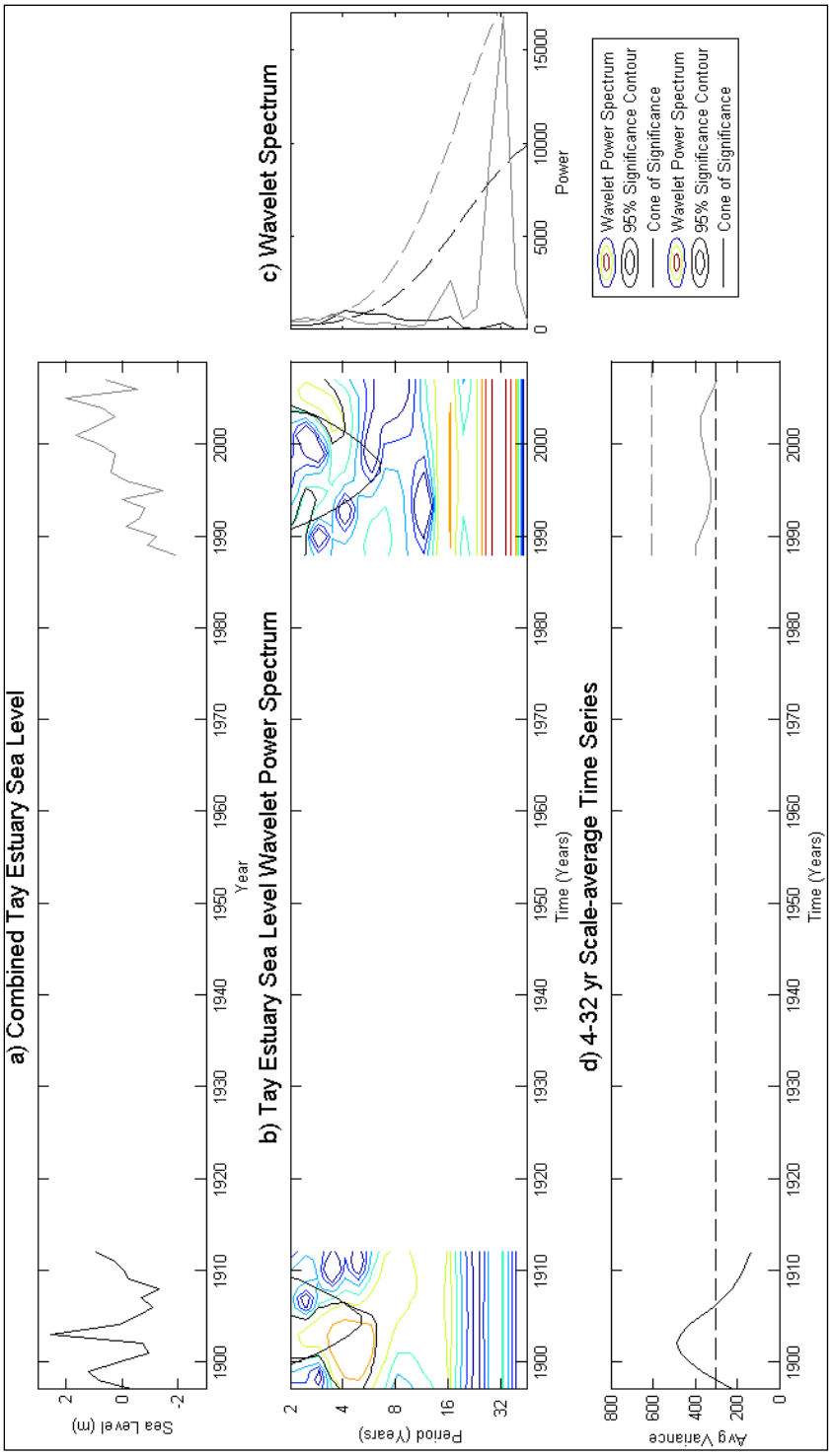

Figure 6.14. Wavelet analysis using the Torrence and Compo (1998) wavelet software. a) Combined Tay Estuary sea level data. b) Tay Estuary sea level power spectrum with attached legend explaining the wavelet power spectrum contours, 95% significance contours and the cone of significance. Contours coloured red and yellow are of high significance. c) The wavelet spectrum illustrates the spikes in variance in relation to the wavelet power spectrum (graph b). The y-axis is shared with graph b. d) The 4-32 year scale-average time series illustrates the smoothed variance in the data along the time series from the scale-average.

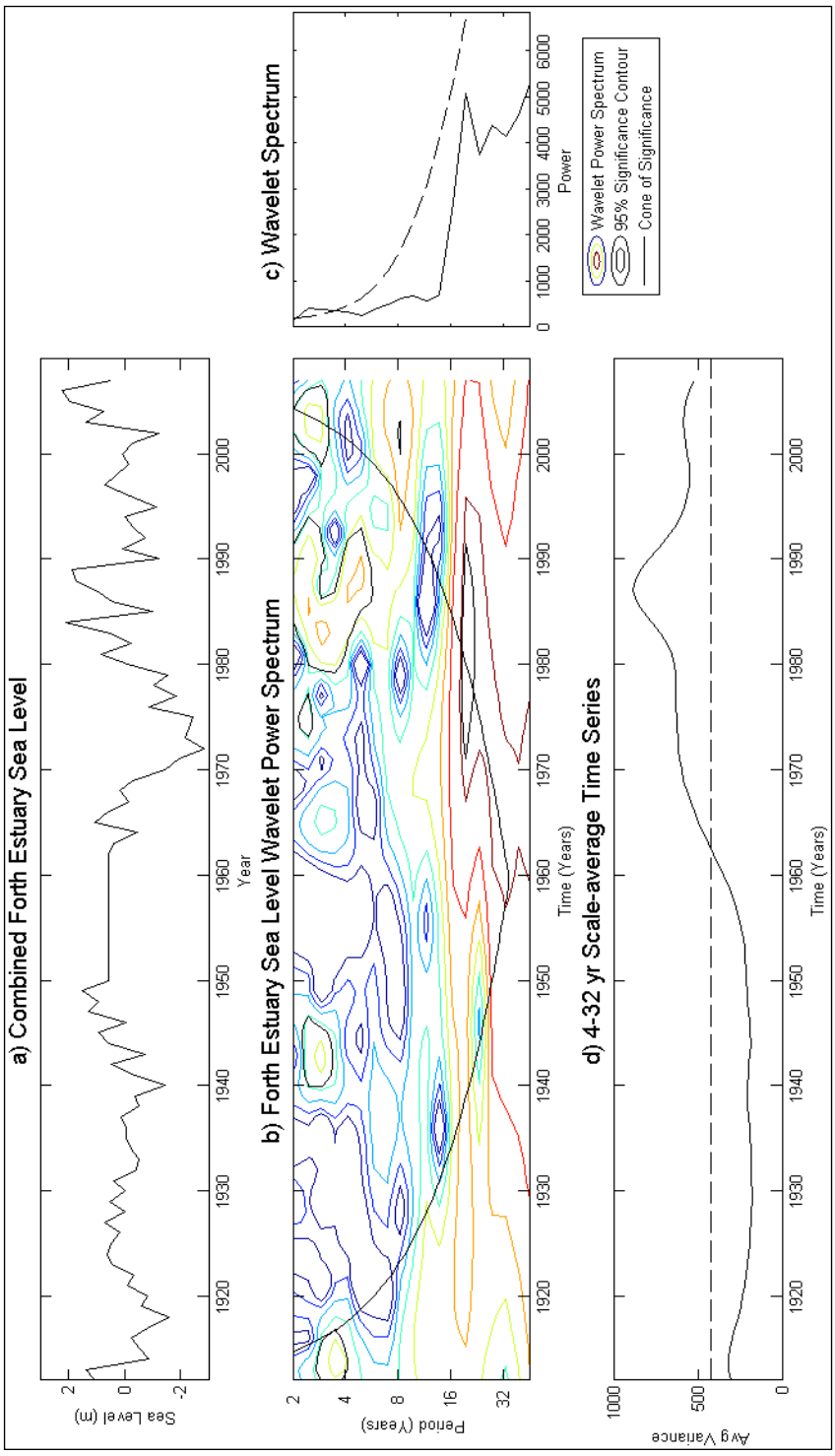

Figure 6.15. Wavelet analysis using the Torrence and Compo (1998) wavelet software. a) Combined Forth Estuary sea level data. b) Forth Estuary sea level power spectrum with attached legend explaining the wavelet power spectrum contours, 95% significance contours and the cone of significance. Contours coloured red and yellow are of high significance. c) The wavelet spectrum illustrates the spikes in variance in relation to the wavelet power spectrum (graph b). The y-axis is shared with graph b. d) The 4-32 year scale-average time series illustrates the smoothed variance in the data along the time series from the scale-average.

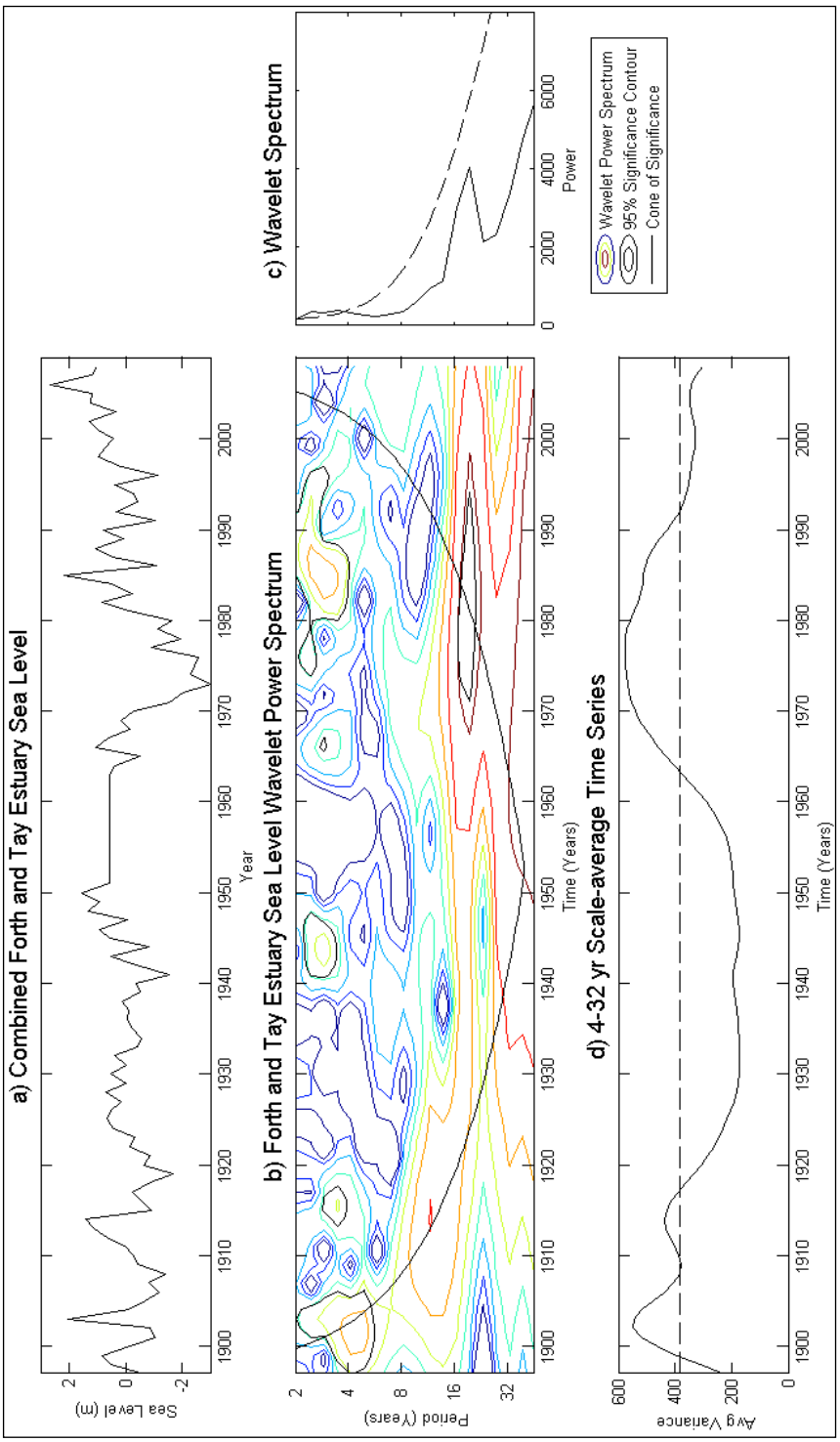

Figure 6.16. Wavelet analysis using the Torrence and Compo (1998) wavelet software. a) Combined Forth and Tay Estuary sea level data. b) Forth and Tay Estuary sea level power spectrum with attached legend explaining the wavelet power spectrum contours, 95% significance contours and the cone of significance. Contours coloured red and yellow are of high significance. c) The wavelet spectrum illustrates the spikes in variance in relation to the wavelet power spectrum (graph b). The y-axis is shared with graph b. d) The 4-32 year scale-average time series illustrates the smoothed variance in the data along the time series from the scale-average.

6.5 Astronomical and Other Forcings

In continuation from Section 6.4, this section aims to identify the local wavelets discovered through wavelet analysis. Some lunar, solar and planetary influences on sea level can be predicted significantly far in advance. These forcings can be combined with more unpredictable elements, such as atmospheric changes. The cycles that occur in sea level data around the North Atlantic include those in Table 6.2.

Cycle	Frequency
Lunar monthly	29.5 days
Solar semi-annual	182.7 days
Solar annual	364.96 days
North Atlantic Oscillation (NAO)	1 to 3 years
Arctic Oscillation (AO)	10 years
NAO low-frequency variation	10 to 30 years
Sunspot/double sunspot (Hale)	11 and 22 years
Lunar nutation/nodal tidal cycle	18.6 years
Saturn-Jupiter cycle	19.9 years
Atlantic Multidecadal Oscillation (AMO) cycle	60 to 70 years

Table 6.2. Planetary driven oceanic cycles active in the study region (Polykov and Johnson, 2000; Czaja and Marshall, 2001; Hurrell, 1995; Gratiot *et al.*, 2008; Knight *et al.*, 2006; Knudsen *et al.*, 2011).

Long cycles, including the AMO, the 87 year Gleissberg solar cycle and the 210 year De Vries-Suess solar cycle, are unlikely to appear clearly in tide gauge data due to temporal limitations in the data. The AMO has been closely observed with Knight *et al.* (2006) in particular noting cold phases occurring in the 1900s to 1920s and 1960s to 1980s as well as a warm phase in the 1930s to 1950s (Figure 6.17). The warm phase coincided with reduced rainfall in the USA as well as increased rainfall and hurricane formation in the Sahel with the cold phases associated with the opposite effect. If this see-saw relationship between cold and warm phases continues at the present rate then the AMO would presently be in the latter stage of a warm phase.

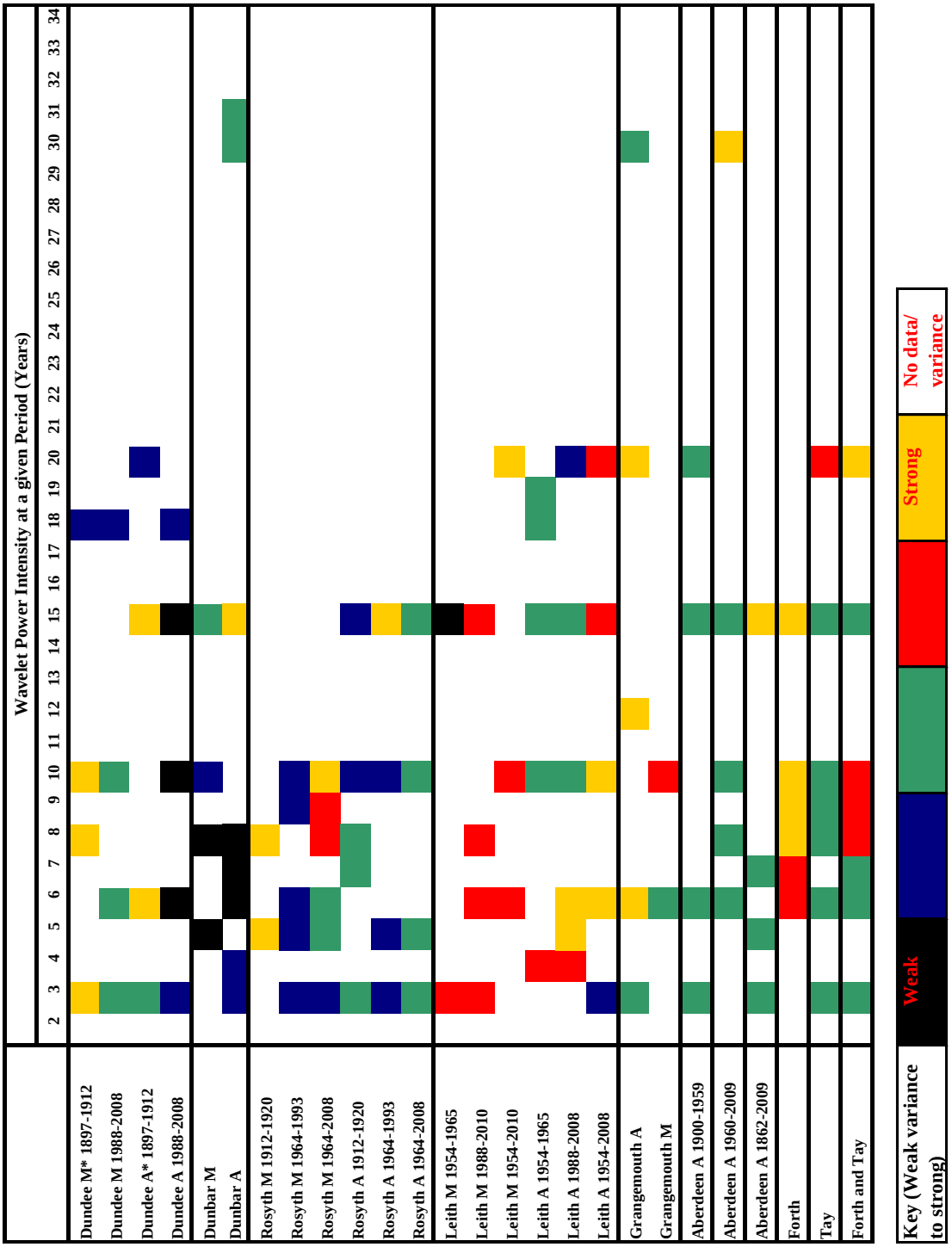

Table 6.3. Wavelet variance at a given period (2-34 years) within the datasets specified. A weak variance represents a consistent sea level cycle that agrees with the wavelet and there are few overlapping, variable cycles. Strong variance can represent a number of overlapping, variable cycles or one cycle with poor agreement with the wavelet. Three combined datasets were used; Forth, Tay and the 'Forth and Tay' Estuaries dataset. Monthly and 1-2 year cycles have been excluded, but are known to exist. As a generalisation, the most common, strong cycles occur around 3-4, 7, 10, 15, 18-20, and 32 years.

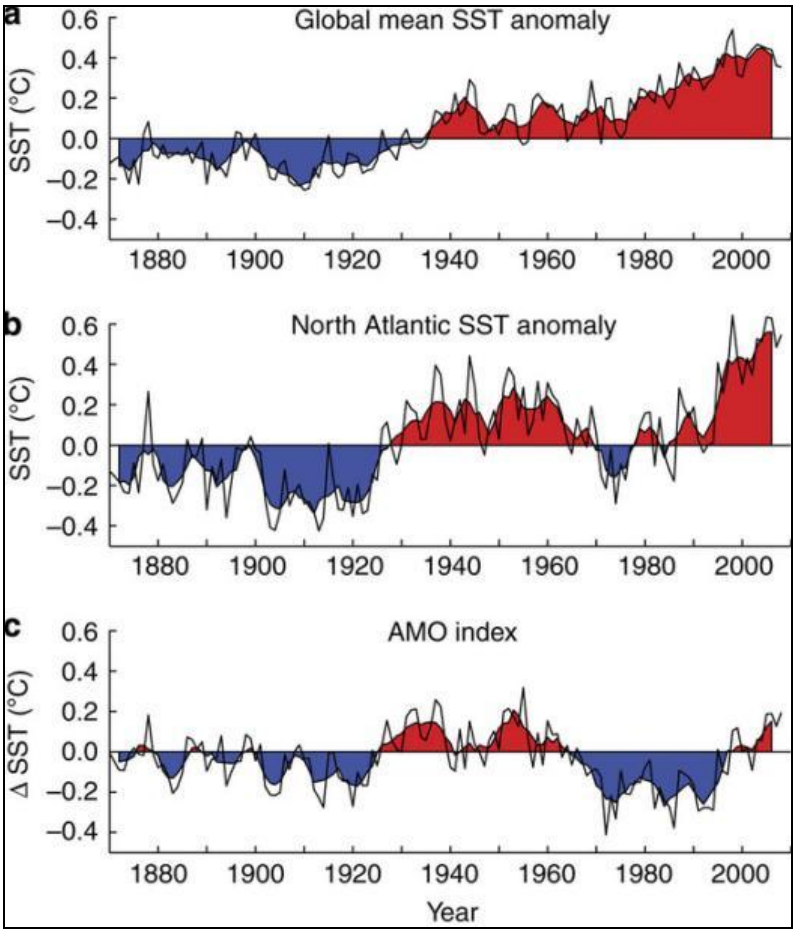

Figure 6.17. (a) Global annual mean sea-surface temperature (SST) anomalies from the UKMO Hadley Centre Sea Ice and Sea Surface Temperature (HadISST) data for the period 1870–2008 (thin black line). (b) Annual mean North Atlantic SST anomalies for the period 1870–2008 (thin black line). (c) The Atlantic Multidecadal Oscillation (AMO) index for the period 1870–2008. The modern AMO index is defined by subtracting the global mean SST anomalies (a) from the North Atlantic SST anomalies (b). Five-year running means are shown by heavy black lines with fill in all panels (Knudsen *et al.*, 2011:2).

Some of the cycles highlighted above, such as the NAO (Figure 6.18) and AO, are Northern Hemispherical cycles limited to the North Atlantic and upper latitudes. For this reason, comparison between national and global sea level trends may vary over a short timescale. More information on the comparison between local, national and global relationships is discussed in the following section.

Referring back to the cycles identified in Section 6.4, the most dominant sea level forcing emulates the NAO, which is responsible for 3, 5 to 7, 10, 15 and 20 year periodic cycles. Comparison between the NAO Index, AO Index and local sea level data has been made in Figure 6.19. The 10 year cycles are coincident with the decadal AO and both the lunar nutation cycles are influential.

Sunspot cycles and the Saturn-Jupiter cycle are known to have a minor influence on sea level with the >1 year solar and lunar cycles identified as forcings.

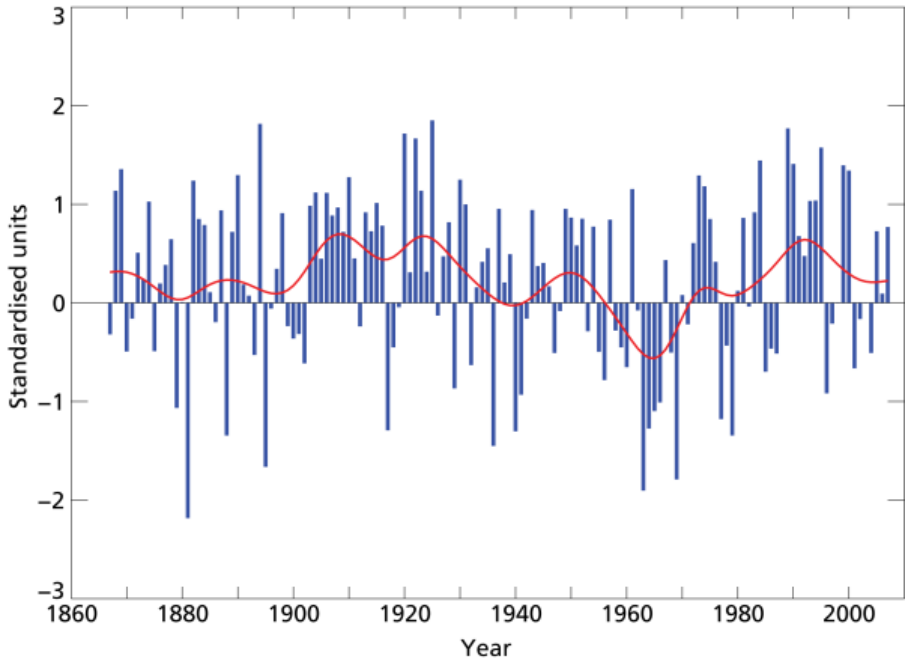

Figure 6.18. The North Atlantic Oscillation Standardised Index over winter periods (Dec-Feb) 1867-2006. The red line emphasises multidecadal variations in the NAO (Jenkins *et al.*, 2008).

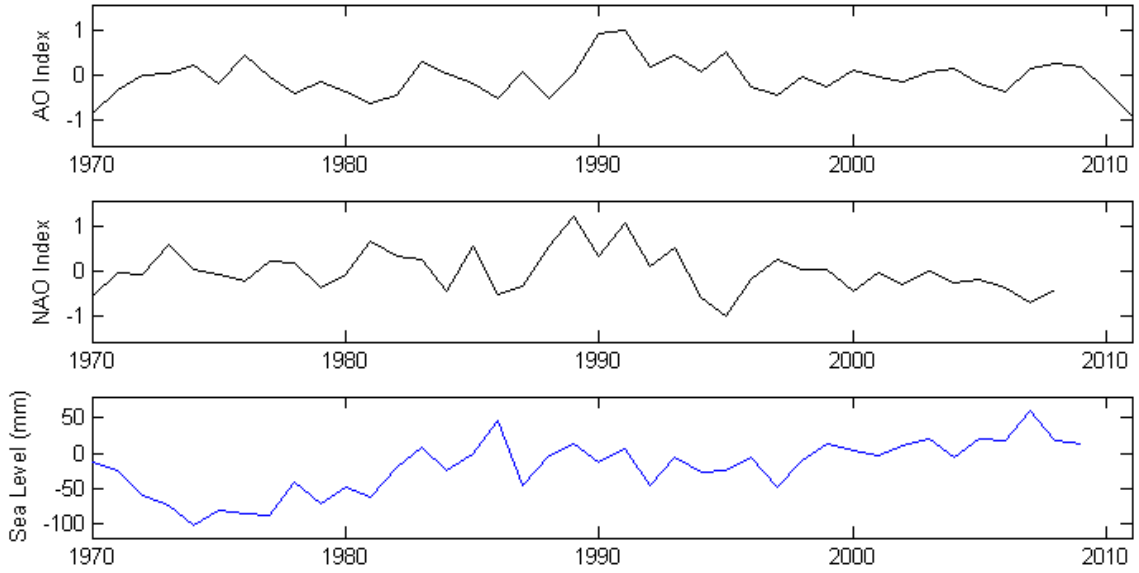

Figure 6.19. AO Index, NAO Index and sea level comparison. The sea level dataset here is the combined dataset constructed from Dunbar, Dundee, Leith, Grangemouth and Rosyth data. The AO and NAO Index data were collected by the US National Weather Service Climate Prediction Center (2011).

6.6 National and Global Sea Level Relationships

The IPCC is a world-leading producer of global climate and sea level change predictions and historical records. As part of the explanation of historic global sea level change the IPCC use global sea level trends from Church and White (2006) and Holgate and Woodworth (2004) as well as satellite altimetry trend lines from Leuliette *et al.* (2004) (Figure 6.20). In support of the findings from the wavelet analysis in Section 6.2.2, the global trend in Figure 6.20 illustrates an increased decadal oscillation in the sea level rise trend.

Jenkins *et al.* (2008) described global sea level trends on behalf of the UKMO and UKCIP using a graph of global sea level change since 1860 (Figure 6.20), which can also be found in IPCC AR4 (Solomon *et al.*, 2007). The linear trend of global sea level between 1900 and 2003 varies from 1.7 mm a^{-1} across the full timescale and 3.1 mm a^{-1} between 1993 and 2003 (Solomon *et al.*, 2007).

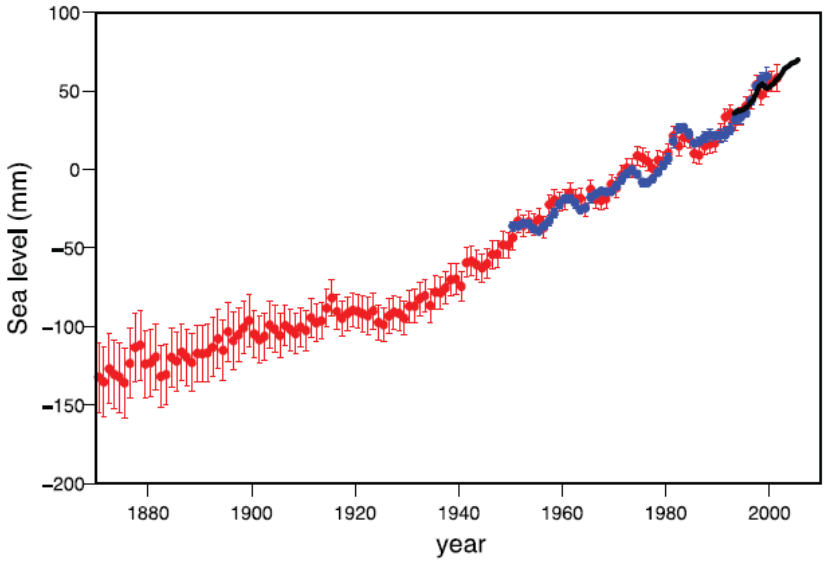

Figure 6.20. "Annual averages of the global mean sea level (mm). The red curve shows reconstructed sea level fields since 1870 (updated from Church and White, 2006); the blue curve shows coastal tide gauge measurements since 1950 (from Holgate and Woodworth, 2004) and the black curve is based on satellite altimetry (Leuliette *et al.*, 2004). The red and blue curves are deviations from their averages for 1961 to 1990, and the black curve is the deviation from the average of the red curve for the period 1993 to 2001. Error bars show 90% confidence intervals," (Solomon *et al.*, 2007:410).

In order to predict climate change until 2095, UKCIP collected historic data on a range of climate variables across the UK. Historic gridded datasets have been generated from data between 1914 and 2009 with the 5 x 5 km resolution grid covering the UK as part of the UKMO PPE. These data are available from the UKMO, specifically air temperature and precipitation data, are available in daily, monthly and annual frequencies since 1960 (DEFRA, 2009).

Since 1914 a linear rise in temperature across the UK has occurred (Figure 6.21). However, during the late 1950s and early 1960s a slight lowering of temperature occurred before another more rapid rise began (DEFRA, 2009).

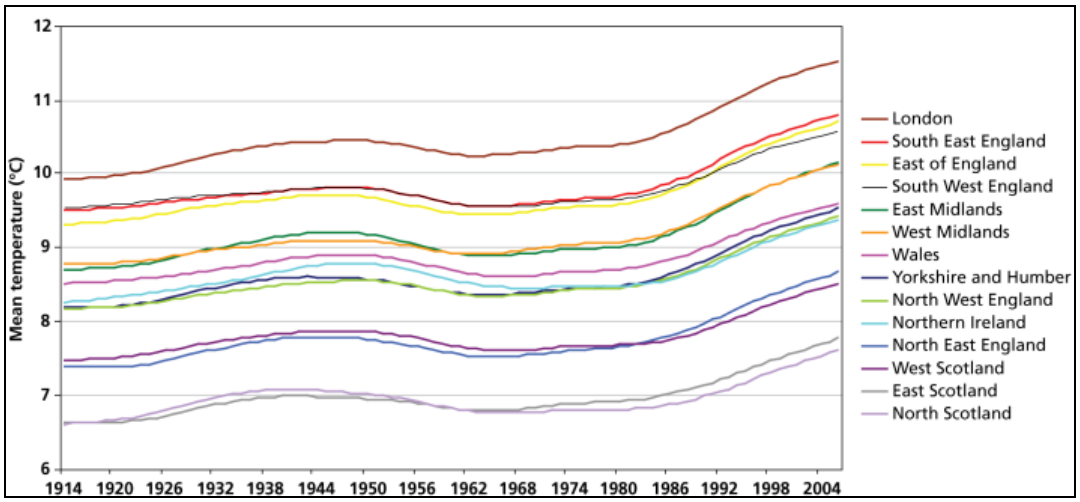

Figure 6.21. UKCP09 daily mean temperature (°C) from 1914 to 2006 filtered by region (DEFRA, 2009).

A detailed illustration of global temperature change between the 1840s and 2000s was compiled for IPCC AR4 (Solomon *et al.*, 2007) (Figure 6.22). These data highlight the oscillatory nature of temperature globally, with various cycles of different frequencies overlapping.

Global temperature data have been analysed by hemisphere. Distinct differences can be seen between the two hemispheres, especially within the 1920s and 1930s. During these two decades the Northern Hemisphere saw a sharp rise in SST, similar to that occurring within the last 30 years, whereas the Southern Hemisphere witnessed a stable rise until the late 1960s (Figure 6.23).

To evaluate the impact a rise in temperature may have on sea level, the IPCC plotted global sea level change against global SST change between 1993 and 1998, as determined by the TOPEX/POSEIDON satellites. This small temporal sample of data indicated a trend in the level of sea level change relative to the change in temperature over that time period. This timescale is too short for appropriate long-term relationship generation, but does show short-term trends (Figure 6.24).

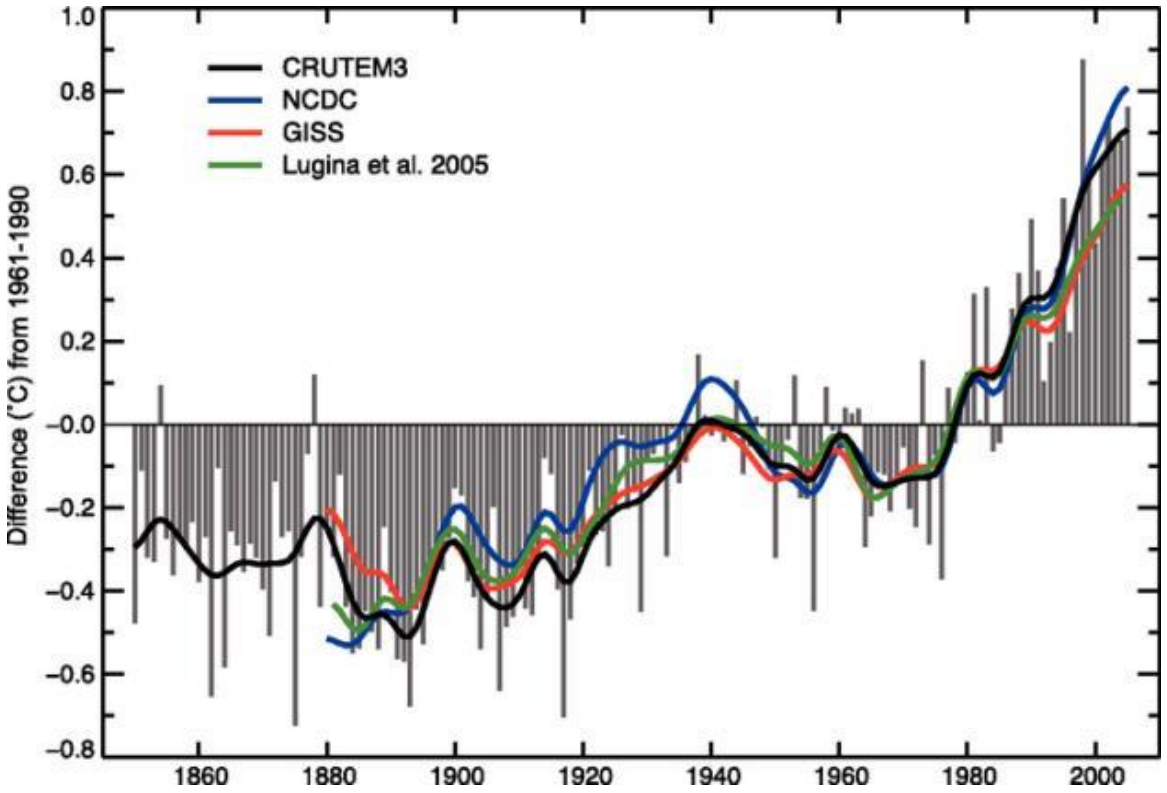

Figure 6.22. Annual anomalies of global land-surface air temperature (°C), 1850 to 2005, relative to the 1961-1990 mean for the UKMO/University of East Anglia Climate Research Unit (CRU) land surface temperature anomaly grid dataset (CRUTEM3), updated from Brohan *et al.* (2006). The smooth curves show decadal variations. The black curve from CRUTEM3 is compared with those from US National Climate Data Center (NCDC) (Smith and Reynolds, 2005; blue), GISS (Hansen *et al.*, 2001; red) and Lugina *et al.* (2005; green),' Solomon *et al.* (2007).

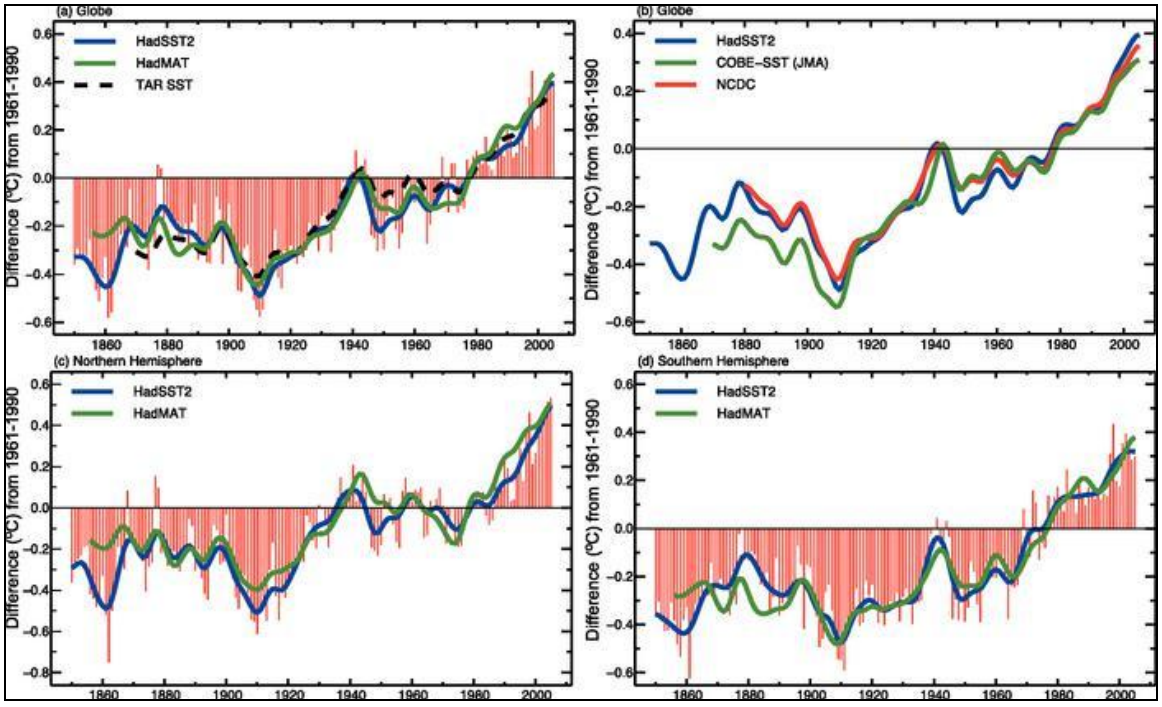

Figure 6.23. (a) Annual anomalies of global SST (UKMO Hadley Centre Sea Surface Temperatures 2 dataset (HadSST2); red bars and blue solid curve), 1850 to 2005, and global NMAT (referred to at the UKMO Hadley Centre Marine Air Temperature (HadMAT) dataset, green curve), 1856 to 2005, relative to the 1961 to 1990 mean (°C) from the UKMO (Rayner *et al.*, 2006). The smooth curves show decadal variations (see Appendix 3.A). The dashed black curve shows equivalent smoothed SST anomalies from the TAR. (b) Smoothed annual global SST anomalies, relative to 1961 to 1990 (°C), from HadSST2 (blue line, as in (a)), from NCDC (Smith *et al.*, 2005; red line) and from the UKMO Hadley Centre Centennial in-situ Observation-Based Estimate Analysis Sea Surface Temperatures (COBE-SST) dataset (Ishii *et al.*, 2005; green line). The latter two series begin later in the 19th century than HadSST2. (c,d) As in (a) but for the Northern Hemisphere and Southern Hemisphere showing only the UKMO series (Solomon *et al.*, 2007).

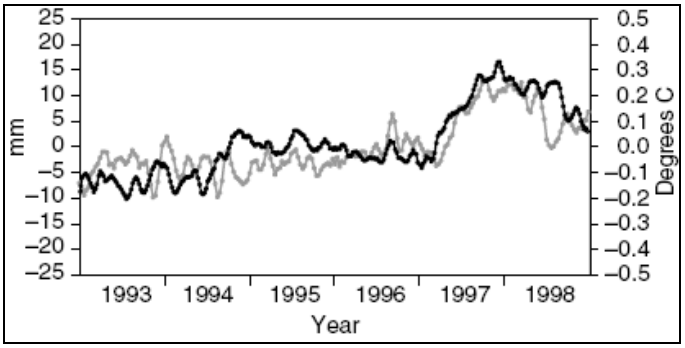

Figure 6.24. Global mean sea level variations (light line) computed from the TOPEX/POSEIDON satellite altimeter data compared with the global averaged sea surface temperature variations (dark line) for 1993 to 1998 (Cazenave *et al.*, 1998, updated). The seasonal components have been removed from both time-series (Houghton *et al.*, 2001:663).

Jones and Jeff (1991) produced SST data for various recording stations along the coast of England and Wales. Two of these stations on the north eastern English coast are Longstone (Farne Islands) and Blyth. Both temperature records indicate cyclic patterns in the annual temperature (Figure 6.25).

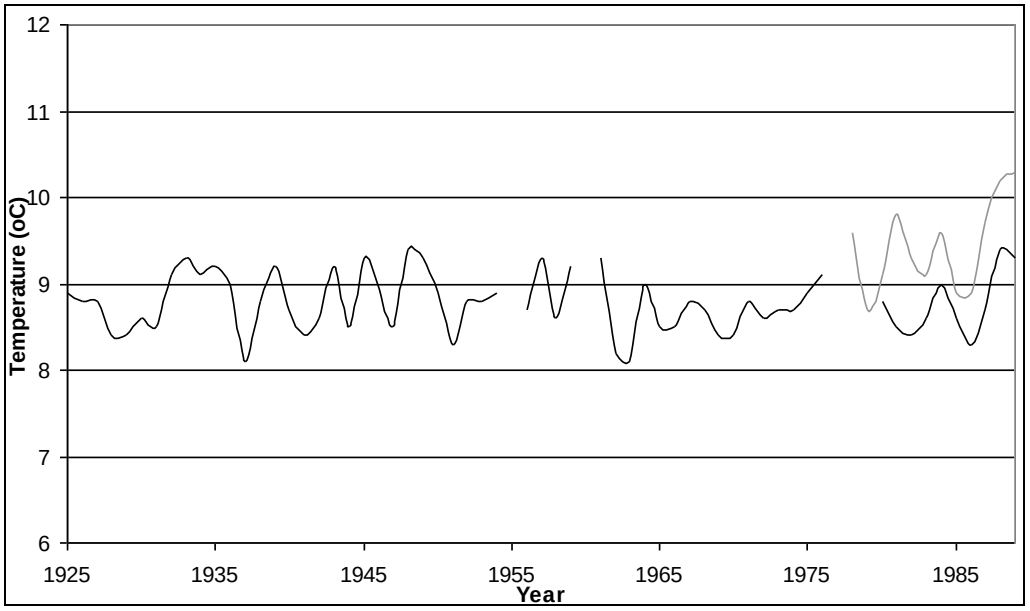

Figure 6.25. Jones and Jeff (1991) annual mean sea surface temperature at Longstone and Blyth. Longstone in black and Blyth in grey.

The relationship between global temperature and sea level is often illustrated by the Archer (2006) graph that suggests a linear positive relationship of 20 m $°C^{-1}$ (Figure 6.26). However, this trend is based on extremely long-term Eocene sea levels, without any observance of interglacial relationships since. Tectonic effects have also not been taken into account (Grinsted, 2009). The Archer (2006) graph has been used in the German Advisory Council on Global Change (WBGU) Report (Schubert *et al.*, 2006), even though there are fundamental flaws with the use of Eocene sea level data for interglacial comparison (Grinsted, 2009).

Rohling *et al.* (2009) plotted global sea level against Antarctic temperature over the past five glacial cycles, which suggested that the sea level-temperature relationship is not linear (Figure 6.27). Sea level response is directly linked to ice volume with sea level response being larger at times of high ice volume. From the resulting data, a positive relationship between Antarctic temperature and global sea level of 3 to 5 m of sea level change to 1°C of temperature change has been calculated. Taking into account polar amplification, which could amplify by 1.5 to 2.3 times, Grinsted (2009) estimates the true relationship to be nearer to 6 to 10 m per 1°C.

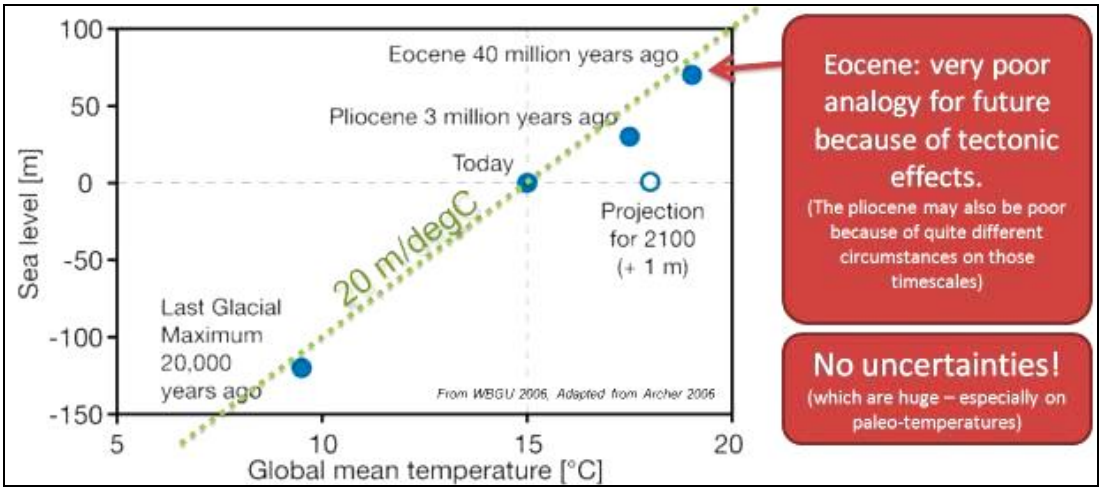

Figure 6.26. Archer (2006) Eocene based sea level-temperature relationship (Grinsted, 2009).

Further discussions regarding SSTs and their relation to sea level are included in Section 6.8.

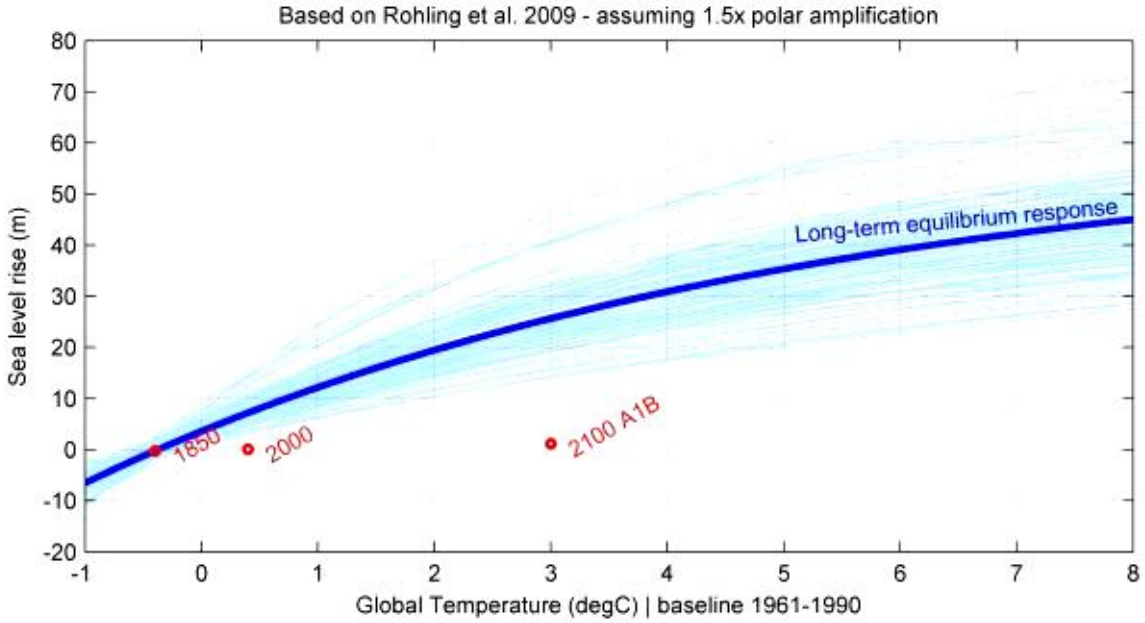

Figure 6.27. Global sea level-temperature relationship based on the last five interglacials, as analysed by Rohling *et al.* (2009) (Grinsted, 2009).

6.7 Other Forcings

The relationship between land ice and sea level has already been commented on in previous sections. In particular, Section 6.6 refers to the IPCC suggestion that the exchange of water between land-based reservoirs, including ice caps, is one of the two major contributions to sea level change. Additionally, it was noted at the end of Section 6.6 that Grinsted (2009) concluded that the size of the ice mass can influence the size of the sea level response to temperature. Figure 6.8 illustrates the

oscillations in “climate-driven land water storage” alongside sea level change, emphasising the relationship (Solomon *et al.*, 2007).

Several studies have predicted large future sea level changes occurring due to large-scale ice melt in Antarctica and Greenland (Houghton *et al.*, 2001). Ice sheet melting could have a significant impact on sea level within the next few hundred years (Mitrovica *et al.*, 2001), but ice sheet melting has not been weighted highly within IPCC AR4. Over “two to five hundred years, the West Antarctic Ice Sheet could disintegrate, raising sea level 6 meters”, (Titus *et al.*, 1991:3).

Some solar cycles have already been discussed in Section 6.5, however other solar influences, such as solar flares, are less predictable. NAO has been connected with solar cycles by Landscheidt (2004). In his analyses, Landscheidt predicted NAO to follow a similar maxima-minima pattern to that of Figure 6.28, being heavily influenced by the greatest perturbations of the Sun’s orbital motion cycle and the secondary harmonic perturbation cycle. The relationship agrees closely and suggests that the NAO cycle will be at its maximum in 2026 and minimum in 2044 (Landscheidt, 2004).

Jevrejeva *et al.* (2009) constructed two models of sea level change between 1000 AD and 2000 AD to compare natural volcanic and solar radiative forcings against natural and anthropogenic forcings. The resultant graph (Jevrejeva *et al.*, 2009) suggested that since the 1850s the anthropogenic influence has significantly increased sea level above the natural solar and volcanic induced levels (Figure 6.29).

As global temperatures are predicted to rise considerably over the next one hundred years due primarily to anthropogenic forcings (Solomon *et al.*, 2007), governments across the globe are attempting to reduce their greenhouse gas (GHG) emissions. If GHG emissions are reduced future temperatures may be lower than predicted, therefore sea levels may not reach the high levels predicted by the IPCC AR4 (Solomon *et al.*, 2007).

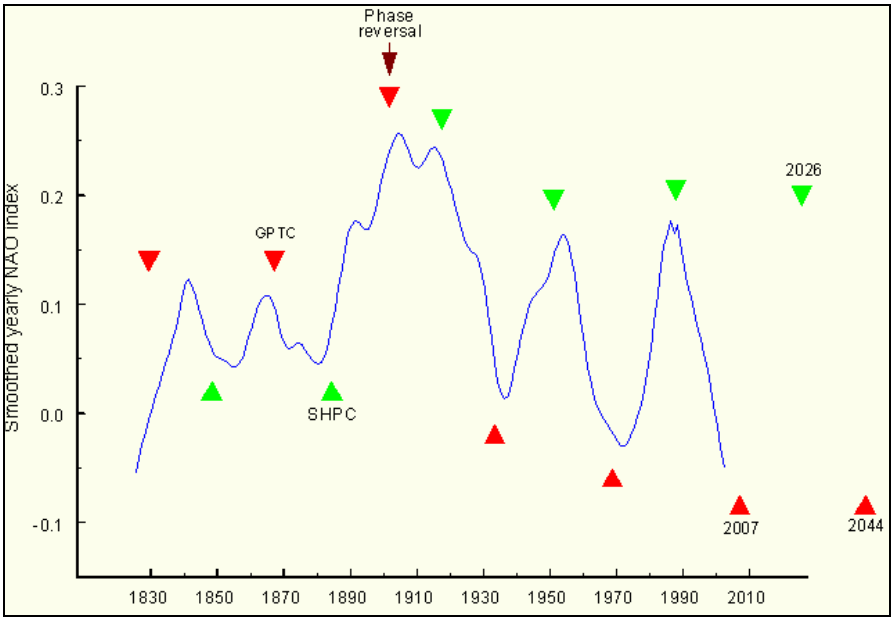

Figure 6.28. Annual means of the NAO index between 1852 and 2002 with predicted NAO turning points until 2050 (Landscheidt, 2004). The red triangles represent the greatest perturbation in the Sun's orbital motion (torque) cycle (GPTC). The green triangles represent the second harmonic of the perturbation cycle (SHPC). Before the phase reversal SHPC coincided with minima events and after phase reversal SHPC coincides with maxima events. Landscheidt (2004) identified a link between the Sun's cycle and the NAO and predicted that future turning points in the NAO cycle will coincide with the next GPTC and SHPC.

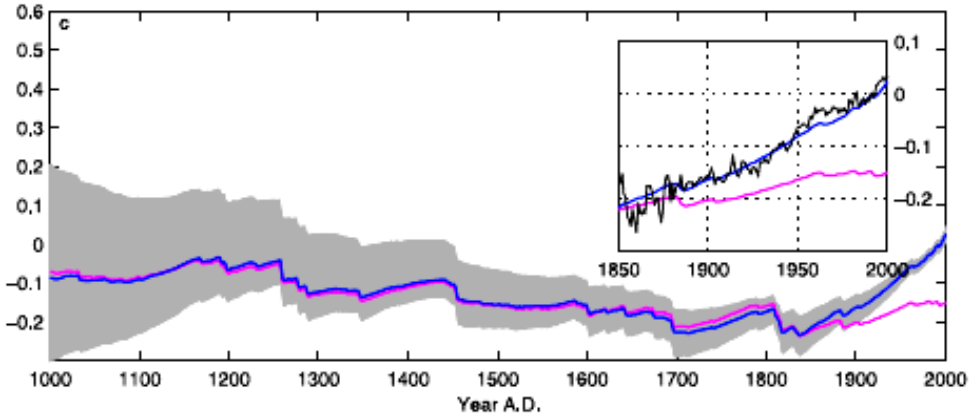

Figure 6.29. Anthropogenic and naturally forced sea level above the 1990 mean between 1000 and 2000 AD. "Blue: modelled sea level using all radiative forcings (including greenhouse gases). Magenta: modelled sea level using only Solar and Volcanic radiative forcings (excluding greenhouse gases)," Jevrejeva *et al.* (2009).

6.8 Discussion

Relationships and trends associated with local sea level change can be generated from the data analysed in this chapter, including relationships between oscillations, linear sea level trends, SST and additional forcing parameters. This section begins by discussing the sea level oscillations analysed in Section 6.4 and identified in Section 6.5. The dominant oscillation frequencies/periods identified within the Forth and Tay Estuaries using wavelet power spectra are 3, 5 to 7, 10, 15 and 20 years. These periods were highlighted as being connected with global cycles by Jevrejeva *et al.* (2006) and are connected with NAO and AO cycles, which are unique to the Northern Hemisphere.

The average trend of global sea level rise between 1900 and 2003 was +1.7 mm a^{-1} (Solomon *et al.*, 2007). Short datasets have been hindcast and forecast to create linear trends between 1900 and 2008. Four of these linear trends, created from datasets longer than thirty years, lie between +0.23 and +0.56 mm a^{-1}. This suggests a long-term difference of approximately 1.1 to 1.5 mm a^{-1} between the global and local datasets, which is slightly greater than the glacio-isostatic rates for the area given by Shennan *et al.* (2009) and used by the UKCP09 (Jenkins *et al.*, 2008).

Satellite altimetry between 1993 and 2003 suggests a global sea level trend of 3.1 mm a^{-1} (Solomon *et al.*, 2007). Between 1993 and 2008 Dundee and Rosyth had average sea level trends of +0.7 and +1.4 mm a^{-1} greater than the global sea level trend (Table 6.1). After the identification and confirmation of increased NAO and AO activity since 1940 through wavelet analysis, as well as the knowledge of coinciding NAO and AO cycle turning points causing negative sea level influence around 1993. It can be confidently implied that any recent short-term increase in sea level trend within the last 20 years is likely to have been accentuated by these two oscillatory cycles.

There is a close relationship between temperature and sea level oscillations, which is utilised by Vermeer and Rahmstorf (2009) in their sea level model (see Chapter 8). Ice-melt induced sea level change, driven by global temperature increase, should be considered a prominent component of large-scale sea level change within the next three or four centuries (Titus *et al.*, 1991). However, it is unlikely that sea level will increase by more than 50 cm before 2100. Therefore, this thesis does not focus on the large-scale predictions acknowledged by Mitrovica *et al.* (2001) and Titus *et al.* (1991).

Anthropogenic influence of sea level has been identified in Figure 6.29 (Jevrejeva *et al.*, 2006). The major drivers of this sea level change are the increase in temperature and water mass due to anthropogenically-driven climate change. A reduction in GHGs, in addition to more sustainable practices, can reduce the rate of temperature increase and the rate of sea level rise.

6.9 Conclusion

This chapter has identified components of sea level behaviour within two estuaries. Four datasets were linearly interpolated between 1900 and 2010; revealing relative sea level trends of +0.23 to +0.56 mm a^{-1}. Tide gauge data were analysed using wavelet analysis methods, identifying oscillatory cycles of 3, 5 to 7, 10, 15 and 20 year frequencies. These oscillations, including the NAO and AO, were found to be influential in the region.

Short-term trends in particular are heavily influenced by these oscillations. The period between 1993 and 2007 is a good example of a period when several oscillations simultaneously contributed to increasing sea levels. For example, the four relative sea level trends identified in Section 6.2 were increased by 6 to 10 times when limited to data from the 1993 to 2008 time period. For this reason, relative sea level datasets were chosen in this thesis for their time spans and combined with other local datasets; removing potential errors that could have occurred during long term sea level analysis.

Chapter 7 – Storm Surge Events

7.1 Introduction

Storm surges, residual tide gauge data and extreme relative sea level events are discussed in this chapter. Several studies have identified and modelled surge events around the UK (e.g. Lowe *et al.*, 2009). This thesis has separated existing surge data, primary and secondary maxima data, and primary residual tide gauge data collected from the Forth and Tay Estuaries. All of these datasets are of vital importance to understand how surges and extreme events impact upon the shorelines of the water bodies.

The main terms used in this chapter that need to be defined are:

- Surge – a heightening or lowering of a water body primarily caused by changes in atmospheric pressure and strong winds (Haslett, 2000; Lowe *et al*., 2001; Sorensen, 2006).
- Residual tide gauge data – data representing the height difference between the observed water level and the predicted water level. Surges can be measured using a variety of techniques. Observed tide gauge data can be compared with sea level projections, therefore calculating the residual tidal/sea level. Residual tide gauge data collected for use in this thesis may include minor prediction errors made by the tide gauge software; therefore these data are not referred to as surge data.

Other influences on surge level in nearshore areas include bottom currents, response to the Coriolis Effect, wind-wave setup, precipitation and runoff (Sorensen, 2006). Surges within a storm period are greater due to increased winds and reduced atmospheric pressure. If a high positive surge occurs simultaneously with an astronomical high tide event, then flooding and potentially infrastructural damage may result.

Surges may be influenced by various local characteristics. Funnel-shaped estuaries increase the height of a storm surge as it progresses upstream (Zsamboky *et al.*, 2011). Onshore winds are affected by land topography, while the offshore wind is influenced by fetch distance (Bretaña, 1987), both of which can affect the surge height.

There is potential for storm surges to coincide with high tides, forming an extreme sea level event, which could result in coastal flooding.

7.1.1 Connections Between Storm Surges and Coastal Flooding

Storm surges are not the sole drivers of coastal flooding, but may be a contributing factor along with tides, waves and relative sea level rise. In macrotidal areas, such as the Forth and Tay Estuaries, the tidal cycle is the dominant short-term control of sea level at the coast. In mesotidal and microtidal areas, waves and surges have the greatest impact on sea level change. The combination of high tides, large storm surge events and high energy waves can be destructive along low-lying and 'soft' geology coastlines.

Fluvial discharge from large river catchments into small estuaries can influence the water level and cause additional rise in specific topographic circumstances. Some flood databases do not separate estuarine, marine and fluvial events. Hickey (1997) identified an increase in the frequency of flooding in Scotland since 1500 and Lozano *et al.* (2004) identified an increase in intense storm events in Europe since 1970. Neither of these studies focused specifically on coastal flooding, combining coastal with both fluvial and pluvial flood events in their statistics.

When looking specifically at storm surge events, studies including Ball *et al.* (2008) suggest that there has been no significant change in storm surge frequency or magnitude within Scotland. However, potentially rising relative sea levels will increase flood risk even if present storm surge heights are maintained (Werritty and Chatterton, 2004; Zong and Tooley, 2003). A decadal to bi-decadal 'flood-rich'/'flood-poor' fluctuation in coastal and fluvial flooding has been identified by Hickey (1997) during the twentieth century within Scotland. This mimics the North Atlantic Oscillation (NAO) cycle, which heavily influences sea level and storminess (Lozano *et al*., 2004; Woodworth *et al.*, 2007). Several high NAO and coastal flooding decades include 1850 to 1860, 1890 to 1900, 1970 to 1980 and 1990 to 2000 (Ball *et al*., 2009).

One particularly extreme and well documented example of a major surge-related event is that of 31st January 1953 when a large surge progressed down the eastern coast of Britain before hitting the Netherlands (Baxter, 2005). As it progressed further south the height increased from 0.6 m at Aberdeen to 0.82 m at Leith, 2.97 m at King's Lynn and 3.36 m at the Netherlands coastline (Hickey, 2001; Lamb, 1991). The 1953 flood resulted in 2,000 deaths and 20,000 km^2 of flooded land within Britain and the Netherlands (Gill, 1982).

The culmination of this large surge and high tide at the Thames Estuary resulted in large areas of flooding in the south east of England. In the Thames region several large population centres and major infrastructure were damaged and destroyed; including damage to Tilbury Docks, 1,000 houses in West Ham, the BP Oil Refinery on the Isle of Grain, Sheerness Naval Dockyards and Canvey Island where 50 people died (UKMO, 2010).

Since 1953, additional defences have been built to protect London and areas upstream along the River Thames from potentially recurring surges (Baxter, 2005). Upstream seawalls and minor defence systems are today supported by the Thames Barrier installation, although upstream areas can still be affected by fluvial-sourced flooding. Climate change has been predicted by some to increase the magnitude of storminess and extreme high sea levels before 2100 (Black and Burns, 2002; Haigh *et al.,* 2010). The Thames Barrier has reduced the potential for marine surge-related flooding of the central London area and the Environment Agency (2012) intends to maintain the existing defence systems while investigating alternatives and possible improvements.

The 1953 event has been used by most insurers to calculate potential flood risk from future flood events. Risk Management Solutions (RMS) is one particular company that models potential flood risk scenarios for multiple insurance providers using the 1953 flood as its guideline worst case scenario for coastal flooding (RMS, 2003).

For this chapter, background information has been collected regarding surge events in the Forth and Tay Estuaries (Section 7.3). This involved reviewing background literature, local historical information, recent events and primary tide gauge data. Several separate techniques have been used within the chapter (Sections 7.4 and 7.5; Chapter 4) to analyse the influence of surges on sea level and identify surges within tide gauge data.

8.2 Sourcing Storm Surge Data

Historical records can build important background information about coastal flood and defence developments along a coastline. Rare records dating back to 120 BC have illustrated the storm surge event that is thought to have caused the migration of the Celts from the German Bight (Lamb, 1991). Very few records of this age have survived to date. In the Forth and Tay Estuaries, historical records are available covering the tide gauge data collection time period, but records are sparse from earlier periods due to political upheaval and the literacy limitations of local people in rural areas.

Flood event databases and other compilations of storm histories have led to greater understanding of cycles and trends of surge events (Lozano *et al*., 2004). One particular database, added to by Ball *et al*. (2009), extends from 1849 to 2007 and holds information on 304 Scottish coastal flood events. Another database, compiled by the British Hydrological Society, holds information about significant fluvial, pluvial and coastal flood events for large river regions within Britain (Black and Law, 2004; Law *et al*., 2010; McDonald *et al*., 2006). Some of the records within this database are

repeated from several sources, but within the region of Forth and Tay Estuaries there are over 200 records between 1210 and 1948 AD, some of which highlight coastal events (Table 7.1).

Historical surge records rely on literate people to record events at the time they occur; therefore some pre-1900 historical events within rural or semi-rural areas may not have been recorded. Since both the Forth and Tay Estuaries have several large population centres, there is increased likelihood that surge events would have been recorded.

The Forth and Tay Estuaries have several riparian local authorities along their courses that publish flooding and coastal management reports (Figure 7.1).

Region	Time period	No. of Events
Firth of Tay	1877-1951	10
Tay	1210-1947	100
Earn	1852-1911	3
Firth of Forth Group	1766-1913	19
Forth	1785-1930	70
Almond Group	1575-1920	18
Tyne (Lothian) Group	1358-1948	17

Table 7.1. The British Hydrological Society Chronology of British Hydrological Events Regional Collection (Law *et al.*, 2010). Most of these events are likely to be from fluvial sources in upstream areas.

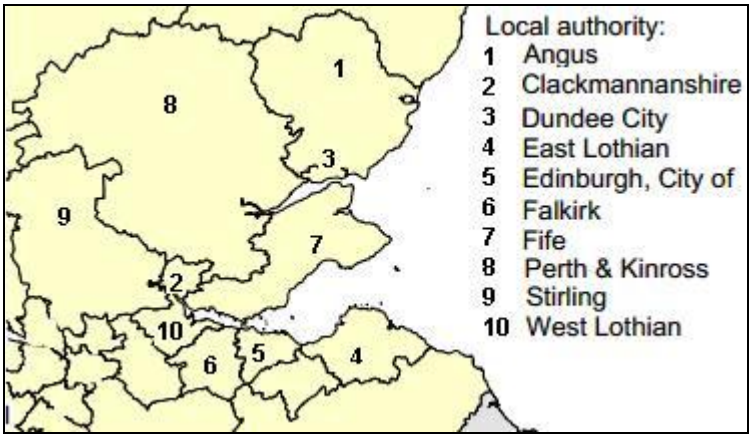

Figure 7.1. Riparian local authority areas connected to the Forth and Tay Estuaries (adapted from source: General Register Office for Scotland, 2010).

Storm surge data can be collected using a variety of different methods (Chapter 4). These range from the simplistic pressure and tide observations made by Proudman and Doodson (1926) to the POL storm surge model (POLCS3) (Lowe *et al.*, 2001). With knowledge of these methods, this

chapter relies heavily on data collected from local tide gauges to identify actual storm surge events since 2003. Two methods have, however, been investigated in more detail: analysis of sea level maxima and analysis of storm surges through residual tide gauge data (Chapter 4).

7.3 Secondary Surge Data

This section compiles all of the secondary data collected from fluvial discharge records, academic journals, government or local authority reports, estate management records, contemporary literature, newspaper reports, bridge inscriptions, chronicles and word of mouth. Secondary maxima data are discussed in Section 7.4 and primary tide gauge data in Section 7.5.

7.3.1 Tay Estuary Secondary Data

McEwen (1987) documented various sources of historic flood data along the River Tay from source to mouth. Some of the data are coastal flooding specific, but pluvial and fluvial events are also included. Accounts documented by McEwen (1987) include inscriptions on Smeaton's Bridge, Perth, and the three chronicle collections relating to the Perth area – *Chronicles of Perth*, *Annals and Archives of Perth*, and the *Buik of Croinclis of Scotland* (McEwen, 1987; Maitland Club, 1831; Peacock, 1849; Bellenden, 1822).

Bridge inscriptions can be unreliable as not all flood events will be marked and large storms may destroy the bridge and its markings (McEwen, 1987). Extreme high waters may also be influenced by combined fluvial and marine surges, making it hard to identify the marine surge contribution. Black and Anderson (1994) documented historical floods that have been marked on Smeaton's Bridge in Perth centre since 1814. The first marked flood was significantly larger, by 0.52 m, than any other to have post-dated it. However, this event was caused by ice-damming of the bridge's arches and not by coastal flooding (Black and Burns, 2002).

In the *Buik of the Croinclis of Scotland*, Boece wrote of the Scottish Prince John's death after he was taken by the flooding River Tay at the Bloody Inches near Scone (Figure 2.1), which is at the upper tidal limit of the Tay Estuary (Bellenden, 1822). This flood was primarily a fluvial event, but is likely to have had a tidal surge influence. Several high water level events at Perth were the result of combined pluvial, fluvial and marine extreme events. Perth, being close to the tidal limit and fed by a large catchment area upstream, is the most likely location along the river course to experience these combined events.

Perth experienced large flood events in 1991, 1993 and 1997. The flooding of Perth in 1991 and 1993 cost a combined £40 million in damages and the 1993 and 1997 events were estimated to be *c*.1 in 150 year flood events (Falconer and McInally, 2002). After the 1991 and 1993 floods, the Perth Flood Alleviation Scheme was completed to provide a 5 hour fluvial warning at Ballathie (Figure 2.1) and a coastal flood warning at Newport-on-Tay, costing £24 million to install (Falconer and McInally, 2002).

Smith (1993) documented the progress of a storm across Perth during January 1993. The flood waters overtopped Perth centre's flood defences and damaged the infrastructure behind. Although there were few measurements recorded, there are numerous photographic illustrations showing the damage done by the storm (see Figure 7.2).

Each riparian local authority along the Tay Estuary has produced reports about flooding in their area. Most identify the date and location of coastal flood events, although the details vary. Perth & Kinross Council has produced a biennial *Flood Prevention Report*. Their 2009 report highlighted several fluvial flood events between 2007 and 2009, but none within the area of tidal influence below Scone (Perth & Kinross Council, 2009). Previous reports are unavailable, but flood events are known to have occurred within the last two decades as described above.

Figure 7.2. Image of the Perth Flood in 1993 (BBC, 2012).

The primary city along the Tay Estuary, Dundee, is subject to fluvial and coastal flooding. Figure 7.3 illustrates 11 minor watercourses draining through the city, many of which are culverted beneath highly populated areas. Generic flooding in the city has been recorded in Dundee City Council's biennial *Flood Prevention Reports* (1997; 1999; 2001; 2003; 2005; 2007; 2009) (Figure 7.4).

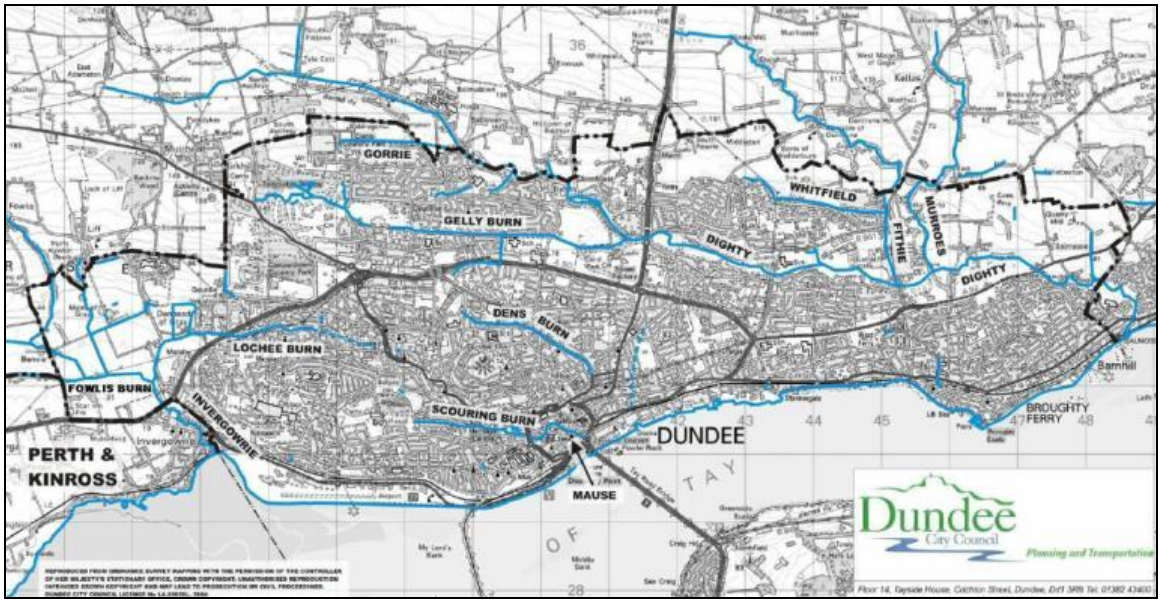

Figure 7.3. Map of watercourses within Dundee City (Dundee City Council, 2005). The Dighty Burn, Gorrie, Scouring Burn and Fithie produce the highest fluvial flood category warnings.

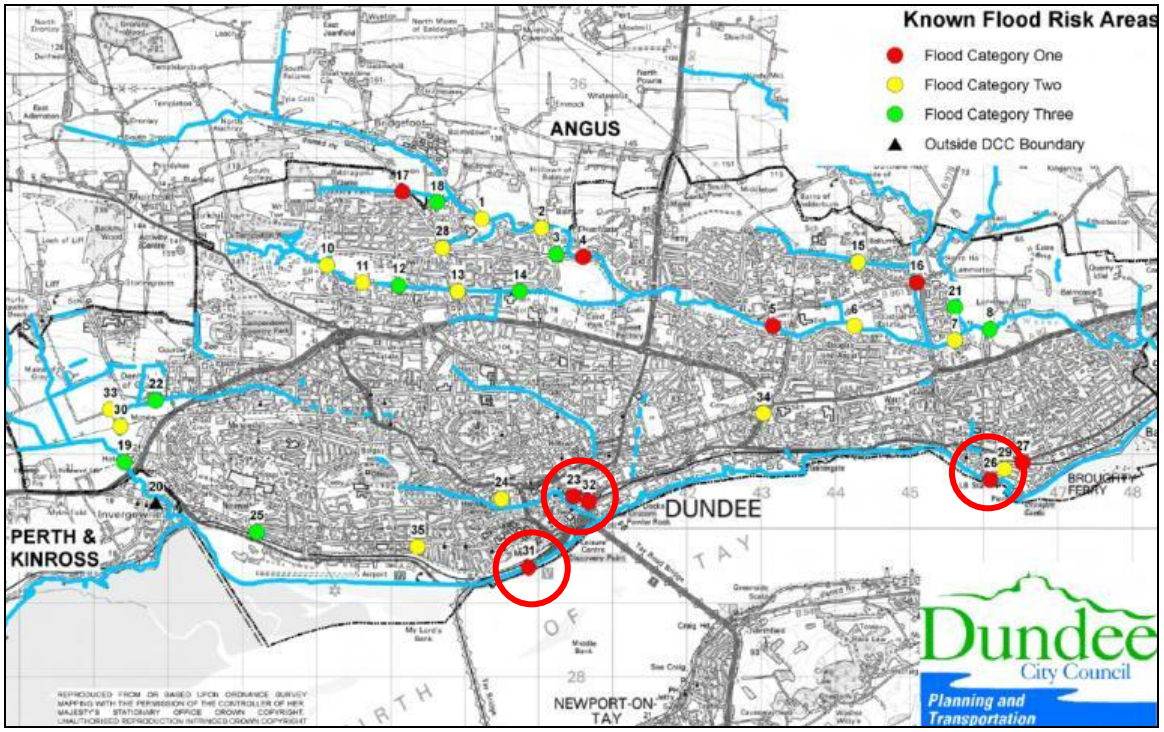

Figure 7.4. Flood risk map of Dundee City (Dundee City Council, 2007). Coastal flooding occurs at points 31 and 26, with high water restriction of outlet flow commonly impacting points 23 and 32 in the city centre.

Most of the sites at risk are along minor watercourses, subject to pluvial and fluvial events. Broughty Ferry and Riverside Drive have been highlighted as areas at high risk from coastal flooding in Dundee. Riverside Drive, trending directly parallel to the coast, experiences mainly

seawall overtopping and poor drainage. Both sites have experienced overtopping on several occasions during the last five years.

Although pluvial and fluvial flooding are not analysed within this thesis, abnormally high tides can cause retention of water within waste water systems due to the methods used at these locations to dispose of waste water during high rainfall periods. Table 7.2 illustrates coastal flood events and pluvial flood events that coincided with high tides, therefore causing water retention, on 11 August 2004, 16 August 2004 and 21 August 2008. These floods appeared across the Forth and Tay Estuaries, although the peak water levels varied across the sites.

Year	Location	Flood event
30th July 1998	Trades Lane – Dock St – Commercial St – Allan St (City Centre)	TAY. High tide prevented flood drainage; fast onset and end; 300mm in street; surface water backing up.
July 2001	Allan St (City Centre)	TAY. High tide prevented flood drainage; fast onset and end; 300mm in street; surface water backing up.
11th Aug 2004	City Centre	Sewer flooding; 1 in 100 year flood event; 1 in 1000 year rainfall event.
11th Aug 2004	Dundee urban fringe	Surface water runoff from overlogged ground; 1 in 100 year flood event; Leuchars reported 1 in 1000 year rainfall event.
16th Aug 2004	City Centre	Sewer flooding; basement flooding and road flooding; 1 in 100 year event.
January 2005	Riverside Drive, Dundee (City Centre)	TAY. Highest Astronomical Tide and 0.7m hurricane storm surge.
21st Aug 2008	City Centre	Sewer flooding of basements and roads due to high rainfall.

Table 7.2. Dundee City flooding 1997 to 2009 influenced by the Tay Estuary, compiled from several Dundee City Council Reports (Dundee City Council, 1997; 1999; 2001; 2003; 2005; 2007; 2009).

Angus Council is responsible for the coastline directly east of the City of Dundee local authority region. The coastal towns in Angus include Monifieth, Carnoustie, Arbroath and Montrose. Angus Council provides a *Flood Schedule of Watercourses*, which gives minimal information about the watercourses within this region and flood events along them (Angus Council, 2005). At least one widespread flood event was noted between 2007 and 2009, but insufficient information was recorded about the event including the date on which it occurred (Angus Council, 2009).

Fife Council produced a *Flood Prevention Report* in 2003 and *Flood Alleviation Reports* in 2007 and 2009; all suggest there were no coastal flooding events between 1999 and 2009 (Fife Council, 2003; 2007; 2009). Fife experienced coastal flooding at the end of March 2010 (Duck, 2011), during which event significant storm damage was caused to the Anstruther coastline in particular (Figure 7.5 and 7.6). More information on this event is likely to be included within the *Flood Alleviation Report* due to be released in 2012.

Overall, riparian local authorities in the Tay Estuary highlighted very few flooding events from coastal overtopping within their reporting periods. The reports highlight the risk of coastal flood events being mistaken or combined with fluvial or pluvial events. However, there is potential for vital information to be included within the next generation of reports, providing a reliable source for future surge or sea level maxima studies.

Figure 7.5. Anstruther during the 30th March 2010 storm. A still image taken from a Youtube video posted by 'georgeaimer' (Youtube, 2011).

Figure 7.6. Anstruther during the 30th March 2010 storm. A still image taken from a Youtube video posted by 'georgeaimer' (Youtube, 2011).

7.3.2 Forth Estuary Secondary Data

Stirling lies at the head of the Forth Estuary; at the tidal limit. Stirling Council's (2009) *Flood Report* highlighted several flood events along the Forth, although these were above the City of Stirling and therefore outside the study area. Clackmannanshire Council, which adjoins Stirling Council's area to its north east, has not reported any coastal flood events, being subject only to fluvial flooding within several tributaries (Clackmannanshire Council, 2007).

Falkirk Council, to the south east of Stirling Council's area, provides several documents relating to flooding and drainage. Falkirk Council's *Flooding and Sustainable Urban Drainage Systems Report* (2009a) provides much information on fluvial and pluvial flood areas from recorded flood events, but the only area under threat from coastal flooding appears within 'Grangemouth Docks' (Falkirk Council, 2009a). No additional information appears regarding this flood event, which was not documented by Forth Ports, the owners of the Port of Grangemouth. Falkirk Council also published *Flood Reports* in 2007 and 2009 (Falkirk Council, 2007; 2009b), which did not document any coastal flood events between 2005 and 2009.

West Lothian Council provide a *Supplementary Planning Guidance* document and a *Flood Prevention Report* for 2006 to 2008 (West Lothian Council, 2010), neither of which identify any coastal flooding events. In the Edinburgh City Council area there are five tributaries that drain into the Forth Estuary, most of which are subject to flooding along their courses (Figure 7.7). Queensferry is the only location in this riparian authority area with a coastal flood warning to the

east of Port Seton Harbour. Within the Edinburgh City Council *Water Quality and Flooding Report* (2010), flood events between 1998 and 2007 were recorded, however none are relevant to this thesis.

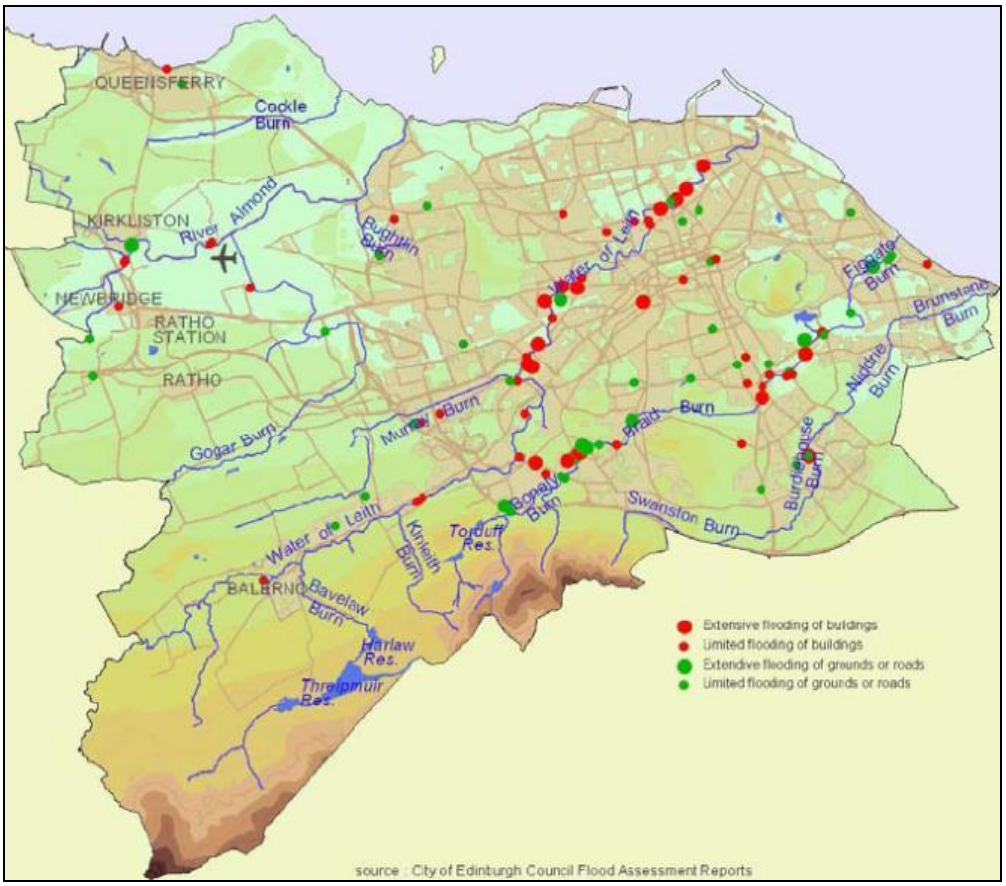

Figure 7.7. Area of flooding within Edinburgh 1998 to 2007 (Edinburgh City Council, 2010).

The Water of Leith is the most significant tributary of the Forth Estuary in this riparian local authority area. It drains directly through major parts of the City of Edinburgh and has a history of fluvial and pluvial flood events (Edinburgh City Council, 2010). The Water of Leith floodplain is heavily developed, increasing the potential for infrastructural damage caused by fluvial flooding, but the council have provided open areas of land in places along its course to promote flooding away from built up areas (Figure 7.8).

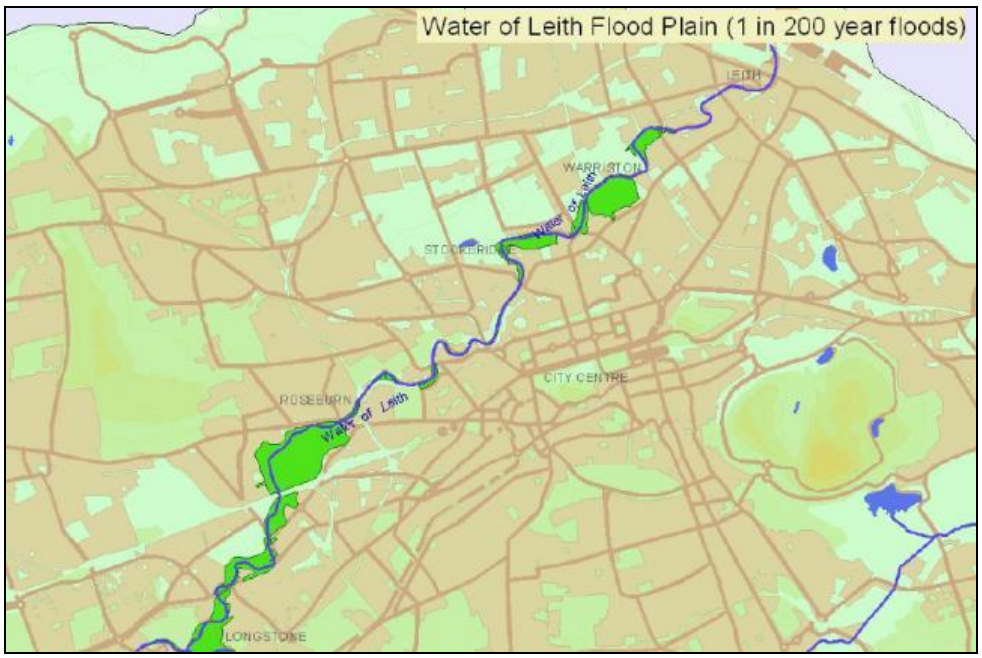

Figure 7.8. Water of Leith Flood Plain (1 in 200 year floods) (Edinburgh City Council, 2010:7).

The Water of Leith drains through the impounded Port of Leith, operated by Forth Ports. Knowledge of tides, fluvial discharge, surge events and daily port lock operations are required to keep the port within operating water levels, without impacting on upstream areas during fluvial flash flood periods. As the gauge is on the seaward side of the port there is no measureable fluvial component.

East Lothian, the most south easterly of the local authority regions, mainly experiences agricultural run-off with minor accounts of fluvial tributary and coastal flooding (East Lothian, 2010). Musselburgh experiences coastal flooding in this region, with additional flooding associated with fluvial water retention during high tides at the River Esk confluence.

Video documentation of the 30th March 2010 flooding event is available through Youtube. These videos have been verified against sightings and word of mouth evidence of the events occurring. Due to the open nature of websites such as 'Youtube', video publication verification is necessary to ensure accuracy. Locations within this collection that were affected by extreme water levels and wave heights include Anstruther (see above), St. Andrews, Kirkcaldy, North Berwick, Fisherrow, Kinghorn, Port Seton, Dunbar, Cramond, Silverknowes and Musselburgh (Youtube, 2011). YouTube.com also highlighted the potential risk to human life when people ignore high wave energy and surge events ('bobduncan3731', Youtube, 2011).

Riparian local authorities in the Forth Estuary indicate that a greater number of flooding events have occurred within their reporting periods than those reported in the Tay Estuary. These reports are likewise influenced by reports of fluvial and pluvial flood events mixed with coastal flooding. Some

of the reports, particularly those produced by Falkirk Council, give very little information about flood events, making it difficult to identify specific areas where flooding has been prevalent.

7.4 Primary and Secondary Maxima Data

This section includes all sea level maxima data compiled from primary tide gauge data and secondary data collated from Graff (1981). Maxima data, the highest recorded high water levels, are likely to include HATs and surge events. The dates on which maxima events occur could correlate with surge events identified by riparian local authorities and with identified residual high level events.

The primary maxima data were collated from Forth Ports tide gauge data at Dundee, Grangemouth, Leith, Methil and Rosyth during the periods specified in Table 7.3. The highest maxima reach approximately 4 m above OD, with most of the top five being sourced at Grangemouth. Had maxima data been available from Perth then analysis could have been conducted to discover if the increase in maxima at Grangemouth was due to maxima progression towards the head of the estuary.

The Dundee, Leith and Grangemouth datasets, being the longest, have been used to demonstrate analysis of sea level maxima in the Forth and Tay Estuaries between 1979 and 2010. All of the high tide data were collected for analysis (Chapter 4). One of the methods used followed Graff's (1981) sea level maxima analysis method, which has previously been used to analyse Forth Estuary data. The data are compiled into three datasets for trend analysis (Chapter 4):

- Highest 20 maxima across the timescale;
- Highest 10 maxima per annum (Figure 7.9 shows the highest 10 maxima per annum for all the sites);
- Graff's (1981) analysis of the 5 year running mean.

The Forth Estuary primary data have been compared with secondary maxima data previously collected by Graff (1981). Both sets of data followed the same analysis method, thereby permitting viable connections to be made between the primary and secondary datasets for Grangemouth and Leith.

Date	Dundee	Date	G.mouth	Date	Leith	Date	Methil	Date	Rosyth
11/08/98	3.67	**12/01/05**	**4.13**	**01/04/10**	**3.96**	10/03/08	3.27	12/01/05	3.93
11/01/05	3.56	**23/12/91**	**4.05**	05/03/10	3.81	09/03/08	3.23	11/09/10	3.74
30/03/10	3.51	**18/02/96**	**4.05**	30/03/10	3.74	29/09/07	3.18	09/10/06	3.71
10/10/06	3.47	**14/10/90**	**4.03**	09/02/97	3.64	26/11/03	3.18	30/03/10	3.69
11/01/93	3.45	06/12/79	3.96	12/01/05	3.60	19/03/07	3.14	30/03/06	3.61
Ave.:	3.53		4.04		3.75		3.20		3.74

Table 7.3. Dundee, Grangemouth, Leith, Methil and Rosyth highest five maxima for each port, 1986-2010 (Dundee) / 2003-2010 (Methil and Rosyth) / 1989-2010 (Leith) / 1979-2010 (Grangemouth). Measured in metres above ODN. The highest five maxima across all the sites are in bold.

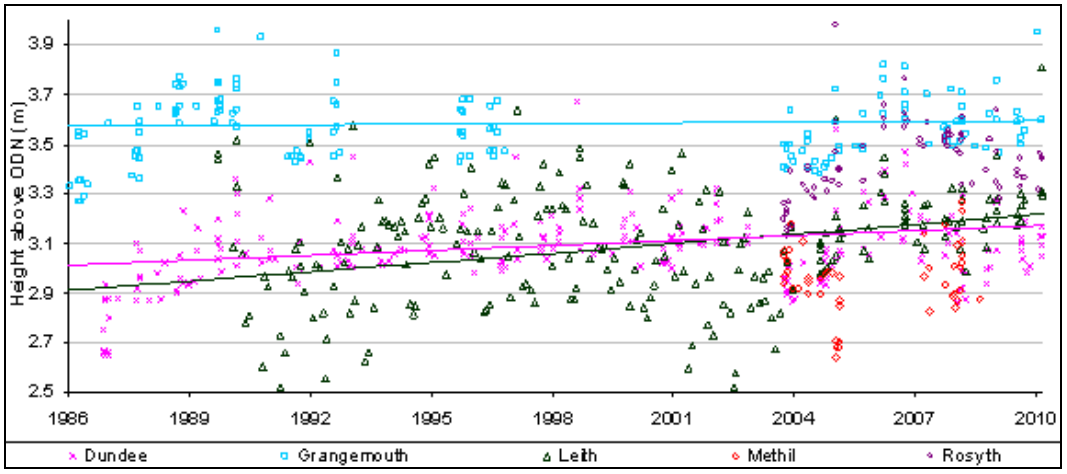

Figure 7.9. Dundee, Grangemouth, Leith, Methil and Rosyth maxima data and trend lines; explained individually in Section 7.4.

7.4.1 Tay Estuary Maxima Data

Presentation of the highest 20 maxima for the Dundee dataset (Figure 7.10) indicates a widespread distribution of the maxima across the timescale, illustrating that the dataset is not skewed by clumping of maxima within a five year time span. The trend line within Figure 7.10 indicates a stable, positive maxima trend.

If the highest 20 maxima for the entire time series were subject to clumping within five year periods due to an intensely stormy period, then comparison could be made using the 10 highest maxima per annum across the entire time series (Figure 7.11). This would highlight if specific years were stormier than others and identify where data gaps occur. Comparison between Figure 7.10 and 7.11

identifies a variance in the rate of maxima sea level rise between the two techniques at Dundee with sea level maxima trends of 3.8 mm a^{-1} and 12.8 mm a^{-1}, respectively between 1989 and 2010 (see Section 7.6).

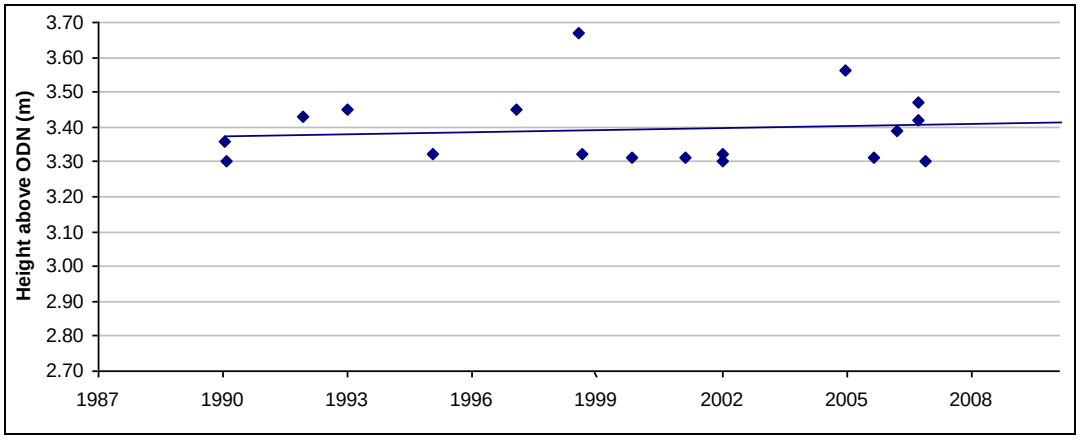

Figure 7.10. Dundee maxima data including the highest 20 maxima between 1987 and 2009, excluding 2003. Maxima are evenly spread throughout the time period with no timeline clumping. Mean average: 3.394 m above OD. Standard Deviation: 0.101 ± 0.044.

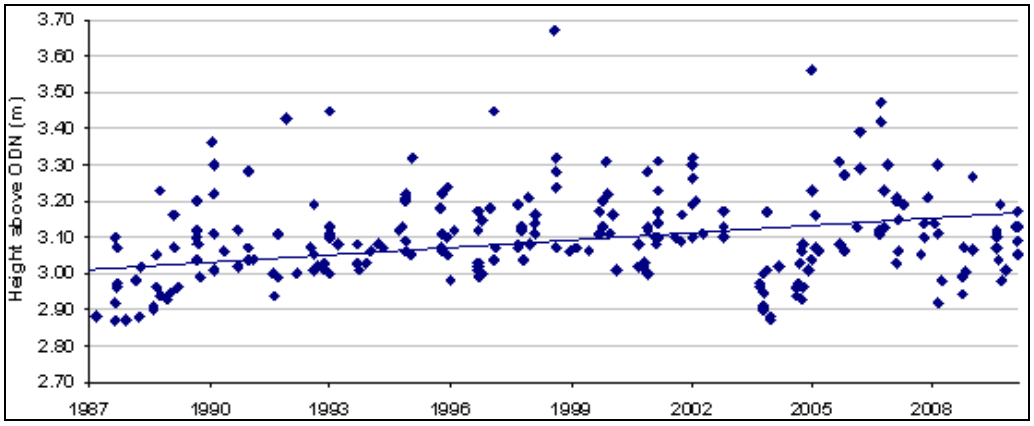

Figure 7.11. Dundee maxima data including the 10 highest maxima for each year between 1987 and 2009, excluding 2003 due to data limitations.

Graff's (1981) method, using a five year running mean, has been used to produce two datasets (Figure 7.12), one only using the singular highest maximum per year and the other using an average of the 10 highest maxima per year. Apart from the obvious reduction in height that appears when using an average, the two datasets show very little difference between the general cyclic trend and linear trend of the maxima mean.

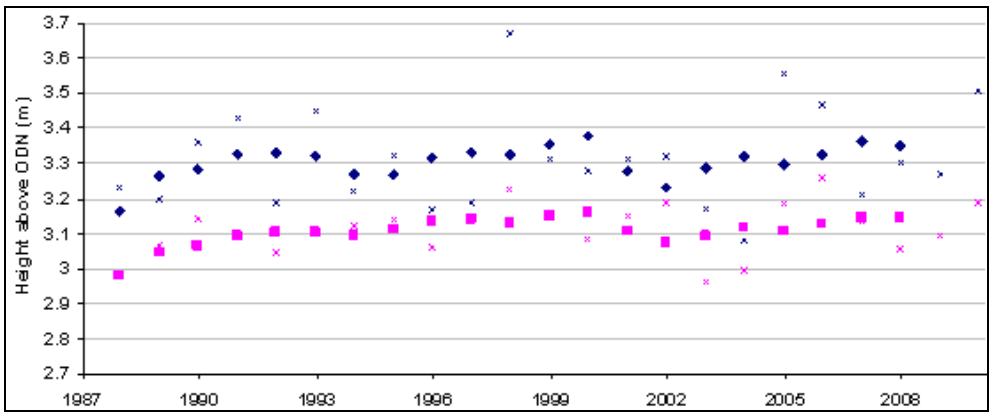

Figure 7.12. Dundee maxima five year running mean following Graff (1981) including the highest maxima from 1987 to 2009, excluding 2003 due to missing data. Blue points represent a five year running mean created from the single highest maxima for each year. Pink points are five year running mean heights created from an average of the highest 10 maxima for each year. Small x-marks represent the annual data that the running-means are based upon.

No previous maxima data for the Tay Estuary are available to compare with the primary data introduced here.

7.4.2 Forth Estuary Maxima Data

Grangemouth, because of its missing data, is a poor comparison with the Dundee dataset (Figure 7.13). For this reason the Grangemouth example relies more heavily on findings from secondary data, using the 10 maxima per annum dataset rather than 20 maxima over the entire time series. The Dundee maxima sea level rise rates are greater than those found at Grangemouth, which are -0.27 mm a^{-1} using 20 maxima over the time series and 3.5 mm a^{-1} using 10 maxima per annum. Figure 7.14 provides an illustration of the time periods for which data were available at Grangemouth.

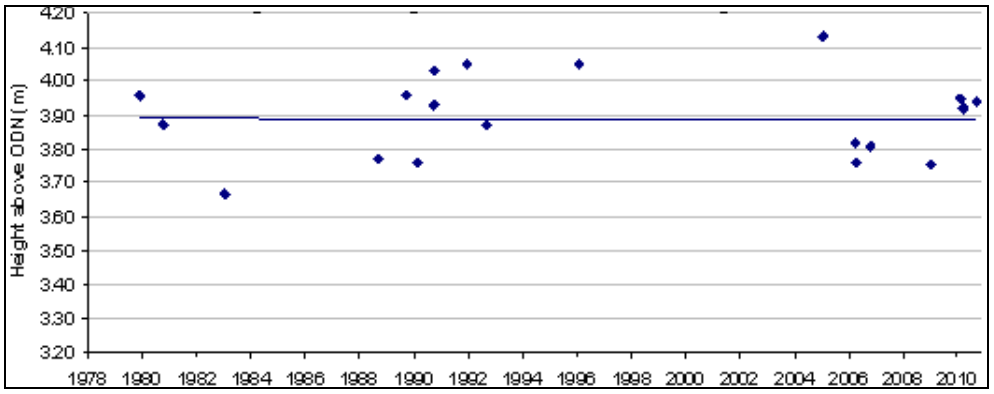

Figure 7.13. Grangemouth maxima data including the highest 20 maxima between 1979 and 2009, excluding 1984, 1985, 1993, 1994, and 1997 to 2003. Maxima are evenly spread throughout the time

period with no timeline clumping. Mean average: 3.888 m above OD. Standard Deviation: 0.124 ± 0.056.

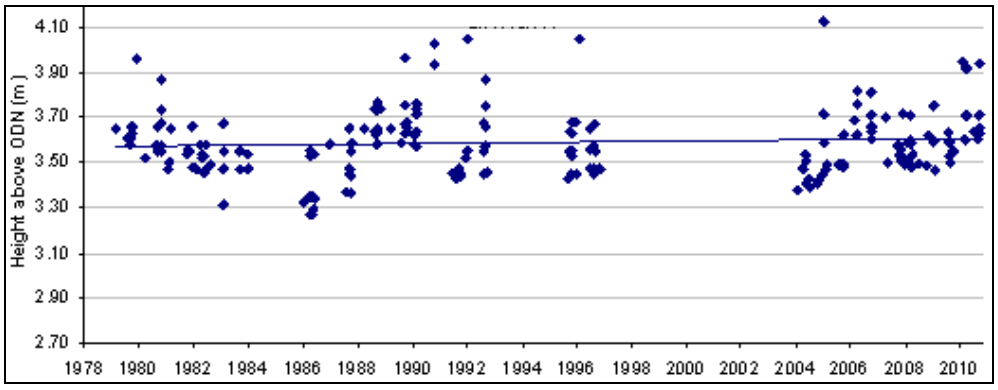

Figure 7.14. Grangemouth maxima data including the 10 highest maxima for every year between 1987 and 2009, excluding 1984, 1985, 1993, 1994, and 1997 to 2003.

Data have been extracted from BODC and Forth Ports tide gauge records based at Leith between 1990 and 2010, so that an extra site can be analysed in the Forth Estuary. These data have been processed for both maxima analysis techniques (Figures 7.15 and 7.16).

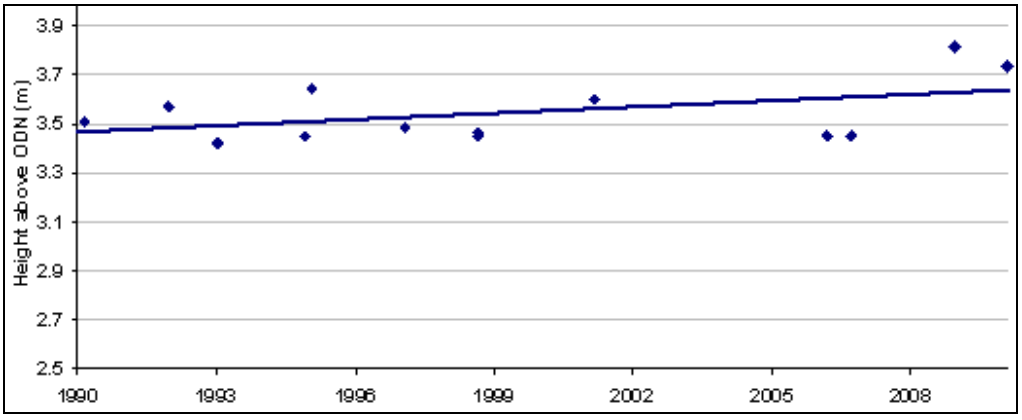

Figure 7.15. Leith maxima data including the highest 20 maxima between 1990 and 2010. Maxima are evenly spread throughout the time period with no timeline clumping. Mean average: 3.43 m above OD. Standard Deviation: 0.066 ± 0.028.

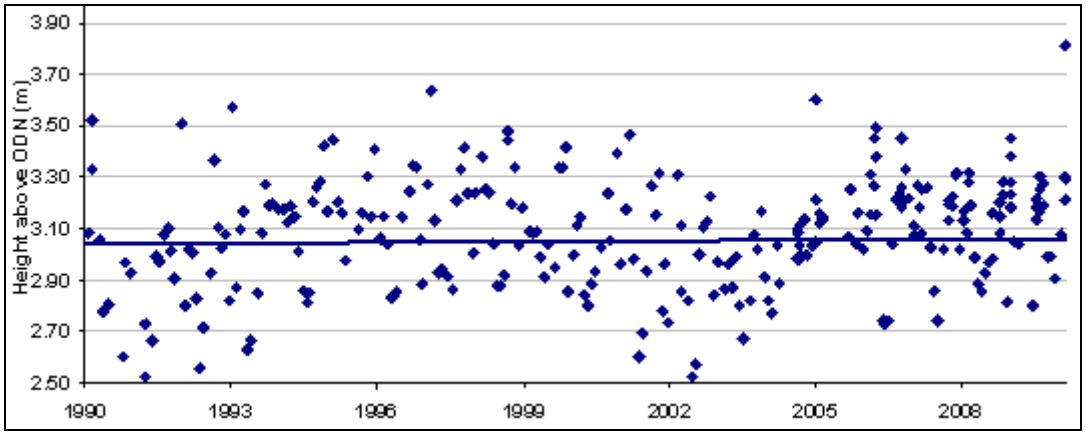

Figure 7.16. Leith maxima data including the 10 highest maxima for every year between 2004 and 2010, along with the highest monthly maxima from 1990 to 2010.

Graff's (1981) method, using a five year running mean, has proved unsuitable for the Grangemouth dataset as the outputs are severely limited by the necessity of five consecutive years of data that are rarely available (Figure 7.17). However, comparison between the Dundee, Leith (Figure 7.18) and Grangemouth patterns highlights simultaneous high periods around 1990 to 1991 and 2006 to 2007 where the datasets overlap, validating the Grangemouth cyclic trends.

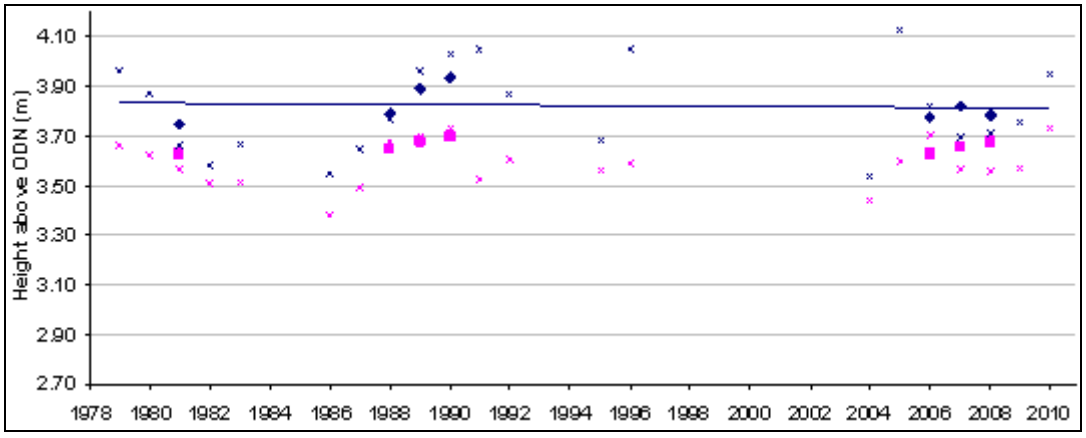

Figure 7.17. Grangemouth maxima five year running mean following Graff (1981) including the highest maxima from 1987 to 2009, including only 1981, 1988 to 1990 and 2006 to 2008. Blue points represent a five year running mean created from the single highest maxima for each year. Pink points are five year running mean heights created from an average of the highest 10 maxima for each year. Small x-marks represent the annual data that the running-means are based upon.

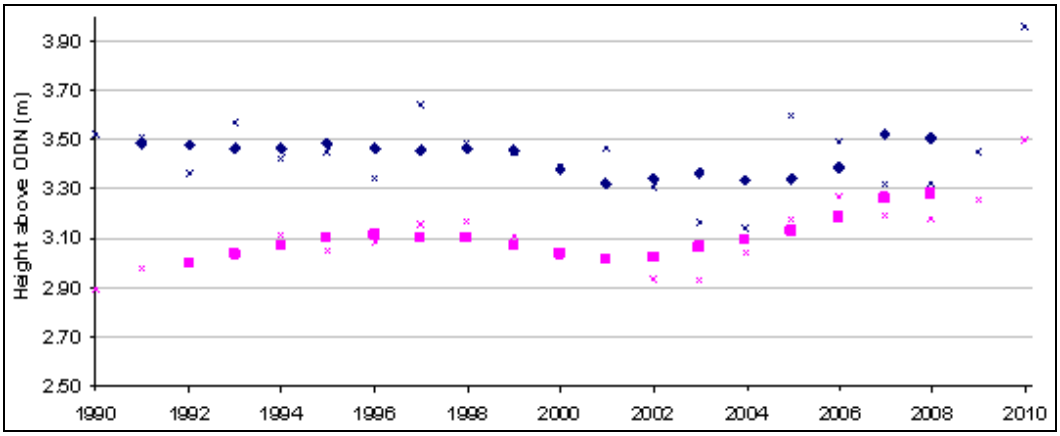

Figure 7.18. Leith maxima five year running mean following Graff (1981) including the highest maxima from 1990 to 2010. Blue points represent a five year running mean created from the single highest maxima for each year. Pink points are five year running mean heights created from an average of the highest 10 maxima for each year (pre-2004 data based upon averaged monthly maxima data). Small x-marks represent the annual data that the running-means are based upon.

Graff (1981) commented on the link between extreme level frequencies at sites within estuarine locations, such as Rosyth and Leith, but there are distinct variations between Rosyth and Grangemouth which Graff attributes to local characteristics. Rosyth, being located just inside the inner estuary adjacent to a significant convergence point that stimulates a double-high tide, would be subject to unique tidal influences.

Graff produced maxima data for five sites in the Forth Estuary (Figure 7.19), a series of frequency distribution curves (Figure 7.20) and partial differential frequency curves (Figure 7.21) to project contemporary (*c.*1981) flood frequency probability. All the Forth Estuary sites displayed a similar gradient in their frequency distribution curves. Grangemouth has a particularly steep curve and high calculated 1/100 year flood in comparison with Leith, whereas Rosyth has a mid-range curve. This illustrates the transitional change in sea level maxima frequency within the estuary.

When comparing sites within the Forth Estuary using partial differential frequency curves, there is a general trend of increasing maxima heights progressing up the estuary from Leith and Kirkcaldy to Grangemouth. Methil does not conform to this trend due to the increased exposure to the prevailing wind and wave fetch compared with Kirkcaldy and Leith, which are partially protected by coastal headlands.

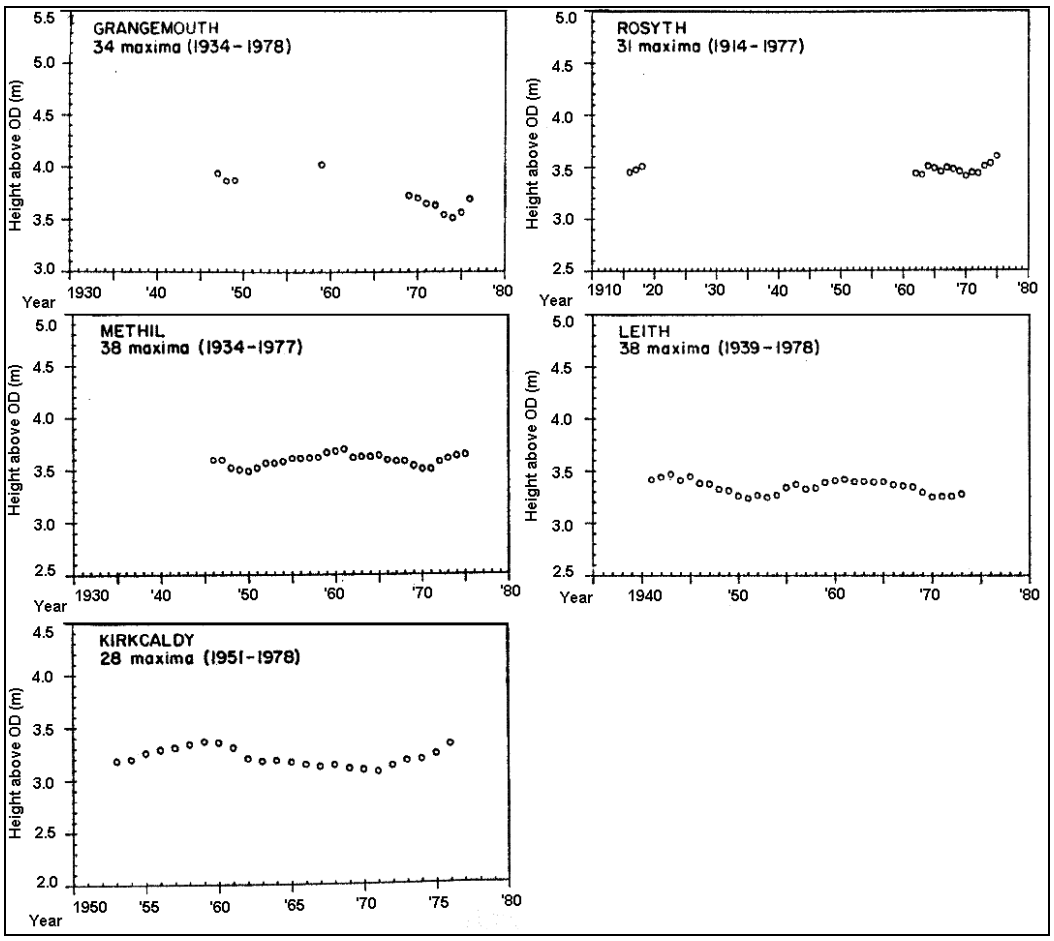

Figure 7.19. 'Distribution of annual sea level maxima, plotted as 5-year running means from full time series available at each port' for Kirkcaldy (Graff, 1981:437). Cyclical trends appear with high points around 1960 and low points around 1950 and 1970.

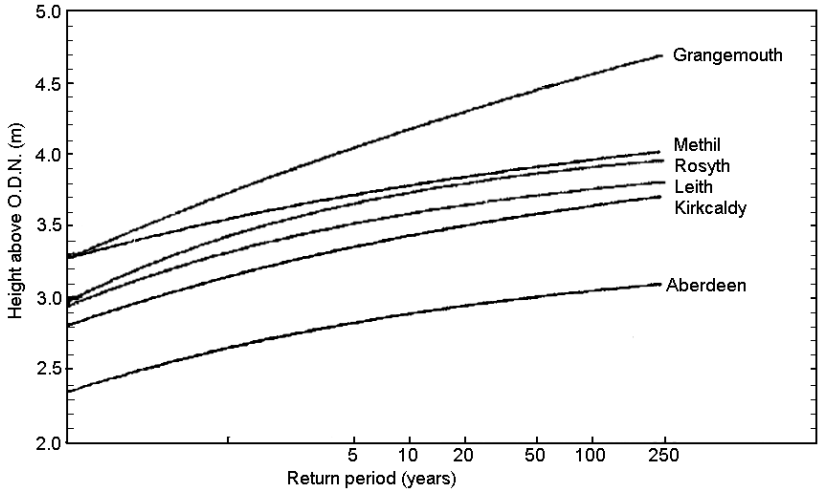

Figure 7.20. 'Frequency distribution curves for north east coast regions between Firth of Forth and Lerwick' (Graff, 1981:406). Graff (1981) created these frequency curves using the Jenkinson (1955) General Extreme Value (GEV) distribution method for maxima and minima. This method itself was developed from the Frechet, Weibull and Gumbel standard extreme value distribution methods (Bali, 2003).

Maxima data from Graff (1981) can be continued using the primary data from Grangemouth and Leith. Figures 7.22 and 7.23 illustrate the two datasets and the timescales they cover. Maxima levels from the Dundee dataset illustrate the cyclic nature determined by Graff (1981) from his long timescale English datasets. These correlate with the NAO, Arctic Oscillation (AO) and Arctic Oscillation Low-Frequency Oscillation (LFO), which heavily influence sea levels across North Atlantic coasts (see Chapter 6). Combination of the primary and secondary data illustrates a continuation of previous maxima trends identified by Graff (1981).

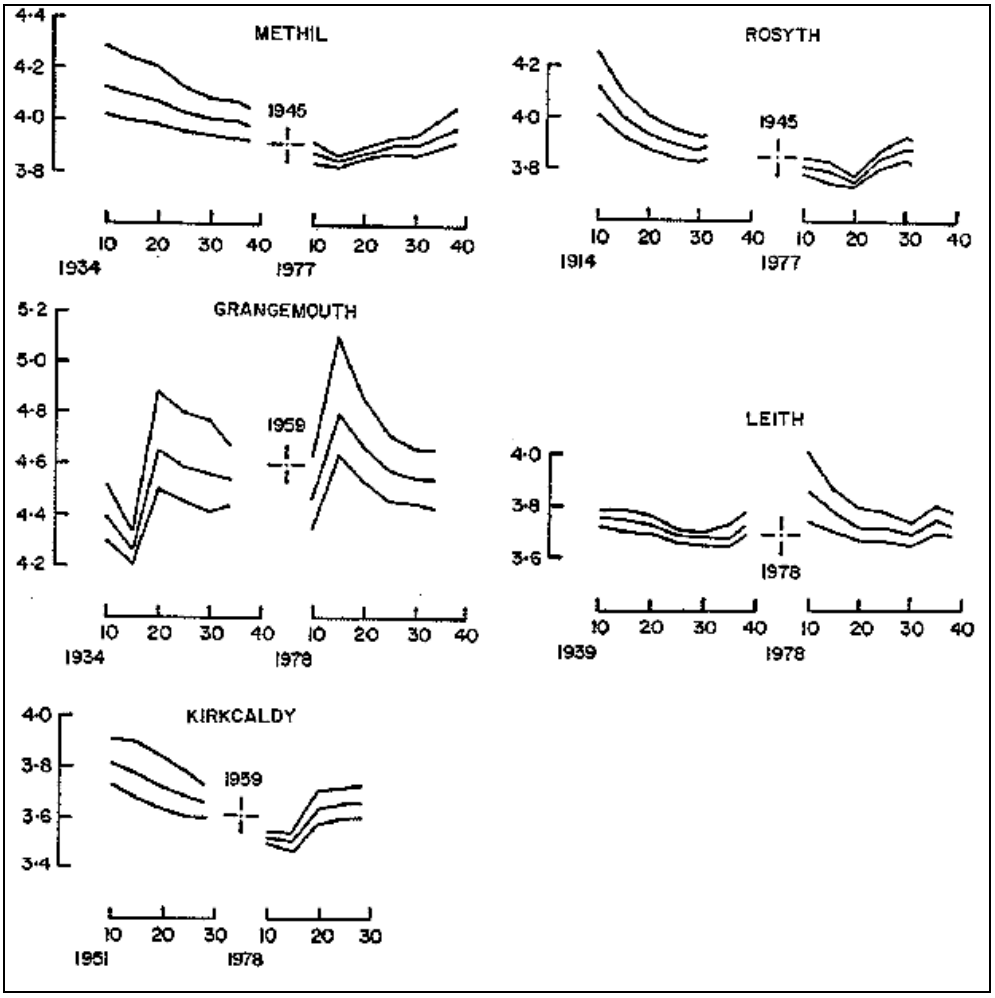

Figure 7.21. 'Partial frequency curves showing extreme level estimates associated with return periods of 50, 100 and 250 years derived from computing the frequency distribution of cumulative subsets of the time series for each port.' 'Left-hand traces show the equivalent frequency levels based on the analysis of increasing subsets of data from past to present. Right-hand traces show the equivalent measures but based on increasing subsets ordered from present to past. When the cumulative data sets reach the full time series length the equivalent frequency levels are equal. Cross represents the maximum observed level recorded throughout the time series.' Ordered 1/250, 1/100, 1/50-year event from top to bottom (Graff, 1981:414-449).

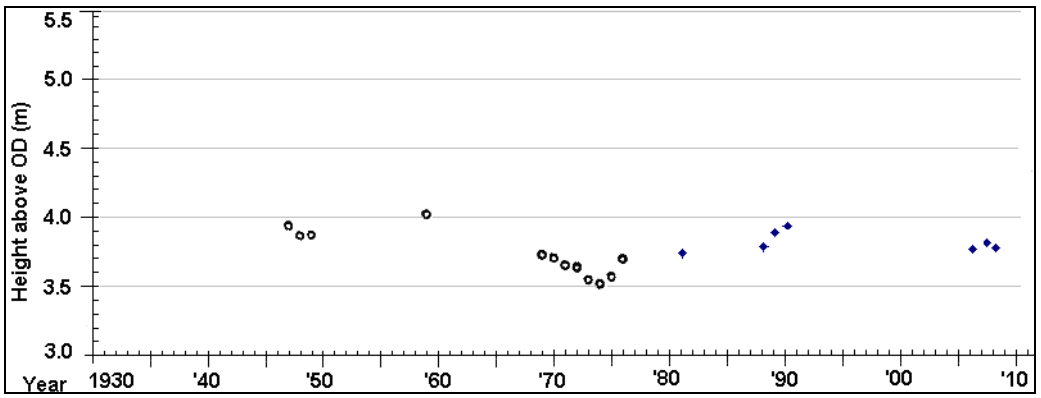

Figure 7.22. Continuation of maxima height at Grangemouth from Graff (1987) (circles) with five year running mean of highest annual maxima (diamonds).

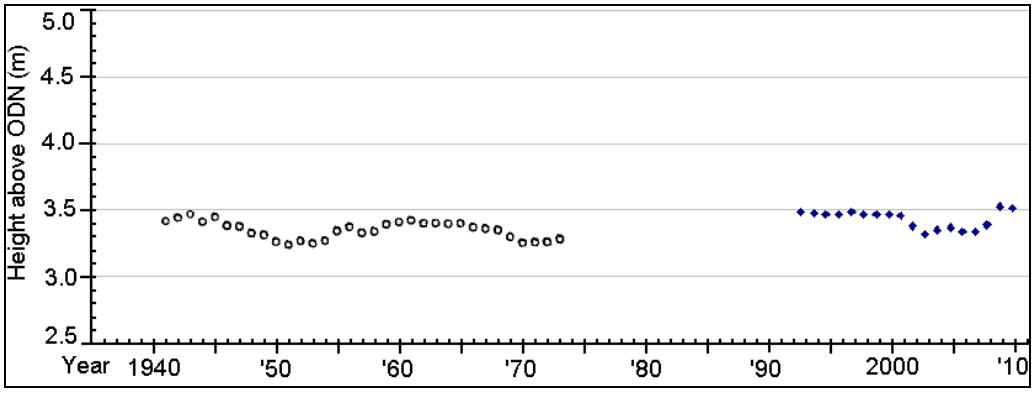

Figure7.23. Continuation of maxima height at Leith from Graff (1987) (circles) with five year running mean of highest annual maxima (diamonds).

Graff's (1981) data for the Firth of Forth were collected directly from the ports. However, the records used are no longer available (they may have been given to Graff, to a museum, disposed of or lost). As such, this study may be one of few surviving accounts of tidal levels in the Forth from this time period.

Comparison between the maxima results from the Forth and Tay Estuaries is made in Section 7.6.

7.5 Primary Tide Gauge Data

Tay Estuary residual tide gauge data are available only for the Port of Dundee between 2003 and 2010. These data are directly comparable with residual data from Leith, which are both mid-estuary locations. Residual tide gauge data are available from four ports in the Forth Estuary; Grangemouth, Rosyth, Leith and Methil. As both the Forth and Tay Estuaries are influenced by the same amphidromic point (see Chapter 2), it is likely that marine-sourced surge events would occur across both estuaries in short succession.

Data from Dundee, Leith and Grangemouth have been plotted in Figure 7.24, identifying similar seasonal trends at Dundee and Leith. Grangemouth residual data have higher amplitudes, possibly due to estuarine influences. Comparison between the five largest tide gauge residual height records at Dundee, Leith and Grangemouth show obvious differences between the sites (Table 7.4), with larger residual heights at Grangemouth than Dundee and Leith. More details about the residual data are given below.

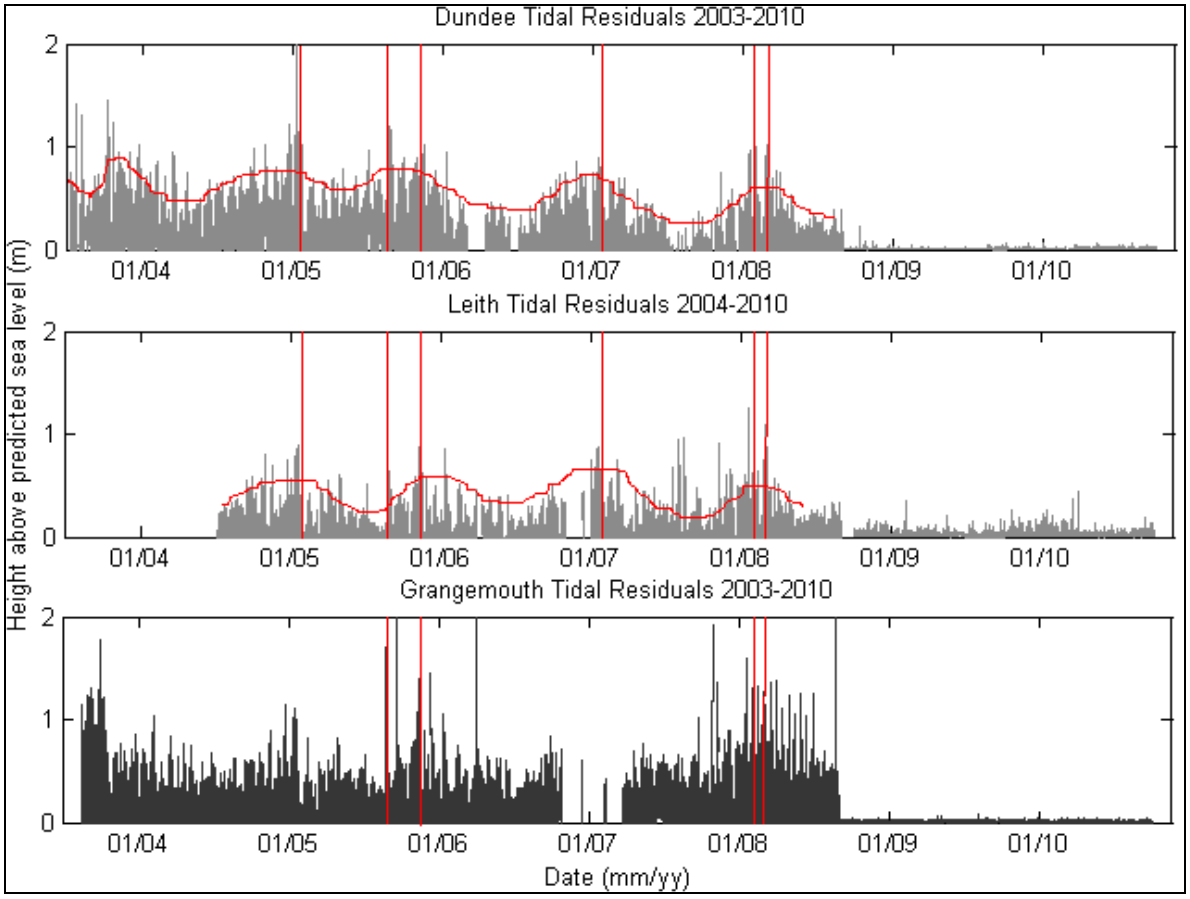

Figure 7.24. Dundee, Leith and Grangemouth tidal residuals between 2003 and 2010 taken from Valeport 710 pressure gauges pre-2008 and Valeport Midas TMS pressure gauges post-2008 at Forth Ports' ports. Annotation depicts the basic annual seasonal trend shape and a selection of time periods where residual high periods occur concurrently between the sites.

Date	Dundee	Date	Leith	Date	Grangemouth
20/01/2005	1.31	01/03/2008	1.09	03/04/2006	2.06
24/08/2005	1.2	08/11/2007	0.92	21/09/2005	1.99
23/12/2004	1.14	20/01/2005	0.89	30/09/2003	1.76
12/01/2005	1.14	08/11/2005	0.88	24/08/2005	1.70
22/12/2004	1.12	12/01/2005	0.87	23/08/2005	1.67
Ave.:	1.18		0.93		1.84

Table 7.4. Dundee, Leith and Grangemouth highest five residual tidal heights, 2003-2008 (Dundee and Grangemouth) / 2004-2008 (Leith) measured in metres above the predicted height.

8.5.1 Primary Tide Gauge Data, 2003 to 2008

The actual heights recorded in the Forth and Tay Estuaries are presented in Table 7.5, Table 7.6 and Table 7.7, using the Leith and Dundee datasets.

	Residual height above the predicted tidal height (cm)						
	50-60	60-70	70-80	80-90	90-100	100-110	Total no. of events
2004	4	3	1				8
2005	9	6	1	3			19
2006	2	0	1	1			4
2007	8	8	3	4	1		24
2008	5	10	2	0	0	1	18
Total	28	27	8	8	1	1	73

Table 7.5. Number of events with residual tide gauge data greater than 50 cm above the predicted tidal level at Leith – 2004 to 2008.

	Residual height above the predicted tidal height (cm)										
	50-60	60-70	70-80	80-90	90-100	100-110	110-120	120-130	130-140	140-150	Total no. of events
2003	31	17	20	6	4	2	3	1	2	2	88
2004	56	52	14	11	4	2	2				141
2005	51	50	24	11	4	2	2	1	1		146
2006	13	7	8	1	1						30
2007	10	5	5	5							25
2008	9	8	4	2	3	2					28
Total	170	139	75	36	16	8	7	2	3	2	458

Table 7.6. Number of events with residual tide gauge data greater than 50 cm above the predicted tidal level at Dundee – 2003 to 2008.

	Residual height above the predicted tidal height (cm)										
	50-60	60-70	70-80	80-90	90-100	100-110	110-120	120-130	130-140	Over 140	Total no. of events
2003	48	40	17	13	12	6	9	9	1	1	156
2004	26	8	6	2	1	2	1				46
2005	63	28	16	7	1	3	1			5	124
2006	57	27	6	3		1				1	95
2007	55	23	7	1	1	1				2	90
2008	58	30	18	3	8	9	4	6		2	138
Total	307	156	70	29	23	22	15	15	1	11	649

Table 7.7. Number of events with residual tide gauge data greater than 50 cm above the predicted tidal level at Grangemouth – 2003 to 2008.

Residual data taken from the Leith records are significantly different to the Dundee residual data between 2004 and 2008, particularly the quantity and magnitudes of events each year. The difference is marked most prominently in 2004 and 2005 (Tables 7.5 to 7.7) when Dundee experienced nearly 150 events with the residual sea level being over 50 cm higher than predicted; 10 of which were greater than 1 m higher than predicted.

The average number of residual tidal heights greater than 50 cm above the predicted height between 2004 and 2008 are 14.6 for Leith and 74 for Dundee; five times greater. Evidence from these

records confirms that, between 2004 and 2008, Leith experienced 73 events where the residual tidal level was between 50 and 110 cm greater than predicted. At Dundee, between 2003 and 2008, 458 events were recorded where the residual tidal level was between 50 and 150 cm greater than predicted.

The changes in residual data through time and the variations in magnitude are presented in Figures 7.25 to 7.28. Figures 7.25 and 7.26 illustrate the variations each year in the total number of events over 50 cm above the predicted height as well as the change in the quantity of high events in each decadal band. The first and last year for both datasets are incomplete, due to the mid-year software and hardware changes to the tide gauges. Figures 7.27 and 7.28 illustrate the variations in the total number of events by magnitude across the entire duration with annual banding for each decadal height band. There is a clear decrease in the number of events as the height increases, but there is no clear increasing or decreasing annular trend.

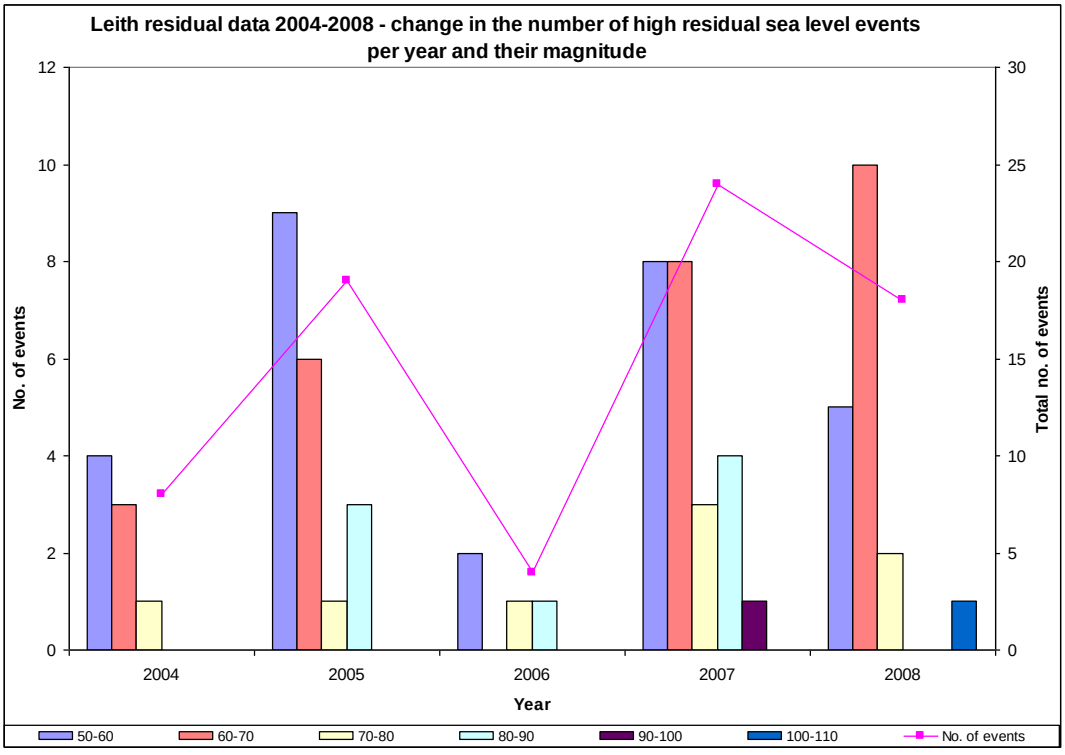

Figure 7.25. Leith residual data, 2004 to 2008. Variation in the number of high residual sea level events over 50 cm above the predicted tidal height per year. The line graph represents the total number of events.

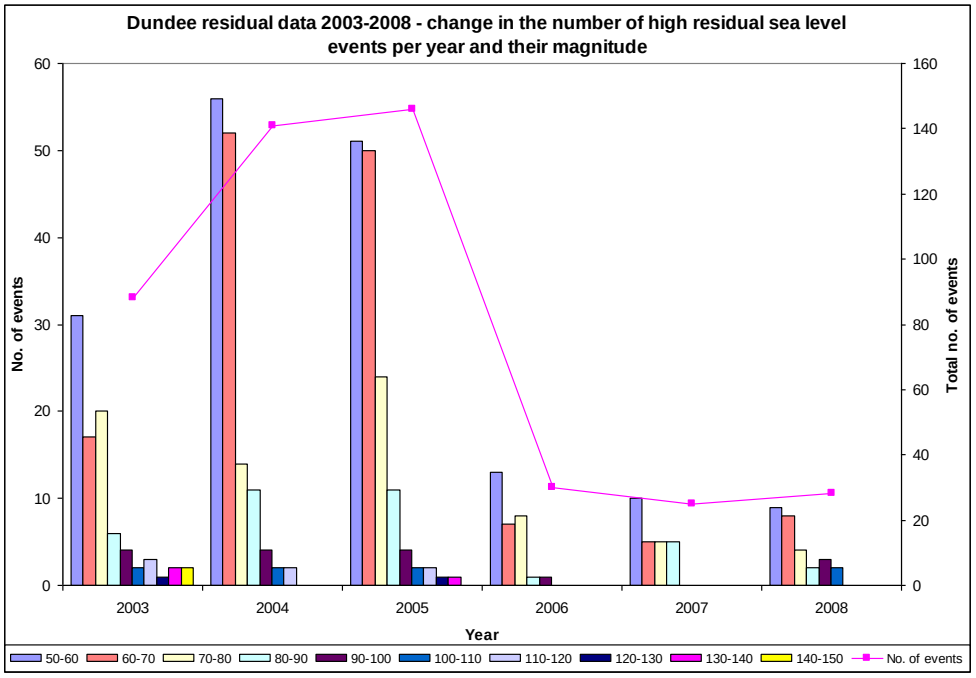

Figure 7.26. Dundee residual data, 2003 to 2008. Variation in the number of high residual sea level events over 50 cm above the predicted tidal height per year. The line graph represents the total number of events.

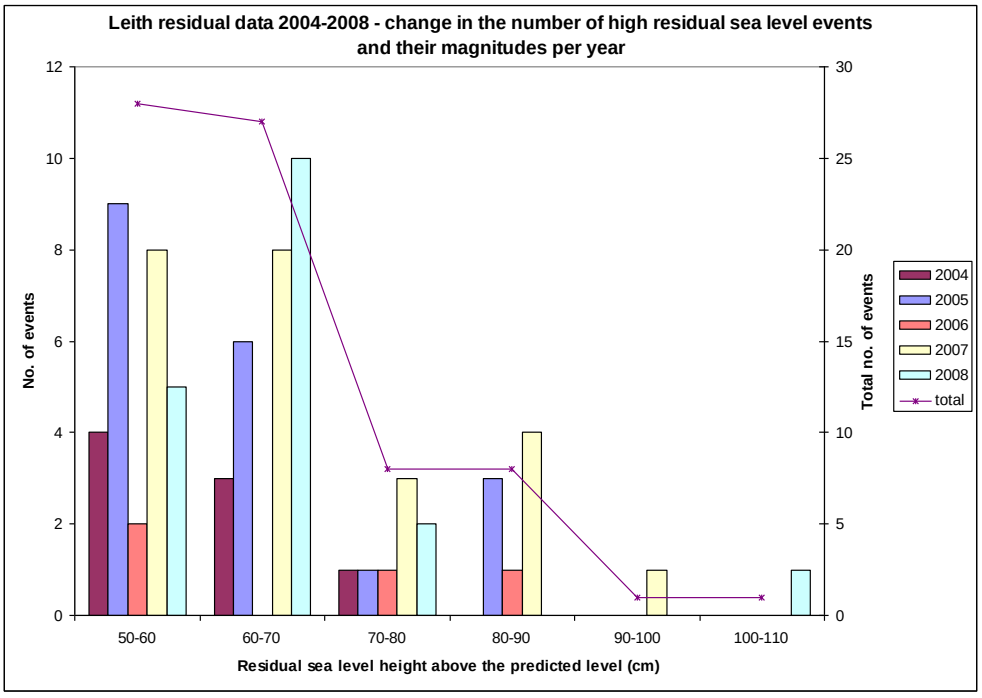

Figure 7.27. Leith residual data, 2004 to 2008. Variation in the number of high residual sea level events per year over 50 cm above the predicted tidal height.

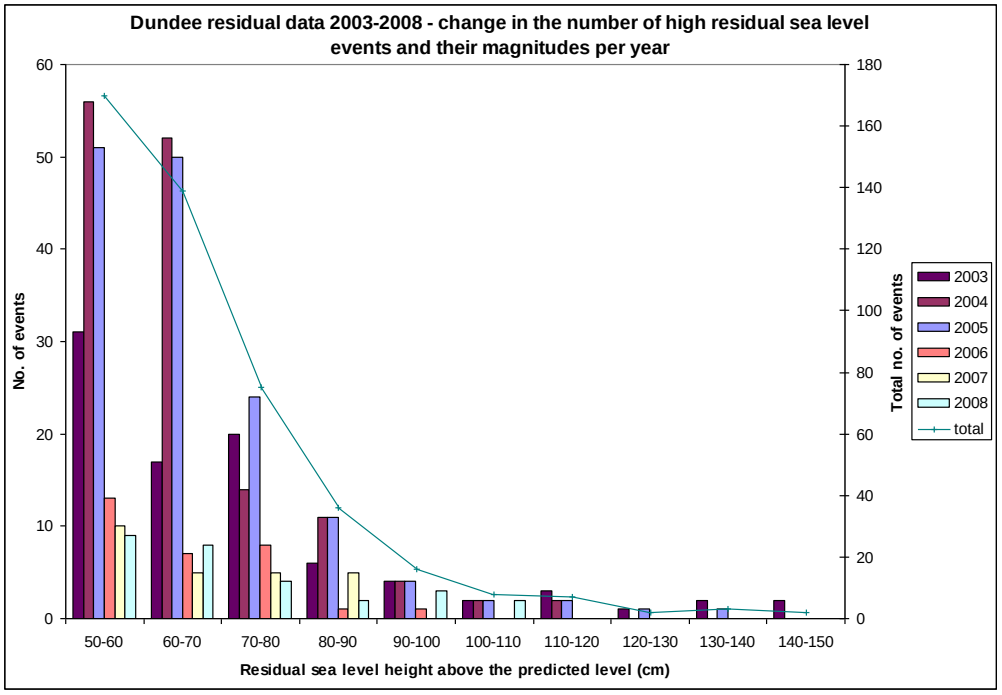

Figure 7.28. Dundee residual data, 2003 to 2008. Variation in the number of high residual sea level events per year over 50 cm above the predicted tidal height.

Examination of the distribution of these residual tidal data in more detail illustrates a seasonal distribution. The majority of high events at both sites occurred in the winter, with some abnormalities in the autumn of 2003 at Dundee. This winter predominance coincides with the general storm surge seasonality.

To ensure that the Dundee and Leith examples are representative of their estuaries, residual tidal data across the Forth Estuary have been compared with those from Leith during several high level events. Figure 7.29 illustrates the Dundee data; the Forth Estuary data; and all five datasets overlapping. The close relationship between the Leith, Grangemouth and Methil residual data suggest that these three sites are closely linked. The Rosyth data are closer in relationship to the height of the Dundee residual levels during this event, but relate to other data from the Forth Estuary during a number of other events. This suggests that there is a margin for discrepancy between residual levels within estuaries.

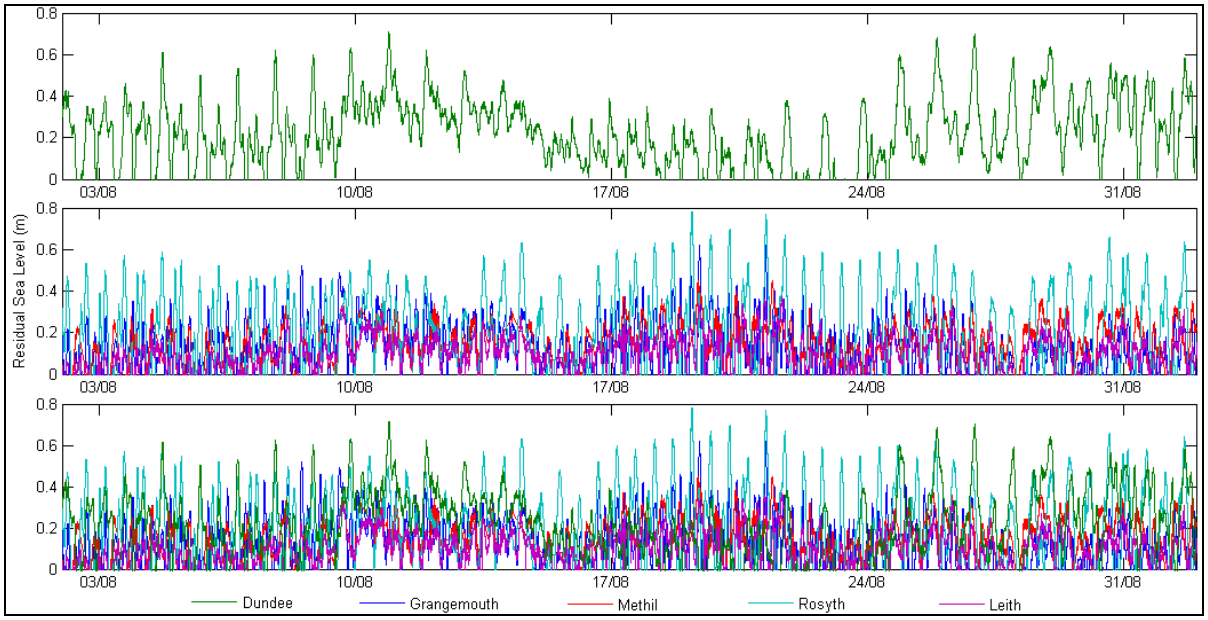

Figure 7.29. Comparison of residual tidal heights across the five Forth Ports tide gauge records during a surge event in August 2004. The Dundee residual tidal heights appear to vary considerably more than those found in the Forth Estuary, with Rosyth having the greatest variation within that region.

In January 2005, Dundee City Council noted flooding associated with the Highest Astronomical Tide combined with a 0.7 m storm surge event. Figure 7.30 illustrates the impact on the residual height of this combination of high winds and high tides.

Another example of an identified surge period took place in August 2004 (Figure 7.31). The recorded surge at Dundee reached approximately 0.7 m in height and flooding was reported by Dundee City Council (2005) in coastal and fluvial flooding areas. Leith experienced a rise in the residual data height of ~0.3 m (Figure 7.31), significantly lower than the surge witnessed at Dundee. Leith also experienced lower residual levels than Dundee during a surge event in January 2005 (Figure 7.30), with surge levels reaching a height of nearly 1 m compared with nearly 1.4 m at Dundee.

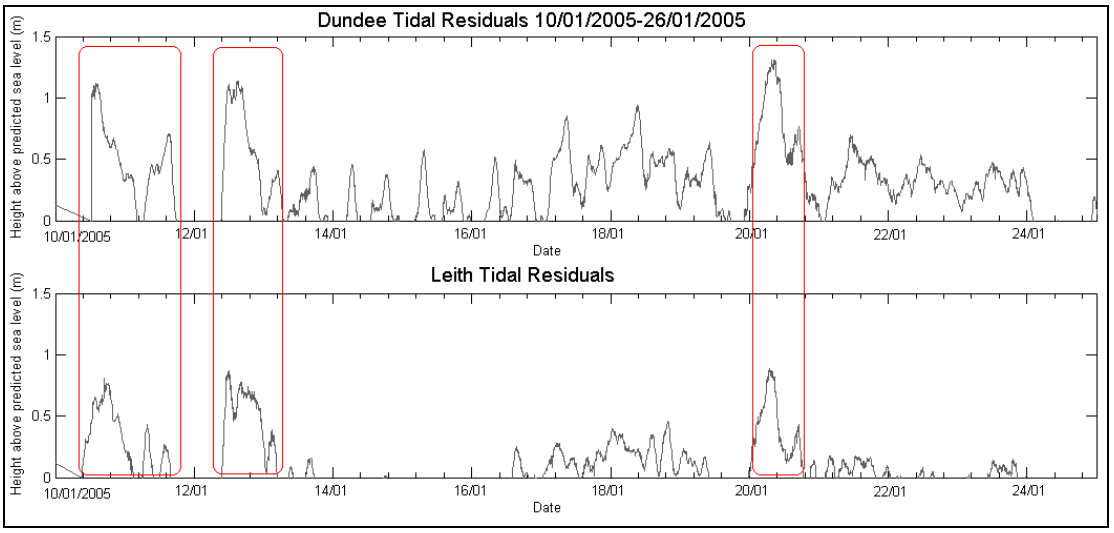

Figure 7.30. Dundee and Leith tidal residuals between 10/01/2005 and 26/01/2005. A representation of residual data from January 2005; an identified surge period. The y-axis has a large scale to encompass the large Dundee residuals. Three surge events have been highlighted inside boxes.

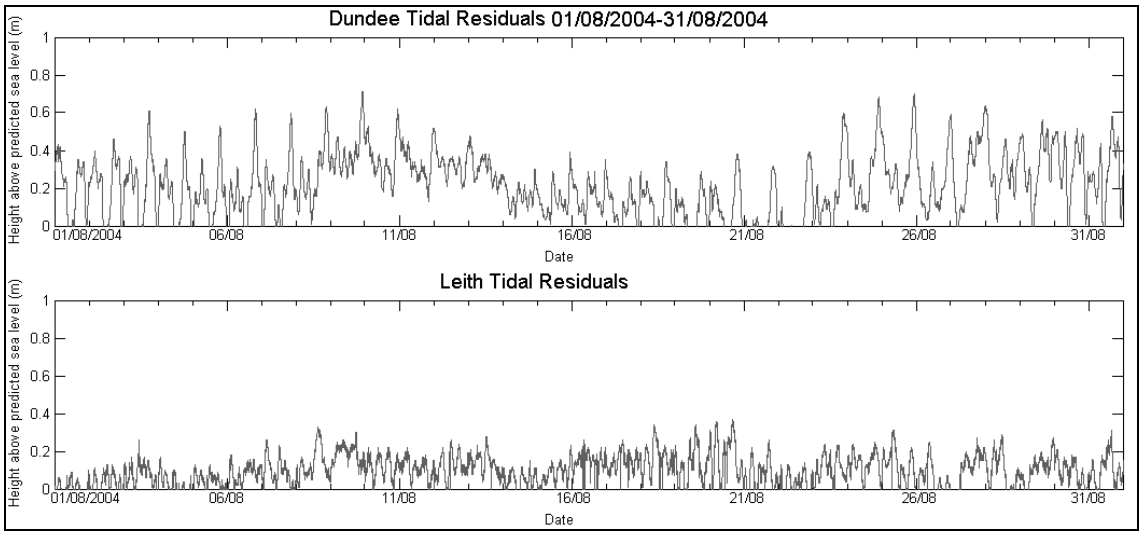

Figure 7.31. Dundee and Leith tidal residuals between 01/08/2004 and 31/08/2004. A representation of residual data from August 2004; an identified surge period.

7.5.2 Primary Tide Gauge Data, 2008 to 2010

All Forth Ports tide gauges were upgraded in September 2008, which included changing the tide gauge hardware and prediction software (Figure 7.23). As a result, residual data produced by the second prediction software were significantly reduced compared with those produced by the previous software (Figure 7.32).

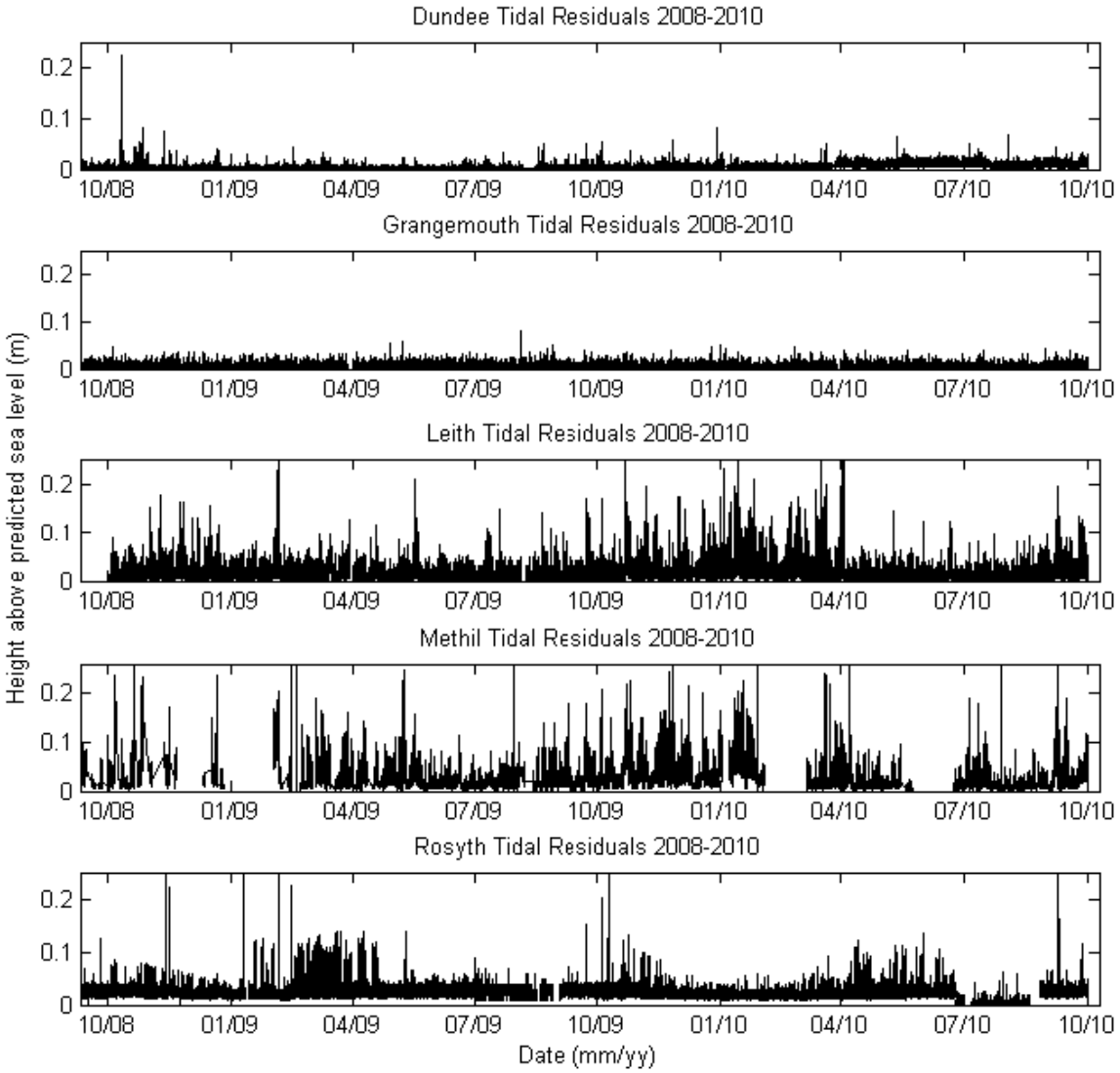

Figure 7.32. Dundee, Grangemouth, Leith, Methil and Rosyth tidal residual data between 2008 and 2010. These data were recorded by Valeport Midas TMS pressure gauges and are considerably smaller in amplitude than those recorded by the Valeport 710 pressure gauges before September 2008.

The largest changes between the pre-2008 and post-2008 residuals were observed at Dundee where the highest record pre-2008 was over 1 m in height, whereas post-2008 the highest record was below 0.1 m. As the pre-2008 events correlated closely with events that were identified by riparian local authority records, these data can be used for surge analysis. However, the post-2008 data are not suitable for surge analysis. Comparison between the Dundee and Leith pre-2008 residual datasets highlights similar seasonal trends and maxima events occurring concurrently within the two estuaries (Figure 7.23).

The large storm event that occurred on March 30th 2010 was observed at the Port of Grangemouth and manually measured approximately 0.8 m above the predicted tidal height. The difference between the observed and predicted tides was caused by a large surge event, not human or

instrumental error. However, the recorded at Grangemouth residual levels during this event remained below 0.035 m above the predicted height (Figure 7.33). These residual levels were calculated using the tide gauge prediction software that was installed in 2008 and cannot be used for storm surge analysis.

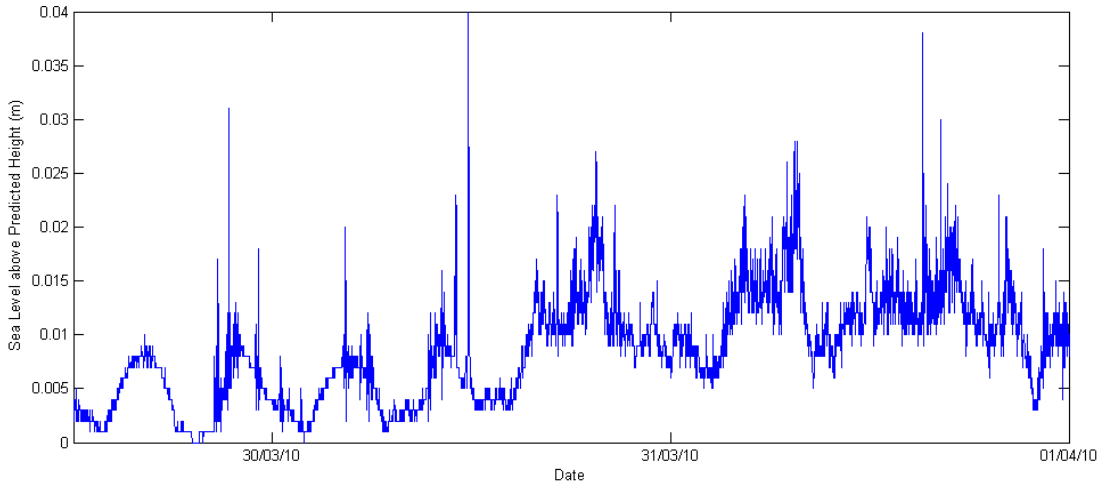

Figure 7.33. Grangemouth tidal residuals between 30/03/2010 and 01/04/2010; an identified surge period. The y-axis ranges from 0 to 0.04 m (4 cm). The primary cycles appear to be approximately 12 hours in duration (the semi-diurnal lunar cycle).

7.6 Discussion

7.6.1 Secondary Data

Surge events do not always cause flooding. Surges themselves can be of variable height and, when combined with the fluctuations of tides in macrotidal regions, they may not overtop the coast. In addition, the actual vulnerability of the coast to high water levels is dependent on the coastal elevation, defence structures and other coastal processes and features. However, comparison of flooding dates identified by secondary sources and residual data from nearby tide gauges suggests that several flood events have occurred simultaneously with surge events in the Forth and Tay Estuaries, including the August 2004 flood event (Section 7.5).

Basic information about a number of historic flood events across the Forth and Tay Estuaries region are available from flood databases, such as that of Law *et al.* (2010). Most of the flood chronologies do not provide enough information about each flood event to identify them as being caused by marine sources, as opposed to fluvial or pluvial sources, i.e. tides, surges or waves (Section 7.2). More indepth investigations into the primary data used to form the flood databases may reveal further details. However, the last entry of British Hydrological Society database associated with the

two estuaries was in 1951, therefore not comparable with residual or maxima data. Comparison between the database entries and surge data could have been used as validation of surge events.

Reports produced by riparian local authorities record the dates and locations of flood events, but rarely the water levels and are often too brief in their description of events. Cross-comparisons between the riparian local authority output shows large variations in the amount of information provided. Dundee's *Flood Prevention Reports* provide consistent temporally comparable flood maps, making it easier to identify the location and degree of flooding across the riparian local authority region. These reports also provide additional information about the probable cause of the flood and the impact. Edinburgh City Council also provides similarly useful maps, which could be adopted by other riparian local authorities.

Several areas subject to flooding between 2000 and 2010 have been identified, including Riverside Drive in Dundee, Broughty Ferry, Anstruther, St. Andrews, Grangemouth, Kirkcaldy, North Berwick, Fisherrow, Kinghorn, North Queensferry, Port Seton, Dunbar, Cramond, Silverknowes and Musselburgh (Section 7.3). The extent to which flooding occurred was not, however, documented.

Video documentation provided on Youtube identified several ports and harbours that were overtopped during storm events. The videos visually represent the impact flooding can have. However, the videos need to be temporally verified, so as to confirm the recordings were date specific and at the most severe point of the storm surge event. With the limitations imposed by the lack of verification, these videos can still be used to confirm that these locations were impacted by the March 30th 2010 surge event, which has been recorded within sea level maxima records.

7.6.2 Sea Level Maxima and Residual Tide Gauge Data

Primary sea level maxima data, extracted from tide gauge data from five sites, were used to investigate maxima trends. The averages calculated from the highest five maxima at each site range from 3.2 m above ODN at Methil to 4.04 m above ODN at Grangemouth. These averages could be affected by missing data, timescale limitations and estuarine funnelling.

Some of the highest maxima identified at one site were also within the highest five maxima at another site. Dates identified include:

- 12/01/2005 – at Grangemouth, Leith and Rosyth;
- 30/03/2010 – at Dundee, Leith and Rosyth.

The 12/01/2005 event did not appear in the highest five maxima at Dundee, but a preceding event on 11/01/2005 was highlighted. These inter-estuary and cross-estuary high maxima agreements confirm that these events affected whole estuaries, not just individual sites.

The method analysing the 20 highest maxima across the timescale at each site aimed to identify if maxima are equally spread across the timescale. If data were limited to a short period of time, this could be due to either a strong period of storminess that could bias the results or to missing data. The highest 20 maxima extracted from tide gauge data at Dundee between 1989 and 2010 are evenly distributed across the timeline. This suggests that the dataset did not experience frequent extreme maxima events over a short period of time.

The method presenting the 10 highest maxima per year removed the temporal variability element that biased the previous method. Both the Dundee and Grangemouth datasets were reanalysed using the top 10 maxima per annum. The average produced using this method is reduced compared to the 20 highest maxima average; for the simple reason that the lower maxima are included. The trend for Dundee increased from 3.8 to 12.8 mm a^{-1}. The difference between the two trends is due to the 20 highest maxima method disregarding the period of lower maxima at the beginning of the recording time period. Ultimately, the maxima are records of extreme water level events, but the maxima may not always include coinciding surge peaks and high tides. If the timing does not agree then the maxima would be lower than their potential, which could have occurred at the beginning of the Dundee dataset.

Sea level maxima data were converted to five year running means to continue the Graff (1981) trends. These trends used the single highest maxima per year to calculate the running means. This study also compared these running means to running means created using the highest 10 maxima per year. The lower trends agree that there is a general cyclical trend in the five year running mean; continuing on from the Graff (1981) data in Figures 7.21 and 7.22. The NAO and AO trends influence these 20 year cycles. The primary data from Grangemouth and Leith were connected to the Graff (1981) data, providing evidence of trend continuation in the maxima data (Section 7.4).

The residual tide gauge data analysis was limited to between 2004 and 2008 due to data limitations. In this time the average residual levels, from the top five recorded residual heights, were 1.18 m above predicted at Dundee and 0.93 m above predicted at Leith. Both sites experienced high residual levels on January 12th 2005, which relates back to extreme maxima findings and confirms the occurrence of a surge event. Unfortunately, accurate residual records are not available for March 30th 2010 to compare with maxima data. Residual heights of up to 1.4 m have been recorded at Dundee and 1.09 m at Leith between 2004 and 2010. More commonly, residual heights reached 0.7

m at Dundee and 0.4 m at Leith. These unpredicted heights, which include surge components, can thus cause a significant increase to the predicted tidal height.

Between 2003 and 2008 the majority of residual events were below 70 cm above the predicted height at Leith. Residual levels at Dundee were statistically higher than those at Leith (Tables 7.5 and 7.6), but not as high as those at Grangemouth (Table 7.7). The residuals were seasonally skewed to be more dominant in the winter. The residual data are not sufficiently long temporally to confirm a rising trend in surge height, but they do confirm that large maxima events have been driven by surge events. The maxima data, being over 20 years in length, are long enough to confirm that maxima trends are rising. However, depending on which method of analysis is used to calculate the maxima trend, the rate of maxima increase is considerably variable.

Sea level maxima data and tide gauge residual data can both be used to inform surge models (Chapter 8). Such models, when combined with sea level projection models, should help to reduce inappropriate development near the coast in areas where flooding may occur.

7.7 Conclusion

Storm surge events have been identified in the Forth and Tay Estuaries using a variety of techniques, including secondary data analyses, maxima data analyses and residual tide gauge data analyses. Secondary data revealed flood chronology databases and online video footage of past coastal flood events. Background information about flood locations is very important, providing general knowledge of where floods may occur in the future.

Several techniques have been tested to analyse recent residual and maxima data taken from tide gauges and secondary sources. Sea level maxima have reached over 3.6 and 4 m above ODN in both the estuaries between 1987 and 2010. These levels can be compared to coastal infrastructure heights to identify whether present day extreme still water levels could overtop.

Storm surges do not always result in flooding, as surges must combine with a high tide to overtop structures. Residual heights reaching 1.4 m in the Tay Estuary and 1.09 m in the Forth Estuary were recorded between 2003 and 2010. If these levels combine with high tides in the future, flooding may occur. Residual and maxima data were compared, confirming that, on occasion, the highest maxima events agreed with the highest residual level events. These dates also agree with secondary data, such as video footage and riparian local authority records, marking these dates as flood events as well as surge events. This thesis uses this storm surge evidence to guide extreme relative sea level projection in Chapter 8.

Chapter 8 – Modelling the Impact of Relative Sea Level Change on the Forth and Tay Estuaries

8.1 Introduction

Modelling is a fundamental tool, essential for understanding potential climate changes. The region of Forth and Tay Estuaries is very small compared with some of the areas covered by internationally renowned climate and sea level change models. Global models, such as the IPCC models (Solomon *et al.,* 2007), often misrepresent local trends due to their coarse resolution, which can have one grid square representing an area larger than this study's area. Several climate and sea level models are discussed in this chapter, introducing the range of projection methods.

The first general circulation model (GCM) was constructed by Phillips (1956), which included realistic atmospheric circulation simulations and led on to the development of 3-D multi-level GCMs (Weert, 2011b). GCMs are designed to replicate present and past climate, but cannot always understand the drivers of climate: 'It is more a case of trying to represent everything, even if things get so complicated that we can't always understand what's going on' (Climateprediction.net, 2010). Simplified models act in the opposite sense to GCMs in this respect. They aim to identify the response of a small number of variants to a projected change, rather than calculating everything at once; therefore they are more appropriate to ascertain drivers and relationships in the climate (Climateprediction.net, 2010).

Since 2000 a series of internationally renowned global models have been produced, including the Intergovernmental Panel on Climate Change (IPCC) series. The models discussed in this chapter have been chosen because they have previously been used for climate change or sea level change projection on global or national scales. This chapter describes the models, their results and how the projected change in sea level would impact upon the shoreline.

8.2 Simplified Models and GCMs

Simplified models are constructed using observed relationships between two or more climate variables. For example, a positive relationship between sea surface temperatures and sea level rise has been identified. Accurate temperature projections, calculated using historical trend, are used to project sea level change where historical sea level data are not available (Rahmstorf, 2007).

GCMs, sometimes referred to as atmospheric-oceanic global climate models (AOGCM), attempt to simulate as many different variables to the highest quality possible, which involves manipulation of

equations within reasonable limits until the model results fit the observed trends to the best possible degree of accuracy (Climateprediction.net, 2010). GCMs are considered to be more accurate than simplified models due to their intensive modelling and boundary conditions, but simplified models are quicker and easier to replicate.

Large GCMs run numerous simulations over long time periods to provide statistically accurate projections of future climate scenarios. These simulation collections are known as ensembles: 'Such ensembles can be generated either by collecting results from a range of models from different modelling centres ('multi-model ensembles' [MME]), or by generating multiple model versions in a particular model structure, by varying internal model parameters within plausible ranges ('perturbed physics ensembles' [PPE])' (Solomon *et al*., 2007:594).

Several GCMs have embedded regional climate models (RCM), which increase the resolution of GCMs in areas typically smaller than 5000 km^2 (Climateprediction.net, 2010). Regional models can be designed to be PPE, with a MME forming the boundary conditions and large scale climate variables (Climateprediction.net, 2010). PPE are also used in large climate models for enhanced analysis of variants, such as gas concentrations or temperature change (Solomon *et al.*, 2007). Large variations can occur between the GCM and RCM due to the difference in model resolution (Figure 8.1) (Solomon *et al.*, 2007; DEFRA, 2011a).

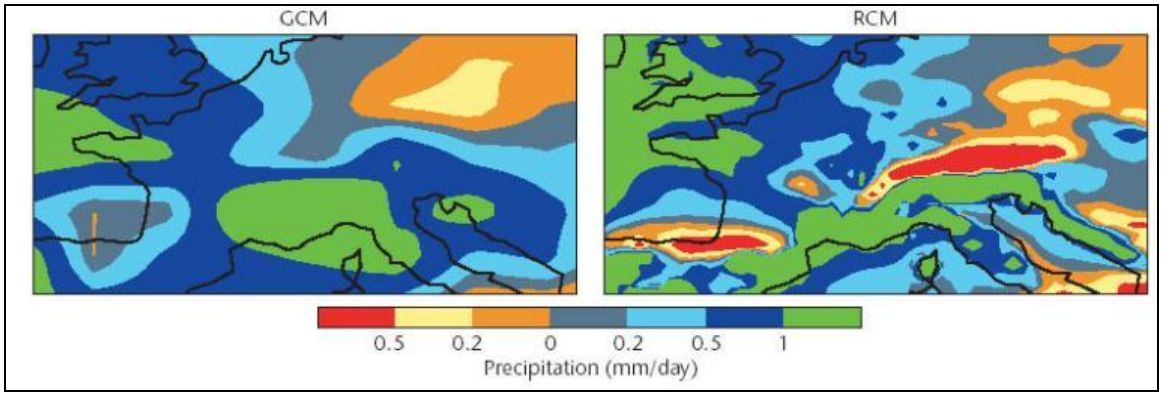

Figure 8.1. Predicted changes in winter precipitation over central/ southern Europe between the present day and 2080. The areas of red, where precipitation has fallen by more than 0.5mm/day, indicate large reductions over the Alps and Pyrenees predicted by the RCM (right), but not the large scale GCM (left) (Climateprediction.net, 2010).

A number of GCMs, RCMs and simplified models have been constructed that overlap this study location, including the:

- UK Meteorological Office (UKMO) unified model (MetUM);
- Intergovernmental Panel on Climate Change (IPCC) series;

- UK Climate Impact Programme (UKCIP) series;
- Rahmstorf's (2007) and Vermeer and Rahmstorf's (2009) simplified temperature-sea level relationship models; and
- Grinsted *et al.*'s (2009) simplified temperature-sea level relationship model.

8.2.1 The UKMO Unified Model (MetUM)

Since 1990 the UKMO has continually improved its climate modelling system; MetUM, which encompasses a selection of atmospheric and ocean projection models. The models include a series of multi-decadal to centennial scale combined atmosphere and ocean GCMs including HadCM3 and HadGEM1 (UKMO, 2011) (Figures 8.2 and 8.3).

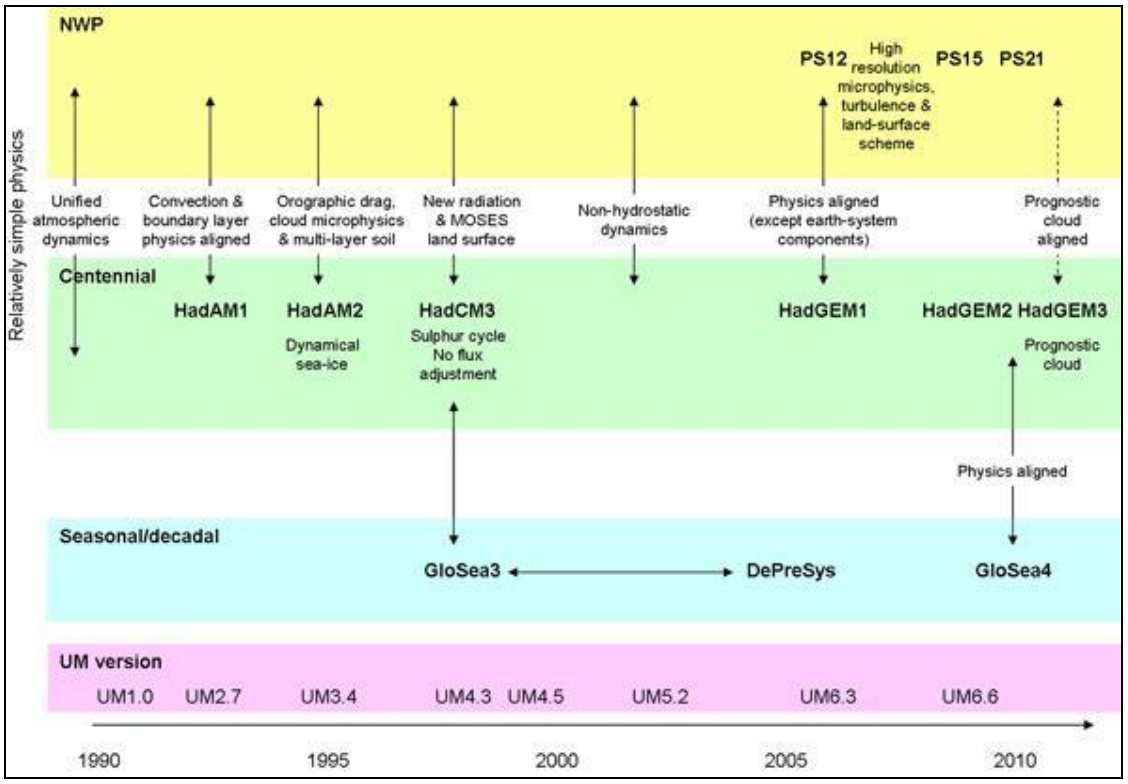

Figure 8.2. History of the MetUM, including its numerical weather prediction (NWP), centennial-scale prediction models and seasonal to decadal prediction models (UKMO, 2011). Abbreviations explained in the Appendix.

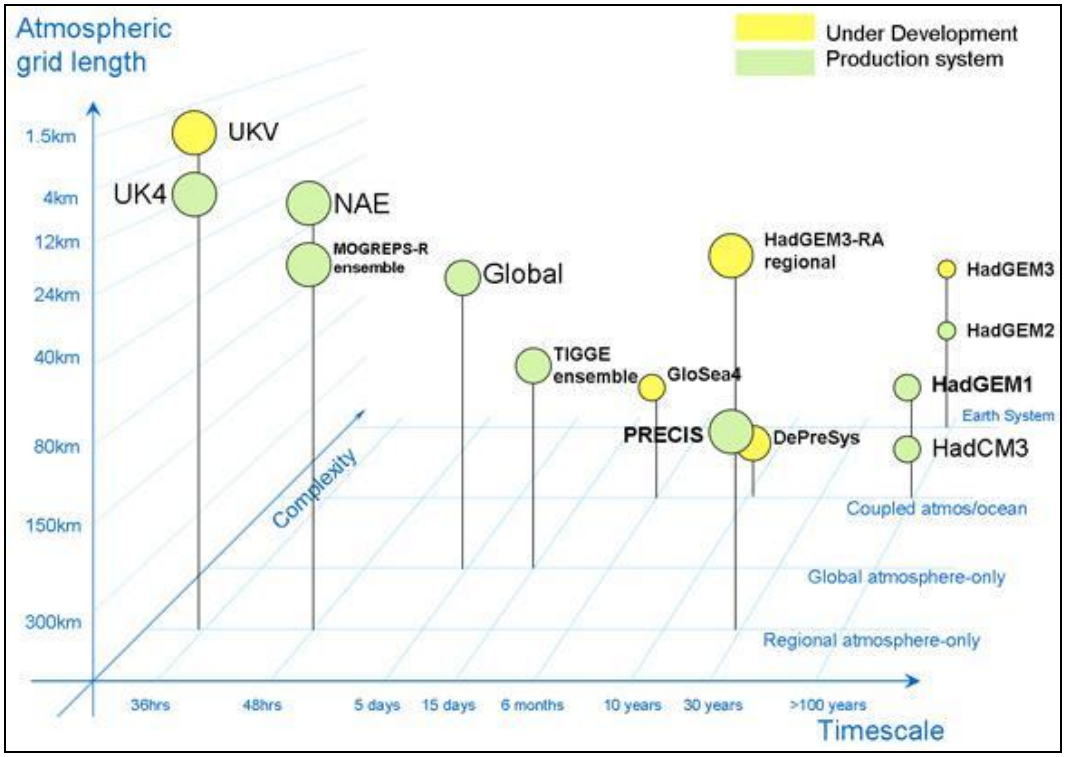

Figure 8.3. The resolution and timescale of the MetUM (UKMO, 2011). Abbreviations explained in the Appendix.

Both HadCM3 and HadGEM1 are MMEs, which use multiple model runs to improve the accuracy of climate variable projections. Several of the MetUM component models have been used in the construction of PPE and MME in the models featured in Sections 8.2.2 to 8.2.4.

8.2.2 IPCC TAR and AR4 Models

The IPCC produced several climate change assessment reports over the last three decades. These reports have used UKMO MetUM MMEs to project 2100 climate variable changes since 1990, including eustatic sea level change. The most recent, the Third Assessment Report (TAR) and Fourth Assessment Report (AR4), have been adopted within various studies to construct new models and for policy guidance (Houghton *et al.*, 2001; Solomon *et al.*, 2007). Extensive information about all of these reports is available on the IPCC website (http://www.ipcc.ch), to which the reader is referred in preference to lengthy discussion here.

TAR and AR4 rely on emissions scenarios published in the IPCC Special Report on Emissions Scenarios (SRES) with the high (A1FI), medium (A1B) and low (B1) scenarios being selected as the policy focal points of several regional climate impact programmes (Nakićenović and Swart, 2000; DEFRA, 2011b). Transition from TAR to AR4 resulted in a decrease in the global sea level

projection range between 1990 and 2100 from 15-95 cm to 18-59 cm (Houghton *et al.*, 2001; DEFRA, 2011b).

TAR and AR4 both use models from the UK Meteorological Office (UKMO) Unified Model (MetUM), namely the Hadley Centre Coupled Model 3 (HadCM3) and the Hadley Centre Global Environment Model 1 (HadGEM1) (UKMO, 2011). Both of these models are combined AOGCM, which use the UKMO models in their PPE. IPCC TAR used considerably fewer models than AR4; only 7 compared to AR4's 23 models (Houghton *et al.*, 2001; Solomon *et al.*, 2007). The MME of AR4 uses 16 of the 23 models and uses MetUM models as a PPE for sea level comparison with the MME (Solomon *et al.*, 2007).

Although there are similarities between the two reports the central estimates of sea level change in TAR are 0.03 to 0.07 m above the AR4 scenario estimates (Church *et al.*, 2004; Solomon *et al.*, 2007) due to the change in temporal scale, 2100 in TAR to 2090-2099 in AR4, as well as an additional omission of permafrost calculations from AR4 (Solomon *et al.*, 2007). The range of each scenario in AR4 is narrower than TAR due to the improved knowledge concerning some of the uncertainties (Solomon *et al.*, 2007).

> *'Sea level is projected to rise between the present (1980–1999) and the end of this century (2090–2099) under the SRES B1 scenario by 0.18 to 0.38 m, A1B by 0.21 to 0.48 m and A1FI by 0.26 to 0.59 m. These are 5 to 95% ranges based on the spread of AOGCM results, not including uncertainty in carbon cycle feedbacks. In all scenarios, the average rate of rise during the 21st century very likely exceeds the 1961 to 2003 average rate (1.8 ± 0.5 mm a^{-1}). During 2090 to 2099 under A1B, the central estimate of the rate of rise is 3.8 mm a^{-1}. For an average model, the scenario spread in sea level rise is only 0.02 m by the middle of the century, and by the end of the century it is 0.15 m',* (Solomon *et al.*, 2007:750).

The resolution of the component models and the output from the regional study imply that AR4 cannot be accurately applied to a study limited to the size of the Forth and Tay Estuaries due to the regionally fluctuating nature of relative sea levels (Gehrel and Long, 2008), therefore highlighting the need for models specific to the study location.

8.2.3 UKCIP Models

In 2002 the UKCIP produced the UK Climate Impacts Projections '02 (UKCIP02); a climate projections report orientated around the UK (Hulme *et al.*, 2002). UKCIP02 was created in response to the release of IPCC TAR. More recently, in 2009, UKCIP released the UKCP09 in response to IPCC AR4. The UKCP09 probabilistic climate projections were produced by combining 12 models

from the IPCC AR4 GCM MME with the UKMO coupled climate model HadSM3 (a PPE) into a Bayesian statistical framework (Murphy *et al.*, 2009; DEFRA, 2011b; DEFRA, 2011a). The Marine Climate Change Impact Partnership (MCCIP) report, which reported marine specific UKCP09 projections, projected the global sea level rise range by 2095 to be between 12 and 76 cm (Jenkins *et al.*, 2007; Lowe *et al.*, 2009), which incorporates the high, medium and low emissions scenarios.

8.2.4 Simplified Models

Global temperature projections are presumed by the UKCIP to be more robust than their sea level projections (DEFRA, 2011b). The two simplified sea level models described here use the past climate variable relationships to project future sea levels from temperature scenarios, i.e. Vermeer and Rahmstorf (2009) and Grinsted *et al.* (2009). Focusing on the temperature-sea level relationship should account for potential thermal expansion and land ice melt, which are the main drivers of global sea level rise (Vermeer and Rahmstorf, 2009).

Vermeer and Rahmstorf's (2009) study was based around improvements made to that of Rahmstorf (2007). To correct potential omissions in the 2007 model, Vermeer and Rahmstorf (2009) produced a semi-empirical method 'dual mode' simple equation that accounted for the time lag in the temperature-sea level relationship:

$$\boldsymbol{dH/dt = a\,(T - T_0)\ [Eq.1] + b\,dT/dt\ [Eq.\ 2]}$$

where:

- a is temperature – determined by the data;
- 'T_0 is a base temperature at which sea level is in equilibrium with climate' (Vermeer and Rahmstorf, 2009:21527) – determined by the data;
- H is sea level;
- dH/dt is the rate of rise in sea level;
- b is the instantaneous sea level response on the timescales under consideration, 'it implies $H \sim T$.

'The rate of rise in sea level H, dH/dt, is proportional to the warming above this base temperature' (Vermeer and Rahmstorf, 2009:21527). This combines the lag effect outlined in the first equation and a more responsive element (Figure 8.4).

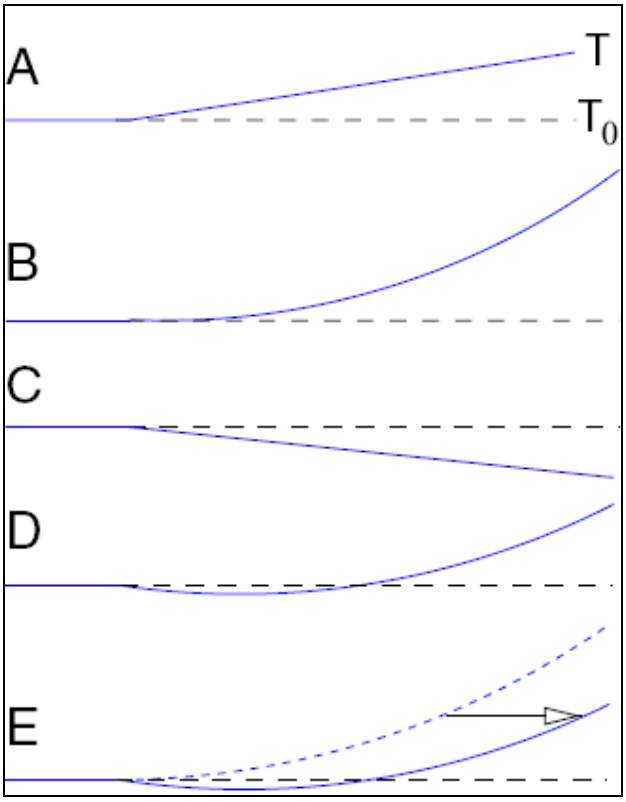

Figure 8.4. 'Schematic of the response to a linear temperature rise. (*A*) Temperature. (*B*) First term on the right of Eq. 2. (*C*) Second term. (*D*) Total sea-level response. (*E*) Comparison to the case Eq. 1, showing that *b* primarily corresponds to a time lag in the sea-level response' (Vermeer and Rahmstorf, 2009:21530).

Vermeer and Rahmstorf (2009) used the IPCC AR4 temperature ranges from six of the SRES scenarios to project global absolute sea level change to 2100. The sea level range across the six scenarios calculated by Vermeer and Rahmstorf (2009) is 81 to 179 cm by 2100 (Table 8.1). The Vermeer and Rahmstorf (2009) model has been adapted for this study for comparison with the UKCP09 results in Section 8.3. These results must be used with caution, because there is always a possibility with simplified models that a vital climate variable has been omitted. Also, this model is similar to other climate models in that it is a wide variability to its results, 81 to 179 cm, which affects it accuracy.

Scenario	Temperature range, ˚C above 1980-2000	Model average, ˚C above 1980-2000	Sea level range, cm above 1990	Model average, cm above 1990
B1	1.4-2.9	2.0	81-131	104
A1T	1.9-3.8	2.6	97-158	124
B2	2.0-3.8	2.7	89-145	114
A1B	2.3-4.3	3.1	97-156	124
A2	2.9-5.3	3.9	98-155	124
A1FI	3.4-6.1	4.6	113-179	143

Table 8.1. Temperature ranges and associated sea-level ranges by the year 2100 for different IPCC emission scenarios. The temperatures used are taken from the simple model emulation of 19 climate models as shown in Figure 10.26 of the IPCC AR4 (Solomon *et al.*, 2007); they represent the mean ± 1 SD across all models, including carbon cycle uncertainty. The sea-level estimates were produced by using Eq. 2 and 342 temperature scenarios and are given here excluding the uncertainty of the statistical fit, which is approximately ± 7% (1 SD) (Vermeer and Rahmstorf, 2009:21531).

8.3 UKCP09 Storm Surge Model

The Proudman Oceanographic Laboratory Continental Shelf tide-surge model 3 (POLCS3) was used in UKCP09 for prediction of storm surge maxima to 2095. POLCS3 projected the change in the ‘skew surge’ height (Figure 8.5 and Figure 8.6). This tends to be smaller than the highest actual residual value if the high tide is temporally advanced or delayed by the surge (Figure 8.5). Lowe *et al.* (2009) calculated the future change in skew surge using 11 models from the UKCP09 PPE. The specific climate variables analysed were chosen to project changes in wind, atmospheric pressure and tides.

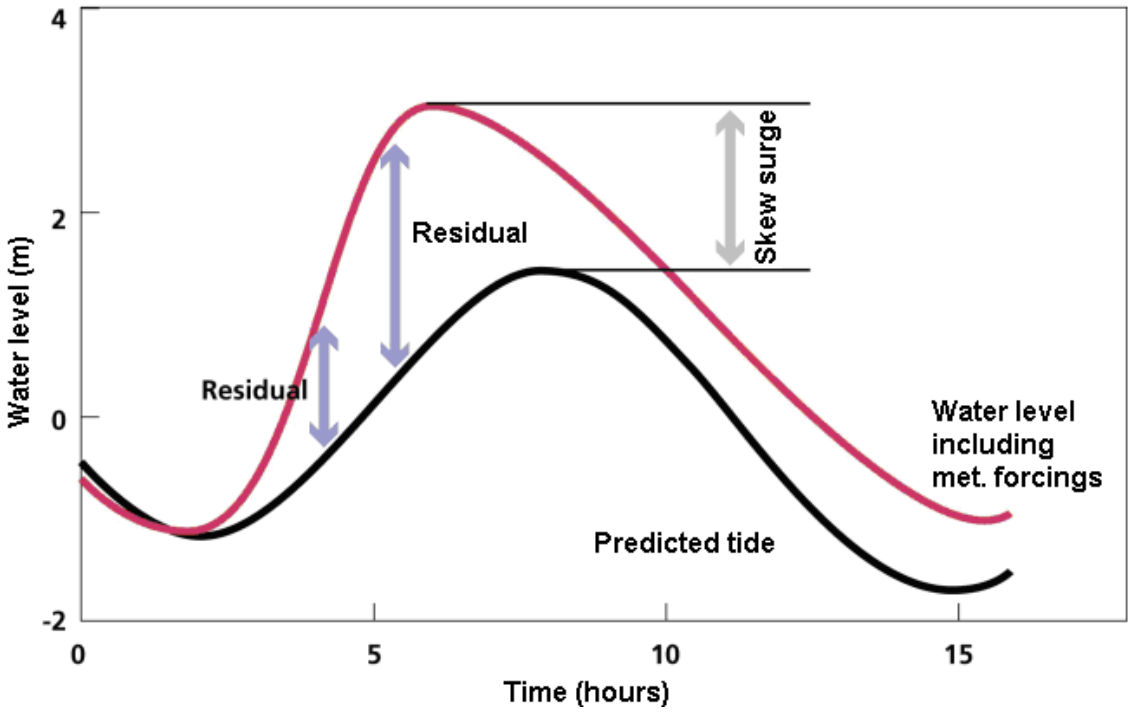

Figure 8.5. How skew surge and surge residuals are evaluated. The surge residual changes through the tidal cycle, usually peaking before the predicted tide (Adapted from Lowe *et al.*, 2009).

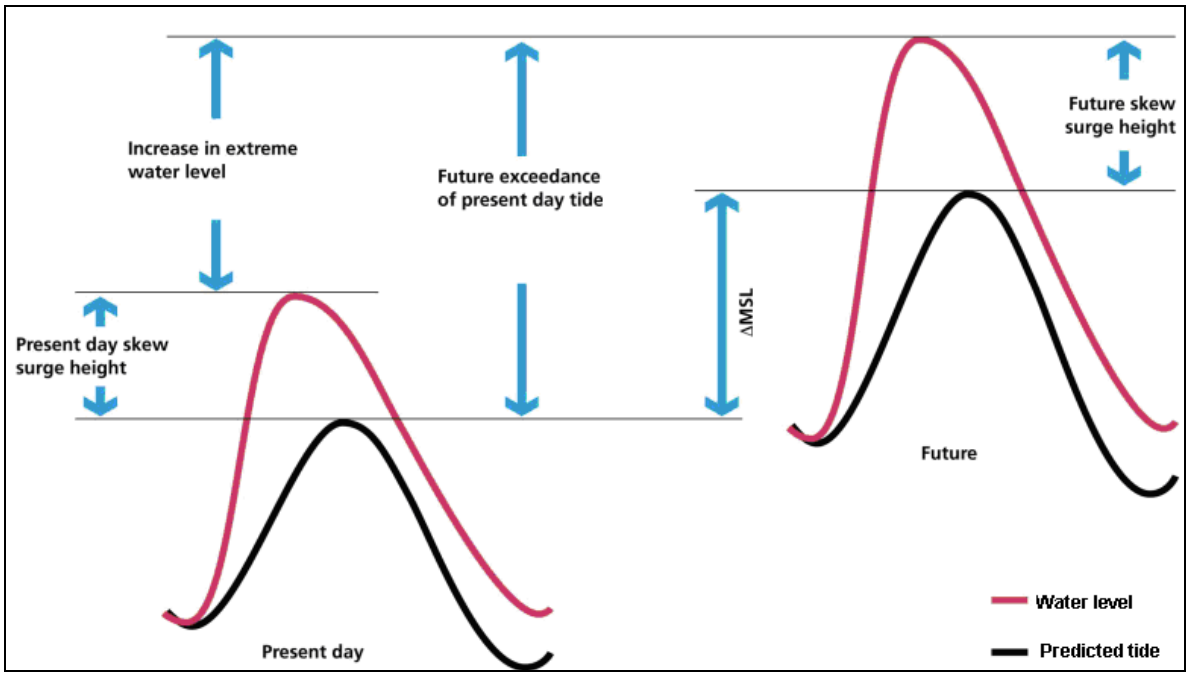

Figure 8.6. Present day and future baselines of skew surge (above HAT) (Adapted from Lowe *et al.*, 2009).

UKCP09 estimated the present day surge level during a HAT (Figure 8.7) and compared it against their modelled 2095 surge level (Figure 8.8).

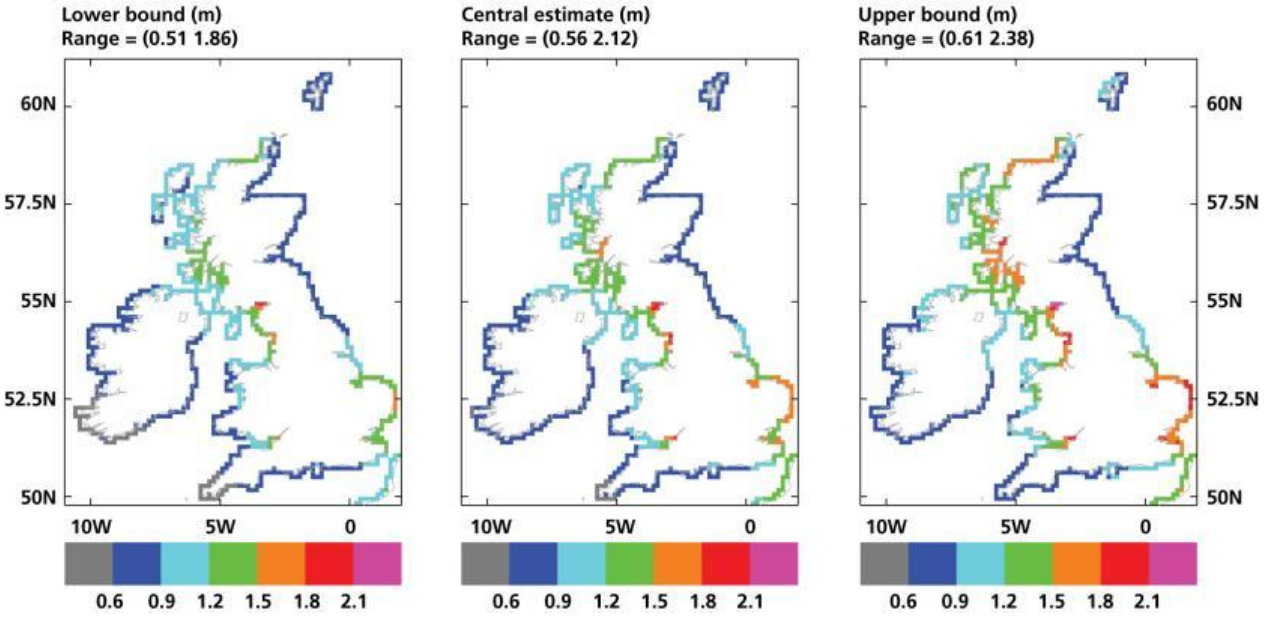

Figure 8.7. 'Illustrative present-day baseline of skew surge (present-day extreme sea level during an astronomical high tide) 50 year return levels (m). The central panel shows the estimated central value. Left and right panels show the lower and upper bounds of the 90% confidence interval,' (Lowe *et al.*, 2009).

The POLCS3 tide-surge model projected that the northern and western coasts of Scotland would continue to be affected by higher surge events than the eastern coast. It also projected increasing surge heights along the northern and western Scottish coasts. The model suggests that the height of a 1:50 year storm surge may increase by *c.*0.8 mm a^{-1}, which is significantly less than the 5 mm a^{-1} that the UK Climate Impact Programme predicted in their 2002 report (Lowe *et al.*, 2009; Hines, 2010).

Figure 8.7 illustrates the variation in potential surge heights around the British Isles for the 50 year return period scenarios. These suggest that presently surge heights of between 0.5 and 1.0 m could occur in the Forth and Tay Estuaries (Figure 8.7) (Lowe *et al.*, 2009). The 2095 UKCP09/POLCS3 projection suggests that surge heights may increase by up to between 0.9 and 1.5 m (Figure 8.8). These projections are significantly higher than the projected changes to relative and absolute sea level over the same period.

Several residual records for the area were higher than the 0.9 m upper boundary of the POLCS3 projections. This difference can be explained by means of Figure 8.5, referring back to the difference between residual heights and surge skew heights, which tend to be smaller. Owing to the reservations regarding the surge projections, the accurate residual data that have been compiled in Chapter 7, will be used as substitutes for the POLCS3 model.

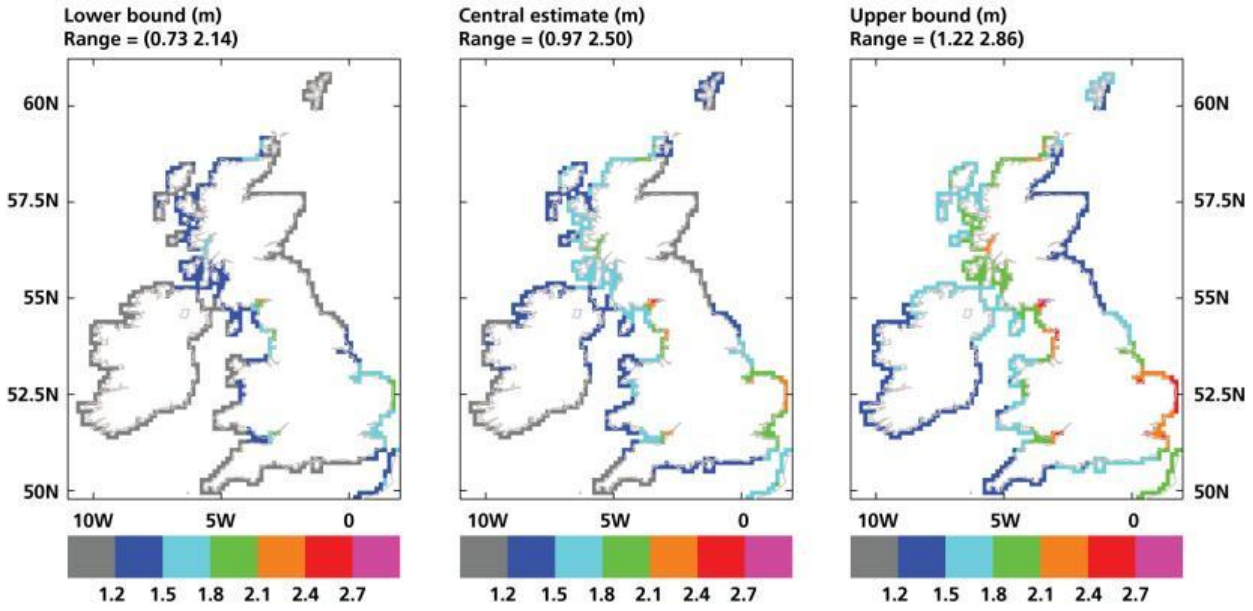

Figure 8.8. 'Exceedance of present-day HAT by projected future extreme water 50 year return levels for 2095 (m). The central panel shows the estimated central value. Left and right panels show the lower and upper bounds of the 90% confidence interval. Grey shows any value < 1.2 m,' (Lowe *et al.*, 2009).

8.4 Modelling East Scotland

Two of the sea level models discussed in Section 8.2 have been adapted for use for the Forth and Tay Estuaries, i.e. UKCP09 and Vermeer and Rahmstorf (2009). The author of this thesis performed simplistic transformations of these models for projection of relative sea level by converting global sea level projections using local GIA rates.

8.4.1 UKCP09

UKCIP provide an online User Interface enabling registered users to create and adapt graphs of various climate variables and scenarios. For relative and absolute sea level elements, data can be collected for the 5th, 50th and 95th percentiles of the low, medium and high emission scenarios. These statistics are geographically limited to grid squares of 1.25° latitude 1.25° longitude (DEFRA, 2011a).

The UKCP09 projections of relative sea level change for three tide gauge recording sites were analysed, namely Dundee, Dunbar and Grangemouth (Figure 8.9). Each of these records has been converted by the UKCIP from 'absolute' sea levels to relative sea level projection using the Bradley *et al.* (2009) VLM GIA rates that were calculated for each grid square (DEFRA, 2011a). Dunbar

has the highest rate of relative sea level rise, followed by Dundee and then Grangemouth, which is due to the location of the three ports in relation to where the ice cap epicentre was during the Last Glacial Maxima. All three sites are projected to experience less than 0.45 m of relative sea level rise under the high emission scenario (50th percentile) (DEFRA, 2011a). These levels were compared with the low emission scenario (5th percentile) absolute (i.e. eustatic) sea level projections (Figure 8.10).

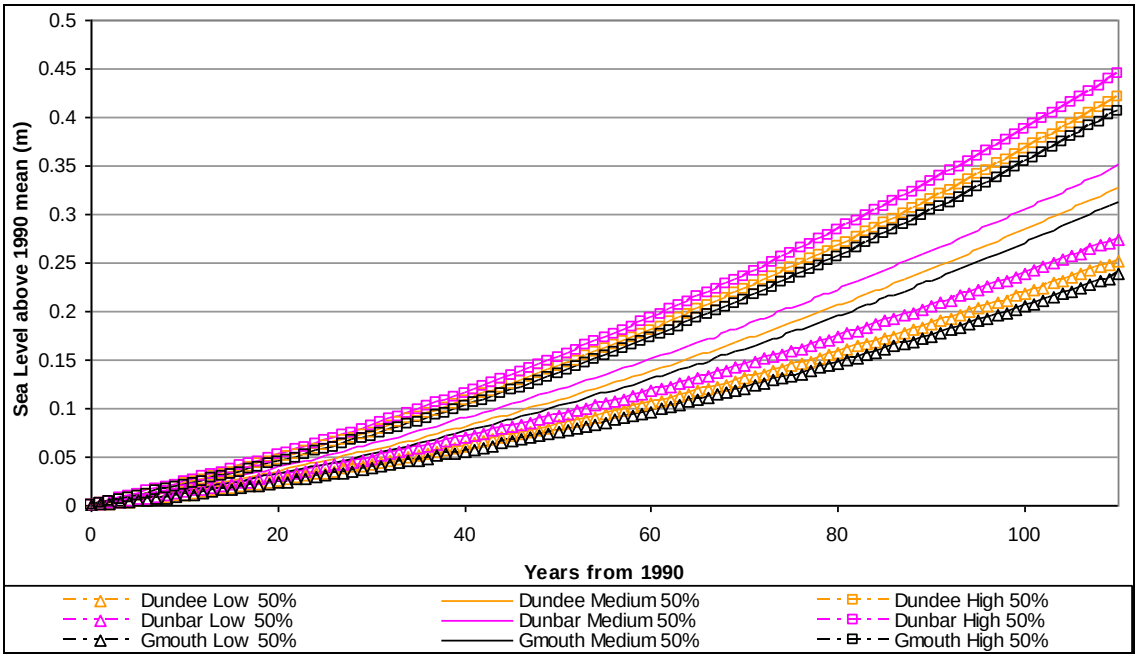

Figure8.9. UKCP09 relative low, medium and high emissions scenario 50th percentile projections for Dundee, Dunbar and Grangemouth, using the Bradley *et al.* (2009) VLM GIA convertion rates (DEFRA, 2011a).

In Figure 8.11, the 1900 to 2010 relative and GIA-corrected combined Forth and Tay Estuaries datasets are compared with the UKCP09 1990 to 2100 projected levels for Dunbar and Grangemouth (DEFRA, 2011a); the two locations experiencing the region's extreme high and low GIA rates. These relative sea level projections are for the low, medium and high emission scenarios.

As well as the site-by-site UKCP09 relative projections, the UKCP09 absolute sea level projections for each scenario are projected. The UKCP09 absolute sea level projections have been converted to present relative sea levels using the Shennan *et al.* (2012) GIA rates for the Forth and Tay Estuaries. These calculated relative sea levels are compared with the existing UKCP09 relative sea levels that were originally calculated using Bradley *et al.*'s (2009) GIA (VLM) rates in Figure 8.11 (simplified in Figure 8.12).

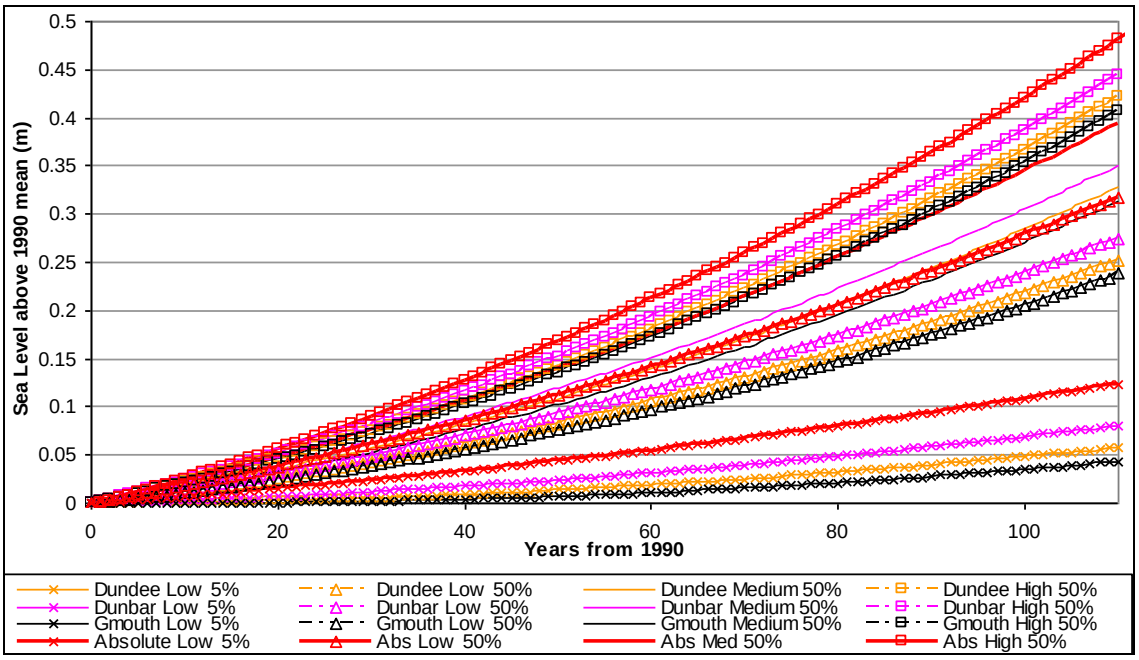

Figure 8.10. UKCP09 extreme low (5th percentile of low emissions scenario), low, medium and high emissions scenario projections for relative sea level at Dundee, Dunbar and Grangemouth, using the Shennan *et al.* (2009) RLLC GIA convertion rates, as well as UKCP09 absolute sea level (sourced from DEFRA, 2011a).

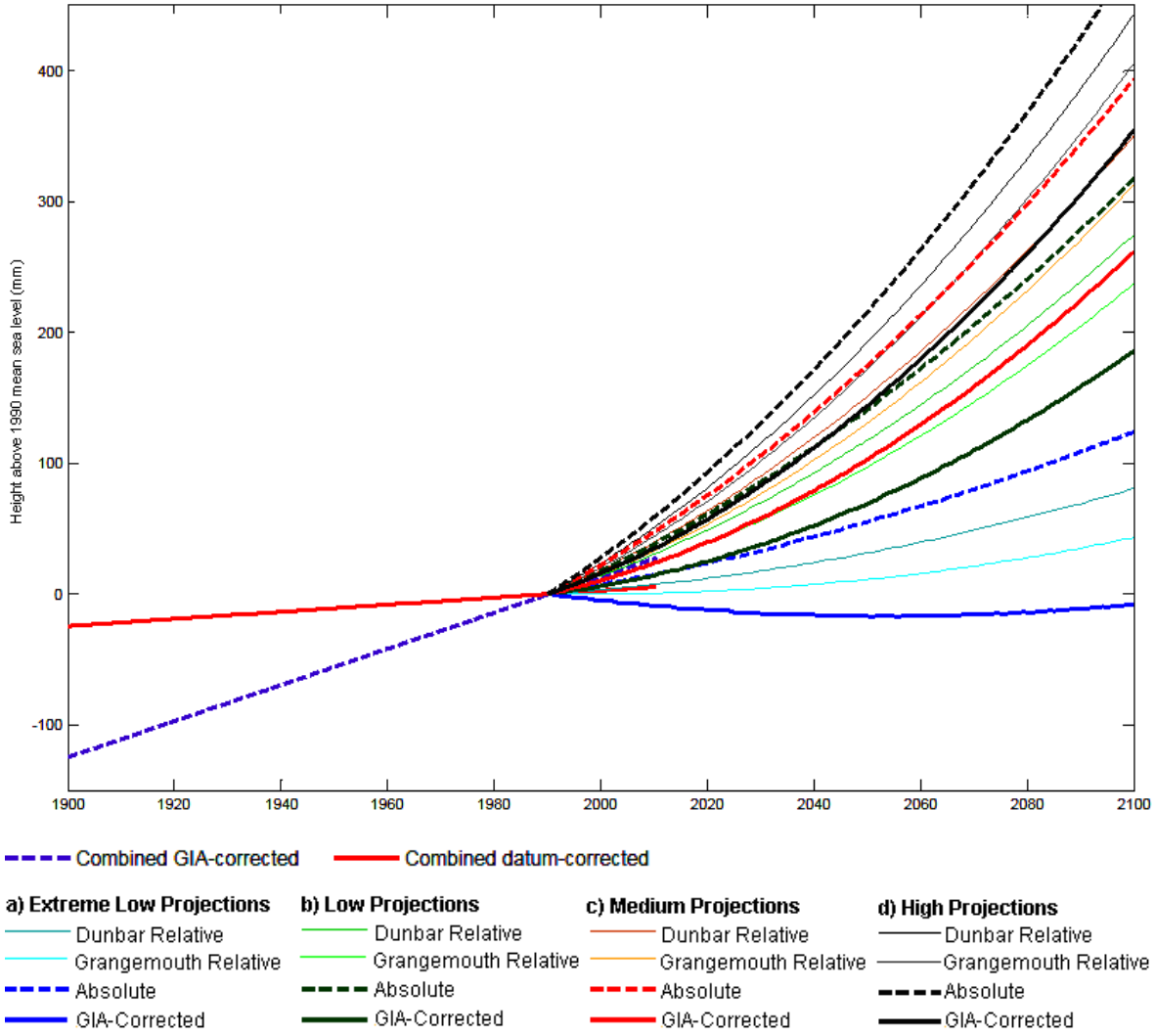

Figure 8.11. Datum-corrected relative sea level rates (1900 to 2010), GIA-corrected absolute (eustatic) sea level (1900 to 2010) and UKCP09 relative and absolute sea level projections (1990 to 2100) (sourced from DEFRA, 2011a). The historical rates and projections overlap by 20 years, highlighting the difference between observed and predicted sea levels over a short time period. Grangemouth and Dunbar were chosen from the study sites to represent the range of relative sea level change projected across the study site. Each emission scenario has been illustrated separately in Figure 8.12.

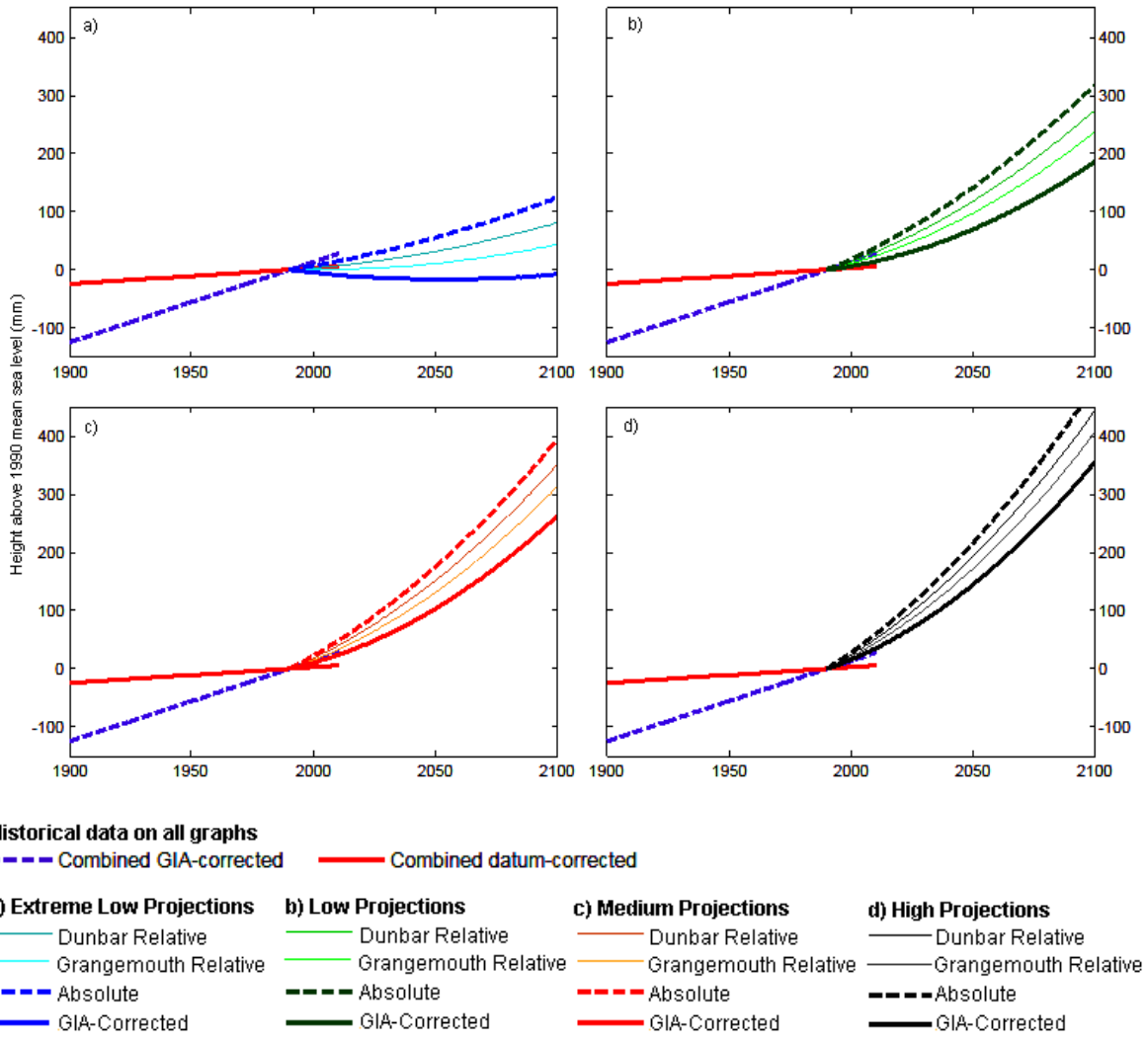

Figure 8.12. Datum-corrected relative sea level (1900 to 2010), GIA-corrected absolute (eustatic) sea level (1900 to 2010) and UKCP09 relative and absolute sea level projections (1990 to 2100) (sourced from DEFRA, 2011a). The historical trend and projections overlap by 20 years, highlighting a difference between observed and predicted sea levels of over 10 cm over a short time period.

The UKCP09 projected relative sea level changes at each site are considerably different to those produced through the Shennan *et al.* (2012) GIA conversion of UKCP09 absolute sea levels (Table 8.2 and Table 8.3). Direct comparison during the overlapping 20 years of the observed 1900 to 2010 linear trends and the 1990 to 2100 UKCP09 projected trends suggests a good relationship between the UKCP09 low emission scenario projection and past trends.

Ultimately the UKCP09 2095 relative sea level projections could be inaccurate by as much as 89 mm in the Forth and Tay Estuaries; specifically at Dunbar (Table 8.2 and Table 8.3). If the UKCP09 was updated to use the Shennan *et al.* (2011; 2012) GIA model, Dunbar's 2095 projected high emission scenario relative sea level change would reduce from 444 mm (shown on Table 8.2) to 355 mm (calculated using the Dunbar specific GIA correction).

	Dundee	Dunbar	Grangemouth	Absolute#	GIA-Corrected*
5% Low	58	81	43	124	0.5
Low	252	275	238	318	137
Medium	328	351	313	394	254
High	421	444	406	487	306
95% High	744	766	729	810	666

Table 8.2. Comparison between UKCP09 projected twenty-first century relative sea level change at Dundee, Dunbar and Grangemouth with # the UKCP09 projected UK absolute sea level change and *the average GIA-corrected sea level for the Forth and Tay Estuaries (i.e. relative sea level) across the low, medium and high emission scenarios as well as the low emission scenario 5th percentile and high emission scenario 95th percentile (sourced from DEFRA, 2011a).

	Dundee	Dunbar	Grangemouth	Absolute#
a) 2100 height difference (mm)	74.5	76.5	70	140
b) Annual height difference (mm)	0.68	0.70	0.64	1.27
c) UKCP09 GIA estimate (mm a^{-1})	0.60	0.39	0.73	N/A
d) Shennan* et al. *(2012) GIA estimate (mm a^{-1})	1.1	0.9	1.2	N/A

Table 8.3. a) The 2100 height difference between three UKCP09 projected relative sea level change estimates and study specific GIA-corrected relative sea level change, as well as # the UKCP09 UK absolute sea level change estimates (source from DEFRA, 2011a). b) Annual variation between UKCP09 projected relative and absolute sea level change and study specific GIA-corrected relative sea level change throughout the data. c) Estimate of UKCP09 GIA correction used at three sites. The average GIA correction across the Grangemouth, Leith, Rosyth, Dunbar and Dundee sites is 1.2 mm a^{-1}, therefore this measurement has been used in calculations here. d) Shennan *et al.*'s (2009) GIA estimates from geological records for Dundee, Dunbar and Grangemouth.

8.4.2 Vermeer and Rahmstorf (2009)

Vermeer and Rahmstorf (2009) adapted their sea level-temperature relationship model into MATLAB code and Moriarty (2011) adapted it into a Microsoft Office Excel spreadsheet. The basic model components of the Vermeer and Rahmstorf (2009) model are a historical global temperature record (GISS, 2011) and the IPCC low, medium and high emissions scenarios (Solomon *et al.*, 2007).

The GISS (2011) global temperature record dates from 1880 to 2010. For the primary scenario, mimicking the original model design, the GISS annual temperature data were inputted into Moriarty's (2011) Excel model for the entire length of the dataset. The model then used the Vermeer and Rahmstorf (2009) equations (Section 8.2.4) to project future temperatures for a set emissions scenario (see Figure 8.13 for the medium emissions scenario example).

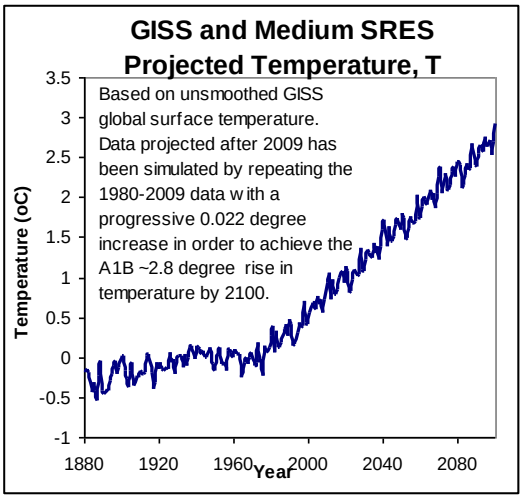

Figure 8.13. Vermeer and Rahmstorf (2009) temperature scenario used to predict sea level change until 2100 (Moriarty, 2011; GISS, 2011).

The temperature projections used cyclical loops of the last recorded 30 year period (1980-2009), adding gradually increasing increments to the temperature value until the year 2100. Annual increments of 0.022 °C were used to reach the IPCC projected medium emission scenario temperature of 2.8 °C. For the high emissions scenario, increments of 0.025 °C a^{-1} were used with steps of 0.002 °C every five years.

To apply the projected temperature scenarios to sea level change, the Vermeer and Rahmstorf (2009) equation was used. The original calculations assumed that the sea level relationship, *a*, equalled 5.6 mm K^{-1} a^{-1}; the corresponding lag effect, *b*, equalled -49 mm K^{-1}; and the base temperature at which sea level was in equilibrium with climate, T_0, equalled -0.41 K^{-1}. Figure 8.14 illustrates the resultant impact on the annual rate of absolute sea level change. The original equation does not account for GIA.

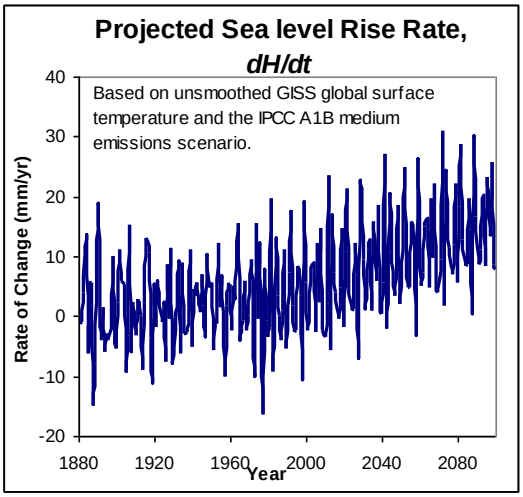

Figure 8.14. Projected sea level rise rate calculated through the Vermeer and Rahmstorf (2009) temperature-sea level relationship (Moriarty, 2011; GISS, 2011).

The results of the model (Figure 8.15) indicate potential sea level rise of 1324.75 mm (1.32 m) under a high emission scenario and 1073.64 mm (1.07 m) under a medium emission scenario by 2100. When the sea level data are corrected for GIA of 1.2 mm a^{-1}, the average medium emission scenario sea level height is reduced to 941.64 mm (0.94 m). However, Moriarty (2011) suggests that another element of analysis can reduce this further.

After reading comments by Moriarty (2011), this study applied Wada *et al.*'s (2010) groundwater depletion calculations to the Vermeer and Rahmstorf (2009) results. Chao *et al.*'s (2008) artificial reservoir storage calculations have been used by Vermeer and Rahmstorf (2009) to correct the GISS temperature data and Church and White (2006) global sea level data that have been used to calculate the historical relationship trends (Moriarty, 2011; Vermeer and Rahmstorf, 2009). In 2010 Wada *et al.* estimated groundwater depletion worldwide and illustrated it to be greater than that of artificial reservoir storage, which is why these calculations have to be accounted for in the Vermeer and Rahmstorf (2009) model.

Figure 8.16 illustrates changes made to the Vermeer and Rahmstorf (2009) projections using the Wada *et al.* (2010) groundwater extraction calculations and Shennan *et al.*'s (2011) GIA rates. Both the absolute and GIA-corrected sea level results decrease by over 400 mm to 641.32 mm (0.64 m) and 509.32 mm (0.51 m), respectively, when these additional calculations are applied.

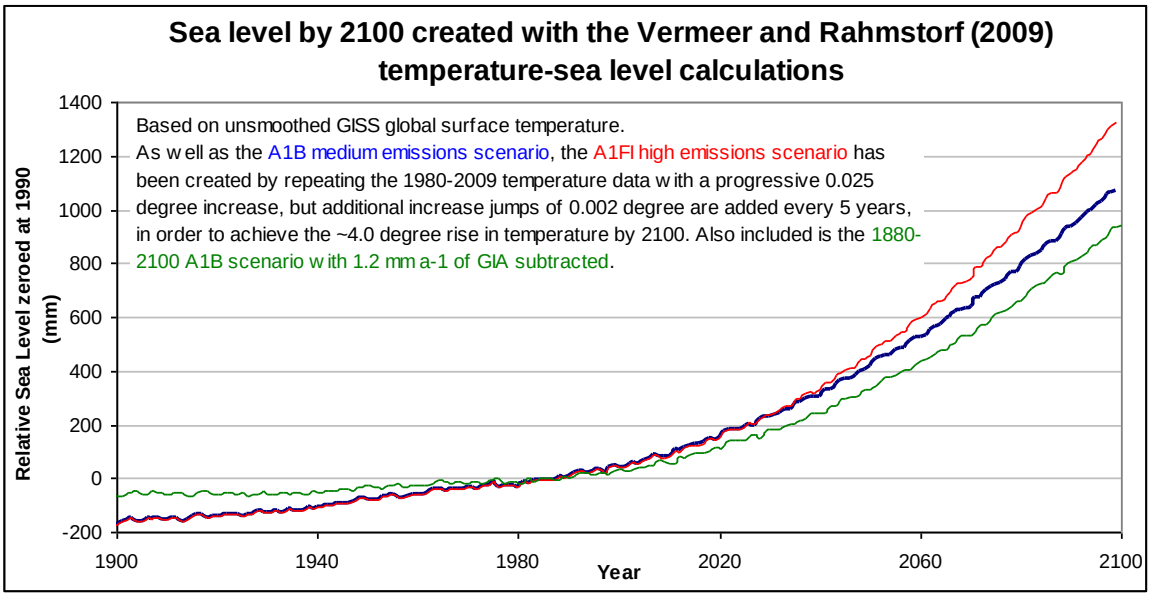

Figure 8.15. Three sea level projections using the Vermeer and Rahmstorf (2009) temperature-sea level calculations (Moriarty, 2011; GISS, 2011).

Although the Vermeer and Rahmstorf (2009) projections have been corrected and suggest reduced relative sea level rise, the medium emission scenario projections are still over 150 mm above the GIA-corrected UKCP09 sea level projections for the Forth and Tay Estuaries. The resultant range of potential medium emission scenario relative sea level change in the Forth and Tay Estuaries from these two modelling techniques is between 243 mm and 542 mm by 2100 (Table 8.4). The calculations for Leith in Table 8.4 are also representative of sea level projections for Dundee, Methil and Rosyth, as the Shennan *et al.* (2011) GIA rates used to correct the Leith data are exactly the same as those for Dundee, Methil and Rosyth. Variation in sea level across the region, using the medium emissions scenario, is calculated to be 38 mm using UKCP09 and 33 mm using Vermeer and Rahmstorf (2009). However, variation between models is more significant, with the results from Vermeer and Rahmstorf (2009) being calculated to be double the height of the UKCP09 projections.

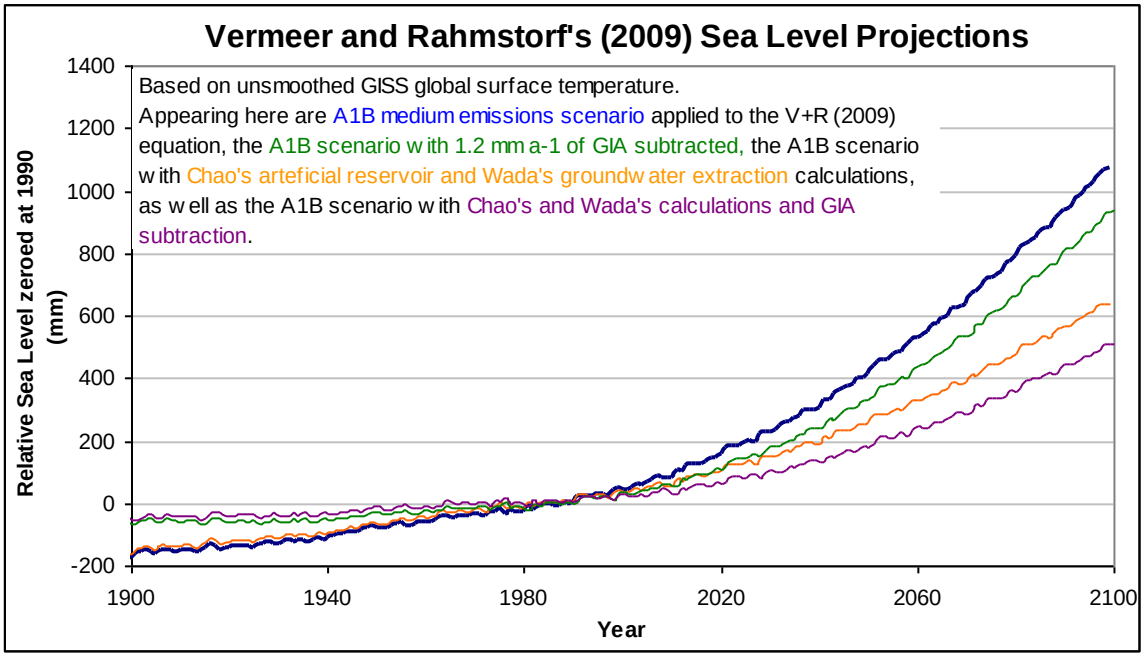

Figure 8.16. Projections of the a) Vermeer and Rahmstorf (2009) A1B scenario sea level by 2100, b) the same with GIA correction suitable for the Forth and Tay Estuaries, c) a, but with Chao and Wada corrections that are discussed in the text, and d) c, but with GIA corrections suitable for the Forth and Tay Estuaries.

	Dunbar (mm)	Leith (mm)	Grangemouth (mm)
UKCP09 Original A1B Scenario	351	328	313
UKCP09 *GIA-Corrected* A1B Scenario	274.5	253.5	243
Vermeer and Rahmstorf (2009) Original	1073	1073	1073
Vermeer and Rahmstorf (2009) *Corrected*	542	520	509

Table 8.4. Regional spread of approximate relative sea level projections across the Forth Estuary using the UKCP09 medium emissions scenario absolute sea level projection that have been corrected for GIA and the Vermeer and Rahmstorf (2009) projections corrected with reference to Wada *et al.* (2010). The Leith projected sea levels are also representative of heights at Rosyth, Methil and Dundee (see text above).

8.5 Sea Level, Surge Heights and the Shoreline

Two methods were used to assess the consequences of predicted future extremes, which included comparison of:

- Projected maxima levels with quay heights;

- Projected relative sea level and surge levels with quay heights.

Both methods rely on the corrected relative sea level projections for 2100.

Several quayside heights have been noted after discussion with Forth Ports' Dredging and Conservancy Superintendent, Peter Crawley, and reference to the Ordnance Survey's benchmark and triangulation point locator website (Table 8.5) (Ordnance Survey, 2011). Additional sources of information about quay heights include technical drawings of defence structures, maps and flooding studies.

Comparing quay heights with potential maxima rise is a simple method of estimating if sea defences can withstand future still water levels. This method has been used by several pre-development flooding assessments along the Forth and Tay Estuaries in the last ten years, including the Skinflats Realignment Scheme (Babtie Group, 2001), Dundee Renewable Energy Plant (Forth Energy, 2010b) and the Leith Renewable Energy Plant (Forth Energy, 2010a).

Before comparing maxima data to quay heights, Graff's (1981) maxima analysis method was applied to the Forth Ports and BODC maxima data. The Dundee, Leith and Grangemouth datasets, being between 20 and 30 years in length, were sufficiently long to identify decadal or shorter frequency trends. The Graff (1981) data did suggest the presence of an 18 to 20 year sea level trend, which is continued in the Leith data (Figure 9.19).

The highest maxima heights across the region are 3.69 m (Dundee), 4.13 m (Grangemouth), 3.96 m (Leith), 3.27 m (Methil) and 3.93 m (Rosyth). The average maxima heights constructed from the top five maxima (and more practical for management purposes) are 3.53 m, 4.04 m, 3.75 m, 3.20 m and 3.74 m, respectively (Chapter 7).

The Leith Renewable Energy Plant Flood Risk Assessment (Forth Energy, 2010a) identifying that the quay heights range from 5.0 m to 6.2 m above ODN. The Flood Risk Assessment went on to compare these heights with extreme water level. A method used by Forth Energy (2010a) was to combine HAT levels at Leith (3.4 m above ODN) and the UKCP09 projected storm surge extreme levels in the Firth of Forth (1.25 m above ODN) to illustrate a maximum extreme still water level of 4.65 m above ODN. Forth Energy (2010a) suggested that a development freeboard of 0.6 m should be applied, meaning that all flood sensitive development in that area should be above 5.25 m above ODN to avoid extreme coastal flood events.

Continuing with this case study, the Port of Leith still water level is maintained near to 3.0 m above ODN and the sealing dam has a maximum height of 5.28 m above ODN (Table 8.5). The quay height measured by the benchmark at the tide gauge house is approximately 5.0 m above ODN, resulting in an additional height of 0.25 m above the recommended freeboard.

Location	Structure Height	Gate Level	Comments
Grangemouth	4.75 m	3.45 m	Maintained dock level 3.25 m INEOS fire pump min. level 3.10 m 10-15 cm dock level variance Suggested 1997 overtopping of old berths
Leith	4.9439 m at tide gauge	At least 3.5 m	Maintained dock level 3.007 m Sealing dam height 5.278 m
Methil	3.99 m at tide gauge	N/A	Only impounded if vessels are working in the port
Dundee	4.38 m at Camperdown and Victoria Docks		Predominantly river berths, some long-duration vessels moor in the enclosed Camperdown and Victoria Docks where the water level is maintained, but variable within a tolerance to aid flushing.
Rosyth	4.7012 m	N/A	
Broughty Ferry	4.0668 m at 4-5 Esplanade (estuary edge)	N/A	Wall height unknown.
Perth	~5 m at Side Shore Rd (estuary edge)	N/A	Wall height unknown.

Table 8.5. Quay heights (measured in metres above ODN, unless stated) at selected ports and significant places along the Tay and Forth Estuaries. All gates are lower than the quay levels. Some heights have been sourced from Peter Crawley (pers. comm.), Alan Melville (pers. comm.) and Derek McGlashan (pers. comm.) at Forth Ports.

Dundee has a HAT of 3.16 m above ODN (Forth Energy, 2010b). If the Forth Energy (2010b) extreme level calculation were adopted, which use the same 1.25 m surge estimates as the Forth Energy (2010a) report, then the maximum still water level would be 4.41 m above ODN. Dundee's Camperdown Dock quayside lies at 4.38 m above ODN. However, the highest recorded maxima at this dock reached 3.69 m above ODN, so the quay height seems adequate as the 0.6 m freeboard appears to have been available.

Comparing the maxima data to previous reports, the highest recorded maxima at Grangemouth of 4.13 m above ODN is approximately 50 cm above HAT (3.65 m above ODN) and 50 cm below the projected 250 year flood height (Forth Energy, 2010c; Babtie Group, 2001; Graff, 1981) (Figure 7.21). Grangemouth's HAT level added to the storm surge element, suggested by Forth Energy (2010c) of 1.25 m, is 4.90 m above ODN. Some areas of the site were recorded as being 3.93 m above ODN (Forth Energy, 2010c).

At Rosyth the highest recorded maxima was 3.39 m above ODN; 6 cm below the HAT (3.45 m above ODN) (Forth Energy, 2010d). With the additional Forth Energy (2010d) suggested surge element of 1.25 m, the extreme still water level is calculated as 4.70 m above ODN, which is near equal to the riverside berth height at the tide gauge. However, ground levels of 4.15 m above ODN have been recorded at this site (Forth Energy, 2010d).

The Methil 1:250 year return period height lies around or just above the benchmark recorded height of the quay. Maxima heights are unreliable for this site due to the erratic nature of the data collection. The quay height is the lowest of all the sites, which suggests that Methil would be at greatest risk from overtopping, but the sparse Forth Ports maxima data and the Graff (1981) maxima data suggest that the sea level maxima at Methil tend to be lower than those recorded at the other Forth Estuary sites.

The primary extreme sea level calculations in this thesis rely on two methods to integrate the projected mean sea level increase with extreme height data:

- Method 1 – site-by-site, the relative sea level model results were added to the site average of the five highest residual tidal records (representing the potential storm surge element) and added to the HAT level. Table 8.6 illustrates a simple example of how this is done, presenting the future extreme sea level with the maximum surge and a development freeboard.
- Method 2 – the maxima data were added to the modelled relative sea level change projections and the freeboard height. Surge levels have not been additionally added to the extreme sea level projection, as the surge element has not been removed from the maxima dataset (Table 8.7).

Port	**a) HAT (mOD)**	**b) Modelled MSLC (mOD)**	**c) Average Residual Tidal Height (mODN)**	**d) Freeboard (mODN)**	**Total Extreme (mOD)**	**e) Total Extreme + Freeboard (mOD)**
Dundee	3.16	0.25* – 0.52^	1.18	0.60	4.59* – 4.86^	5.19* – 5.46^
Leith	3.40	0.25 – 0.52	0.93	0.60	4.58 – 4.85	5.18 – 5.45
Rosyth	3.45	0.25 – 0.52	0.93	0.60	4.63 – 4.94	5.23 – 5.50
Grangemouth	3.65	0.24 – 0.51	1.84	0.60	5.73 – 6.00	6.33 – 6.60#

Table 8.6. Method 1 - Calculations used to convert the 2100 relative mean sea level projections of *UKCP09 and ^Vermeer and Rahmstorf (2009) into (e) extreme high still water estimates. This involves adding the (a) HAT, (b) UKCP09 and Vermeer and Rahmstorf (2009) corrected relative mean sea level change (MSLC), (c) average of the five highest residual tidal readings recorded at each location, and (d) a 0.60 m freeboard. # Grangemouth's residuals are based on peak events

approximately 60 cm higher than the surrounding residuals, which are also subject to estuarine influences (Chapter 7).

Table 8.8 directly compares the two methods by illustrating the extreme high sea level projections with freeboard included. The surge element between the two methods ranges between 0.4 and 0.7 m (excluding Grangemouth). With the 0.60 m freeboard included, the quaysides would witness overtopping by the highest maxima events. Subtraction of the freeboard reveals that without surge events the quaysides would rarely be affected by the highest maxima according to Method 2.

Port	a) Highest Maxima (mOD)	b) Modelled MSLC (mOD)	c) Freeboard (mOD)	Total Extreme (mOD)	d) Total Extreme + Freeboard (mOD)
Dundee	3.67	0.25* – 0.52^	0.60	3.92* – 4.19^	4.52* – 4.79^
Leith	3.96	0.25 – 0.52	0.60	4.21 – 4.48	4.81 – 5.08
Rosyth	3.93	0.25 – 0.52	0.60	4.18 – 4.45	4.78 – 5.05
Grangemouth	4.13	0.24 – 0.51	0.60	4.37 – 4.64	4.97 – 5.24

Table 8.7. Method 2 - Calculations used to convert the 2100 relative mean sea level projections of *UKCP09 and ^Vermeer and Rahmstorf (2009) into (d) extreme high still water estimates. This involves adding the (a) highest maxima heights recorded for each site, (b) UKCP09 and Vermeer and Rahmstorf (2009) corrected relative mean sea level change (MSLC), to a (c) 0.60 m freeboard.

Port	Method 1 + Freeboard (mOD)	Method 2 + Freeboard (mOD)	Quay Heights (mOD)
Dundee	5.19 – 5.46	4.52 – 4.79	4.38
Leith	5.18 – 5.45	4.81 – 5.08	4.94
Rosyth	5.23 – 5.50	4.78 – 5.05	#4.15
Grangemouth	6.33 – 6.60	4.97 – 5.24	#3.93

Table 8.8. Comparison between two methods of 2100 extreme high sea level projection with 0.60 m freeboard; Method 1 (Table 8.6) and Method 2 (Table 8.7). Quay heights are supplied for direct comparison. #These heights may represent areas away from the quayside that are present on the site with actual quay heights being 60 or 70 cm higher.

8.6 Discussion

8.6.1 Climate Model Accuracy and Past Critiques

Focusing initially on the construction of the UKCP09 model, UKCP09 uses HadSM3 as a base model, which is not as accurate at modelling energy transference over the atmosphere-ocean interface as HadCM3 (DEFRA, 2011a). For this reason the UKCP09 used the IPCC AR4 MME for projection of sea level change instead (Jenkins *et al.*, 2007). The borrowed AR4 resolutions used in the UKCP09 sea level calculations are coarse and in places the grid squares are some distance from the coast (Figure 8.17).

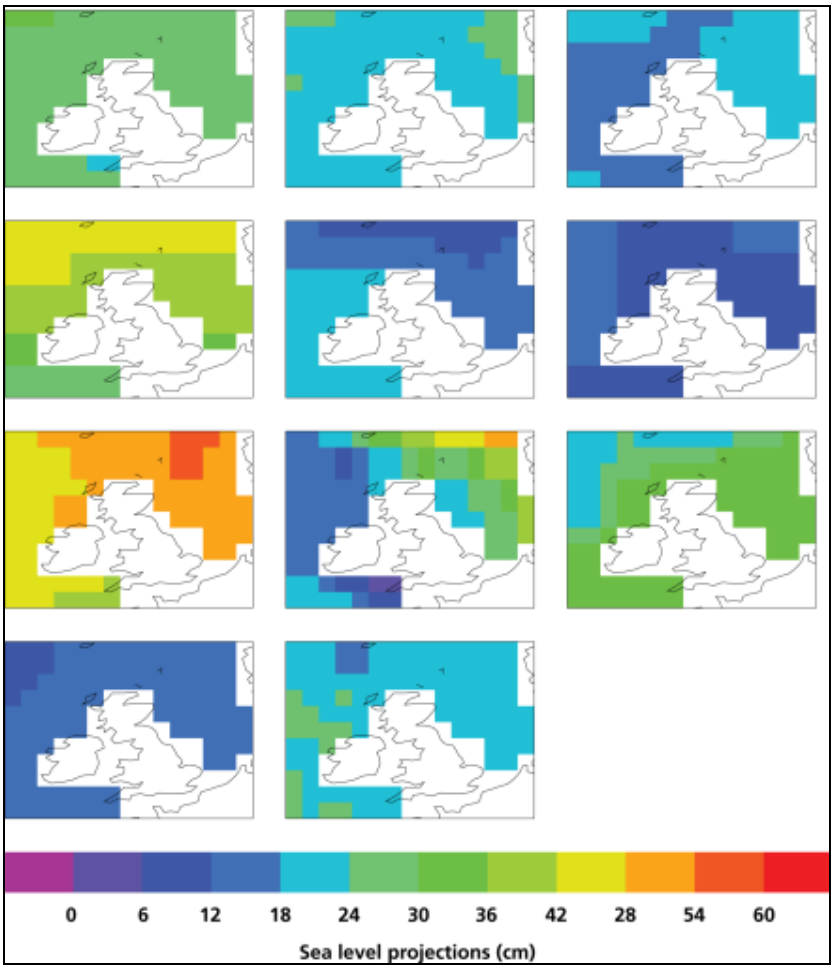

Figure 8.17. 'Sea level projections (cm) around the UK (not including land ice melt) for the end of the 21st century (2080–2099 relative to 1980–1999) for the medium emissions scenario. The data are from 11 model runs included in the MME (originally collated as part of the IPCC Fourth Assessment, processed and provided by Jonathan Gregory). Here, the data are projected to fit the resolution of the HadCM3 model (1.25° x 1.25°), and a common UK land region imposed' (Jenkins *et al.*, 2007).

Climate models that calculate sea level do not need historic sea level data for comparison; several models use temperature or pressure data relationships instead, as close relationships have been

determined between these variables and sea level (Climateprediction.net, 2010). However, simplified models can easily overlook the impact of specific climate variables.

Vermeer and Rahmstorf (2009) produced global sea level projections using a model developed purely from the global sea level-temperature relationship. This produced a non-linear projection of sea level change rates for the twenty-first century (Figure 8.4B). Several issues were highlighted with the Rahmstorf (2007) method (DEFRA, 2011b; Holgate *et al.*, 2007; Schmith *et al.*, 2007; Grinsted, 2009).

Rahmstorf (2010) compared the Vermeer and Rahmstorf (2009) estimated sea level range with that of IPCC AR4 (Solomon *et al.*, 2007), Rahmstorf (2007), Horton *et al.* (2008), Grinsted *et al.* (2009) and Jevrejeva *et al.*, (2010) (Figure 8.18). The Vermeer and Rahmstorf (2009) model agrees to some degree with Grinsted *et al*. (2009) and Jevrejeva *et al.* (2010), but it is considerably higher than the IPCC AR4 and Horton *et al.* (2008) models. The model variability for all of the models shown in Figure 8.18 is considerably, with the variability ranging from approximately 80 cm to over 180 cm. Considering that the lower limit of the IPCC AR4 model projected a global sea level rise of less than 25 cm, this range in projection is significant.

There are valid queries regarding the Vermeer and Rahmstorf (2009) model that have been acknowledged by the IPCC (Taboada and Anadón, 2010). One is that twenty-first century temperature rise is projected to be up to six times larger than the rise during the twentieth century (medium emissions scenario); therefore the relationship between temperature and sea level may change (DEFRA, 2011b).

Grinsted (2009) suggested that most models that use twentieth century temperature-sea level relationships to project large scale change cannot accurately hindcast past multi-centennial sea level change, including those of Vermeer and Rahmstorf (2009) and Grinsted *et al.* (2009). However, Grinsted (2009) continued to explain that neither of these relationship models was designed for the projection of multi-centennial analyses. The model accuracy for both models is radically improved when used over centennial time scales, which they were both originally designed for (Grinsted, 2009).

The MATLAB code designed for reproduction of the Vermeer and Rahmstorf (2009) projections has been criticised by Moriarty (2011) for being difficult to use. During adaptation of the code for use in the Forth and Tay Estuaries, it was discovered that the MATLAB code relied on several externally-sourced MATLAB Functions. Moriarty (2011) merged these m-files within an Excel spreadsheet version, which is simpler to use, includes all calculations in one file and is easily adaptable.

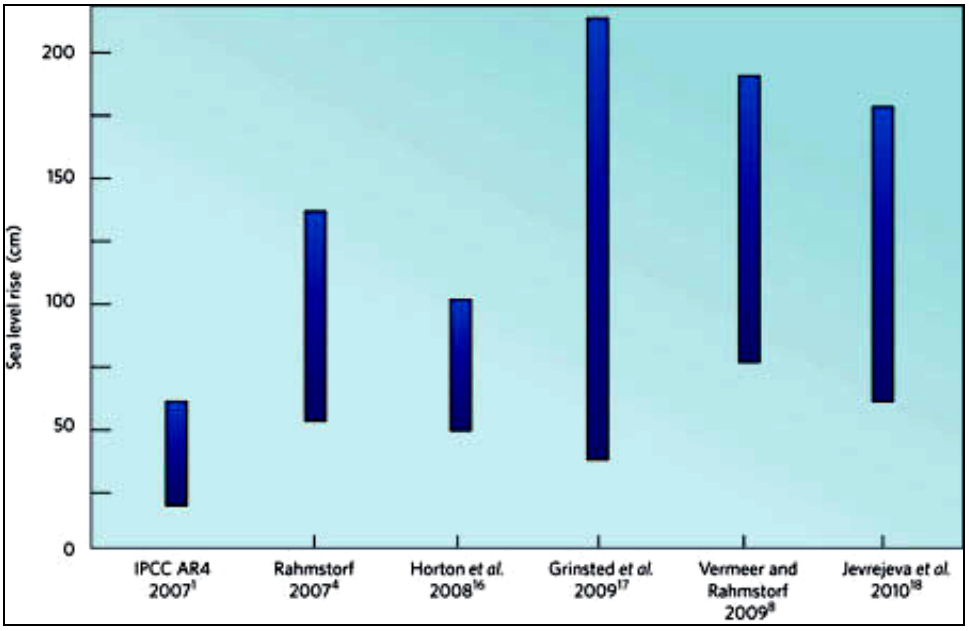

Figure 8.18. Estimates for twenty-first century global sea level rise from semi-empirical models (Solomon *et al.*, 2007; Rahmstorf, 2007; Horton *et al.*, 2008; Grinsted *et al.*, 2009; Vermeer and Rahmstorf, 2009; Jevrejeva *et al.*, 2010). For exact definitions of the time periods and emissions scenarios considered, see Rahmstorf (2010).

Adaptation of the Vermeer and Rahmstorf (2009) model in this thesis included adaptation of the Moriarty (2011) Excel spreadsheet. Temperature increases were imposed on replicated temperature data from previous decades throughout future projections, which provides a more realistic projection of decadal to multidecadal cycles. The temperature increases were set at increments that would gradually increase the average annual temperature until it reached the 2100 projected temperature level.

8.6.2 Sea Level Projections and Shoreline Structures

Quay heights at several economically-important sites were compared with present day sea level maxima heights and projected future maxima and HAT. Present day sea level maxima data are safely beneath the recorded quay heights, protecting the quays from overtopping for all but the extreme high level events. Gate heights should be taken into account, as several quays have maintained water heights that would be threatened by overtopping by the lowest point of the dock; i.e. the gate.

Two basic methods were used to project future extreme sea levels utilising maxima data and HAT heights (Section 8.4). Both methods included adding a 0.60 m freeboard to accommodate a safe development distance. Excluding the freeboard height, Method 1 produced extreme heights with

upper limits possibly 50 cm greater than some of the respective quaysides (Tables 8.6 and 8.8). Grangemouth in particular may experience flooding. Again excluding the freeboard height, Method 2 suggested there could be extremes of up to 71 cm above one of the quaysides (Tables 8.7 and 8.8). Method 1 requires extreme surge events to occur concurrently with HAT, which is improbable, so the heights are suggested to be less reliable than the results for Method 2. The extreme levels from Method 2 are more likely to occur by 2100, but on a very irregular basis.

8.7 Conclusion

In this chapter, past sea level and surge trends have been used to validate and construct sea level projections until 2100. Two renowned models were adapted to fit the Forth and Tay Estuaries, i.e. UKCP09 and that of Vermeer and Rahmstorf (2009). Under the IPCC A1B medium emission scenario, UKCP09 predicted absolute (i.e. eustatic) sea level rise for the UK of 0.394 m between 1990 and 2095 (Table 8.2). Vermeer and Rahmstorf (2009) predicted greater rates of absolute sea level rise of between 0.97 and 1.58 m (Table 8.1).

After GIA-correction, basic UKCP09 projection results (Table 8.4) suggest future medium emission scenario sea level increases of between 0.25 m and 0.58 m between 1990 and 2100 across the region. Under the same scenario, the GIA-corrected Vermeer and Rahmstorf (2009) projections suggest sea level increases of between 0.40 m and 0.73 m (Table 8.4). The Vermeer and Rahmstorf (2009) calculations were dramatically changed by the inclusion of Wada *et al.*'s (2010) groundwater depletion equation and Shennan *et al.*'s (2009) GIA corrections. After the Wada *et al.* (2010) corrections were applied, the regional projections by Vermeer and Rahmstorf (2009) overlapped the UKCP09 projections.

Projected extreme sea levels including a 0.6 m freeboard, extracted from the two methods in Section 8.5, range from 4.52 m above ODN to 6.60 m above ODN with Grangemouth projections including estuarine influences. Using the maxima data dependent Method 2, the lowest quayside recorded at each location may be overtopped by the highest extreme sea level events projected to occur by 2100. Using the higher and less probable Method 1 results, the lowest quaysides at each location may be overtopped by over 1 m by the highest extreme sea level events projected to occur by 2100.

Chapter 9 – Discussion and Conclusions

Outlined within this chapter are the key findings of the thesis and their significance to the wider scientific community. These findings are related to the original aims and hypotheses as detailed in Chapter 1 and referred to throughout the chapter.

9.1 Tide Gauge Data

Data, recorded by float or pressure tide gauge systems, were transcribed and corrected before sea level analysis. Tide gauge collection methods and error margins are discussed in this section.

Aim 1 was to *identify the appropriate process needed for accurate tide gauge data correction*. After searching thoroughly through international, national and local archives for tide gauge data relating to the Forth and Tay Estuaries, data were collected from seven source institutes covering sixteen data locations; with each institute processing data differently. Some institutes were gifted data from different sources, which provided different levels of information about the gauge system, maintenance regimes and potential human error (Powell *et al.*, 2012). None of the presently published studies about tide gauge data or sea level change have provided collection and correction information to the extent described here.

To ensure consistency between the datasets, high frequency datasets, including the minute-by-minute datasets, 15 minute interval datasets and continuous paper records, were converted into high and low tide daily averages. The use of high and low tide daily averages, instead of daily averages composed from hourly data, ensures that the extreme high and lows are accounted for and reduces potential for loss of whole days of data when several hours of data are missing. The daily averages from both of these methods are comparable, allowing data used in the thesis to be directly compared with other studies.

Aim 2 was to *develop appropriate methods to create a process to piece together regional sea level trend(s) from multiple datasets*. To achieve this aim a large database of raw tide gauge data from the Forth Estuary, the Tay Estuary and Aberdeen was created (Chapter 5). Errors that were expected within the datasets including gaps, spikes, datum jumps and time slips (Woodworth *et al.*, 1999; Holgate *et al.*, 2007; Powell *et al.*, 2012), were corrected prior to data use. The final corrected datasets produced the following results, confirming **Hypothesis 1;** that *tide gauge data from the Forth and Tay Estuaries can be used to form a reliable dataset between 1900 and 2010*:

- Datum-corrected relative sea level data;
- GIA-corrected eustatic sea level data;

- Oscillation identification results;
- Long-term relative and eustatic sea level trends; and
- Historical storm surge results.

Twelve datasets, across five locations, were chosen for further analysis after datum correction; Dundee, Grangemouth, Rosyth, Leith and Dunbar. Data from each site spans over 20 years with all except Grangemouth having at least 20 years of consecutive monthly sea level data points. When the data were unified to form a combined dataset from 1900 to 2010, a relative sea level rise of between 10 and 12 cm was suggested (Chapter 5). These data are used to represent this region accurately as a historical trend (Section 9.4) and were robust enough for projection use (Section 9.6), agreeing with **Hypothesis 3;** that *multiple short datasets can be used to create a longer regional time series that allows for enough data for genuine relative sea level histories to be created, leading to robust enough data for projections*.

Tide gauge data errors, associated with gauge inaccuracies and recording limitations, have been documented in Tables 4.1 to 4.10. Table 4.10 is particularly useful, as it explains that the largest recording inaccuracy for the tide gauges is between ±0-160 mm. It is likely that these data have lower inaccuracies than estimated here, as additional cross-location comparisons have taken place.

The thesis has used existing methods to correct some errors. Notably, Woodworth *et al.* (1999) explained how the data could be corrected for datum jumps. Thus the Woodworth *et al.* (1999) correction method, as demonstrated in the correction of a PSMSL Aberdeen record to agree with another PSMSL Aberdeen record that had a slightly higher datum level, has been used. This correction allowed the continuation of one of the largest tide gauge records in the UK. Similar techniques were used to convert all of the datasets from their individual datums to OD.

Natural cycles were used in cross-site comparisons to validate data. Datasets have comparable peaks and troughs with neighbouring datasets. This knowledge can be used to reduce local influences and is necessary for regional comparison of relative sea levels. Data were obtained from Aberdeen for comparison with those from the Forth and Tay Estuaries and as a control record, because the Aberdeen data are commonly used in sea level studies and are known to be reliable.

All of these methods have reduced potential for mechanical and human errors that would influence the results presented here.

9.2 Land Movement Correction

Land movement considered in this thesis includes GIA, mining subsidence and infrastructural subsidence. This was an essential part of the correction and validation process. Shennan *et al.*'s (2012) GIA relative land level change (RLLC) model was used to confirm present day GIA rates in the Forth and Tay Estuaries, as well as to convert relative sea level data into eustatic sea level data. Shennan *et al.* (2012) calculate GIA RLLC rates to be between 0.9 and 1.2 mm a^{-1} across the Forth and Tay Estuaries with the highest rates being at the estuary heads, decreasing towards their mouths. The model was used in place of an advanced ice-Earth model, because large global models, such as ICE-4G, cannot accurately model the topographic change in areas of the Scottish mountains and the formation of raised beaches within the Forth and Tay Estuaries (Berge-Nguyen *et al.*, 2008).

One method employed to model the potential eustatic sea level trends of the Forth and Tay Estuaries was to remove Shennan *et al.*'s (2012) GIA levels from five local sites along with Aberdeen. This involved plotting the datum-corrected relative sea levels for the region and converting these relative sea level data from OD to each site's 1990 mean datum, i.e. the mean 1990 sea level will then equal 0 m. These data were then compared with data that GIA has been removed from between 1900 and 2010. The Aberdeen dataset underwent the same manipulation process. There was a residual difference between the Aberdeen GIA-corrected and Forth and Tay Estuaries GIA-corrected datasets (Figure 5.57 and 5.58).

The resultant 'GIA-corrected' sea level trends from 1900 were considerably closer to the eustatic rate than the original relative sea level dataset (Figure 5.59). The difference in height between the Aberdeen and the combined Forth and Tay Estuaries datasets in 1900 is reduced from ~77 mm to ~24 mm by removing the Shennan *et al.* (2012) GIA RLLC rate. This is illustrated and explained in Chapter 5 (Figure 5.57 and Figure 5.58).

The reduced difference between the two datasets is substantial and the final inaccuracy is equivalent to a GIA error of 0.27 mm a^{-1} between 1900 and 1990 in either the Aberdeen dataset or the combined Forth and Tay Estuaries dataset. This additional variation could be due to miscalculation by Shennan *et al.* (2012) or a number of gauge and local issues at any of the sites. These GIA-corrected data can be used in comparison with tide gauge data from any geographical location that has been corrected for datum and converted to eustatic sea levels by removing the calculated GIA height.

Previous studies have used Bradley *et al.* (2009) to represent present day GIA rates (Rennie and Hansom, 2011; Lowe *et al.*, 2009), not fully understanding that Bradley *et al.* (2009) designed their model to observe changes to the solid rock surface and not the ocean geoid, i.e. only presenting

Vertical Land Motion (VLM) heights instead of RLLC. This issue has also influenced one of the models discussed in Section 9.6.

To summarise the land and infrastructural movement assessments discussed in Chapter 4, corrections of tide gauge data for land movement are not necessary as none of the tide gauge sites are experiencing mining or infrastructural subsidence. However, if eustatic sea level needs to be calculated, GIA corrections of between 0.9 and 1.2 mm a^{-1} need to be applied.

9.3 Sea Level Oscillations

As part of **Aim 3**, it was necessary to evaluate and understand the usefulness of local tide gauge data for sea level oscillation identification. Relative sea level records were analysed for decadal and multi-decadal cycles, such as the North Atlantic Oscillation (NAO), Arctic Oscillation (AO), Atlantic Multi-Decadal Oscillation (AMO) and the North Atlantic Oscillation Low Frequency Oscillation (LFO), which were introduced in Section 2.3.

Relative sea levels have been higher than in 2008, specifically between the late 1940s and early 1950s, when coinciding AMO, NAO and Saturn-Jupiter cycle high periods with AO and LFO low periods (with inverse effects on sea level) were major contributors to significant high relative sea levels in Aberdeen. Since the 1980s a fast rate of sea level rise has occurred coinciding with an increasing AMO and decreasing LFO. These dominant cycles warp short-term 15 year tide gauge datasets.

Using the Department of Atmospheric and Oceanic Sciences at the University of Colorado's (ATOC, 2011) Morlet wavelet analysis MATLAB Function, based on Torrence and Compo's (1998) calculations and modulated by a Gaussian envelope, all of the data from the Forth and Tay Estuaries were analysed for sea level oscillations (Section 6.4). The Dunbar dataset was also processed with three separate techniques: Welch's Power Spectral Density Estimate, the Ricker 'Mexican Hat' Scalogram and Fast Fourier Transform using the Microsoft Excel Add-In 'Data Analysis Toolpak'. All three agreed with the Morlet wavelet transform-based analyses, but were either too complicated for the general viewer to read (Ricker 'Mexican Hat' Scalogram) or too over-simplified to identify more than the single largest oscillation.

The Morlet wavelet transform-based analysis results agree closely with the finding of Jevrejeva *et al.* (2006) with oscillations identified being approximately 3-4, 5-7 and 10 years in frequency. This accurate identification of several oscillations in the primary tide gauge data corroborate part of **Hypothesis 2**, i.e. *primary and secondary data can identify multi-annual to multi-decadal sea level trends*. Other oscillations identified are approximately 15, 18-20 and 30 years in frequency. These

oscillations correlate with some of the NAO, AO and LFO frequencies of 1-3, 10 and 30 years (Polykov and Johnson, 2000; Czaja and Marshall, 2001; Hurrell, 1995).

The longer frequency Atlantic Multi-Decadal Oscillation (AMO), of 60-70 year frequencies, would not appear in these analyses, but may still influence the relative sea level. Other astronomical cycles that correlate with the frequencies found in the data from the Forth and Tay Estuaries include the 18.6 year lunar nutation (nodal) cycle, the 11 and 22 year sunspot/double sunspot cycles and the 19.9 year Saturn-Jupiter orbital cycle.

9.4 Past Relative Sea Level Change

As part of **Aim 3**, local tide gauge data were evaluated to assess how useful they are for historical sea level analysis. Without these data the thesis would not be able to accurately compare local relative sea levels with historic global sea level trends.

Relative sea level data have been investigated within several studies, including those of Douglas (1997) and Woodworth *et al.* (1999). Highly reliable global sea level records have been produced, representing twentieth century eustatic sea level trends. Douglas (1997), Jevrejeva *et al.* (2008) and Church and White (2006) identified the average global sea level rise to be between 18.5 and 19.5 cm between 1900 and 1995/2004. Church and White (2011), using a tide gauge dataset from 1880 to 2009, suggested the global sea level rise has been 1.7 ± 0.2 mm a^{-1} (Solomon *et al.*, 2007).

Douglas (1997) set out a list of accuracy guidelines that data must comply with to be included within results. Some of these guidelines are that datasets must be over 60 years in length, not located at convergent plate boundaries, over 80% complete, show agreement with nearby gauges and not located in regions of high glacio-isostatic movement. As the datasets in this thesis tend to be short in duration, another method has been used to combine individual dataset to form a reliable, combined dataset.

Four of the datasets collected and corrected for the thesis have relative sea level rates of +0.23 to +0.56 mm a^{-1} between 1900 and 2010 (Section 6.2); significantly lower than the 1.7 mm a^{-1} calculated by Church and White (2011) as the average global sea level trend, which is not as accurate as local trends due to geographical variability in sea level. However, when these rates are corrected for the Shennan *et al.* (2011) RLLC GIA rate for this region (0.9 to 1.2 mm a^{-1}), the resultant sea level rates are very close to the Church and White (2011) rate, at approximately +1.43 to 1.46 mm a^{-1}. The minor difference between the GIA-corrected dataset and the Church and White (2011) rate could be due to the geographical variation in eustatic sea level. The four longest datasets, Dunbar, Dundee, Leith and Rosyth, have been used for long term analyses.

Grangemouth, having a lot of missing data within its timeline, cannot be used for long or short term trend analyses, but does correlate with short overlapping parts of the Dundee data and cycles. Grangemouth data are representative of parts of the generic decadal sea level cycles and adequately represent relative sea levels at times when data are available. Therefore, Grangemouth data can be used as part of a regional sea level compiled database.

9.5 Sea Level Surge and Maxima Data

This section discusses the analysis of sea level maxima data and residual tidal data. Part of **Aim 3** was to evaluate the usefulness of local tide gauge data for surge and maxima analysis. The residual tidal data and maxima data, extracted from the local tide gauge data between 1979 and 2010 are discussed in Sections 9.5.1 and 9.5.2. **Aim 5** was to identify if areas of the Forth and Tay Estuaries would be under threat from future sea level flooding. The two flood maps discussed in Section 9.5.3 could have been essential to this aim, were it not for the points highlighted. These data also corroborated part of **Hypothesis 2**, suggesting that *primary and secondary data can identify surge events*.

9.5.1 Sea Level Maxima Data Use

Sea level maxima data used in this thesis, include secondary data from Graff (1981) at Grangemouth and Leith between 1939 and 1978 as well as three primary datasets from the Forth and Tay Estuaries between 1979 and 2010; specifically Dundee, Grangemouth and Leith. The top five recorded maxima heights at five ports in the Forth and Tay Estuaries are documented in Table 7.5; the majority of which have an average height between 3.5 and 4.0 m above OD.

Before comparing the Graff (1981) secondary data and primary data, primary data were processed into three datasets:

- Highest 20 maxima across the timescale;
- Highest 10 maxima per annum;
- Graff's (1981) analysis of the five year running means (Chapter 7).

Section 7.4 provides in depth information about the results from these three methods. The first method can identify periods where a number of maxima events have occurred within a short time frame. This method is adequate for event identification in continuous datasets, but not in sporadic datasets such as that from Grangemouth.

Method 2, using the highest 10 maxima per annum, removes the temporal variability of the data selection. These data are directly comparable across locations and provide a large amount of maxima information. Instead of using one highest maxima level per year, which could be construed as a natural anomaly, the use of the 10 highest maxima per year provides supportive evidence of data validity. The highest maxima height from the primary Grangemouth dataset was higher than 4 m above OD and four out of the top five recorded maxima across the Forth and Tay Estuaries were recorded at Grangemouth.

Method 3, using the Graff (1981) five year running mean sea level maxima method, converted the mean average of the top 10 maxima per year into five year running sea level maxima means. Some of the annual data were lost during this process, as to form a five year running mean for a single year it is essential to have two years of data before and after. As Grangemouth has data missing at different time periods, more data were lost from this dataset than the others. The data are presented in Figures 7.12, 7.22, 7.23 and Table 7.5. The highest maxima recorded at Grangemouth were 4.13 m above OD.

Graff's (1981) 1950 to 1975 maxima data for several locations around the Scottish coast were used by Pethick (1999) and Rennie and Hansom (2010) to depict sea level trend reversal, i.e. a sudden change from a decreasing relative sea level trend to an increasing relative sea level trend; suggested to have occurred in the early 1970s due to a reduction in GIA levels. This research suggests this was actually a turning point in the 30 year North Atlantic Oscillation (NAO) cycle that was more evident in the longer timescale English maxima records. If these studies had observed longer datasets than the Graff (1981) Scottish datasets, the authors would have observed that relative sea levels around Scotland have been rising since before the mid-1860s when the Aberdeen dataset started recording.

Sea level oscillations and cycles, such as the NAO, are closely linked with storminess (Hickey, 1997; Woodworth *et al.*, 2007; Ball *et al.*, 2009), which has been discussed further in Chapter 7.

9.5.2 Residual Tidal Data Use

Comparison of flooding dates identified by secondary sources and residual data from nearby tide gauges suggests that several flood events have occurred simultaneously with surge events in the Forth and Tay Estuaries, including the August 2004 flood event (Section 7.5).

Reports produced by local riparian authorities are often too brief in their description of events. Several areas subject to flooding between 2000 and 2010 have been identified, including Riverside Drive in Dundee, Broughty Ferry, Anstruther, St. Andrews, Grangemouth, Kirkcaldy, North

Berwick, Fisherrow, Kinghorn, North Queensferry, Port Seton, Dunbar, Cramond, Silverknowes and Musselburgh (Section 7.3). The extent to which flooding occurred was not, however, documented.

Residual tidal heights are available at five locations in the Forth and Tay Estuaries, namely the Forth Ports locations at Grangemouth, Rosyth, Leith, Methil and Dundee. Two sites have been selected for review, Leith and Dundee, as representative datasets for their estuaries. Data are available between 2003 and 2010, but data after September 2008 are suspect and have been excluded from analyses (see Chapter 7). Residual data used here have been produced using the tide gauge prediction software.

To analyse whether the highest tidal residuals correlate with recorded surge/flood events, the highest five residual tidal heights for Dundee, Leith and Grangemouth were compared with surge events recorded by local authorities (Table 7.6). The average for each site was 1.18, 0.93 and 1.84 m above predicted, respectively. Residual heights of up to 1.31 m have been recorded at Dundee, 1.09 m at Leith and 2.06 m at Grangemouth between 2003 and 2010. More commonly, residual heights reached 0.7 m at Dundee, 0.4 m at Leith and 0.7 m at Grangemouth. Only one of the surge/flood events recorded by riparian local authorities correlates with any of the highest residual tidal levels, on 12 January 2005, when a 'hurricane' scale storm surge occurred (Dundee City Council, 2005). This date also agrees with the highest sea level maxima data at Grangemouth, Leith and Rosyth (Table 7.5 and 7.6).

9.6 Relative Sea Level Projection

Aim 4 was to *review simplistic sea level projections made by international and national sea level models adapted for the Forth and Tay Estuaries*. To achieve this aim, simplified models and General Circulation Models (GCMs) were analysed. For high levels of accuracy, sea level models should be based on sea level datasets of 15 years or over; preferably 30 to 50 years, to maintain standard errors of below 0.5 to 0.3 mm a^{-1} respectively (Woodworth *et al.*, 1999). IPCC AR4 suggests 50 years of data are needed for reliable sea level scenario creation, but itself relies on the temperature-sea level relationship to project sea level change (Solomon *et al.*, 2007).

GCMs attempt to simulate as many different variables to the highest quality possible; this involves manipulation of equations within reasonable limits until the model results fit the observed trends to the best possible degree of accuracy (climateprediction.net, 2010). GCMs are considered by some to be more accurate than simplified models due to their intensive modelling and boundary conditions.

Simplified models are quicker and easier to replicate (Chapter 8) and focus on the observed relationships between two or more climate variables, but some can omit important elements.

For this thesis, it was unfeasible to construct an entire GCM for sea level projection, but one GCM and one simplified model were adapted, as discussed below.

9.6.1 GCMs – UKCP09 Adaptation

The UKCP09 regional GCM provides a set of probabilistic projections based on the UKMO Multi-Model Ensemble (MME). The UKCP09 projections are available through an easy-access User Interface, which uses three IPCC SRES emissions scenarios; B1 (low), A1B (medium) and A1FI (high) (DEFRA, 2011a; Nakićenović *et al.*, 2000).

Some suggestions for improvement are that the UKCP09 sea level projections need to be based on original historical sea level data. The UKCP09 sea level projections are actually based on historic 1961 to 2000 gridded temperature data created by the UKMO. Global temperature projections are presumed by UKCIP to be more robust than their sea level projections, due to the comparable number of model runs of the projection models (DEFRA, 2011b). Also, the model needs to be of a finer resolution for regional analyses (DEFRA, 2011b; UKCIP, 2009).

The GIA VLM rates of Bradley *et al.* (2009), which are used in UKCP09, ignore present day land level movement caused by changes to the ocean geoid. Across the three emissions scenarios, UKCP09 projected a relative sea level rise range for the Forth and Tay Estuaries of 30.9 to 35.1 cm above the 1990 mean (Table 8.5) (DEFRA, 2011a).

The UKCP09 projected relative sea level change for three tide gauge recording sites, namely Dundee, Dunbar and Grangemouth, which have been compared (Figure 8.12). Each of these records has been designed by UKCIP to project relative sea levels using the Bradley *et al.* (2009) VLM GIA rates calculated for each grid square (DEFRA, 2011a). Taking into account the pattern of GIA change across two estuaries, as expected Dunbar has the highest rate of sea level rise, followed by Dundee and then Grangemouth. All three sites are projected to experience less than 0.45 m of sea level rise under the high emission scenario (50th percentile) (DEFRA, 2011a).

The UKCP09 projected relative sea level changes at each site are considerably different to those of the projected sea level changes corrected for GIA using Shennan *et al.*'s (2012) GIA RLLC rates (Table 8.3 and Table 8.4). Dunbar, in particular, has been allocated a GIA rate by UKCIP that is approximately 0.70 mm a^{-1} smaller than the Shennan *et al.* (2009) rate, which was available before UKCP09 was released (Table 8.4).

Ultimately the UKCP09 2095 relative sea level projections could be inaccurate by as much as 8.9 cm in the Forth and Tay region across the 1900 to 2010 timeline; specifically at Dunbar (Table 8.3 and Table 8.4) due to the GIA model choice. If the UKCP09 was updated to use the Shennan *et al.* (2011; 2012) GIA model, Dunbar's 2095 projected high emission scenario relative sea level change would reduce from 35.1 cm to 27.5 cm.

9.6.2 Simplified Models – Vermeer and Rahmstorf (2009) Temperature-Sea Level Relationship Model

Vermeer and Rahmstorf (2009) used GISS temperature data and Church and White's (2006) sea level data, along with IPCC SRES emission scenarios (Nakićenović *et al.*, 2000) to project a global sea level rise of 0.75 to 1.9 m by 2100.

To visualise how relative sea levels are projected to change between 1990 and 2100, in comparison to the 1900 to 2010 relative sea level data, both the Vermeer and Rahmstorf (2009) corrected simplified model and the UKCP09 corrected probabilistic projections model were plotted with the historical trend in Figures 8.15 and 8.19. This comparison between the models and historical trend, a method aligned with **Aim 3** of this thesis, illustrates that these projections are significantly higher than the twenty-first century relative sea level trend at this location.

The Vermeer and Rahmstorf (2009) model has been critiqued previously for being difficult to recreate (Moriarty, 2011; Grinsted, 2009a; b; Tamboada and Anadon, 2010); particularly concerning their MATLAB Function. During adaptation of the code for use in the Forth and Tay Estuaries, it was discovered that it relied on several externally-sourced MATLAB Functions, increasing the potential for errors to occur. Moriarty's (2011) Excel spreadsheet version is considerably simpler to use, includes all calculations in one file and is easily adaptable.

Another concern that has been highlighted by the UKCIP is that twenty-first century temperature rise is projected to be up to six times larger than the rise during the twentieth century (medium emissions scenario), therefore the relationship between temperature and sea level may change (DEFRA, 2011b). If this is the case, then all temperature-sea level relationship based sea level projections, including the UKCP09 and IPCC AR4 projections, would change and may become inaccurate.

The Vermeer and Rahmstorf (2009) model results, seen in Figure 8.18, indicate potential sea level rise of 1324.75 mm (1.32 m) under a high emission scenario and 1073.64 mm (1.07 m) under a medium emission scenario by 2100. When the sea level data are corrected for GIA of 1.1 mm a^{-1} (the average for the Forth and Tay Estuaries), the average medium emission scenario sea level

height is reduced to 941.64 mm (0.94 m), but Moriarty (2011) suggests another element of analysis can reduce this further.

Moriarty (2011) reviewed two highly relevant studies that could have a great impact on Vermeer and Rahmstorf's calculations; those of Chao *et al.* (2008) and Wada *et al.* (2010). Chao *et al.*'s (2008) artificial reservoir storage calculations have been used by Vermeer and Rahmstorf (2009) to correct the GISS temperature data and Church and White's (2006) global sea level data (Moriarty, 2011; Vermeer and Rahmstorf, 2009). Their calculations explained that throughout the twentieth century global artificial reservoirs have withheld increasingly large quantities of water from the sea and therefore reduced the overall potential sea level change.

Chao *et al.*'s (2008) study neglected to investigate the fluctuation of groundwater levels, which could counterbalance the artificial reservoir retention. In 2010 Wada *et al.* estimated the rate of groundwater depletion and found it to be greater than that of artificial reservoir storage. Therefore, Wada *et al.*'s (2010) calculations should also be included in Vermeer and Rahmstorf's equation.

The Vermeer and Rahmstorf (2009) calculations were dramatically changed by the inclusion of Wada *et al.*'s (2010) groundwater depletion equation and Shennan *et al.*'s (2009) GIA corrections. Under the medium emissions scenario, with the Chao *et al.* (2008) and Wada *et al.* (2010) corrections, the Vermeer and Rahmstorf (2009) projections suggest sea level increases of between 0.51 m and 0.54 m (Table 8.5).

Although the Vermeer and Rahmstorf (2009) projections have been corrected and suggest reduced relative sea level rise, the medium emission scenario projections are still over 0.15 m above the GIA-corrected UKCP09 sea level projections for the Forth and Tay Estuaries (Table 8.5).

9.7 Projected Storm Surges

The IPCC AR4 and UKCP09 both projected that storm surges would decrease in frequency and increase in magnitude by 2100 (Solomon *et al.*, 2007; Lowe *et al.*, 2009). The UKCP09 used the POLCS3 tide-surge model to project surge change (Dixon and Tawn, 1994; 1995; 1997; Flather *et al.*, 2001; Williams and Flather, 2004; Lowe *et al.*, 2004; Jones and Davies, 2009). The POLCS3 model projections for Scotland outlined that the northern and western coastlines would continue to experience higher surge events than that of eastern Scotland. It also projected increasing surge heights; the model suggesting that the height of a 1:50 year storm surge may increase by ~0.8 mm a^{-1}, which is significantly less than the 5 mm a^{-1} that the UK Climate Impact Programme predicted in their 2002 report (Lowe *et al.*, 2009; Hines, 2010). However, when the trend is converted into an

overall increase by 2095, surge heights are projected to increase from a range of 0.5-1.0 m to 0.9-1.5 in the Forth and Tay Estuaries (Figure 8.10) (Lowe *et al.*, 2009).

The projected surge increases are significantly higher than the projected relative and eustatic sea level changes for the same period. This is particularly perplexing as relative sea levels are projected to increase by an insignificant fraction of the overall nearshore depth, whilst surges are projected to increase by one third of their original nearshore height. There is no comparison in the scale of change between the projections of the two processes. This element of incomparability reduces confidence in the POLCS3 tide-surge model, therefore this model was not utilised in this thesis.

However, even though the projections of the POLCS3 model are questionable, the original results for the Forth and Tay Estuaries are very similar to the average residual height recorded in the region (Chapter 7). Several residual records for the area were higher than the 0.9 m upper boundary of the POLCS3 projections. This difference can be explained by means of Figure 8.8, referring back to the difference between residual heights and surge skew heights, which tend to be smaller. As the residual tidal records and the sea level maxima data are reliable and accurate site specific records, they were used as part of the projection models discussed below to identify if areas of the Forth and Tay Estuaries would be under threat from future sea level flooding, achieving **Aim 5** of this thesis (see Section 9.5 for storm surge heights).

9.8 Final Projection Results

The main purpose of the projections produced by the thesis was to achieve **Aim 5**, to *identify if areas of the Forth and Tay Estuaries would be under threat from future sea level flooding.* After GIA-correction, UKCP09 projection results (Table 8.5) propose future medium emission scenario relative sea level rise of between 0.24 m and 0.27 m between 1990 and 2100 across the region. Under the same scenario and with Wada *et al.*'s (2010) groundwater abstraction corrections, the GIA-corrected Vermeer and Rahmstorf (2009) projections suggest sea level increases of between 0.51 m and 0.54 m (Table 8.5), as stated in Section 9.6.

Two basic methods were used to project future sea level maxima and highest astronomical tide heights (Section 8.4):

- Method 1, projected relative sea level and surge levels with quay heights – HAT + modelled relative sea level change + residual tidal heights + freeboard by 2100;
- Method 2, projected maxima levels with quay heights – average highest maxima + modelled relative sea level change + freeboard by 2100.

Both methods rely on the corrected UKCP09 relative sea level projections for 2100. Using Method 1, Table 8.9 presents the calculated extreme relative sea level projections for the region to be between 5.18 and 5.64 m OD. Method 2 projected a range of heights between 4.52 to 5.24 m OD, which are considerably lower than the results from Method 1.

Comparing quay heights with potential maxima rise is a simple method of estimating if sea defences can withstand future still water levels. The highest maxima heights across the region, measured above OD, were 3.69 m (Dundee), 4.13 m (Grangemouth), 3.96 m (Leith), 3.27 m (Methil) and 3.93 m (Rosyth). The average maxima heights constructed from the top five maxima and more practical for management purpose are 3.53 m, 4.04 m, 3.75 m, 3.20 m and 3.74 m OD, respectively. The quayside heights are estimates of the lowest parts of the seaward quaysides, but do not account for lower port gates or lower quaysides inside docks. These locations also need to be accounted for on a site by site basis.

For impounded ports, lock gate heights should be taken into account, as several ports have maintained water heights, where quays could be threatened by overtopping of the lowest point of the dock; i.e. the gate. Quay height and sea level maxima comparison has been used by several pre-development flooding assessments along the Forth Estuary in the last ten years, including (amongst others) the Skinflats Realignment Scheme (Babtie Group, 2001) and the Leith Renewable Energy Plant (Forth Energy, 2010a).

The Leith Renewable Energy Plant Flood Risk Assessment (Forth Energy, 2010a), considered fluvial and coastal flood risk of the area around Imperial Dock, Albert Dock and Edinburgh Dock. In this area the land height ranges from 5.0 m to 6.2 m OD. These heights were compared with extreme water level and potential storm surge levels published by SEPA (2006) and UKCIP (DEFRA, 2011a) as well as the Highest Astronomical Tide (HAT) level.

Combined HAT levels at Leith (3.4 m OD) and UKCP09 projected storm surge extreme levels in the Forth Estuary (1.25 m OD) were utilised by Forth Energy (2010a) to illustrate a maximum extreme still water level of 4.65 m OD. Babtie (2001) indicated the 50 year and 100 year surges can increase the projected sea level by 1.5 m and 1.65 m, respectively, which would add 0.25 to 0.40 m. It was the Forth Energy (2010a) report that suggested using a 0.6 m freeboard. Together the 3.4 m HAT and 1.25 m surge would create an extreme height estimate of 5.25 m OD.

In Chapter 8, Dundee and Grangemouth are analysed using the Forth Energy (2010a; 2010b; 2010c) storm surge extreme level method, identifying the HAT, adding the pre-calculated extreme level for 2100 and the freeboard height. For these two scenarios, the lowest point of Dundee's quayside could be overtopped by the highest extreme sea level and the lowest point of Grangemouth's quayside could be overtopped by over 1.5 m by the highest extreme sea level. Neither site could

accommodate a freeboard level (Tables 8.9 and 8.11). Again, excluding the freeboard height, Method 2 suggested there could be extremes of up to 20 cm below the quayside height at Dundee (Tables 8.10 and 8.11). Method 2 is the more reliable method.

9.9 Conclusions

Before initiation of this thesis, there were no existing relative sea level studies focusing on the Forth and Tay Estuaries. As a product of this study, a historical relative sea level database has been constructed, identifying relative sea level trends of +0.23 to +0.56 mm a^{-1} between 1900 and 2010 in the region. To create historical trends from tide gauge data from the Forth and Tay Estuaries, the thesis used reliable collection and correction methods developed for this purpose. As such, this process has achieved two of the research aims and the first hypothesis of the thesis.

- **Aim 1 -** *Identify the appropriate correction process needed for accurate tide gauge data correction and explain these.*
- **Aim 2 -** *Develop appropriate methods to create a process to piece together regional sea level trend(s) from multiple datasets.*
- **Hypothesis 1** - *Tide gauge data from the Forth and Tay Estuaries can be used to form a reliable dataset between 1900 and 2010*.

Taking this further, analysis of recorded sea level maxima heights and tide gauge residual heights using both primary and secondary data identified the highest surge events across the Forth and Tay Estuaries. There were extreme residual heights of up to 1.31 m at Dundee, 1.09 m at Leith and 1.84 m at Grangemouth between 2003 and 2010, but more commonly residual heights reached 0.7 m at Dundee, 0.4 m at Leith and 0.7 m at Grangemouth. The highest five maxima recorded at Grangemouth, Dundee, Leith, Rosyth and Methil ranged between 3.27 and 4.13 m above OD (Table 7.5). These results, along with the historical sea level analysis and sea level oscillation identification discussed in Chapter 9, achieved Aim 3 and confirmed with the second hypothesis of this thesis.

- **Aim 3 -** *Evaluate the usefulness of local tide gauge data for historical sea level analysis, surge and maxima analysis, sea level oscillation identification and sea level projections.*
- **Hypothesis 2** - *Primary and secondary data can identify multi-annual to multi-decadal sea level trends and surge events*.

In 2009, part way through this research, two sea level projection models were made available; the UKCP09 probabilistic projections General Circulation Model (GCM) and the Vermeer and Rahmstorf (2009) temperature-sea level relationship simplified model. Both models were adapted in Chapter 8, correcting inaccuracies thereby decreasing the original projections.

For the Forth and Tay Estuaries, the UKCP09 projections were originally 31.3 to 35.1 cm above the 1990 mean. These values decreased to between 24.3 and 27.5 cm above the 1990 mean by replacing the Bradley *et al.* (2009) GIA Vertical Land Motion (VLM) calculations with the Shennan *et al.* (2012) GIA Relative Land Level Change (RLLC) calculations, which are deemed more appropriate.

The Vermeer and Rahmstorf (2009) sea level projections, originally calculated to be 107.5 cm above the 1990 mean, was reduced greatly by correction made in the thesis. Two corrections were made for GIA and groundwater extraction using Shennan *et al.*'s (2012) and Wada *et al.*'s (2010) calculations. Using historical trends to aid these projections, the final projections for the Forth and Tay Estuaries made using this method were 50.9 to 54.2 cm above the 1990 mean; significantly greater than those produced with the UKCP09 GCM.

These corrections followed critiques made about the two models and the corrected results have not previously been published. The process of adapting these models accomplished Aim 4 and confirmed the third hypothesis of this thesis.

- **Aim 4** - *Review simplistic sea level projections made by international and national sea level models adapted for the Forth and Tay Estuaries.*

- **Hypothesis 3** - *Multiple short datasets can be used to create a longer regional time series that allows for enough data for genuine relative sea level histories to be created, leading to sufficiently robust data for projections*.

The relative sea level projections to 2100 were then used to estimate extreme sea levels across the Forth and Tay Estuaries and to compare these levels against present day quayside heights, thereby achieving Aim 5 of this thesis.

- **Aim 5** - *Identify if areas of the Forth and Tay Estuaries would be under threat from future sea level flooding.*

These extreme sea level calculations, based on an adaptation of the Forth Energy (2010) extreme sea level calculation for Leith, took into account the projected relative sea level range, a development freeboard, and either sea level maxima heights or tidal residual heights with respect to HAT (i.e. the storm surge component). The results suggest that by 2100, the most extreme sea level heights could reach quayside levels at several ports in the Forth and Tay Estuaries.

9.10 Recommendations

The recommendations given here are directed towards sea level researchers and local policy-makers, encouraging them to use the methods developed here along with the local relative sea level results:

- The sea level data collection and correction methods produced during this thesis are based on a selection of highly renowned studies, including that of Woodworth *et al.* (1999). It is suggested that future studies should follow these methods to reduce errors;
- The observed relative sea level data and trends identified here for the Forth and Tay Estuaries should be recognised by local policy-makers as being substantially lower than the global average;
- This thesis acknowledges the impact that sea level oscillations can have on short-term relative sea level data trends and suggests that similar approaches should be undertaken elsewhere;
- Sea level maxima and tidal residual data can be used to estimate the upper extreme relative sea levels that have occurred at specific locations;
- The UKCP09 and Vermeer and Rahmstorf (2009) models need to be corrected for GIA and groundwater extraction before being used to project relative sea level change to 2100;
- Sea level projections to 2100 can be combined with surge levels and a development freeboard to create extreme relative sea level projections, which can be compared with present day quayside heights to identify areas that may be at risk in the future. However, policy-makers should be aware that these calculations project the highest and most infrequent extremes.

9.11 Suggestions for Future Research

This chapter has highlighted the key findings and their significance to the wider community, including:

- An original, reliable tide gauge dataset dating between 1900 and 2010;
- Reliable relative sea level rates for the Forth and Tay Estuaries between 1900 and 2010;
- Original storm surge and sea level oscillation observations;
- Reliable storm surge heights between 1979 and 2010;
- Reliable corrections of two sea level projection models, projecting relative sea level change until 2100;

- Reasonable projections of potential extreme relative sea level heights at selected quaysides in the Forth and Tay Estuaries by 2100.

Ultimately this method has created a reliable relative sea level dataset. Therefore, local projections of relative sea level can be based on science and observation rather than sea level models designed to predict changes across UK-scale or continent-wide regions. This arms individual infrastructure owners/developers with the evidence to make genuinely informed decisions, rather than relying on the generic (often sensational).

In the course of this research, several suggestions for future research have emerged, which include:

- The potential for data collection and correction methods to be transferred to another location, producing more accurate, location specific, relative sea level data;
- The attachment of GPS recorders at several tide gauge sites across the region, to facilitate the monitoring of land movement over a long time period, to estimate the *actual* observed land movement. The data acquired could then be compared with the GIA RLLC rates of Shennan *et al.* (2012);
- The creation of a modelling tool that can predict how much each sea level oscillations can influence sea levels at set locations around the British Isles, thereby increasing the accuracy of long-term projections;
- Expansion of the investigation into how estuarine morphology impacts upon surge progression, by comparing data from several estuaries of varying shapes and sizes, such as the Clyde, Humber and Severn;
- Enhanced 3D sea level modelling to include estuarine influences, local temperature-sea level relationships, GIA and topography;
- The potential for the original UKCP09 probabilistic projections to be corrected from Bradley *et al.*'s GIA VLM model to Shennan *et al.*'s (2012) GIA RLLC model;
- Investigations into the link between sedimentation and relative sea level rise, which relies on data from port dredging regimes;
- Investigation of land movement at OS Benchmark and GPS locations across the UK through dGPS surveys;
- The potential for similar investigations into other estuaries, producing extreme relative sea level calculations and comparing these heights to local quayside or other infrastructure heights.

References

Aagaard, T., Black, K. P. and Greenwood, B. (2002) *Cross-shore suspended sediment transport in the surf zone: a field-based parameterization.* Marine Geology, vol. 185, pp. 283-302.

Abbott, M. B. and Price, W. A. (eds.) (1994) Coastal, Estuarial and Harbour Engineers' Reference Book. London: E & FN Spon.

Al-Jabbari, M. H., McManus, J. and Al-Ansari, N. A. (1980) *Sediment and solute discharge into the Tay Estuary from the River System*. Proceedings of the Royal Society of Edinburgh B, vol. 78, pp. 15-32.

Anderson, J. M. (1989) *Remote sensing in the Tay Estuary using airborne Thematic Mapper*. Chapter In: McManus, J and Elliott, M. (edts.) Developments in Estuarine and Coastal Study Techniques. Fredensborg: Olsen & Olsen, pp. 15-19. In: Bates, C. R. and Oakley, D. J. (2004) *Bathymetric sidescan investigation of sedimentary features in the Tay Estuary, Scotland*. International Journal of Remote Sensing, vol. 25, pp. 5089-5104.

Angus Council. (2005) Flood Prevention Report (5th Biennial Report). (20/07/2009) http://www.angus.gov.uk/ac/documents/floodprevention

Angus Council. (2009) Flood Prevention Report (7th Biennial Report). (20/07/2009) http://www.angus.gov.uk/ac/documents/floodprevention/

Angus Council. Shoreline Management Plan 1st Edition. Volume 2, Appendix 2 : 2.1 Wind, wave & tidal characteristics.

Antonov, J. L., Levitus, S. and Boyer, P. (2002) *Steric sea level variations during 1957-1994: Importance of salinity*. Journal of Geophysical Research, vol. 107, 8013.

Archer, D. (2006) Global Warming – Understanding the Forecast. Blackwell Publishers, Oxford, UK.

Armstrong, M., Paterson, I. B. and Browne, M. A. E. (1985) *Geology of the Perth and Dundee district*. Memoir of the British Geological Society, S. 48W, 48E and 49. London, HMSO.

Babtie Group. (2001) Feasibility and Implications of Managed Realignment at Skinflats. Babtie Group in conjunction with Northern Ecological Services and Coastal Research Group, University of Glasgow. Report to the Forth Estuary Forum. Scottish Natural Heritage.

Bali, T. G. (2003) *An extreme value approach to estimating volatility and value at risk*. Journal of Business, vol. 76, pp. 83-108.

Ball, T., Werritty, A., Duck, R. W., Edwards, A., Booth, L. and Black, A. R. (2008) FRM10: Coastal Flooding in Scotland: A Scoping Study Technical Summary. (10/10/2010) www.sniffer.org.uk

Ball, T., Booth, L., Duck, R.W., Edwards, A., Hickey, K. and Werritty, A. (2009) *Coastal Flooding in Scotland: Past, present and future.* Proceedings of Institution of Civil Engineers, 'Breakwaters (2009)' Conference, Aberdeen.

Barbosa, S. M., Fernandes, M. J. and Silva, M. E. (2006) *Long-range dependence in North Atlantic sea level*. Physica A, vol. 371, pp. 725-731.

Bates, C. R., Moore, C. G. and Malthus, T., Mair, J. M. and Karpouzli, E. (2004) Broad scale mapping of habitats in the Firth of Tay and Eden Estuary, Scotland. Scottish Natural Heritage Commissioned Report No. 007. Edinburgh: Scottish Natural Heritage.

Baxter, J. M., Boyd, I. L., Cox, M., Cunningham, L., Holmes, P., Moffat, C. F. (edts.) (2008) Scotland's Seas: Towards Understanding their State. Aberdeen: Fisheries Research Services.

Beardmore, N. (1862) Manual of Hydrology. Waterlow & Sons, London.

Bearman, G. (edt.) (1999) Waves, Tides and Shallow-Water Processes (2nd Ed.). Oxford: Butterworth-Heinemann.

Bellenden, J. (ed.) (1822) The buik of the croinclis of Scotland. H. Boece, Prose version, 3 Vols. In: McEwen, L. J. (1987) *Sources for establishing a Historic Flood Chronology (Pre-1940) within Scottish River Catchments*. Scottish Geographical Journal, vol. 103, pp. 132-140.

Berge-Nguyen, M., Cazenave, A., Lombard, A., Llovel, W., Kiarre, J. and Cretaux, J. F. (2008) *Reconstruction of past decades sea level using thermosteric sea level, tide gauge, satellite altimetry and ocean reanalysis data*. Global and Planetary Change, vol. 62, pp. 1-13.

Berger, W. (2012) *Hans E. Suess (1909-1993): Radiocarbon, Sun and Climate Pioneer*. Scripps Institution of Oceanography Technical Report, UC San Deigo. (01/11/2012) http://escholarship.org/uc/item/5bc4c0w7#page-13

Besley, P., Stewart, T. and Allsop, N. W. H. (1998) Overtopping of vertical structures: new prediction methods to account for shallow water conditions. In: Allsop, N W. H. (ed.) Coastlines, structures and breakwaters. London: Thomas Telford Publishing, pp. 46-57.

Bingley, R. M., Teferle, F. N., Orliac, E. J., Doodson, A. H., Williams, S. D. P., Blackman, D. L., Baker, T. F., Riedmann, M., Haynes, M., Aldiss, D. T., Burke, H. C., Chackfield, B. C. and Traigheim, D. (2007) Absolute fixing of tide gauge benchmarks and land levels measuring change in land and sea levels around the coast of Great Britain and along the Thames Estuary using GPS, absolute gravimetry, persistent scatterer interferometry and tide gauges. DEFRA/ EA Joint R&D FCERM Programme R&D technical report FD2319/TR, April 2009.

Bird, E. (2008) Coastal Geomorphology: An Introduction (2nd Ed.). Chichester: John Wiley & Sons.

Black, A. R. and Anderson, J. L. (1994) *The Great Tay Flood Disaster of January 1993*. UK 1993 Hydrological Yearbook Hydrology Data UK Series, pp. 29-34.

Black, A. R. and Burns, J. C. (2002) *Re-assessing the flood risk in Scotland*. The Science of the Total Environment, vol. 294, pp. 169-184.

Black, A. R. and Law, F. M. (2004) Development and utilization of a national web-based chronology of hydrological events. *Hydrological Science Journal*, vol. 49, pp. 237-246.

Blackburn, M., Methven, J. and Roberts, N. (2008) *Large-scale context for the 2007 floods in summer 2007*. Weather, vol. 63, pp. 280-288.

Boulton, G. and Hagdorn, M. (2006) *Glaciology of the British Isles Ice Sheet during the last glacial cycle: form, flow, streams and lobes*. Quaternary Science Reviews, vol. 25, pp 3359-3390.

British Broadcasting Company (BBC) Learning Zone Broadband Class Clips: Clip 4309, River Tay – Floods in 1993. (01/02/2012) http://www.bbc.co.uk/learningzone/clips/river-tay-floods-in-1993/4309.html

Bradley, S., Milne, G. A., Teferle, F. N., Bingley, R. M. and Orliac, E. J. (2009) *Glacial isostatic adjustment of the British Isles: new constraints from GPS measurements of crustal motion*. Geophysical Journal International, vol. 178, pp. 14-22.

Bradley, S., Milne, G., Shennan, I. and Edwards, R. (2011) *An improved Glacial Isostatic Adjustment model for the British Isles.* Journal of Quaternary Science, vol. 26, pp. 541–552.

Bretaña, G. (1987) Admiralty manual of navigation, volume 1. Ministry of Defence: Norwich.

Broecker, W. S. (1998) *Palaeocean circulation during the last deglaciation: a bipolar seesaw*. Palaeoceanography, vol. 13, pp. 119-121.

Browne, M. A. E. (1987) *The physical geography and geology of the estuary and Firth of Forth, Scotland*. Proceedings of the Royal Society of Edinburgh B, vol. 93, pp.235-244.

Brunel, C. and Sabatier, F. (2009) *Potential influence of sea-level rise in controlling shoreline position on the French Mediterranean Coast.* Geomorphology, vol. 107, pp. 47-57.

Buller, A. T. and McManus, J. (1971) *Channel stability in the Tay Estuary: controls by bedrock and unconsolidated post-glacial sediment.* Engineering Geology, vol. 5, pp. 227-237.

Buller, A. T., McManus, J. and Williams, D. J. A. (1971) Investigations in the estuarine environments of the Tay (Tay Estuary Research Centre). A – Physical Aspects. An Interim Report. Research Report No. 1. Dundee: TERC.

Bungenstock, F. and Schäfer, A. (2009) *The Holocene relative sea-level curve for the tidal basin of the barrier island Langeoog, German Bight, Southern North Sea*. Global and Planetary Change, vol. 66, pp. 34-51.

Burroughs, W. (edt.) (2003) Climate into the 21st Century. Cambridge: Cambridge University Press.

Cadell, H. M. (1913) The Story of the Forth. Glasgow: James Maclehose and Sons.

Camuffo, D. (1999) *Lunar influences on Climate.* Earth, Moon and Planets, vol. 85-86(0), pp.99-113.

Carrell, S. Hurricane-force winds hit Scotlamd as UK storms cause chaos. (08/12/2011) www.guardian.co.uk

Cazenave, A. and Nerem, R.S. (2004) *Present-day sea level change: observations and causes.* Reviews of Geophyics, vol. 42, RG3001.

Chapman, S. and Westfold, K. C. (1956) *A comparison of the annual mean solar and lunar atmospheric tides in barometric pressure, as regards their worldwide distribution of amplitude and phase*. Journal of Atmospheric and Terrestrial Physics, vol. 8, pp. 1-23.

Charlton, J. A., McNicholl, W. and West, J. R. (1975) Tidal *and freshwater induced circulation in the Tay Estuary.* Proceedings of the Royal Society of Edinburgh B, vol. 75, pp. 11-27.

Chao, B. F., Wu, Y. H. and Li, Y. S. (2008) *Impact of artificial reservoir water impoundment on global sea level*. Science, vol. 320, pp. 212–214.

Charlton, J. A. (1980) *The tidal circulation and flushing capacity of the outer Tay Estuary*. Proceedings of the Royal Society of Edinburgh B, vol. 78, pp. 33–46.

Charlton, J. A., McNicholl, W. and West, J. R. (1975) Tidal *and freshwater induced circulation in the Tay Estuary.* Proceedings of the Royal Society of Edinburgh B, vol. 75, pp. 11-27.

Chelton, D. B. and Davis, R. E. (1982) *Monthly mean sea-level variability along the west coast of North America*. Journal of Physical Oceanography, vol. 12, pp. 575-584.

Chowdhury, Md. R., Chu, P. -S., Schroeder, T. A. and Zhao, X. (2008) *Variability and predictability of sea-level extremes in the Hawaiian and U.S.-Trust Islands – a knowledge base for coastal hazards management*. Journal of Coastal Conservation, vol. 12, pp. 93-104.

Christie, A. (1980) P00095. (12/12/2012) http://geoscenic.bgs.ac.uk/asset-bank/action/viewAsset?id=2293&index=16&total=181&categoryId=1129&categoryTypeId=1&collection=Raised%20beaches&sortAttributeId=0&sortDescending=false

Church, J. A., Whilte, N. J., Coleman, R., Lambeck, K. and Mitrovica, J. X. (2004) *Estimates of regional distribution of sea level rise over the 1950-2000 period.* American Meteorological Journal, vol. 17, pp. 2609-2625.

Church, J. A. and White, N. J. (2006) *A 20th-century acceleration in global sea-level rise*. Geophysical Research Letters, vol. 30, L01602.

Church, J. A. and White, N. J. (2011), *Sea-level rise from the late 19th to the early 21st Century.* Surveys in Geophysics, vol. 32, pp. 585-602.

Clackmannanshire Council. (2007) Biennial Report – November 2007 as required by the Flood Prevention and Land Drainage (Scotland) Act 1997. (20/10/09) http://www.clacksweb.org.uk/document/1231.pdf

Clarke, S. and Elliott, A. J. (1998) *Modelling suspended sediment concentrations in the Firth of Forth. Estuarine*, Coastal Shelf Science, vol. 47, pp. 235-250.Cunningham, D. (1887) The River Tay Report. D. R. Clark & Sons: Dundee.

Climateprediction.net (2010) Modelling the climate. (10/01/2011) http://climateprediction.net/content/modelling-climate

Coal Authority (2010a) Coal Mining Report: Musselburgh Harbour Mouth, Mussleburgh, West Lothian. Report Reference 00029492-10, Unpublished.

Coal Authority (2010b) Coal Mining Report: Port of Rosyth Harbour Mouth, Rosyth, Fife. Report Reference 00029479-10, Unpublished.

Coal Authority (2010c) Coal Mining Report: Port of Grangemouth Tide Gauge Housing, Grangemouth, West Lothian. Report Reference 00029480-10, Unpublished.

Coal Authority (2010d) Coal Mining Report: Port of Methil Harbour Mouth, Methil Harbour, Fife. Report Reference 00029493-10, Unpublished.

Collins, J. A. (1972). *Prediction of shallow-water spectra.* Journal of Geophysical Research, vol. 77, pp. 2693-2707.

Courier, The. Scotland battered by hurricane-force storm (08/12/2011) www.thecourier.co.uk.

Cullingford, R. A. and Smith, D. E. (1966) *Late-glacial shorelines in Eastern Fife*. Transactions of the Institute of British Geographers, vol. 39, pp. 31-51.

Cullingford, R. A., Smith, D. E. and Firth, C. R. (1996) *The altitude and age of the main postglacial shoreline in Eastern Scotland.* Quaternary International, vol. 9, pp. 38-52.

Cunningham, D. (1895) The Estuary of the Tay. Great George Street, Westminster, S. W.: London.

Curry, J. A. (2003) Readings on Ice Ages (Milankovitch Cycles). School of Earth and Atmosphere Sciences, Georgia Institute of Technology. (Retrieved on 01/03/2003) http://curry.eas.gatech.edu/Courses/6140/Chapter10/Ency_Atmos/Ice_age.pdf

Czaja, A. and Marshall, J. (2001) *Observations of atmosphere-ocean coupling in the North Atlantic.* Quarterly Journal of the Royal Meteorological Society, vol. 127, pp. 1893-1916.

Davis, J. E., Latychev, K., Mitrovica, J. X., Kendall, R. and Tamisiea, M. E. (2008) *Glacial isostatic adjustment in 3-D earth models: Implications for the analysis of tide gauge records along the US east coast.* Journal of Geodynamics, vol. 46, pp. 90-94.

Dawson, S., Powell, V. A., Duck, R. W. and McGlashan, D. J. (2012) *"Discussion of Rennie, A.F. and Hansom, J.D. 2011. Sea level trend reversal: land uplift outpaced by sea level rise on Scotland's coast. Geomorphology, 125 (1), 193-202."* Geomorphology, In Press.

Dawson N., Söhle I., Wilson L.J., Dean B.J., Webb A. and Reid J.B. (2007) *The numbers of inshore waterbirds using the Firth of Forth during the non-breeding season, and an assessment of the area's potential for qualification as a marine SPA*. JNCC Report No. 402. Peterborough: JNCC.

De la Vega-Leinert, A. C. and Nicholls, R. J. (2008) *Potential Implications of SLR for Great Britain.* Journal of Coastal Research, vol. 24, pp. 342-357.

Denny, M. W. and Paine, R. T. (1998) *Celestial Mechanics, Sea-Level Changes, and Intertidal Ecology*. Biological Bulletin, vol. 194, pp. 108-115.

Department of the Environment, Food and Rural Affairs (DEFRA) (2009) What is UKCP09? (12/12/2009) www.ukclimateprojections.defra.gov.uk

Department of the Environment, Food and Rural Affairs (DEFRA) (2011a) UK Climate Projections User Interface. (12/07/2011) http://ukclimateprojections-ui.defra.gov.uk/ui/admin/login.php

Department of the Environment, Food and Rural Affairs (DEFRA) (2011b) Mitigating Climate Change – Defra's role. (11/07/2011) www.defra.gov.uk

Dixon, M. J. and Tawn, J. A. (1994). Extreme sea-levels at the UK A-class sites: site-by-site analyses. Proudman Oceanographic Laboratory. POL Internal Document No. 65.

Dixon, M. J. and Tawn, J. A. (1997) Estimates of Extreme Sea Conditions: Spatial Analyses for the UK Coast. Proudman Oceanographic Laboratory. POL Internal Report No. 112, MAFF.

Dobereiner, C. (1982) Aggradation and Deposition of Fine Particles in the Tay Estuary. University of Dundee, Unpublished Thesis.

Dobson, J., Edwards, A., Hill, A. and Park, R. (2000) *Decadal Changes in the Forth Estuary and Firth of Forth in Relation to the North Sea 1980-2000*. In series: Leatherland, T. M. Long-Term Trends In Water Quality Of The Tidal Forth. Scottish Environment Protection Agency East Region.

Domingues, M. O., Mendes, O. Jr. and Mendes da Costa, A. (2005) *On wavelet techniques in atmospheric sciences*. Advances in Space Research, vol. 35, pp. 831-842.

Donnelly, J. P., Cleary, P., Newby, P. and Ettinger, R. (2004) *Coupling instrumental and geological records of sea-level change: evidence from southern New England of an increase in the rate of sea-level rise in the late 19th century*. Geophysical Research Letters, vol. 31, L05203, doi:10.1029/2003GL018933.

Douglas, B. C. (1997) Global sea level acceleration. Journal of Geophysical Research, vol. 97, pp. 699–12 706.

Duck, R. W. (2005) Evolving understanding of the Tay Estuary, Scotland: exploring the linkages between frontal systems and bedforms. Chapter In: Fitzgerald, D. M. and Knight, J. (edts.) High Resolution Morphodynamics and Sedimentary Evolution of Estuaries. Coastal Systems and Continental Margins Volume 8. The Netherlands: Springer, pp. 299-313.

Duck, R. (2011) This Shrinking Land: Climate Change and Britain's Coast. Dundee: Dundee University Press.

Duncan, P. J. (1996) The small ports and landing places of the River Tay: circa 1750 to 1850. Unpublished PhD Thesis, University of Dundee.

Dundee City Council. (1997) Flood Prevention Report 1997. Dundee: Dundee City Council.

Dundee City Council. (1999) Flood Prevention Report 1999. Dundee: Dundee City Council.

Dundee City Council. (2001) Flood Prevention Report 2001. Dundee: Dundee City Council.

Dundee City Council. (2003) Flood Prevention Report 2003. Dundee: Dundee City Council.

Dundee City Council. (2005) Flood Prevention Report 2005. Dundee: Dundee City Council.

Dundee City Council. (2007) Flood Prevention Report 2007. Dundee: Dundee City Council.

Dundee City Council. (2009) Flood Prevention Report 2009. Dundee: Dundee City Council.

Dundee City Council (2011) Dundee Economic Profile November 2011. (20/11/2011) www.dundeecity.gov.uk

Dyer, K. R. (1997) Estuaries: A Physical Introduction (2nd Ed.). West Sussex: John Wiley & Sons Ltd.

Dyke, P. P. G. (1987) *Water circulation in the Firth of Forth, Scotland*. Proceedings of the Royal Society of Edinburgh B, vol. 93, pp. 273-284.

East Lothian Council. Report of Flood Risk. (12/12/2010) www.eastlothian.gov.uk

Edinburgh City Council. Water Quality and Flooding. River Flow and Flooding. (12/06/2010) http://www.edinburgh.gov.uk/

Elliott, A. J. and Neill, S. P. (2007) *The tidal flux in the Firth of Forth*. Proceedings of the Institution of Civil Engineers, Journal of Maritime Engineering, vol. 160, pp. 25-32.

Environment Agency. Thames Estuary 2100. (12/04/2012) http://www.environment-agency.gov.uk/homeandleisure/floods/125045.aspx

Escarameia, M. (1998) River and channel revetments: a design manual. London: Thomas Telford Publishing.

Fagherazzi, S. and Wiberg, P. L. (2009) *Importance of wind conditions, fetch, and water levels on wave-generated shear stresses in shallow intertidal basins.* Journal of Geophysical Research, vol. 114, F03022.

Falconer and McInally (2002) Perth Flood Alleviation Scheme and the 1993 flood. Report by Perth & Kinross Council, Perth.

Falkirk Council. (2007) Flood Report 2007. (10/10/2010) www.falkirk.gov.uk

Falkirk Council. (2009a) Flooding and Sustainable Urban Drainage Systems. Supplimentary Planning Guidance Note. (12/07/2010) http://www.falkirk.gov.uk/

Falkirk Council. (2009b) Flood Report 2009. (10/10/2010) www.falkirk.gov.uk

Feynman, J. and Ruzmaikin, A. (2011) *The Sun's strange behavior: Maunders Minimum or Gleissberg Cycle*. Solar Physics, vol. 272, pp. 351-363.

Fife Council. (2003) Flood Prevention Report 2003. (10/10/2010) www.fife.gov.uk

Fife Council. (2007) Flood Alleviation Report 2007. (10/10/2010) www.fife.gov.uk

Fife Council. (2009) Flood Alleviation Report 2009. (10/10/2010) www.fife.gov.uk

Fife Council. (2011) Shoreline Management Plan Consultation: Policy Statement and Maps. (12/10/2011) http://admin.1fife.org.uk/uploadfiles/publications/c64_PolicyStatementsandMaps.pdf

Finan, K. (2007) Water quality changes in the Tay Estuary: does public perception match reality? University of Dundee, Unpublished MPhil Thesis.

Finkl, C. W. and Walker, H. J. (2002) Beach nourishment. In: Chen, J., Eisma, D., Hotta, K. and Walker, J. Engineering Coasts. Coastal Systems and Continental Margins Series. The Netherlands: Kluwer Academic Publishers, pp. 1-22.

Firth, C. R. and Stewart, I. S. (2000) *Postglacial tectonics of the Scottish glacio-isostatic uplift centre*. Quaternary Science Review, vol. 19, pp. 1469-1493.

Firth, C. R., Collins, P. E. F. and Smith, D. E. (1997) Coastal processes and management in Scottish estuaries IV: the Firth of Forth. Edinburgh: SNH Review, No. 87.

Flather, R., Baker, T., Woodworth, P., Vassie, I. and Blackman, D. (2001) Integrate effects of climate change on coastal extreme sea levels. Proudman Oceanographic Laboratory Internal Document No. 140. (13/12/2009) www.pol.ac.uk

Fleming, K. M. (2000). Glacial Rebound and Sea-level Change Constraints on the Greenland Ice Sheet. Australian National University. PhD Thesis. In: Rohde, R. (2009a) Holocene sea level trends. (13/10/10) www.globalwarmingart.com

Fleming, K., Johnston, P., Zwartz, D., Yokoyama, Y., Lambeck, K. and Chappell, J. (1998). *Refining the eustatic sea-level curve since the Last Glacial Maximum using far- and intermediate-field sites*. Earth and Planetary Science Letters, vol. 163, pp. 327-342.

Forbes, B. M. (2011) River Earn Bridge. (12/07/2011) www.flickr.com

Forth Energy (2010a) Leith Renewable Energy Plant Environmental Impact Assessment. (12/12/2010) www.forthenergy.co.uk

Forth Energy (2010b) Dundee Renewable Energy Plant Environmental Impact Assessment. (12/12/2010) www.forthenergy.co.uk

Forth Energy (2010c) Grangemouth Renewable Energy Plant Environmental Impact Assessment. (12/12/2010) www.forthenergy.co.uk

Forth Energy (2010d) Rosyth Renewable Energy Plant Environmental Impact Assessment. (12/12/2010) www.forthenergy.co.uk

Forth Estuary Forum. The Forth Estuary Forum. (06/01/2010) www.forthestuaryforum.co.uk

Forth Ports. Forth Ports – The Ports. (11/10/2010) http://www.forthports.co.uk/ports/index.jsp

Forth River Purification Board. (1995) The Forth: a catchment under pressure. Edinburgh: Forth River Purification Board.

French, P. W. (2001) Coastal Defences: Processes, problems and solutions. London: Routeledge.

Friedrichs, C. T. and Aubrey, D. G. (1988) *Non-linear tidal distortion in shallow well-mixed estuaries: a synthesis*. Estuarine, Coastal and Shelf Science, vol. 27, pp. 521-545.

Galvin, C. J. (1968) *Breaker type classification on three laboratory beaches*. Journal of Geophysical Research, vol. 73, pp. 3651-3660.

Gaur, A. S. and Vora, K. H. (1999) *Ancient shorelines of Gujarat, India, during the Indus civilization (Late Mid-Holocene): A study based on archaeological evidences*. Current Science, vol. 77, pp. 180-185.

Gehrels, R. and Long, A. (2008) *Sea Level is not Level: the case for a new approach to predicting UK sea-level rise*. Geography, vol. 93, pp. 11-16.

General Register Office for Scotland. (2010) Council Area Profiles. (12/1/2011) www.gro-scotland.gov.uk

GeoWise Limited and Coastal Research Group, Glasgow University (CRGGU) (1999) Use of GIS to map land claim and identify potential areas for coastal managed realignment in the Forth Estuary. Unpublished Confidential Report.

Geyer, W. R. and Farmer, D. M. (1989) *Tide-induced variation of the dynamics of a salt wedge estuary*. Journal of Physical Oceanography, vol. 19, pp. 1060-1073.

Gibson, J. (2011) UK Coastal Zone Law. (09/11/2011) http://web.uct.ac.za/staff/jgibson/iczm/home.htm

Gil, E. and De Toro, C. (2005) *Improving tide-gauge data processing: A method involving tidal frequencies and inverted barometer effect*. Computer Geoscience, vol. 31, pp. 1048-1058.

Gill, A. E. (1982) Atmosphere-Ocean Dynamics. Academic Press: California.

Gilvear, D., Tyler, A. and Davids, C. (2004) *Detection of estuarine and tidal river hydromorphology using hyper-spectral and LiDAR data: Forth estuary, Scotland*. Estuarine, Coastal and Shelf Science, vol. 61, pp. 379-392.

Goddard Institute for Space Studies (GISS) Air Surface Temperature Anomaly. (12/03/2011) http://data.giss.nasa.gov/gistemp/graphs/Fig.A.txt

Google Maps. (2012) Map. (12/10/2012) http://maps.google.com

Graff, J. (1981) *An investigation of the frequency distribution of annual sea level maxima at ports around Great Britain*. Estuarine, Coastal and Shelf Science, vol. 12, pp. 389-449.

Graham, A. (1979) *Old harbours and landing-places on the east coast of Scotland*. Proceedings of the Society for Antiquities in Scotland, vol. 108, pp. 333-365.

Gratoit, N., Anthony, E. J., Gardel, A., Gaucherel, C., Proisy, C. and Wells, J. T. (2008) *Significant contributions of the 18.6 year tidal cycle to regional coastal changes.* Nature Geoscience, vol. 1, pp. 169-172.

Gray, J. M. and Brooks, C. L. (1971) *The Loch Lomond Readvance moraines of Mull and Menteith*. Scottish Journal of Geology, vol. 8, pp. 95-103.

Gray, S. T., Graumlich, L. J., Betancourt, J. L. and Pederson, G. T. (2004) *A tree-ring based reconstruction of the Atlantic Multidecadal Oscillation since 1567 A.D.* Geophysical Research Letters, vol. 31, L12205.

Greenwood, M. F. D. and Hill, A. S. (2003) *Temporal, spatial and tidal influences on benthic and demersal fish abundance in the Forth Estuary.* Estuarine & Coastal Shelf Science, vol. 58, pp. 211-225.

Gregory, J. M., Lowe, J. A. and Tett, S. F. B. (2006) *Simulated Global-Mean Sea Level Changes over the Last Half-Millennium*. Journal of Climate, vol. 19, pp. 4576-4591.

Grinsted, A. (11/11/2009) Relationship between sea level rise and global temperature. (10/07/2011) www.glaciology.net

Grinstead, A., Moore, J. C. and Jevrejeva, S. (2009) *Reconstructing sea level from paleo and projected temperatures 200 to 2100AD*. Climate Dynamics, vol. 34, pp. 461-472.

Grinsted, A., Moore, J. C. and Jevrejeva, S. (2010) *Reconstructing sea level from paleo and projected temperatures 200 to 2100AD.* Climate Dynamics, doi:10.1007/s00382-008-0507-2.

Hadley, D. (2009) *Land use and the coastal zone*. Land Use Policy, vol. 26, pp. S198-S203.

Haigh, I., Nicholls, R. and Wells, N. (2010) *Assessing changes in extreme sea levels: Application to the English Channel, 1900-2006*. Continental Shelf Research, vol. 30, pp. 1042-1055.

Hansom, J. D. and McGlashan, D. J. (2005) *Scotland's Coast: Understanding Past and Present Processes for Sustainable Management*. Scottish Geographical Journal, vol. 120, pp. 99-116.

Hardisty, J. (2007) Estuaries: Monitoring and Modeling the Physical System. Oxford: Blackwell Publishing.

Harrison, S. J. (1987) *Climate conditions over the estuary and Firth of Forth, Scotland*. Proceedings of the Royal Society of Edinburgh B, vol. 93, pp. 245-258.

Haslett, S. K. (2008) Coastal Systems (2nd Ed.) London: Routledge.

Hendershott, M. C. (2012) *Ocean tides*. Eos, Transactions of the American Geophysical Union, vol. 54, pp. 76-86.

Hesp, P. A. (2002) *Foredunes and blowouts: initiation, geomorphology and dynamics*. Geomorphology, vol. 48, pp. 245-268.

Hickey, K. R. (2001) *The storm of 31 January to 1 February 1953 and its impact in Scotland.* Scottish Geographical Journal, vol. 117, pp. 283-295.

Hicks, S. D., Goodheart, A. J. and Iseley, C. W. (1965) *Observations of the tide on the Altantic Continental Shelf.* Journal of Geophysical Research, vol. 70, pp. 1827-1830.

Holgate, S. J. (2007) *On the decadal rates of sea level change during the twentieth century*. Geophysical Research Letters, vol. 34. In: World Climate Report. Shocking Facts about Climate Change. (16/03/2009) http://www.worldclimatereport.com/index.php/2007/02/09/shocking-facts-about-sea-level-rise/

Holgate, S. J., and Woodworth, P. L. (2004) *Evidence for enhanced coastal sea level rise during the 1990s*. Geophysical Research Letters, vol. 31, L07305.

Horton, R., Herweijer, C., Rosenzweig, C., Liu, J. P., Gornitz, V. and Ruane, A.C. (2008) *Sea level rise projections for current generation CGCMs based on the semi-empirical method*. Geophysical Research Letters, vol. 35, L02715.

Houghton, J. T., Ding, Y., Griggs, D. J., Noguer, M., van der Linden, P. J., Dai, X., Maskell, K. and Johnson, C. A. (edts.) (2001) Climate Change 2001: The Scientific Basis. Contribution of Working Group I to the Third Assessment Report of the Intergovernmental Panel on Climate Change. Cambridge: Cambridge University Press.

Hudspeth, R. T. (2006) Waves and Wave Forces on Coastal and Ocean Structures. Advanced Series on Ocean Engineering – Volume 21. New Jersey: World Scientific.

Hulme, M., Jenkins, G. J., Lu, X., Turnpenny, J. R., Mitchell, T. D., Jones, R. G., Lowe, J., Murphy, J. M., Hassell, D., Boorman, P., McDonald, R. and Hill, S. (2002) Climate Change Scenarios for the United Kingdom: The UKCIP02 Scientific Report. Norwich: Tyndall Centre for Climate Change Research, University of East Anglia.

Hunt, A. G. and Malin, P. E. (1998) *Possible triggering of Heinrich Events by ice-load-induced earthquakes*. Nature, vol. 393, pp. 155-158.

Hurrell, J.W. (1995) *Decadal Trends in the North Atlantic Oscillation: Regional Temperatures and Precipitation*. Science, vol. 269, pp. 676-679.

Imray Laurie Norie & Wilson Ltd. (2007) No. C27 Scotland – East Coast. Firth of Forth. St. Ives: Imray Laurie Norie & Wilson Ltd.

Ingle, J. C. (ed.) (1966) *The movement of beach sand: an analysis using fluorescent grains. In: Developments in Sedimentology*. Development in Sedimentology Volume 5. Essex: Elsevier Publishing.

Intergovernmental Panel on Climate Change (IPCC) (1991) Climate Change: The Response Strategies. Contribution of Working Group III to the First Assessment Report of the Intergovernmental Panel on Climate Change. Cambridge: Cambridge University Press.

Ishii, M., Kimoto, M., Sakamoto, K. and Iwasaki, S. I. (2006) *Steric sea level changes estimated from historical ocean subsurface temperature and salinity analyses*. Journal of Oceanography, vol. 62, pp. 155–170.

Jenkins, P. A. (2003) *Fingerprinting of bed sediments in the Tay Estuary*. University of Dundee PhD thesis, Unpublished.

Jenkins, P. A., Duck, R. W., Rowan, J. S. and Walden, J. (2002) *Fingerprinting of bed sediment in the Tay Estuary, Scotland: an environmental magnetism approach*. Hydrology and Earth System Sciences, vol. 6, pp. 1007-1016.

Jenkins, P. A., Duck, R. W. and Rowan, J. S. (2005) *Fluvial contribution to the sediment budget of the Tay Estuary, Scotland, assessed using mineral magnetic fingerprinting.* Sediment Budgets 1 – Proceedings of symposium S1 held during the Seventh IAHS Scientific Assembly at Foz do Iguacu, Brazil, April 2005. IAHS Publication 291, pp.134.

Jenkins, G. J., Perry, M. C. and Prior, M. J. (2007) The Climate of the United Kingdom and Recent Trends. Met Office Hadley Centre, Exeter, UK.

Jenkinson, A. F. (1955) *The frequency distribution of the annual maximum (or minimum) of meteorological elements.* Quaternary Journal of the Royal Meteorological Society, vol. 81, pp. 158-171.

Jennings, G., Furness, B. and McGlashan, D. (2010) *Ecology of an urban common tern colony in Leith Docks, Scotland.* 1st World Seabird Conference Poster Session 2, Victoria, Canada, 7-11 September.

Jevrejeva, S., Grinsted, A., Moore, J. C. and Holgate, S. (2006) *Nonlinear trends and multiyear cycles in sea level records.* Journal of Geophysical Research, vol. 111, C09012.

Jevrejeva, S., Moore, J. C. and Grinsted, A. (2010) *How will sea level respond to changes in natural and anthropogenic forcings by 2100?* Geophysical Research Letters, vol. 37, pp. 1-5.

Jevrejeva, S., Moore, J. C., Grinsted, A. and Woodworth, P. L. (2008) *Recent global sea level acceleration started over 200 years ago?* Geophysical Research Letters, vol. 35, L08715, doi:10.1029/2008GL033611.

Jones, J. E. and Davies, A. M. (2009) *Storm surge computations in estuarine and near-coastal regions: the Mersey estuary and Irish Sea area*. Ocean Dynamics, vol. 59, pp. 1061-1076.

Journey through the Galaxy. (2006) Earth's Moon. (16/02/2009) http://filer.case.edu/sjr16/advanced/earth_moon.html

Kaye, C. A. and Stuckey, G. W. (1973) *Nodal tidal cycle of 18.6 yr.: its importance in sea-level curves of the east coast of the United States and its value in explaining long-term sea-level changes.* Geology, vol. #, pp. 141-144.

Kearney, M. S. and Stevenson, J. C. (1991) *Island land loss and marsh vertical accretion rate: evidence for historical sea level changes in Chesapeake Bay*. Journal of Coastal Research, vol. 7, pp. 403–415.

Khayrallah, N. and Jones, A. M. (1975) *A survey of the benthos of the Tay Estuary*. Proceedings of the Royal Society of Edinburgh B, vol. 75, pp. 113-135.

Kjerve, B. (ed.) (1988) Hydrodynamics of Estuaries. Volume I Estuarine Physics. Florida: CRC Press.

Knight, J. R., Follard, C. K. and Scaife, A. A. (2006) *Climate impacts of the Atlantic Multidecadal Oscillation.* Geophysical Research Letters, vol. 33, L17706, doi:10.1029/2006GL026242.

Knudsen, M. F., Seidenkrantz, M.-S., Jacobsen, B. H. and Kuijpers, A. (2011) *Tracking the Atlantic Multidecadal Oscillation through the last 8,000 years*. Nature Communications, vol. 2, 178.

Kopp, R., Simons, F., Mitrovica, J., Maloof, A. and Oppenheimer, M. (2009) *Probabilistic assessment of sea level during the last interglacial stage*. Nature, vol. 462, pp. 863–867.

Kostaschuk, R. A., Church, M. A. and Luternauer, J. L. (1992) *Sediment transport over salt-wedge intrusions: Fraser River estuary, Canada*. Sedimentology, vol. 39, pp. 305-311.

Kravtsov, S., Dewar, W. K., Berloff, P., McWilliams, J. C. and Ghil, M. (2007) *A highly nonlinear coupled mode of decadal variability in a mid-latitude ocean-atmosphere model*. Dynamics of Atmospheres and Oceans, vol. 43, pp, 123-150.

Kumar, P. and Foufoula-Georgious, E. (1997) *Wavelet Analysis for Geophysical Applications*. Reviews of Geophysics, vol. 35, pp. 385-412.

Lamb, H. (1991) Historic storms of the North Sea, British Isles and Northwest Europe. Cambridge: Cambridge University Press.

Lamb, G. L. (1995) Introductory Applications of Partial Differential Equations : With Emphasis on Wave Propagation and Diffusion. New York: John Wiley & Sons.

Lambeck, K. (1993) Glacial *rebound of the British Isles-1: preliminary model results*. Geophysical Journal International, vol. 115, pp. 941–959.

Land Information New Zealand. The Cause and Nature of Tides. (24/07/2009) http://www.linz.govt.nz/hydro/tidal-info/tidal-intro/cause-nature/index.aspx

Landscheidt, T. (2004) Decadal-Scale NAO Forecast Based on Solar Motion Cycles. Schroeter Institute for Research in Cycles of Solar Activity, Germany. (12/03/2012) www.john-daly.com/theaodor/naonew.htm

Law, F. M., Black, A. R., Scarrott, R. M. J., Miller, J. B. and Bayliss, A. G. British Hydrological Society's Chronology of British Hydrological Events. (20/01/2010) www.dundee.ac.uk/geography/cbhe

Lee, D. T. L. and Yamamoto, A. (1994) Wavelet Analysis: Theory and Applications. Hewlett-Packard Company.

Lennon G. W. (1963) *A frequency investigation of abnormally high tidal levels at certain west coast ports.* Proceedings of the Institution of Civil Engineers, vol. 25, pp. 451-483.

Leuliette, E. W., Nerem, R. S. and Mitchum, G. T. (2004) *Calibration of TOPEX/Poseidon and Jason altimeter data to construct a continuous record of mean sea level change*. Marine Geodesy, vol. 27, pp. 79–94.

Liu, S-K. (2000) Chapter 120 – Effect of Climate Change and Sea level on Coastal Systems. In: Sheppard, C. (edt.) Seas at the Millennium: An Environmental Evaluation. Elsevier Science Ltd.

Livingston, W. and Penn, M. (2010) *Are sunspots different during this solar minimum?* EOS, vol. 90, pp. 257-258.

Lombard, A., Garric, G. and Penduff, T. (2009) *Regional patterns of observed sea level change: insights from a 1/4o global ocean/sea-ice hindcast*. Ocean Dynamics, vol. 59, pp. 433-449.

Lowe, J. A., Gregory, J. M. and Flather, R. A. (2001) *Changes in the occurrence of storm surges around the UK under a future climate scenario using a dynamic storm surge model driven by the Hadley Centre climate models*. Climate Dynamics, vol. 18, pp. 179-188.

Lowe, J. A., Howard, T. P., Pardaens, A., Tinker, J., Holt, J., Wakelin, S., Milne, G., Leake, J., Wolf, J., Horsburgh, K., Reeder, T., Jenkins, G., Ridley, J., Dye, S. and Bradley, S. (2009) UK Climate Projections science report: Marine and coastal projections. Exeter: UKMO Hadley Centre.

Lowe, J. A., Woodworth, P. L., Knutson, T., McDonald, R. E., McInnes, K. L., Woth, K., von Storch, H., Wolf, J., Swail, V., Bernier, N. B., Gulev, S., Horsburgh, K. J., Unnikrishnan, A. S., Hunter, J. R. and Weisse, R. (2010) Chapter 11 – Past and Future Changes in Extreme Sea Levels and Waves. In: Church, J. A., Woodworth, P. L., Aarup, T. and Stanley, W. Understanding Sea-Level Rise and Variability. Chichester: John Wiley & Sons Ltd.

Lozano, I., Devoy, R. J. N., May, W. and Andersen, U. (2004) *Storminess and vulnerability along the Atlantic coastlines of Europe: analysis of storm records and of greenhouse gases induced climate scenario.* Marine Geology, vol. 210, pp. 205-225.

Lydolf, P. E. (1985) Weather and Climate. Lanham: Rowman and Littlefield.

Macdonald, N., Werritty, A., Black, A. R. and McEwen, L. J. (2006) *Historical and pooled flood frequency analysis for the River Tay at Perth, Scotland*. Area, vol. 38, pp. 34-46.

Mackintosh, D. (2009) Ports and Harbours of the UK. (16th January 2009) www.ports.org.uk

Maitland Club. (1831) Chronicles of Perth. Maitland Club, vol. 10. In: McEwen, L. J. (1987) *Sources for establishing a Historic Flood Chronology (Pre-1940) within Scottish River Catchments*. Scottish Geographical Journal, vol. 103, pp. 132-140.

Marcos, M., Wöppelmann, G., Bosch, W. and Savcenko, R. (2007) *Decadal sea level trends in the Bay of Biscay from tide gauges, GPS and TOPEX*. Journal of Marine Systems, vol. 68, pp. 529-536.

Marchuk, G. I. and Kagan, B. A. (1989) Dynamics of ocean tides. Dordrecht: Kluwer Academic Publishers.

Marine Climate Change Impact Partnership (MCCIP) (2008) Marine Climate Change Impacts: Annual Report Card 2007-2008. (17th November 2008) www.mccip.org.uk/arc

Marshall, J., Kushnir, Y., Battisti, D., Chang, P., Czaja, A., Dickson, R., Hurrell, J., McCartney, M., Vanan, R. S. and Visbeck, M. (2001) *North Atlantic climate variability: phenomena, impacts and mechanisms.* International Journal of Climatology, vol. 21, pp. 1863-1898.

Massel, S. R. (2001) *Wavelet analysis for processing of ocean surface wave records*. Ocean Engineering, vol. 28, pp. 957-987.

Masselink, G. and Anthony, E. J. (2001) *Location and height of intertidal bars on macrotidal ridge and runnel beaches.* Earth Surface Processes and Landforms, vol. 26, pp. 759-774.

Masselink, G. and Hughes, M. (2003) An Introduction to Coastal Processes. Hodder Arnold.

Masselink, G. and Short, A. D. (1993) *The effect of tide range on beach morphodynamics and morphology: a conceptual beach model*. Journal of Coastal Research, vol. 9, pp. 785-800.

Masters, J. (2010) Jeff Masters' Wunder Blog. How much will global sea level rise this century? (11/12/2010) Weather Underground Inc. http://www.wunderground.com/blog/JeffMasters/comment.html?entrynum=1255&tstamp=&page=36

Maul, G. A., Hendry, M. D. and Pirazzoli, P. A. (1996) *Sea Level, Tides, and Tsunamis.* Coastal and Estuarine Studies, vol. 51, pp. 83-119.

McCartney, M. S., Curry, R. G. and Bezdex, H. F. (1997) *North Atlantic's transformation pipeline chills and redistributes subtropical water*. Oceanus, vol. 39, pp. 19–23.

McCully, J. G. (2006) Beyond the Moon: A Conversational, Common Sense Guide to Understanding the Tides. London: World Scientific Publishing Co. Pte. Ltd.

Macdonald, N., Werritty, A., Black, A. R. and McEwen, L. J. (2006) *Historical and pooled flood frequency analysis for the River Tay at Perth, Scotland*. Area, vol. 38, pp. 34-46.

McDonald, J. E. (1952) *The Coriolis Effect*. Scientific American, vol. 186, pp. 72-78.

McEwen, L. J. (2006) *Flood seasonality and generating conditions in the Tay catchment, Scotland from 1200 to present*. Area, vol. 38, pp. 47-64.

McGlashan, D. J. (2003) *Managed relocation: an assessment of its feasibility as a coastal management option.* The Geographical Journal, vol. 169, pp. 6-20.

McKean, C. (2006) Battle for the North. The Tay and Forth Bridges and the 19th Century Railway Wars. London: Granta Books.

McKean, C., Harris, B. and Whatley, C. A. (2009) Dundee: Renaissance to Enlightenment. Dundee: Dundee University Press Ltd.

McLusky, D. S., Bryant, D. M. and Elliott, M. (1992) *The impact of land-claim on macrobenthos, fish and shorebirds on the Forth Estuary, eastern Scotland.* Aquatic Conservation, vol. 2, pp. 211-222

McManus, J. (1970) *The geological setting of the Lower Tay Estuary with particular reference to the fill of the buried channel.* The Quarterly Journal of Engineering Geology, vol. 3, pp. 197-205.

McManus, J. (1985) *Gradients of Change in the Estuarine Environments of the Tay.* Proceedings of the University of Dundee Summer School 'Remote Sensing Applications in Civil Engineering' Dundee 19 Aug-8 Sept. 1984, pp. 143-149.

McManus, J. (1986) *Land-derived sediment and solute transport to the Forth and Tay Estuaries, Scotland*. Journal of the Geological Society of London, vol. 143, pp. 927-934.

McManus, J. (1998) *Temporal and Spatial Variations in Estuarine Sedimentation*. Estuaries, vol. 21, pp. 622-634.

McManus, J., Buller, A. T. and Green, C. D. (1980) *Sediments of the Tay Estuary VI: sediments of the lower and outer reaches.* Proceedings of the Royal Society of Edinburgh B, vol. 78, pp. 133-154.

McManus, J., Diez, J. J., Duck, R. W., Escobar, V. A., Anderson, J. M. and Esteban, V. (1993) *Comparison of Scottish Firths and Spanish Rías.* Bulletin of the International Association of Engineering Geology, vol. 47, pp. 127-132.

Meehl, G.A., Stocker, T.F., Collins, W.D., Friedlingstein, P., Gaye, A.T., Gregory, J.M., Kitoh, A., Knutti, R., Murphy, J.M., Noda, A., Raper, S.C.B., Watterson, I.G., Weaver A.J. and Zhao, Z.-C. (2007) Global Climate Projections. In: Solomon, S., Qin, D., Manning, M., Chen, Z., Marquis, M., Averyt, K. B., Tignor, M. and Miller, H. L. (eds.) (2007) Climate Change 2007: The Physical Science Basis. Contribution of Working Group I to the Fourth Assessment Report of the Intergovernmental Panel on Climate Change. Cambridge: Cambridge University Press, Chapter 10.

Mitchum, G. T. (2004) Altimeter Drift from Tide Gauges. (19th March 2009) www.aviso.oceanobs.com

Miller, L. and Douglas, B. C. (2006) *On the rate and causes of twentieth century sea-level rise*. Philosphical Transactions of the Royal Society A, vol. 364, pp. 805-820.

Milne, G. A., Long, A. J. and Bassett. S. E. (2005) *Modelling Holocene relative sea-level observations from the Caribbean and South America*. Quaternary Science Reviews, vol. 24, pp. 1183-1202.

Milne, G. A., Shennan, I., Youngs, B. A. R., Waugh, A. I., Teferle, F. N., Bingley, R. M., Bassett, S. E., Cuthbert-Brown, C. and Bradley, S. L. (2006) *Modelling the glacial isostatic adjustment of the UK region.* Philosophical Transactions of the Royal Society, vol. 364, pp. 931-948.

Mitrovica, J. X. and Milne, G. A. (2003) *On post-glacial sea level: 1. General Theory*. Geophysical Journal International, vol. 154, pp. 253-267.

Mitrovica, J. X., Tamisiea, M. E., Davis, J. L. and Milne, G. A. (2001) *Recent mass balance of polar ice sheets inferred from patterns of global sea-level change.* Nature, vol. 409, pp. 1026-1029.

Mitsuyasu, H. (2002) *A historical note on the study of ocean surface waves*. Journal of Oceanography, vol. 58, pp. 109-120.

Moriarty, T. Critique of global sea level linked to global temperature by Vermeer and Rahmstorf. (12/07/2011) http://climatesanity.wordpress.com

Murphy, J. M., Sexton, D. M. H., Jenkins, G. J., Boorman, P. M., Booth, B. B. B., Brown, C. C., Clark, R. T., Collins, M., Harris, G. R., Kendon, E. J., Betts, R. A., Brown, S. J., Howard, T. P., Humphrey, K. A., McCarthy, M. P., McDonald, R. E., Stephens, A., Wallace, C., Warren, R., Wilby, R., Wood, R. A. (2009) UK Climate Projections Science Report: Climate change projections. Exeter: UK Meteorological Office Hadley Centre.

Mortari, R. (2004) *A new method of stating recent sea level rises and a comparison with tide gauge records.* Global and Planetary Change, vol. 40, pp. 183-194.

Muni Reddy, M. G. and Neelamani, S. (2005) *Hydrodynamic studies on vertical seawall defenced by low-crested breakwater*. Ocean Engineering, vol. 32, pp. 747-764.

Murray, A. (1983) The Forth Railway Bridge. Edinburgh: Mainstream Publishing Company (Edinburgh) Ltd.

Nakada, M. and Inoue, H. (2005) *Rates and causes of recent global sea-level rise inferred from long tide gauge data records*. Quaternary Science Review, vol. 24, pp. 1217-1222.

Nakićenović, N. and Swart, R. (eds.) (2000) IPCC Special Report Emission Scenarios. Cambridge: Cambridge University Press.

National Research Council of the National Academies. Ocean acidification. Starting with the science. (12/01/2011) http://dels.nas.edu/resources/static-assets/materials-based-on-reports/booklets/OA1.pdf

Nicholls, R. (2010) *Impacts of and responses to sea-level rise.* In: Church, J., Woodworth, P., Aarup, T. and Wilson, W. (ed.) Understanding sea-level rise and variability. West Sussex: Wiley-Blackwell, pp. 17-51.

Nicholls, R. J., Marinova, N., Lowe, J. A., Brown, S., Vellinga, P., de Gusmao, D., Hinkel, J. and Tol, R. S. J. (2011) *Sea-level rise and its possible impacts given a 'beyond 4°C world' in the twenty-first century*. Philosophical Transactions of the Royal Society A, vol. 369, pp. 161-181.

Nicholson, J., and O'Connor, B.A. (1986) *Cohesive Sediment Transport Model*. Journal of Hydraulic Engineering, vol. 112 pp. 621 -640.

O'Connor, B. A. (1994) Three-dimensional sediment-transport models. In: Abbott, M. B. and Price, W. A. (edts.) Coastal, Estuarial and Harbour Engineers Reference Book. London: Chapman & Hall.

Ordnance Survey. Get-a-map. (12/1/2010) www.ordnancesurvey.co.uk

Oost, A. P., de Haas, H., IJnsen, F., van den Boogert, J. M. and de Boer, P. L. (1993) *The 18.6 yr nodal cycle and its impact on tidal sedimentation.* Sedimentary Geology, vol. 87, pp. 1-11.

Ove Arup & Partners Ltd. Scotland. (2007) Environmental Statement. (12/10/2010) http://www.leithdocksdevelopment.com/

Peacock, D. (1849) Perth: its annals and its archives. Thomas Richarson: Perth. In: McEwen, L. J. (1987) *Sources for establishing a Historic Flood Chronology (Pre-1940) within Scottish River Catchments*. Scottish Geographical Journal, vol. 103, pp. 132-140.

Pedoja, K., Husson, l., Regard, V., Cobbold, P. R., Ostanciaux, E., Johnson, M. E., Kershaw, S., Saillard, M., Martinod, J., Furgerot, L., Weill, P. and Delcaillau, B. (2011) *Relative sea-level fall since the last interglacial stage: Are coasts uplifting worldwide?* Earth-Science Reviews, vol. 108, pp. 1-15.

Permanent Service for Mean Sea Level (PSMSL). Permanent Service for Mean Sea Level (11/01/2011) www.pol.ac.uk/psmsl/

Perth Harbour Authority. Perth Harbour Facilities. (11/10/2010) http://www.perthharbour.co.uk/perth-harbour-facilities.html

Perth & Kinross Council (2007) Key Facts and Figures. (12/1/2011) www.pkc.gov.uk

Perth and Kinross Council. (2009) Biennial Report on Flood Prevention Responsibilities 2009. Perth and Kinross Council Report No. 09/504.

Perth & Kinross Council (2011) Key Facts – population. (12/11/2011) www.pkc.gov.uk

Pethick, J. (1999) *Future Sea-level Changes in Scotland: Options for Coastal Management*. In: Baxter, J. M., Duncan, K., Atkins, S. M. and Lees, G. (edts.) Living Coastline. The Natural Heritage of Scotland Series 7. London: Stationery Office.

Pfeffer, W. T., Harper, J. T. and O'Neel, S. (2008) *Kinematic Constraints on Glacier Contributions to 21st-Century Sea-Level Rise.* Science, vol. 321, pp. 1340-1343.

Phillips, 0. M. (1957) *On the generation of waves by turbulent wind*. Journal of Fluid Mechanics, vol. 2, pp. 417.

Phillips, O. M. (1956) In: Weert, S. (2009) *Timeline/Milestones*. The Discovery of Global Warming. (12/03/2011) www.aip.org/history/climate

Phillips, M. R. and Jones, A. L. (2006) *Erosion and tourism infrastructure in the coastal zone: problems, consequences and management*. Tourism Management. vol. 27, pp. 517-524.

Phillips, M. R., Powell, V. A. and Duck, R. W. (2009) *Coastal Regeneration at Llanelli, South Wales, UK: lessons not learned*. In: Book of Abstracts of the 10th International Coastal Symposium, 13–18 April, Lisbon, Portugal, Edition e-GEO, Universidade Nova de Lisboa, Lisbon, p. 229.

Phillips, T. (2009) Harmonic Analysis And Prediction Of Tides. State University of New York. (12/07/2009) www.math.sunysb.edu/~tony/tides/harmonic.html

Pilarczyk, K. (2010) Remarks on Coastal Stabilization and Alternative Solutions. In: Kim, Y. C. (ed.) Handbook of Coastal and Ocean Engineering. Singapore: World Scientific Publishing Co. Pte. Ltd., pp. 521-552.

Pinet, P. R. (2008) Invitation to Oceanography (5th Ed.) London: Jones & Bartlett Publishers.

Polyakov, I. and Johnson, M. A. (2000) *Arctic Decadal and Interdecadal Variability*. Geophysical Research Letters, vol. 27, pp. 4097-4100

Pontin, R. A. and Reid, J. A. (1975) *The freshwater input to the Tay Estuary*. Proceedings of the Royal Society of Edinburgh B, vol. 75, pp. 1-9.

Port of London Authority. (2011) About Us. (12/06/2011) www.pla.co.uk

Powell, V. A., McGlashan, D. J. and Duck, R. W. (2012) *Use of local tidal records to identify relative sea level change: accuracy and error for decision makers*. Journal of Coastal Conservation, In Press.

Pugh, D. (2004) Changing Sea Levels: Effects of Tides, Weather and Climate. Cambridge: Cambridge University Press.

Proudman Oceanographic Laboratory (POL). (2008) Tide Gauge Network. (03/02/2009) www.pol.ac.uk/ntslf/tgi/

Rahmstorf, S. (2007) *A semi-empirical approach to projecting future sea-level rise*. Science, vol. 315, pp. 368-370.

Ramsay, D. L. and Brampton, A. H. (2000) *Coastal Cells in Scotland: Cell 2 – Fife Ness to Cairnbulg Point*. Scottish Natural Heritage Research, Survey and Monitoring Report, no. 144.

Reeves, D. E. and Karunarathna, H. (2009) *On the prediction of long-term morphodynamic response of estuarine systems to sea level rise and human interference*. Continental Shelf Research, vol. 29, pp. 938-950.

Rennie, A. F. and Hansom, J. D. (2011) *Sea level trend reversal: land uplift outpaced by sea level rise on Scotland's coast*. Geomorphology, vol. 125, pp. 193-202.

Revelle, R. and Suess, H. E. (1957) Carbon Dioxide exchange between atmosphere and ocean and the question of an increase of atmospheric CO2 during the past decades. Tellus, vol. 9, pp. 18.

Richardson, J. S. (1839) Account of embanking land from the River Tay on the estate of Pitfour, Perthshire. Prize Essays and Transactions of the Highland and Agricultural Society of Scotland, vol. 12, pp. 298-302.

Risk Management Solutions (RMS). (2003) 1953 U.K. Floods: 50 year Retrospective. Risk Management Solutions: California.

Ritchie, G. G. and Thompson, J. H. (1930) Dundee Harbour Trust Centenary 1830-1930. History and development of the harbour at Dundee. Dundee: Dundee Harbour Trust.

Robinson, A. H. W. (1960) *Ebb-flood channel systems in sandy bays and estuaries*. Geography, vol. 45, pp. 183-199.

Rohde, R. (2009a) Holocene sea level trends. (13/10/10) www.globalwarmingart.com

Rohling, E., Grant, K., Hemleben, C., Siddall, M., Hoogakker, B., Bolshaw, M. and Kucera, M. (2008) *High rates of sea-level rise during the last interglacial period*. National Geoscience, vol. 1, pp. 38–42.

RPA Smith. Methil: Early History and Docks. (12/11/2011) www.rpasmith.co.uk/methildocks.htm

Roy, I. and Haigh, J. D. (2010) *Solar cycle signals in sea level pressure and sea surface temperature*. Atmospheric Chemistry and Physics, vol. 10, pp. 3147-3153.

Royal Society, The (2005) Ocean acidification due to increasing atmospheric carbon dioxide. London: The Royal Society.

Ruessink, B. G. and Jeuken, M. C. J. L. (2002) *Dunefoot dynamics along the Dutch coast*. Earth Surface Processes and Landforms, vol. 27, pp. 1043-1052.

Saiu, E., McManus, J. and Duck, R. W. (1994) *Impact of industrial growth and decline on coastal equilibrium, Eastern Scotland*. Conference Proceedings of Coastal Zone Canada '94 'Cooperation in the Coastal Zone', vol. 5, pp. 2205-2219.

Schindler, D. W. (1999). *The Mysterious Missing Sink*. Nature, vol. 398, pp. 105-106.

Schmith, T., Johansen, S. and Thejll, P. (2007*) Comment on "A semi-empirical approach to projecting future sea-level rise"*. Science, vol 315, pp 368.

Scottish Environmental Protection Agency (SEPA) (2006) Flood risk map. (12/06/2011) www.sepa.org.uk

Scottish Executive (2005) Seas the Opportunity: A Strategy for the Long Term Sustainability of Scotland's Coasts and Seas. Edinburgh: Scottish Executive.

Scottish Government (2000) PFI Scotland Edition 8: July 2000. Tay Waste Water Project. (11/3/2011) www.scotland.gov.uk

Scottish Natural Heritage (SNH). 86: Firth of Tay. (13/01/2010) www.snh.gov.uk

Severinghaus, J. P., Sowers, T., Brook, E. J., Alley, R. B. and Bender, M. L. (1998) *Timing of abrupt climate change at the end of the Younger Dryas interval from thermally fractionated gases in polar ice*. Nature, vol. 391, pp. 141-146.

Shennan, I. (1989) *Holocene crustal movements and sea-level changes in Great Britain*. Journal of Quaternary Science, vol. 4, pp. 77–89.

Shennan, I., Bradley, S., Milne, G., Brooks, A., Bassett, S. and Hamilton, S. (2006) *Relative sea-level changes, glacial isostatic modelling and ice-sheet reconstructions from the British Isles since the Last Glacial Maximum*. Journal of Quaternary Science, vol. 21, pp. 585–599.

Shennan, I. and Horton, B. P. (2002) *Holocene land- and sea-level changes in Great Britain*. Journal of Quaternary Science, vol. 17, pp. 511–526.

Shennan, I., Milne, G., Bradley, S. (2009) *Late Holocene relative land- and sea-level change: providing information for stakeholder*. GSA Today, vol. 19, pp. 52-53.

Shennan, I., Milne, G. and Bradley, S. (2011) *Late Holocene vertical land motion and relative sea-level changes: lessons from the British Isles*. Journal of Quaternary Science, In Press.

Shennan, I., Milne, G. and Bradley, S. (2012) *Late Holocene vertical land motion and relative sea-level changes: lessons from the British Isles*. Journal of Quaternary Science, vol. 27, pp. 64-70.

Shennan, I., Peltier, W. R., Drummond, R. and Horton, B. (2002) *Global to local scale parameters determining relative sea-level changes and the post-glacial isostatic adjustment of Great Britain*. Quaternary Science Review, vol. 21, pp. 397-408.

Short, A. D. (1991) *Macro-meso tidal beach morphodynamics – an overview*. Journal of Coastal Research, vol. 7, pp. 417-436.

Sibley, A. (2010) Analysis of extreme rainfall and flooding in Cumbria 18-20 November 2009. Weather, vol. 65, pp. 287-292.

Singer, S. F. and Avery, D. T. (2008) Unstoppable Global Warming. Lanham: Rowman & Littlefield Publishing, Inc.

Sissons, J. B. (1967) The Evolution of Scotland's Scenery. Edinburgh: Oliver and Boyd Ltd.

Sissons, J.B., Smith, D.E. and Cullingford, R.A. (1966) *Lateglacial and postglacial shorelines in South-East Scotland.* Transactions of the Institute of British Geographers, vol. 39, pp. 9–18.

Smith, G. (30/10/2008) *Probe after ship runs aground in Tay*. Herald Scotland. (30/1/2011) www.heraldscotland.com

Smith, R. (1993) The Great Flood: a chronicle of the events and people of Perth and Kinross during the flood of January 1993. Perth and Kinross Council: Perth.

Smith, D. E., Davies, M. H., Brooks, C. L., Mighall, T. M., Dawson, S., Rea, B. R., Jordan, J. T. and Holloway, L. K. (2010) *Holocene relative sea levels and related prehistoric activity in the Forth lowlands, Scotland, United Kingdom*. Quaternary Science Reviews, vol. 29, pp. 2382-2410.

Solomon, S., Qin, D., Manning, M., Chen, Z., Marquis, M., Averyt, K. B., Tignor, M. and Miller, H. L. (eds.) (2007) Climate Change 2007: The Physical Science Basis. Contribution of Working Group I to the Fourth Assessment Report of the Intergovernmental Panel on Climate Change. Cambridge: Cambridge University Press.

Soo An, H. (1977) *A numerical experiment of the M2 tide in the Yellow Sea*. Journal of Oceanographical Society of Japan, vol. 33, pp. 103-110.

Sorensen, R. M. (1993) Basic Wave Mechanics: for Coastal and Ocean Engineers. Chicester: John Wiley & Sons.

Stedman, J. R. (2004) *The predicted number of air pollution related deaths in the UK during the August 2003 heatwave*. Atmospheric Environment, vol. 38, pp. 1087-1090.

Steers, J. A. (1973) *The coastline of Scotland*. Proceedings of the Geologist Association, vol. 103, pp. 237-257.

Stirling Council. (2009) Flood Report November 2009. (12/07/2010) http://www.stirling.gov.uk/

Suthons C. T. (1963) *Frequency of occurrence of abnormally high sea levels on the east and south coasts of England*. Proceedings of the Institution of Civil Engineers, vol. 25, pp. 433-450.

Sylvester, R. (1974) Coastal Engineering, II: Sedimentation, Estuaries, Tides, Effluents and Modelling. Amsterdam: Elsevier Scientific Publishing.

Talk Photography. (2011) Rowan Gorilla VI - Dundee. (11/5/2011) http://www.talkphotography.co.uk/

Tay Estuary Forum. (2009) Management Plan: Tay Estuary and adjacent coastline. River North Esk to Fife Ness. Dundee: Tay Estuary Forum.

Tay Estuary Research Centre (TERC) (1991) Chart of the Upper Forth: Alloa to Kincardine Bridge. Tay Estuary Research Centre. University of St. Andrews. In: GeoWise Limited and Glasgow University Coastal Research Group. (2008) Use of GIS to map land claim and identify potential areas for coastal managed realignment in the Forth Estuary. Management Report. Unpublished.

Teasdale, P. A., Collins, P. E. F., Firth, C. R. and Cundy, A. B. (2011) *Recent estuarine sedimentation rates from shallow inter-tidal environments in western Scotland: implications for future sea-level trends and coastal wetland development.* Quaternary Science Reviews, vol. 30, pp. 109-129.

Teferle, F. N., Bingley, R. M., Orliac, E. J., Williams, S. D. P., Woodworth, P. L., McLaughlin, D., Baker, T. F., Shennan, I., Milne, G. A. and Bradley, S. L. (2009) *Crustal motions in Great Britain: evidence from continuous GPS absolute gravity and Holocene sea level data*. Geophysical Journal International, vol. 18, pp. 23-46.

Titus, J. G., Park, R. A., Leatherman, S. P., Weggel, J. R., Greene, M. S., Mausel, P. W., Brown, S., Gaunt, G., Trehan, M. and Yohe, G. (1991) *Greenhouse Effect and Sea Level Rise: The Cost of Holding Back the Sea*. Coastal Management, vol. 19, pp. 171-204.

Torrence, C. and Compo, G. P. (1998) *A Practical Guide to Wavelet Analysis*. Bulletin of the American Meteorological Society, vol. 79, pp. 61-78.

UK Climate Impact Programme (UKCIP). UK Climate Projections 2009. (11/07/2010) www.ukcip.org.uk

UK Hydrographic Office. (2008) Admiralty Charts and Publications: Admiralty Tide Tables 2008 Volume 1 UK and Ireland (Including Euro Channel Ports). Taunton: UKHO.

UK Meteorological Office (UKMO). (2011) The Unified Model. (12/06/2011) http://www.metoffice.gov.uk/research/modelling-systems/unified-model

UK Meteorological Office (UKMO). Floods and Flooding. (12/11/2010) www.metoffice.gov.uk

Unal, Y. S. and Ghil, M. (1995) *Interannual and interdecadal oscillation patterns in sea level*. Climate Dynamics, vol. 11, pp. 255-278.

University of Bangor. Hydroacoustic Communications in the Firth of Forth. (10/08/2009) www.cao.bangor.ac.uk/

University of Colorado Department of Atmospheric and Oceanic Sciences (ATOC) (2011) Wavelets. (12/05/2011) http://atoc.colorado.edu.

University of Maine. (2003) SMS-491: Physical solutions of everyday problems in aquatic sciences. Lecture 6: Surface gravity waves. (13/06/2009) http://misclab.umeoce.maine.edu/boss/classes/SMS_491_2003/Week_6.htm

US National Weather Service Climate Prediction Center (2011) AAO, AO, NAO, PNA. (12/01/2011) www.cpc.ncep.noaa.gov

van Rijn, L. C. (1990) Principles of fluid flow and surface waves in rivers, estuaries, seas and oceans. Amsterdam: Aqua Publications.

Vellinga, P., Katsman, C., Sterl, A., Beersma, J., Hazeleger, W., Church, J., Kopp, R., Kroon, D., Oppenheimer, M., Plag, H.-P., Rahmstorf, S., Lowe, J., Ridley, J., von Storch, H., Vaughan, D., van de Wal, R., Wiesse, R., Kwadijk, J., Lammersen, R. and Miranova, N. (2008) Exploring high-end climate change scenarios for flood protection of The Netherlands. International Scientific Assessment carried out at request of the Delta Committee. Scientific report WR-2009-05. KNMI, Alterra, The Netherlands. (14/10/2010) http://www.knmi.nl/bibliotheek/knmipubWR/WR2009-05.pdf

Vermeer, M. and Rahmstorf, S. (2009) *Global sea level linked to global temperature*. PNAS, vol. 106, pp. 21527-21532.

Wada, Y. L., van Beek, P. H., van Kempen, C. M., Reckman, J. W. T. M., Vasak, S. and Bierkens, M. F. P. (2010) *Global depletion of groundwater resources*, Geophysical Research Letters, vol. 37, L20402.

Watson, C., Coleman, R. and Handsworth, R. (2008) *Tide gauge calibration: a case study at Macquarie Island using GPS buoy techniques*. Journal of Coastal Research, vol. 24 (4), pp. 1071-1079.

Webb, A. J. and Metcalfe, A. P. (1987) *Physical aspects, water movement, and modelling studies of the Forth estuary, Scotland.* Proceedings of the Royal Society of Edinburgh B, vol. 93, pp. 259-272.

Weerts, H. J. T., Westerhoff, W. E., Cleveringa, P., Bierkens, M. F. P., Veldkamp, J. G. and Rijsdijk, K. F. (2005) *Quaternary geological mapping of the lowlands of The Netherlands, a 21st century perspective*. Quaternary International, vol. 133-134, pp. 159-178.

Weert, S. (2011a) *Simple Models of Climate Change*. The Discovery of Global Warming. (12/03/2011) www.aip.org/history/climate

Weert, S. (2011b) *General Circulation Models of Climate.* The Discovery of Global Warming. (12/03/2011) www.aip.org/history/climate

Werritty, A., Black, A. R., Duck, R. W., Finlinson, W., Thurston, N., Shackley, S. and Crichton, D. (2002) Climate Change: Flooding Occurrences Review. Central Research Unit, Scottish Executive: Edinburgh. In: Werritty, A. and Chatterton, J. (2004) Foresight, Future Flooding. Office of Science and Technology: London.

Werritty, A. and Chatterton, J. (2004) Foresight, Future Flooding. Office of Science and Technology: London.

Whatley, C. A., Harris, B. and Haskell, L. (2011) Victorian Dundee. Dundee: Dundee University Press.

Whittington, G. (edt.) (1996) Fragile Environments: The use and management of Tentsmuir NNR, Fife. Edinburgh: Scottish Cultural Press.

Williams, J. A. and Flather, R. A. (2004) The operational storm surge model: maintenance, performance and development January 2003-March 2004. POL Internal Document No. 164.

Williams, D. and West, J. R. (1975) *Salinity distribution in the Tay Estuary*, Proceedings of the Royal Society of Edinburgh B, vol. 75, pp. 29-39.

Woodroffe, C. (1993) *Sea Level*. Progress in Physical Geography, vol. 17, pp. 259-268.

Woodward, H. B. (1904) Stanford's Geological Atlas, based on Reynold's Geological Atlas of 1860 and 1889. (12/11/2011) http://large.stanford.edu

Woodworth, P. L. (1990) *A search for accelerations in records of European mean sea level*. International Journal of Climatology, vol. 10, pp. 129–143.

Woodworth, P., Church, J., Aarup, T. and Wilson, W. (2010) Introduction. In: Church, J., Woodworth, P., Aarup, T. and Wilson, W. (ed.) Understanding sea-level rise and variability. West Sussex: Wiley-Blackwell, pp. 1-16.

Woodworth, P. L. and Jarvis, J. (1991) A feasibility study of the use of short historical and short modern tide gauge records to investigate long term sea level changes in the British Isles. Proudman Oceanographic Internal Document no. 23.

Woodworth, P. L., Tsimplis, M. N., Flather, R. A. and Shennan, I. (1999) *A review of the trends observed in British Isles mean sea level data measured by tide gauges*. Geophysical Journal International, vol. 136, pp. 651-670.

West Lothian Council. Supplimentary Planning Guideline: West Lothian Flood Risk and Drainage. (12/12/2010) www.westlothian.gov.uk

Woodworth, P L., Flather, R A., Williams, J A., Wakelin, S L. and Jevrejeva, S. (2007) *The dependence of UK extreme sea levels and storm surges on the North Atlantic Oscillation*. Continental Shelf Research, vol. 27, pp. 935-946.

Wöppelmann, G., Martin Miguez, B., Bouin, M.-N. and Altaimi, Z. (2007) *Geocentric sea-level trend estimates from GPS analyses at relevant tide gauges world-wide*. Global and Planetary Change, vol. 57, pp. 396-406.

Yan, Z., Tsimplis, M. N. and Woolf, D. (2004) *Analysis of the relationship between the North Atlantic Oscillation and sea-level changes in northwest Europe*. International Journal of Climatology, vol. 24, pp. 743-758.

YouTube.com. YouTube – Broadcast Yourself. (13/1/2011) www.youtube.com

Zong, Y. and Tooley, M. J. (2003) *A historical record of coastal floods in Britain: Frequencies and associated storm tracks*. Natural Hazards, vol. 29, pp. 13-36.

Zsamboky, M., Fernández-Bilbao, A., Smith, D., Knight, J. and Allan, J. (2011) Impacts of climate change on disadvantaged UK coastal communities. Joseph Rowntree Foundation. (12/04/2012) www.jrf.org.uk

Appendices

Appendix 1 – Abbreviations

A1B – SRES medium emissions scenario

A1FI – SRES high emissions scenario

AG – absolute gravimetry

AO – Arctic Oscillations

AR4 - Intergovernmental Panel on Climate Change Fourth Assessment Report

B1 - SRES low emissions scenario

BODC – British Oceanographic Data Centre

CGPS – continuous global positioning system

DATARING - Data Acquisition for Tidal Applications by the Remote Interrogation of Network Gauges

DEFRA – Department of the Environment, Food and Rural Affairs

GCM – global climate model/ general circulation model

GIA – glacio-isostatic adjustment

GISS - Goddard Institute for Space Studies, related to global temperature data

HadCM3 – UKMO Hadley Centre Climate Model 3

HadGEM1 – UKMO Hadley Centre Global Environment Model 3

IPCC – Intergovernmental Panel on Climate Change

LFO – Arctic Oscillation Low-Frequency Oscillation

MCCIP – Marine Climate Change Impact Partnership

MetUM – UKMO Unified Model

MME – multi-model ensemble

NAO – North Atlantic Oscillation

NTSLF – National Tidal and Sea Level Facility

POL – Proudman Oceanographic Laboratory

POLCS3 - Proudman Oceanographic Laboratory Continental Shelf tid-surge model 3

PPE – perturbed physical ensemble

PSI – persistent scatter interferometry

PSMSL - Permanent Service for Mean Sea Level

RLLC – relative land-level change, associated with GIA

RCM – regional climate model

SEPA – Scottish Environment Protection Agency

SNH – Scottish Natural Heritage

SRES – IPCC Special Report on Emissions Scenarios

SST – sea surface temperature

TAR – Intergovernmental Panel on Climate Change Third Assessment Report

UKCIP – UK Climate Impact Programme

UKCP09 – UK Climate Projections 2009

UKHO – UK Hydrographic Office

UKMO – UK Meteorological Office

VLM – vertical land motion, associated with GIA

Appendix 2 – Literature Review Additional Information

Symbol	Name	Speed (^{o}/h)	Amplitude (m)	Phase at Midnight, 9/1/91 (^{o})
M_2	Principal lunar semi-diurnal	2T-2s+2h = 28.984	0.971	-127.24
N_2	Lunar elliptical semi-diurnal	2T-3s+2h+p = 28.439	0.212	263.60
S_2	Principal solar semi-diurnal	2T = 30.000	0.164	-343.66
K_1	Luni-solar diurnal	T+h = 15.041	0.090	142.02
L_2	N_2 modulator	2T-s+2h-p = 29.528	0.084	-4.72
O_1	Lunar diurnal	T-2s+h = 13.943	0.065	505.93
Sa	Solar annual	h = 0.041	0..059	301.50
NU_2	Lunar eplliptical 2nd Order	2T-3s++4h-p = 28.512	0.048	45.70
K_2	Luni-solar semi-diurnal	2T+2h = 30.082	0.044	-2.55
Mm	Lunar monthly	s-p = 0.544	0.033	86.82
P_1	Solar diurnal	T-h = 14.958	0.031	340.11

Table A2.1. 11 out of 23 constituents that are over 0.1 foot amplitude identified by Phillips (2009); refer to oscillation section for speed constituent explanation.

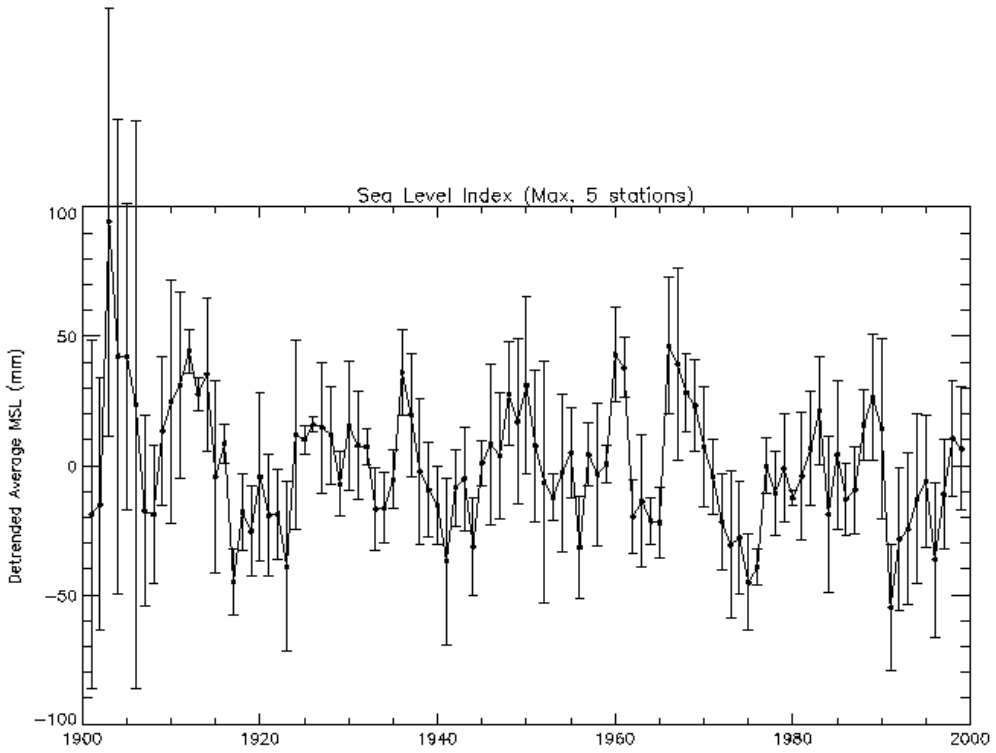

Figure A2.1. An index of changes in UK-average sea level (Flather *et al.*, 2001:8).

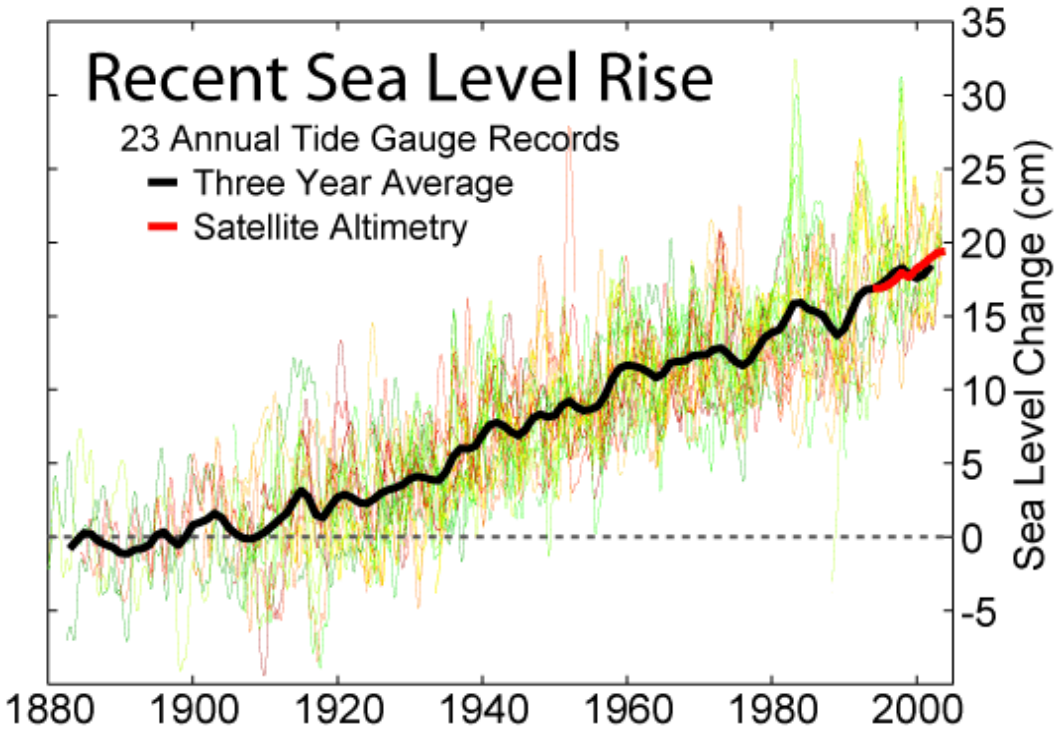

Figure A2.2. Recent sea level rise compiled from 23 tide gauge records by Douglas (1997) and illustrated by Rohde (2009b).

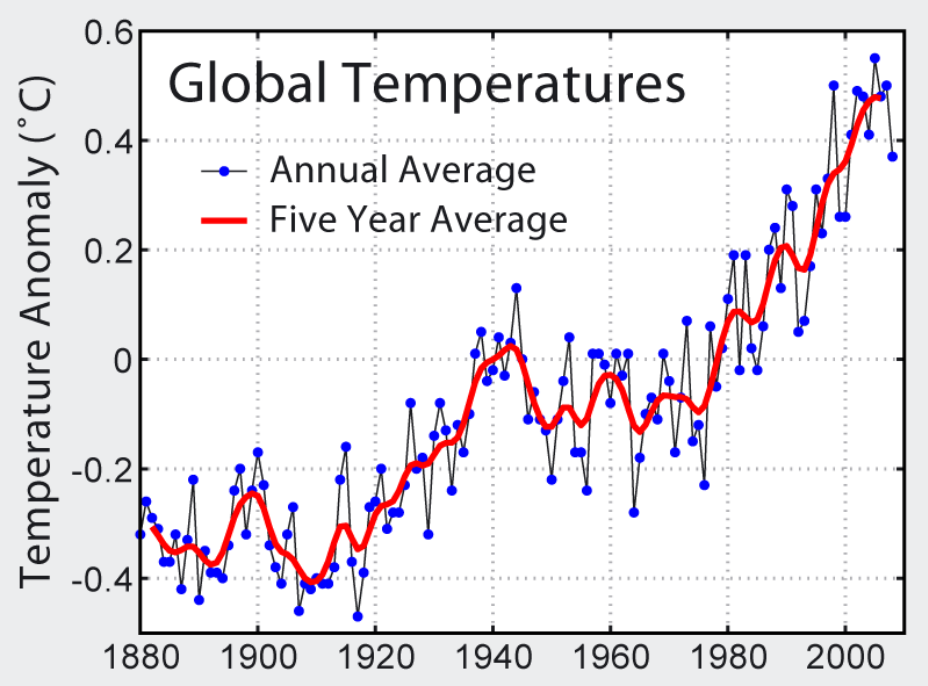

Figure A2.3. Global temperature rise since 1880 compiled from Hansen *et al.* (2006), Houghton *et al.* (2001) and Follard *et al.* (2001) by Rohde (2009c).

Site No.	No. of sea level index points	No. of limiting dates	Site Name	Rate since 4 kyr BP (mm a^{-1})	SE	Best estimate (mm a^{-1})	Reference(s)
1	4	0	Shetlands			<0.0	Hoppe, 1965
2	6	9	Orkney			<0.0	De la Vega and Smith, 1996
3	11	3	Wick	0.08	0.14	0.42	Dawson and Smith, 1997
4	7	0	Dornoch Firth			0.65	Smith *et al.*, 1992
5	9	0	Moray Firth			1.11	Haggart, 1987; Forth and Haggart, 1989
6	7	1	NW Scotland (Coigach)			0.56	Shennan *et al.*, 2000a
7	2	1	Hebrides				Ritchie, 1985
8	7	1	Skye	0.83	0.05	0.81	Selby *et al.*, 2000
9	7	0	NW Scotland (Applecross)	0.4	0.01	0.49	Shennan *et al.*, 2000a
10	11	0	NW Scotland (Kintail)	0.44	0.11	0.73	Shennan *et al.*, 2000a
11	36	0	NW Scotland (Arisaig)	1.13	0.12	1.01	Shennan *et al.*, 1993; 1994; 1995b; 1999; 2000a
12	14	2	NW Scotland (Kentra)	1.06	0.03	1	Shennan *et al.*, 1995a; 1996; 2000a
13	19	5	NE Scotland			0.61	Smith *et al.*, 1982; 1999
14	4	0	Aberdeen			0.69	Smith *et al.*, 1983
15	7	0	Montrose			0.97	Smith and Cullingford, 1985
16	36	0	Tay Valley			1.08	Smith *et al.*, 1985a; 1985b; Haggart and Smith, 1988a
17	21	0	Forth Valley			1.63	Robinson, 1993
18	10	0	Islay	1.46	0.06	1.52	Dawson *et al.*, 1998
19	6	0	Ardyne				Peacock *et al.*, 1978
20	5	0	Clyde	1.54	0.04	1.53	Haggart, 1988a
21	10	0	Ayr			1.98	Donner, 1970; Jardine, 1975; 1982
22	3	0	SE Scotland	1.15		1.15	Robinson, 1982
23	12	5	NE England (North)	0.71		0.71	Shennan *et al.*, 2000d
24	8	2	NE England (Central)			0.11	Plater and Shennan, 1992; Shennan *et al.*, 2000d
25	26	1	NE England (South)	-0.09	0.06	0.17	Plater and Shennan, 1992; Shennan *et al.*,

							2000d
26	30	0	Tees	-0.38	0	-0.17	Gaunt and Tooley, 1974; Tooley, 1978a; 1978b; Plater and Poolton, 1992; Shennan, 1992; Plater *et al.*, 2000; Horton *et al.*, 1999
27	30	2	N Solway Firth	0.96	0.34	1.13	Jardine, 1975; 1982; Lloyd *et al.*, 1999; Haggart, 1999
28	14	1	S Solway Firth	0.66	0.22	0.87	Huddart *et al.*, 1977; Tooley 1978a; Lloyd *et al.*, 1999
29	6	0	Cumbria			0.95	Huddart *et al.*, 1977; Tooley 1978a; Zong and Tooley, 1996
30	12	2	Isle of Man			0.45	Tooley, 1977
31	28	3	Morecambe Bay	0.5	0.33	0.69	Tooley, 1974; 1978a; Zong, 1998
32	42	1	Lancashire	0.1	0.15	0.47	Tooley, 1974; 1978a; 1978c; 1985; Huddart, 1992
33	15	0	Mersey	-0.28	0.03	-0.21	Tooley, 1974; 1978a; 1978c; Bedlington, 1993; Cowell and Innes, 1994
34	9	0	N Wales			-0.29	Tooley, 1978a; Kidson and Heyworth, 1982; Bedlington, 1993
35	14	3	Mid Wales	-0.41	0.05	-0.38	Heyworth and Kidson, 1982
36	31	30	Humber (inner estuary)	-1.31	0.09	-0.86	Smith, 1958; Gaunt and Tooley, 1974; van de Noort and Ellis, 1995; 1997; 1998; Millett and McGrail, 1987; Long *et al.*, 1998; Andrews *et al.*, 2000a; Metcalfe *et al.*, 2000; Rees *et al.*, 2000
37	34	8	Humber (outer estuary)	-1.03	0.08	-0.78	Gaunt and Tooley, 1974; van de Noort and Ellis, 1995; 1997; 1998; Millett and McGrail, 1987; Long *et al.*, 1998; Andrews *et al.*, 2000a; Metcalfe *et al.*, 2000; Rees et al., 2000
38	30	3	Lincolnshire Marshes	-0.97	0.11	-0.62	Waller, 1994; Horton *et al.*, 2000
39	194	28	Fens	-1.3	0.04	-0.86	Shennan, 1986a; 1986b; Waller, 1994;

							Brew *et al.*, 2000
40	31	18	Norfolk	-1.37	0.16	-0.76	Funnel and Pearson, 1989; Andrews *et al.*, 2000b
41	25	5	East Anglia	-1.7	0.17	-0.61	Coles and Funnel, 1981; Brew *et al.*, 1992
42	1	0	S Wales (Pembrokeshire)				Heyworth and Kidson, 1982
43	5	3	S Wales (Glamorgan)	-2.52			Heyworth and Kidson, 1982
44	70	0	Bristol Channel	-1.06	0.08	-0.76	Heyworth and Kidson, 1982; Smith and Morgan, 1989; Jennings *et al.*, 1998; Haslett *et al.*, 1998; 2001
45	11	0	Essex	-0.85	0.22	-0.85	Greensmith and Tucker, 1980; Devoy, 1982; Wilkinson and Murphy, 1986
46	50	24	Thames	-1.46	0.13	-0.74	Greensmith and Tucker, 1980; Devoy, 1979; 1982; Barham *et al.*, 1995; Siddel *et al.*, 2000; Wilkinson *et al.*, 2000
47	71	0	Kent	-1.14	0.07	-0.67	Tooley and Switsur, 1988; Long, 1992; Long and Innes, 1993; 1995; Long *et al.*, 1996; Waller *et al.*, 1999; Spencer *et al.*, 1998
48	11	3	Sussex	-0.63	0.27	-0.42	Devoy, 1982; Jennings and Smyth, 1987
49	11	4	Hampshire	-0.71	0.03	-0.58	Long and Tooley, 1995; Long *et al.*, 2000
50	4	0	SW England (Dorset)	-0.49		-0.49	Devoy, 1982; Long *et al.*, 1999
51	6	2	SW England (Dorset)	-1.43	0.18	-1.23	Devoy, 1982
52	7	0	SW England (Cornwall)	-1.27	0.21	-1.12	Healy, 1995; 1999

Table. A2.2. 'Summary data for each site, including number of validated sea-level index points and limiting dates, net rate of relative land uplift (positive sign, equal to relative sea-level fall) calculated from data 0–4 kyr BP, with the standard error (SE), best estimate of the rate of relative land uplift after allowing for evidence of sediment consolidation (see text), for five sites the best estimate after allowing for modelled tidal range changes during the late Holocene, and the key literature references' (Shennan and Horton, 2002: 519). All extended references can be found in Shennan and Horton (2002).

European, UK and devolved national authorities' legislation and policy documents:

- **EC Floods Directive 2007,**
- **UK Coastal Protection Act 1949,**
- **Water Resources Act 1991,**
- **UK Marine and Coastal Access Act 2009,**
- **UK Flood and Water Management Act 2010,**
- **Marine (Scotland) Act 2010,**
- **UK Planning Policy Statement (PPS) 25 Development and Flood Risk,**
- **UK Marine Policy Statement 2011,**
- **The National Flood and Coastal Erosion Risk Management Strategy for England 2011,**
- **National Strategy for Flood and Coastal Erosion Risk Management to Wales,**
- **National Flood Emergency Framework for England 2011,**
- **Changing Our Ways: Scotland's Climate Change Programme,**
- **The threat posed by tsunami to the UK (DEFRA, 2005),**
- **Ready Scotland – advisory website (Scottish Government, 2011),**
- **Wales Prepared – advisory website (Wales Resilience Forum, 2011).**

Box A2.1. A selection of UK government and devolved national authority legislation and policy documents orientated around sea level and climate change.

Appendix 3 – Coal Mining Reports

The Coal Authority

Issued by:
The Coal Authority, Mining Reports Office, 200 Lichfield Lane, Berry Hill, Mansfield, Nottinghamshire NG18 4RG
ON-Line Service: www.groundstability.com - Phone: 0845 762 6848 - DX 716176 MANSFIELD 5

VICTORIA POWELL,
PERTH ROAD,
DUNDEE,
ANGUS,
DD1 4HN

Person dealing with this matter:	**Eric Fretwell**
Our reference:	**00029480-10**
Your reference:	
Electronic Ref:	
RRUID:	007.00028233690001
Date of your enquiry:	**06 July 2010**
Date we received your enquiry:	**06 July 2010**
Date of issue:	**06 July 2010**

This report is for the property described in the address below and the attached plan.

Coal Mining Report

Port Of Grangemouth Tide Gauge Housing, Grangemouth, West Lothian

This report is based on and limited to the records held by the Coal Authority, at the time we answer the search.

Coal mining	Yes

Information from the Coal Authority

Underground Coal Mining

Past

According to the records in our possession, the property is not within the zone of likely physical influence on the surface from past underground workings.

Present

The property is not in the likely zone of influence of any present underground coal workings.

Future

The property is not in an area for which the Coal Authority is determining whether to grant a licence to remove coal using underground methods.

The property is in an area for which a licence to remove coal using underground methods was granted in October 1994.

The property is not in an area that is likely to be affected at the surface from any planned future workings.

However reserves of coal exist in the local area which could be worked at some time in the future.

No notice of the risk of the land being affected by subsidence has been given under section 46 of the Coal Mining Subsidence Act 1991.

Mine entries

There are no known coal mine entries within, or within 20 metres of, the boundary of the property.

Coal-mining geology

The Authority is not aware of any evidence of damage arising due to geological faults or other lines of weakness that have been affected by coal mining.

Opencast Coal Mining

Past

The property is not within the boundary of an opencast site from which coal has been removed by opencast methods.

Present

The property does not lie within 200 metres of the boundary of an opencast site from which coal is being removed by opencast methods.

Future

The property is not within 800 metres of the boundary of an opencast site for which the Coal Authority is determining whether to grant a licence to remove coal by opencast methods.

The property is not within 800 metres of the boundary of an opencast site for which a licence to remove coal by opencast methods has been granted.

Coal-mining subsidence

The Coal Authority has not received a damage notice or claim for the property since 1 January 1984. There is no current Stop Notice delaying the start of remedial works or repairs to the property.

The Authority is not aware of any request having been made to carry out preventive works before coal is worked under section 33 of the Coal Mining Subsidence Act 1991.

Mine gas

There is no record of a mine gas emission requiring action by the Coal Authority within the boundary of the property.

Hazards related to coal mining

The property has not been subject to remedial works, by or on behalf of the Authority, under its Emergency Surface Hazard Call Out procedures.

Withdrawal of Support

The property is in an area for which a notice of entitlement to withdraw support was published in 1980.

The property is not in an area for which a notice has been given under section 41 of the Coal Industry Act 1994, revoking the entitlement to withdraw support.

Working Facilities Orders

The property is not in an area for which an Order has been made under the provisions of the Mines (Working Facilities and Support) Acts 1923 and 1966 or any statutory modification or amendment thereof.

Payments to Owners of Former Copyhold Land

The property is not in an area for which a relevant notice has been published under the Coal Industry Act 1975/Coal Industry Act 1994.

Comments on Coal Authority information

Where development proposals are being considered, technical advice should be obtained before beginning work on site. All proposals should apply good engineering practice developed for mining areas.

Additional remarks

This report is prepared in accordance with the Law Society's Guidance Notes 2006, the User Guide 2006 and the Coal Authority Terms and Conditions 2006. The report is compliant with Home Information Pack and Home Report (Scotland) requirements.

Location map

Approximate position of property

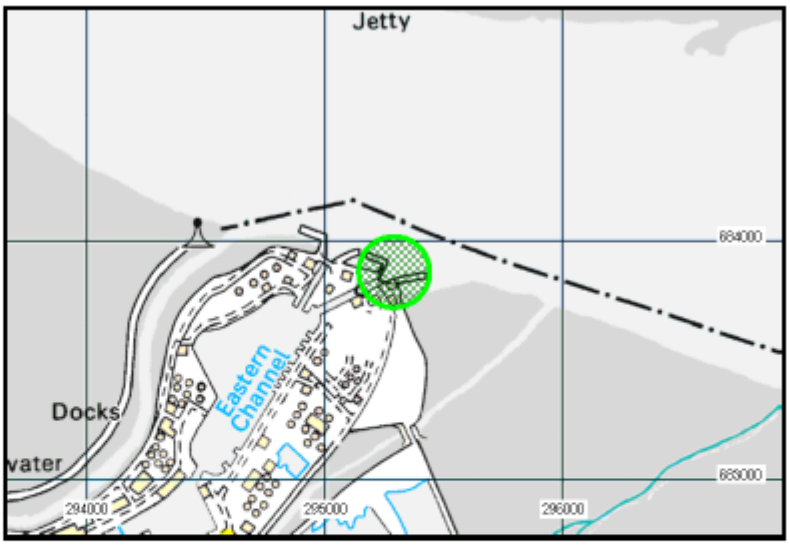

Enquiry boundary

Key

Approximate position of enquiry boundary shown

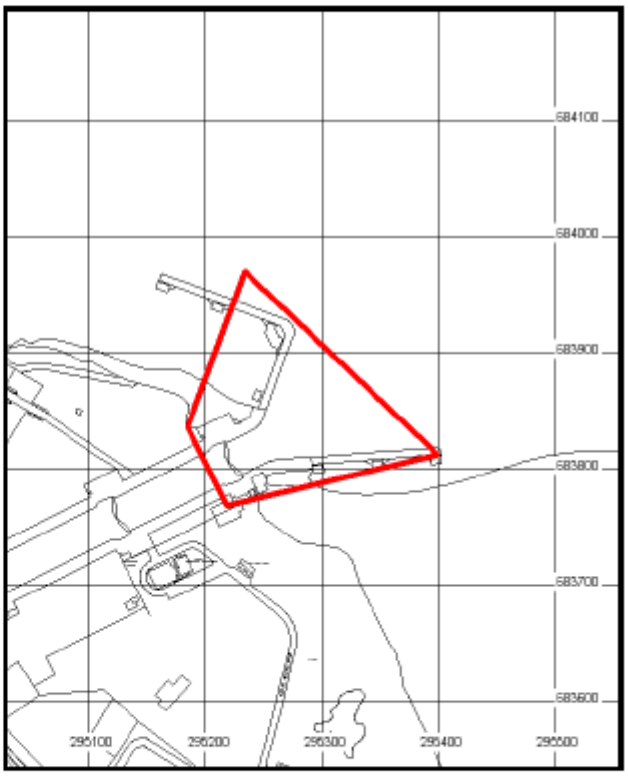

Mapping sourced from Ordnance Survey

Issued by:
The Coal Authority, Mining Reports Office, 200 Lichfield Lane, Berry Hill, Mansfield, Nottinghamshire NG18 4RG
ON-Line Service: www.groundstability.com - Phone: 0845 762 6848 - DX 716176 MANSFIELD 5

VICTORIA POWELL,
PERTH ROAD,
DUNDEE,
ANGUS,
DD1 4HN

Person dealing with this matter:	**Eric Fretwell**
Our reference:	**00029493-10**
Your reference:	
Electronic Ref:	
RRUID:	007.00028233840001
Date of your enquiry:	**06 July 2010**
Date we received your enquiry:	**06 July 2010**
Date of issue:	**06 July 2010**

This report is for the property described in the address below and the attached plan.

Coal Mining Report

Port Of Methil Harbour Mouth, Methil Harbour, Fife

This report is based on and limited to the records held by the Coal Authority, at the time we answer the search.

Coal mining	Yes

Information from the Coal Authority

Underground Coal Mining

Past

The property is in the likely zone of influence from workings in 5 seams of coal at 250m to 660m depth, and last worked in 1963.

Any ground movement from these coal workings should have stopped by now.

Present

The property is not in the likely zone of influence of any present underground coal workings.

Future

The property is not in an area for which the Coal Authority is determining whether to grant a licence to remove coal using underground methods.

The property is in an area for which a licence to remove coal using underground methods was granted in January 2009. The grant of this licence is conditional on the applicant securing any other rights, permissions (including planning permission) and consents to enable operations to be carried out.

The property is not in an area that is likely to be affected at the surface from any planned future workings.

However reserves of coal exist in the local area which could be worked at some time in the future.

No notice of the risk of the land being affected by subsidence has been given under section 46 of the Coal Mining Subsidence Act 1991.

Mine entries

There are no known coal mine entries within, or within 20 metres of, the boundary of the property.

Coal-mining geology

The Authority is not aware of any evidence of damage arising due to geological faults or other lines of weakness that have been affected by coal mining.

Opencast Coal Mining

Past

The property is not within the boundary of an opencast site from which coal has been removed by opencast methods.

Present

The property does not lie within 200 metres of the boundary of an opencast site from which coal is being removed by opencast methods.

Future

The property is not within 800 metres of the boundary of an opencast site for which the Coal Authority is determining whether to grant a licence to remove coal by opencast methods.

The property is not within 800 metres of the boundary of an opencast site for which a licence to remove coal by opencast methods has been granted.

Coal-mining subsidence

The Coal Authority has not received a damage notice or claim for the property since 1 January 1984. There is no current Stop Notice delaying the start of remedial works or repairs to the property.

The Authority is not aware of any request having been made to carry out preventive works before coal is worked under section 33 of the Coal Mining Subsidence Act 1991.

Mine gas

There is no record of a mine gas emission requiring action by the Coal Authority within the boundary of the property.

Hazards related to coal mining

The property has not been subject to remedial works, by or on behalf of the Authority, under its Emergency Surface Hazard Call Out procedures.

Withdrawal of Support

The property is not in an area for which a notice of entitlement to withdraw support has been published.

The property is not in an area for which a notice has been given under section 41 of the Coal Industry Act 1994, revoking the entitlement to withdraw support.

Working Facilities Orders

The property is not in an area for which an Order has been made under the provisions of the Mines (Working Facilities and Support) Acts 1923 and 1966 or any statutory modification or amendment thereof.

Payments to Owners of Former Copyhold Land

The property is not in an area for which a relevant notice has been published under the Coal Industry Act 1975/Coal Industry Act 1994.

Comments on Coal Authority information

Where development proposals are being considered, technical advice should be obtained before beginning work on site. All proposals should apply good engineering practice developed for mining areas.

Additional remarks

This report is prepared in accordance with the Law Society's Guidance Notes 2006, the User Guide 2006 and the Coal Authority Terms and Conditions 2006. The report is compliant with Home Information Pack and Home Report (Scotland) requirements.

Location map

Approximate position of property

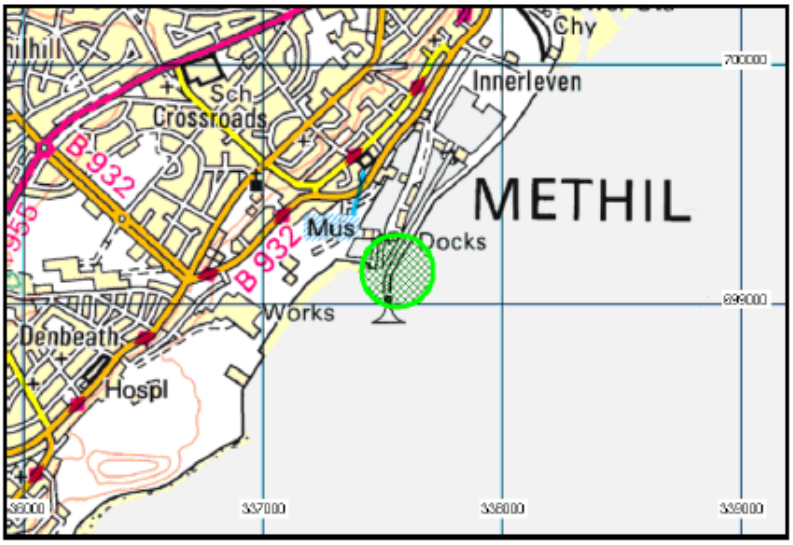

Enquiry boundary

Key

Approximate position of enquiry boundary shown

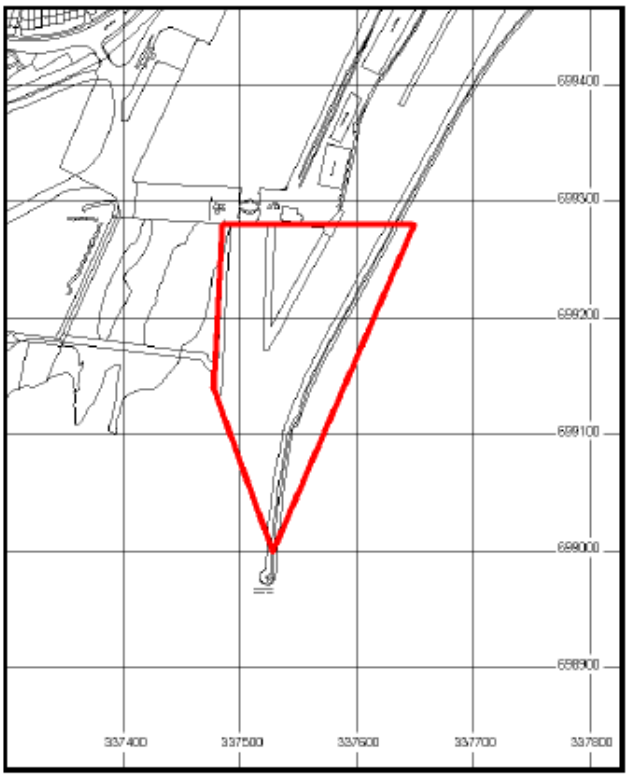

Mapping sourced from Ordnance Survey

Issued by:
The Coal Authority, Mining Reports Office, 200 Lichfield Lane, Berry Hill, Mansfield, Nottinghamshire NG18 4RG
ON-Line Service: www.groundstability.com - Phone: 0845 762 6848 - DX 716176 MANSFIELD 5

VICTORIA POWELL,
PERTH ROAD,
DUNDEE,
ANGUS,
DD1 4HN

Person dealing with this matter:	**Eric Fretwell**
Our reference:	**00029492-10**
Your reference:	
Electronic Ref:	
RRUID:	007.00028233910001
Date of your enquiry:	**06 July 2010**
Date we received your enquiry:	**06 July 2010**
Date of issue:	**06 July 2010**

This report is for the property described in the address below and the attached plan.

Coal Mining Report

Musselburgh Harbour Mouth, Musselburgh, West Lothian

This report is based on and limited to the records held by the Coal Authority, at the time we answer the search.

Coal mining	Yes

Information from the Coal Authority

Underground Coal Mining

Past

The property is in the likely zone of influence from workings in 6 seams of coal at 200m to 1040m depth, and last worked in 1986.

Any ground movement from these coal workings should have stopped by now.

Present

The property is not in the likely zone of influence of any present underground coal workings.

Future

The property is not in an area for which the Coal Authority is determining whether to grant a licence to remove coal using underground methods.

The property is not in an area for which a licence has been granted to remove coal using underground methods.

The property is not in an area that is likely to be affected at the surface from any planned future workings.

However reserves of coal exist in the local area which could be worked at some time in the future.

No notice of the risk of the land being affected by subsidence has been given under section 46 of the Coal Mining Subsidence Act 1991.

Mine entries

There are no known coal mine entries within, or within 20 metres of, the boundary of the property.

Coal-mining geology

The Authority is not aware of any evidence of damage arising due to geological faults or other lines of weakness that have been affected by coal mining.

Opencast Coal Mining

Past

The property is not within the boundary of an opencast site from which coal has been removed by opencast methods.

Present

The property does not lie within 200 metres of the boundary of an opencast site from which coal is being removed by opencast methods.

Future

The property is not within 800 metres of the boundary of an opencast site for which the Coal Authority is determining whether to grant a licence to remove coal by opencast methods.

The property is not within 800 metres of the boundary of an opencast site for which a licence to remove coal by opencast methods has been granted.

Coal-mining subsidence

The Coal Authority has not received a damage notice or claim for the property since 1 January 1984. There is no current Stop Notice delaying the start of remedial works or repairs to the property.

The Authority is not aware of any request having been made to carry out preventive works before coal is worked under section 33 of the Coal Mining Subsidence Act 1991.

Mine gas

There is no record of a mine gas emission requiring action by the Coal Authority within the boundary of the property.

Hazards related to coal mining

The property has not been subject to remedial works, by or on behalf of the Authority, under its Emergency Surface Hazard Call Out procedures.

Withdrawal of Support

The property is not in an area for which a notice of entitlement to withdraw support has been published.

The property is not in an area for which a notice has been given under section 41 of the Coal Industry Act 1994, revoking the entitlement to withdraw support.

Working Facilities Orders

The property is not in an area for which an Order has been made under the provisions of the Mines (Working Facilities and Support) Acts 1923 and 1966 or any statutory modification or amendment thereof.

Payments to Owners of Former Copyhold Land

The property is not in an area for which a relevant notice has been published under the Coal Industry Act 1975/Coal Industry Act 1994.

Additional remarks

This report is prepared in accordance with the Law Society's Guidance Notes 2006, the User Guide 2006 and the Coal Authority Terms and Conditions 2006. The report is compliant with Home Information Pack and Home Report (Scotland) requirements.

Location map

Approximate
position
of property

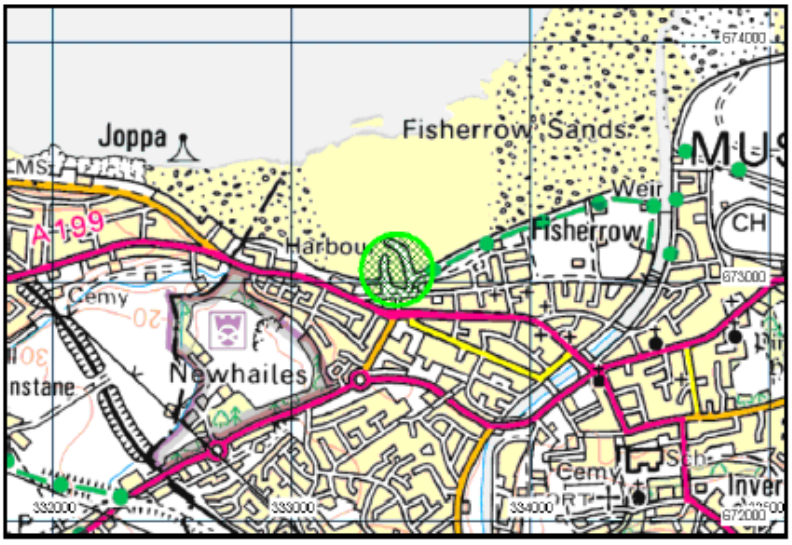

Enquiry boundary

Key

Approximate position of enquiry boundary shown

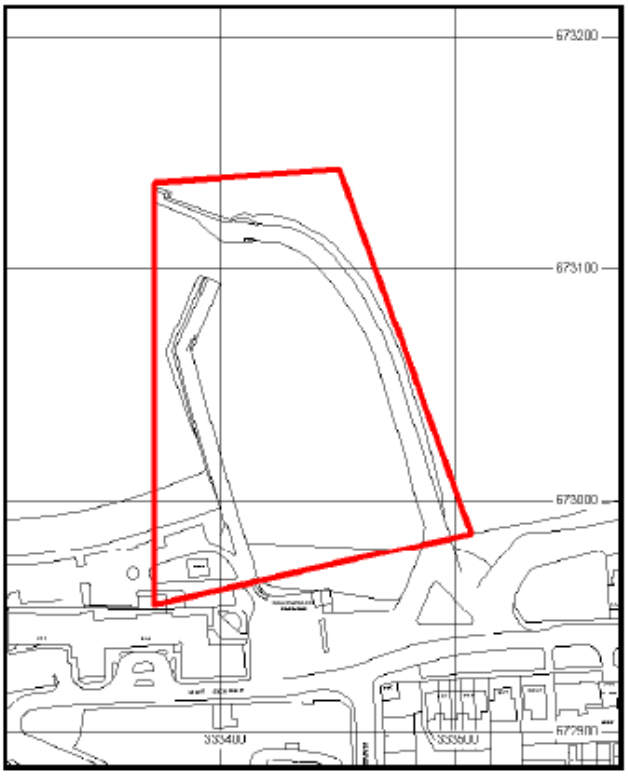

Mapping sourced from Ordnance Survey

The Coal Authority

Issued by:
The Coal Authority, Mining Reports Office, 200 Lichfield Lane, Berry Hill, Mansfield, Nottinghamshire NG18 4RG
ON-Line Service: www.groundstability.com - Phone: 0845 762 6848 - DX 716176 MANSFIELD 5

VICTORIA POWELL,
PERTH ROAD,
DUNDEE,
ANGUS,
DD1 4HN

Person dealing with this matter:	**Eric Fretwell**
Our reference:	**00029479-10**
Your reference:	
Electronic Ref:	
RRUID:	007.00028233750001
Date of your enquiry:	**06 July 2010**
Date we received your enquiry:	**06 July 2010**
Date of issue:	**06 July 2010**

This report is for the property described in the address below and the attached plan.

Coal Mining Report

Port Of Rosyth Harbour Mouth, Rosyth, Fife

This report is based on and limited to the records held by the Coal Authority, at the time we answer the search.

Coal mining	Yes

Information from the Coal Authority

Underground Coal Mining

Past

According to the records in our possession, the property is not within the zone of likely physical influence on the surface from past underground workings.

Present

The property is not in the likely zone of influence of any present underground coal workings.

Future

The property is not in an area for which the Coal Authority is determining whether to grant a licence to remove coal using underground methods.

The property is not in an area for which a licence has been granted to remove coal using underground methods.

The property is not in an area that is likely to be affected at the surface from any planned future workings.

However reserves of coal exist in the local area which could be worked at some time in the future.

No notice of the risk of the land being affected by subsidence has been given under section 46 of the Coal Mining Subsidence Act 1991.

Mine entries

There are no known coal mine entries within, or within 20 metres of, the boundary of the property.

Coal-mining geology

The Authority is not aware of any evidence of damage arising due to geological faults or other lines of weakness that have been affected by coal mining.

Opencast Coal Mining

Past

The property is not within the boundary of an opencast site from which coal has been removed by opencast methods.

Present

The property does not lie within 200 metres of the boundary of an opencast site from which coal is being removed by opencast methods.

Future

The property is not within 800 metres of the boundary of an opencast site for which the Coal Authority is determining whether to grant a licence to remove coal by opencast methods.

The property is not within 800 metres of the boundary of an opencast site for which a licence to remove coal by opencast methods has been granted.

Coal-mining subsidence

The Coal Authority has not received a damage notice or claim for the property since 1 January 1984. There is no current Stop Notice delaying the start of remedial works or repairs to the property.

The Authority is not aware of any request having been made to carry out preventive works before coal is worked under section 33 of the Coal Mining Subsidence Act 1991.

Mine gas

There is no record of a mine gas emission requiring action by the Coal Authority within the boundary of the property.

Hazards related to coal mining

The property has not been subject to remedial works, by or on behalf of the Authority, under its Emergency Surface Hazard Call Out procedures.

Withdrawal of Support

The property is not in an area for which a notice of entitlement to withdraw support has been published.

The property is not in an area for which a notice has been given under section 41 of the Coal Industry Act 1994, revoking the entitlement to withdraw support.

Working Facilities Orders

The property is not in an area for which an Order has been made under the provisions of the Mines (Working Facilities and Support) Acts 1923 and 1966 or any statutory modification or amendment thereof.

Payments to Owners of Former Copyhold Land

The property is not in an area for which a relevant notice has been published under the Coal Industry Act 1975/Coal Industry Act 1994.

Additional remarks

This report is prepared in accordance with the Law Society's Guidance Notes 2006, the User Guide 2006 and the Coal Authority Terms and Conditions 2006. The report is compliant with Home Information Pack and Home Report (Scotland) requirements.

Location map

Approximate position of property

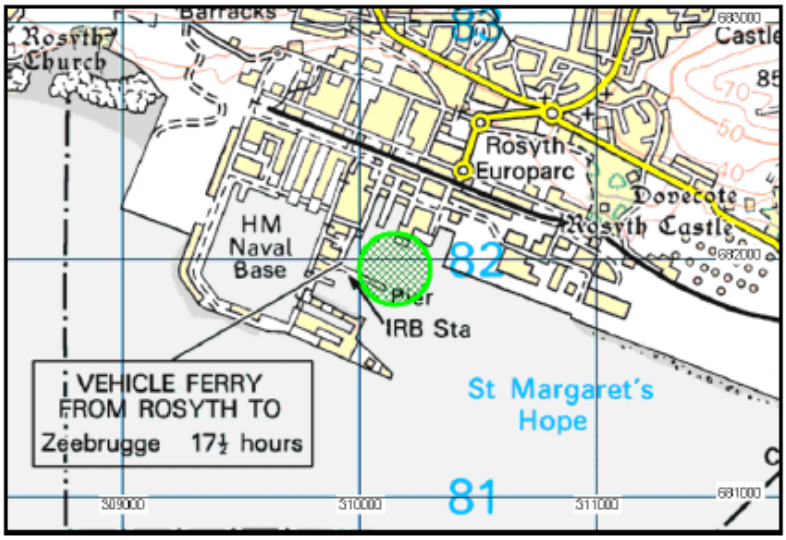

Enquiry boundary

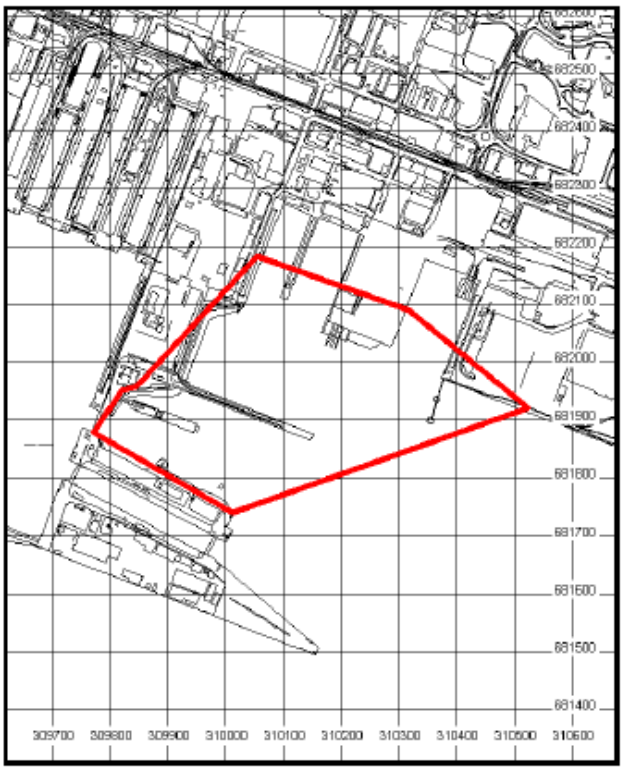

Key

Approximate position of enquiry boundary shown

Mapping sourced from Ordnance Survey

Figure A6.1. Photograph of TERC buoys on the west side of Newport Pier in November 1979. Cracks appearing near the concrete extension join (courtesy of R Duck).

Figure A6.2. Photograph of the west side of Newport Pier in January 1982 showing infill of extension join cracks and nearby patches (courtesy of R Duck).

Figure A6.3. Photograph of the east side of Newport Pier in February 1990 some of the damage caused by a storm event (courtesy of R Duck).

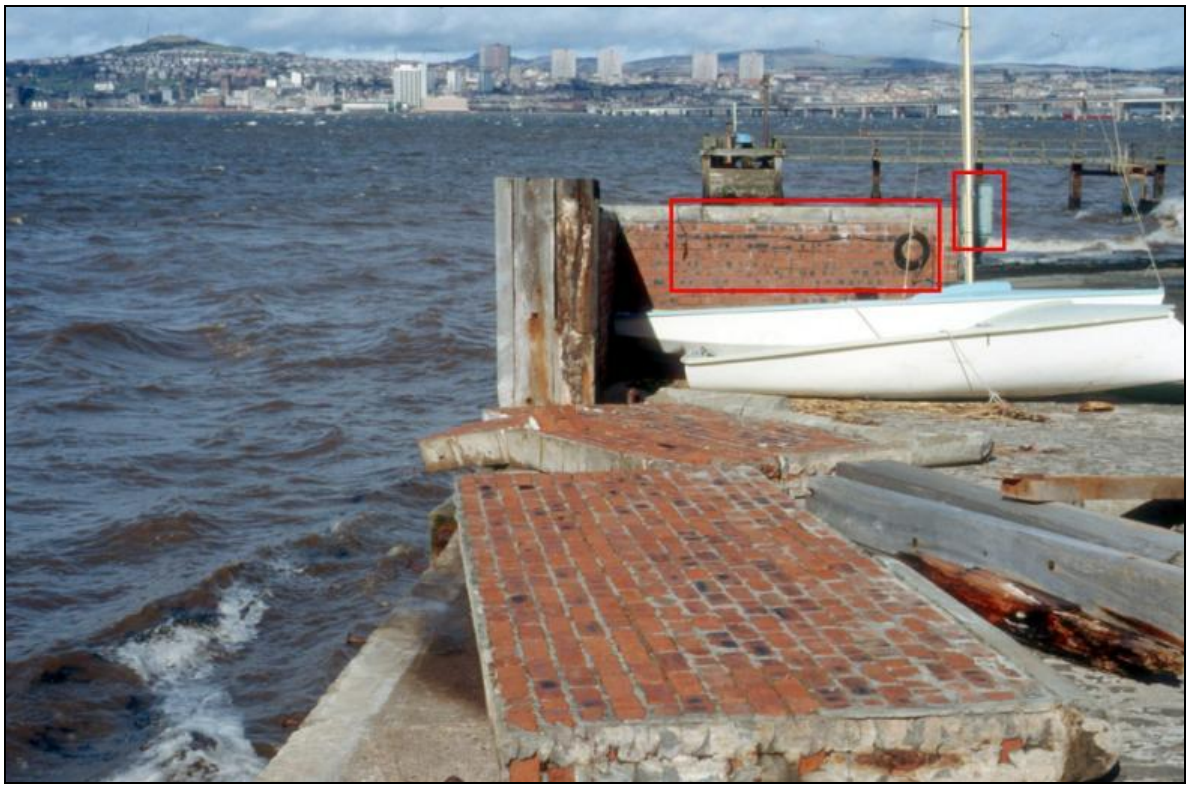

Figure A6.4. Photograph of the west side of Newport Pier in February 1990 showing some of the damage caused by a storm event. On the remaining standing wall the tide gauge housing the connecting tranducer cable shown within the two red boxes (courtesy of R Duck).

Figure A6.5. Photograph of the west side of Newport Pier in June 2002. Red squares represent patch repairs to the pier surface. Red lines highlight cracks along the pier surface. The foremost patch is visible in the 1994 photograph (Figure 6.80) along with the hollow formed at the location of the right most crack (courtesy of R Duck).

Appendix 5 – Methods

Box A5.1. Tide gauge background information

Early records of sea level change were made manually by transcribing high and low tide levels from tide boards and markers located on coastal infrastructure (e.g. at lock entrances in ports). Tide boards and meters were initially used to monitor levels of the tide to ensure appropriate under keel clearance for vessels calling at ports and harbours. As tidal cycles became better understood, primarily due to the increased level of study by several engineers, harbour management and scientists (see Rossiter, 1972, and Matthäus, 1972), these readings were used to calculate tidal predictions and allowed harbour managers to predict timings for safe ship transit.

Tide gauges consist of several different features, including:

- *Measuring components* – sensors and transducers;
- *Protective or supportive components* – tubes, stilling wells and masts;
- *Storing or controlling components* – pen-recorders, self-contained dataloggers and PCs (Martin and Perez, 2010).

Each sensor varies in accuracy due to their collection method. Four types of sensor include:

- *Float gauges* – The level of the water is measured at which a float rests by feeding a wire through a counter-weighted drum measuring system (Permanent Service for Mean Sea Level (PSMSL), 2011). This gauge may be protected by a stilling well to reduce the impact of waves and may be connected to a pen or digital recording device;
- *Acoustic gauges* – A fixed position gauge that relies on acoustic pulses that reflect vertically from the water surface. Again this gauge may be attached to a digital recording device;
- *Pressure gauges* –Water level is measured with respect to changes in pressure exerted by the water column. This may be of a bubbler design that measures pressure relative to a pressurised air tub that is subject to the full tidal cycle. Alternatively, pressure transducers measure direct water pressure below MLWS throughout the tidal cycle, which for complete accuracy is compared with an atmospheric pressure recording to remove this element for the tidal record. For

accuracy the direct pressure transducer may be kept in a stilling well. Both of these systems could be connected to a pen recorder or digital recorder;

- *RADAR gauges* – This detects microwave pulses reflected by the sea surface, either by the time lag of the signal (pulse RADAR) or the phase shift change between emitted and detected waves (optical phase ranging) (Martin and Perez, 2010). Both of these are fixed gauge systems and can be recorded digitally.

To promote high accuracy of recording tide gauges Martin and Perez (2010) made the following suggestions:

- Use connected GPS to avoid timing and land level change errors;
- Install a protective tube or stilling well to protect the sensor against waves, vandalism and theft;
- Use of a stilling well or protective coverage around the tide board and gauge during calibration to a tide board.

Tide gauge systems vary in their software limitations, user-interface 'friendliness', ease of data transmission and the price (Martin and Perez, 2010). Considering all of these aspects RADAR gauges appear to be one of the best options for relative sea level recording, however there are no RADAR gauges operating in the Forth and Tay Estuaries. The historic and current tide gauge measuring components (with descriptions sourced from PSMSL, 2011) on the Forth and Tay, used as sources in this thesis include (Table 5.1):

- *Full-Tide Bubbler* – This pressure sensor processes dry pressurised air down to a pressure point located within two open-bottomed containers underwater. Here the pressure is measured as the pressure within the air line is equal to the weight of the water column;
- *Mid-Tide Bubbler* – The measuring point is located in the centre of the gauge, exposing the measuring point during half of the tidal cycle allowing accurate levelling into the geodetic network. This type of gauge can then be used side-by-side with a full-tide bubbler to link the full-tide gauge with the geodetic network by comparing tidal curves;
- *Ott Pneumatic Gauge* – Pressure from a bubbler system is applied to one end of a pivoted beam. The other end of the beam is counter balanced by an electric motor that is geared to a double helix shaft attached to the pen arm;

- *Munro Float Gauge* – The 45 cm diameter float is contained in a stilling well. It is connected to the gauge via a wire and drum along which a counter-weight drum wire and smaller float are connected. The float wire drum is attached to a slotted tape that moves the pen carriage with the tide. The Ott Pneumatic gauge uses a similar recording system to this and the paper output could easily be thought to have come from a Munro recorder;
- *Direct Pressure Transducer* - This is designed to produce a digital output from the air pressure measurements. This data can then be transferred or directly sent to a PC unit;
- *Precision Potentiometer* – Potentiometers are designed to reduce noise/voltage level output while still providing a large output of data. They can be used during the tide gauge calibration process. Potentiometers have been described as 'an instrument for measuring or adjusting electrical potential' (PSMSL, 2011);
- *DATARING Datalogger* – DATARING dataloggers are a specific type of digital data collection equipment that are commonly attached to pressure transducers, pressure gauges and float gauges that can either transmit data to a connected computer or store the data for future collection. Additional sensor readings can be collected parallel to tidal data, including wind speed, wind direction, water density, datum offset and calibration factors. Data can be averaged over 15 minute periods and accessed locally or remotely.

The tide gauges listed above have been used in the Forth and Tay Estuaries or at Aberdeen Harbour. Their design accuracy and human error variations are of vital study importance and this information should be used in the analysis of the data (Table 5.1).

Box A5.2 Macros

VictoriaData.xls – Module1 (Code) Find_TurningPoints

```
Sub Find_TurningPoints()
'=============
' Author Victoria Powell Version 2.0 25 November 2008
' Synopsis:
'     This macro looks for turing points in a data set containing minutes
'     throughout the day and tide height values.  The tidal data is noisy and
'     contains a number of turning points that are not tidal changes.  So
'     We only accept a turning point is valid if its 10 (+/-5) nearest neighbours
'     are larger (or smaller - high tide) or equal to it.
```

```
'============
    Dim ExcelLastCell As Object, lRow As Long, lLastDataRow As Long, l As Long

    Set ExcelLastCell = ActiveSheet.Cells.SpecialCells(xlLastCell)
    lLastDataRow = ExcelLastCell.Row
    lRow = ExcelLastCell.Row              ' lRow is used to indicate the end of the data set.

    xAnswer = "The Turning Points are..."
    cAnswer = " "
    DataCol = "B"   '  <<<<< change this value if the tide levels are in a different column

 ' =========
 '    The following code prepares a new sheet to accept the results.
 '    NB.  Make sure the data set sheet is active before running
 ' ==========

    rSheet = ActiveSheet.Name
    Set WS = Sheets.Add
    WS = ActiveSheet.Name
    Range("A1") = "The Tidal Turning Points Are..."
    Range("A1").Font.Size = 14
    Sheets(rSheet).Activate
    pRow = 2
' =========
 '    This loop rolls forward the cursor to the start of the real data
 '    The numbers represent valid possible dates in column A
' ==========
    nRow = 1                  ' nRow is the cursor in the data set

    While Range(DataCol & nRow) = " "
        nRow = nRow + 1
    Wend
    nRow = nRow + 5

' =========
 '    This loop is the start of the data set processing
 '    We need to finish five rows early so we don't run off the end of the file
' ==========
    While nRow < (lRow - 5)

       xValue = DataCol & nRow

       If Range(xValue) > Range(xValue).Offset(-1, 0) And _
          Range(xValue) > Range(xValue).Offset(-2, 0) And _
          Range(xValue) > Range(xValue).Offset(-3, 0) And _
          Range(xValue) > Range(xValue).Offset(-4, 0) And _
          Range(xValue) > Range(xValue).Offset(-5, 0) And _
          Range(xValue) >= Range(xValue).Offset(1, 0) And _
```

```
          Range(xValue) >= Range(xValue).Offset(2, 0) And _
          Range(xValue) >= Range(xValue).Offset(3, 0) And _
          Range(xValue) >= Range(xValue).Offset(4, 0) And _
          Range(xValue) >= Range(xValue).Offset(5, 0) Then
' -------- found a tidal high point -----------------------
          cAnswer = " High tide is at " & Range("A" & nRow) & " height " & Range(xValue)
          xAnswer = xAnswer & Chr(13) & cAnswer
          Call pResult(nRow, pRow, WS, rSheet, cAnswer)

        ElseIf Range(xValue) < Range(xValue).Offset(-1, 0) And _
              Range(xValue) < Range(xValue).Offset(-2, 0) And _
              Range(xValue) < Range(xValue).Offset(-3, 0) And _
              Range(xValue) < Range(xValue).Offset(-4, 0) And _
              Range(xValue) < Range(xValue).Offset(-5, 0) And _
              Range(xValue) <= Range(xValue).Offset(1, 0) And _
              Range(xValue) <= Range(xValue).Offset(2, 0) And _
              Range(xValue) <= Range(xValue).Offset(3, 0) And _
              Range(xValue) <= Range(xValue).Offset(4, 0) And _
              Range(xValue) <= Range(xValue).Offset(5, 0) Then
' -------- found a tidal Low point -----------------------
          cAnswer = " Low tide is at " & Range("A" & nRow) & " height " & Range(xValue)
          xAnswer = xAnswer & Chr(13) & cAnswer
          Call pResult(nRow, pRow, WS, rSheet, cAnswer)
        End If
        nRow = nRow + 1
     Wend
' ------ now print the answer on screen --------
     MsgBox xAnswer



' ------ now print a chart on the results sheet --------
    Range("A11:C1475").Select
    ActiveWindow.ScrollRow = 1
    Charts.Add
    ActiveChart.ChartType = xlXYScatterSmooth
    ActiveChart.SetSourceData Source:=Sheets("7S030802").Range( _
        "A11:A1475," & DataCol & "11:" & DataCol & "1475"), PlotBy:=xlColumns
    ActiveChart.SeriesCollection(1).XValues = "='7S030802'!R12C1:R1475C1"
    ActiveChart.Location Where:=xlLocationAsObject, Name:=WS
    With ActiveChart
        .HasTitle = True
        .ChartTitle.Characters.Text = "Tide Cycle"
        .Axes(xlCategory, xlPrimary).HasTitle = False
        .Axes(xlValue, xlPrimary).HasTitle = False
    End With
    With ActiveChart.Axes(xlCategory)
        .HasMajorGridlines = False
        .HasMinorGridlines = False
```

```
    End With
    With ActiveChart.Axes(xlValue)
        .HasMajorGridlines = True
        .HasMinorGridlines = False
    End With
    ActiveChart.HasLegend = False

End Sub

Sub pResult(ThisRow, pRow, WS, rSheet, cAnswer)
'=============
' Author Victoria Powell Version 2.0 25 November 2008
' Synopsis:
'  This prints a results line when found.  Must be used with above
'=============
    Range("A" & ThisRow & ":C" & ThisRow).Select

    With Selection.Interior
        .ColorIndex = 6
        .Pattern = xlSolid
    End With

    Sheets(WS).Range("A" & pRow).Value = cAnswer
    Sheets(rSheet).Select

    pRow = pRow + 1

End Sub
```

Final Macro-bas – Module2 (Code) Find_High_Low_Tides

```
Sub Find_High_Low_Tides()

'=============
' Author Victoria Powell Version 2.0 25 November 2008
' Synopsis:
'       This macro looks for turning points in a data set containing minutes
'       throughout the day and tide height values.  The tidal data is noisy and
'       contains a number of turning points that are not tidal changes.  So
'       We only accept a turning point is valid if its 10 (+/-5) nearest neighbours
'       are larger (or smaller - high tide) or equal to it.
'============
    Dim ExcelLastCell As Object, lRow As Long, lLastDataRow As Long, l As Long

    Set ExcelLastCell = ActiveSheet.Cells.SpecialCells(xlLastCell)
    lLastDataRow = ExcelLastCell.Row
    lRow = ExcelLastCell.Row            ' lRow is used to indicate the end of the data set.
```

```
   xAnswer = "The Turning Points are..."
   cAnswer = " "
   DataCol = "B"   '  <<<<< change this value if the tide levels are in a different column

' =========
'    The following code prepares a new sheet to accept the results.
'    NB.  Make sure the data set sheet is active before running
' ==========

   rSheet = ActiveSheet.Name
   Set WS = Sheets.Add
   WS = ActiveSheet.Name
   Range("A1") = "The Tidal Turning Points Are..."
   Range("A1").Font.Size = 14
   Sheets(rSheet).Activate
   pRow = 2
' =========
'    This loop rolls forward the cursor to the start of the real data
'    The numbers represent valid possible dates in column A
' ==========
   nRow = 1                  ' nRow is the cursor in the data set

   While Range(DataCol & nRow) = "B"
      nRow = nRow + 1
   Wend
   nRow = nRow + 9

' =========
'    This loop is the start of the data set processing
'    We need to finish five rows early so we don't run off the end of the file
' ==========
   While nRow < (lRow - 9)

      xValue = DataCol & nRow

      If Range(xValue) > Range(xValue).Offset(-1, 0) And _
        Range(xValue) > Range(xValue).Offset(-2, 0) And _
        Range(xValue) > Range(xValue).Offset(-3, 0) And _
        Range(xValue) > Range(xValue).Offset(-4, 0) And _
        Range(xValue) > Range(xValue).Offset(-5, 0) And _
        Range(xValue) > Range(xValue).Offset(-6, 0) And _
        Range(xValue) > Range(xValue).Offset(-7, 0) And _
        Range(xValue) > Range(xValue).Offset(-8, 0) And _
        Range(xValue) > Range(xValue).Offset(-9, 0) And _
        Range(xValue) >= Range(xValue).Offset(1, 0) And _
        Range(xValue) >= Range(xValue).Offset(2, 0) And _
        Range(xValue) >= Range(xValue).Offset(3, 0) And _
```

```
        Range(xValue) >= Range(xValue).Offset(4, 0) And _
        Range(xValue) >= Range(xValue).Offset(5, 0) And _
        Range(xValue) >= Range(xValue).Offset(6, 0) And _
        Range(xValue) >= Range(xValue).Offset(7, 0) And _
        Range(xValue) >= Range(xValue).Offset(8, 0) And _
        Range(xValue) >= Range(xValue).Offset(9, 0) Then
' -------- found a tidal high point -----------------------
        cAnswer = " High tide is at " & Range("A" & nRow) & " height " & Range(xValue)
        xAnswer = xAnswer & Chr(13) & cAnswer
        Call pResult(nRow, pRow, WS, rSheet, cAnswer)

      ElseIf Range(xValue) < Range(xValue).Offset(-1, 0) And _
            Range(xValue) < Range(xValue).Offset(-2, 0) And _
            Range(xValue) < Range(xValue).Offset(-3, 0) And _
            Range(xValue) < Range(xValue).Offset(-4, 0) And _
            Range(xValue) < Range(xValue).Offset(-5, 0) And _
            Range(xValue) < Range(xValue).Offset(-6, 0) And _
            Range(xValue) < Range(xValue).Offset(-7, 0) And _
            Range(xValue) < Range(xValue).Offset(-8, 0) And _
            Range(xValue) < Range(xValue).Offset(-9, 0) And _
            Range(xValue) <= Range(xValue).Offset(1, 0) And _
            Range(xValue) <= Range(xValue).Offset(2, 0) And _
            Range(xValue) <= Range(xValue).Offset(3, 0) And _
            Range(xValue) <= Range(xValue).Offset(4, 0) And _
            Range(xValue) <= Range(xValue).Offset(5, 0) And _
            Range(xValue) <= Range(xValue).Offset(6, 0) And _
            Range(xValue) <= Range(xValue).Offset(7, 0) And _
            Range(xValue) <= Range(xValue).Offset(8, 0) And _
            Range(xValue) <= Range(xValue).Offset(9, 0) Then
' -------- found a tidal Low point -----------------------
        cAnswer = " Low tide is at " & Range("A" & nRow) & " height " & Range(xValue)
        xAnswer = xAnswer & Chr(13) & cAnswer
        Call pResult(nRow, pRow, WS, rSheet, cAnswer)
      End If
      nRow = nRow + 1
    Wend
' ------ now print the answer on screen --------
    MsgBox xAnswer


End Sub

Sub pResult(ThisRow, pRow, WS, rSheet, cAnswer)
'=============
' Author Victoria Powell Version 2.0 25 November 2008
' Synopsis:
'  This prints a results line when found.  Must be used with above
'=============
```

```
    Range("A" & ThisRow & ":C" & ThisRow).Select

    With Selection.Interior
      .ColorIndex = 6
      .Pattern = xlSolid
    End With

    Sheets(WS).Range("A" & pRow).Value = cAnswer
    Sheets(rSheet).Select

    pRow = pRow + 1

End Sub
```

Box A5.3 Datum Conversion

Ordnance Datum Newlyn's UK-wide levelling was completed in 1921, therefore the UKHO Chart Datum/ Ordnance Datum record cannot be any older than that. Chart Datum results record as follows:

- Dunbar – 2.41m below ODN (post 1921), 6.80m below OBM 4.21mN (1948), 8.24m below OBM 5.65mN (1959), 7.91m below OBM 5.65mN (29/06/1960), 6.80m below OBM 4.21mN (1970), LAT datum 2.80m below ODN (1971).
- Leith – 2.72m below ODN (post 1921), 7.64m below OBM 4.92mN (1953), 4.13m below 0 of tide gauge (1953), 2.72m below ODN (1968), 7.39m below OBM 4.67N (1969), 7.00m below permanent tide pole (1968), 8.16m below OBM 5.49mN (1969), LAT 2.9m below ODN (1972), 7.85m below OBM 4.94mN (1972), 7.51m below OBM 4.61mN (1972), 7.83m below OBM 4.93mN (1972), 10.20m below OBM 7.30mN (1972), 7.02m below permanent tide pole, 2008 TIDE TABLE lock sill 6.71m AD, AD 2.9m below ODN, MLWS 7.467M, MHWS 12.293M.
- Rosyth – 2.87m below ODL (1951), 7.08m below OBM 4.22mL (1951), 2.87m below 0 of tide gauge (pre1956, when new tide gauge set to chart datum), 2.54m below ODN (1951), 7.79m below OBM 5.06ftN (1964), 7.08m below OBM 4.35ftN (1964), LAT datum is 2.95m below ODN (1971), TIDE TABLE 2008 outer sill 7.57m below AD.
- Dundee – 2.31m below ODN (1955), 7.04m below OBM 4.73mN (1968), 7.26m below OBM 4.95mN (1968), 1.91m above 0 on tide pole (1968), LAT datum is 2.90m below ODN (1971).
- Newburgh – 1.50m below ODL and 1.31m below ODN (1951), 0.98m above tide gauge (1951), 2.30m below 0 of tide gauge (1967), LAT datum is 1.3m below ODN (1971).
- Perth – equal to ODL and 0.06m above ODN (1951, 1955), LAT is ODN (1971).
- Grangemouth – 2.95m below ODL and 2.62m below ODN (1957), LAT datum 2.75m below ODN (1971), TIDE TABLE 2008 outer sill 5.97m above AD, AD 2.75M below ODN, MHWS 5.7M, MHWN 4.5M, MLWS 1.9M, MLWS 0.5M.
- Methil – 3.03m below ODL and 3.12m below ODN (connection not explained) (1917), considerable subsidence due to mining until 1957, 3.00m below ODN (1957), 11.08m below OBM 8.08mN (1966), LAT datum 2.9m below ODN (1971), TIDE TABLE 2008 AD 2.37M below ODN, MHWS 8.63M, MHWN 7.03M, MLWN 4.73M, MLWS 3.53M.
- Burntisland – 3.03m below ODL and 2.66m below ODN (1917, 1955), 7.87m below OBM? (1914), 3.28m above tide gauge (1914), 8.21m below OBM 5.34mN (1968), 10.63m below OBM 7.76mN (1968), LAT datum 2.85m below ODN (1971), 2008 TIDE TABLE AD 2.85m below ODN, MHWS 8.69M, MHWN 7.59M, MLWN 5.19M, MLWS 3.89M.

- Broughty Ferry – 2.31m below ODN (1968), 7.02m below OBM 4.71mN (1968), 7.74m below OBM 5.43mN (1969), LAT datum 2.90m below ODN (1971).
- Kirkcaldy – 3.03m below ODL (1917), 3.03m below ODN (1955), 0.87m above 0 on tide gauge (1917), LAT datum 2.9m below ODN (1971).
- Kincardine – 2.86m below ODN (1948), LAT datum 2.85m below ODN (1971).
- Dunmore – 2.38m below ODN (1947), LAT datum 2.65m below ODN (1971).
- Alloa – 2.62m below ODL and 2.38m below ODN (1927, 1955), 2.3m below ODN (1967), 6.75m below OBM 4.29mN (1967, 1971), LAT datum 2.30m below ODN (1972).
- Stirling – 0.49m above ODL and 0.61m above ODN (pre 1955), LAT datum 0.30m above ODN (1971).
- Granton – 2.73m below ODN (1952), 9.84m below OBM 6.90mN (1953), 2.52m below ODL (1957), LAT datum 2.95m below OD (1971).
- Anstruther Easter – 2.79m below ODN (1958), 19.96m below OBM 16.97mN (1958), 7.98m below OBM 4.98mN (1958), LAT datum 2.90m below ODN (1971).
- Buddon Ness (Tay Estuary Bar) – 2.31m below ODN (1940), 7.76m below OBM 5.27mN (1940), 7.60m below OBM 5.11mN (1968), 0.06m below Dundee Harbour Trust tide pole (1968), LAT datum 2.90m below ODN (1971).
- Arbroath – 2.47m below ODN (pre1963), 9.76m below OBM 6.78mN (pre1963), 2.59m below ODN (1963), 9.37m below OBM 6.78mN (1963), 6.49m below OBM 3.90mN (1968), 6.74m below OBM 4.15mN (1968), LAT datum 2.8m below ODN (1971).

Location	**(a) CD (mm)**	**(b) LAT (mm)**	**(c) Other**
Leith	6790/6779	2900	
Methil		2900	
Dundee		2900	
Rosyth	6700	2950	2870 ODL
Dunbar	6692		2300 MSL
Aberdeen	6745	2250	
Newburgh	2450		
Earn-Tay Confluence	N/A		
Perth Harbour		60	
Stannergate		2900	
Newport-on-Tay		2900	
Grangemouth		2750	
Arbroath		3200	
Bridge of Earn		200	
Musselburgh		200	
Perth (Scone)		2100	

Table A5.1. List of datum conversions to OD Newlyn. (a) Conversion height between ODN and PSMSL's RLR data, except at Newburgh where only the local datum height is known. (b) Conversion height between ODN and LAT. (c) Conversion height between ODN and other local datum.

POL Datum Conversion Charts

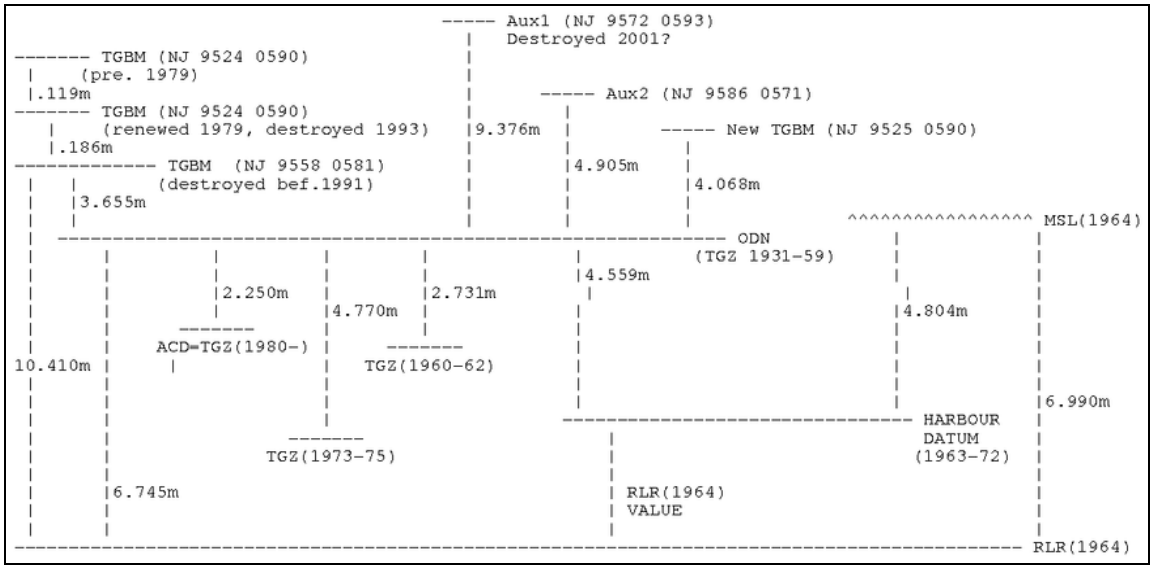

Figure A5.1. PSMSL Aberdeen 1 RLR datum conversion map (PSMSL, 2010).

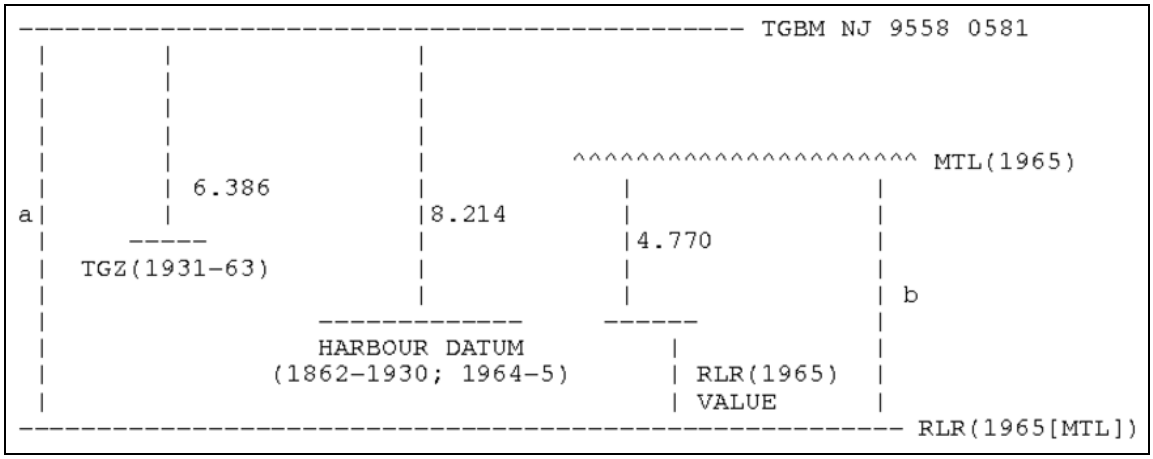

Figure A5.2. PSMSL Aberdeen 2 RLR datum conversion map (PSMSL, 2010).

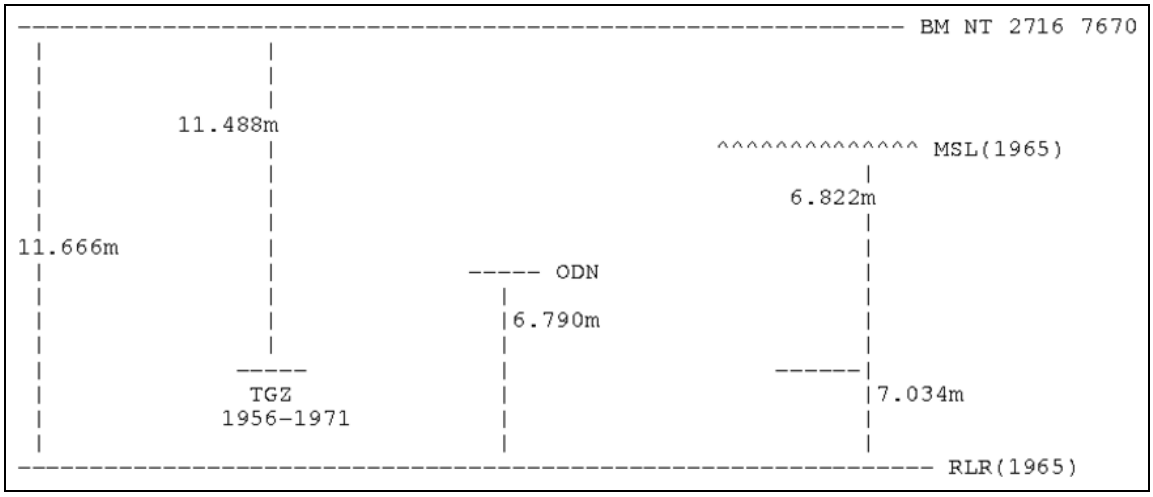

Figure A5.3. PSMSL Leith 1 RLR datum conversions (PSMSL, 2010).

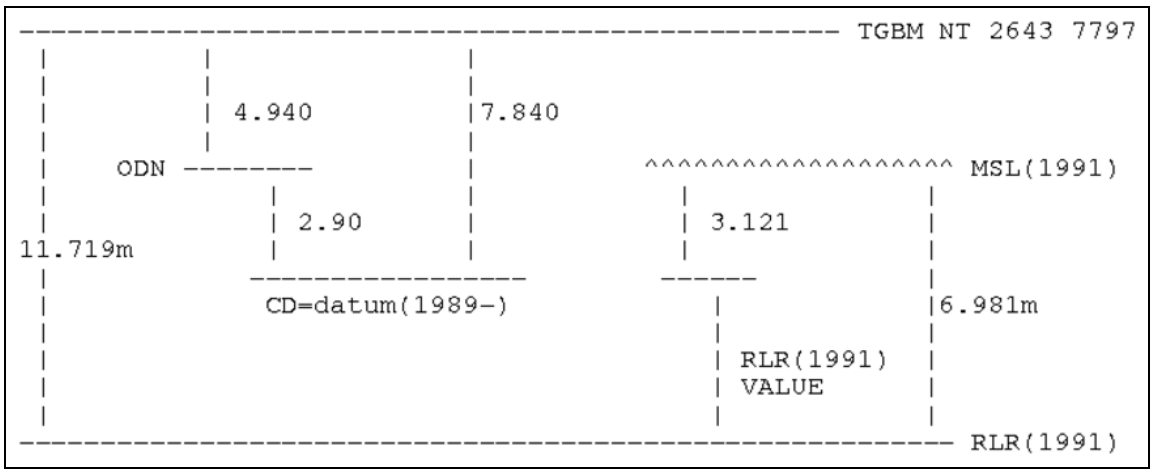

Figure A5.4. PSMSL Leith 2 RLR datum conversions (PSMSL, 2010).

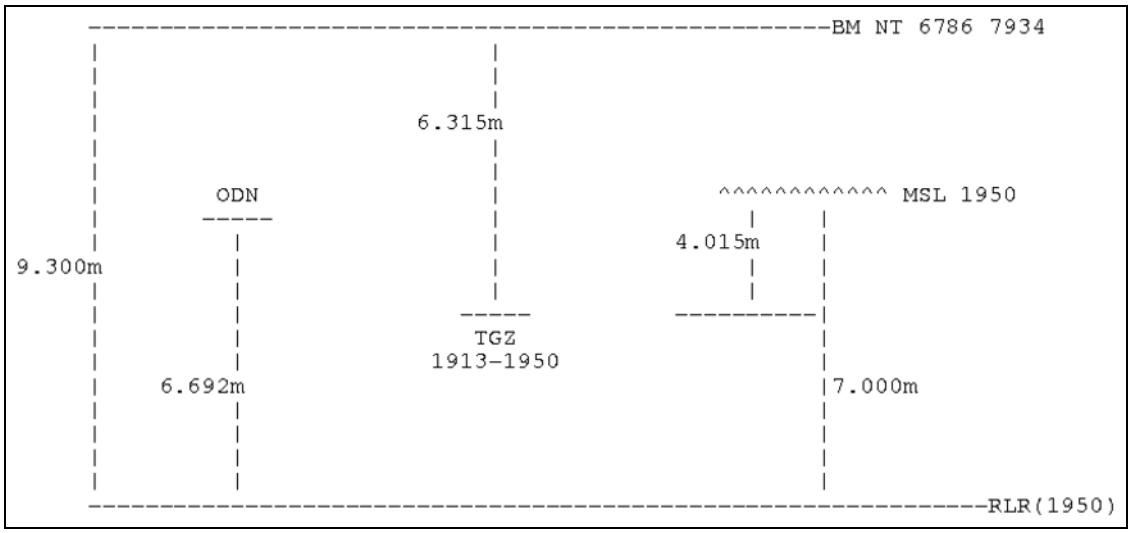

Figure A5.5. PSMSL Dunbar RLR datum conversions (PSMSL, 2010).

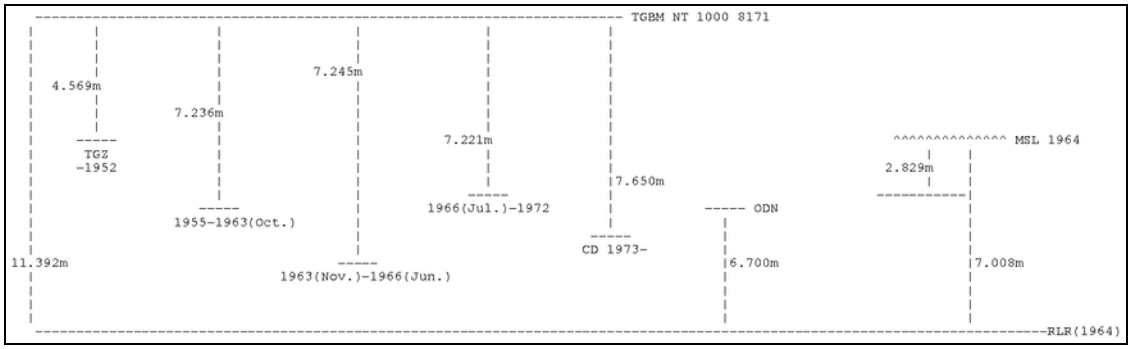

Figure A5.6. PSMSL Rosyth RLR Datum conversions (PSMSL, 2010).

Appendix 6 – Temperature Data

	Accuracy (mm)	Accuracy (%)	Resolution (mm)
e.g. Lea	10	5.0	0.5
All POL gauges	10		
*Valeport 710**	10 (at 10 m depth)	±0.1	1.0
*Valeport MIDAS TMS**	10 (at 10 m depth)	±0.1	1.0
A. Ott Pressure	5 (at 10 m depth) #	-	-
SEPA 5 m Pressure Transistor ~	5 (at 5 m depth)	±0.1	

Table A6.1. Tide Gauge Reliability (Format taken from Martin and Perez, 2010) * Valeport (2011); # International Association of Hydraulic Engineering and Research Hydraulic Instrumentation Section, (2011); - Philip Woodworth and Kevin Horsburgh, (pers. comm., 2011) ~ Julie Carter (pers. comm., 2011).

Sensor	Location	Gauge Accuracy (mm)	Additional Error (mm)	Overall Accuracy (mm)
All POL gauges#	Dunbar; Aberdeen; Rosyth; Leith;	±10.0	±10-150	±0-160
*Munro gauge # **	Aberdeen; Leith; Grangemouth	±10.0#	±100-150*	±90-160
*Valeport 710**	Dundee; Grangemouth; Methil; Leith; Rosyth; Perth; Newburgh; Tay-Earn Confluence	±10.0	±50-100	±30-110
*Valeport MIDAS TMS**	Dundee; Grangemouth; Methil; Leith; Rosyth	±10.0	±50-100	±30-110
SEPA 5 m Pressure Transistor ~	Musselburgh	±5.0	0	±5.0
?	Newport-on-Tay; Stannergate; Bridge of Earn; Arbroath;	?	?	?

Table A6.2. Tide gauge accuracies (Format taken form Watson *et al*., 2008) (*Peter Crawley (pers. comm., 2011), # Philip Woodworth and Kevin Horsburgh (pers. comm., 2011), ~ Julie Carter (pers. comm., 2011).

Appendix 7 – Wavelet Analysis

[page left intentionally blank]

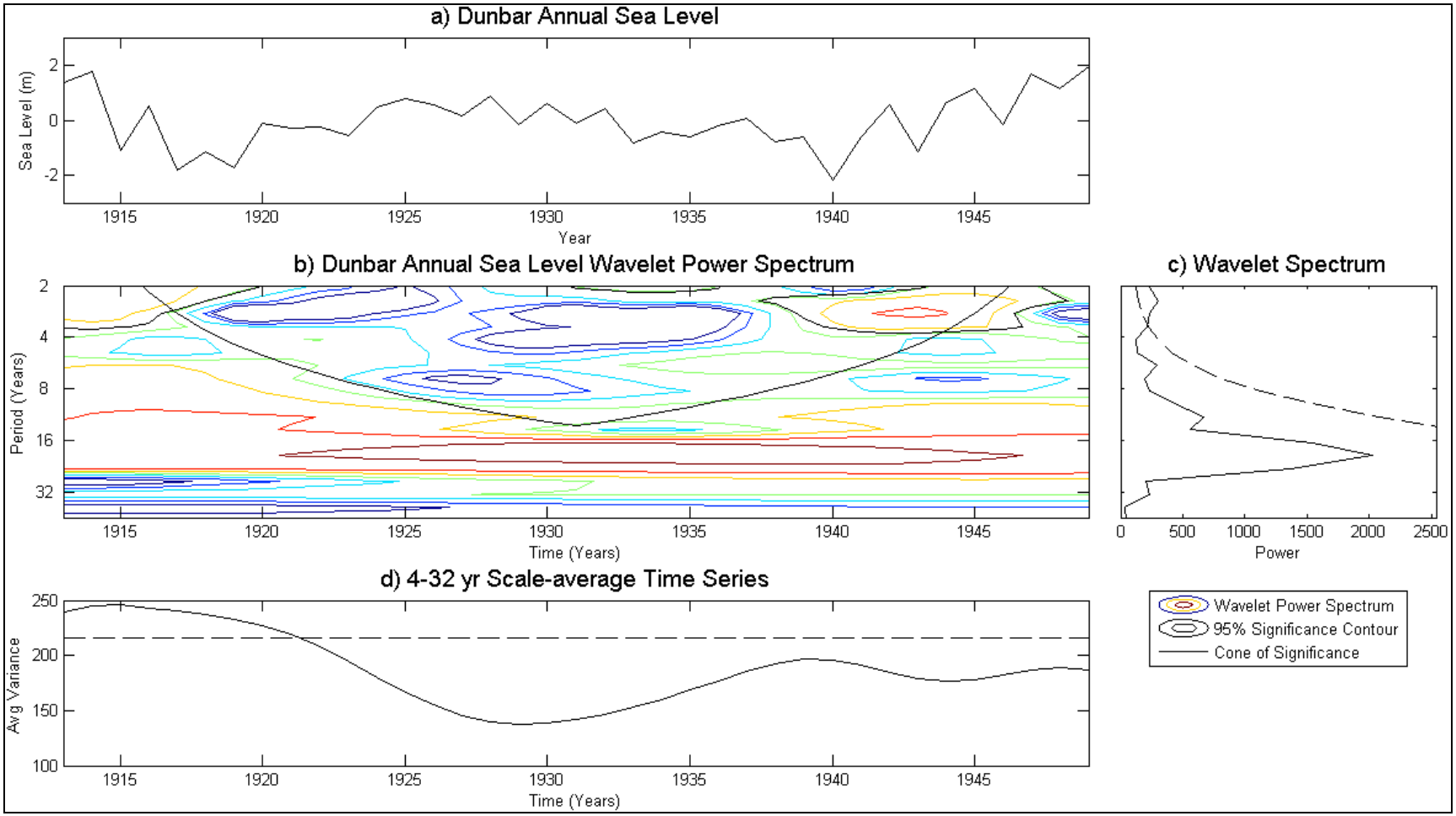

Figure A7.1. Wavelet analysis using the Torrence and Compo (1998) wavelet software. a) Complete Dunbar annual time series sea level data. b) Dunbar annual sea level power spectrum with attached legend explaining the wavelet power spectrum contours, 95% significance contours and the cone of significance. Contours coloured red and yellow are of high significance. c) The wavelet spectrum illustrates the spikes in variance in relation to the wavelet power spectrum (graph b). The y-axis is shared with graph b. d) The 4-32 year scale-average time series illustrates the smoothed variance in the data along the time series from the scale-average.

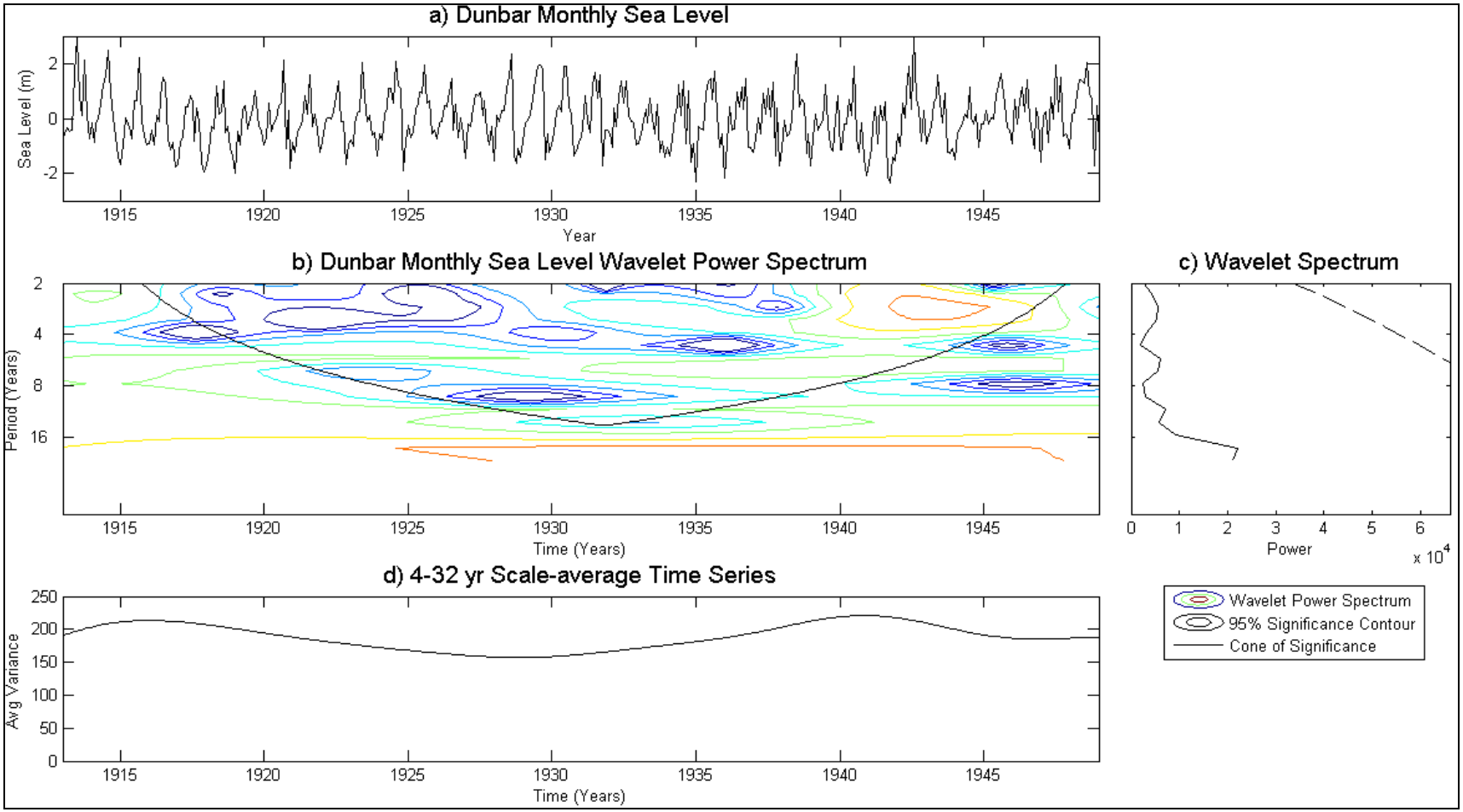

Figure A7.2. Wavelet analysis using the Torrence and Compo (1998) wavelet software. a) Complete Dunbar monthly time series sea level data. b) Dunbar monthly sea level power spectrum with attached legend explaining the wavelet power spectrum contours, 95% significance contours and the cone of significance. Contours coloured red and yellow are of high significance. c) The wavelet spectrum illustrates the spikes in variance in relation to the wavelet power spectrum (graph b). The y-axis is shared with graph b. d) The 4-32 year scale-average time series illustrates the smoothed variance in the data along the time series from the scale-average.

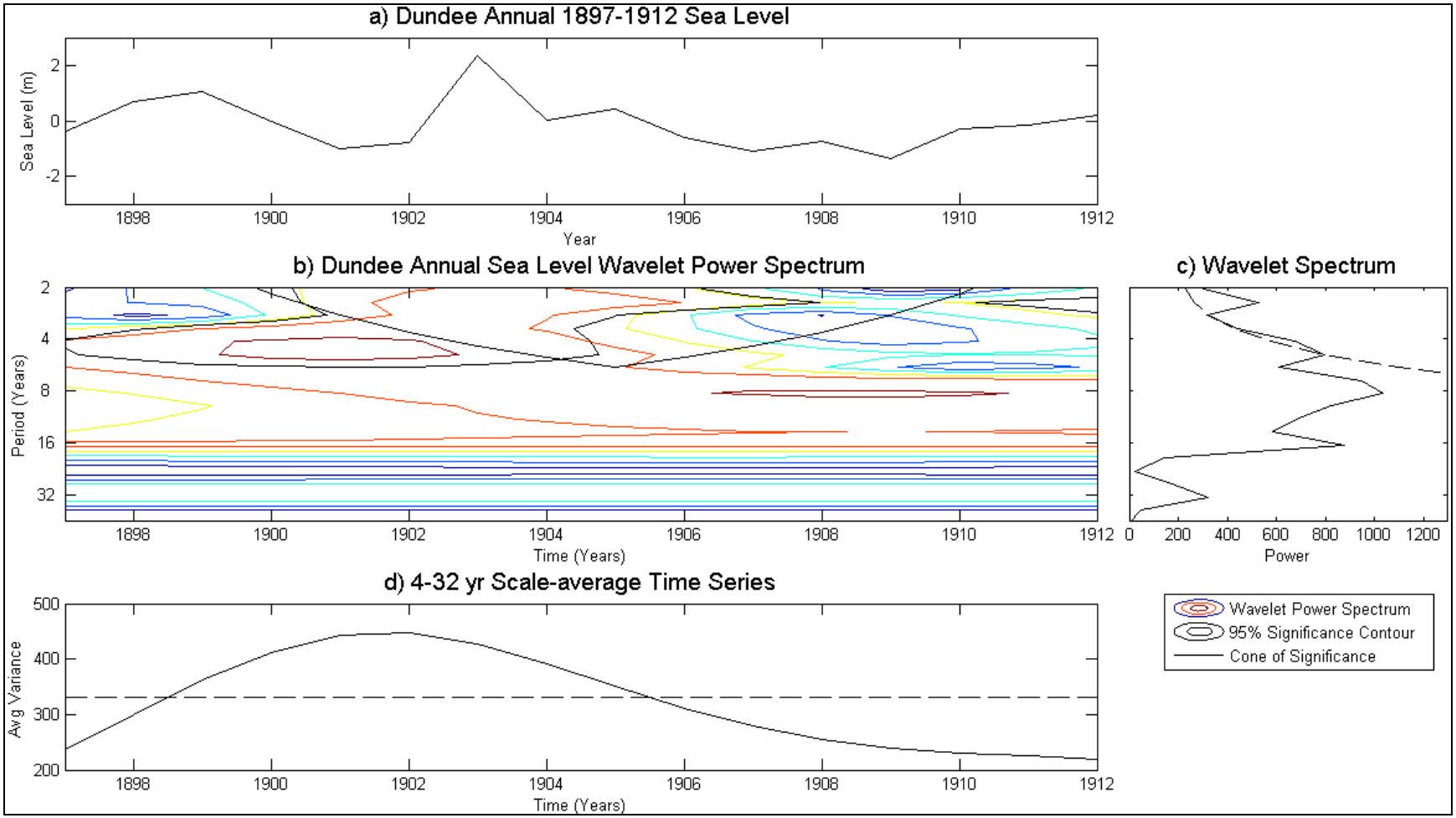

Figure A7.3. Wavelet analysis using the Torrence and Compo (1998) wavelet software. a) Dundee Annual 1897-1912 time series sea level data. b) Dundee annual sea level power spectrum with attached legend explaining the wavelet power spectrum contours, 95% significance contours and the cone of significance. Contours coloured red and yellow are of high significance. c) The wavelet spectrum illustrates the spikes in variance in relation to the wavelet power spectrum (graph b). The y-axis is shared with graph b. d) The 4-32 year scale-average time series illustrates the smoothed variance in the data along the time series from the scale-average.

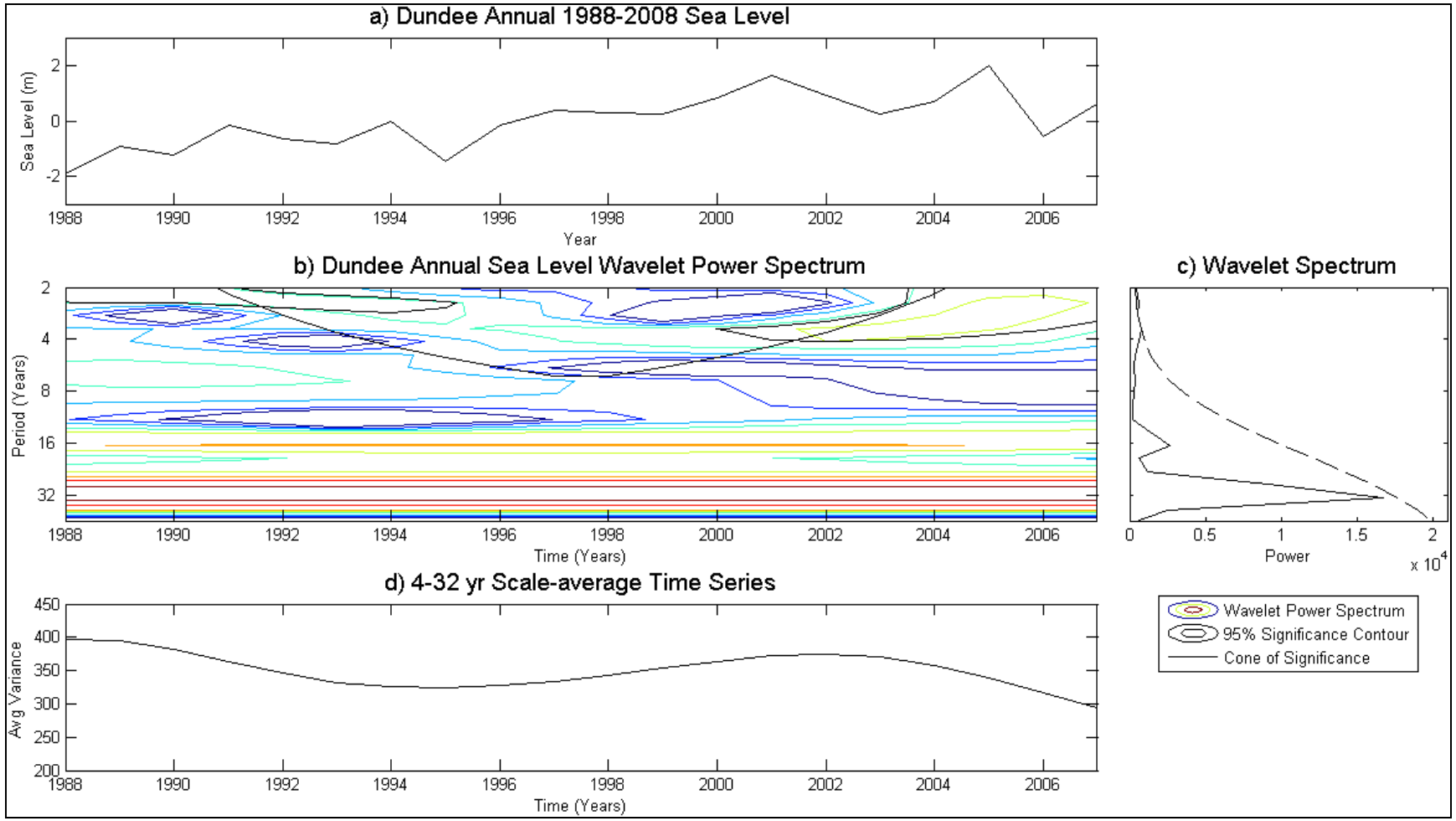

Figure A7.4. Wavelet analysis using the Torrence and Compo (1998) wavelet software. a) Dundee Annual 1988-2008 time series sea level data. b) Dundee annual sea level power spectrum with attached legend explaining the wavelet power spectrum contours, 95% significance contours and the cone of significance. Contours coloured red and yellow are of high significance. c) The wavelet spectrum illustrates the spikes in variance in relation to the wavelet power spectrum (graph b). The y-axis is shared with graph b. d) The 4-32 year scale-average time series illustrates the smoothed variance in the data along the time series from the scale-average.

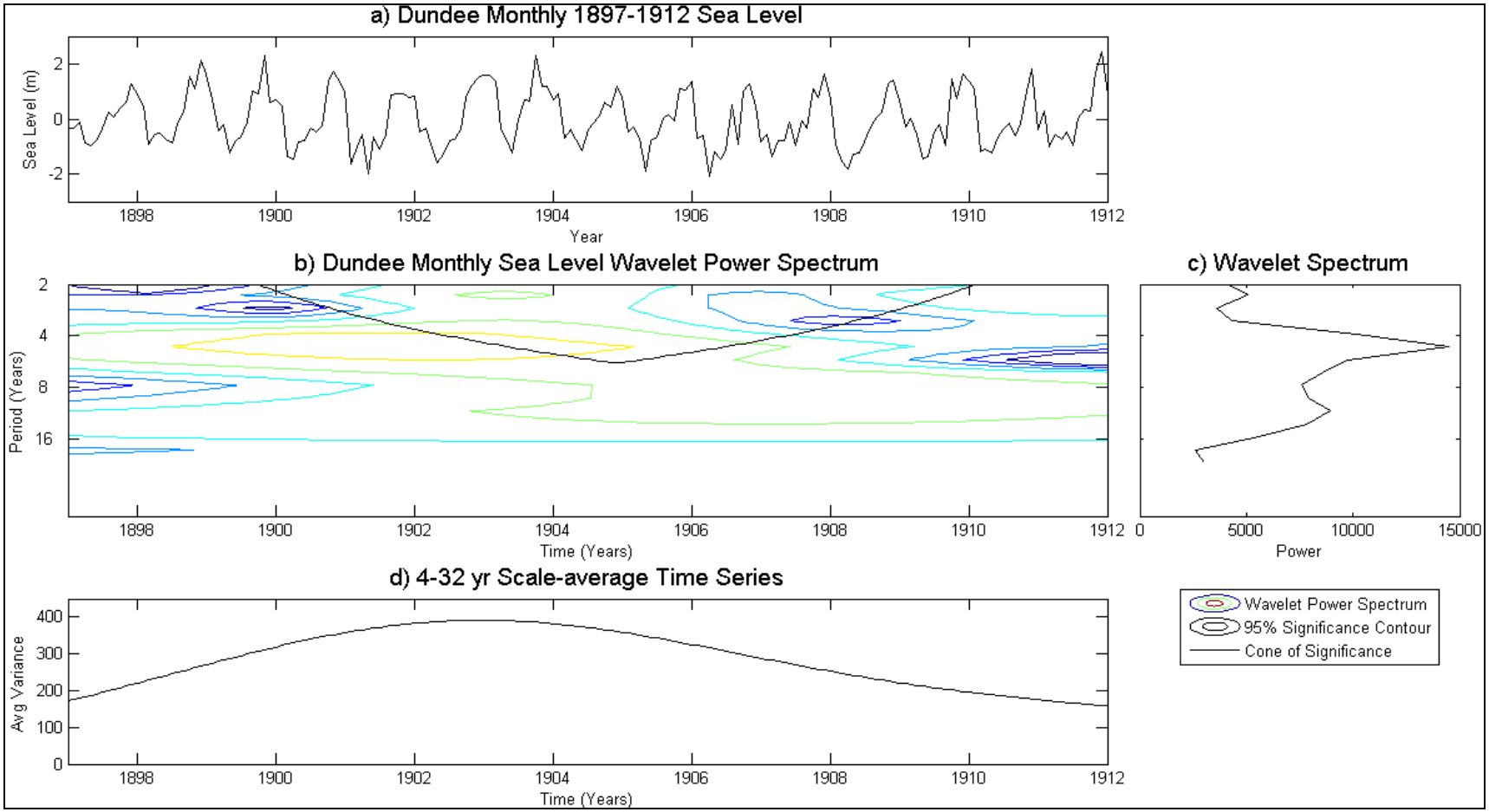

Figure A7.5. Wavelet analysis using the Torrence and Compo (1998) wavelet software. a) Dundee Monthly 1897-1912 time series sea level data. b) Dundee monthly sea level power spectrum with attached legend explaining the wavelet power spectrum contours, 95% significance contours and the cone of significance. Contours coloured red and yellow are of high significance. c) The wavelet spectrum illustrates the spikes in variance in relation to the wavelet power spectrum (graph b). The y-axis is shared with graph b. d) The 4-32 year scale-average time series illustrates the smoothed variance in the data along the time series from the scale-average.

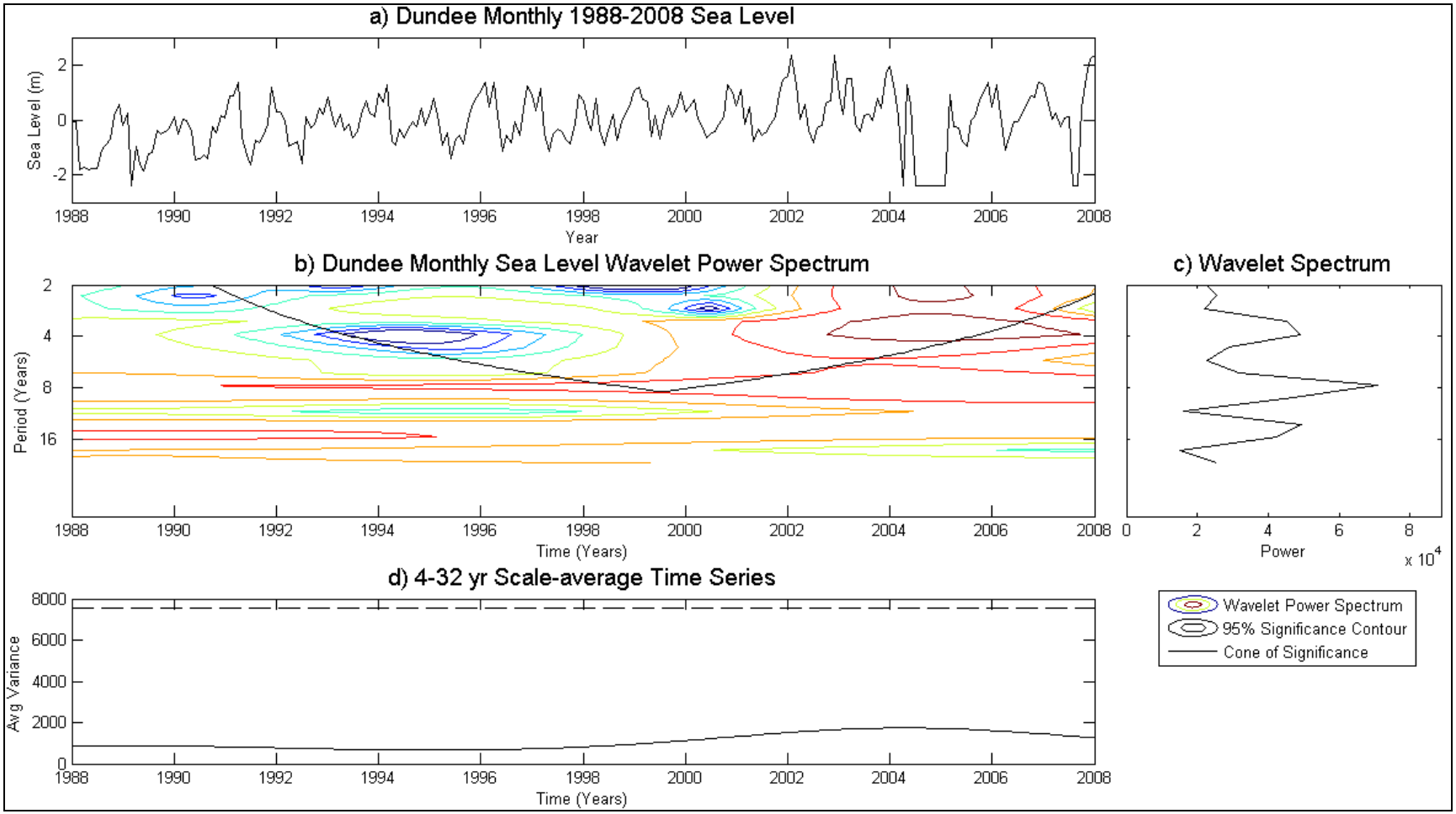

Figure A7.6. Wavelet analysis using the Torrence and Compo (1998) wavelet software. a) Dundee Monthly 1988-2008 time series sea level data. b) Dundee monthly sea level power spectrum with attached legend explaining the wavelet power spectrum contours, 95% significance contours and the cone of significance. Contours coloured red and yellow are of high significance. c) The wavelet spectrum illustrates the spikes in variance in relation to the wavelet power spectrum (graph b). The y-axis is shared with graph b. d) The 4-32 year scale-average time series illustrates the smoothed variance in the data along the time series from the scale-average.

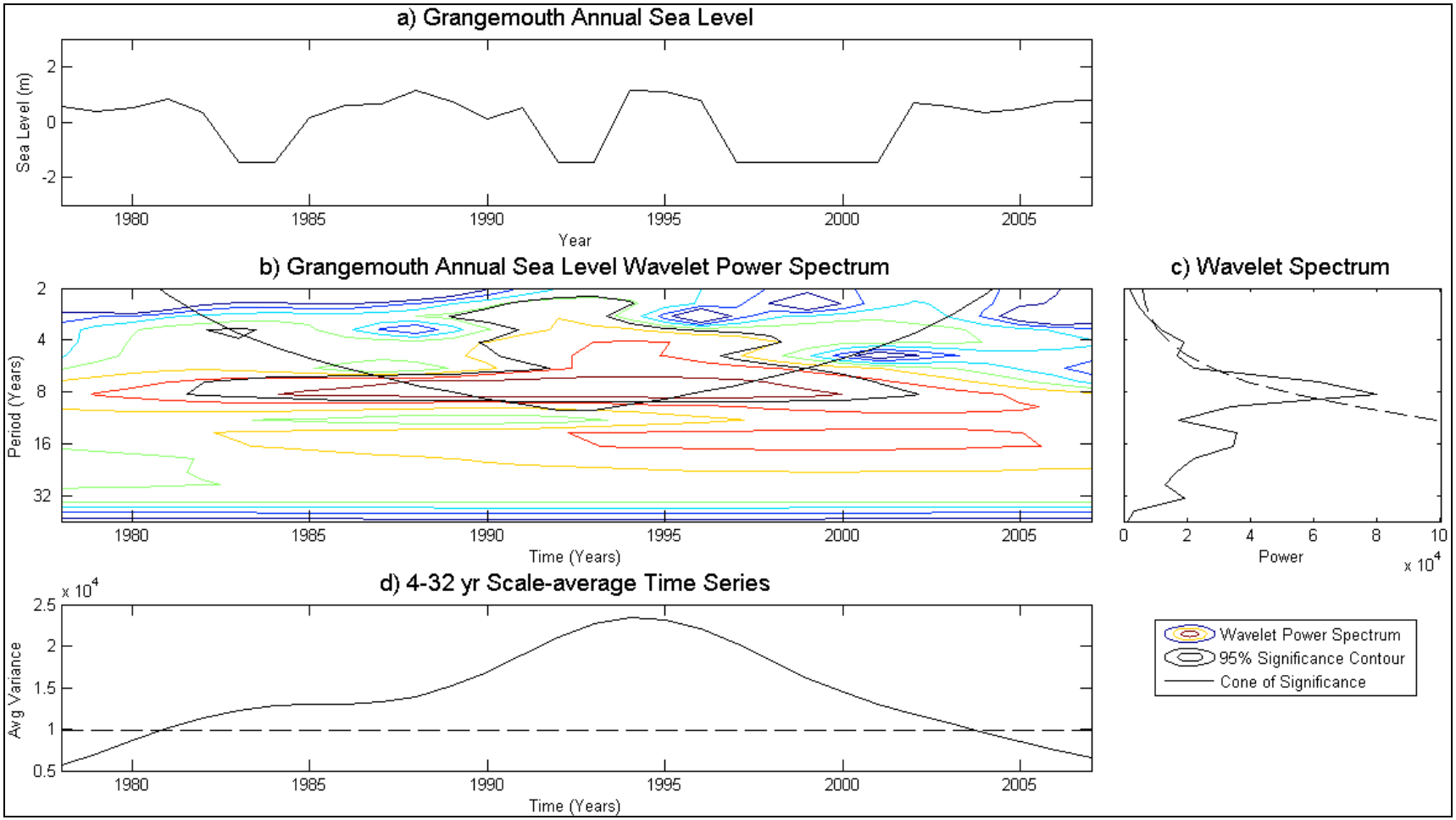

Figure A7.7. Wavelet analysis using the Torrence and Compo (1998) wavelet software. a) Grangemouth annual time series sea level data. b) Grangemouth annual sea level power spectrum with attached legend explaining the wavelet power spectrum contours, 95% significance contours and the cone of significance. Contours coloured red and yellow are of high significance. c) The wavelet spectrum illustrates the spikes in variance in relation to the wavelet power spectrum (graph b). The y-axis is shared with graph b. d) The 4-32 year scale-average time series illustrates the smoothed variance in the data along the time series from the scale-average.

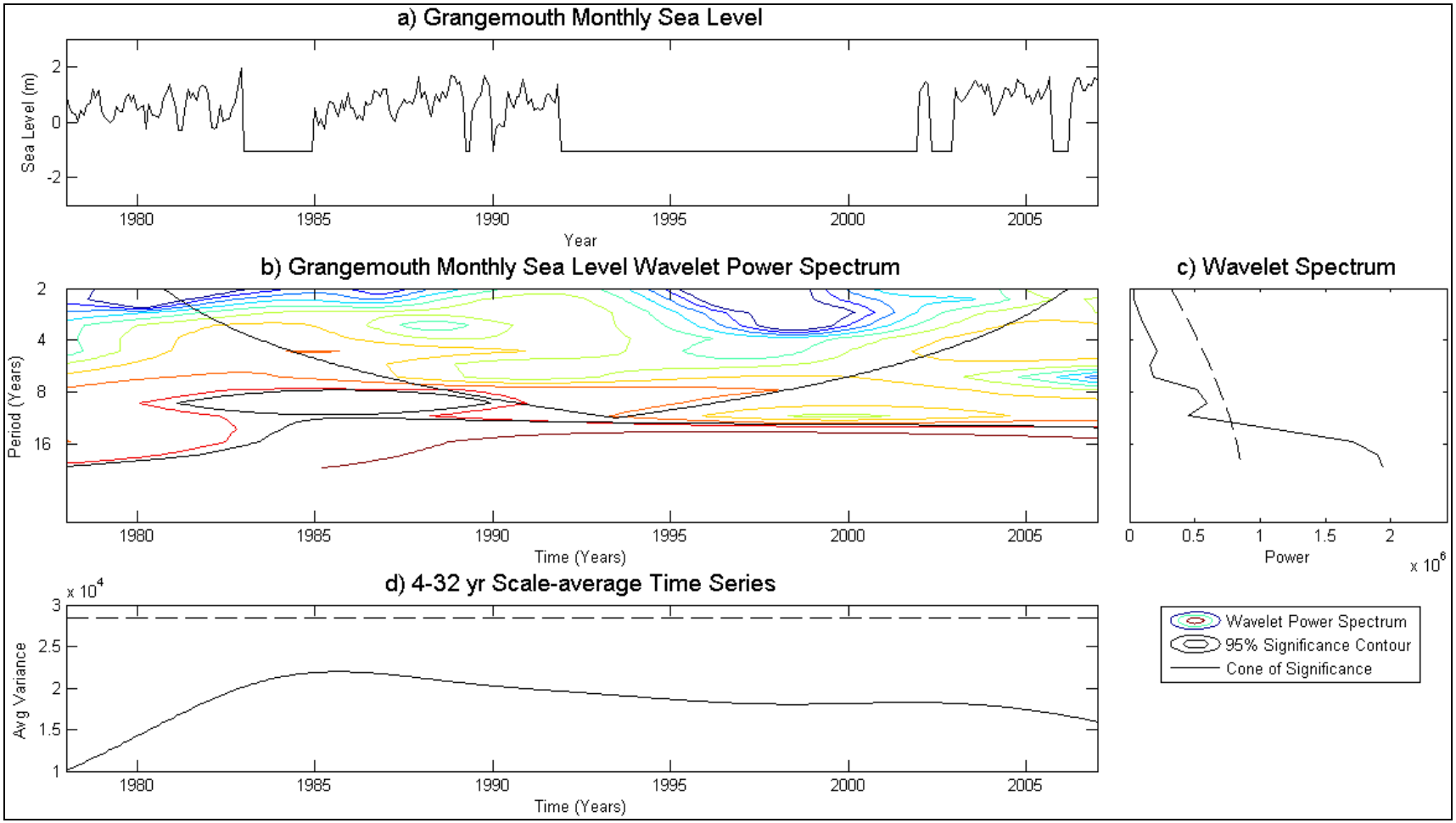

Figure A7.8. Wavelet analysis using the Torrence and Compo (1998) wavelet software. a) Grangemouth monthly time series sea level data. b) Grangemouth monthly sea level power spectrum with attached legend explaining the wavelet power spectrum contours, 95% significance contours and the cone of significance. Contours coloured red and yellow are of high significance. c) The wavelet spectrum illustrates the spikes in variance in relation to the wavelet power spectrum (graph b). The y-axis is shared with graph b. d) The 4-32 year scale-average time series illustrates the smoothed variance in the data along the time series from the scale-average.

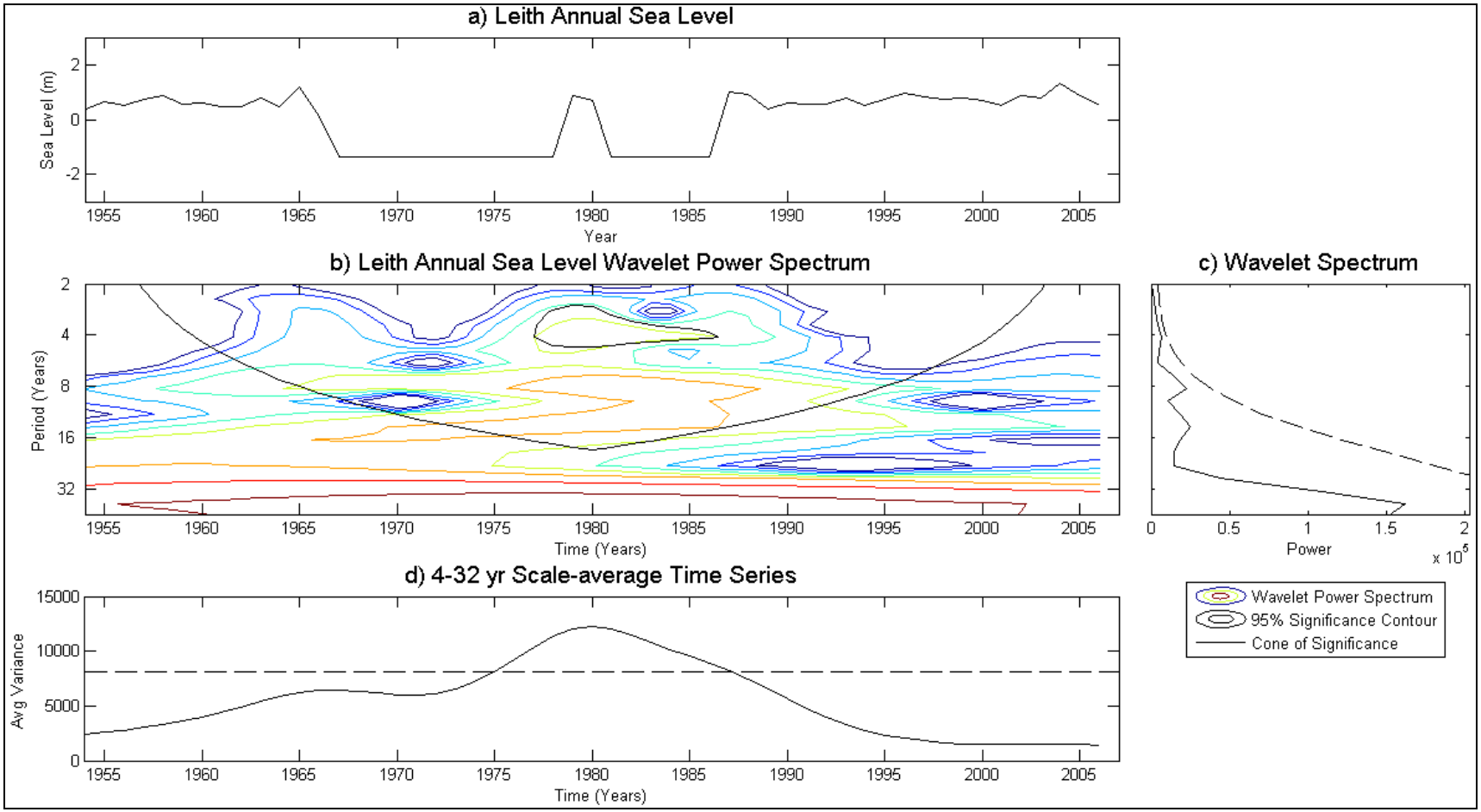

Figure A7.9. Wavelet analysis using the Torrence and Compo (1998) wavelet software. a) Complete Leith annual time series sea level data. b) Leith annual sea level power spectrum with attached legend explaining the wavelet power spectrum contours, 95% significance contours and the cone of significance. Contours coloured red and yellow are of high significance. c) The wavelet spectrum illustrates the spikes in variance in relation to the wavelet power spectrum (graph b). The y-axis is shared with graph b. d) The 4-32 year scale-average time series illustrates the smoothed variance in the data along the time series from the scale-average.

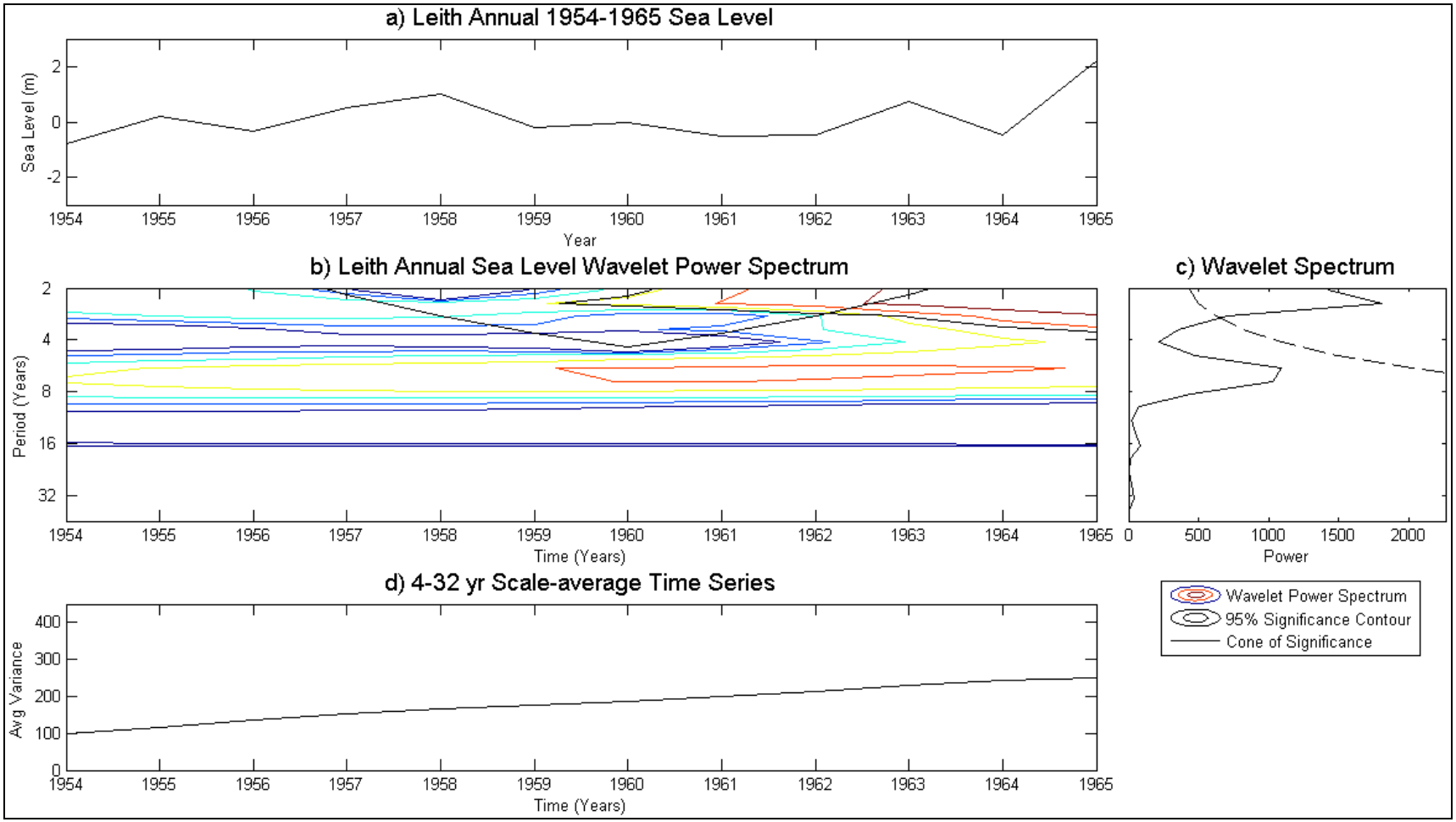

Figure A7.10. Wavelet analysis using the Torrence and Compo (1998) wavelet software. a) Leith 1954-1965 annual sea level data. b) Leith annual sea level power spectrum with attached legend explaining the wavelet power spectrum contours, 95% significance contours and the cone of significance. Contours coloured red and yellow are of high significance. c) The wavelet spectrum illustrates the spikes in variance in relation to the wavelet power spectrum (graph b). The y-axis is shared with graph b. d) The 4-32 year scale-average time series illustrates the smoothed variance in the data along the time series from the scale-average.

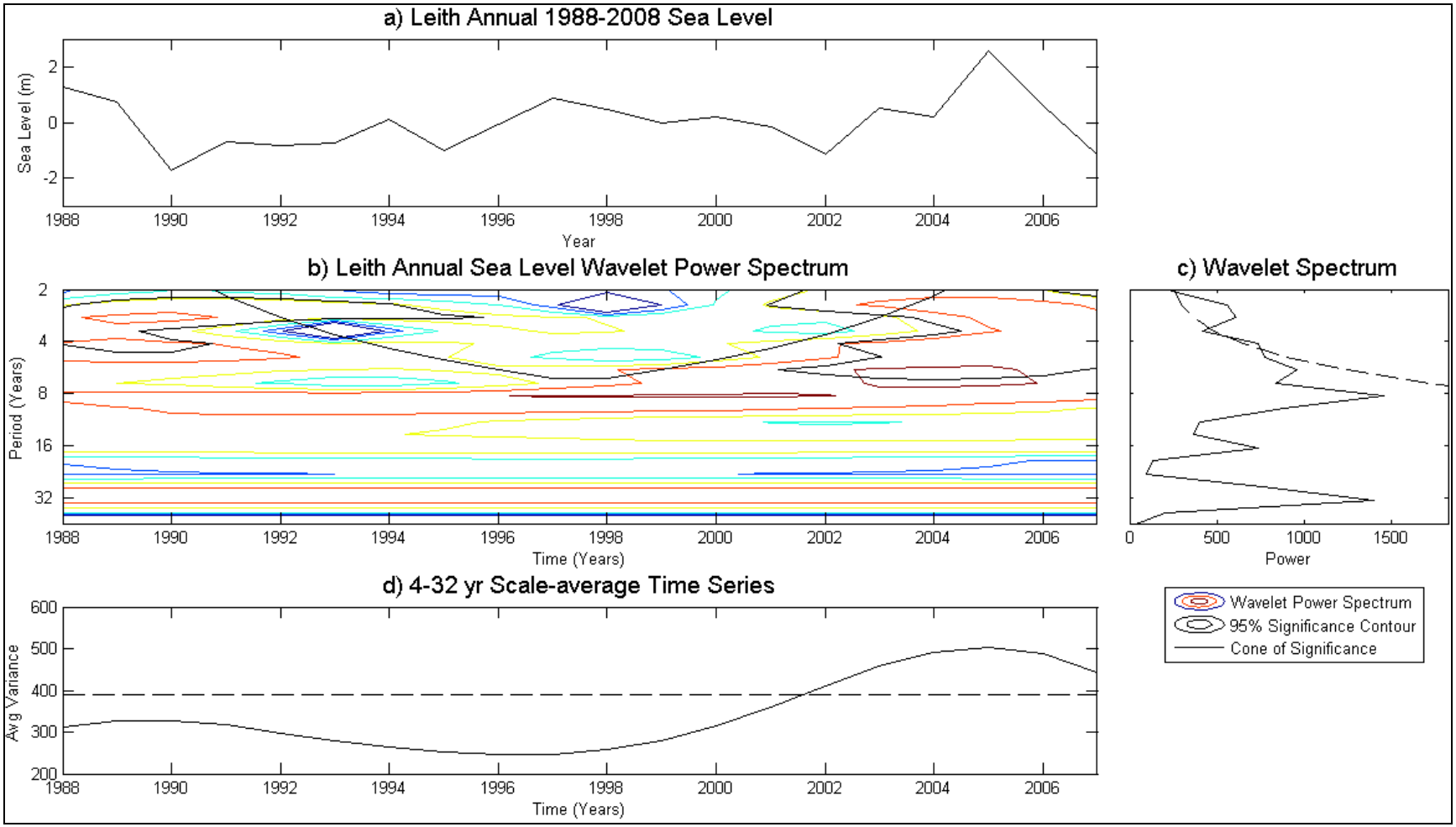

Figure A7.11. Wavelet analysis using the Torrence and Compo (1998) wavelet software. a) Leith 1988-2008 annual sea level data. b) Leith annual sea level power spectrum with attached legend explaining the wavelet power spectrum contours, 95% significance contours and the cone of significance. Contours coloured red and yellow are of high significance. c) The wavelet spectrum illustrates the spikes in variance in relation to the wavelet power spectrum (graph b). The y-axis is shared with graph b. d) The 4-32 year scale-average time series illustrates the smoothed variance in the data along the time series from the scale-average.

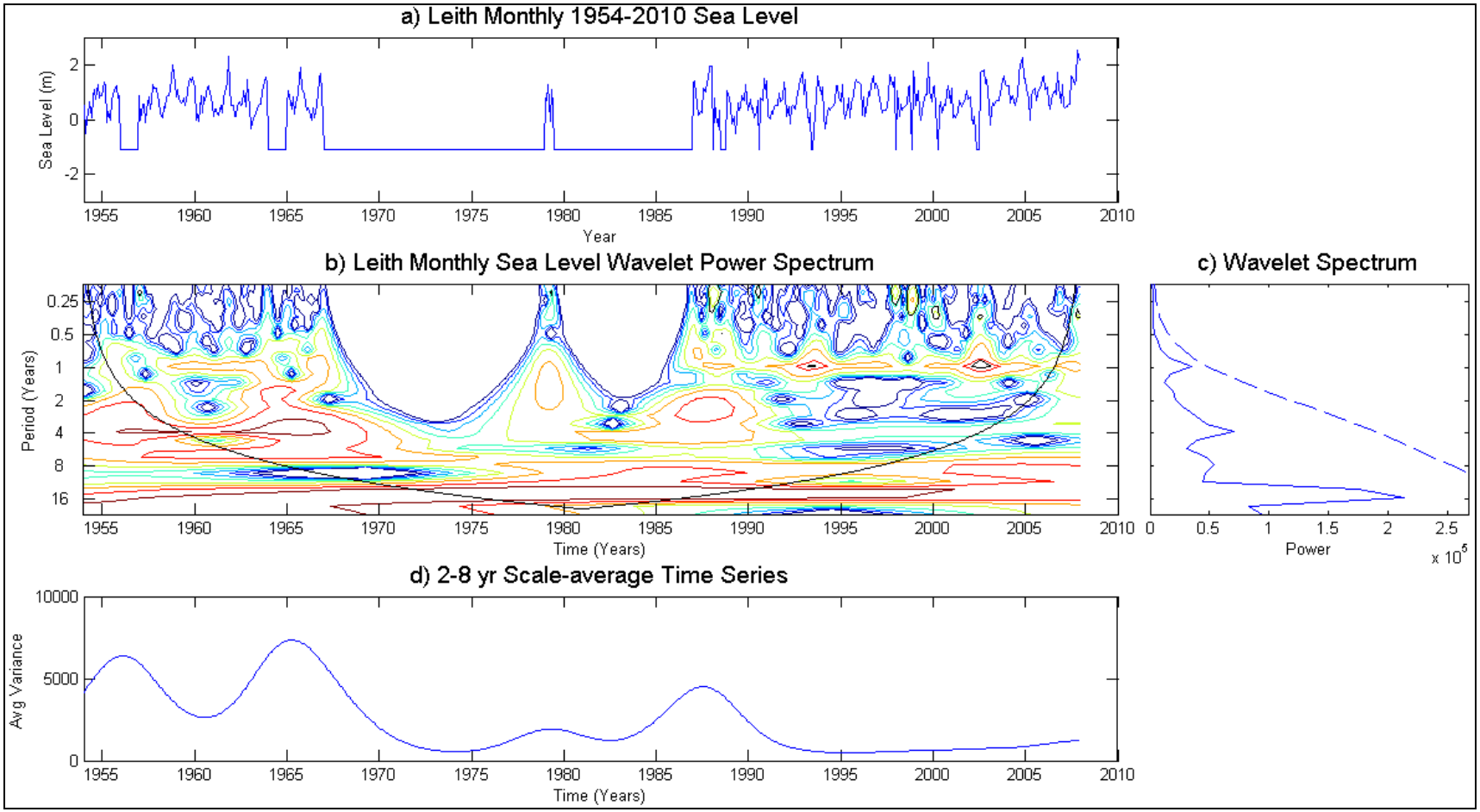

Figure A7.12. Wavelet analysis using the Torrence and Compo (1998) wavelet software. a) Leith 1954-2010 monthly sea level data. b) Leith monthly sea level power spectrum with attached legend explaining the wavelet power spectrum contours, 95% significance contours and the cone of significance. Contours coloured red and yellow are of high significance. c) The wavelet spectrum illustrates the spikes in variance in relation to the wavelet power spectrum (graph b). The y-axis is shared with graph b. d) The 4-32 year scale-average time series illustrates the smoothed variance in the data along the time series from the scale-average.

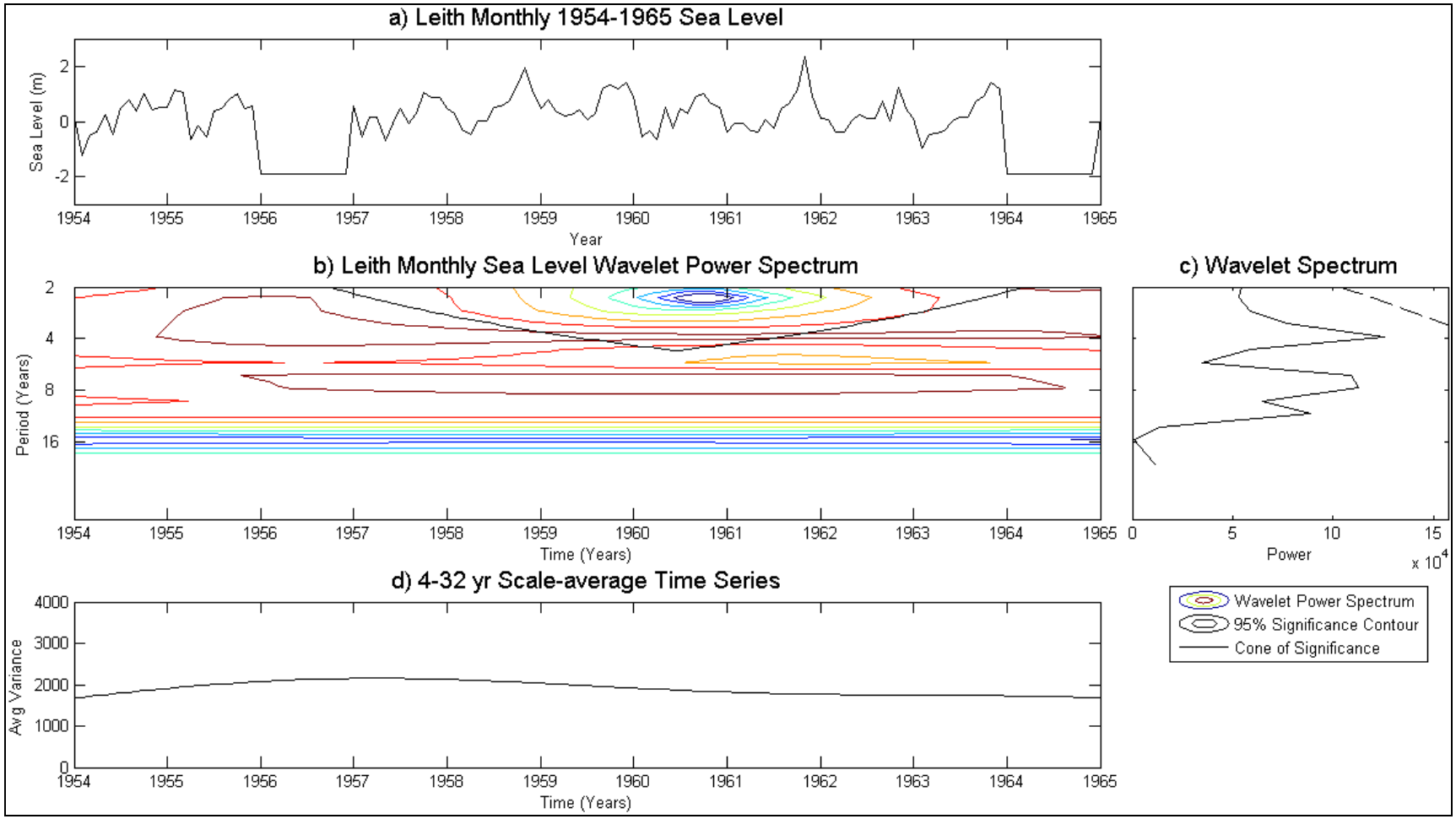

Figure A7.13. Wavelet analysis using the Torrence and Compo (1998) wavelet software. a) Leith 1954-1965 monthly sea level data. b) Leith monthly sea level power spectrum with attached legend explaining the wavelet power spectrum contours, 95% significance contours and the cone of significance. Contours coloured red and yellow are of high significance. c) The wavelet spectrum illustrates the spikes in variance in relation to the wavelet power spectrum (graph b). The y-axis is shared with graph b. d) The 4-32 year scale-average time series illustrates the smoothed variance in the data along the time series from the scale-average.

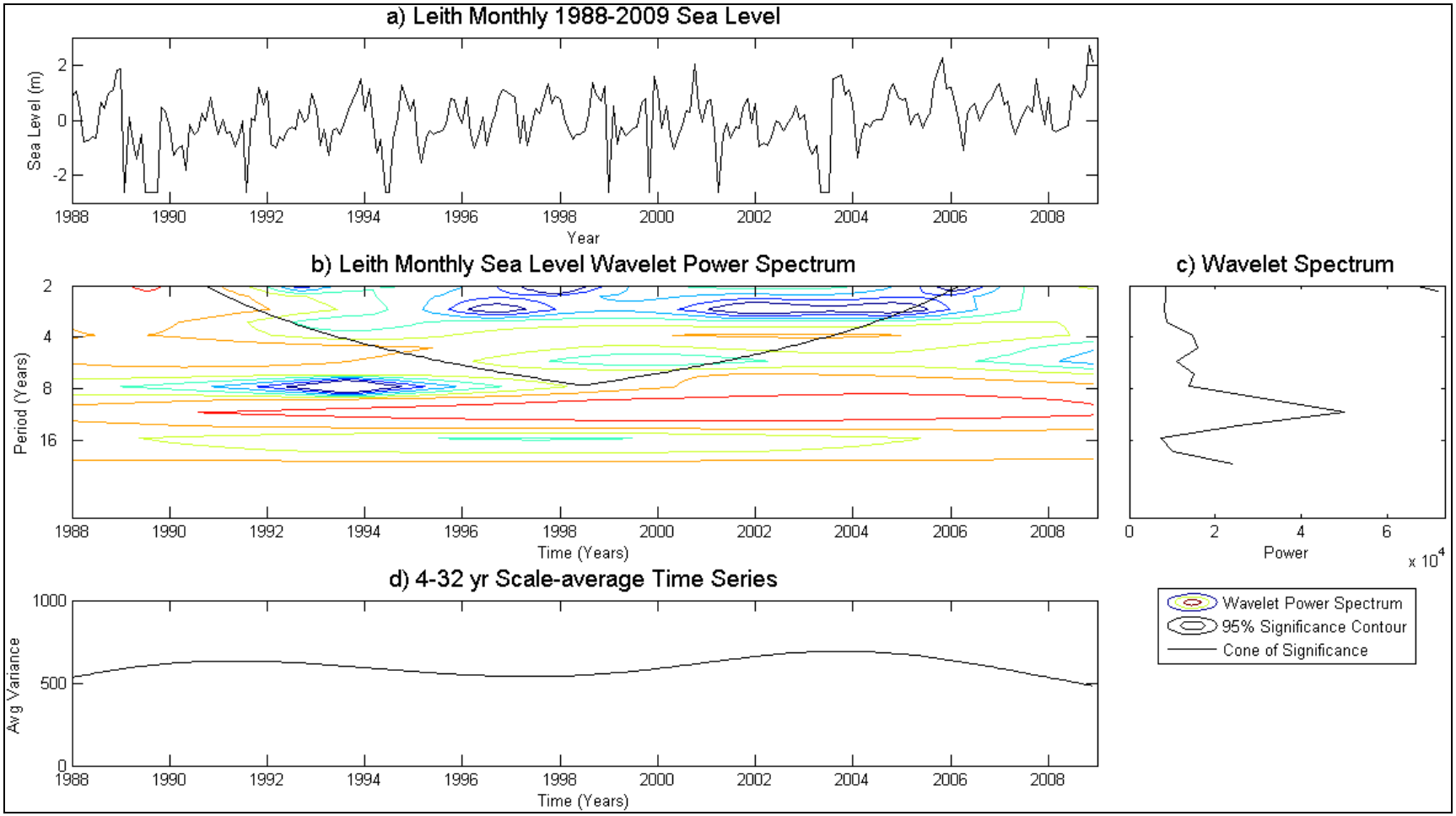

Figure A7.14. Wavelet analysis using the Torrence and Compo (1998) wavelet software. a) Leith 1988-2009 monthly sea level data. b) Leith monthly sea level power spectrum with attached legend explaining the wavelet power spectrum contours, 95% significance contours and the cone of significance. Contours coloured red and yellow are of high significance. c) The wavelet spectrum illustrates the spikes in variance in relation to the wavelet power spectrum (graph b). The y-axis is shared with graph b. d) The 4-32 year scale-average time series illustrates the smoothed variance in the data along the time series from the scale-average.

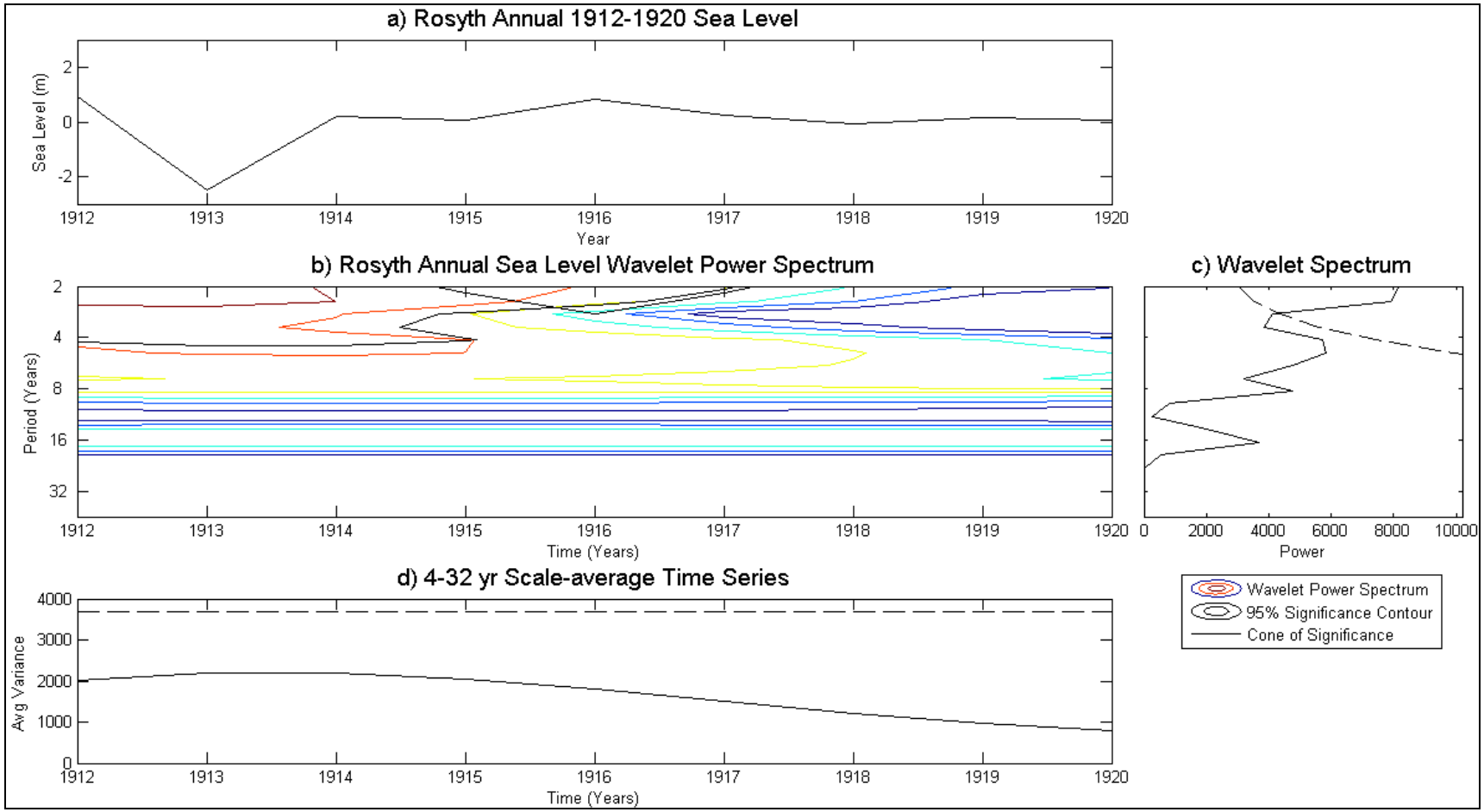

Figure A7.15. Wavelet analysis using the Torrence and Compo (1998) wavelet software. a) Rosyth annual 1912-1920 sea level data. b) Rosyth annual sea level power spectrum with attached legend explaining the wavelet power spectrum contours, 95% significance contours and the cone of significance. Contours coloured red and yellow are of high significance. c) The wavelet spectrum illustrates the spikes in variance in relation to the wavelet power spectrum (graph b). The y-axis is shared with graph b. d) The 4-32 year scale-average time series illustrates the smoothed variance in the data along the time series from the scale-average.

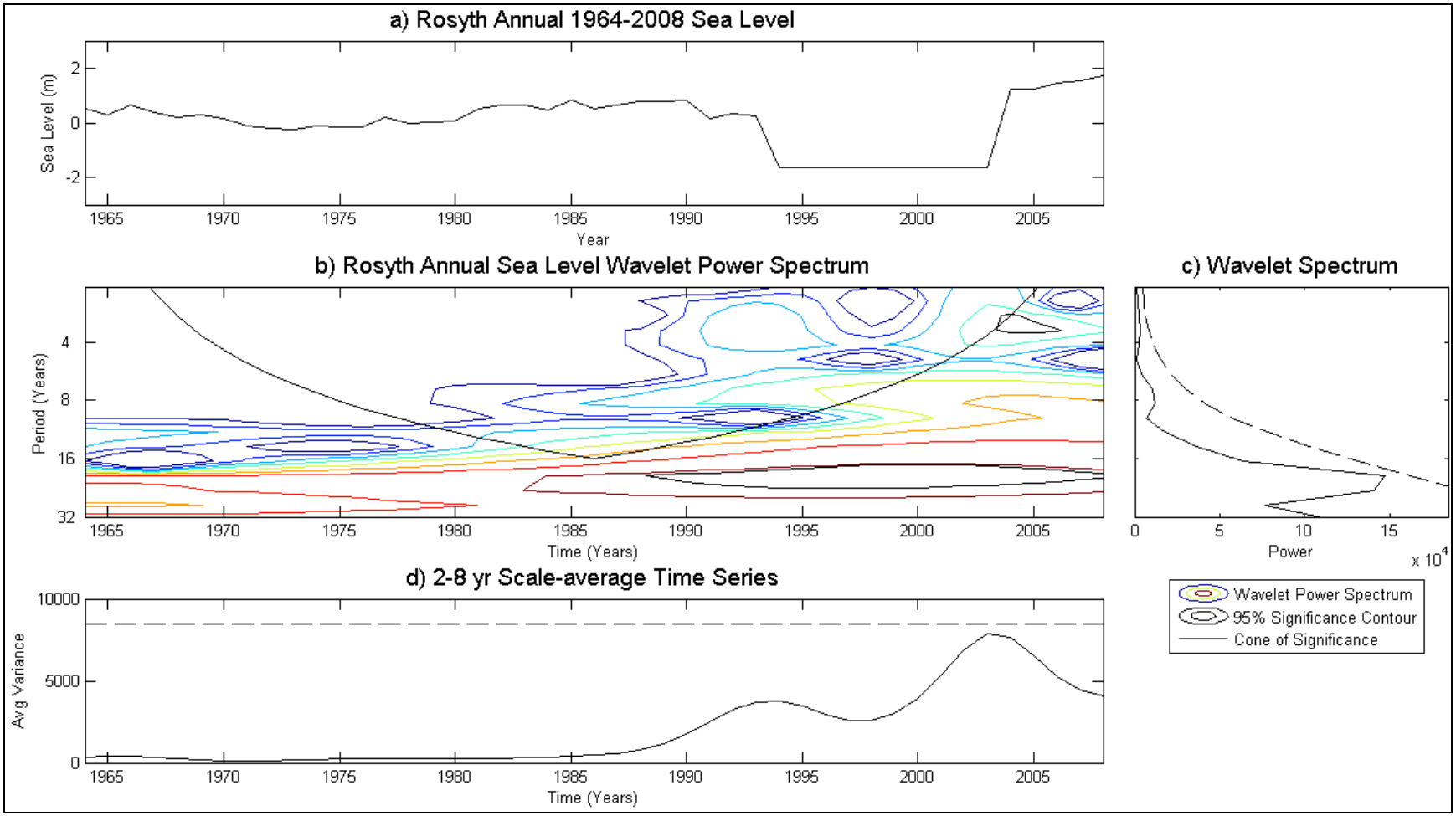

Figure A7.16. Wavelet analysis using the Torrence and Compo (1998) wavelet software. a) Rosyth annual 1964-2008 sea level data. b) Rosyth annual sea level power spectrum with attached legend explaining the wavelet power spectrum contours, 95% significance contours and the cone of significance. Contours coloured red and yellow are of high significance. c) The wavelet spectrum illustrates the spikes in variance in relation to the wavelet power spectrum (graph b). The y-axis is shared with graph b. d) The 4-32 year scale-average time series illustrates the smoothed variance in the data along the time series from the scale-average.

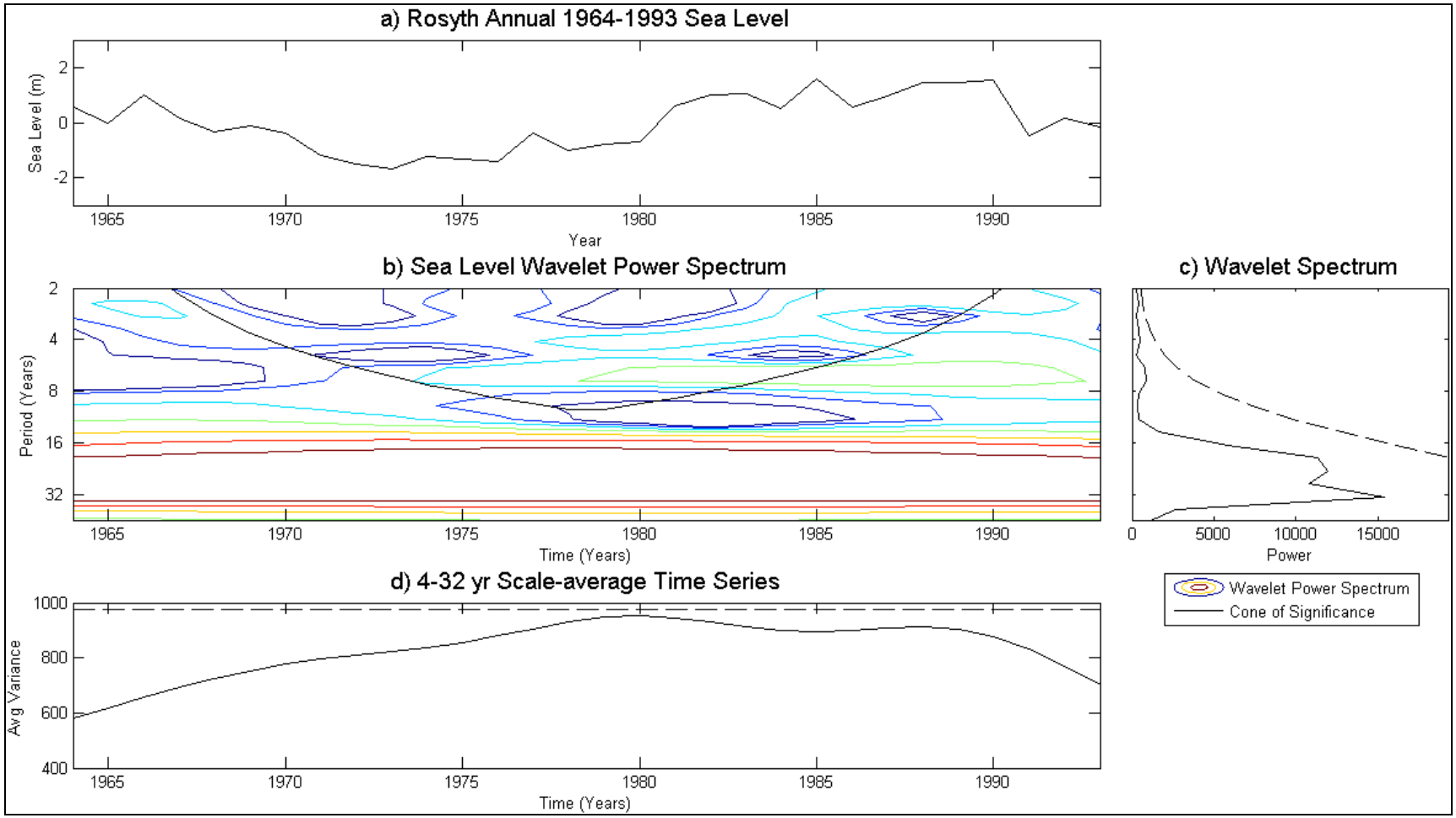

Figure A7.17. Wavelet analysis using the Torrence and Compo (1998) wavelet software. a) Rosyth annual 1964-1993 sea level data. b) Rosyth annual sea level power spectrum with attached legend explaining the wavelet power spectrum contours, 95% significance contours and the cone of significance. Contours coloured red and yellow are of high significance. c) The wavelet spectrum illustrates the spikes in variance in relation to the wavelet power spectrum (graph b). The y-axis is shared with graph b. d) The 4-32 year scale-average time series illustrates the smoothed variance in the data along the time series from the scale-average.

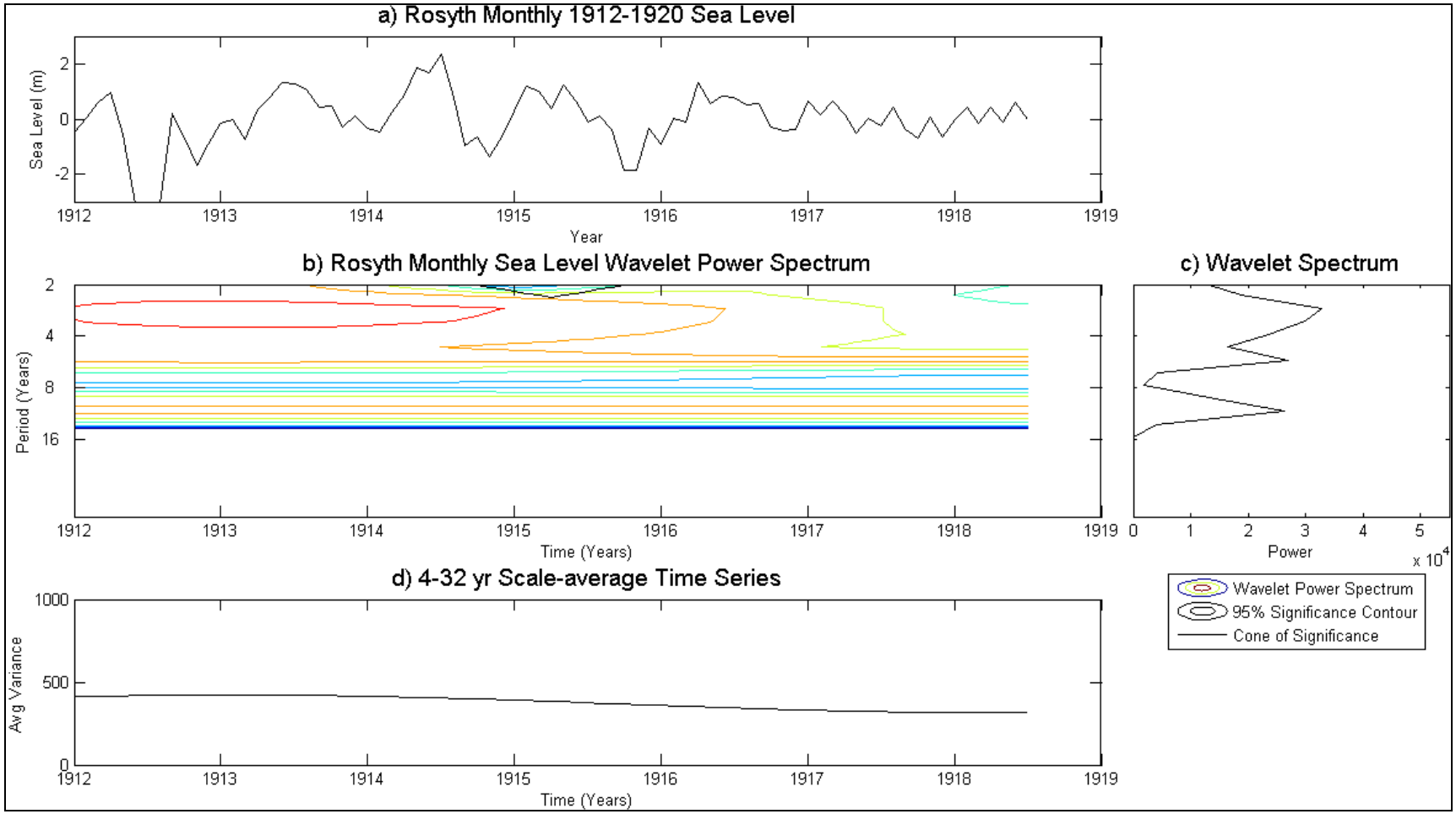

Figure A7.18. Wavelet analysis using the Torrence and Compo (1998) wavelet software. a) Rosyth monthly 1912-1920 sea level data. b) Rosyth monthly sea level power spectrum with attached legend explaining the wavelet power spectrum contours, 95% significance contours and the cone of significance. Contours coloured red and yellow are of high significance. c) The wavelet spectrum illustrates the spikes in variance in relation to the wavelet power spectrum (graph b). The y-axis is shared with graph b. d) The 4-32 year scale-average time series illustrates the smoothed variance in the data along the time series from the scale-average.

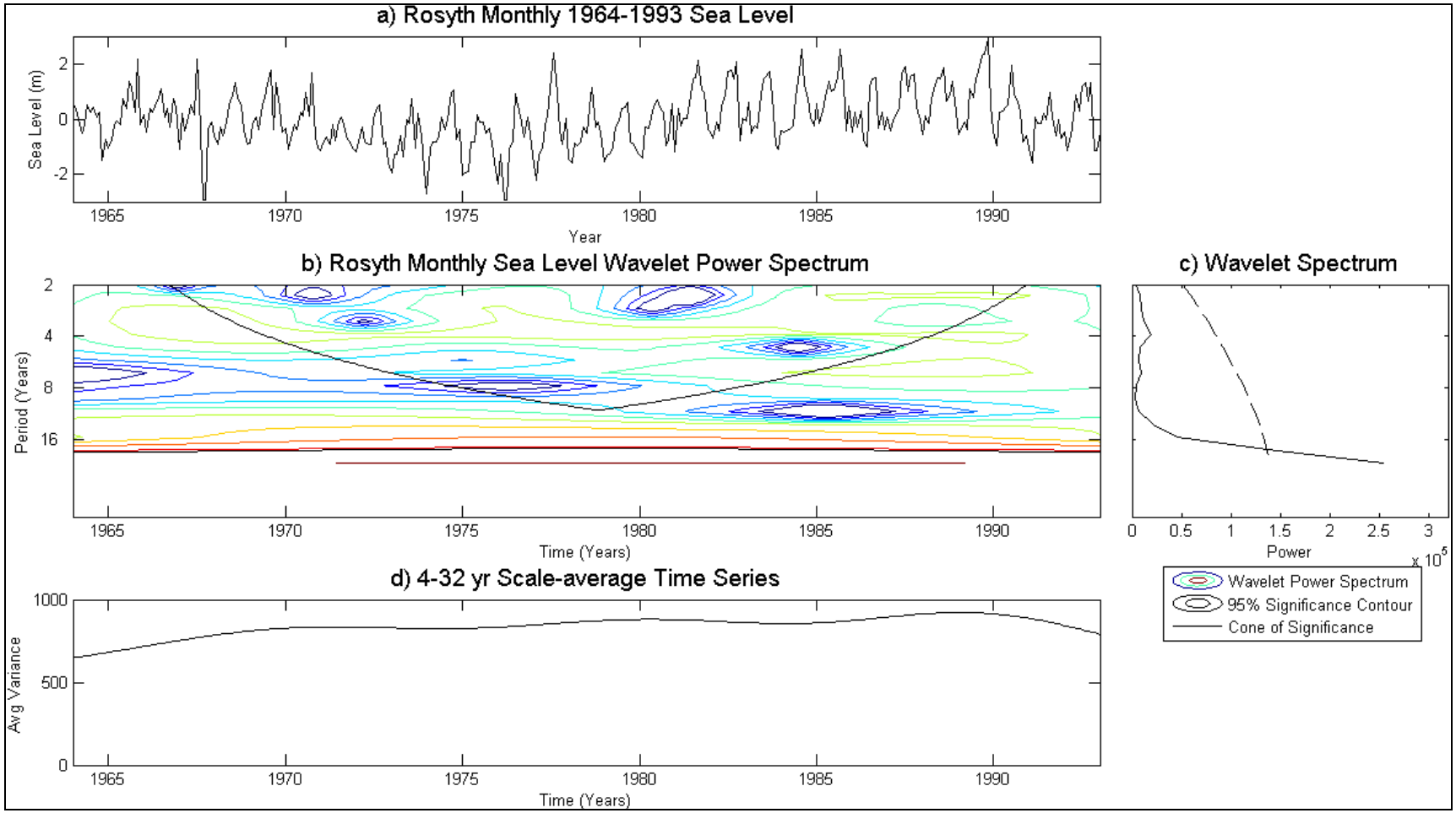

Figure A7.19. Wavelet analysis using the Torrence and Compo (1998) wavelet software. a) Rosyth monthly 1964-1993 sea level data. b) Rosyth monthly sea level power spectrum with attached legend explaining the wavelet power spectrum contours, 95% significance contours and the cone of significance. Contours coloured red and yellow are of high significance. c) The wavelet spectrum illustrates the spikes in variance in relation to the wavelet power spectrum (graph b). The y-axis is shared with graph b. d) The 4-32 year scale-average time series illustrates the smoothed variance in the data along the time series from the scale-average.

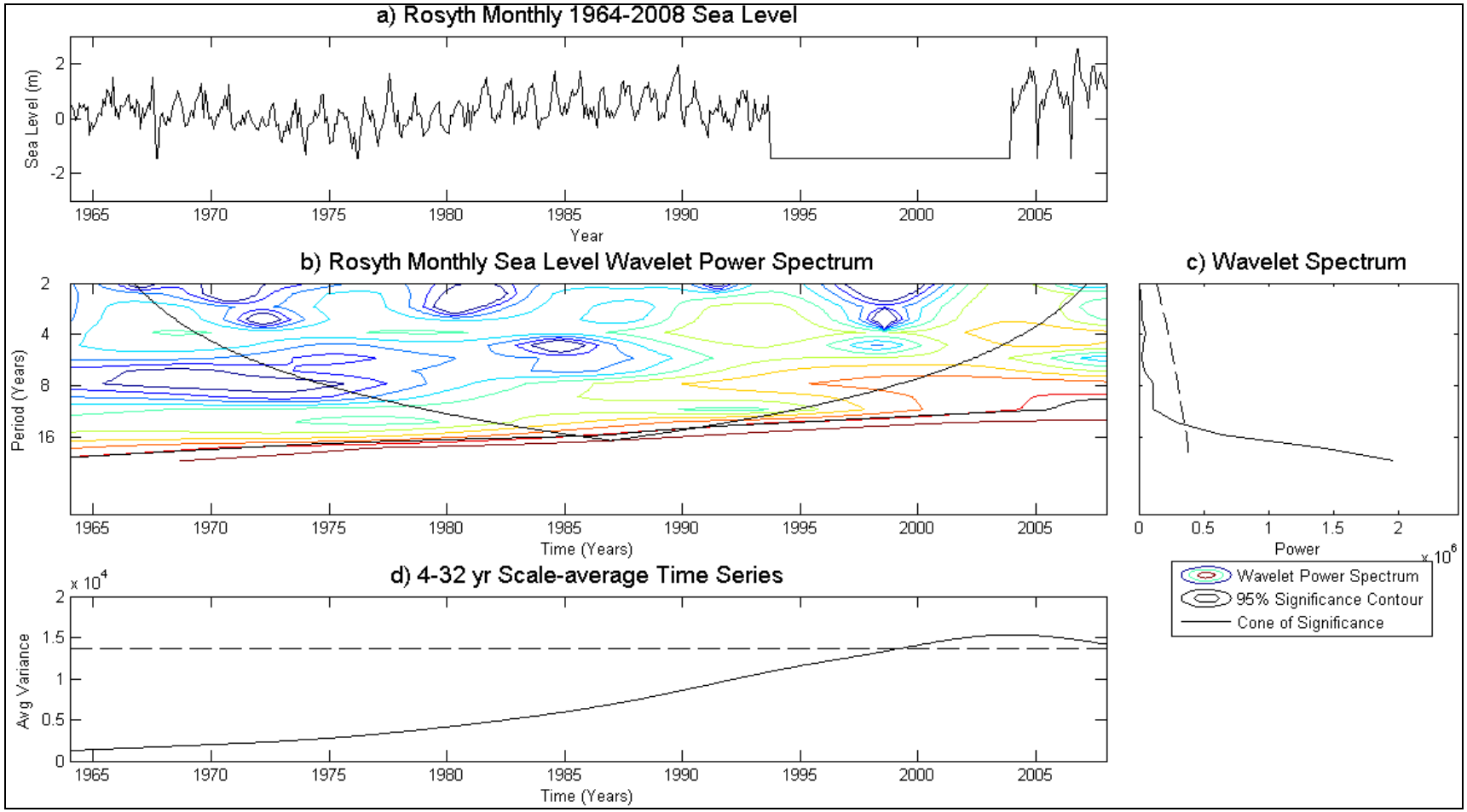

Figure A7.20. Wavelet analysis using the Torrence and Compo (1998) wavelet software. a) Rosyth monthly 1964-2008 sea level data. b) Rosyth monthly sea level power spectrum with attached legend explaining the wavelet power spectrum contours, 95% significance contours and the cone of significance. Contours coloured red and yellow are of high significance. c) The wavelet spectrum illustrates the spikes in variance in relation to the wavelet power spectrum (graph b). The y-axis is shared with graph b. d) The 4-32 year scale-average time series illustrates the smoothed variance in the data along the time series from the scale-average.